New Mexico
Petroleum Recovery Research Center

A Division of
New Mexico Institute of Mining and Technology
Telephone (505) 835-5142

Socorro, NM 87801

May 19, 1988

Gavilan-West Puerto Chiquito Mancos Operators
New Mexico Oil Conservation Division Preliminary Hearing
Santa Fe, NM 87501

Gentlemen:

Enclosed are data collected during the 6/30/87 to 2/23/88 test period. Various calculations have been performed with the data to reach conclusions. Your review of the data, analytical methods, and your comments would be greatly appreciated. Please respond in a timely manner so that corrections can be made to this preliminary report prior to the June 13, 1988 Gavilan-West Puerto Chiquito Mancos hearing.

Sincerely,

Bill Weiss

William W. Weiss
Field Petroleum Engineer

WWW:jeg
enc.

A REVIEW OF THE GAVILAN - WEST PUERTO CHIQUITO MANCOS RESERVOIR PERFORMANCE DURING THE PERIOD OF JULY, 1987 - FEBRUARY, 1988.

Background

The New Mexico OCD requested that operators of the two subject pools, Gavilan and West Puerto Chiquito, conduct pressure buildup tests on key wells. The purpose of the tests was to measure static pressures and reservoir characteristics when the quality of the data was sufficient to analyze. The commission also ordered a variation in well-producing rates via the allowables ruling. The variation in producing rates suggests that the reservoir may be rate-sensitive shown by the fact that lower GOR's were observed during periods of high production rates.

Included in the pressure study were wells Wildfire #1, High Adventure #1, Loddy #1, and Boyt & Lola #1, operated by Sun E&P; Bearcat #1 by Mesa Grande Resources; Howard Federal #43-15 by Reading and Bates; Hill Federal #2Y (later switched to Hill Federal #1) by Meridian; Johnson Federal 12#5 by Mallon; Lindrith B-#37 by Mobil, and Canada Ojita Unit (C.O.U.) wells E-6, B-32, A-20, and K-13 operated by BMG.

In addition to the thirteen wells requested by the commission, operators generously provided information from other wells which is incorporated in this review.

The two subject pools both produce from the Mancos Shale at a depth of about 6,200 to 7,800 feet. Production is from the "A", "B", and "C" zones in what is described as a tight naturally-fractured reservoir consisting of shaley siltstone and low-porosity, fine-grained sand. Some characteristics of the Mancos Reservoir are similar to the larger Spraberry Trend Field of West Texas which has been mentioned extensively in the literature.

Production from the Gavilan Pool is by primary means only, while the West Puerto Chiquito Pool has produced primary and secondary oil via a gas injection program during the past twenty years. The C.O.U. well E-10, alone has produced over 2,000,000 barrels of oil--strong evidence that gas injection is a successful secondary recovery process.

Static Pressures

Static pressures were measured on 6/30/87, 11/19/87, and 2/23/88 in the designated wells with all other pool wells shutin. Pressures which were obtained with a downhole bomb are illustrated in Figures 1-3. Notice in Figures 2 and 3 a small pressure decline during 11/19 -2/23 which indicates pressure support from C.O.U.

The method of arriving at the +370-ft pressure is outlined in Matthews and Russell's "Pressure Buildup and Flow Tests in Wells," Monograph Volume #1, pages 117 and 118, published by the SPE. Briefly, bomb pressure was corrected to the top of the "B" zone based on the tubing gradient. The pressure was then adjusted to a +370 ft datum based on the reservoir gradient. The reservoir gradient was determined from the volume-weighted, average fluid density from the Loddy #1 PVT data. The volume parameters were the gas- and oil-producing rates prior to the test, corrected to reservoir conditions. The work sheets are included in the appendix.

Examination of the pressure data illustrates the presence of a pressure gradient from east to west across the pools--the exception being the undeveloped east side of Gavilan. Pressure gradients of this nature are not uncommon in gas injection projects. For example, the isobaric lines shown in Figure 4 are taken from a CO_2 flood located in North Texas. The well density is 80 acres in this tight, heterogeneous carbonate reservoir, and the production response shown in Figure 5 clearly demonstrates that the reservoir is contiguous, even with a 300-psi pressure drop across the 80 acres. The same is true of the Gavilan-West Puerto Chiquito Pools.

Figure 6 illustrates the directional dependency of the pressure gradients resulting from gas injection in West Puerto Chiquito. Notice that the pressure drop per 1000-ft is about a factor of 10 larger in the east-west direction than in the north-south direction.

Pressure Buildup Tests

Transmissibility, kh/μ, and flow capacity, kh, were calculated from the transient buildup data whenever the data permitted. Since the GOR's were above those of solution gas, the analytical method used to find reservoir parameters included converting gas and oil flow rates to one reservoir flow rate. Formation volume factors and fluid viscosities were arrived at by volume averaging the Loddy #1 PVT data in a manner similar to that used to find reservoir fluid density.

The technique used to analyze most of the transient data consisted of using Agarwal time, T x dt/T + dt, as the time parameter to eliminate short, producing-time effects, and plotting the pressure difference vs. time on logarithmic paper along with the first derivative of the pressure difference curve in order to find the proper semi-log straight line. Most of the buildups had storage and skin effects, which were identified by a unit slope on the logarithmic plots. The middle-time (MTR) straight line began at about 50 times the end of the unit slope line. The first derivative plot confirms the unit-slope-line rule. The C.O.U well analyses were complicated by the presence of a constant pressure boundary caused by gas injection. In an effort to maintain consistency with the Gavilan analyses, the pseudo-steady state (MTR) straight line was used in all analyses. The single exception was the November data from the B-37 well which fit a dual porosity model very nicely and was so analyzed. Work sheets are included in the appendix.

Table I summarizes the analyses of the pressure buildup data. The transmissibility and capacity are mapped on Figures 7 and 8, respectively.

As mentioned earlier, the 11/19/87 buildup data from the B-37 well was of sufficient quality, and free of boundary effects, that the dual porosity analytic model described by Raghaven in the December, 1983 JPT could be applied. Using the analytical techniques presented in Raghaven's article, "New Pressure Transient Analysis Methods for Naturally Fractured Reservoirs," produced the following results:

Fracture capacity, $k_f h_f$	=	1,477 md-ft
Matrix capacity, $k_m h_m$	=	9.16 md-ft
Transfer coefficient λ'	=	1.27×10^{-7}
Fracture Storativity, $\phi_f C_f h_f$	=	1.106×10^{-5}
Dimensionless matrix storativity, ω'	=	27 (about 4% of total porosity is in the fracture system)

These results support Mobil's observation that the reservoir is a dual porosity system.

Interference Tests

BMG recorded bottomhole pressures at various observation wells while stimulating seven Canada Ojitos Unit wells. The pressure pulse generated by the hydraulic fracture treatment was recorded as a deviation from the pressure trend as seen on the attached curves included in the appendix. The pressure differential resulting from the frac job was analyzed with a type curve from Ramey's "A Drawdown and Buildup Type Curve for Interference Testing," and Kamal's "Well Interference and Pulse Tests" analytical method.

Problems with determining the proper formation volume factors, viscosities, and compressibilities, all of which are saturation dependent, were encountered. Accepting the problems in estimating saturations the Kamal method results are illustrated in Figure 9 as capacity, kh, in Darcy feet and as storage ϕh, in Figure 10. Again, the N-S major permeability trend is evident. The Ramey-type curve gave similar results but was considered more subjective than Kamel's analytical method.

Frac pulse response of F-7 at E-6 and D-17 was analyzed using the well-known method introduced by Ramey to determine direction and magnitude of the permeability trend in an anisotropic reservoir. The major trend is 33,600 md-ft north with a 370 md-ft trend normal to the major axis. The results include an estimate for $\phi \mu c_t$ of 3.5 x 10^{-7} which was observed in the frac pulse test analyses and the B-37 buildup. The results are illustrated on Figure 11 and detailed in the appendix.

The interference test data supported by static pressure measurements indicate that the permeability is much greater in the N-S direction than in the E-W direction. Similar differences in major and minor permeabilities were reported by Elkins and Skov in their "Determination of Fracture Orientation from Pressure Interference." Their data concerning the Spraberry Trend is summarized in Figure 12.

Rate Sensitivity

During the 6/30/87 to 2/23/88 test period, a GOR vs. BOPD trend developed which indicated increased recovery efficiency at high production rates. A total of 87 wells were monitored. The GOR's were based on monthly averages except where producing time was less than three months, then daily rates were utilized.

Logarithmic plots of rate vs. GOR were made for the 87 wells. A total of the 46 wells had a goodness of fit to a logarithmic straight line of 85% or better. Only one well had a positive slope indicating poor recovery efficiency at high rates, the remaining wells indicate increased recovery efficiency at high rates. The wells with their correlation coefficients are tabulated in Table II. All wells are included in the appendix.

Explanations for the favorable rate sensitivity vary. Three possibilities are:

1. Counter-current gas flow with the formation of a secondary gas cap displacing oil downward.

2. Formation of a large pressure difference between the fractures and the matrix enhancing the transfer of oil to the fracture system.

3. Formation of an unusually large number of gas bubbles in oils subject to rapid pressure decline which in turn reduces the oil saturation.

The concept of the formation of gas bubbles with resulting reduced oil saturation was proposed 25 years ago by Amoco in a paper titled "The Role of Bubble Formation in Oil Recovery by Solution Gas Drives in Limestones," which followed a paper by Kennedy and Olsen on the same subject. Since then, little has been done to advance the concept.

Increasing the pressure difference between the fractures and the matrix was suggested by Elkins as a means of improving recovery efficiency in the Spraberry Trend. If this was applied in the field, the results were not well documented in the literature. The concept does have merit in the Mancos where the surface area available for flow from the very tight matrix is largely due to the fracture system.

Normally, rate-sensitivity is associated with a displacement process and is readily described with the fractional flow equation:

$$f_g = \frac{1 - \dfrac{4.9 \times 10^{-4}\, k\, k_{ro}\, A\, (\Delta\rho) \sin\Theta}{q_t\, \mu_o}}{1 + \dfrac{kro}{krg}\dfrac{\mu g}{\mu o}}$$

Dake eq 10.21
Page 359

With the formation of a secondary gas cap, oil is displaced downward and the sin(-90°) becomes a minus one which allows the fraction of gas flowing, f_g, to decrease as the total rate, q_t, increases.

This equation was applied to well B-37 utilizing the parameters derived from the November pressure buildup test, 320 acres drainage, relative permeability ratios from Slider's textbook, curve #16 on page 456 which is for large fractures connected together, and Loddy #1 PVT data. Figures 13-16 depict the theoretical match to the actual data obtained, utilizing only the fractional flow equation. The trend of the theoretical curve is similar to the production trend in the B-37, E-6, and Johnson-Federal 12#5 wells; however, the Bearcat #1 does not follow suit.

The match of the theoretical to the actual shown on Figure 17 for the B-37 well was obtained by reducing the permeability-area product in the fractional flow equation from 8.75×10^7 md-ft^2 to 8.75×10^5 md-ft^2 suggesting the secondary gas cap is not continuous throughout the 320 acre drainage area.

The permeability calculated from the well B-37 buildup test was used to match the producing f_g trend in the critical rate, q_{crt}, equation

$$q_{crt} = \frac{4.9 \times 10^{-4}\, kk_{rg}\, A\, \Delta\gamma \sin \Theta}{\mu_g\ (M-1)}$$

results in a 50 STB/D critical flow rate.

Counter to the production data supporting the improvement in the recovery efficiency, is recovery efficiency as a function of pressure drop. During the period of high-production rates, the recovery efficiency averaged 98 barrels/psi for the nine wells illustrated in Figure 18. However, during the low production rate period, illustrated in Figure 19, the recovery efficiency increased to 136 barrels/psi. Results are tabulated in Table III.

This dichotomy can be explained by pressure support external to the individual well-drainage areas. Notice that the Bearcat #1 and Howard-Federal #43-15 demonstrate little variation in recovery efficiency as a function of pressure drop since they do not have external pressure support. However, wells E-6, A-20, and B-32 show improvement during the period of low production rates when gas injection was able to support withdrawals. In fact, pressure did not drop at B-32 during the low rate period, yet the well produced 42,200 barrels of oil during this period.

In a similar manner, the B-37, Loddy #1, and High Adventure #1 enjoyed external pressure support, apparently from outside the pool boundaries.

Conclusions

The Gavilan-West Puerto Chiquito Mancos Pools appear to be a common reservoir. It is clear that the reservoir fracture system is sufficient to allow fluid migration across pool boundaries.

The anisotropic nature of the reservoir should be further defined in order to investigate a secondary recovery process. Production rates in a secondary mode would be dependent on balancing injection and production rates rather than the poorly understood, currently postulated producing mechanisms.

It is worth noting that the Spraberry Trend Field has produced over a billion barrels of oil with about 25% of it as a result of primary recovery.

Table I

Transient Test Results

Well	Test Date	$\frac{kh}{\mu}$ md-ft/cp	kh md-ft	k_oh md-ft	k_gh md-ft
E-6	11/19/87	18,320	1,523	1,290	232
B-32	11/19/87	21,700	5,123	4,925	196
Fisher Federal #2-1	2/23/88	5,710	231	154	76
Johnson Federal 12#5	11/19/88	3,110	131	88	44
Hill Federal 2Y	6/30/87	1,240	141	126	15
Hill Federal #1	11/19/87	7,020	117	12.3	98
Bearcat #1	6/30/87	2,500	165	133	32
Lindrith B-37	11/19/87	19,020	1,477	1,242	235
Howard Federal 43-15	11/19/87	3,690	65	14.2	50.5
High Adventure #1	11/19/87	11,150	1,126	992	134
Loddy #1	11/19/87	2,085	140	113	27

TABLE II.

Gavilan Dome
Rate Sensitivity Correlation Coefficients

Operator	Well Name	c.c.	Slope
AMOCO	SCC	1.00	NEG
M.G.	PRO#2	1.00	NEG
B.M.G.	L-11	1.00	NEG
B.M.G.	J-6	1.00	NEG
MALLON	JF 12#5	1.00	NEG
MERIDIAN	HF 3	1.00	NEG
MERIDIAN	HF #1	0.99	NEG
SUN	JA A2	0.99	NEG
SUN	NS 2	0.98	NEG
M.G.	BC#1	0.98	NEG
M.G.	RL#3	0.98	NEG
MOBIL	B 37	0.98	NEG
SUN	FS A2	0.97	NEG
MALLON	RF 2#16	0.97	NEG
MERIDIAN	HF 2Y	0.97	NEG
MALLON	HF 1#11	0.97	NEG
MERRION	KRY 1	0.96	NEG
M.G.	HC #1	0.96	NEG
MERIDIAN	HAF 2	0.96	NEG
SUN	DRDO 1	0.96	NEG
B.M.G.	E-10	0.96	NEG
SUN	HR 1	0.95	NEG
SUN	NS 1	0.95	NEG
MOBIL	B 73	0.95	NEG
SUN	ET 1	0.93	NEG
SUN	LOD 1	0.93	NEG
M.G.	GH#1	0.92	NEG
M.G.	MAR#1	0.92	NEG
B.M.G.	N-31	0.92	NEG
MERIDIAN	HAF 3	0.92	NEG
M.G.	INV#1	0.91	NEG
SUN	FT E1	0.91	NEG
MALLON	FF 2#1	0.90	NEG
M.G.	GAV #3	0.90	NEG
B.M.G.	A-20	0.90	POS
MALLON	PF 13#6	0.89	NEG
B.M.G.	E-6	0.89	NEG
SUN	BL 2	0.89	NEG
SUN	FT 1	0.88	NEG
MOBIL	B 34	0.88	NEG
SUN	ML 2	0.87	NEG
B.M.G.	F-19	0.87	NEG
SUN	NS 3	0.86	NEG
MOBIL	B 38	0.86	NEG
MOBIL	B 74	0.86	NEG
MALLON	DF 3#15	0.85	NEG

Of the sample
with c.c. > .85

Negative Slopes	
ammount	percentage
45	97.83%

Positive Slopes	
ammount	percentage
1	2.17%

85% Correlation Coefficient Cut Off Point

TABLE II.

Gavilan Dome
Rate Sensitivity Correlation Coefficients

Operator	Well Name	c.c.	Slope
B.M.G.	C-34	0.84	POS
SUN	LL 1	0.80	NEG
SUN	GG 1	0.80	NEG
R&B	IN 34-16	0.79	NEG
B.M.G.	O-9	0.76	NEG
B.M.G.	B-29	0.76	POS
R&B	HF 43-15	0.76	NEG
DUGAN	LIND 1	0.75	NEG
M.G.	RL#2	0.73	NEG
SUN	HA 2	0.71	NEG
B.M.G.	L-3	0.68	NEG
B.M.G.	F-30	0.66	NEG
SUN	JA B3	0.66	NEG
SUN	NH 1	0.65	NEG
SUN	WW 1	0.62	NEG
B.M.G.	F-18	0.58	NEG
M.G.	BRO#1	0.54	NEG
SUN	HA 1	0.52	NEG
B.M.G.	D-17	0.52	NEG
MOBIL	B 72	0.49	NEG
SUN	FS B3	0.48	NEG
SUN	FS 1	0.46	NEG
SUN	BB 1	0.44	NEG
B.M.G.	L-27	0.43	NEG
B.M.G.	O-33	0.43	NEG
B.M.G.	B-32	0.36	POS
AMOCO	SGC 1	0.35	NEG
M.G.	GAV #1	0.32	POS
AMOCO	BCU 2	0.31	NEG
MALLON	HF 1#8	0.31	NEG
SUN	JA 1	0.29	NEG
B.M.G.	K-8	0.20	NEG
B.M.G.	F-7	0.18	POS
B.M.G.	N-22	0.17	POS
B.M.G.	A-16	0.16	NEG
MERRION	OCG 1	0.15	POS
B.M.G.	G-5	0.13	POS
SUN	ML 1	0.08	POS
HIXON	DIV 3	0.06	NEG
B.M.G.	G-32	0.05	NEG
HIXON	TAP 4	0.01	POS

TABLE III.

Gavilan Dome, Recovery Efficiency
Barrel per PSI Pressure Drop

6/30-11/19

Operator	Well Name	dP psia	Cum Oil bbl	Cum/dP bbl/psia
B.M.G.	E-6	208	41118	198
B.M.G.	A-20	217	2443	11
B.M.G.	B-32	237	83828	354
M.G.	Bearcat #1	271	2929	11
Mobil	Lind B 37	270	26385	98
R & B	HF 43-15	261	1020	4
Sun	High Adventure #1	291	24002	82
Sun	Loddy #1	230	7296	32

11/19-2/23

Operator	Well Name	dP psia	Cum Oil bbl	Cum/dP bbl/psia
B.M.G.	E-6	16	4424	277
B.M.G.	A-20	19	2400	126
B.M.G.	E-10	-12	2317	-193
B.M.G.	B-32	0	42177	1000+
Merridian	Hill Federal #1	4	453	113
M.G.	Bearcat #1	33	531	16
Mobil	Lind B 37	36	13011	361
R & B	HF 43-15	37	393	11
Sun	High Adventure #1	54	14052	260
Sun	Loddy #1	53	3318	63

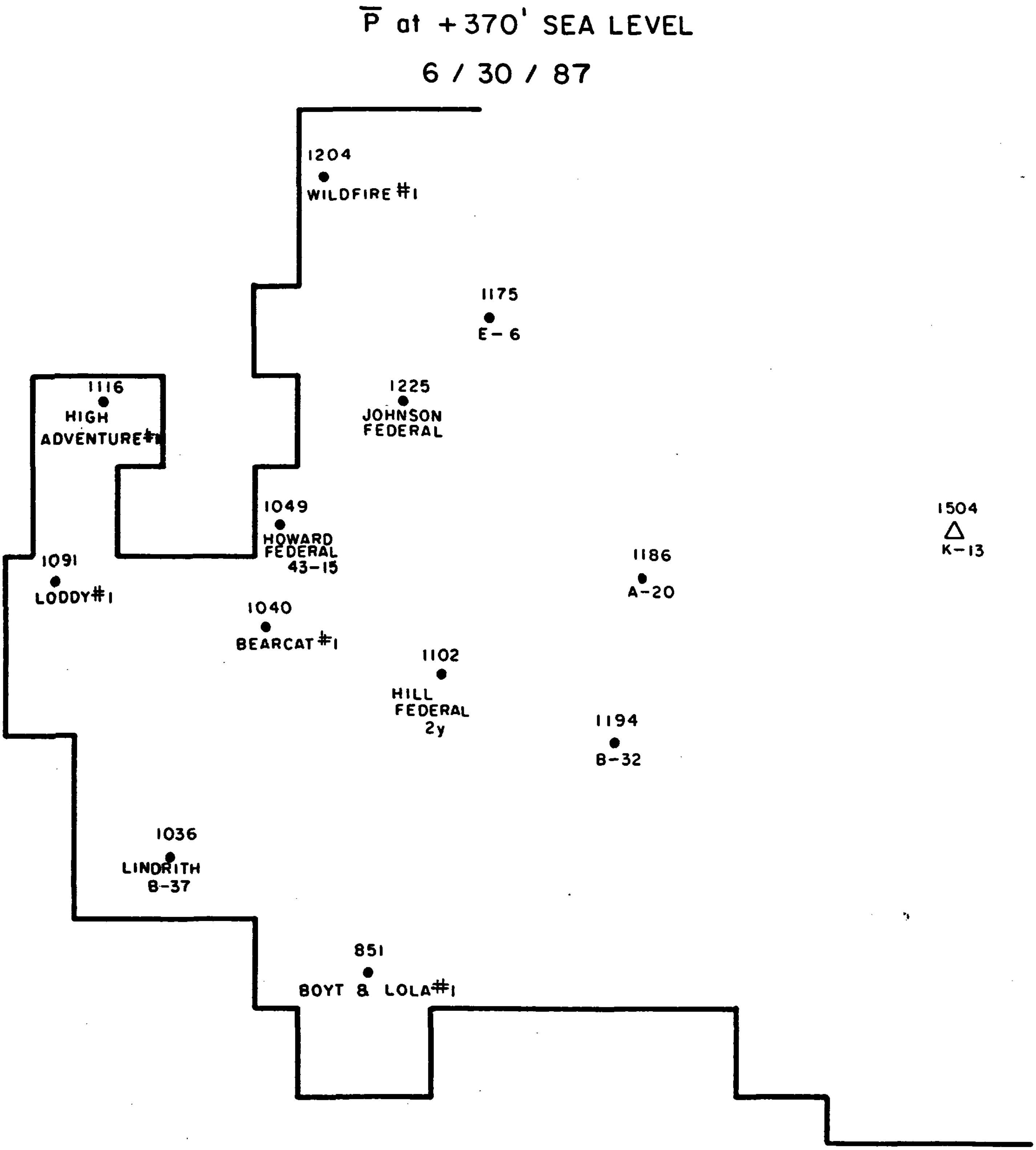
$\overline{P}$ at +370' SEA LEVEL
6 / 30 / 87
1204
WILDFIRE #1
1175
E-6
1116
HIGH
ADVENTURE #1
1225
JOHNSON
FEDERAL
1049
HOWARD
FEDERAL
43-15
1504
K-13
1186
A-20
1091
LODDY #1
1040
BEARCAT #1
1102
HILL
FEDERAL
2y
1194
B-32
1036
LINDRITH
B-37
851
BOYT & LOLA #1

Figure 1

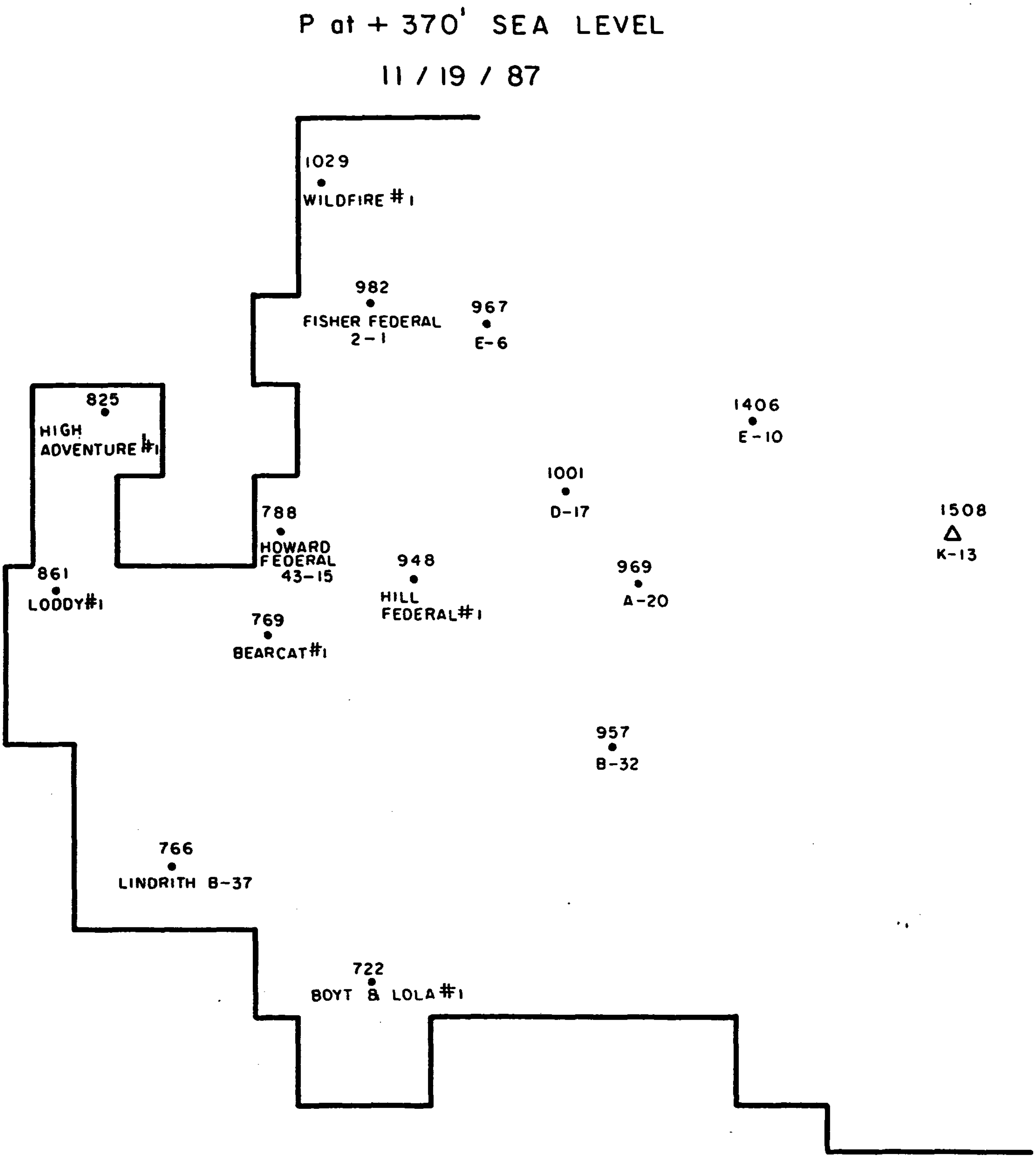

P at + 370' SEA LEVEL
11 / 19 / 87
1029
WILDFIRE #1
982
FISHER FEDERAL
2-1
967
E-6
825
HIGH
ADVENTURE #1
1406
E-10
1001
D-17
1508
K-13
788
HOWARD
FEDERAL
43-15
861
LODDY #1
948
HILL
FEDERAL #1
969
A-20
769
BEARCAT #1
957
B-32
766
LINDRITH B-37
722
BOYT & LOLA #1

Figure 2

$\overline{P}$ at +370' SEA LEVEL 2/23/88

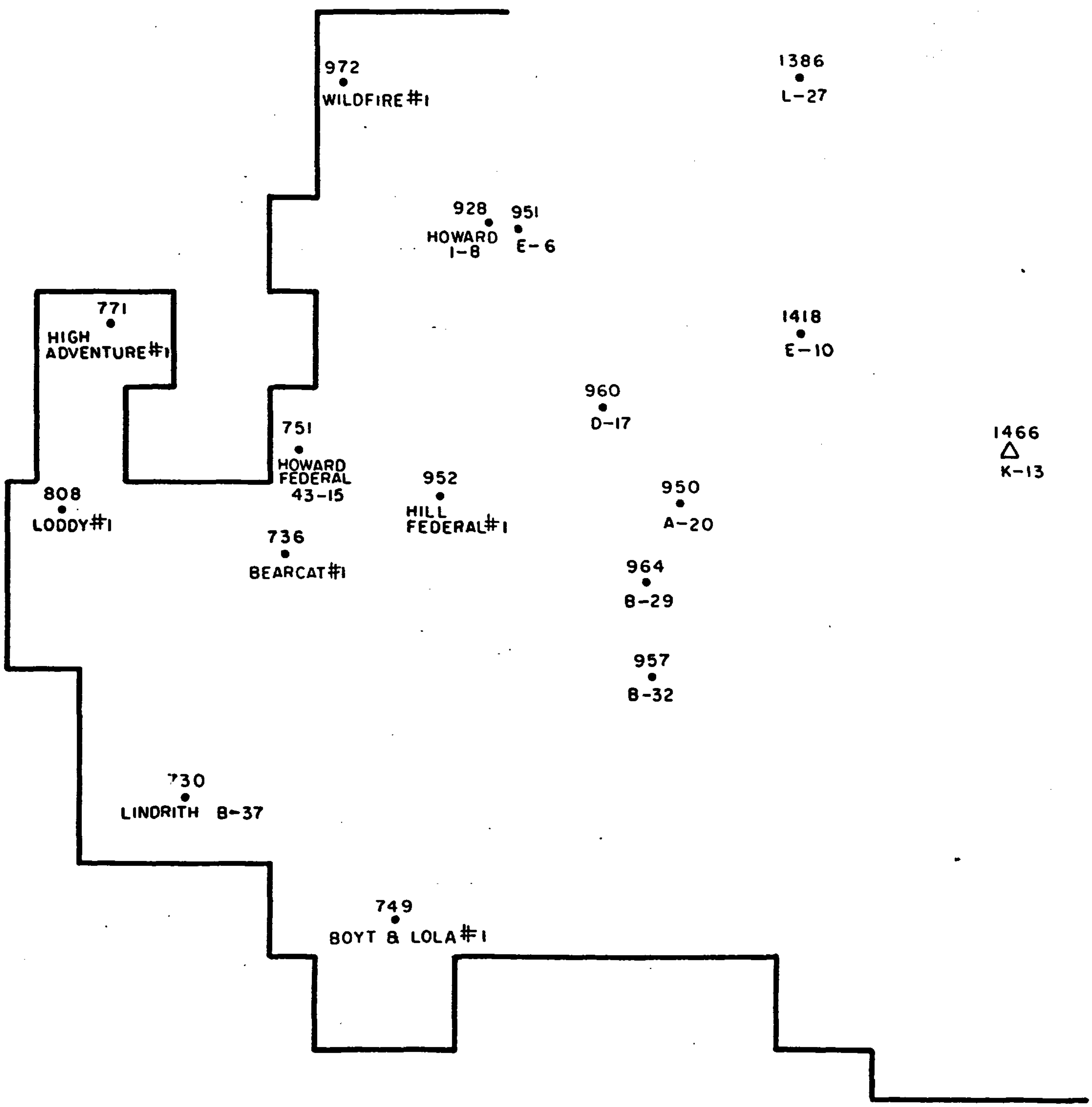

Figure 3

CO_2 FLOOD ISOBARS

SPE / DOE 17327

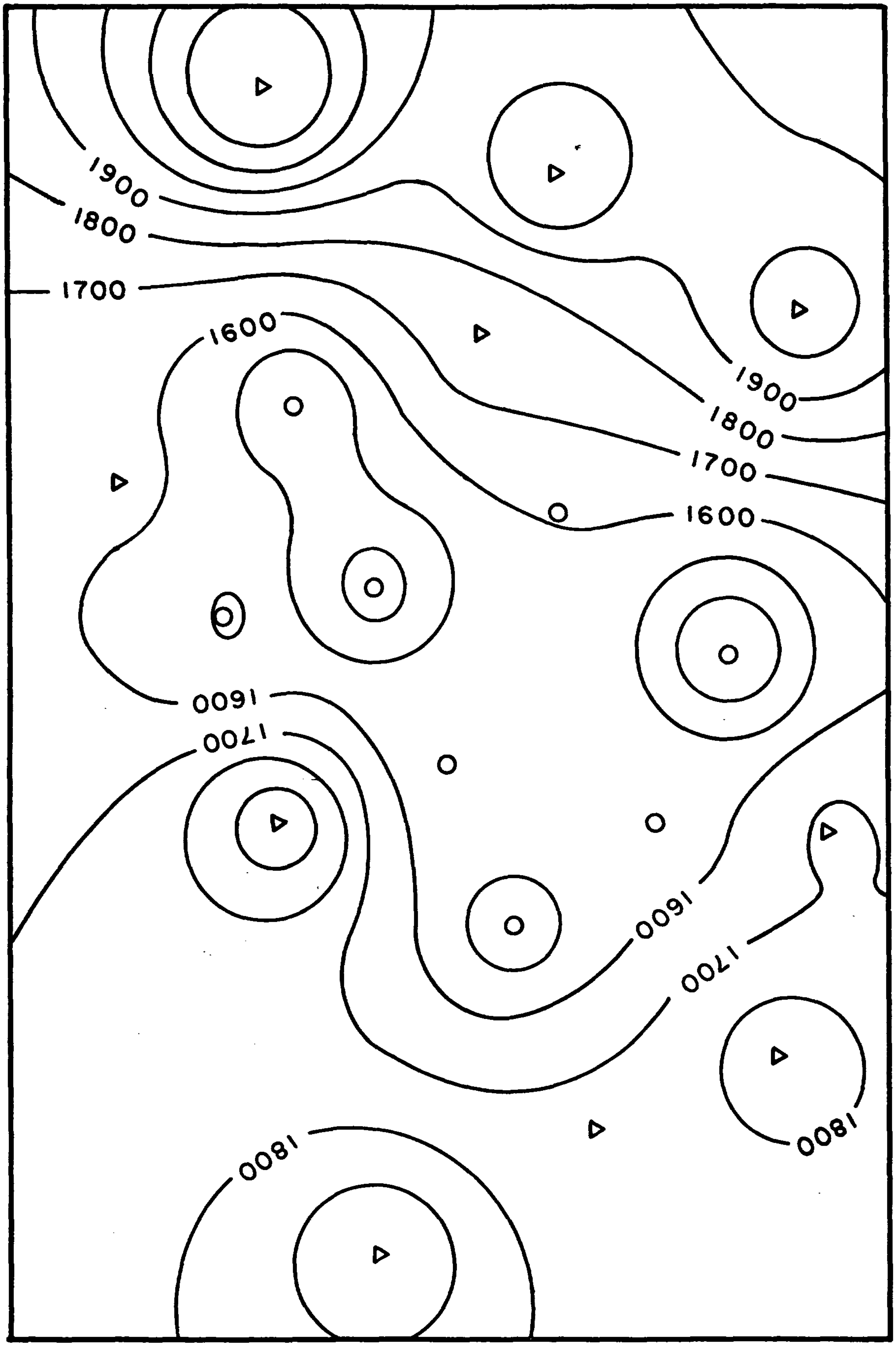

Figure 4

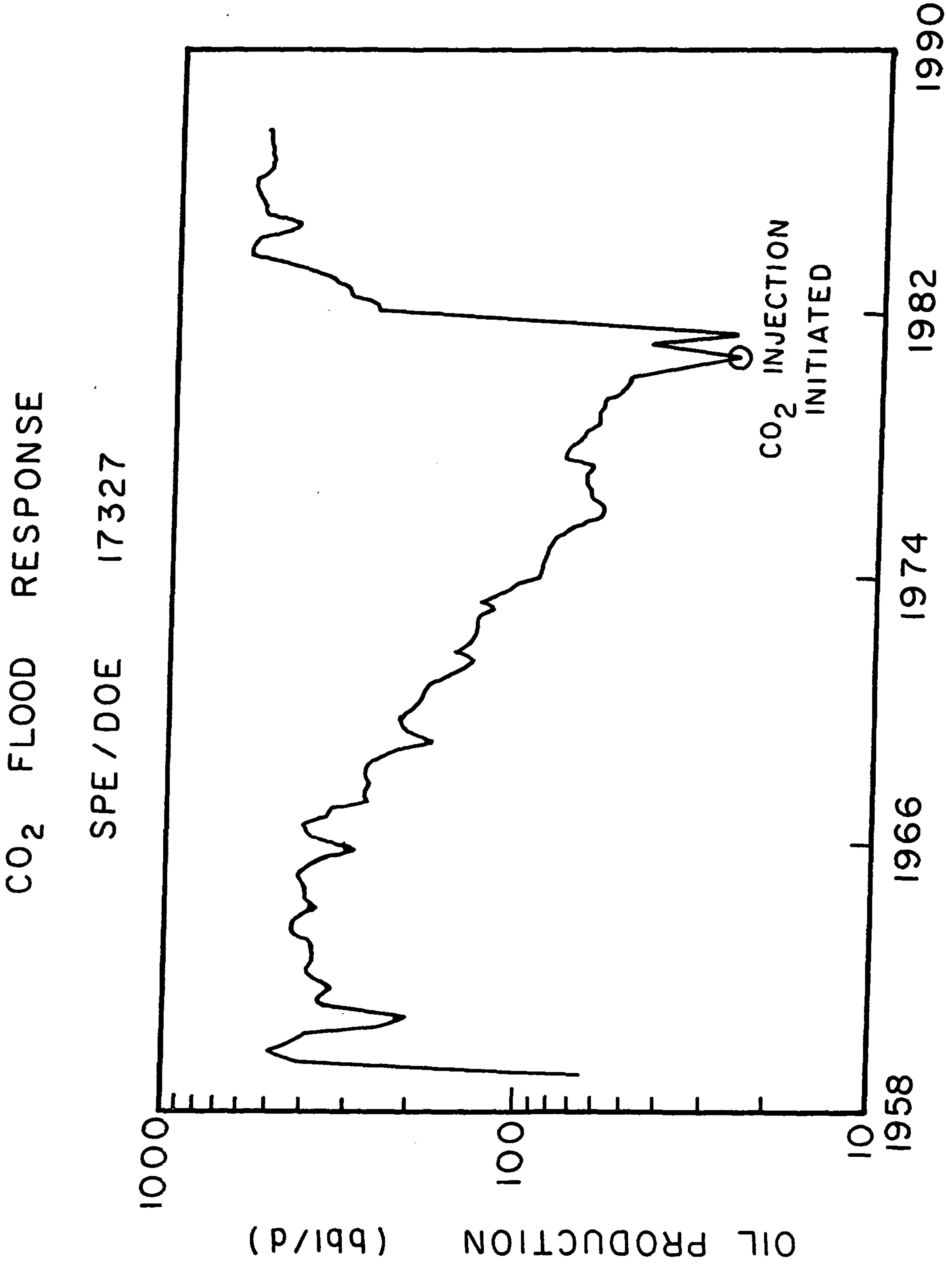

CO_2 FLOOD RESPONSE
SPE/DOE 17327
CO_2 INJECTION INITIATED
OIL PRODUCTION (bbl/d)
1000
100
10
1958
1966
1974
1982
1990

Figure 5

PRESSURE GRADIENTS , psi/1000   2/23/88

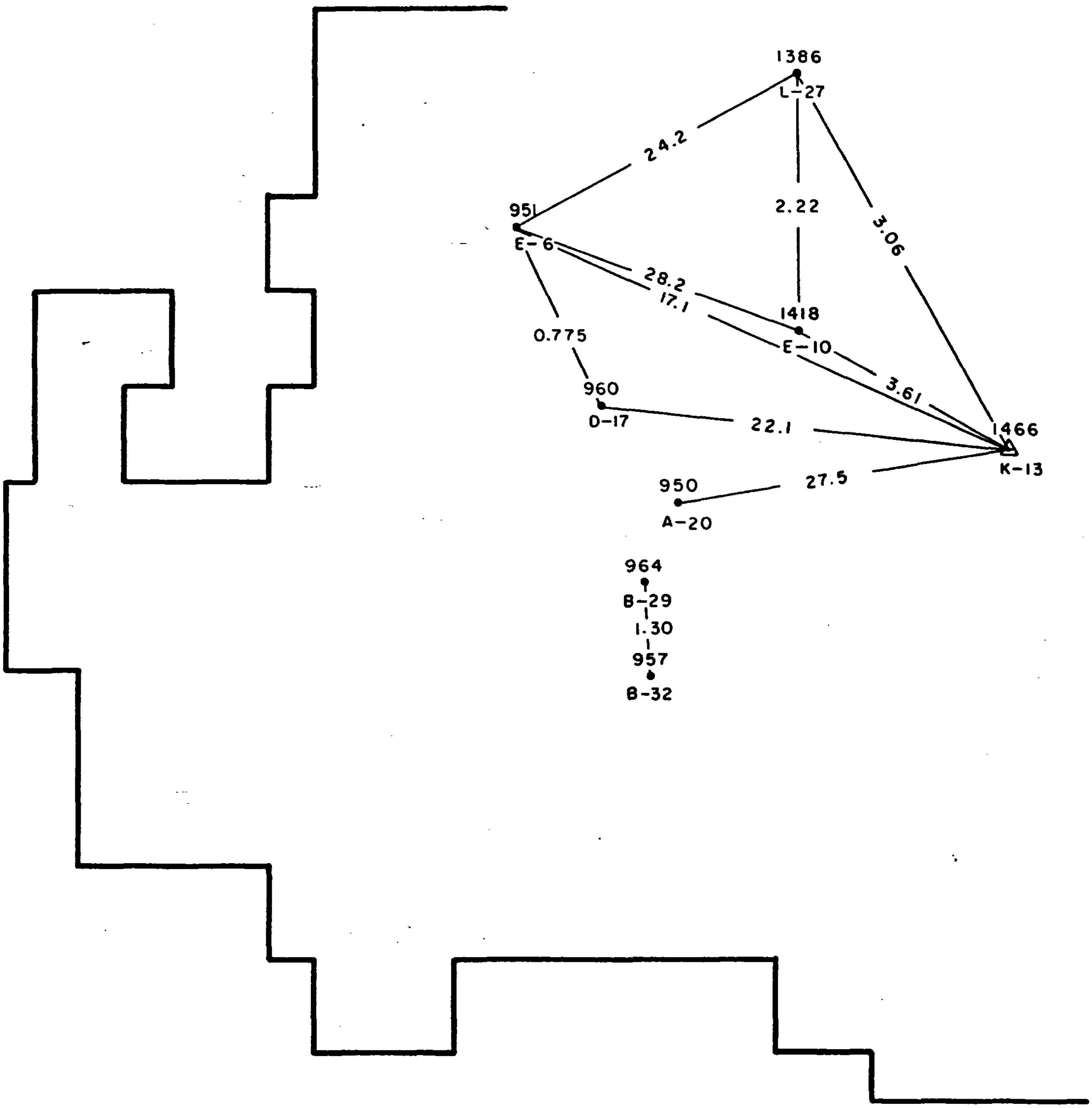

Figure 6

TRANSMISSABILITY $\frac{Kh}{\mu}$, $\frac{md \cdot ft}{cp}$ FROM BUILDUPS

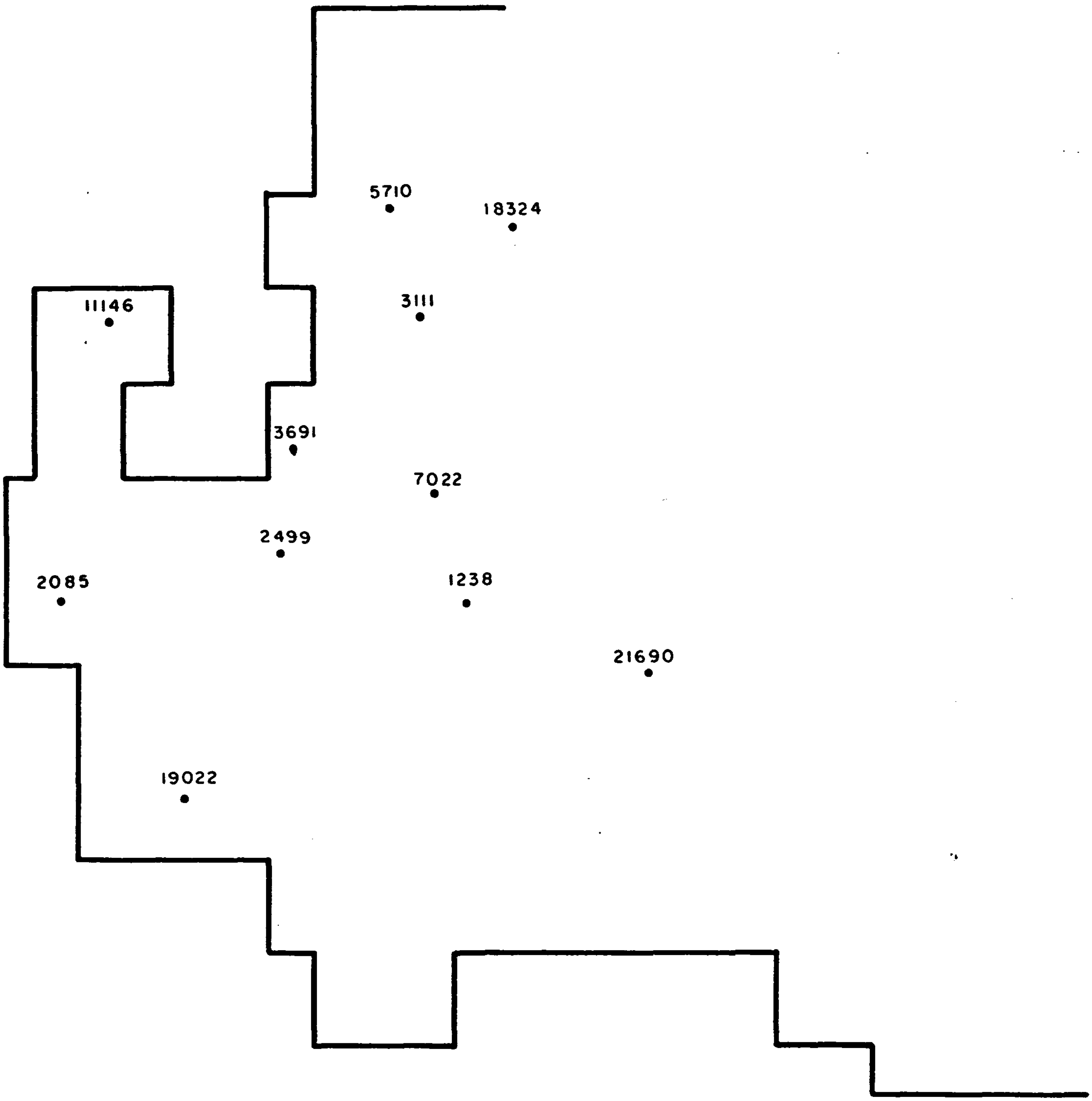

Figure 7

FLOW CAPACITY $\overline{K}_t h$, md·ft FROM BUILDUPS

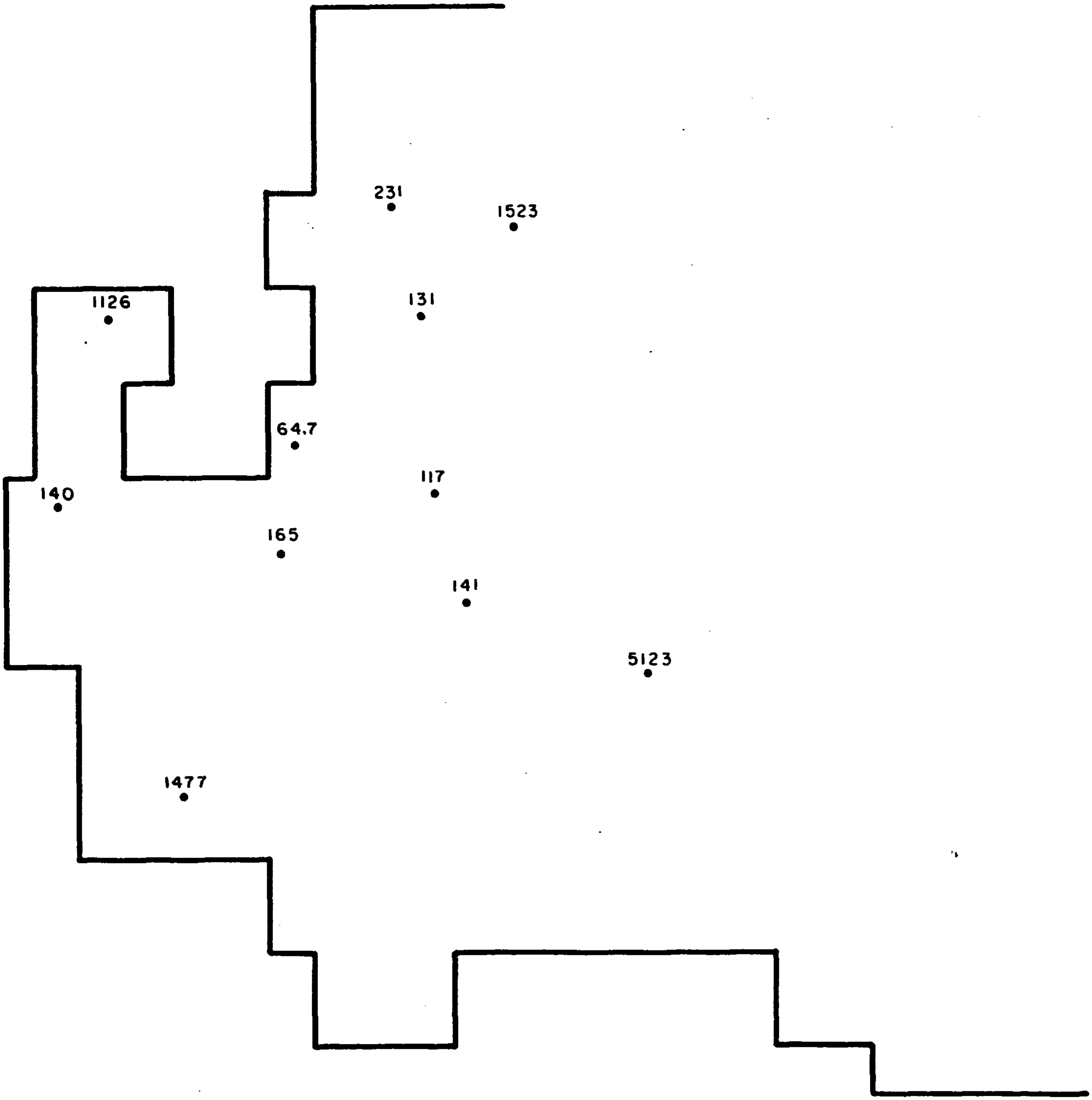

Figure 8

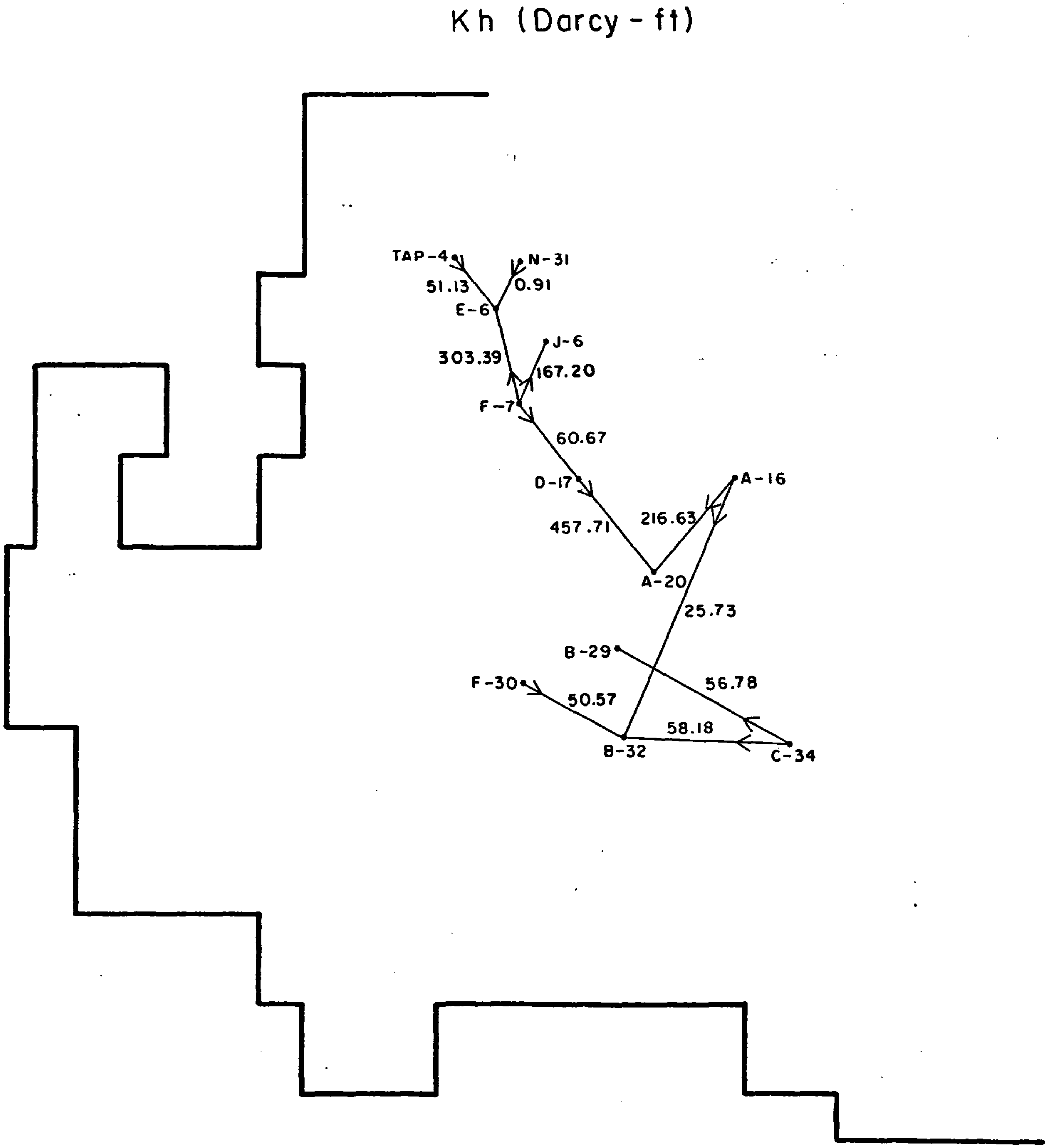

Kh (Darcy - ft)
TAP-4
N-31
51.13
0.91
E-6
J-6
303.39
167.20
F-7
60.67
D-17
A-16
216.63
457.71
A-20
25.73
B-29
56.78
F-30
50.57
58.18
B-32
C-34

Figure 9

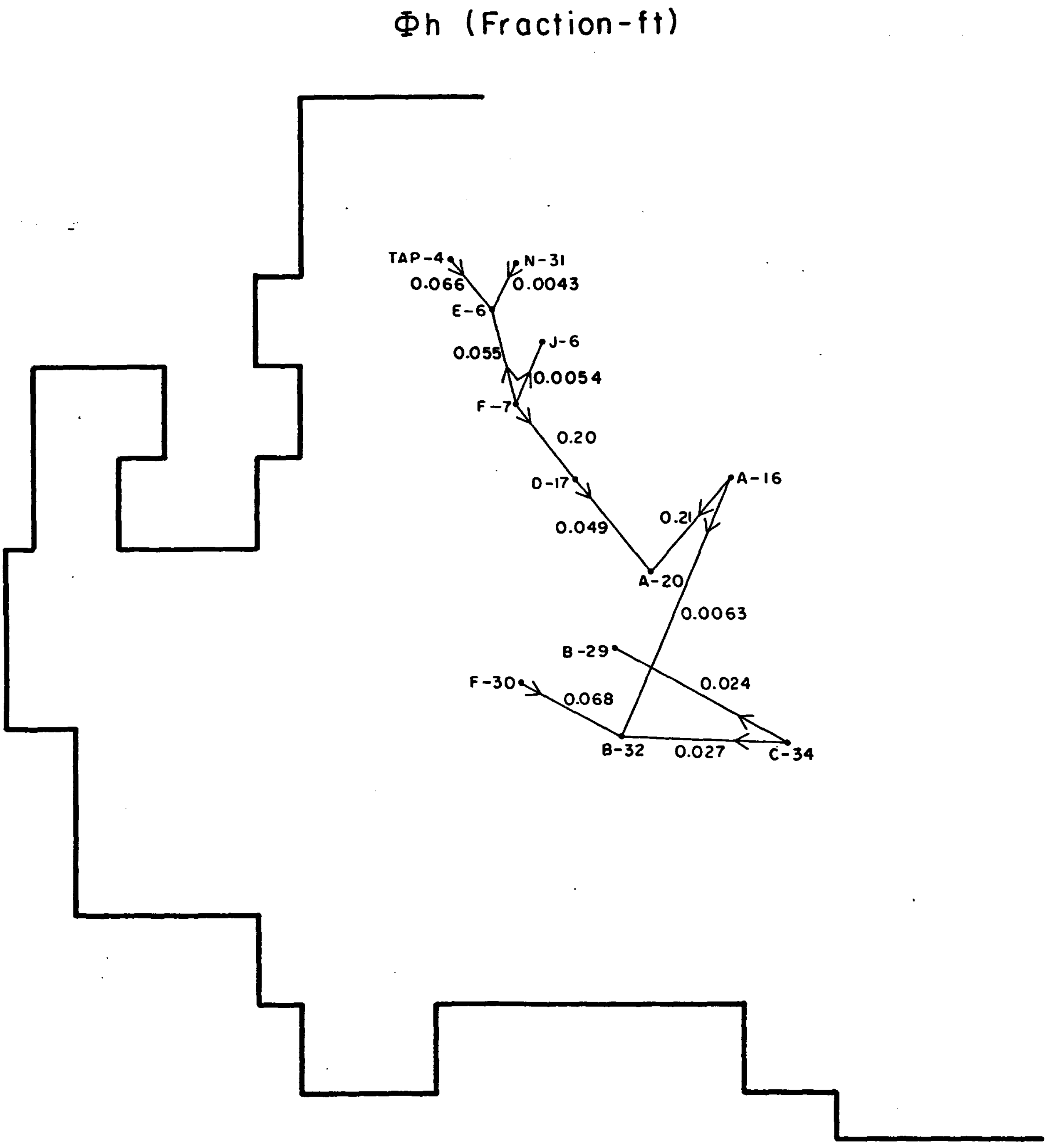
Φh (Fraction-ft)
TAP-4
N-31
0.066
0.0043
E-6
J-6
0.055
0.0054
F-7
0.20
D-17
A-16
0.21
0.049
A-20
0.0063
B-29
F-30
0.024
0.068
B-32
0.027
C-34

Figure 10

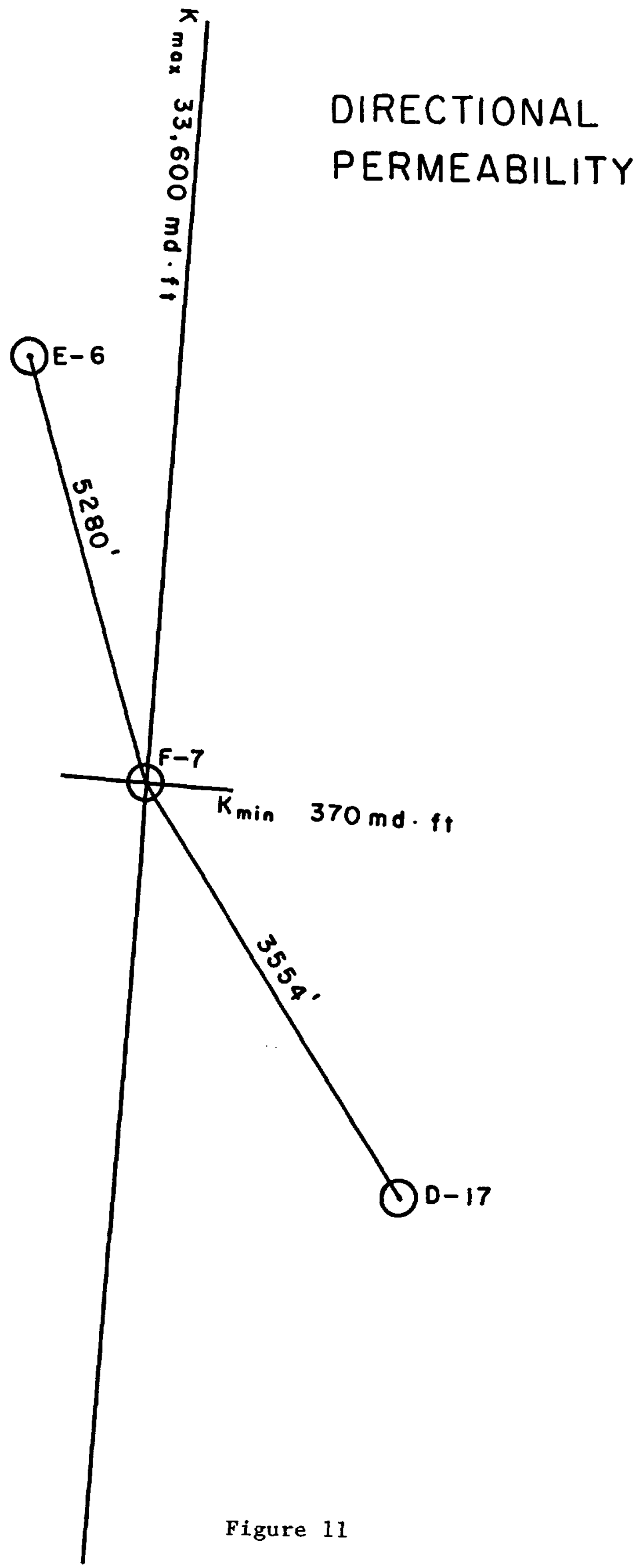
DIRECTIONAL
PERMEABILITY
K max 33,600 md · ft
E-6
5280'
F-7
K min 370 md · ft
3554'
D-17

Figure 11

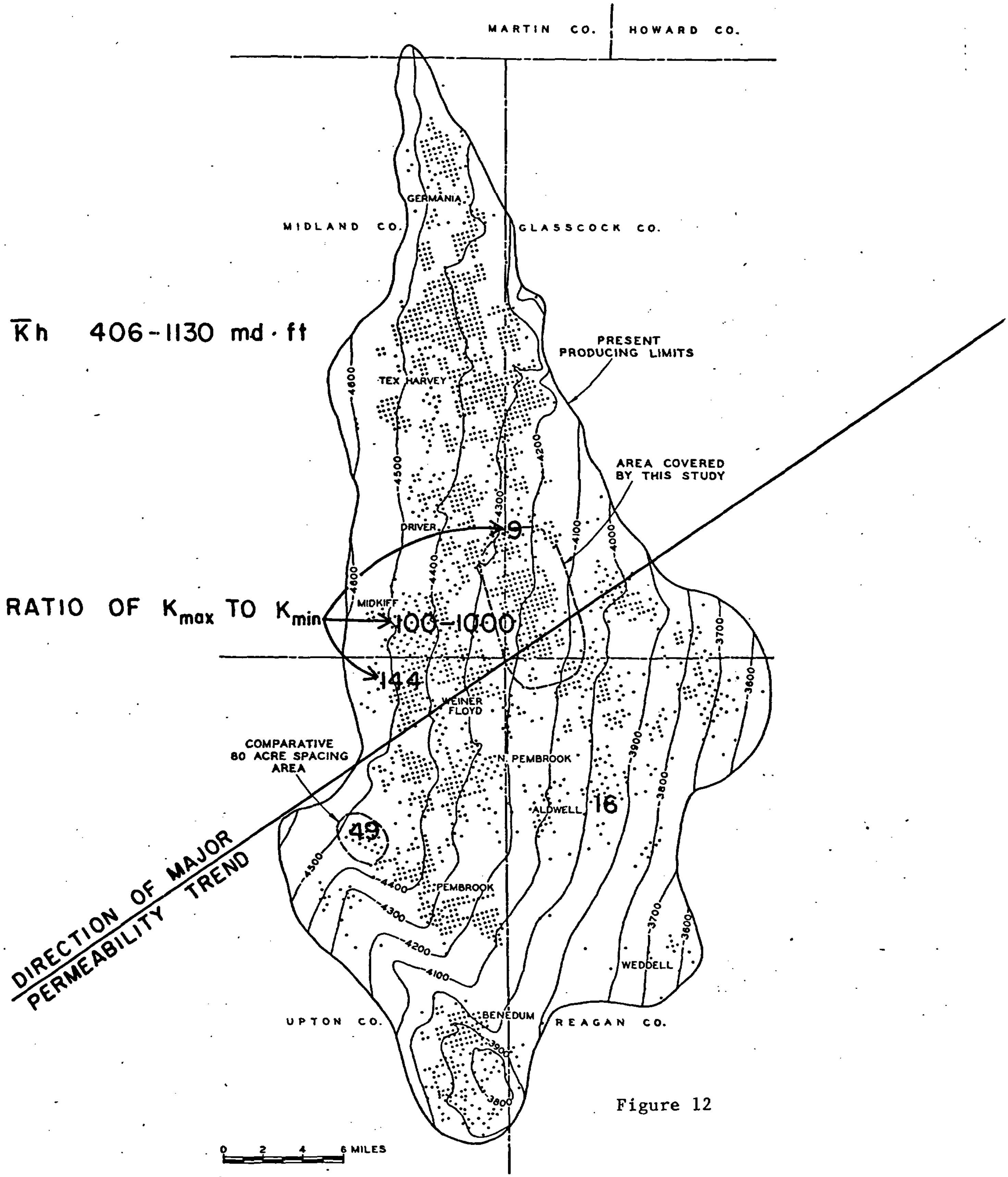

FIG. 1 — SPRABERRY TREND FIELD, CONTOURS ON TOP OF SPRABERRY FORMATION.

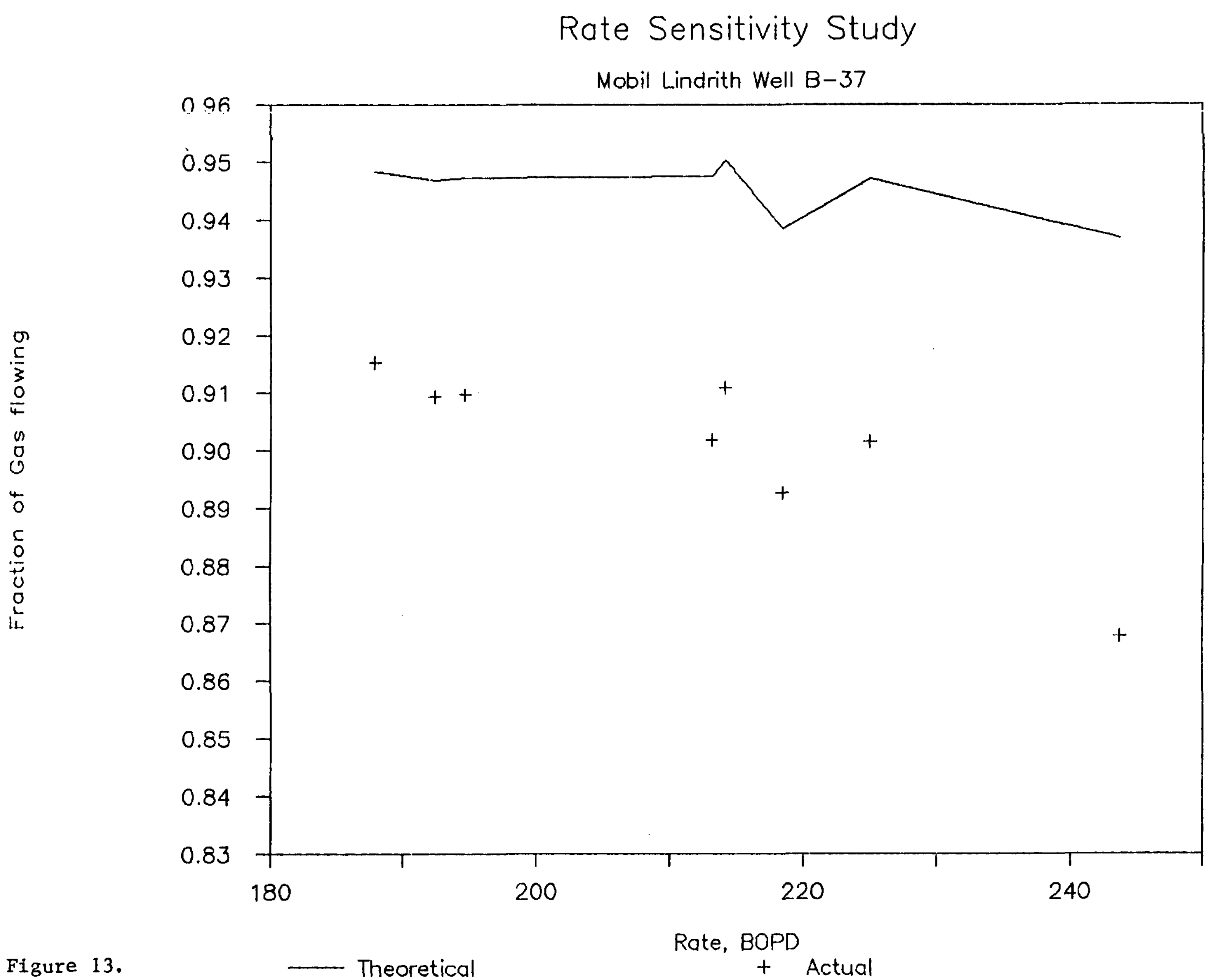
Rate Sensitivity Study
Mobil Lindrith Well B-37
Fraction of Gas flowing
0.96
0.95
0.94
0.93
0.92
0.91
0.90
0.89
0.88
0.87
0.86
0.85
0.84
0.83
180
200
220
240
Rate, BOPD
Theoretical
+ Actual

Figure 13.

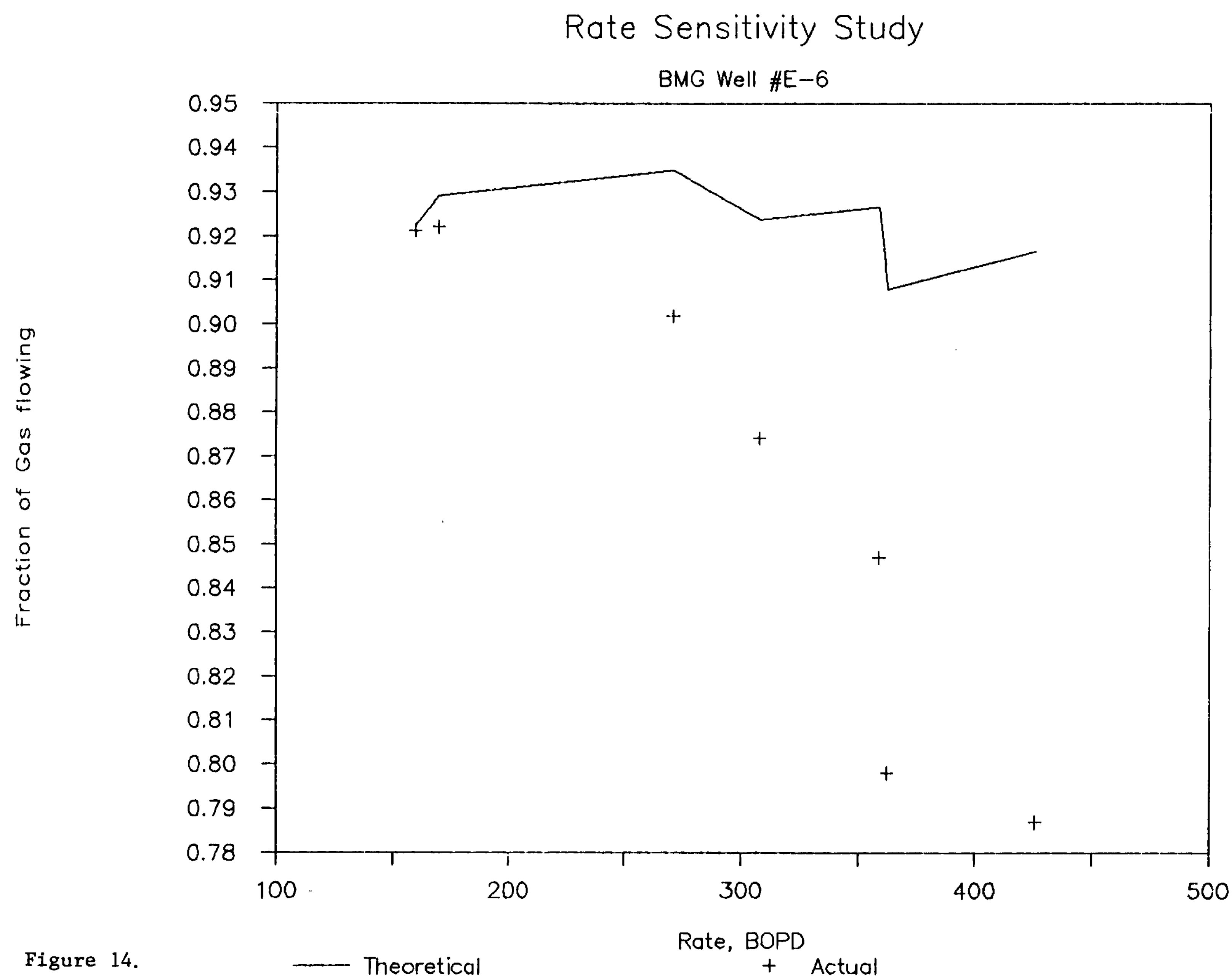
Rate Sensitivity Study
BMG Well #E-6
Fraction of Gas flowing
0.95
0.94
0.93
0.92
0.91
0.90
0.89
0.88
0.87
0.86
0.85
0.84
0.83
0.82
0.81
0.80
0.79
0.78
100
200
300
400
500
Rate, BOPD
Theoretical
+ Actual

Figure 14.

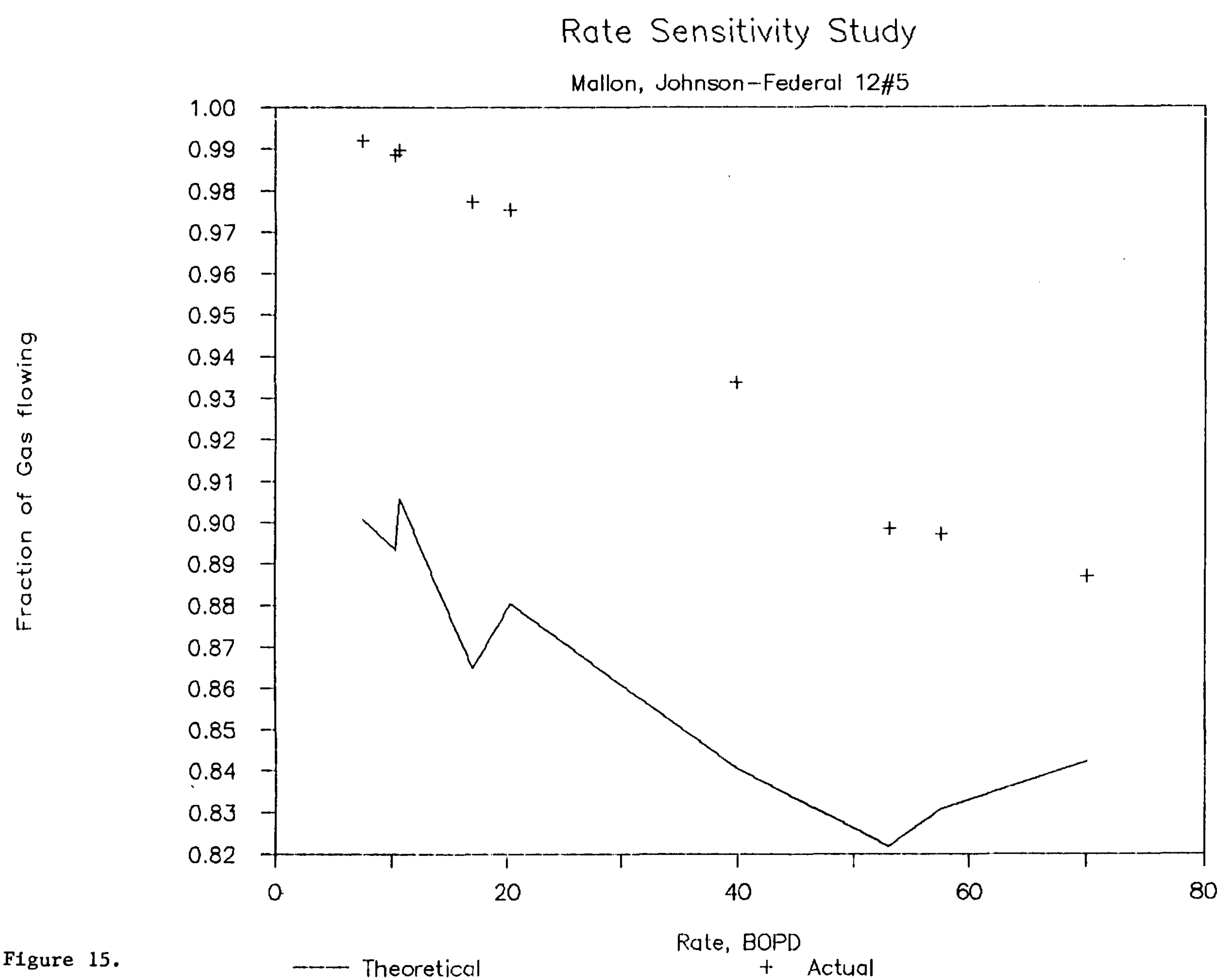
Rate Sensitivity Study
Mallon, Johnson-Federal 12#5
Fraction of Gas flowing
1.00
0.99
0.98
0.97
0.96
0.95
0.94
0.93
0.92
0.91
0.90
0.89
0.88
0.87
0.86
0.85
0.84
0.83
0.82
0
20
40
60
80
Rate, BOPD
Theoretical
Actual

Figure 15.

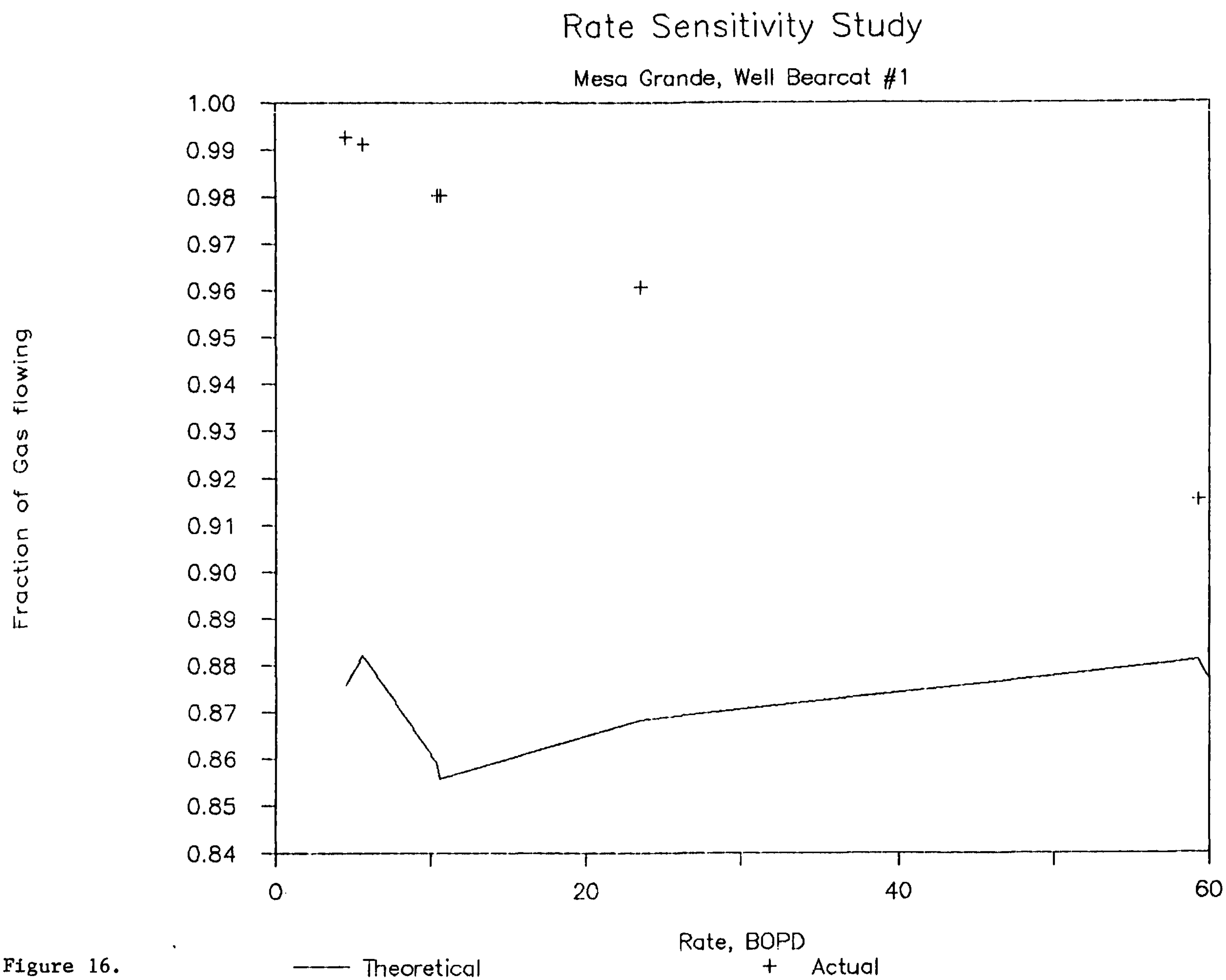
Rate Sensitivity Study
Mesa Grande, Well Bearcat #1
1.00
0.99
0.98
0.97
0.96
0.95
0.94
0.93
0.92
0.91
0.90
0.89
0.88
0.87
0.86
0.85
0.84
Fraction of Gas flowing
0
20
40
60
Rate, BOPD
Theoretical
+ Actual

Figure 16.

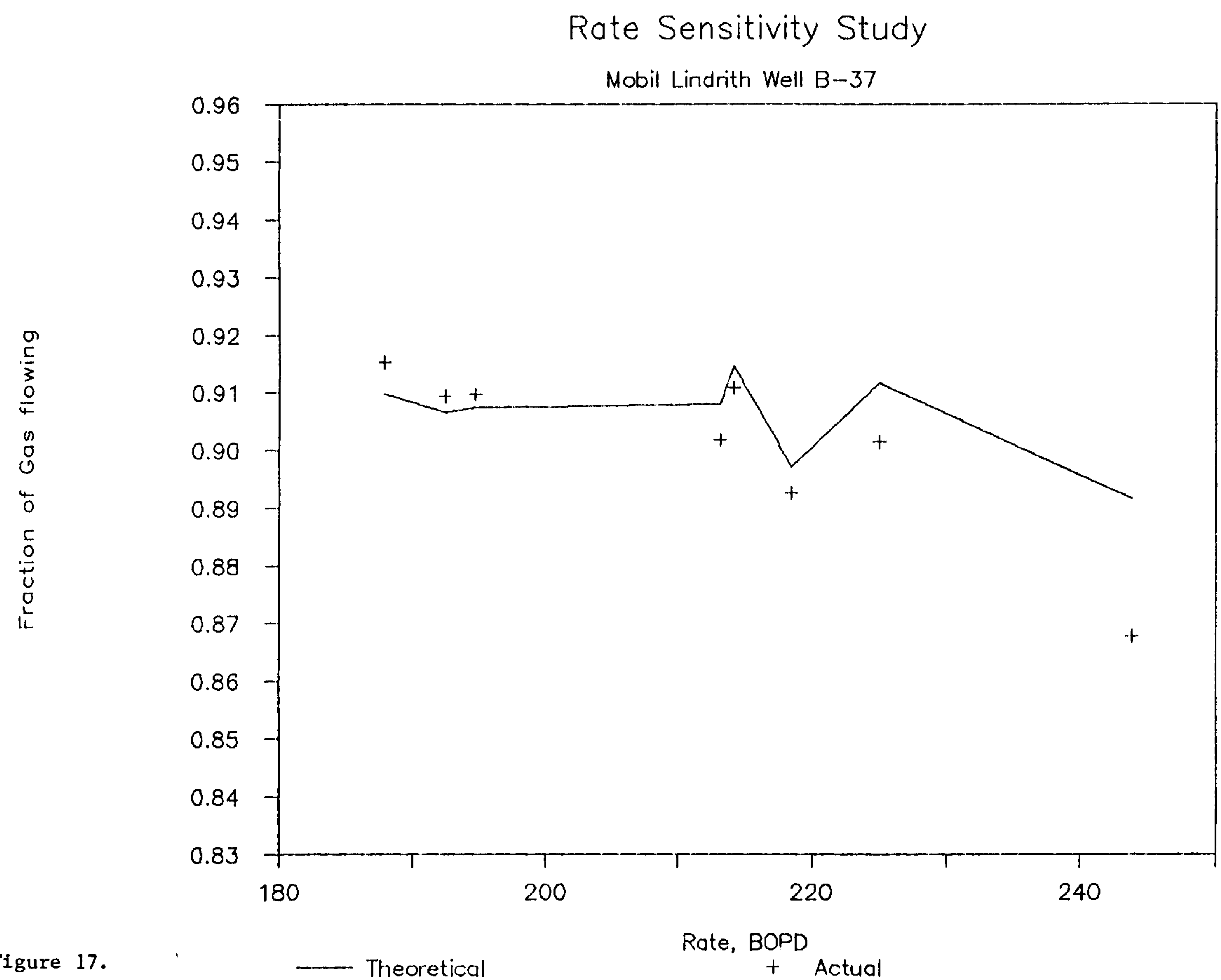
Rate Sensitivity Study
Mobil Lindrith Well B-37
Fraction of Gas flowing
0.96
0.95
0.94
0.93
0.92
0.91
0.90
0.89
0.88
0.87
0.86
0.85
0.84
0.83
180
200
220
240
Rate, BOPD
Theoretical
Actual

Figure 17.

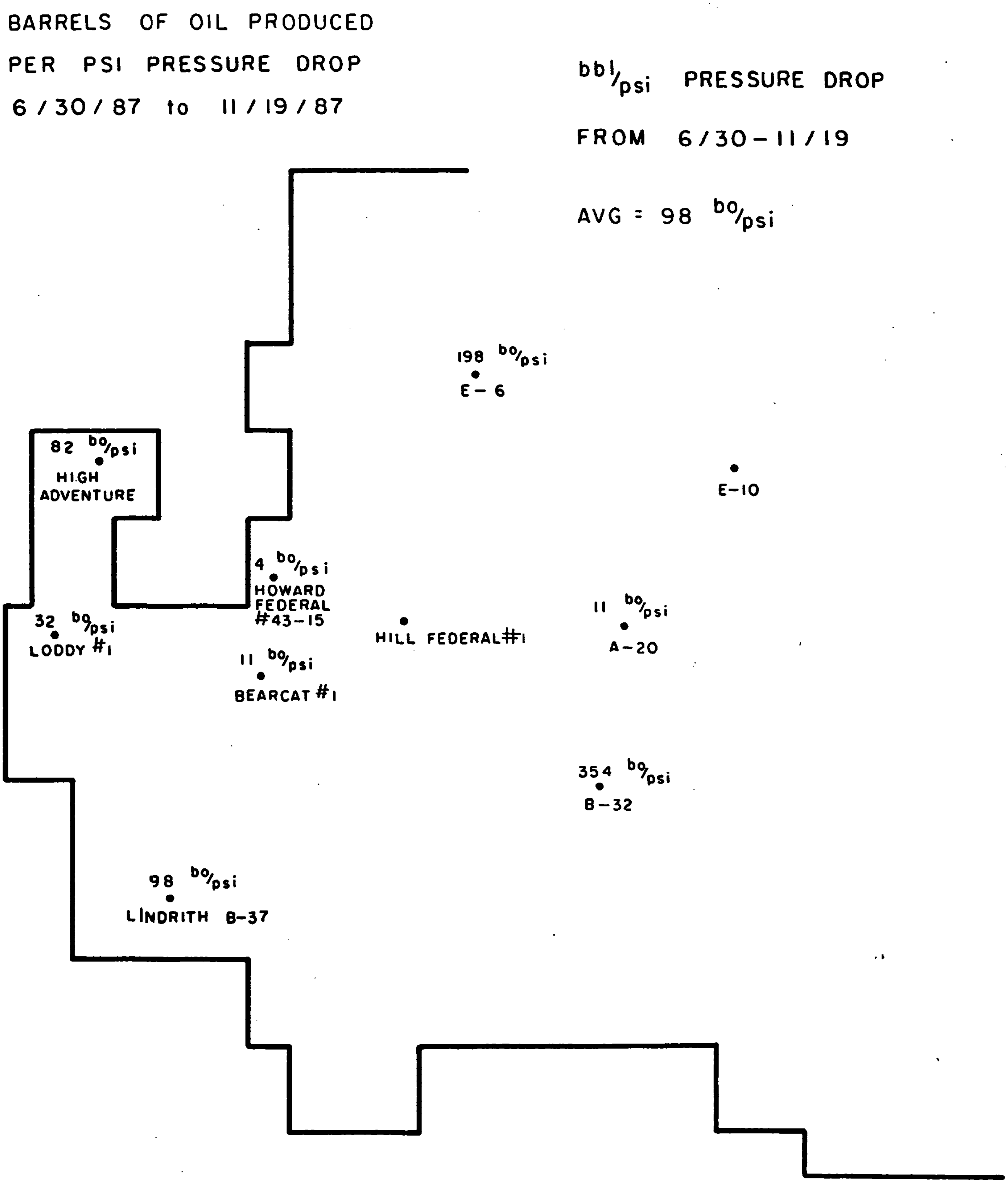
BARRELS OF OIL PRODUCED
PER PSI PRESSURE DROP
6 / 30 / 87 to 11 / 19 / 87
bbl/psi PRESSURE DROP
FROM 6/30-11/19
AVG = 98 bo/psi
198 bo/psi
E-6
82 bo/psi
HIGH ADVENTURE
E-10
4 bo/psi
HOWARD FEDERAL #43-15
11 bo/psi
A-20
32 bo/psi
LODDY #1
HILL FEDERAL #1
11 bo/psi
BEARCAT #1
354 bo/psi
B-32
98 bo/psi
LINDRITH B-37

Figure 18

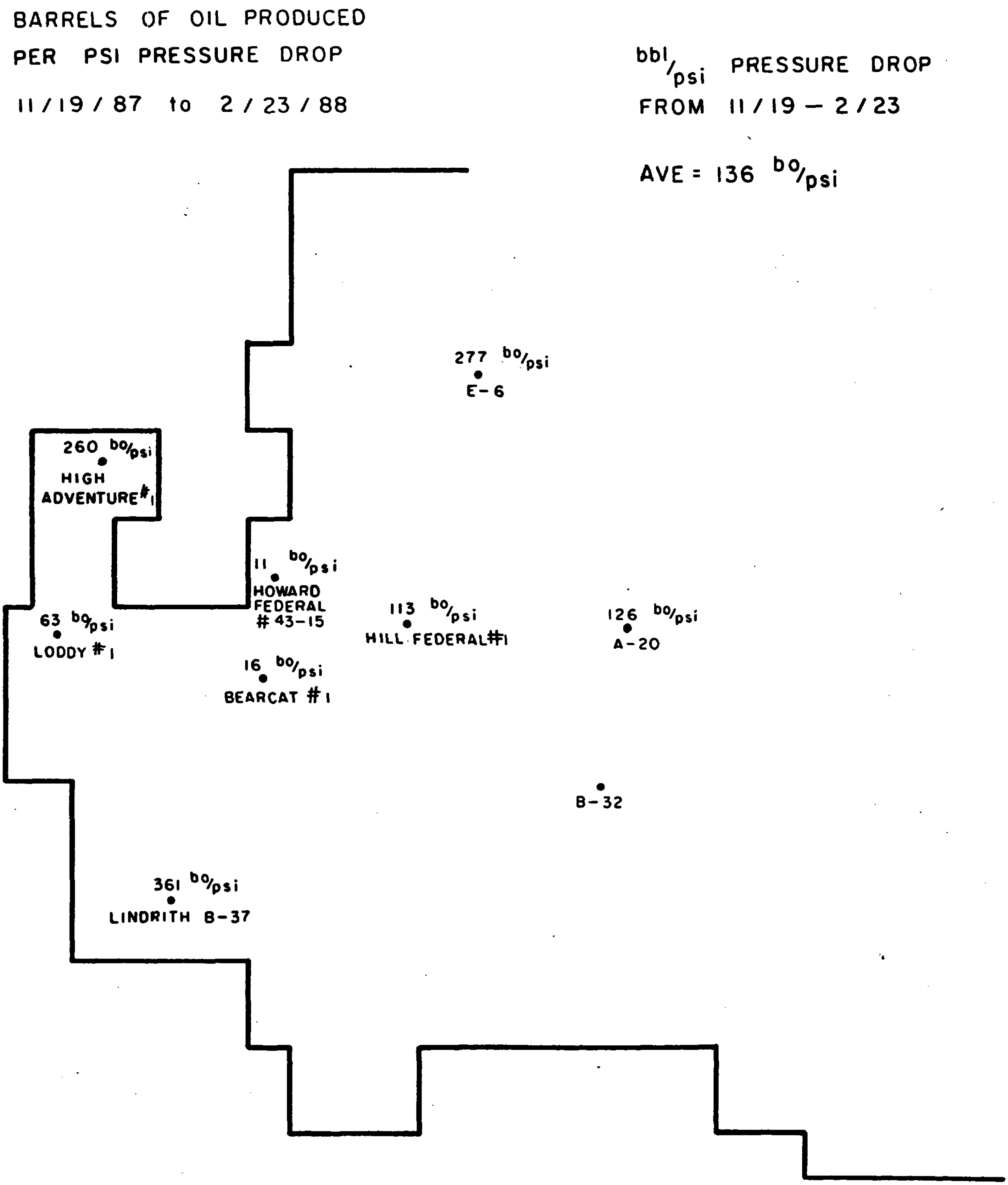
BARRELS OF OIL PRODUCED
PER PSI PRESSURE DROP
11 / 19 / 87 to 2 / 23 / 88
bbl/psi PRESSURE DROP
FROM 11 / 19 – 2 / 23
AVE = 136 bo/psi
277 bo/psi
E-6
260 bo/psi
HIGH ADVENTURE #1
11 bo/psi
HOWARD FEDERAL # 43-15
63 bo/psi
LODDY #1
113 bo/psi
HILL FEDERAL #1
126 bo/psi
A-20
16 bo/psi
BEARCAT #1
B-32
361 bo/psi
LINDRITH B-37

Figure 19

APPENDIX 1

Static Pressure Worksheets

	KB		Subsea
Operator	BMG		
Well	E-6		
Elevation	7505		
Top of B Zone	7148		+357
Test Date		6/30/87	
Bomb Depth	7277		+ 228
Bomb Pressure, psig		1214.2	
Fluid Level	7137		+368
Wellbore Gradient			
Oil, psi/ft	(0.3)(228-357)		-38.7
Gas, psi/ft			
Pressure at Top of B Zone		1175.5	
Top of B Zone to +370 ft	13		
Production			
BO/D		321	
Mcf/D		1471	
Volume Weighted Reservoir Density, psi/ft		0.06350	
dP to +370 ft		.83	
Pressure at +370 ft datum		1174.7	

$(321)(1.342) = 430.8$

$\left[1471 - \frac{(321)(501)}{1000}\right] 2.328 = 3050.1$

$(.7088)(430.8) = 305.3$

$(.067265)(3050.1) = 205.2$

$(.433)(.1466)$

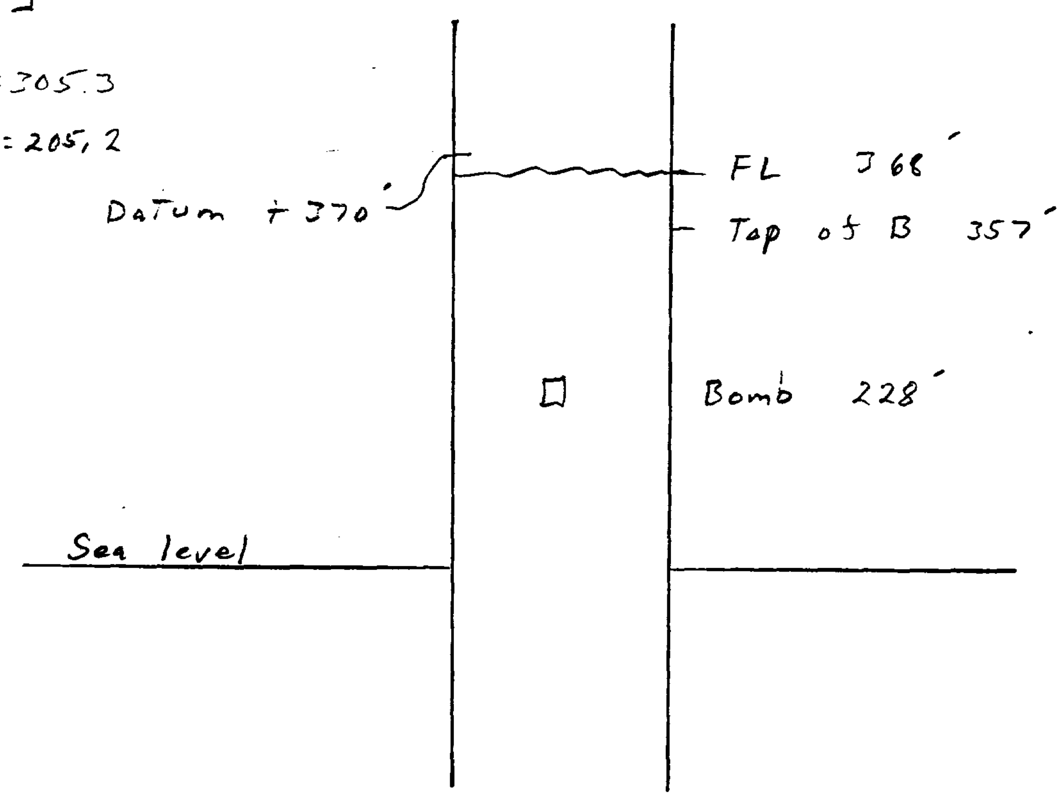

	KB		Subsea
Operator	BMG		
Well	E-6		
Elevation	7505		
Top of B Zone	7148		+357
Test Date		11/19/87	
Bomb Depth	7337		+168
Bomb Pressure, psig		1014.9	
Fluid Level	7132		+323
Wellbore Gradient			
Oil, psi/ft	0.3(168-323)		-46.5
Gas, psi/ft	0.03(323-357)		-1.0
Pressure at Top of B Zone		967.4	
Top of B Zone to +370 ft	13		
Production			
BO/D		291	
Mcf/D		1250	
Volume Weighted Reservoir Density, psi/ft		0.05437	
dP to +370 ft		0.7	
Pressure at +370 ft datum		966.7	

(291) (1.317) = 383.2

$\left[1250 \quad \frac{291(443)}{1000}\right] 2.865 = 3211.9$

(.7143) (383.2) = 273.8

(.055291)(3211.9) = 177.6

(.433)(.1256) = 0.0543

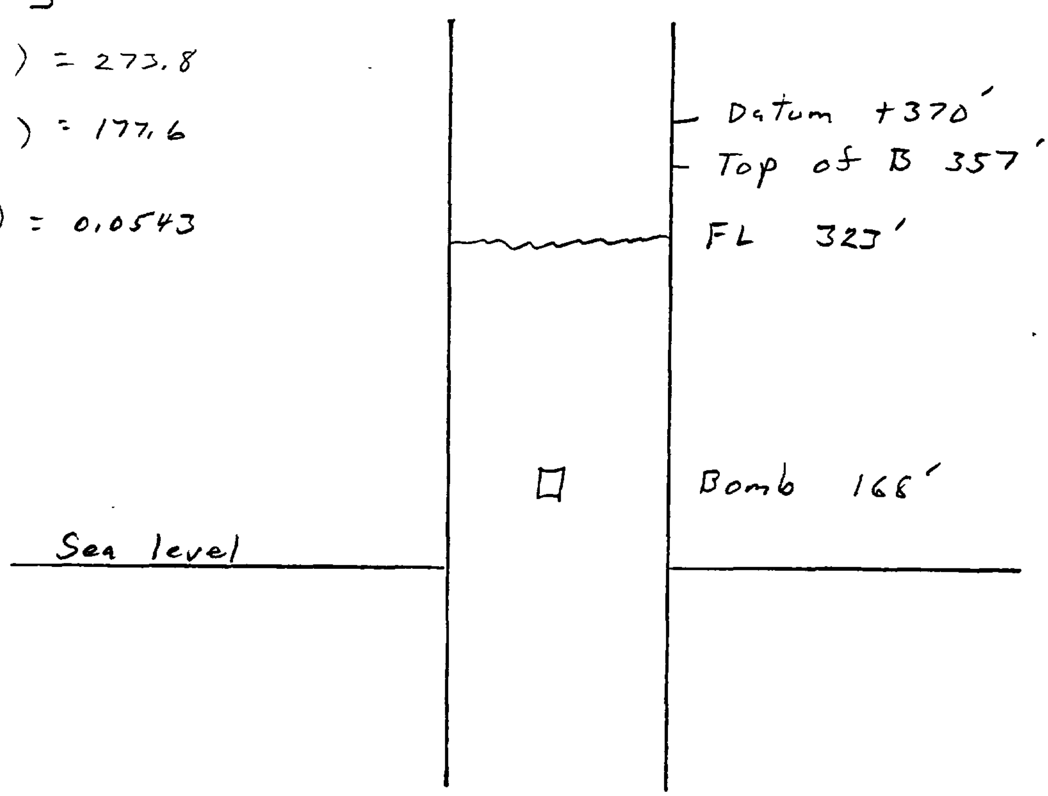

	KB		Subsea
Operator	BMG		
Well	E-6		
Elevation	7505		
Top of B Zone	7148		+357
Test Date		2/23/88	
Bomb Depth	7277		+228
Bomb Pressure, psig		955.2	
Fluid Level			
Wellbore Gradient			
Oil, psi/ft			
Gas, psi/ft	(.03)(228-357)		-3.9
Pressure at Top of B Zone		951.3	
Top of B Zone to +370 ft	13		
Production			
BO/D		160	
Mcf/D		840	
Volume Weighted Reservoir Density, psi/ft		0.04788	
dP to +370 ft		0.6	
Pressure at +370 ft datum		950.7	

$(160)\ (1.314) = 210.24$

$\left[840 - \frac{(160)(437)}{1000}\right] 2.932 = 2257.9$

$(.7148)(210.2) = 150.3$

$(.054314)(2257.9) = 122.6$

$(.433)(.1106) = 0.04788$

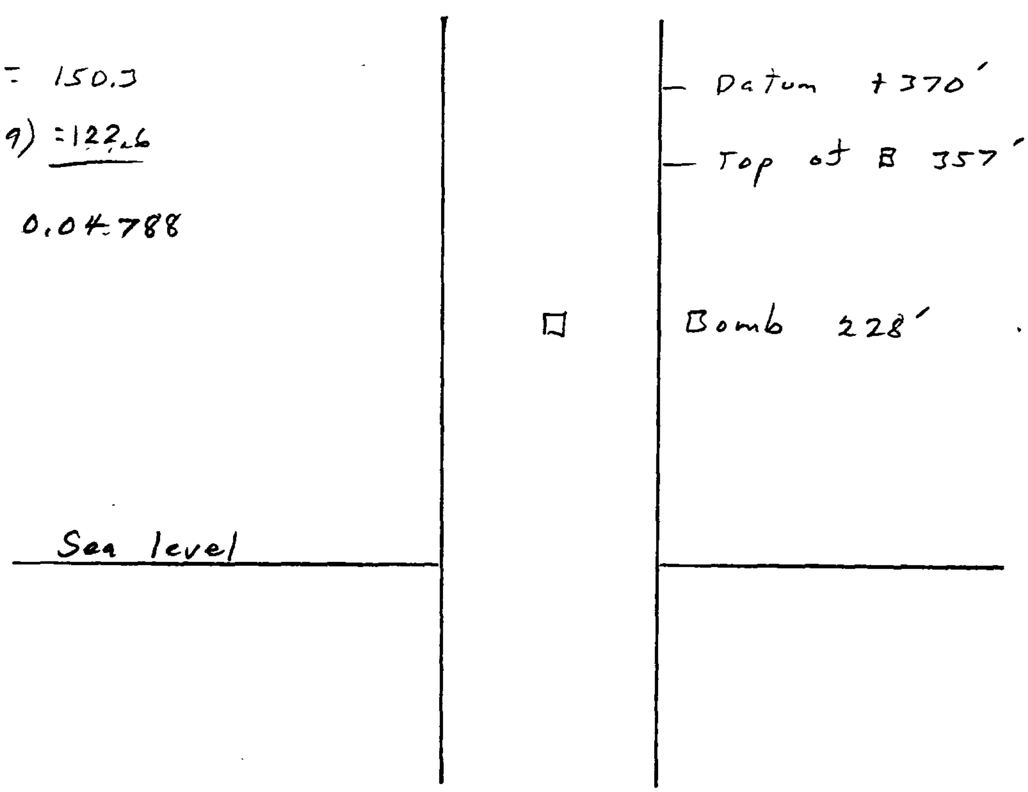

	KB		Subsea
Operator	BMG		
Well	E-10		
Elevation	7341		
Top of B Zone	6820		+521
Test Date		11/19/87	
Bomb Depth	7012		+329
Bomb Pressure, psig		1403	
Fluid Level			
Wellbore Gradient			
Oil, psi/ft			
Gas, psi/ft	(.03)(329-521)		-5.8
Pressure at Top of B Zone		1397.2	
Top of B Zone to +370 ft	151'		
Production			
BO/D		234	
Mcf/D		1760	
Volume Weighted Reservoir Density, psi/ft		0.0580	
dP to +370 ft		8.8	
Pressure at +370 ft datum		1406.0	

$(234)(1.370) = 320.6$

$\left[1760 - \frac{234(565)}{1000}\right] 2.081 = 3387.4$

$(.7015)(320.6) = 224.9$

$(.080205)(557.4) = 211.7$

$(.433)(.1339) = 0.0580$

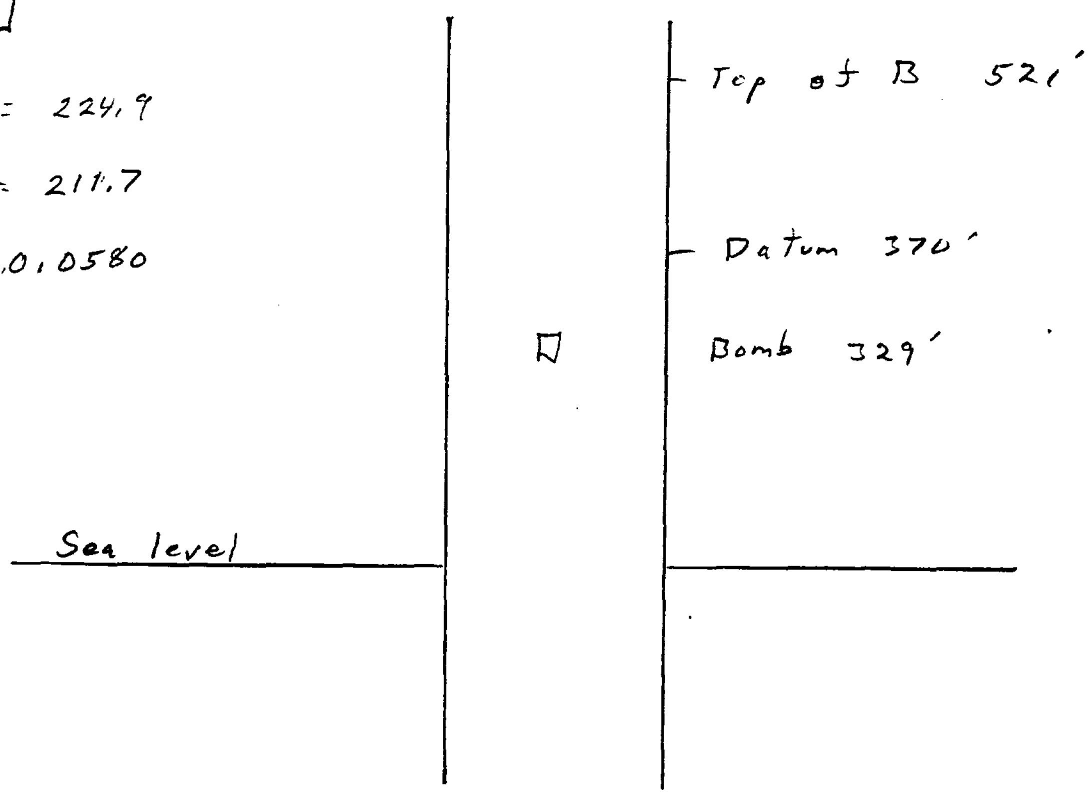

	KB		Subsea
Operator	BMG		
Well	E-10		
Elevation	7341		
Top of B Zone	6820		+521
Test Date		2/23/88	
Bomb Depth	7012		+329
Bomb Pressure, psig		1415	
Fluid Level			
Wellbore Gradient			
Oil, psi/ft			
Gas, psi/ft	(.03)(329-521)		-5.8
Pressure at Top of B Zone		1409.2	
Top of B Zone to +370 ft	151		
Production			
BO/D		23	
Mcf/D		1600	
Volume Weighted Reservoir Density, psi/ft		.058	
dP to +370 ft		8.8	
Pressure at +370 ft datum		1418.0	

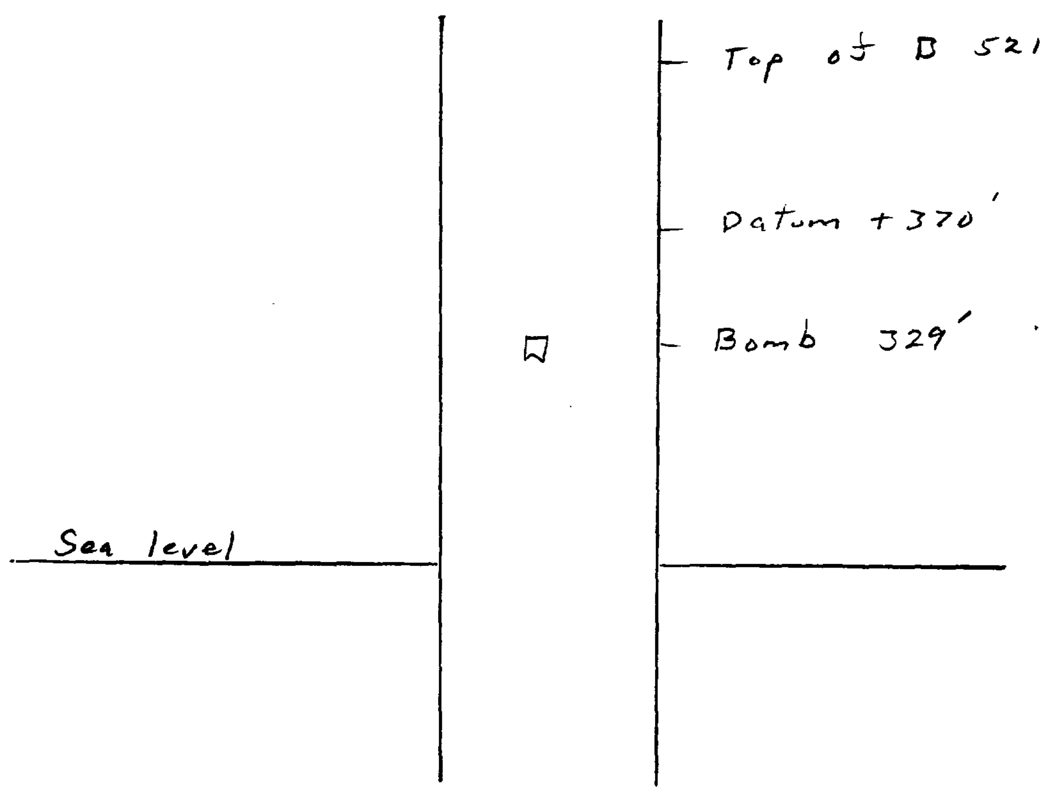

	KB		Subsea
Operator	BMG		
Well	K-13		
	KB		Subsea
Elevation	7100		
Top of B Zone			
Test Date		6/30/87	
Bomb Depth	5862		+1238
Bomb Pressure, psig		1477.8	
Fluid Level			
Wellbore Gradient			
Oil, psi/ft			
Gas, psi/ft	(0.03)(1238-370)		26.04
Pressure at Top of B Zone			
Top of B Zone to +370 ft			
Production			
BO/D			
Mcf/D			
Volume Weighted Reservoir Density, psi/ft			
dP to +370 ft			
Pressure at +370 ft datum		1503.8	

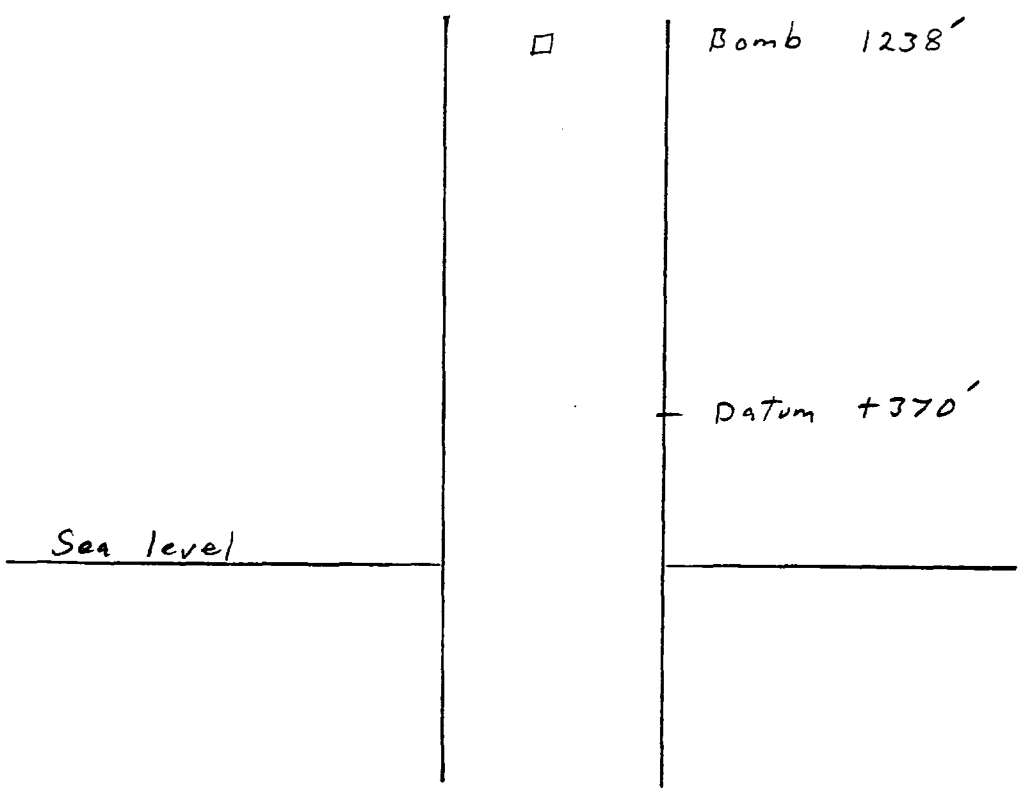

	KB		Subsea
Operator	BMG		
Well	K-13		
Elevation	7100		
Top of B Zone			
Test Date		11/19/87	
Bomb Depth	5862		+ 1238
Bomb Pressure, psig		1482	
Fluid Level			
Wellbore Gradient			
Oil, psi/ft			
Gas, psi/ft	(.03)(1238-370)		26.04
Pressure at Top of B Zone			
Top of B Zone to +370 ft			
Production			
BO/D			
Mcf/D			
Volume Weighted Reservoir Density, psi/ft			
dP to +370 ft			
Pressure at +370 ft datum		1508	

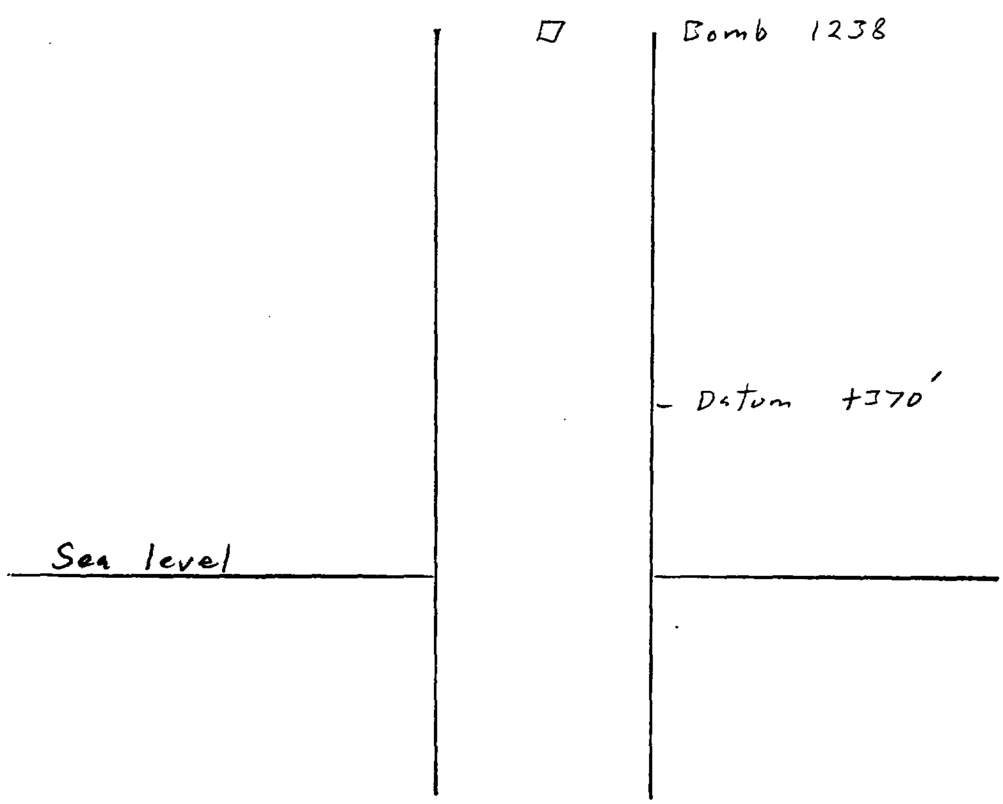

	KB		Subsea
Operator	BMG		
Well	K-13		
	KB		Subsea
Elevation	7106		
Top of B Zone			
Test Date		2/23/88	
Bomb Depth	5862		+1238
Bomb Pressure, psig		1440	
Fluid Level			
Wellbore Gradient			
Oil, psi/ft			
Gas, psi/ft	(.03)(1238-370)		26
Pressure at Top of B Zone			
Top of B Zone to +370 ft			
Production			
BO/D			
Mcf/D			
Volume Weighted Reservoir Density, psi/ft			
dP to +370 ft			
Pressure at +370 ft datum		1466	

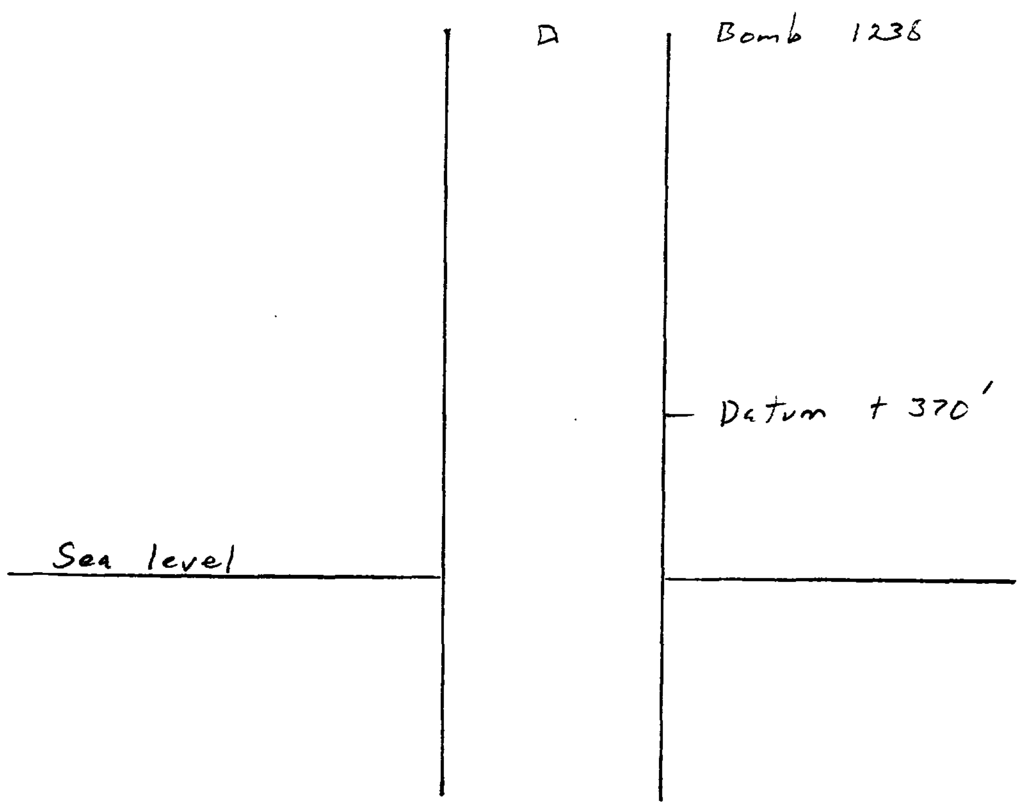

Operator	BMG		
Well	D-17		
	KB		Subsea
Elevation	7477		
Top of B Zone	7130		+347
Test Date		11/19/87	
Bomb Depth	7112		+365
Bomb Pressure, psig		1001	
Fluid Level			
Wellbore Gradient			
Oil, psi/ft			
Gas, psi/ft	(.03)(365-347)		.5
Pressure at Top of B Zone		1001.5	
Top of B Zone to +370 ft	23		
Production			
BO/D			
Mcf/D			
Volume Weighted Reservoir Density, psi/ft		.035	
dP to +370 ft		0.8	
Pressure at +370 ft datum		1000.7	

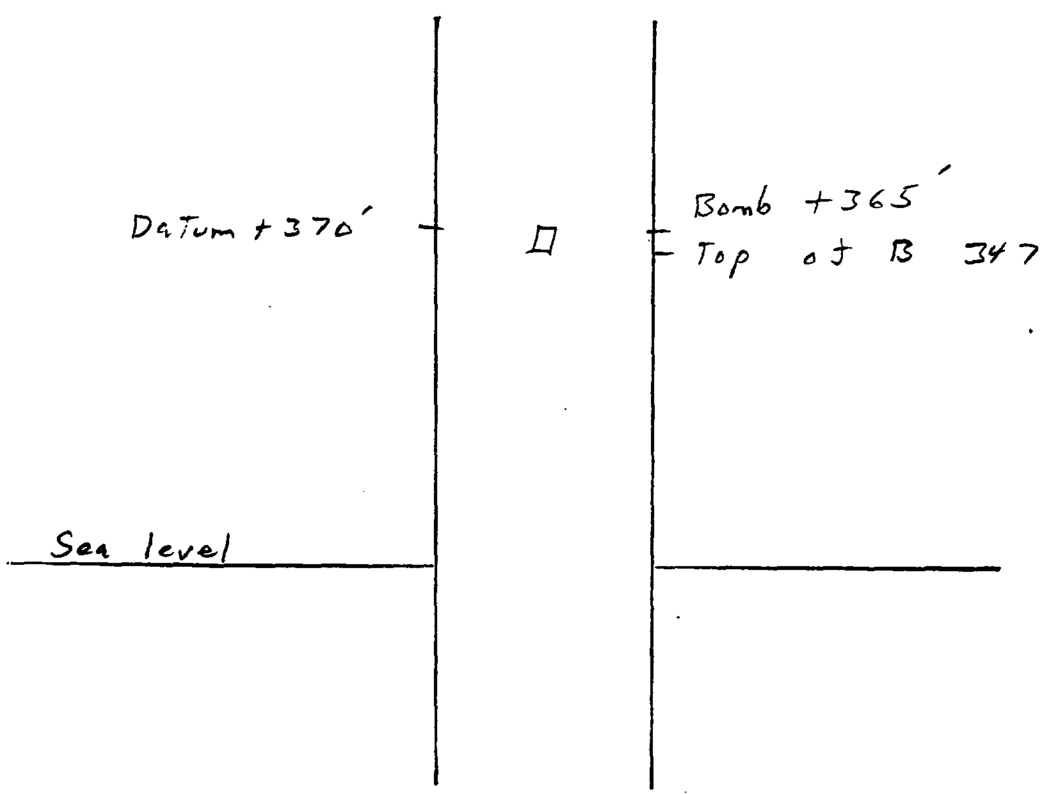

	KB		Subsea
Operator	BMG		
Well	D-17		
	KB		Subsea
Elevation	7477		
Top of B Zone	7130		+347
Test Date		2/23/88	
Bomb Depth	7112		+365
Bomb Pressure, psig		960	
Fluid Level			
Wellbore Gradient			
Oil, psi/ft			
Gas, psi/ft	(.03)(365-347)		0.5
Pressure at Top of B Zone		960.5	
Top of B Zone to +370 ft	23		
Production			
BO/D			
Mcf/D			
Volume Weighted Reservoir Density, psi/ft		.035	
dP to +370 ft		0.8	
Pressure at +370 ft datum		959.7	

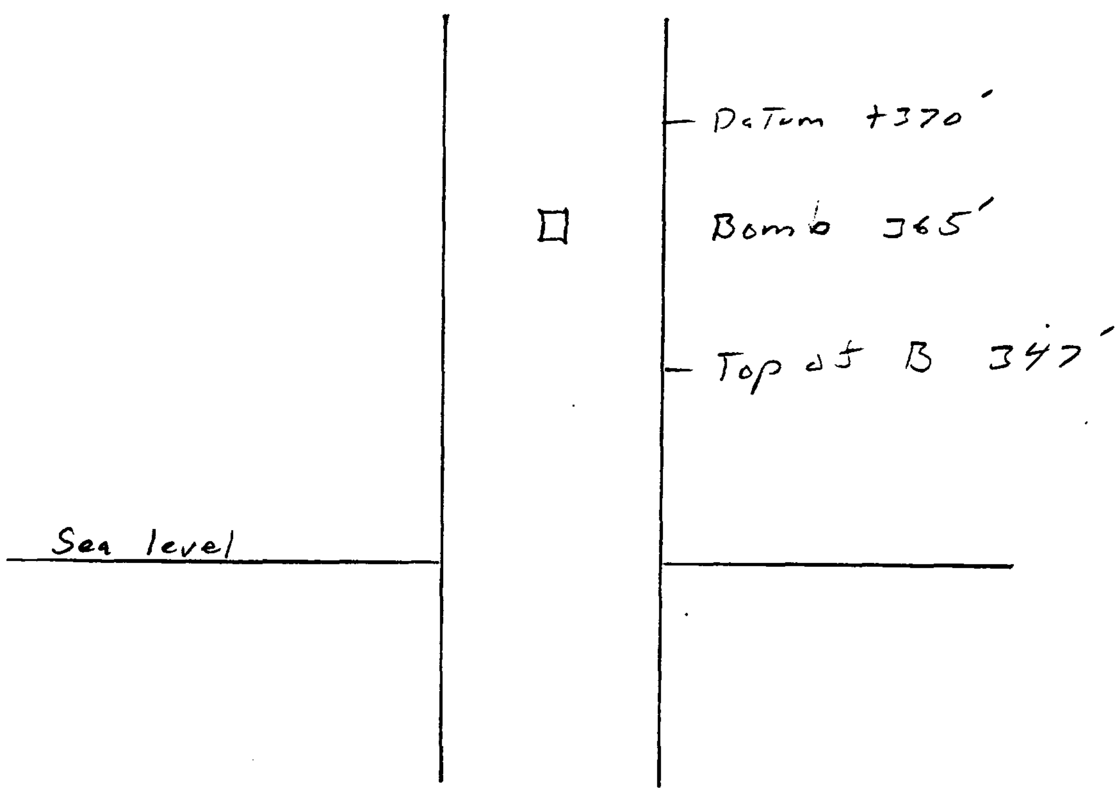

	KB		Subsea
Operator	BMG		
Well	A-20		
Elevation	7444		
Top of B Zone	7038		+406
Test Date		6/30/87	
Bomb Depth	7166		+278
Bomb Pressure, psig		1224.6	
Fluid Level	6992		+454
Wellbore Gradient			
Oil, psi/ft	(0.3)(278-406)		-38.4
Gas, psi/ft			
Pressure at Top of B Zone		1186.2	
Top of B Zone to +370 ft	36		
Production			
BO/D		37	
Mcf/D		220	
Volume Weighted Reservoir Density, psi/ft		0.05628	
dP to +370 ft		2.0	
Pressure at +370 ft datum		1186.0	

(37) (1.344) = 49.7

$\left[220 - \frac{(37)(505)}{1000}\right] 2.3 = 463$

(.7074)(49.4) = 35.2

(0.067899)(463) = 31.4

(.433)(.1300) = .05628

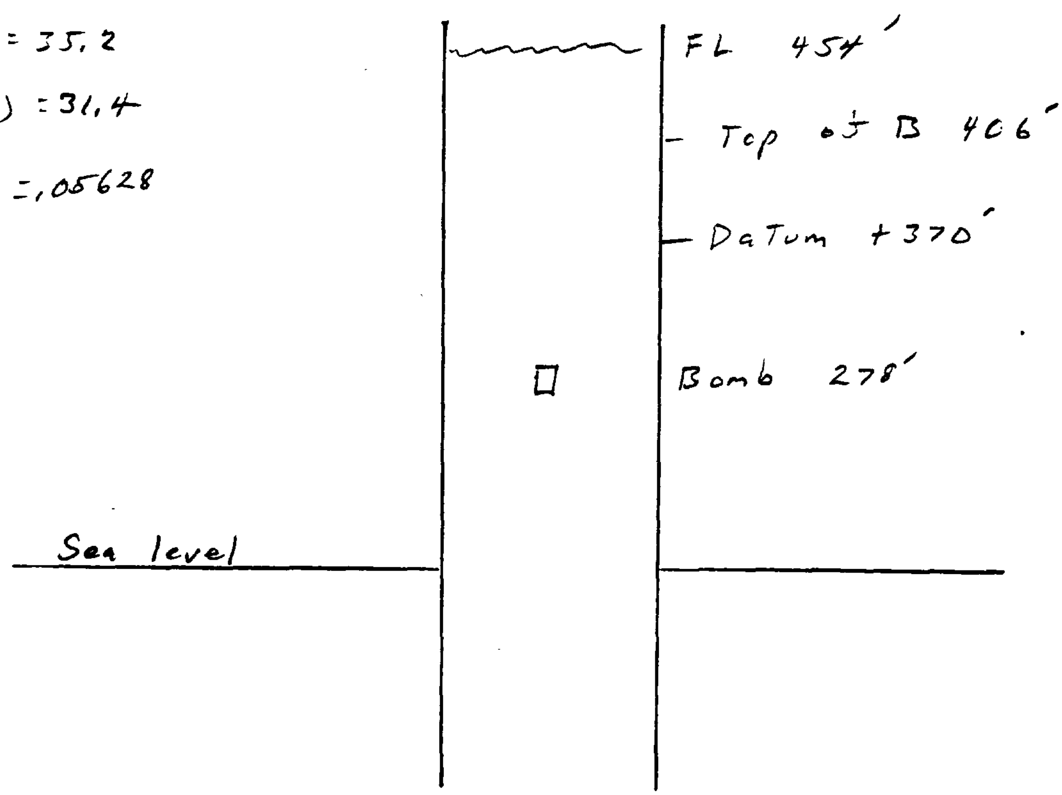

	KB		Subsea
Operator	BMG		
Well	A-20		
Elevation	7444		
Top of B Zone	7038		+406
Test Date		11/19/87	
Bomb Depth	7166		+278
Bomb Pressure, psig		971.1	
Fluid Level			
Wellbore Gradient			
Oil, psi/ft			
Gas, psi/ft	(0.03)(278-406)		-3.8
Pressure at Top of B Zone		967.3	
Top of B Zone to +370 ft	36		
Production			
BO/D		37	
Mcf/D		220	
Volume Weighted Reservoir Density, psi/ft		0.0458	
dP to +370 ft		1.6	
Pressure at +370 ft datum		968.9	

$(37)(1.316) = 48.7$

$\left[220 - \frac{(37)(441)}{1000}\right] 2.891 = 588.8$

$(.7144)\ 48.7 = 34.8$

$(.055291)\ 588.8 = 32.6$

$(.433)\ .1057 = 0.0458$

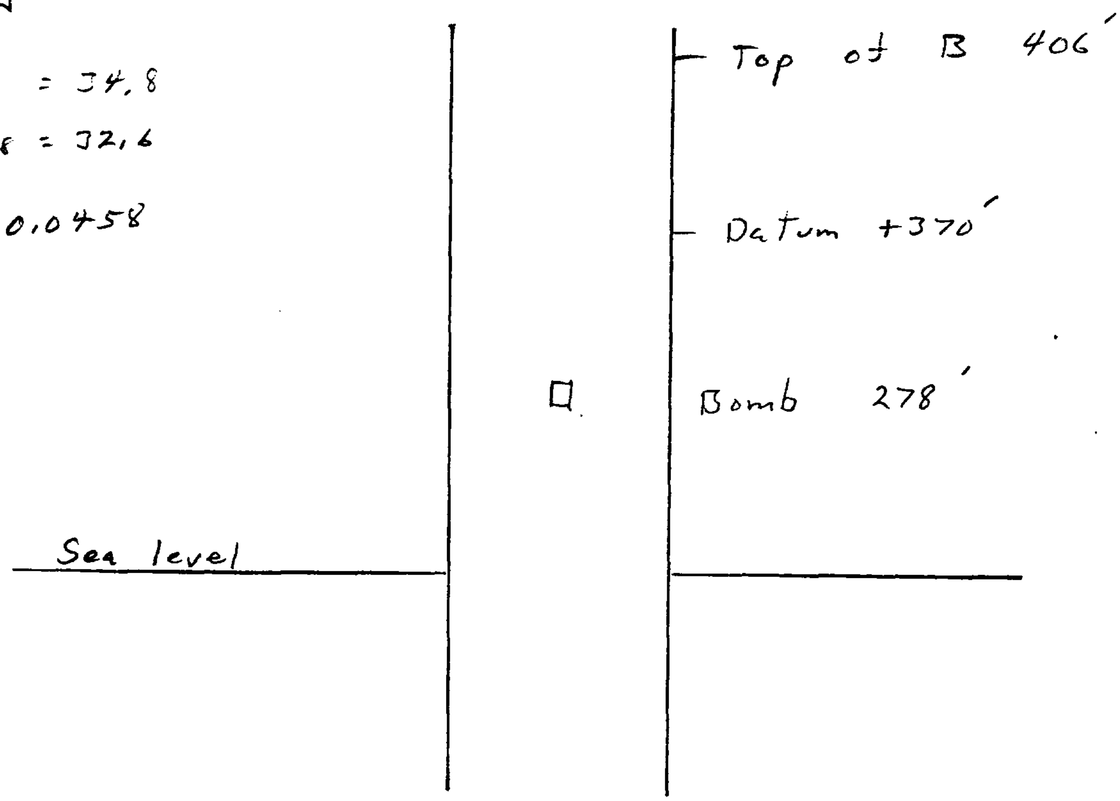

	KB		Subsea
Operator	BMG		
Well	A-20		
Elevation	7444		
Top of B Zone	7038		+406
Test Date		2/23/88	
Bomb Depth	7166		+278
Bomb Pressure, psig		952.4	
Fluid Level	None		
Wellbore Gradient			
Oil, psi/ft			
Gas, psi/ft	(.03)(278-406)		-3.8
Pressure at Top of B Zone		948.6	
Top of B Zone to +370 ft	36		
Production			
BO/D		45	
Mcf/D		360	
Volume Weighted Reservoir Density, psi/ft		.0395	
dP to +370 ft		1.4	
Pressure at +370 ft datum		950.0	

$(45)(1.314) = 59.1$

$\left[360 - \frac{(45)(437)}{1000}\right] 2.932 = 997.9$

$(.7148)(59.1) = 42.3$

$(.054314)(997.9) = 54.2$

$(.433)(.09130) = .0395$

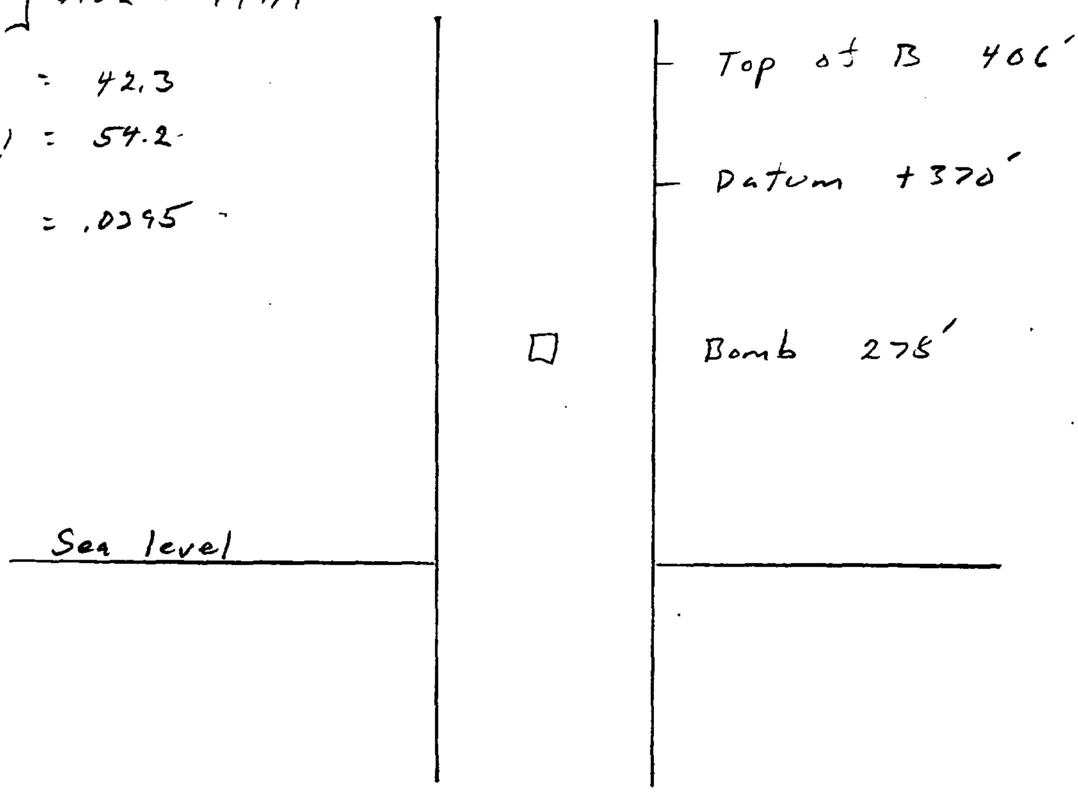

Operator	BMG		
Well	L-27		
	KB		Subsea
Elevation	7475		
Top of B Zone	7032		+443
Test Date		2/26/88	
Bomb Depth	6822		+653
Bomb Pressure, psig		1377	
Fluid Level			
Wellbore Gradient			
Oil, psi/ft			
Gas, psi/ft	(.03)(653-443)		6.3
Pressure at Top of B Zone		1383.3	
Top of B Zone to +370 ft	73		
Production			
BO/D			
Mcf/D			
Volume Weighted Reservoir Density, psi/ft		.035	
dP to +370 ft		2.6	
Pressure at +370 ft datum		1385.9	

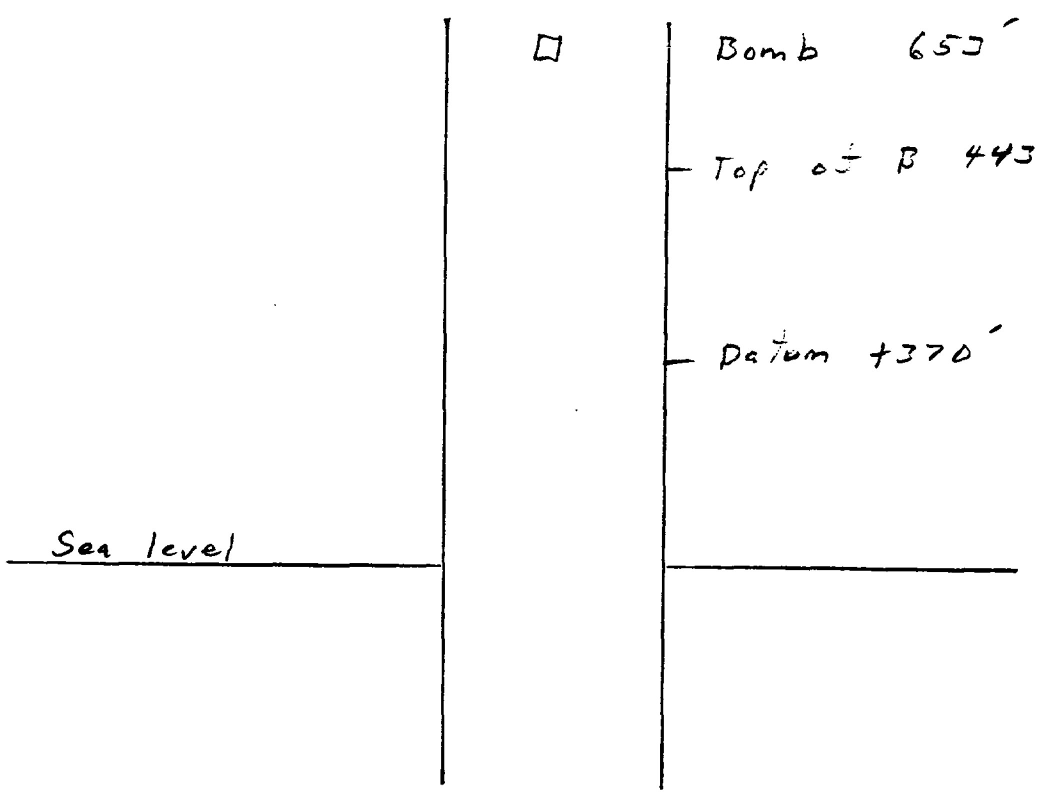

	KB		Subsea
Operator	BMG		
Well	B-29		
Elevation	7508		
Top of B Zone	7085		+423
Test Date		2/23/88	
Bomb Depth	7212		+296
Bomb Pressure, psig		962	
Fluid Level			
Wellbore Gradient			
Oil, psi/ft			
Gas, psi/ft	(03)(296-423)		-3.8
Pressure at Top of B Zone		958.2	
Top of B Zone to +370 ft	53		
Production			
BO/D		1136	
Mcf/D		1590	
Volume Weighted Reservoir Density, psi/ft		0.1117	
dP to +370 ft		5.9	
Pressure at +370 ft datum		964.1	

$(1136)\,1.316 = 1488.2$

$\left[1590 - \frac{(1136)(430)}{1000}\right] 3.015 = 3321.1$

$(.7154)\ 1488.2 = 1064.6$

$(.052877)\ 3321.1 = 175.6$

$(.433)(.2579) = .1117$

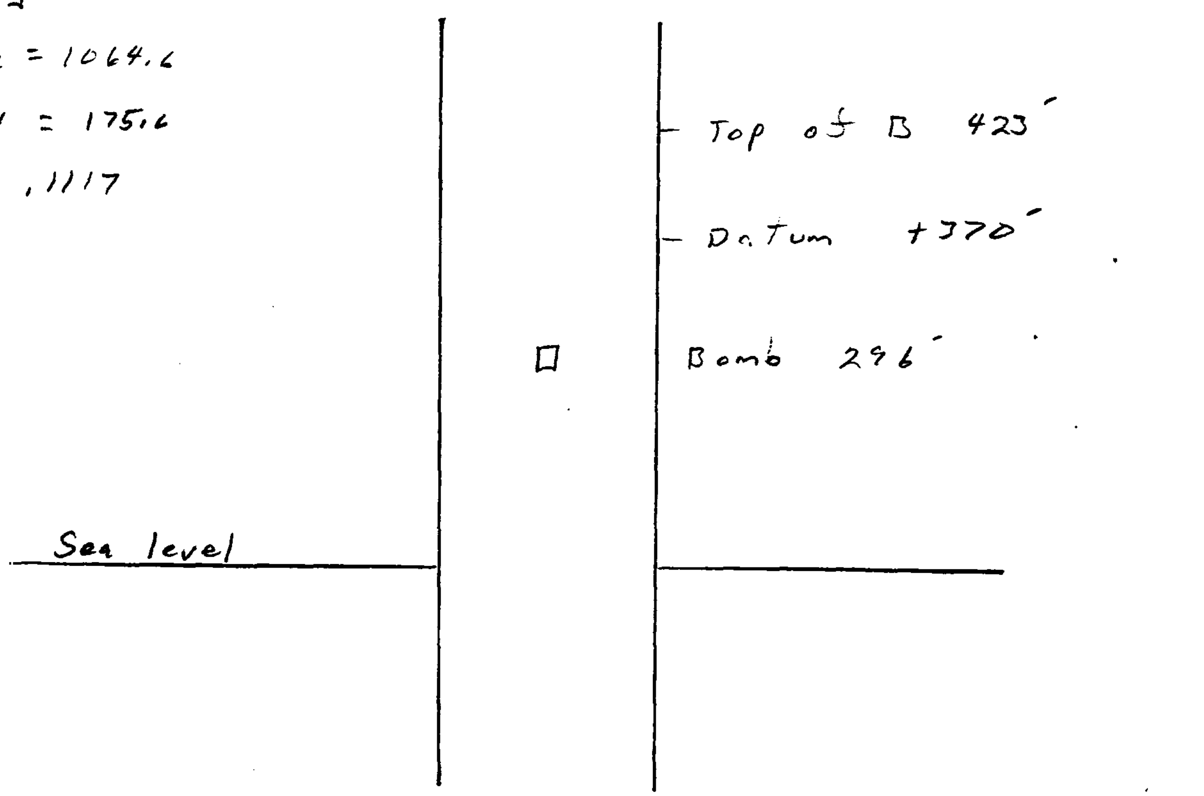

	KB		Subsea
Operator	BMG		
Well	B-32		
Elevation	7611		
Top of B Zone	7190		+421
Test Date		6/30/87	
Bomb Depth	7316		+295
Bomb Pressure, psig		1203.4	
Fluid Level	7262		+349
Wellbore Gradient			
Oil, psi/ft	(.3)(295-349)		-16.2
Gas, psi/ft	(.03)(349-421)		-2.2
Pressure at Top of B Zone		1185	
Top of B Zone to +370 ft	51		
Production			
BO/D		520	
Mcf/D		470	
Volume Weighted Reservoir Density, psi/ft		0.1832	
dP to +370 ft		+ 9.3	
Pressure at +370 ft datum		1194.3	

$(520)\ (1.331) = 692.1$

$\left[470 - \frac{(520)(476)}{1000}\right] 2.524 = 561.5$

$(.7115)(692.1) = 492.4$

$(.067841)(561.5) = 38.1$

$(.433)(0.4232) = .1832$

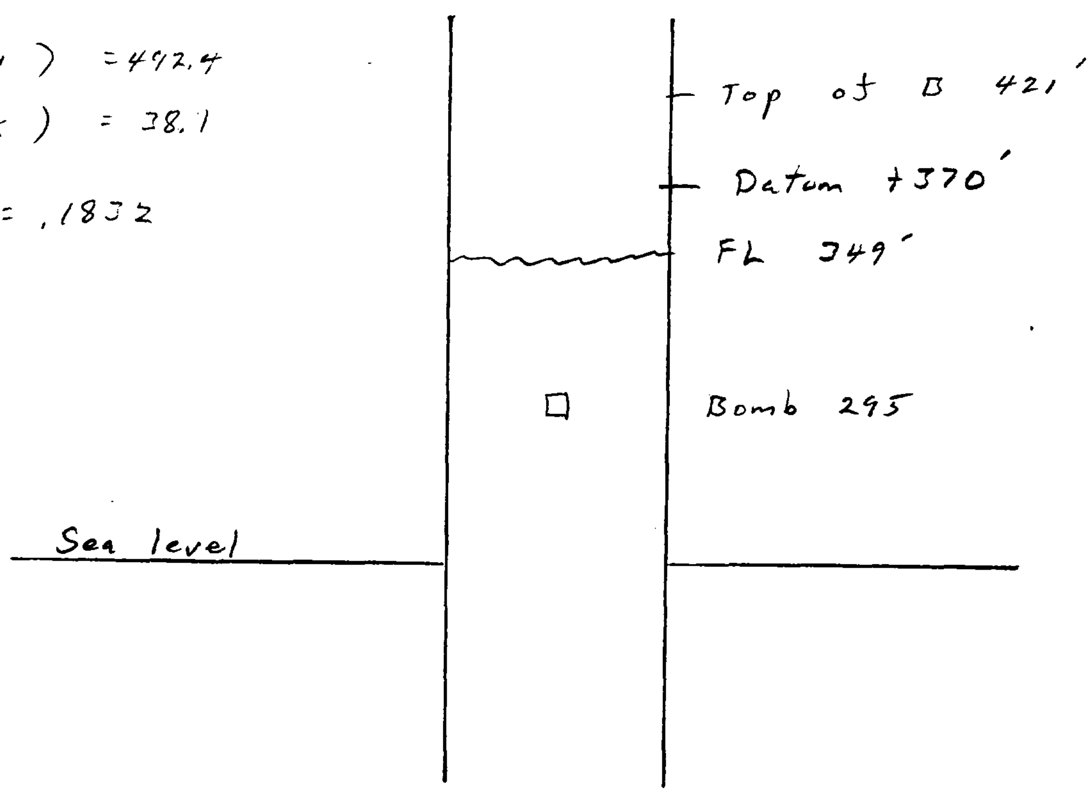

	KB		Subsea
Operator	BMG		
Well	B-32		
Elevation	7611		
Top of B Zone	7190		+421
Test Date		11/19/87	
Bomb Depth	7302		+309
Bomb Pressure, psig		970.5	
Fluid Level	None		
Wellbore Gradient			
Oil, psi/ft			
Gas, psi/ft	(.03)(309-421)		-3.4
Pressure at Top of B Zone		967.1	
Top of B Zone to +370 ft	51		
Production			
BO/D		766	
Mcf/D		920	
Volume Weighted Reservoir Density, psi/ft		.05684	
dP to +370 ft		2.9	
Pressure at +370 ft datum		970.0	

(766) (1.316) = 1008.1

$$\left[920 - \frac{(766)(442)}{1000}\right] 2.875 = 1671.6$$

(0.7143) (1008) = 720

(0.055291)(1671) = 92.4

(.433)(.3032) = .1313

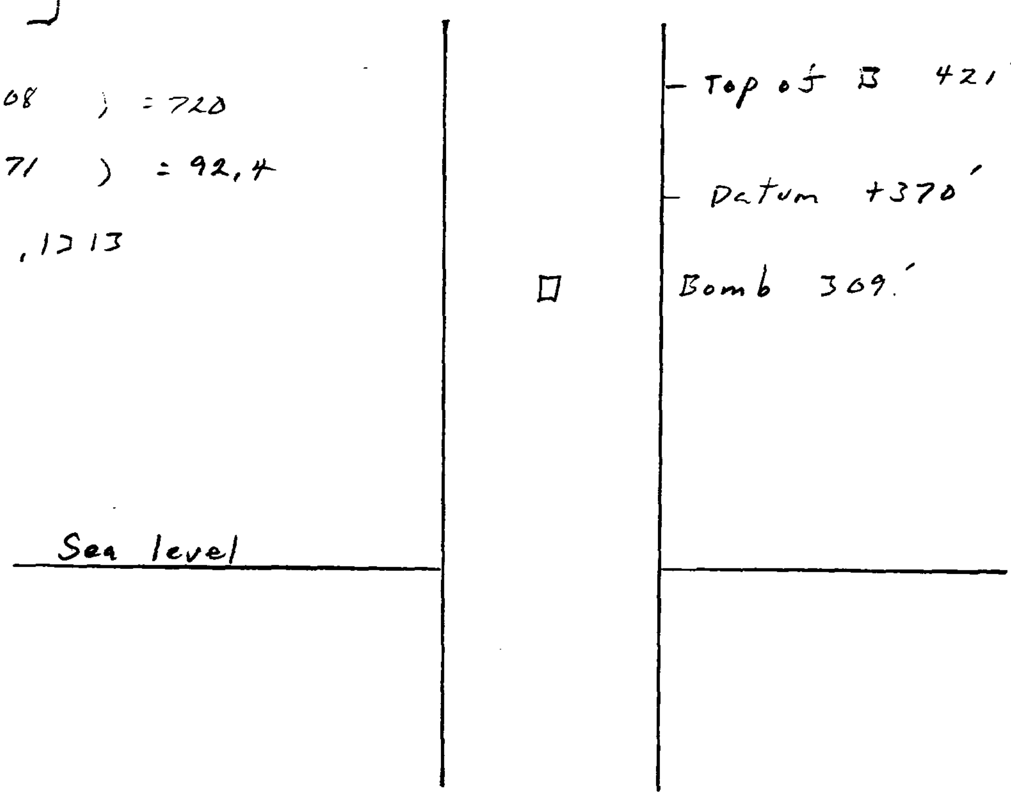

	KB	Subsea
Operator	BMG	
Well	B-32	
Elevation	7611	
Top of B Zone	7190	+421
Test Date	2/23/88	
Bomb Depth	7302	+309
Bomb Pressure, psig	953.8	
Fluid Level		
Wellbore Gradient		
Oil, psi/ft		
Gas, psi/ft	.03(309-421)	-3.4
Pressure at Top of B Zone	950.4	
Top of B Zone to +370 ft	51	
Production		
BO/D	754	
Mcf/D	770	
Volume Weighted Reservoir Density, psi/ft	0.1238	
dP to +370 ft	+ 6.3	
Pressure at +370 ft datum	956.7	

(754) 1.288 = 971.2

$\left[770 - \frac{754(280)}{1000}\right] 3.792 = 1833.4$

(.7229) 971.2 = 702

(.054314) 1833.4 = 99.8

(.433)(0.2858)

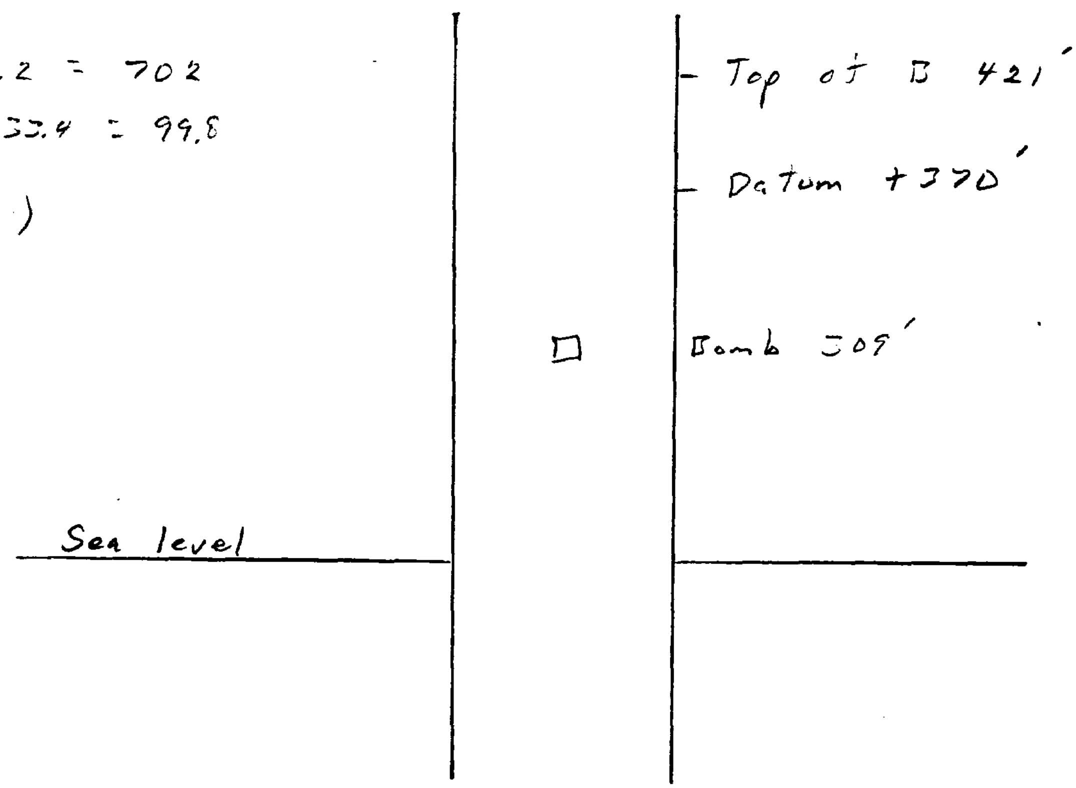

	KB		Subsea
Operator	Mallon		
Well	Johnson Federal 12-5		
Elevation	7430		
Top of B Zone	7029		+401
Test Date		6/30/87	
Bomb Depth	7611		-181
Bomb Pressure, psig		1427	
Fluid Level	5205		+2225
Wellbore Gradient			
Oil, psi/ft	(0.355)(-181-401)		-206.6
Gas, psi/ft			
Pressure at Top of B Zone		1220.4	
Top of B Zone to +370 ft	94		
Production			
BO/D		30	
Mcf/D		382	
Volume Weighted Reservoir Density, psi/ft		0.04324	
dP to +370 ft		4.1	
Pressure at +370 ft datum		1224.5	

$(30)(1.348) = 40.4$

$\left[382 - \frac{(30)(515)}{1060}\right] 2.234 = 818.9$

$(.7072)(40.4) = 28.6$

$(.069860)(818.9) = 57.2$

$(.433)(.09986) = .04324$

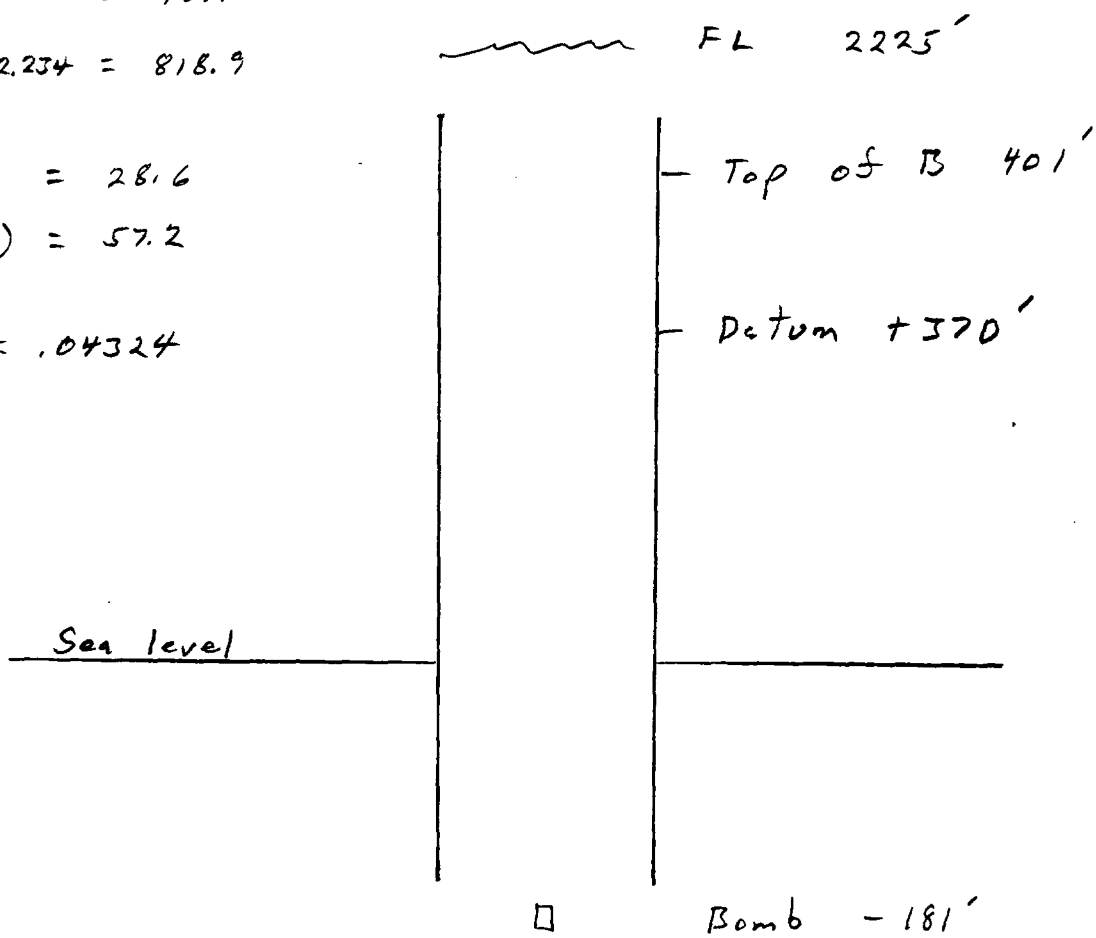

	KB		Subsea
Operator	Mallon		
Well	Fisher Federal 2-1		
Elevation	7654		
Top of B Zone	7307		+347
Test Date		11/19/87	
Bomb Depth	7875		-221
Bomb Pressure, psig		1177	
Fluid Level	7297		+357
Wellbore Gradient			
Oil, psi/ft	(0.34)(-221-347)		-193.1
Gas, psi/ft			
Pressure at Top of B Zone		983.8	
Top of B Zone to +370 ft	23		
Production			
BO/D		228	
Mcf/D		575	
Volume Weighted Reservoir Density, psi/ft		0.08429	
dP to +370 ft		1.9	
Pressure at +370 ft datum		981.9	

$(228)\ (1.3185) = 300.6$

$\left[575 - \frac{(228)(448)}{1000}\right] 2.808 = 1127.8$

$(.7140)(300.6) = 214.6$

$(.05627)(1127.8) = 63.5$

$(.433)(.19467) = .08429$

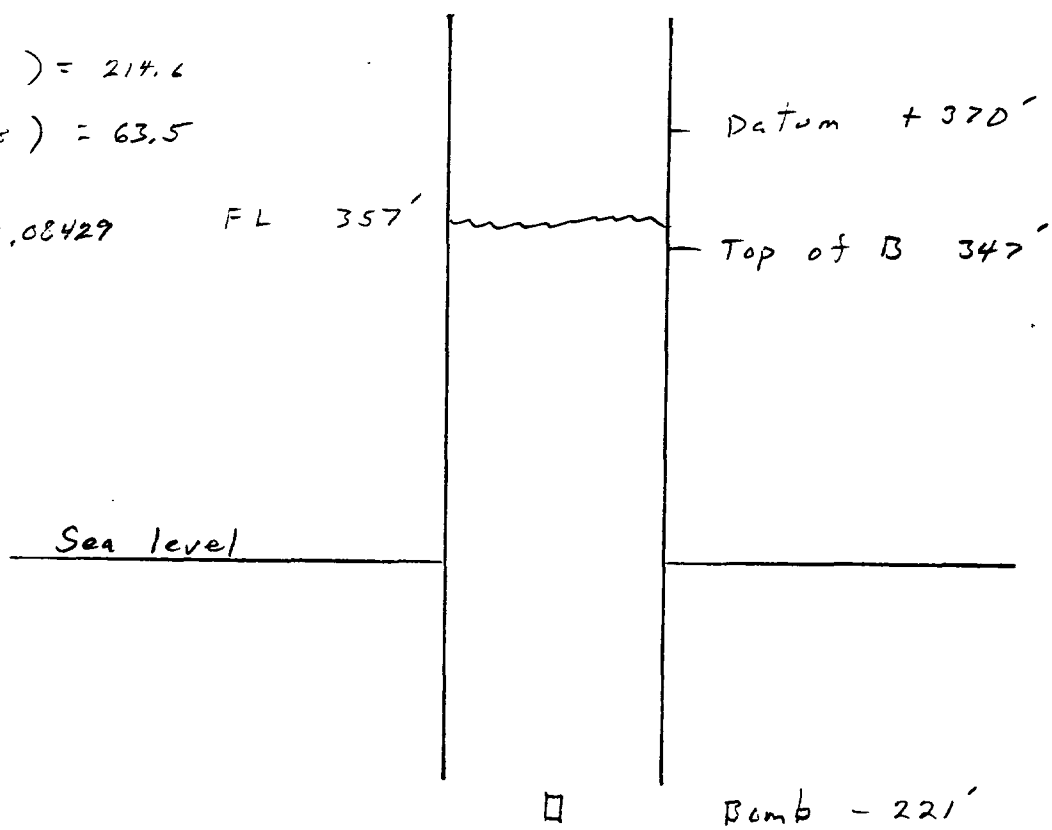

	KB		Subsea
Operator	Mallon		
Well	Howard 1-8		
Elevation	7522		
Top of B Zone	7150		+372
Test Date		2/23/88	
Bomb Depth	7300		+222
Bomb Pressure, psig		980	
Fluid Level	4523		+2999
Wellbore Gradient			
Oil, psi/ft	.345 (222-372)		-51.8
Gas, psi/ft			
Pressure at Top of B Zone		928	
Top of B Zone to +370 ft	2		
Production			
BO/D		120	
Mcf/D		1021	
Volume Weighted Reservoir Density, psi/ft		.03754	
dP to +370 ft		0.1	
Pressure at +370 ft datum		928.1	

$(120)\ (1.310) = 157.2$

$\left[1021 - \frac{(120)(430)}{1000}\right] 3.015 = 2922.7$

$(.7154)(157.2) = 112.5$

$(.052877)(2922.7) = 154.5$

$(.433)(.08671) = .03754$

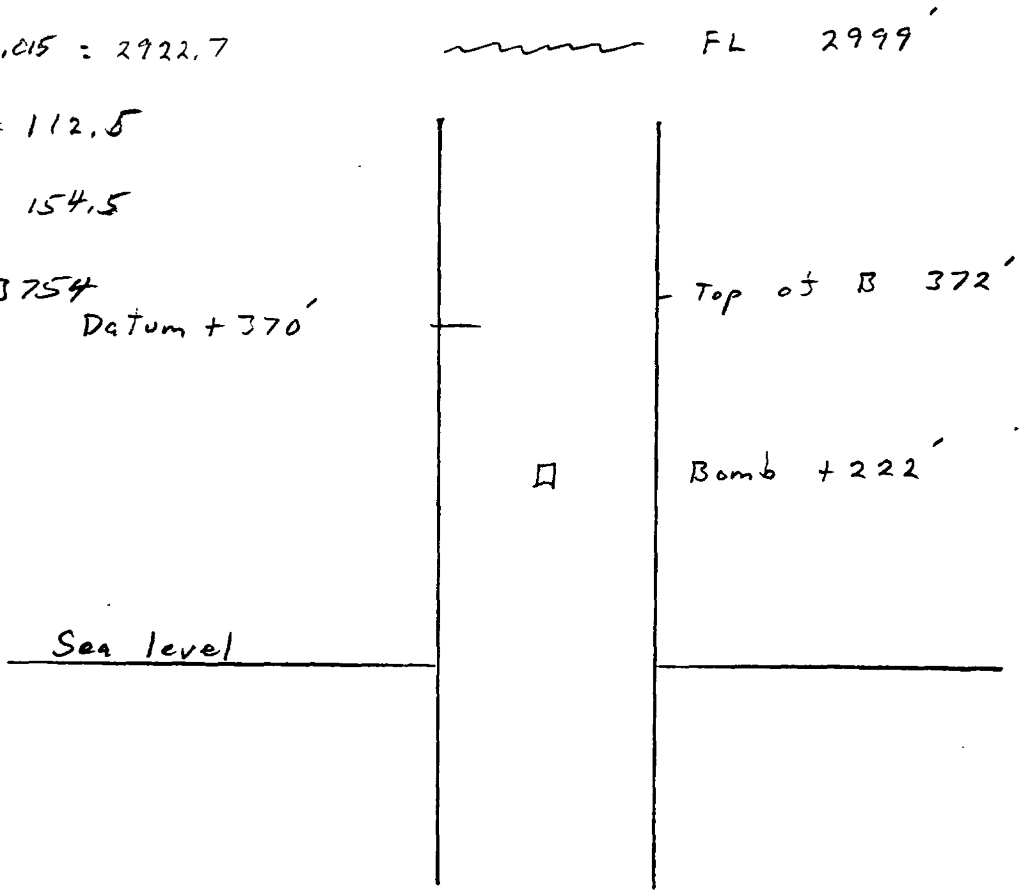

	KB		Subsea
Operator	Mesa Grande		
Well	Bearcat #1		
	KB		Subsea
Elevation	7249		
Top of B Zone	6777		+472
Test Date		6/30/87	
Bomb Depth	6800		+449
Bomb Pressure, psig		1036	
Fluid Level			
Wellbore Gradient			
Oil, psi/ft			
Gas, psi/ft	(.03)(449-472)		-.66
Pressure at Top of B Zone		1035.4	
Top of B Zone to +370 ft	102'		
Production			
BO/D		52	
Mcf/D		347	
Volume Weighted Reservoir Density, psi/ft		0.04657	
dP to +370 ft		4.8	
Pressure at +370 ft datum		1040.2	

$(52)(1.325) = 68.9$

$\left[347 - \frac{(52)(463)}{1000}\right] 2.67 = 862.2$

$(.7129)(68.9) = 49.1$

$(.05920)(862.2) = 51.0$

$(.433)(.1076) = .04657$

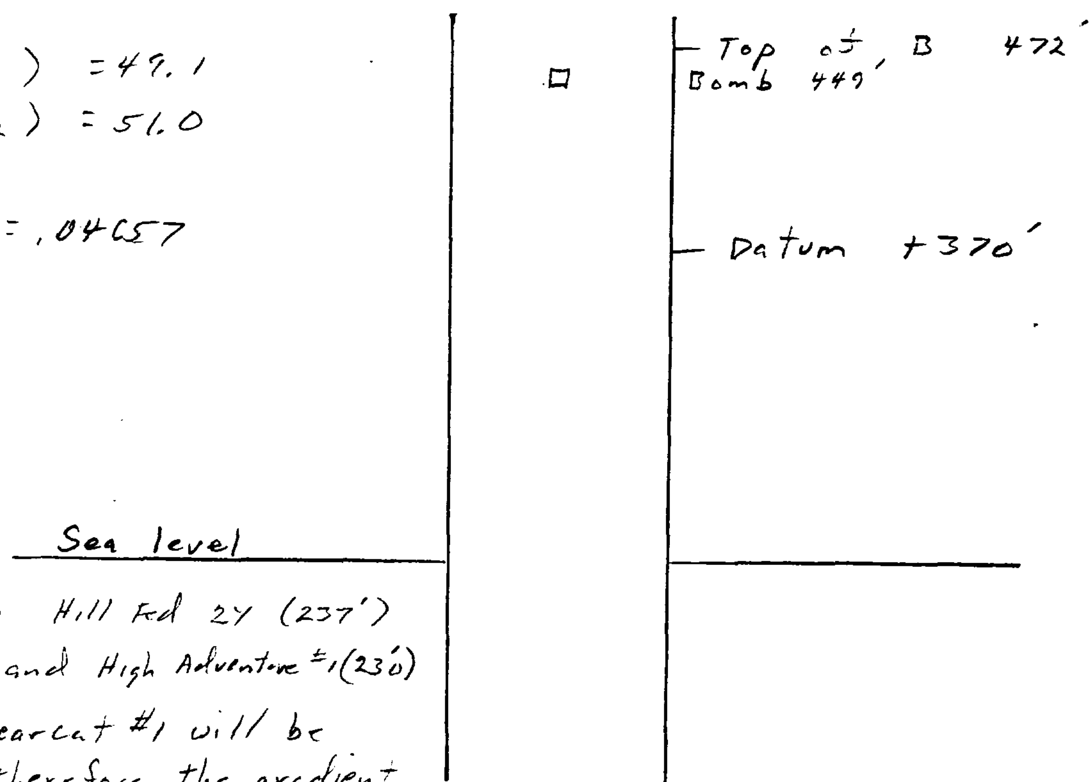

By analogy to Hill Fed 24 (237') Loddy #1 (205') and High Adventure #1 (230') the FL of Bearcat #1 will be +200' to +250' therefore the gradient is gas only

	KB	Subsea
Operator	Mesa Grande	
Well	Bearcat #1	
Elevation	7249	
Top of B Zone	6777	+472
Test Date	11/19/87	
Bomb Depth	6770	+479
Bomb Pressure, psig	765	
Fluid Level	below +370'	
Wellbore Gradient		
Oil, psi/ft		
Gas, psi/ft	(.03)(479-472)	.15
Pressure at Top of B Zone	765.15	
Top of B Zone to +370 ft	102	
Production		
BO/D	10.6	
Mcf/D	192	
Volume Weighted Reservoir Density, psi/ft	.035	
dP to +370 ft	3.6	
Pressure at +370 ft datum	768.7	

$(10.6)(1.289) = 13.7$

$\left[192 - \frac{(10.6)(385)}{1000}\right]3.7 = 695.3$

$(.722)(13.7) = 9.9$

$(.04414)(695.3) = 30.6$

$(.433)(.05725) = .0248$

use 0.035 psi/ft (wet gas)

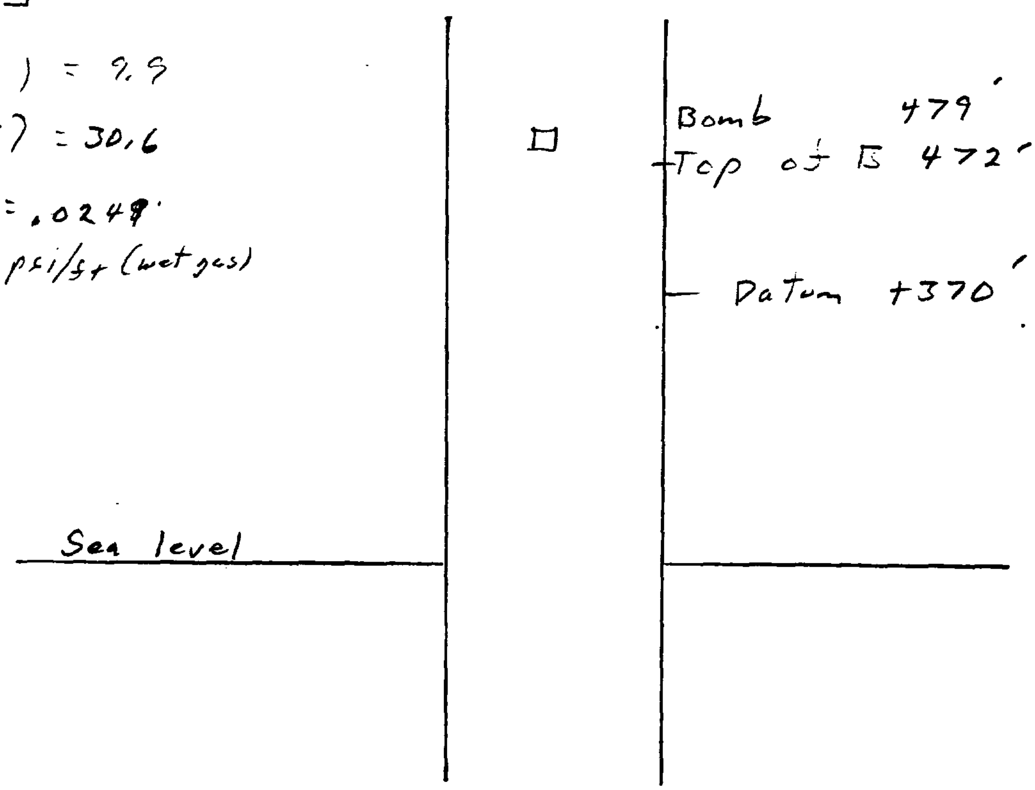

	KB	Subsea
Operator	Mesa Grande	
Well	Bearcat #1	
Elevation	7249	
Top of B Zone	6777	+472
Test Date	2/23/88	
Bomb Depth	6770	+479
Bomb Pressure, psig	732	
Fluid Level	below +370'	
Wellbore Gradient		
Oil, psi/ft		
Gas, psi/ft	(.03)(479-472)	.15
Pressure at Top of B Zone	732.15	
Top of B Zone to +370 ft	102	
Production		
BO/D	5.7	
Mcf/D	213	
Volume Weighted Reservoir Density, psi/ft	0.035	
dP to +370 ft	3.6	
Pressure at +370 ft datum	735.7	

$(5.7)(1.285) = 7.3$

$\left[213 - \frac{5.7(373)}{1000}\right] 3.92 = 826.6$

$(.7239)(7.3) = 5.3$

$(.04239)(826.6) = 35.0$

$(.433)(.04837) = 0.0209$

use wet gas 0.035

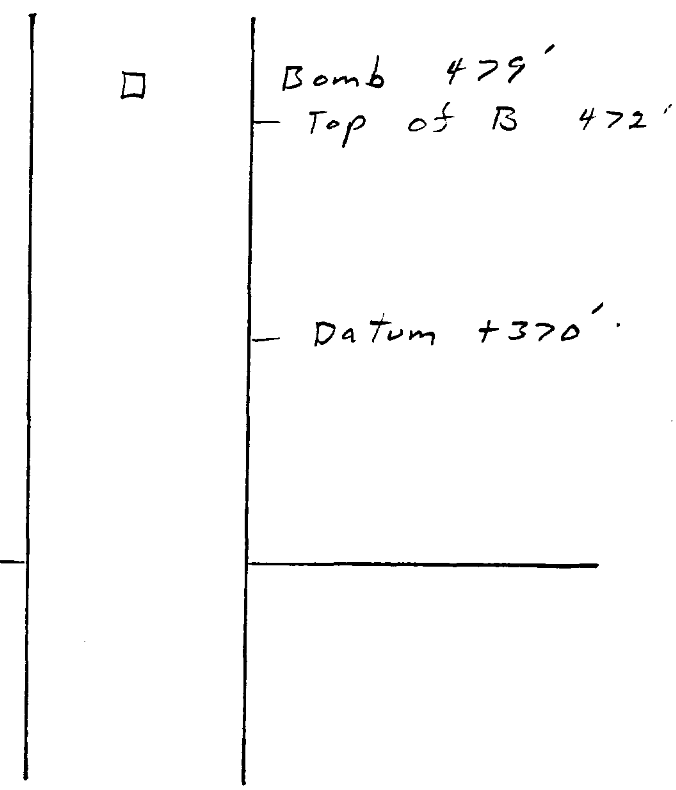

	KB		Subsea
Operator	Meridian		
Well	Hill Federal 24		
Elevation	7467		
Top of B Zone	7013		+454
Test Date		6/30/87	
Bomb Depth	7400		+67
Bomb Pressure, psig		1165	
Fluid Level (oil)	7230		+237
Wellbore Gradient	7300	water	+167
Oil, psi/ft	(.3)(.237-167)		21.0
Gas, psi/ft	(.03)(467-237)		6.3
H2O, .433 psi/ft	(.433)(167-67)		43.3
Pressure at Top of B Zone		1094.4	
Top of B Zone to +370 ft	84		
Production			
BO/D		100	
Mcf/D		240	
Volume Weighted Reservoir Density, psi/ft		.08803	
dP to +370 ft		7.4	
Pressure at +370 ft datum		1101.8	

(100)(1.333) = 133.3

$$\left[240 - \frac{(100)(479)}{1000}\right] 2.511 = 482.4$$

(.7113)(133.3) = 94.8

(.062944)(482.4) = 30.4

(.433)(0.2033) = 0.08803

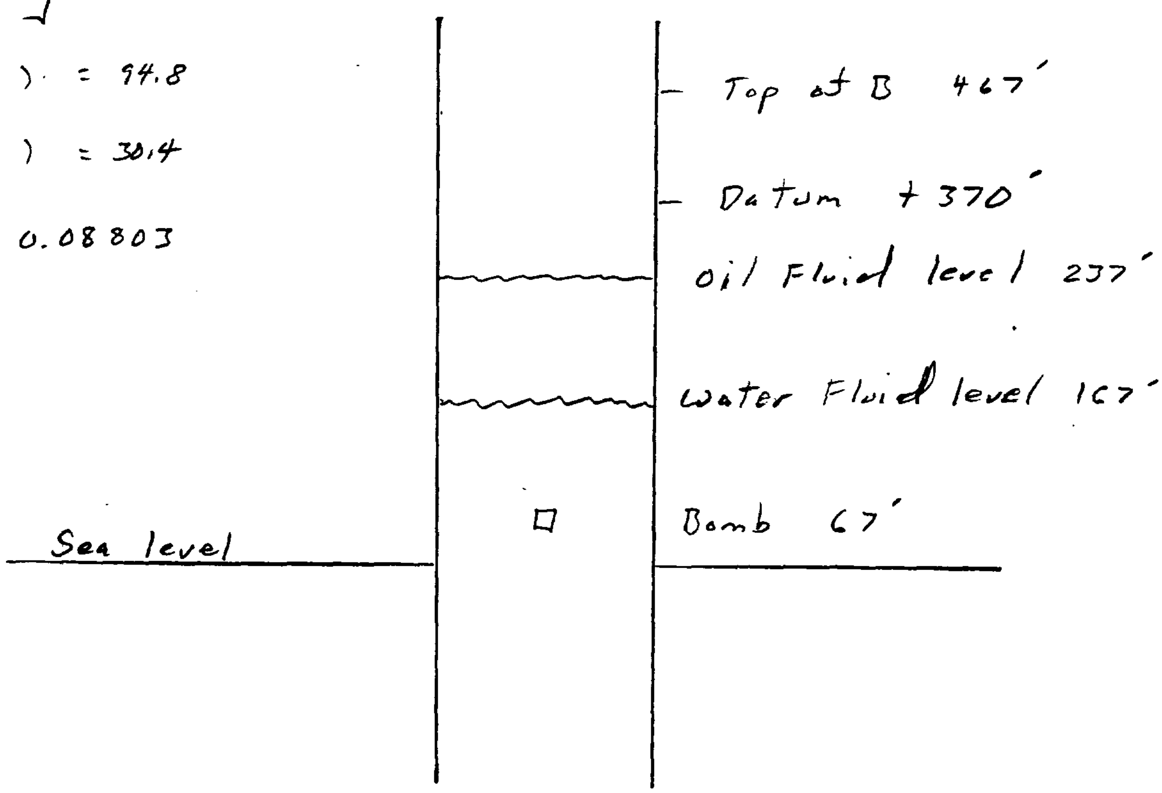

	KB		Subsea
Operator	Meridian		
Well	Hill Federal #1		
Elevation	7480		
Top of B Zone	7017		+463
Test Date		11/19/87	
Bomb Depth	7555		-75
Bomb Pressure, psig		988	
Fluid Level	7456		+24
Wellbore Gradient			
Oil, psi/ft	(.3)(-75-24)		-29.7
Gas, psi/ft	(.03)(24-463)		-13.2
Pressure at Top of B Zone		945.1	
Top of B Zone to +370 ft	93'		
Production			
BO/D		27	
Mcf/D		880	
Volume Weighted Reservoir Density, psi/ft		0.035	
dP to +370 ft		3.3	
Pressure at +370 ft datum		948.4	

$(27)(1.314) = 35.5$

$\left[880 - \frac{(27)(436)}{1000}\right] 2.95 = 2561.3$

$(.7149)(35.5) = 25.4$

$(.05403)(2561) = 138.4$

$(.433)(.06307) = .027$

use wet gas 0.035 psi/ft

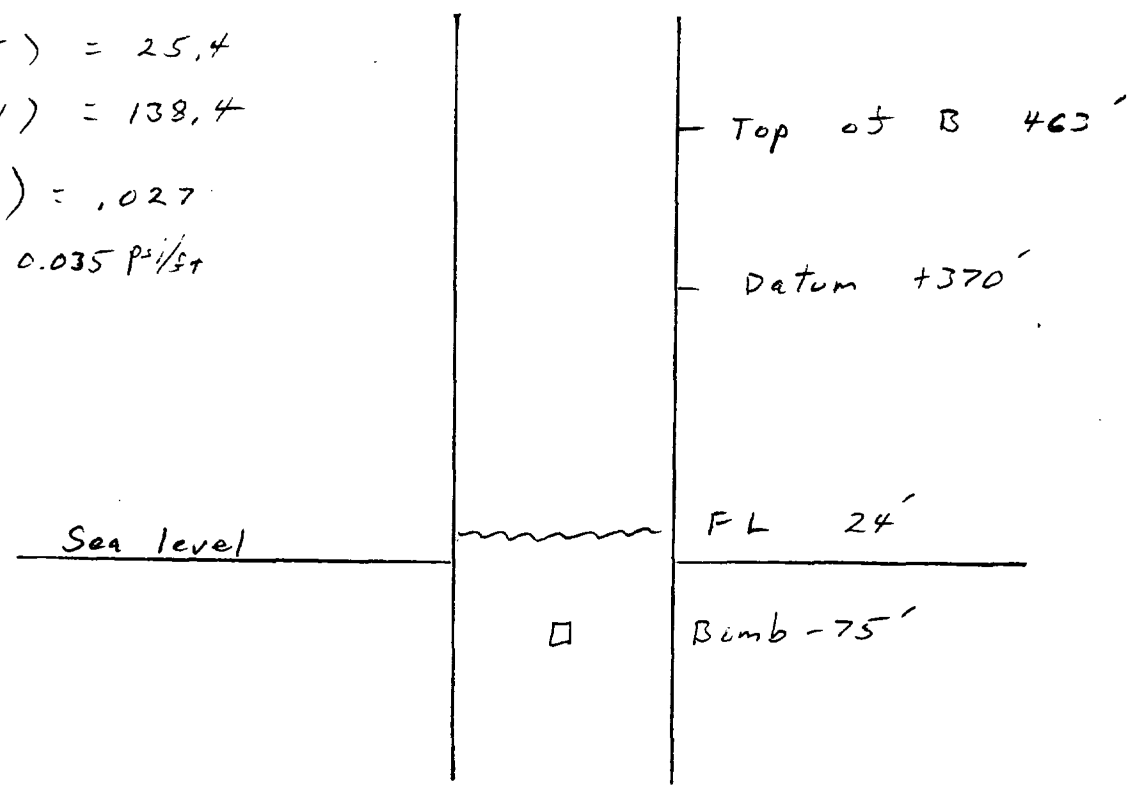

	KB		Subsea
Operator	Meridian		
Well	Hill Federal #1		
Elevation	7480		
Top of B Zone	7017		+463
Test Date		2/23/88	
Bomb Depth	7555		−75
Bomb Pressure, psig		966	
Fluid Level	7552		−72
Wellbore Gradient			
Oil, psi/ft	.3(75−72)		−0.9
Gas, psi/ft	.03(463+72)		−16.05
Pressure at Top of B Zone		949	
Top of B Zone to +370 ft	93		
Production			
BO/D		11	
Mcf/D		962	
Volume Weighted Reservoir Density, psi/ft		0.035	
dP to +370 ft		3.3	
Pressure at +370 ft datum		952.3	

$(11) \quad (1.314) = 14.5$

$\left[962 - \frac{(11)(437)}{1000}\right] 2.932 = 2806.5$

$(.7148)(14.5) = 10.3$

$(.054314)(2806.5) = 152.4$

$(.433)(.05769) = .02498$

use 0.035 wet gas

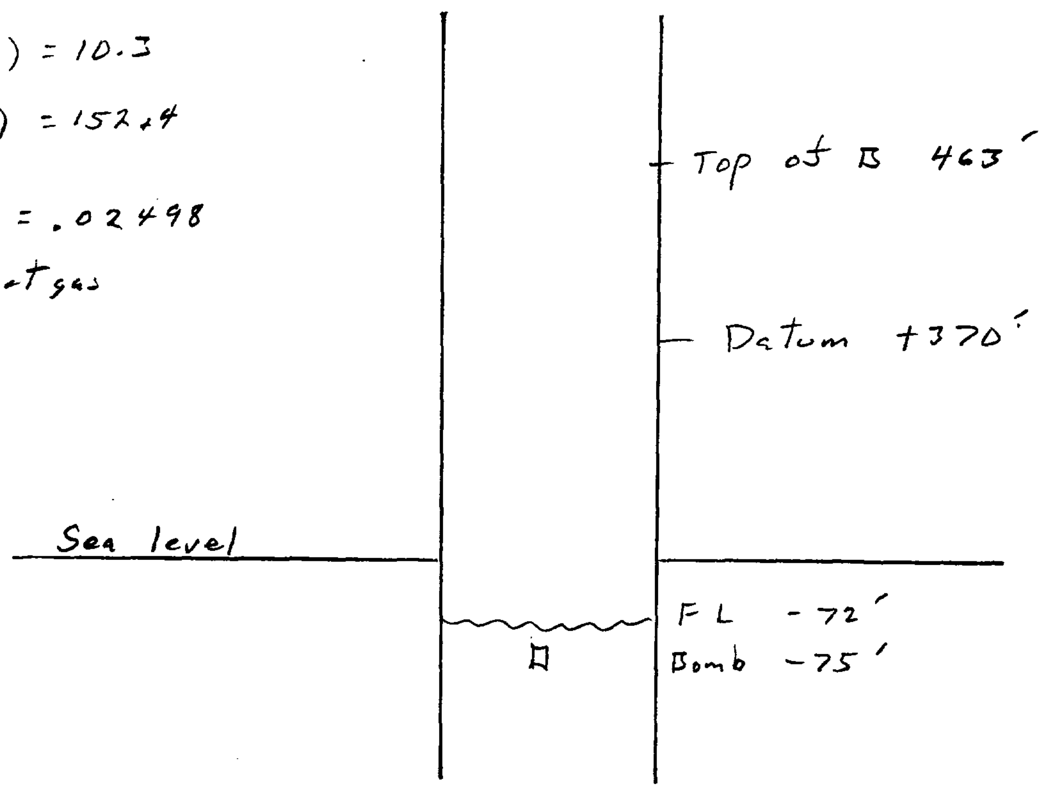

5/2/88

	KB		Subsea
Operator	Mobil		
Well	Lindrith B-37		
Elevation	7134		
Top of B Zone	6683		+ 451
Test Date		6/30/87	
Bomb Depth	6814		+ 334
Bomb Pressure, psig		1059	
Fluid Level			+ 419
~~Distance to Top of B Zone~~			
Wellbore Gradient			
Oil, psi/ft		0.3 (419-334)	
Gas, psi/ft		0.03 (451-419)	
Pressure at Top of B Zone		1059-26 = 1032	
Top of B Zone to +370 ft		81	
Production			
BO/D		54	
Mcf/D		435	
Volume Weighted Reservoir Density, psi/ft		0.04270	
dP to +370 ft		3.5	
Pressure at +370 ft datum		1035.5	

$(54)(1.323) = 71.4$

$\left[435 - \frac{(54)(459)}{1000}\right] 2.7 = 1107.6$

$\overline{\quad 1179 \quad}$

$(71.4)(.7131) = 50.9$

$(1107.6)(.05903) = 65.4$

$.433(.0986) = .04270$

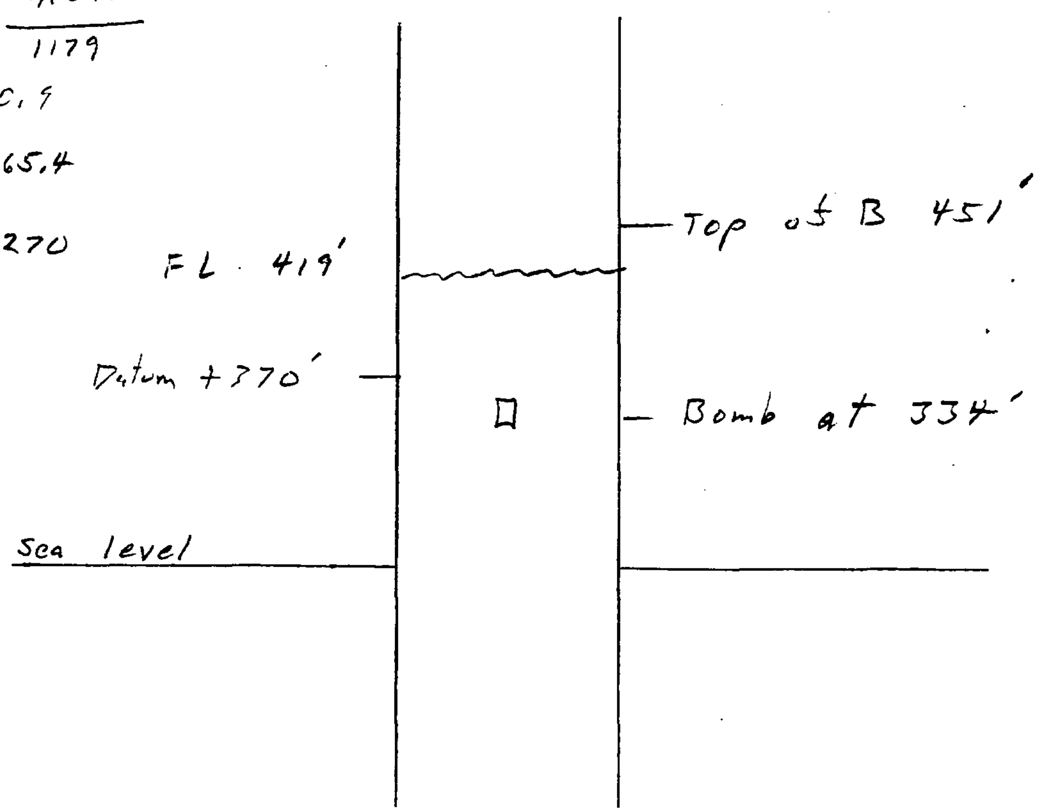

	KB	Subsea
Operator	Mobil	
Well	Lindrith B-37	
Elevation	7134	
Top of B Zone	6683	+451
Test Date	11/19/87	
Bomb Depth	6814	+334
Bomb Pressure, psig	797	
Fluid Level		+522
~~Distance to Top of B Zone~~		
Wellbore Gradient		
Oil, psi/ft	0.3 (451-334)	
Gas, psi/ft	0.03	
Pressure at Top of B Zone	762	
Top of B Zone to +370 ft	81	
Production		
BO/D	214	
Mcf/D	889	
Volume Weighted Reservoir Density, psi/ft	0.04422	
dP to +370 ft	3.6	
Pressure at +370 ft datum	765.6	

$(214)(1.291) = 276.3$

$\left[889 - \frac{(214)(357)}{1000}\right] 3.656 = 2947.4$

3223.7

$(276.3)(.7218) = 199.4$

$(2947.4)(.04404) = 129.8$

$\rho_{Avg} = (.10212)(.433)$

$= .04422$

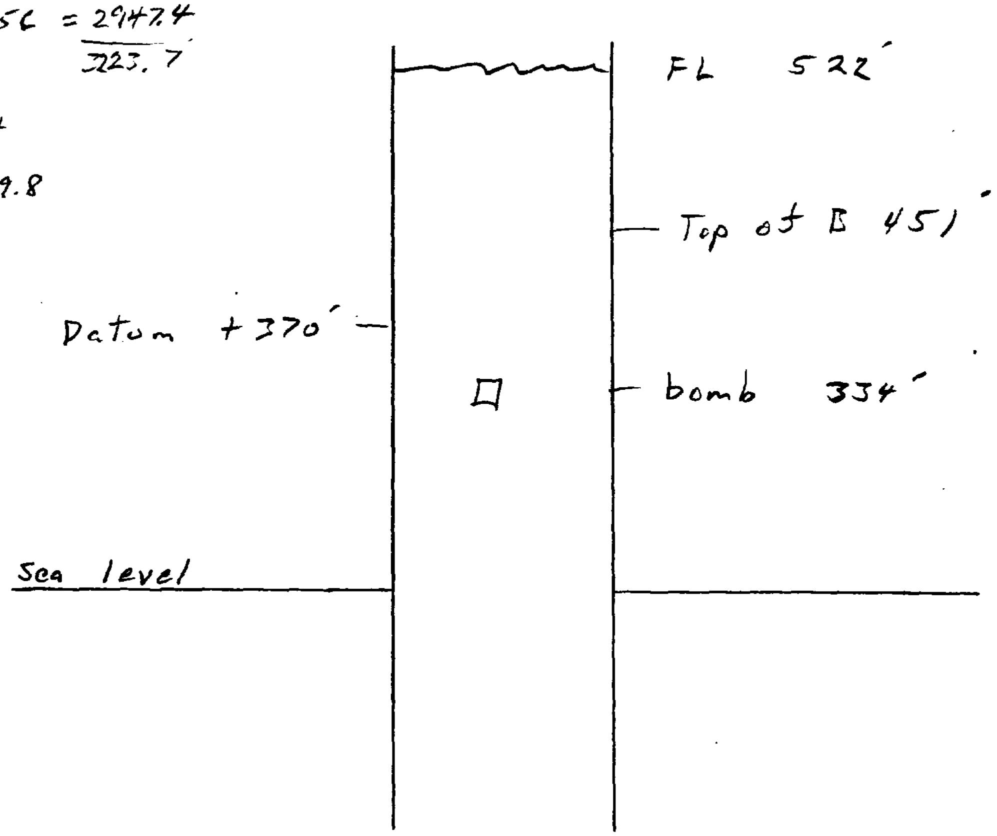

	KB		Subsea
Operator	Mobil		
Well	Ludrith B-37		
Elevation	7134		
Top of B Zone	6683		+451
Test Date		2/23/88	
Bomb Depth	6894		+240
Bomb Pressure, psig		774	
Fluid Level	6744		+390
~~Distance to Top of B Zone~~			
Wellbore Gradient			
Oil, psi/ft		.3 (390-240) = 45	
Gas, psi/ft		.03 (451-390) = 1.8	
Pressure at Top of B Zone		774-47 = 727	
Top of B Zone to +370 ft		81	
Production			
BO/D		188	
Mcf/D		816	
Volume Weighted Reservoir Density, psi/ft		0.04070	
dP to +370 ft		3.3	
Pressure at +370 ft datum		730.3	

$(188)(1.284) = 241.4$

$\left[816 - \frac{(188)(372)}{1000}\right] 3.928 = 2930.5$

3172

$(.7241)(241.4) = 174.8$

$(.04209)(2930.5) = 123.3$

$\rho_{AV} = .09399\ (433)$

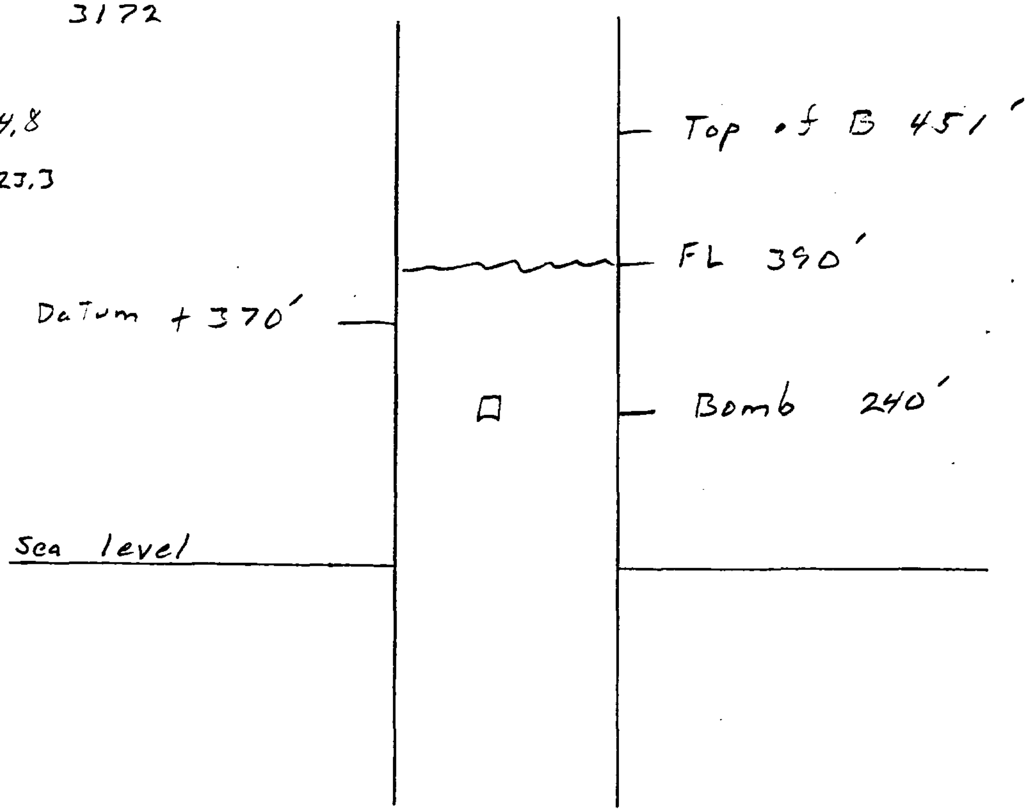

	KB		Subsea
Operator	Reading & Bates		
Well	Howard Federal 43-15		
Elevation	7269		
Top of B Zone	6799		+ 470
Test Date		6/30/87	
Bomb Depth	6802		+ 467
Bomb Pressure, psig		1045	
Fluid Level	None		
~~Distance to Top of B Zone~~			
Wellbore Gradient			
Oil, psi/ft			
Gas, psi/ft		.03	
Pressure at Top of B Zone		1045 - (.03)(2) = 1045	
Top of B Zone to +370 ft		100'	
Production			
BO/D		4.3	
Mcf/D		239	
Volume Weighted Reservoir Density, psi/ft		0.035	
dP to +370 ft		3.5	
Pressure at +370 ft datum		1048.5	

$(4.3)(1.327) = 5.7$

$\left[239 - \frac{(4.3)(466)}{1000}\right] 2.632 = 623.8$

629.5

$(.7125)(5.7) : 4.06$

$(.05978)(623.8) : 37.3$

$\rho_A = (.0657\ gm/cc)(0.433\ psi/ft) = 0.0284$

use 0.035 (wet gas)

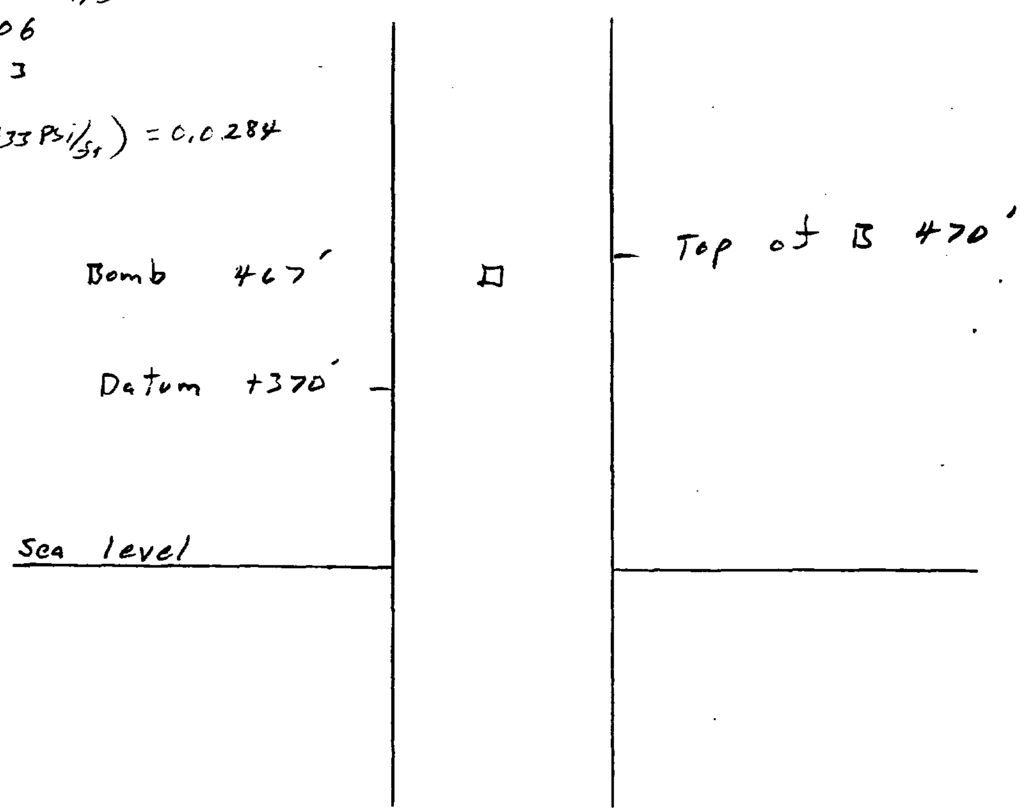

Operator	Reading + Bates		
Well	Howard Federal #3-15		
	KB		Subsea
Elevation	7269		
Top of B Zone	6799		+470
Test Date		11/19/87	
Bomb Depth	6512		+757
Bomb Pressure, psig		776	
Fluid Level			
~~Distance to Top of B Zone~~			
Wellbore Gradient			
Oil, psi/ft			
Gas, psi/ft		0.03 (757-470) =	
Pressure at Top of B Zone		776 + 8.6 = 784.6	
Top of B Zone to +370 ft		100	
Production			
BO/D		9.2	
Mcf/D		637	
Volume Weighted Reservoir Density, psi/ft		0.035	
dP to +370 ft		3.5	
Pressure at +370 ft datum		788.1	

$(9.2)(1.292) = 11.8$

$\left[637 - \frac{(9.2)(390)}{1000}\right] 3.6 = 2280$

$(.7210)(11.8) = 8.57$

$(.04526)(2280) = 103.2$

$(.437)(0.04877) = 0.02112$

use 0.035

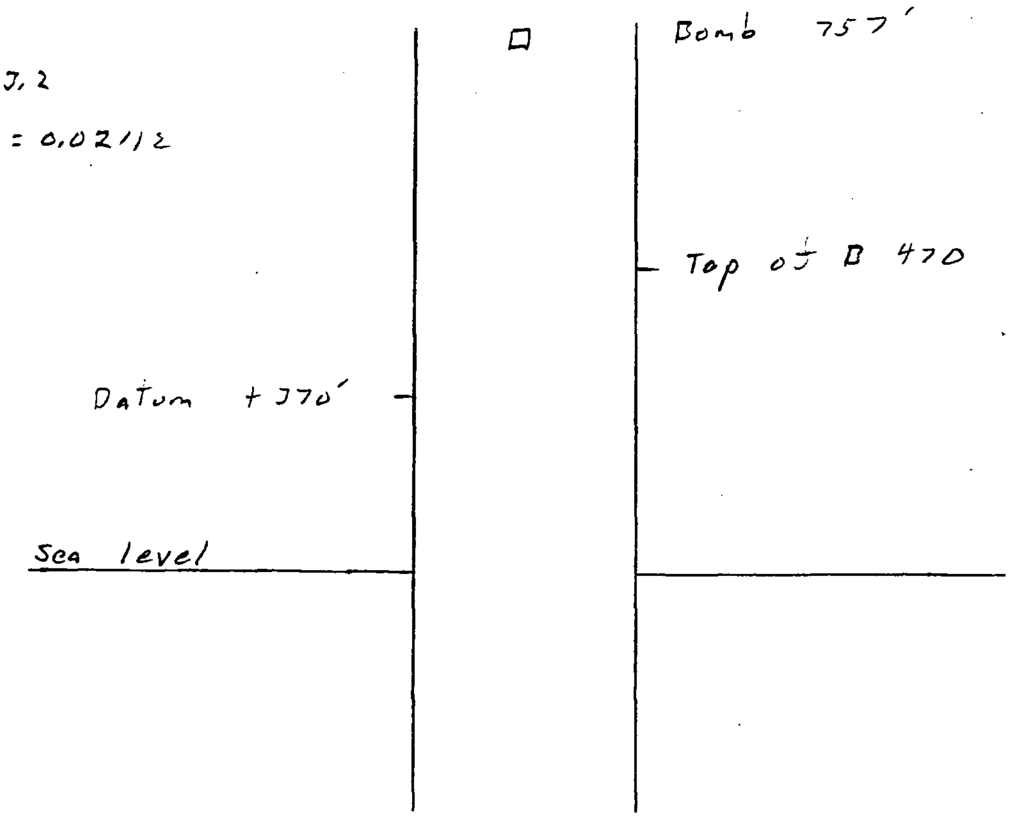

	KB		Subsea
Operator	Reading & Bates		
Well	Howard Federal 43-15		
Elevation	7269		
Top of B Zone	6799		+470
Test Date		2/23/88	
Bomb Depth	6512		+757
Bomb Pressure, psig		739	
Fluid Level	None		
~~Distance to Top of B Zone~~			
Wellbore Gradient			
Oil, psi/ft			
Gas, psi/ft		.03 (470 - 757)	
Pressure at Top of B Zone		739 + 8.6 = 747.6	
Top of B Zone to +370 ft		100	
Production			
BO/D		3.6	
Mcf/D		240	
Volume Weighted Reservoir Density, psi/ft		0.035	
dP to +370 ft		3.5	
Pressure at +370 ft datum		751.1	

$(3.6)\,(1.288) = 4.63$

$\left[240 - \frac{(3.6)(380)}{1000}\right] 3.792 = 904.9$

909.5

$(.7229)(4.63) = 3.35$

$(.0\cancel{43344})(904.9) = 39.2$

$\rho_A = (.04681)(.433) = 0.02027$

use wet gas 0.035

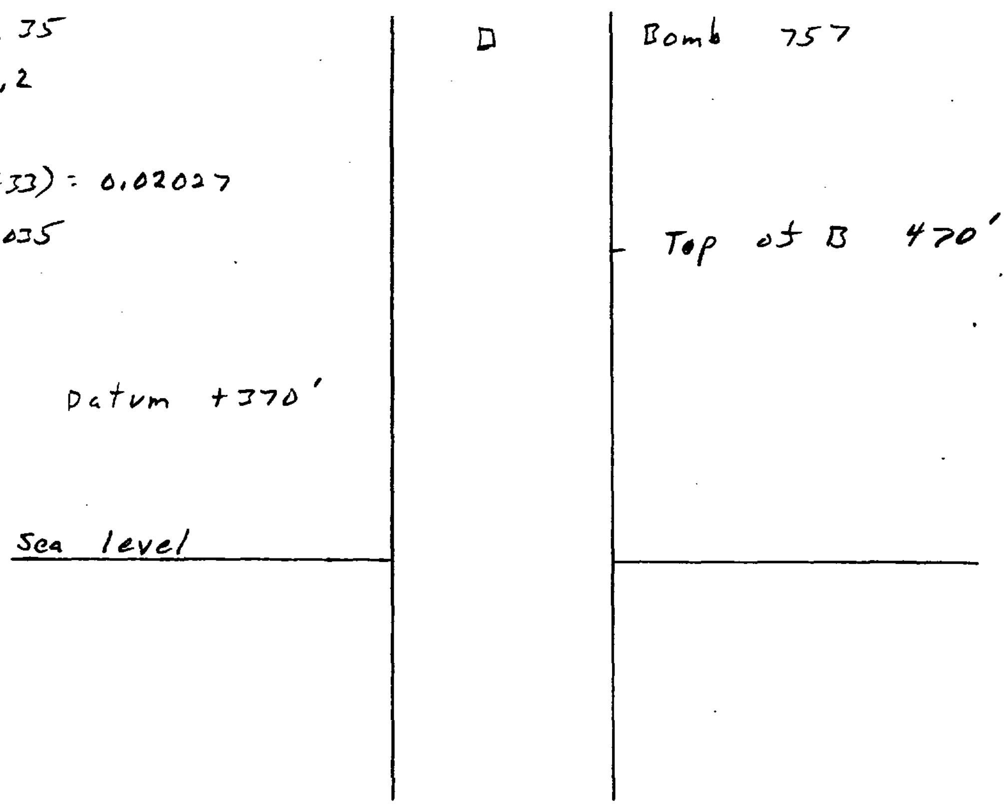

	KB		Subsea
Operator	Sun		
Well	Boyt & Lola #1		
Elevation	7351		
Top of B Zone	6848		+ 503
Test Date		6/30/87	
Bomb Depth	7000		+ 351
Bomb Pressure, psig		853	
Fluid Level			+ 363
~~Distance to Top of B Zone~~			
Wellbore Gradient			
Oil, psi/ft		0.3	
Gas, psi/ft		0.03	
Pressure at Top of B Zone		845	
Top of B Zone to +370 ft — 133'			
Production			
BO/D		1.8	
Mcf/D		9.7	
Volume Weighted Reservoir Density, psi/ft		.04210	
dP to +370 ft		5.6	
Pressure at +370 ft datum		850.6	

$(0.3)(363-351) = 3.6$
$(.03)(503-363) = 4.2$ } 7.8

853
$-\ 8$
845

$(1.8)(1.301) = 2.3$

$\left[9.7 - \frac{(1.8)\,409}{1000}\right] 3.309 = 29.6$

32.03

$(.7183)(2.3) = 1.68$

$(.04848)(29.6) = 1.43$

$(.433)(.0973) = .04210$

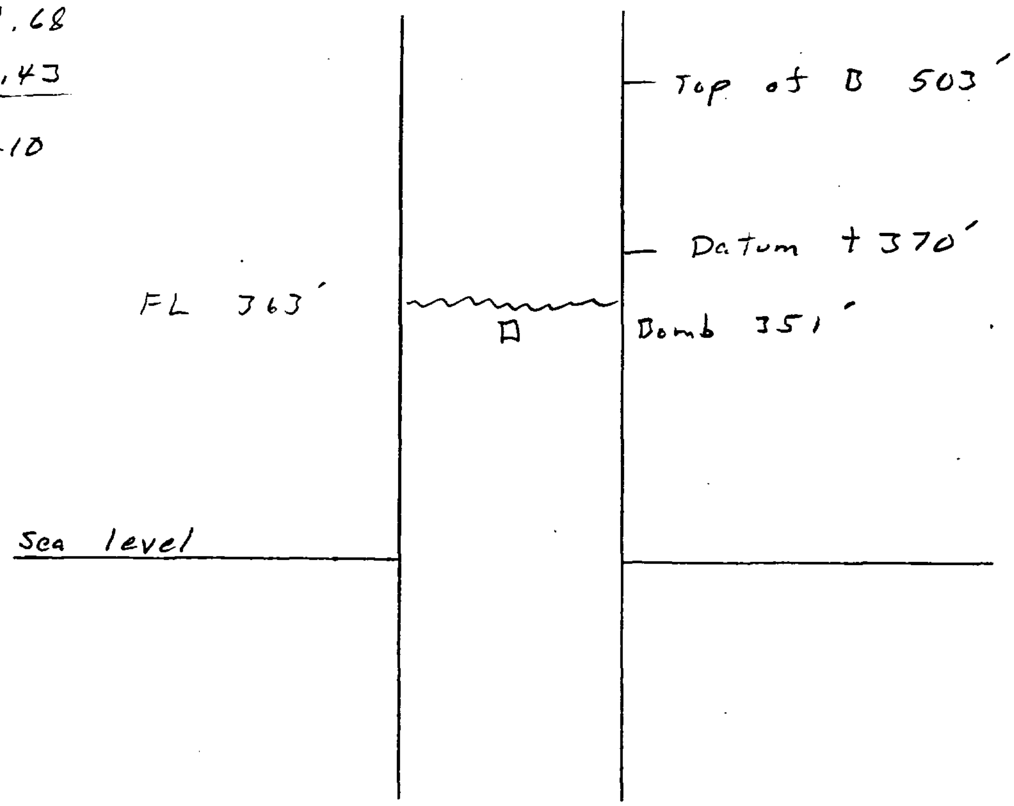

	KB		Subsea
Operator	Sun		
Well	Boyt + Lola #1		
	KB		Subsea
Elevation	7351		
Top of B Zone	6848		+503
Test Date		11/19/87	
Bomb Depth	7060		+351
Bomb Pressure, psig		762	
Fluid Level			+571
Distance to Top of B Zone			
Wellbore Gradient			
Oil, psi/ft		.3(503-351) = 45.6	
Gas, psi/ft			
Pressure at Top of B Zone	762 - 46	716.4	
Top of B Zone to +370 ft	133'		
Production			
BO/D		1.8	
Mcf/D		9.7	
Volume Weighted Reservoir Density, psi/ft		0.04241	
dP to +370 ft		5.6	
Pressure at +370 ft datum		722.0	

$(1.8)(1.315) = 2.4$

$\left[9.7 - \frac{(1.8)(440)}{1000}\right] 29 = 25.8$

28.2

$(.7146)(2.4) = 1.69$

$(.04155)(25.8) = 1.07$

$(.433)(.09794) = .04241$

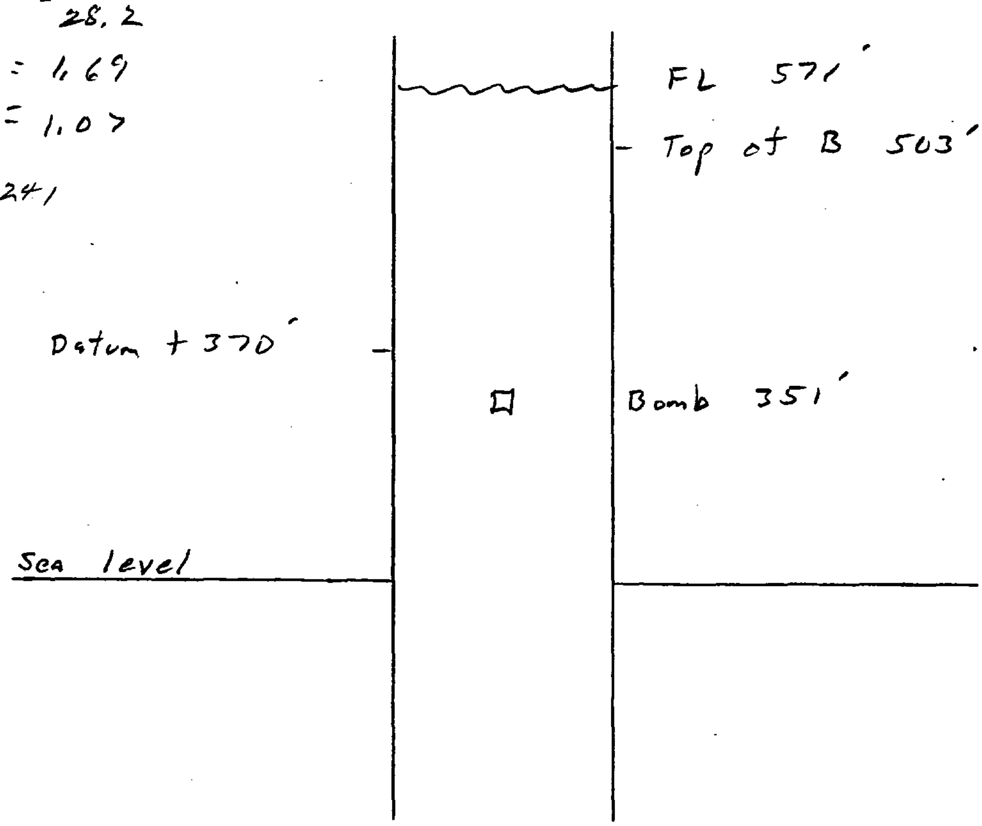

	KB		Subsea
Operator	Sun		
Well	Boyt + Lola #1		
Elevation	7351		
Top of B Zone	6848		+ 503
Test Date		2/23/88	
Bomb Depth	7000		+ 351
Bomb Pressure, psig		790	
Fluid Level			+ 561
~~Distance to Top of B Zone~~			
Wellbore Gradient			
Oil, psi/ft		(0.3)(503-351) = 45.6	
Gas, psi/ft			
Pressure at Top of B Zone	790 - 45.6	= 744.4	
Top of B Zone to +370 ft	133'		
Production			
BO/D		1.8	
Mcf/D		9.7	
Volume Weighted Reservoir Density, psi/ft		.03727	
dP to +370 ft		5.0	
Pressure at +370 ft datum		749.4	

$(1.8)(1.288) = 2.3$

$\left[9.7 - \frac{(1.8)(380)}{1000}\right] 3.792 = 34.2$

$(.7229)(2.3) = 1.67$

$(.04302)(34.2) = 1.47$

$(433)(.08606) = .03727$

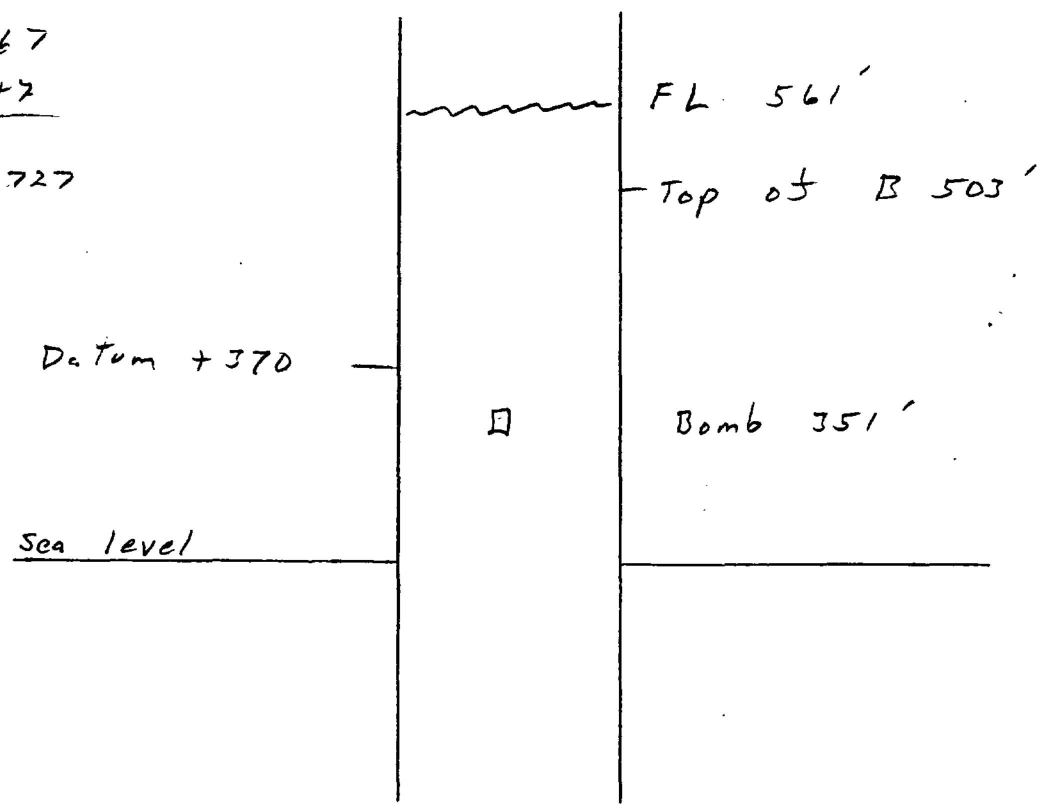

Operator	Sun		
Well	High Adventure #1		
	KB		Subsea
Elevation	7332		
Top of B Zone	7150		+ 182
Test Date		6/30/87	
Bomb Depth	7310		+ 22
Bomb Pressure, psig		1164	
Fluid Level	7102		+ 230
Wellbore Gradient			
Oil, psi/ft	0.3 (182-22)		48
Gas, psi/ft			
Pressure at Top of B Zone	1164-48	= 1116	
Top of B Zone to +370 ft	188'		
Production			
BO/D		225	GOR
Mcf/D		604	2684
Volume Weighted Reservoir Density, psi/ft		.07474	
dP to +370 ft		14.1	
Pressure at +370 ft datum		1101.9	

$(225)(1.334) = 300.2$

$\left[604 - \frac{(225)(482)}{1000}\right] 2.46 = \frac{1485.8}{1786}$

$(.7110)(300.2) = 213.4$

$(.063860)(1485.8) = 94.9$

$(.433)(.1720) = 0.07474$

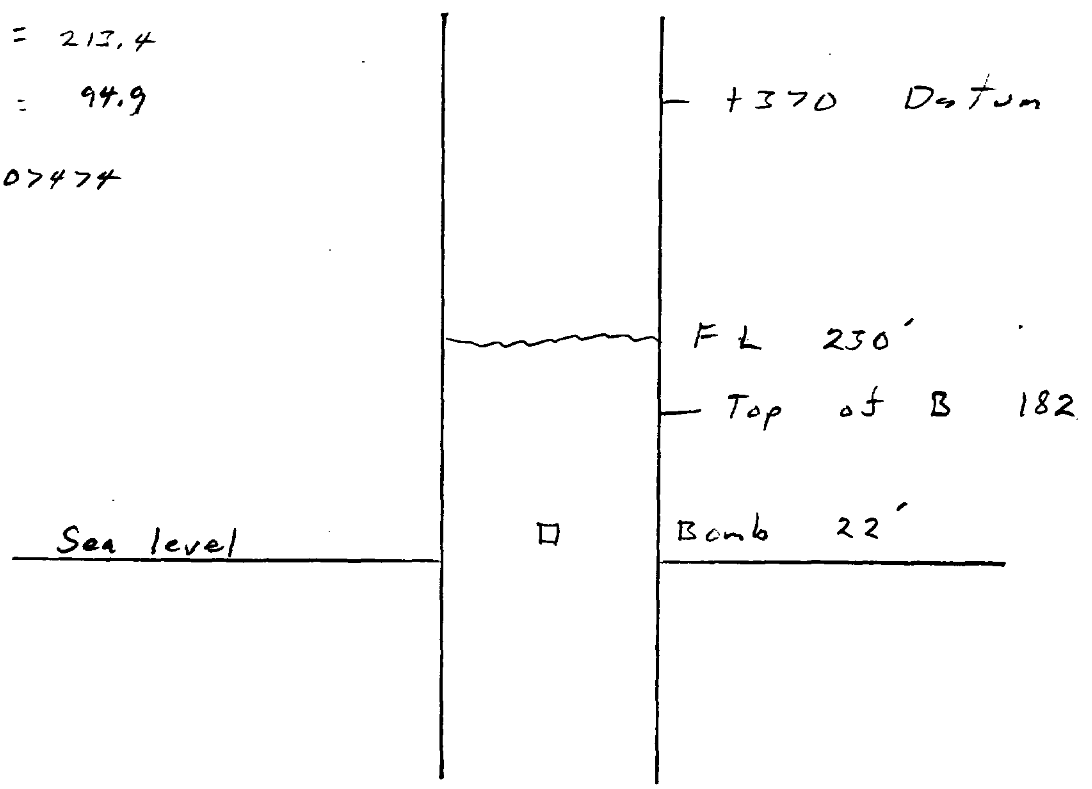

	KB		Subsea
Operator	Sun		
Well	High Adventure #1		
Elevation	7332		
Top of B Zone	7150		+182
Test Date		11/19/87	
Bomb Depth	7400		-68
Bomb Pressure, psig		911	
Fluid Level			+210'
Wellbore Gradient			
Oil, psi/ft	(.3)(-68-182)		-75
Gas, psi/ft			
Pressure at Top of B Zone		836	
Top of B Zone to +370 ft	188		
Production			
BO/D		228	
Mcf/D		689	
Volume Weighted Reservoir Density, psi/ft		0.05798	
dP to +370 ft		10.9	
Pressure at +370 ft datum		825.1	

(228)(1.30) = 296.4

$\left[689 - \frac{228(405)}{1000}\right] 3.385 = 2019.6$

(.719)(296.4) = 213.1

(.04805)(2019.6) = 97.0

(.433)(.1339) = .05798

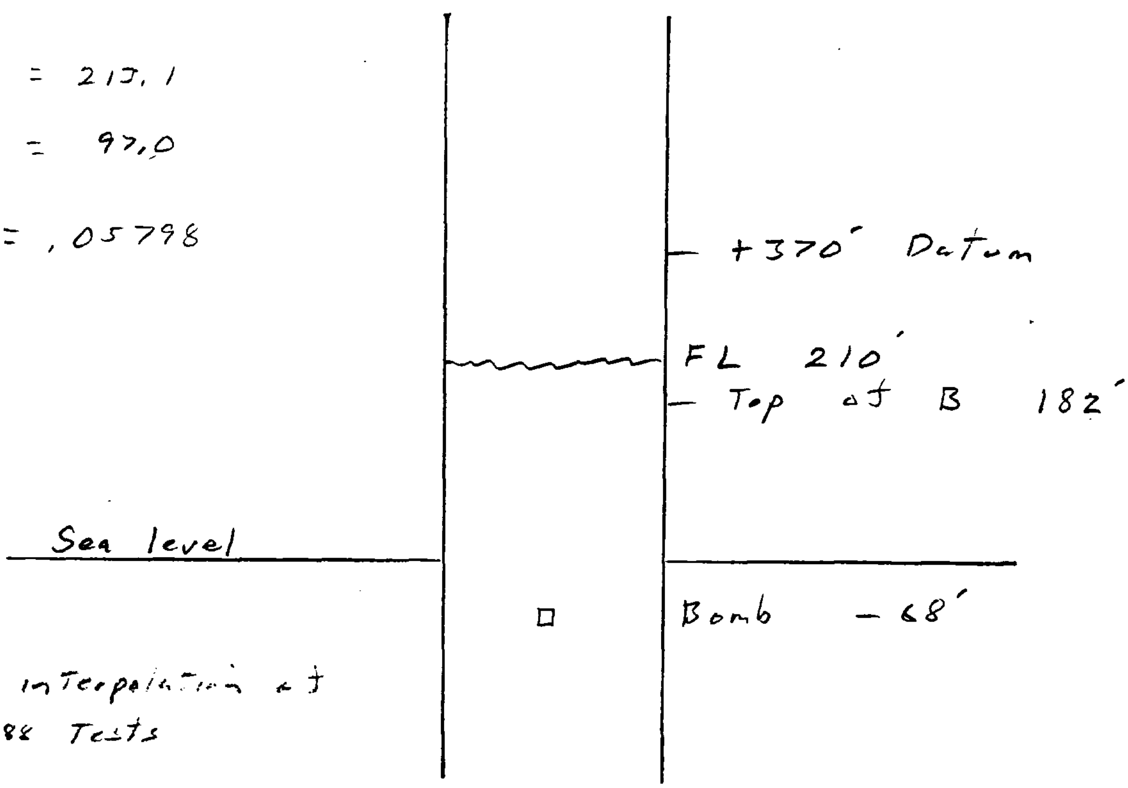

Fluid level by interpolation of 6/30/87 + 11/19/88 Tests

$\frac{1116 - 785}{911 - 785} = \frac{230 - 197}{FL_{11/19} - 197}$

FL = 210'

Operator	Sun		
Well	High Adventure #1		
	KB		Subsea
Elevation	7332		
Top of B Zone	7150		+182
Test Date		2/23/88	
Bomb Depth	7400		−68
Bomb Pressure, psig		860	
Fluid Level	7135		+197
Wellbore Gradient			
Oil, psi/ft	(.3)(−68−182)		−75
Gas, psi/ft			
Pressure at Top of B Zone		785	
Top of B Zone to +370 ft	188'		
Production			
BO/D		269	GOR
Mcf/D		584	2171
Volume Weighted Reservoir Density, psi/ft		0.07269	
dP to +370 ft		13.7	
Pressure at +370 ft datum		771.3	

$(269)(1.292) = 347.5$

$\left[584 - \frac{269(390)}{1000}\right] 3.6 = 1724.7$

$(.7210)(347.5) = 250.5$

$(.05647)(1724.7) = 97.4$

$(.433)(.16789) = 0.07269$

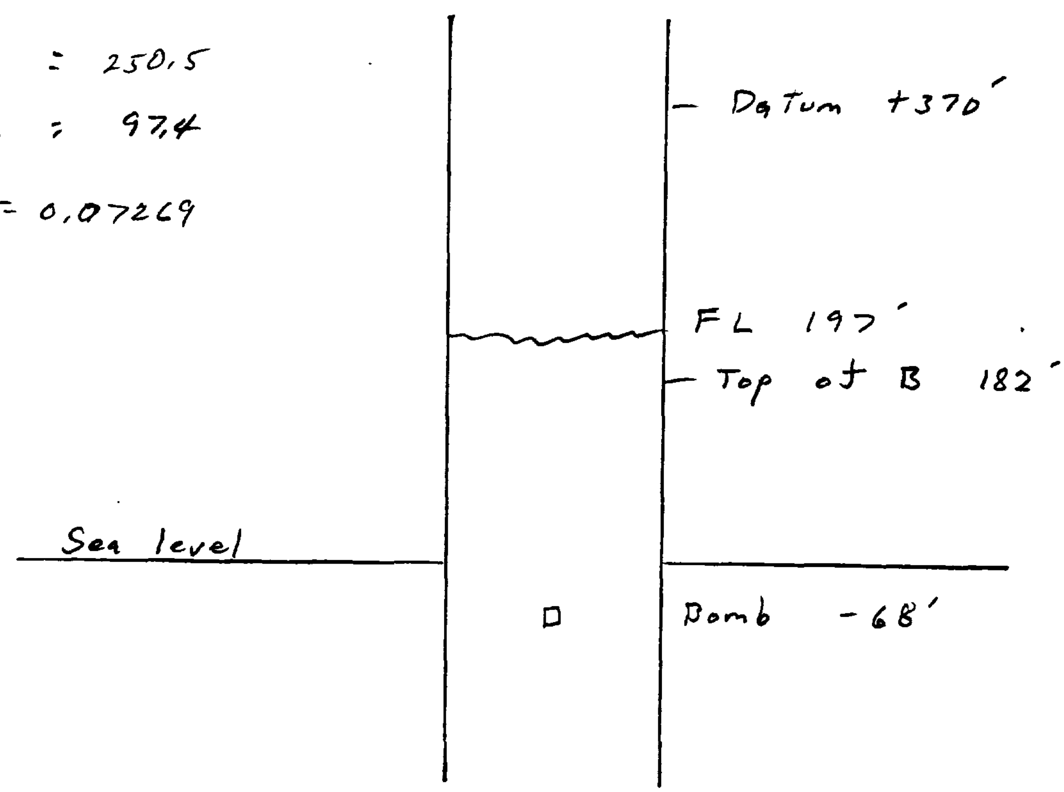

	KB		Subsea
Operator	Sun		
Well	Loddy #1		
Elevation	7167		
Top of B Zone	6927		+ 240
Test Date		6/30/87	
Bomb Depth	7100		+ 67
Bomb Pressure, psig		1140	
Fluid Level	6962		+ 205
Wellbore Gradient			
Oil, psi/ft	(.3)(205-67)		41.4
Gas, psi/ft	(.03)(240-205)		1.1
Pressure at Top of B Zone		1097.5	
Top of B Zone to +370 ft	130'		
Production			
BO/D		61	
Mcf/D		433	
Volume Weighted Reservoir Density, psi/ft		.04819	
dP to +370 ft		6.3	
Pressure at +370 ft datum		1091.2	

(61) (1.333) = 81.3

$$\left[433 - \frac{(61)(480)}{1000}\right] 2.497 = 1008.1$$

(.7113) (81.3) = 57.8

(.062944) (1008.1) = 63.5

(.433) (.1113) = .04819

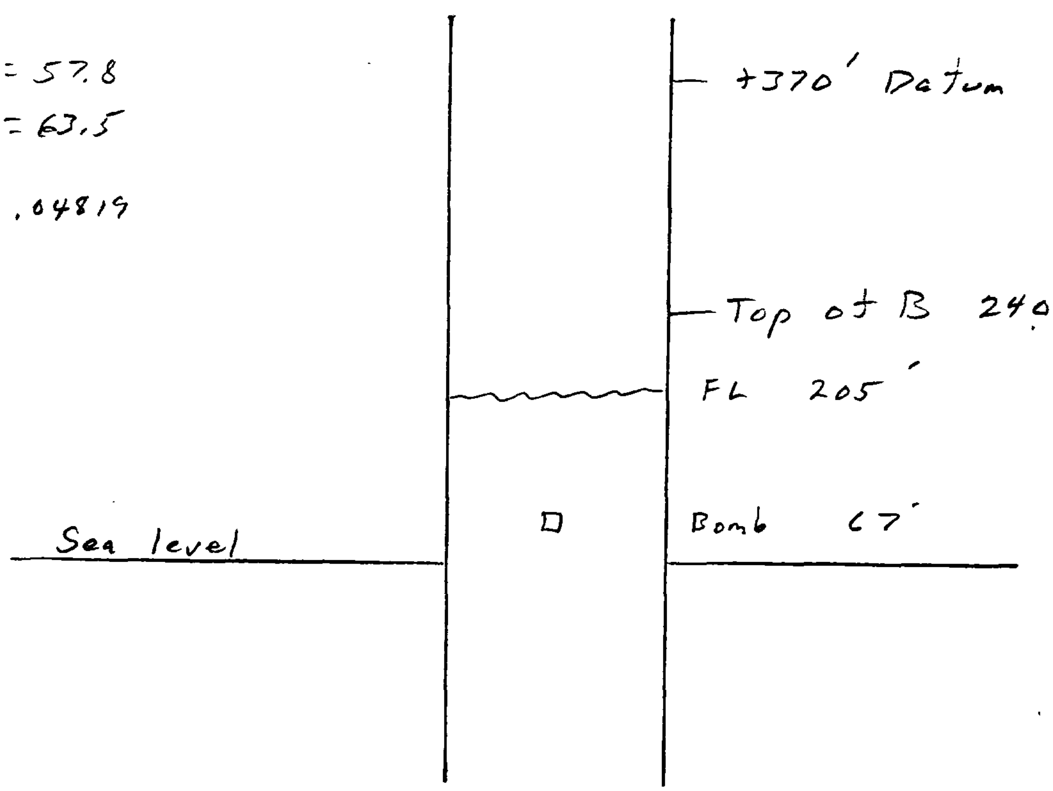

Operator	Sun	
Well	Loddy #1	
	KB	Subsea
Elevation	7167	
Top of B Zone	6927	+240
Test Date	11/19/87	
Bomb Depth	7100	+67
Bomb Pressure, psig	902	
Fluid Level		+182
Wellbore Gradient		
Oil, psi/ft	(.3)(182-67)	34.5
Gas, psi/ft	(.03)(240-182)	1.7
Pressure at Top of B Zone	866.8	
Top of B Zone to +370 ft	130	
Production		
BO/D	58	
Mcf/D	338	
Volume Weighted Reservoir Density, psi/ft	0.4187	
dP to +370 ft	5.4	
Pressure at +370 ft datum	861.4	

$(58)(1.303) = 77.1$

$\left[338 - \frac{(58)(412)}{1000}\right] 3.25 = 1020.8$

$(.7178)(77.1) = 55.4$

$(.049729)(1020.8) = 50.8$

$(.433)(.09670) = 0.4187$

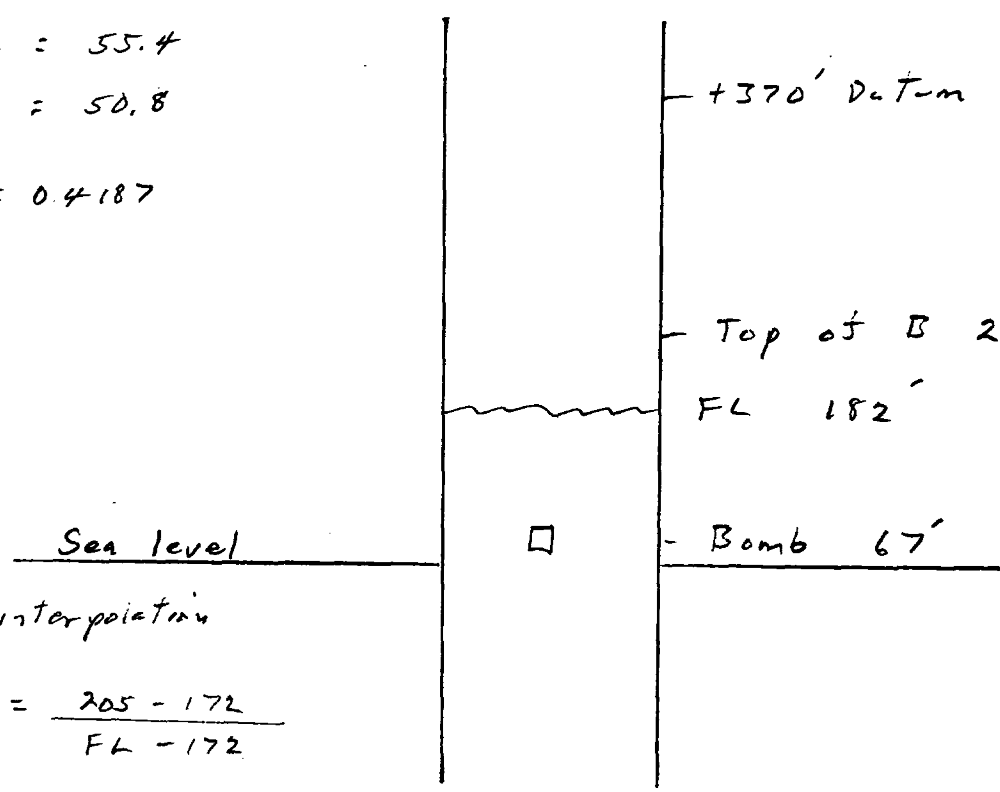

Fluid level by interpolation

$$\frac{1097.5 - 812.5}{902 - 812.5} = \frac{205 - 172}{FL - 172}$$

$FL = 182$

	KB		Subsea
Operator	Sun		
Well	Loddy #1		
Elevation	7167		
Top of B Zone	6927		+240
Test Date		2/23/88	
Bomb Depth	7100		+67
Bomb Pressure, psig		84.6	
Fluid Level			+ 172
Wellbore Gradient			
Oil, psi/ft	(.3)(172-67)		31.5
Gas, psi/ft	(.03)(240-172)		2.04
Pressure at Top of B Zone		812.5	
Top of B Zone to +370 ft	130		
Production			
BO/D		52	
Mcf/D		369	
Volume Weighted Reservoir Density, psi/ft		.03569	
dP to +370 ft		4.6	
Pressure at +370 ft datum		867.8	

$(52)(1.295) = 67.3$

$\left[369 - \frac{(52)(399)}{1000}\right] 3.46 = 1205.0$

$(.7200)(67.3) = 48.5$

$(.04679)(1205) = 56.4$

$(.433)(0.08243) = 0.03569$

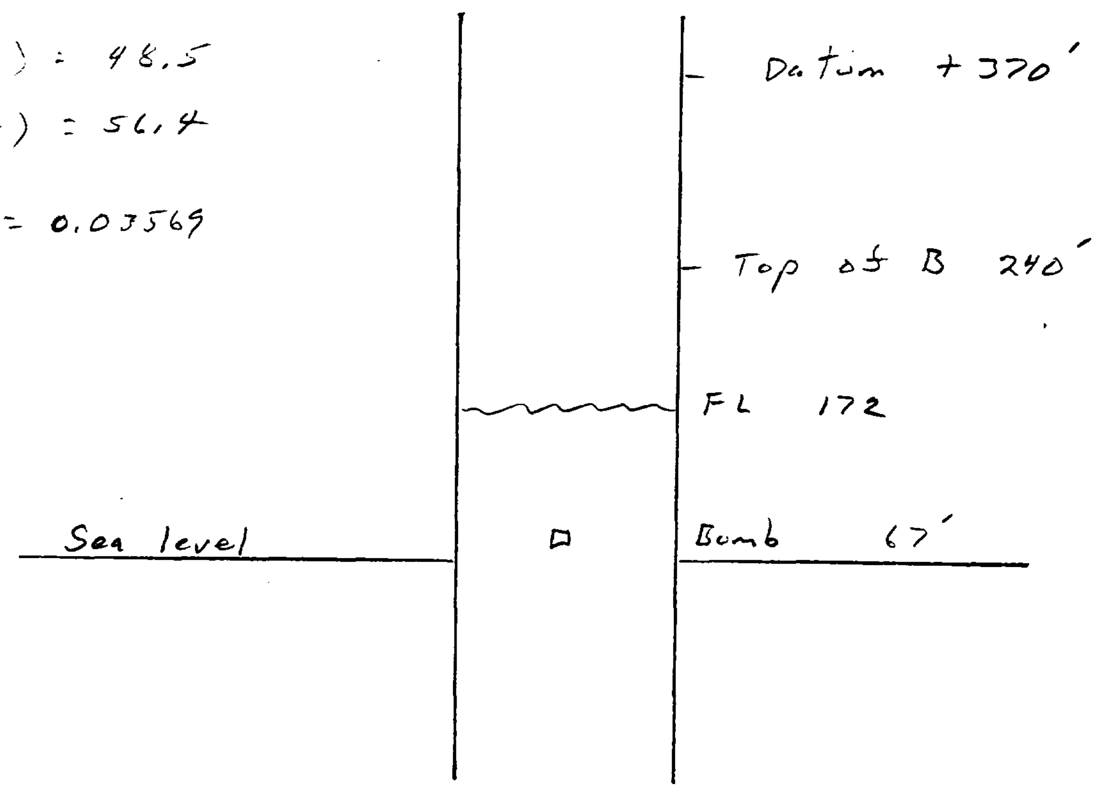

	KB		Subsea
Operator	Sun		
Well	Wildfire #1		
Elevation	7727		
Top of B Zone	7408		+ 319
Test Date		6/30/87	
Bomb Depth	7600		+ 127
Bomb Pressure, psig		1263	
Fluid Level	7120		+ 607
Wellbore Gradient			
Oil, psi/ft	(.3)(319-127)		57.6
Gas, psi/ft			
Pressure at Top of B Zone		1205.4	
Top of B Zone to +370 ft	51		
Production			
BO/D		Not Produced	
Mcf/D			
Volume Weighted Reservoir Density, psi/ft		.035	
dP to +370 ft		1.8	
Pressure at +370 ft datum		1203.6	

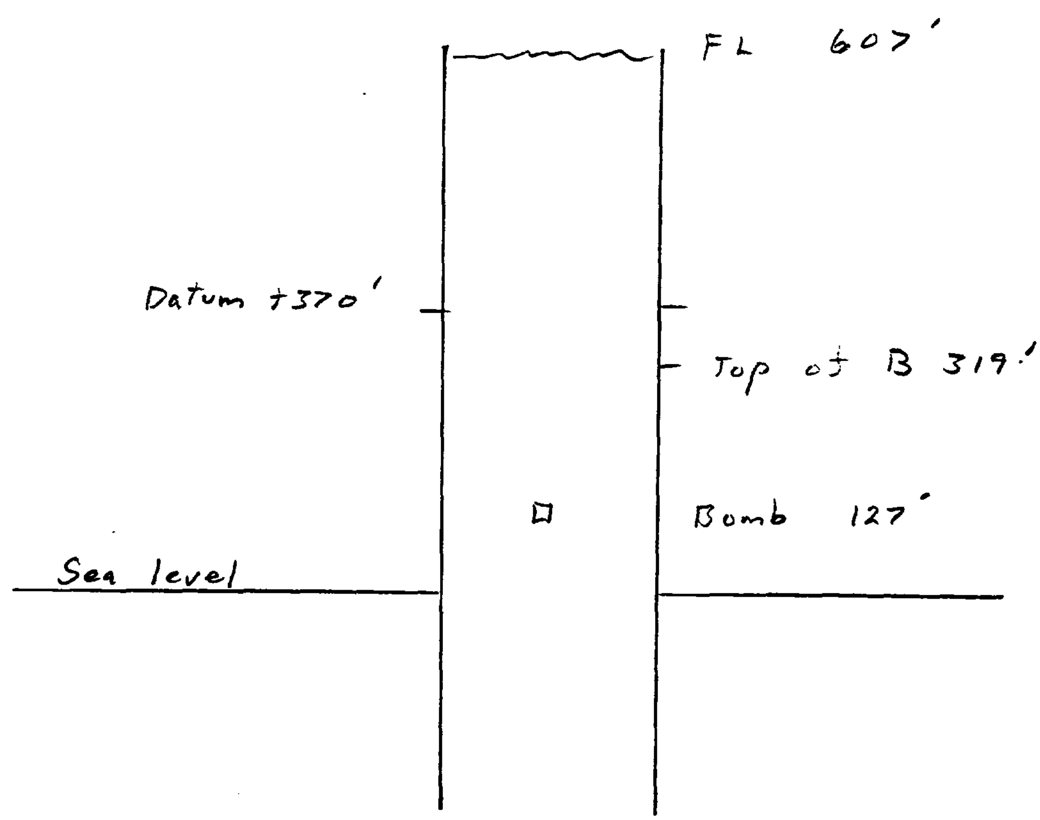

	KB		Subsea
Operator	Sun		
Well	Wildfire #1		
Elevation	7727		
Top of B Zone	7408		+319
Test Date		11/19/87	
Bomb Depth	7400		+327
Bomb Pressure, psig		1028	
Fluid Level	7252		+475
Wellbore Gradient			
Oil, psi/ft	(.3)(327-319)		2.4
Gas, psi/ft			
Pressure at Top of B Zone		1030.4	
Top of B Zone to +370 ft	51		
Production			
BO/D		Not Produced	
Mcf/D			
Volume Weighted Reservoir Density, psi/ft		0.035	
dP to +370 ft		1.8	
Pressure at +370 ft datum		1028.6	

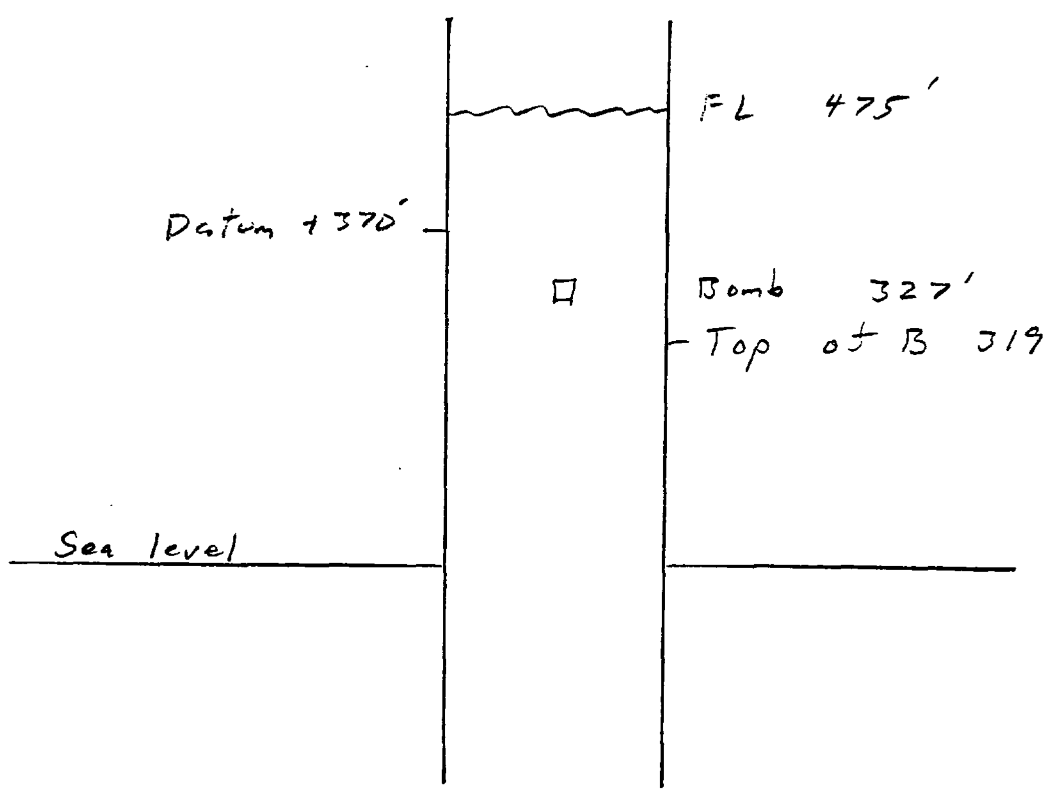

	KB		Subsea
Operator	Son		
Well	Wildfire #1		
Elevation	7727		
Top of B Zone	7408		+319
Test Date		2/23/86	
Bomb Depth	7400		+327
Bomb Pressure, psig		972	
Fluid Level	7205		+522
Wellbore Gradient			
Oil, psi/ft	.3(327-319)		2.4
Gas, psi/ft			
Pressure at Top of B Zone		974	
Top of B Zone to +370 ft	51		
Production			
BO/D		Not Produced	
Mcf/D			
Volume Weighted Reservoir Density, psi/ft		0.035	
dP to +370 ft		1.8	
Pressure at +370 ft datum		972.2	

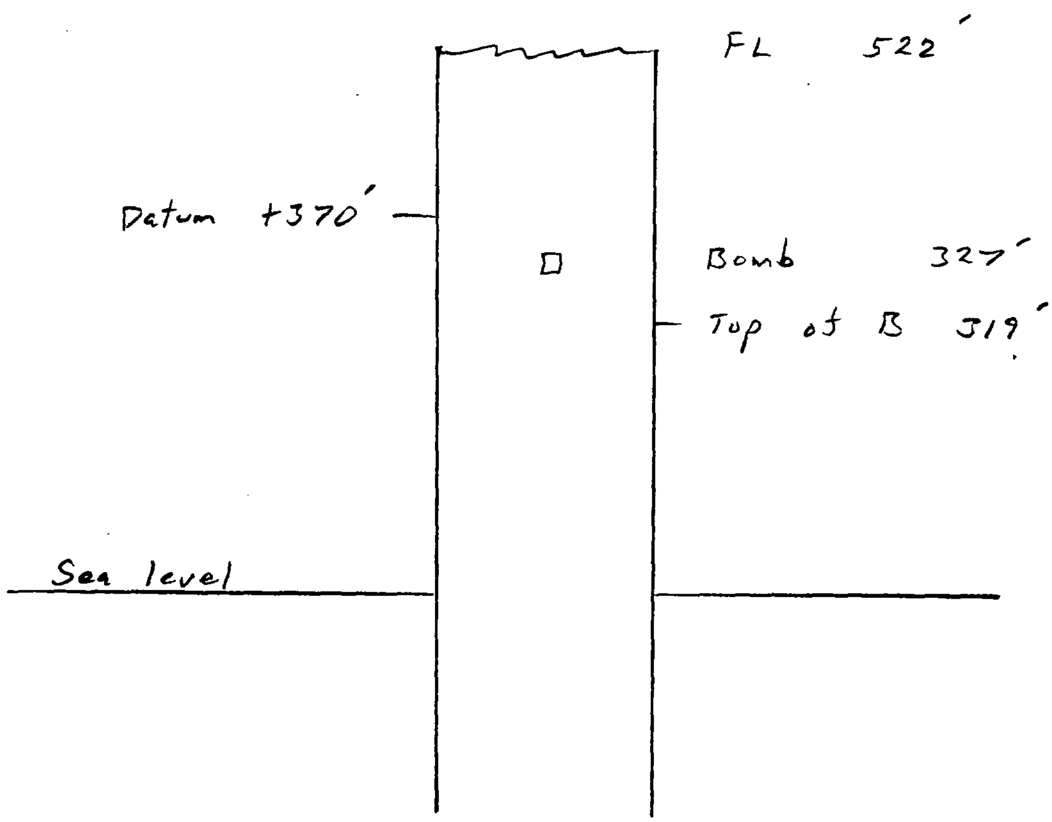

APPENDIX 2

Pressure Buildup Worksheets

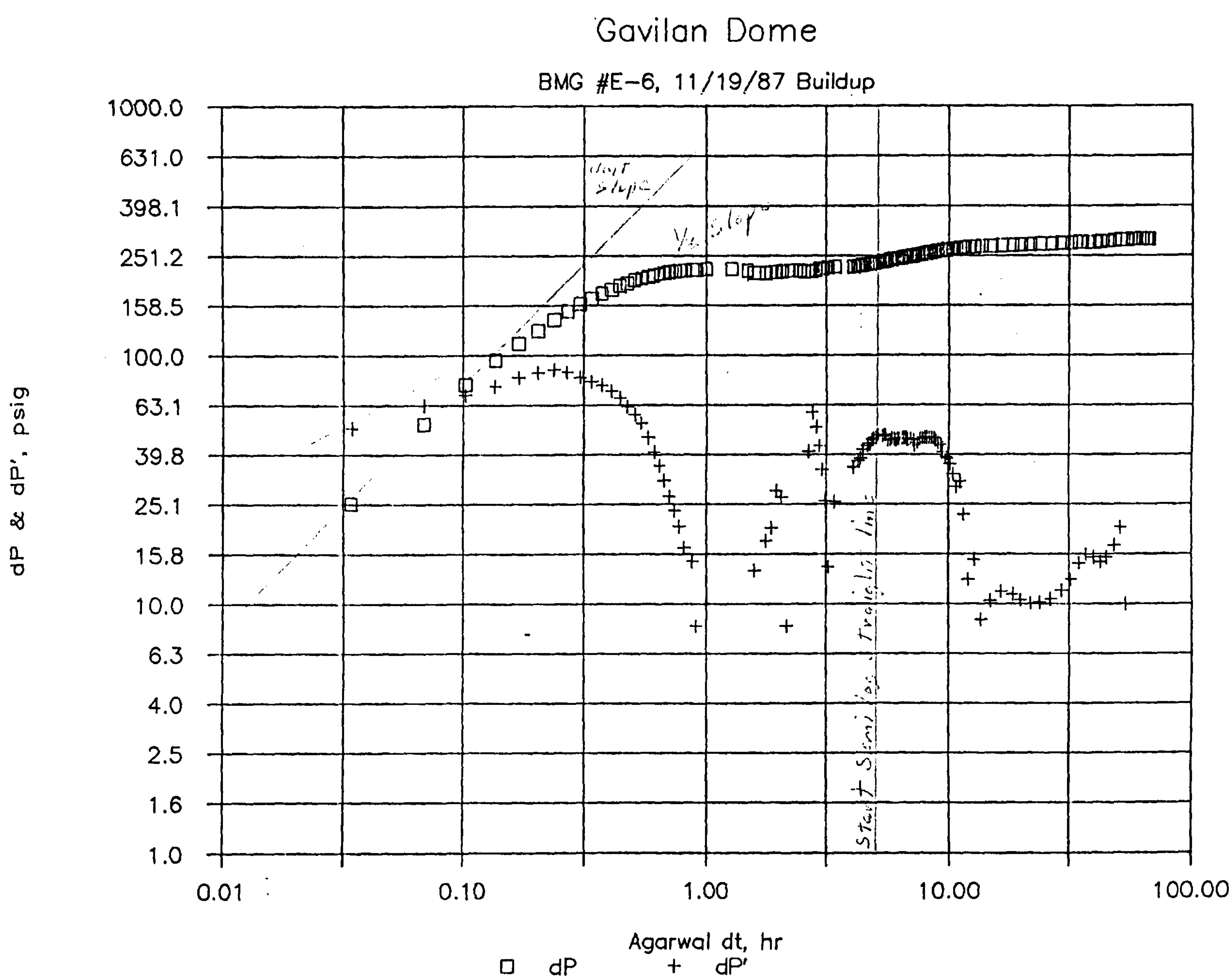

Gavilan Dome
BMG #E-6, 11/19/87 Buildup
1000.0
631.0
398.1
251.2
158.5
100.0
63.1
39.8
25.1
15.8
10.0
6.3
4.0
2.5
1.6
1.0
dP & dP', psig
0.01
0.10
1.00
10.00
100.00
Agarwal dt, hr
□ dP
+ dP'
Start Semi log straight line

Gavilan Dome, 11/19/87 Buildup
BMG, E-6, q = 281 B/D GOR = 4500

Initial work
From Standings Correlations
GOR = 4000
$\beta = 11,0$
$q_o = 281$
$m = 36.05$

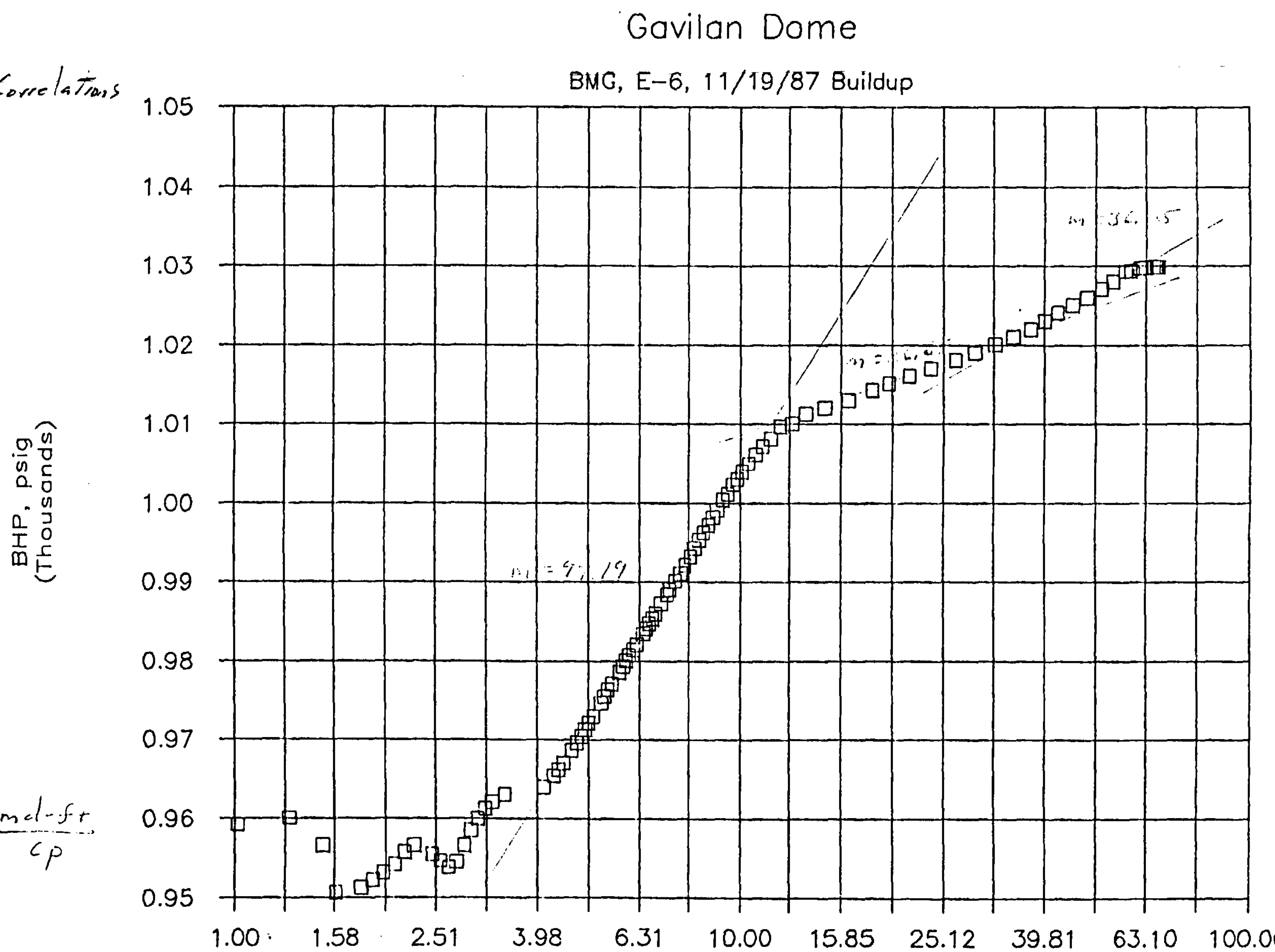

$$\frac{kh}{\mu} = \frac{162.6\, q_o \beta}{m}$$

$$\frac{kh}{\mu} = 13,942 \ \frac{md\text{-}ft}{cp}$$

Using q_{Rt} concept

$$q_{Rt} = q_o B_o + \left(q_g - \frac{q_o R_s}{1000}\right) B_g + q_w B_w$$

$$\frac{kh}{\mu} = 14,156$$

From Loddy PVT
$B_g = 2.778 \ RB/mcf$
$R_s = 452$

$B_o = 1.242$
$q_g = 4000 \times 281$

$B_g = 5.04 \times 10^{-3} \frac{TZ}{P}$
$q_{Rt} = 3179$ RB

Initial Work

E-6 $q_o = 281$ B/D GOR = 4296 $q_g = 1207$ Mcf/D

Boundry Dominated Flow. Therefore use Flow Regime 1 (doesn't work on 4/24)
for analyses $m = 99.19$ Max pressure = 1030 psig

Transform gas flow rate to RB

$$\left(q_g - \frac{q_o R_s}{1000}\right) B_g$$

where q_g, Mscf/D
R_s; scf/bbl
B_g, RB/Mscf

$$\left[1207 - \frac{(281)(466)}{1000}\right] 2.632 = 2832 \text{ RB/D}$$

Total flowrate $= (281)(1.327) + 2832$
$= 3205$ RB/Day

$$\lambda h_t = \frac{(162.6)\, q_{Rt}}{m} = 5254 \frac{\text{md}\cdot\text{ft}}{\text{cp}} \quad (m = 99.19 \text{ psi/cycle})$$

Flow Regime #1

if $m = 36.05$ last slope

$$\lambda h_t = 14{,}456 \frac{\text{md}\cdot\text{ft}}{\text{cp}} = \left(14{,}456 \frac{\text{md}\cdot\text{ft}}{\text{cp}}\right)(.0831 \text{ cp}) = 1200 \text{ md}\cdot\text{ft}$$

Average viscosity $(1.327)(281 \text{ BO/D})(.605) = 255.6 \frac{\text{RB}\cdot\text{cp}}{\text{D}}$
$+ (2832 \text{ RBG/D})(.0143) = 40.5 \frac{\text{RB}\cdot\text{cp}}{\text{D}}$

3204 RB/D $\quad$ 266.1 $\frac{\text{RB}\cdot\text{cp}}{\text{D}}$

$$\frac{266.1 \frac{\text{RB}\cdot\text{cp}}{\text{D}}}{3204 \text{ RB}} = 0.0831 \text{ cp}$$

Average Rate, STB/D
$(1,076)(2.632) = 2832$ STB/D
$+ 281(1.327) = 373$ STB/D
3205 STB/D

Average FVF $\frac{3205}{[illegible]} = 2.361$

4/14/86

②

doesn't work with $m = 99.19$ psi/cy

$$Kh_{absolute} = \left(5254 \frac{md \cdot ft}{cp}\right)(.0831\ cp) = \cancel{1200}\ 437\ md \cdot ft$$

$$K_o h = \frac{(162.6)(281)(1.327)(.605)}{36.05} = 1018\ md \cdot ft$$

$$K_g h = \frac{(162.6)(2832)(\quad)(0.0143)}{36.05} = 783\ md \cdot ft$$

BMG E-6 11/19/87 Buildup Last effort 4/15/cc

(3)

10 hr → 55 hr Agarwal Time (Averaged slope)

cc = 99.5%, Intercept = 977.9 psig slope = 28.44

$$\frac{Kh}{\mu}_{absolute} = \frac{162.6\, q_{B}\, R_t}{m} = \frac{(162.6)(3205)}{28.44} = 18324 \ \frac{md.ft}{cp}$$

$$Kh_{absolute} = \left(18324 \ \frac{md.ft}{cp}\right)(0.0831\, cp) = 1523 \ md.ft$$

$$K_o h = \frac{(162.6)(281)(1.327)(.605)}{28.44} = 1290 \ md.ft$$

$$K_g h = \frac{(162.6)(2832)(0.0143)}{28.44} = 232 \ md.ft$$

Gavilan Dome,. Buildup

BMG B-32, 11/19/87

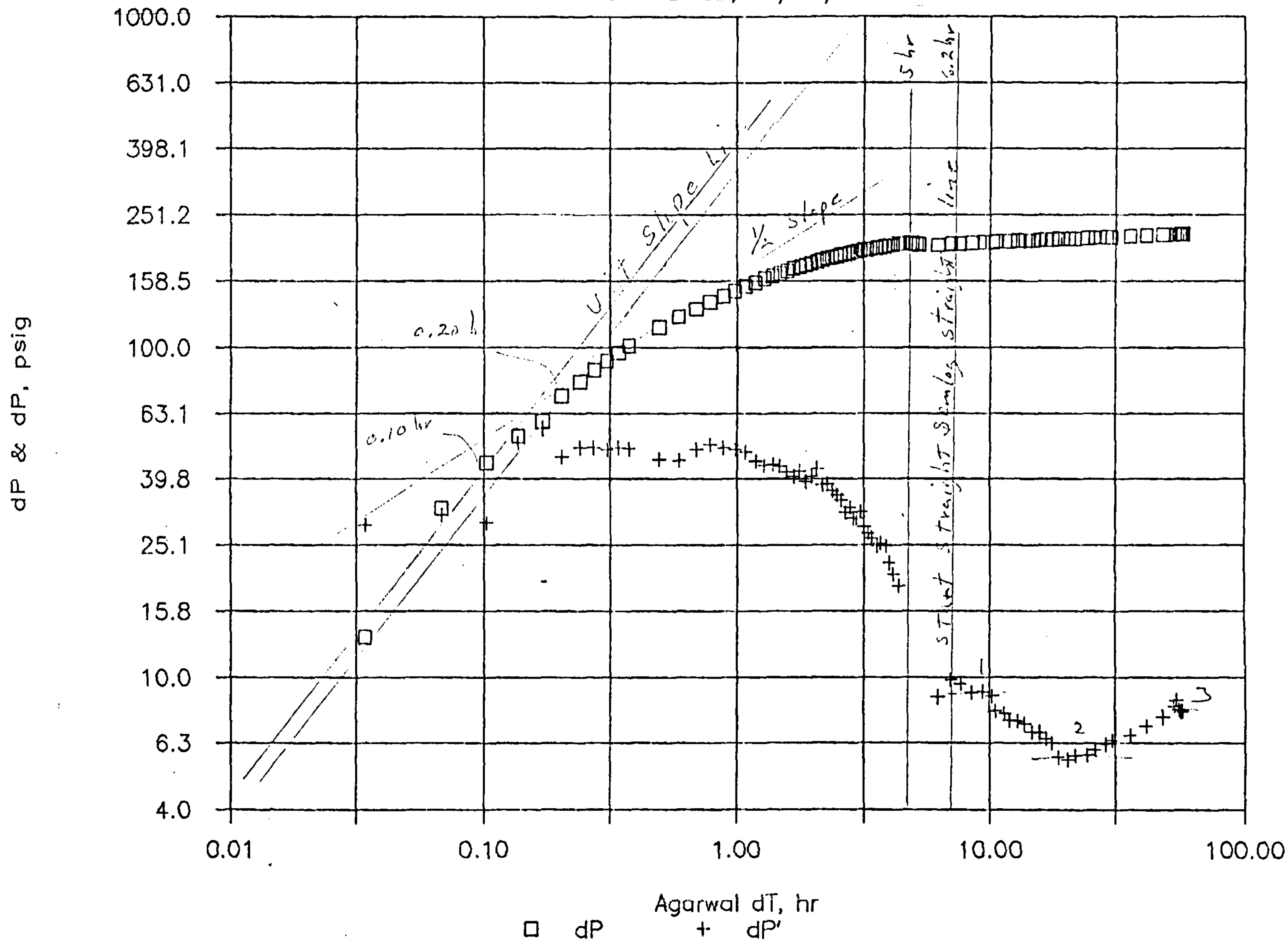

4/13/88 wwc

From Loddy #1
PVT data @ 1000psig
GOR = 1200
$\beta = 1.242$
$q = 719$ BOPD
$m = 19.18$

$\frac{kh}{\mu} = \frac{162.6\, q\, \beta}{m}$

$\frac{kh}{\mu} = 7570 \frac{md \cdot ft}{cp}$

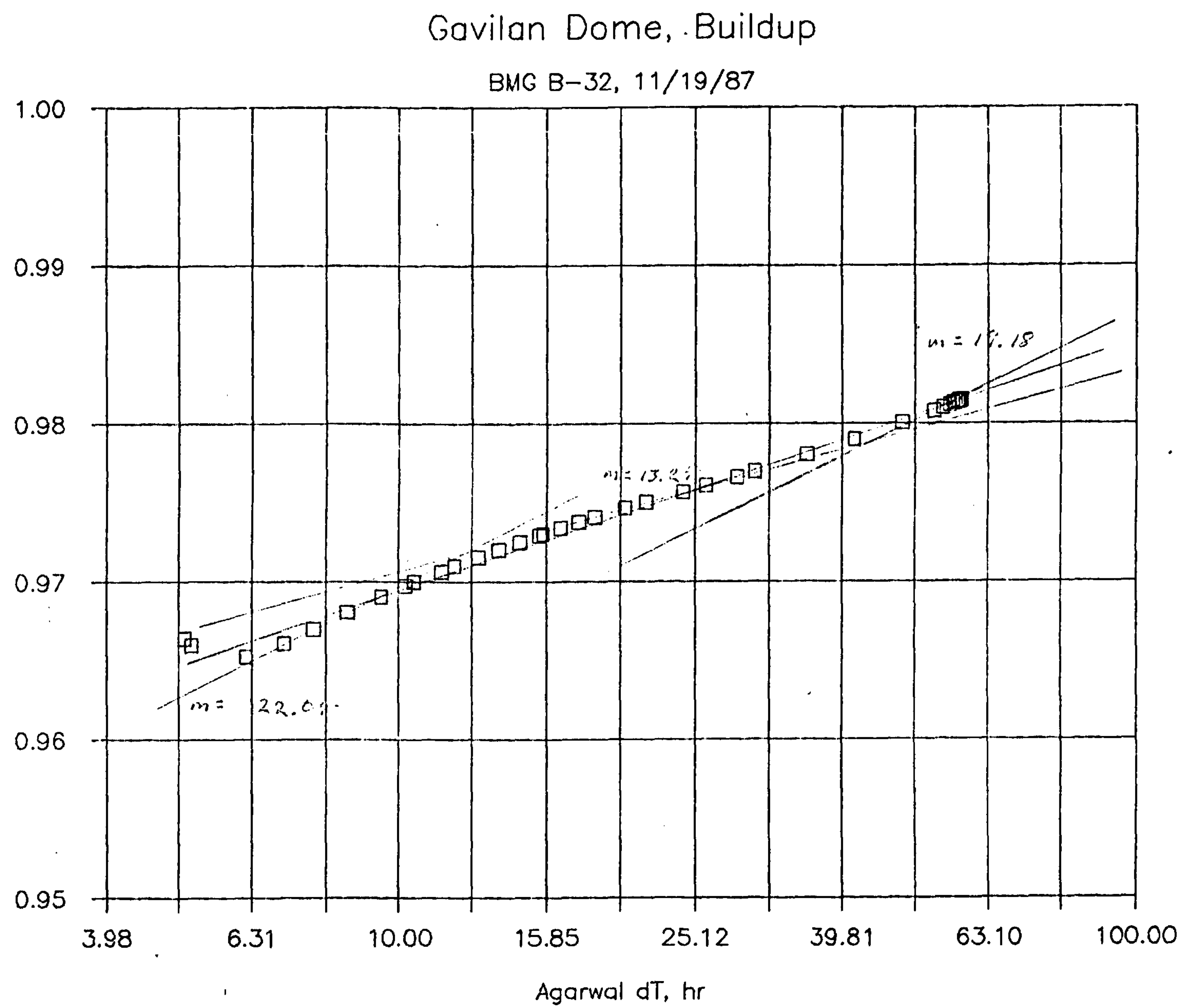

11/19/87 Buildup

$q_{o} = 719$ BOPD GOR = 1,242

$q_{g} = 893$ Mcf/D Max pressure 955

$B_o = 1.314$ $B_g = 2.932$ $\mu_o = 0.635$ $\mu_g = 0.01403$ $R_s = 437$
$\rho_o = .7148$ $\rho_g = .000891$

$q_o, RB = (719)(1.314) = 944.8$ RB/D

579 bbl/D equivalent

$q_g, RB = \left[893 - \frac{(719)(437)}{1000}\right] 2.932 = 1697$ RB/D

$q_t = q_o + q_g = 2642$ RB/D

Volume average viscosity + density

$(944.8)(0.635) = 599.9$
$(1697)(0.01403) = 23.8$
623.8

$\mu_{Average} = 0.2361$ cp

$(944.8)(0.7148) = 675.3$
$(1697)(.000891) = 1.5$
676.9

$\rho_{Average} = 0.2562$ gm/cc

$\frac{0.2562}{1} = \frac{x}{0.433 \text{ psi/ft}}$

Reservoir gradient, $x = 0.1109$ psi/ft

$\frac{K_t h}{\mu} = \frac{(162.6)(2642 \text{ RB/D})}{19.8} = 21,696 \frac{\text{md}\cdot\text{ft}}{\text{cp}}$, $Kh = 5123$ md·ft $h \approx 150'$

$K = 34.2$ md

$K_o h = \frac{(162.6)(944.8)(.635)}{19.8} = 4927$ md·ft

$K_g h = \frac{(162.6)(1697)(0.01403)}{19.8} = 196$ md·ft

Mallon

7/29/88

Fisher Federal 2-1

11/19/87 Buildup $m = 69.0$ $q_o = 39.8$ $q_g = 347.47$

$\bar{p}$ 978 $B_o = 1.317$ $B_g = 2.85$ $\mu_o = 0.628$ $\mu_g = 0.01409$ $R_s = 444$

$q_o, RB = (39.8)(1.317) = 52.4166$

$q_g, RB = \left[347.47 - \frac{(39.8)(444)}{1000}\right] 2.85 = 939.9$

$q_t, RB = 992.3$ RB/D

$(52.4)(.628) =$

$(939.9)(.01409) =$

46.15

$\mu_{Average} = 0.0465$ cp

$\lambda_t h = \frac{(162.6)(992.37)}{m} = 2338 \frac{md \cdot ft}{cp}$

$Kh = 109$ md

2/23/88 Buildup $m = 87$ $q_o = 98$ $q_g = 1013$

$\bar{p} \sim 925$ $B_o = 1.310$ $B_g = 3.015$ $\mu_o = 0.643$ μ_g 0.01396 $R_s = 430$

$q_o = (1.310)(98) = 128.4$ RB/D

$q_g = \left[1013 - \frac{(98)(430)}{1000}\right] 3.015 = 2927.1$ "

3055

$q_t = 3055$ RB/D

$(128.4)(.643) = 82.56$

$(2927.1)(0.01396) = 40.86$

123.42

$\mu_{Average} : 0.0404$

$\lambda_t h = \frac{(162.6)(3055)}{87}$

$\lambda_t h = 5710 \frac{md \cdot ft}{cp}$

$\bar{K}h = 231$ md·ft

$K_o h = \frac{(128.4)(.643)(162.6)}{87} = 154$

$K_g h = \frac{(2927.1)(.01396)(162.6)}{87} = 76.4$

Meridian

Hill Federal 2-4

6/30/97 Buildup

$m = 108.4$ $q_o = 107.2$ $q_g = 327.0$ $\bar{P} = 1111$

$B_o = 1.334$ $B_g = 2.477$ $\mu_o = .588$ $\mu_g = 0.01442$ $R_s = 482$

$$q_o = (107.2)(1.334) = 143.0$$

$$q_g = \left[\left(327 - \frac{(107.2)(482)}{1000}\right)\right] 2.477 = \frac{682}{825 \text{ RB/D}}$$

$$(143)(.588) = 84$$
$$(682)(0.01442) = \frac{9.8}{93.92}$$

$$\lambda_t h = \frac{(162.6)(825)}{108.4} = 1237.5 \frac{\text{md-ft}}{\text{cp}}$$

$\mu_{Average} = 0.1138$

$\bar{k} h = 141 \text{ md}$

$$k_o h = \frac{(162.6)(143)(.588)}{108.4} = 126$$

$$k_g h = \frac{(162.6)(682)(.01442)}{108.4} = 15$$

Meridian
Hill Federal #1

11/19/87 Buildup

$m = 168.9$ $q_o = 24$ $q_g = (820)(3)$ $\bar{P} = 943$

$B_o = 1.312$ $B_g = 2.965$ $\mu_g = 0.01401$ $\mu_o = .637$ $R_s = 435$

$q_{bo} = (24)(1.312) = 31.5$

$q_{bg} = \left[(820)(3) - \frac{(24)(435)}{1000}\right] 2.965 = 7262.9$

$q_{bt} = 7294$ RB

$(31.5)(0.637) = 20.06$

$(7262.9)(.01401) = 101.75$

121.81

Average $\mu = 0.01670$

$\lambda_t h = \frac{(162.6)(7294)}{168.9} = 7022 \ \frac{md.ft}{cp}$

$\bar{K} h = 117.3$ md. ft

$K_o h = \frac{(162.6)(20.06)(.637)}{168.9} = 12.3$

$K_g h = \frac{(162.6)(7262.9)(.01401)}{168.9} = 98.0$

Bear Cat #1 4/24/86

6/30/87 Buildup

$q_o = 47.11$ BO/D | Max BHP 1052 psig | $B_o = 1.327$

$q_g = 268.95$ Mcf/D | $P_{1\,hr} = 950.2$ psig | $B_g = 2.632$

$h = 90'$ (perforated) | $m = 46.36$ psig/cycle | $\mu_o = .605$

$\mu_g = .01428$

$R_s = 466$

q_o, RB $= (47.11)(1.327) = 62.5$ RB/D

q_g, RB $= \left[268.95 - \frac{(47.11)(466)}{1000}\right] 2.632 = 650.1$ RB/D

$q_t = q_o + q_g = 712.6$ RB/D

Volume average viscosity

$(62.5)(0.605) = 37.8$

$(650.1)(0.01428) = \underline{9.28}$

47.1

$\frac{47.1}{712.6} = 0.06610$ cp

$\lambda_t h = \frac{162.6\ q_t}{m} = \frac{(162.6)(712.6)}{46.36} = 2499\ \frac{\text{md}\cdot\text{ft}}{\text{cp}}$

$K_o h = \frac{162.6\ q_o B_o \mu_o}{m} = \frac{(162.6)(62.5)(.605)}{46.36} = 132.6$ md·ft

$K_g h = \frac{162.6\ q_g (RB) \mu_g}{m} = \frac{(162.6)(650.1)(0.01428)}{46.36} = 32.6$ md·ft

$Kh_{Absolute} = \left(2499\ \frac{\text{md}\cdot\text{ft}}{\text{cp}}\right)(0.0661\ \text{cp}) = 165.2$ md·ft

$K_{Absolute} = 1.8$ md

end of storage
at .033 hr

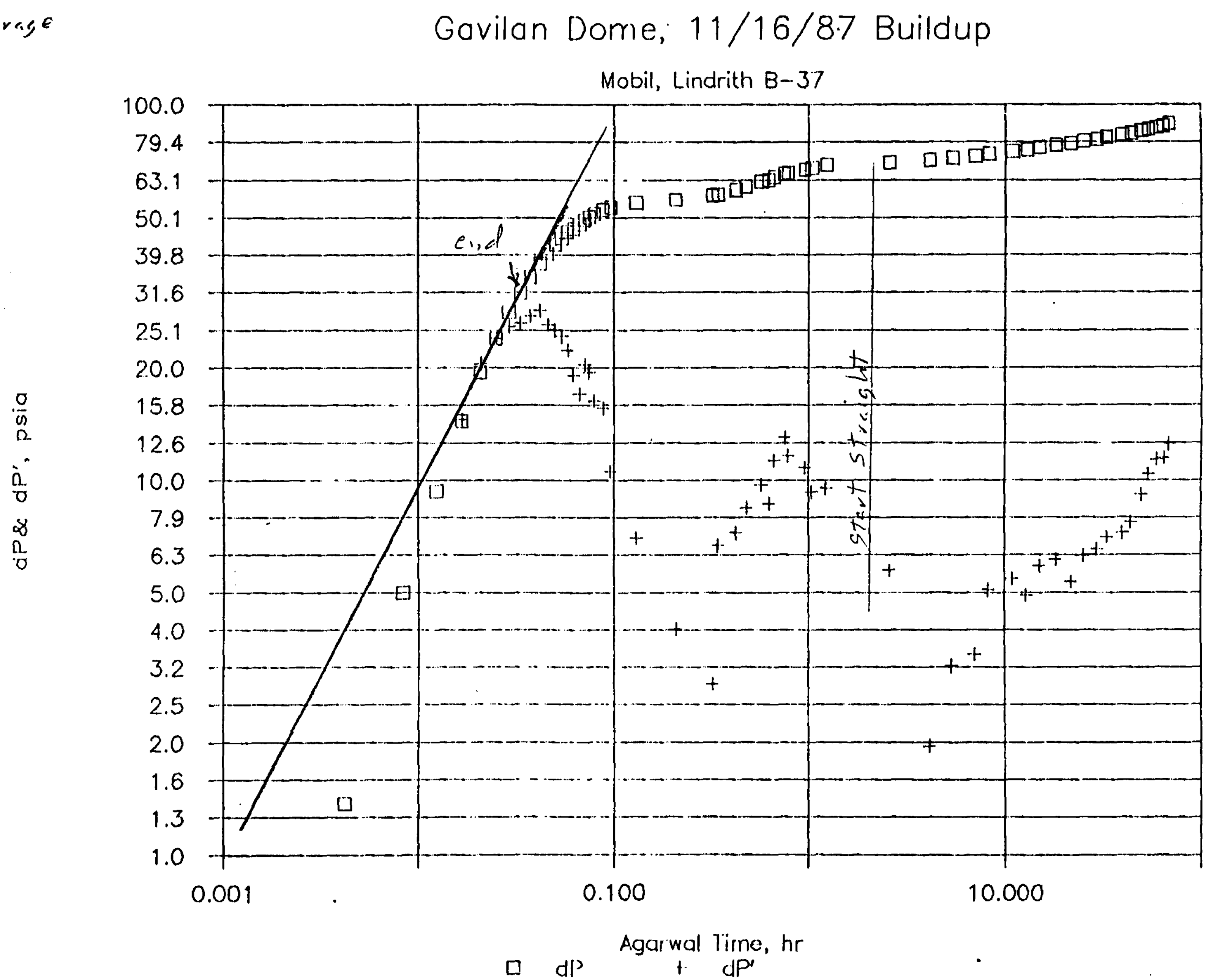

Fig 1

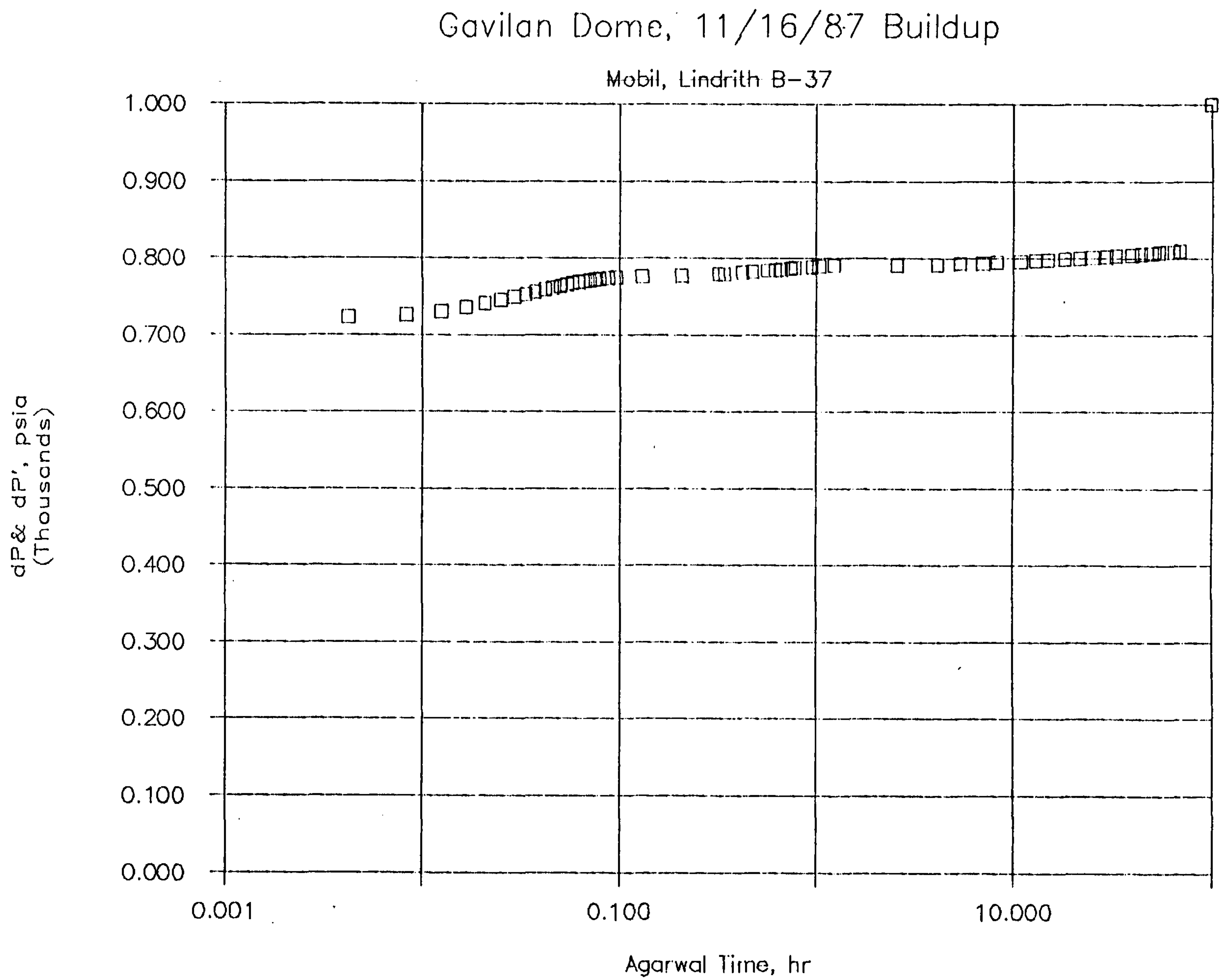
Gavilan Dome, 11/16/87 Buildup
Mobil, Lindrith B-37
dP& dP', psia
(Thousands)
1.000
0.900
0.800
0.700
0.600
0.500
0.400
0.300
0.200
0.100
0.000
0.001
0.100
10.000
Agarwal Time, hr

Fig 2

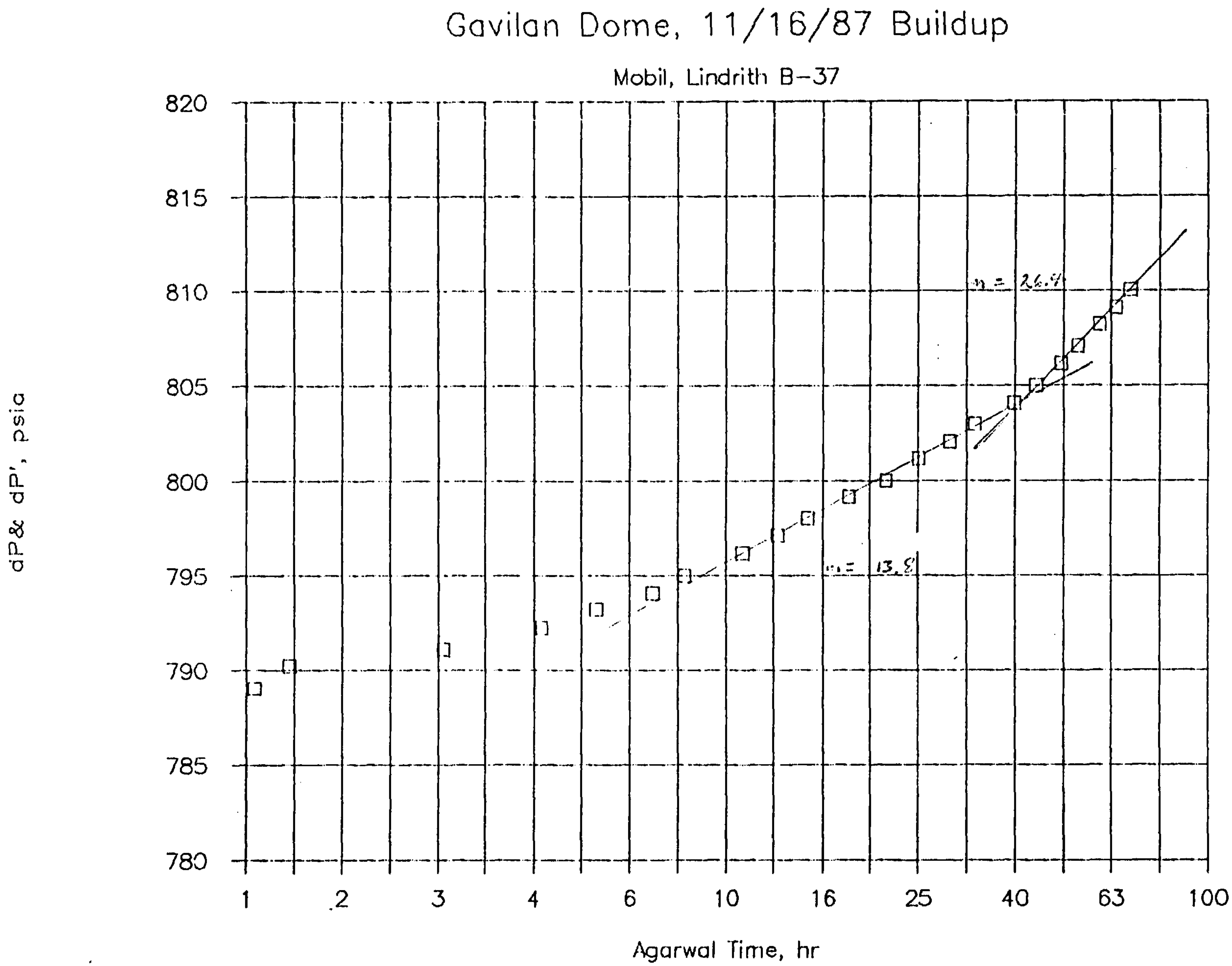
Gavilan Dome, 11/16/87 Buildup
Mobil, Lindrith B-37
820
815
810
805
800
795
790
785
780
dP& dP', psia
1
2
3
4
6
10
16
25
40
63
100
Agarwal Time, hr
m = 26.4
m = 13.8

Fig 3

Mobil Lindrith "B" Unit ①
Well #37 4/24/88
11/16/87 Buildup

Max Pressure 810 psig Loddy PVT Data
Rates 221.2 BOPD, 889.1 McF/D GOR = 3907 scf/bbl
m = 26.4 psig/cycle $h = 233$ ft
Flow Rates, Reservoir bbl

gas $\left[889.1 - \frac{221.2(400)}{1000}\right] 3.5 = 2802$ RB/D

oil $(221.2)(1.295) = 286$ RB/D

$q_t = 3088$ RB/D

$\lambda h_t = \frac{(162.6)(3088)}{26.4} = 19{,}022 \frac{md \cdot ft}{cp}$

Average viscosity

$(2802)(.0136) = 38.11$
$(286)(.705) = 201.63$
239.7

$\frac{239.7 \text{ RB} \cdot cp}{3088 \text{ RB}} = 0.0776\ cp$

$\left(\frac{Kh}{\mu}\right)_{absolute} = 19{,}022 \frac{md \cdot ft}{cp}$ or 1477 md.ft (6.3md)

$K_o h = \frac{(162.6)(286)(.705)}{26.4} = 1242$ md.ft (5.3md

$K_g h = \frac{(162.6)(2802)(0.0136)}{26.4} = 235$ md.ft (1.0md

Skin estimate

(2)
4/24/

$$S = 1.151\left[\frac{761.4-721.2}{26.4} - \log\frac{6.3}{(.001)(1.265\times10^{-3})(.0776)(.229^2)} + 3.23\right]$$

(C1) (C2)

$S = -5$

Then from type curve for wells with storage + skin

at $S = -5$ $\quad P_D = \dfrac{(1477)(87)}{(141.2)(3088)(.0776)} = 3.80$ $\qquad \dfrac{\Delta P K h}{141.2 q B \mu} = 1$

at $\Delta P = 87$ psig $\quad \Delta t = 59.523$

From Type curve at $P_D = 3.8$ & $S = -5$ $\quad t_D = 1.9\times10^{7}$

$$\phi = \frac{(2.637\times10^{-4})(6.3)(59.523)}{(1.9\times10^{7})(0.0776)(1.265\times10^{-3})(.229^2)} \qquad t_D = \frac{2.637\times10^{-4} K t}{\phi \mu C_t r_w^2}$$

$\phi = 10.11\times10^{-2}$

$\phi h = 0.236$

$$K_m = \frac{(532.3)(1.011\times10^{-3})(1.265\times10^{-3})(233^2)(0.0776)}{41.6}$$

$K_m = 0.069$ md

$$\lambda' = 12\left(\frac{.069}{6.3}\right)\left(\frac{0.229^2}{233^2}\right) = 1.27\times10^{-7}$$

$$\phi_f C_f h_f = 8.33\times10^{-4}\left[\frac{(1477)(1.011\times10^{-3})(1.265\times10^{-3})(233)(1.27\times10^{-7})(12.833)}{(0.0776)(.229^2)}\right]^{1/2}$$

$\phi_f C_f h_f = 1.106\times10^{-5}$

$$\phi_f = \frac{1.106\times10^{-5}}{(1.\ldots\times10^{-3})(0.\ldots)} = 3.75\times10^{-5}$$

3

4/24/88

$$\omega' = \frac{\phi_m}{\phi_f} = \frac{1.011 \times 10^{-3}}{3.75 \times 10^{-5}} = 27$$

or ~ 3.7% of total porosity is in fractures

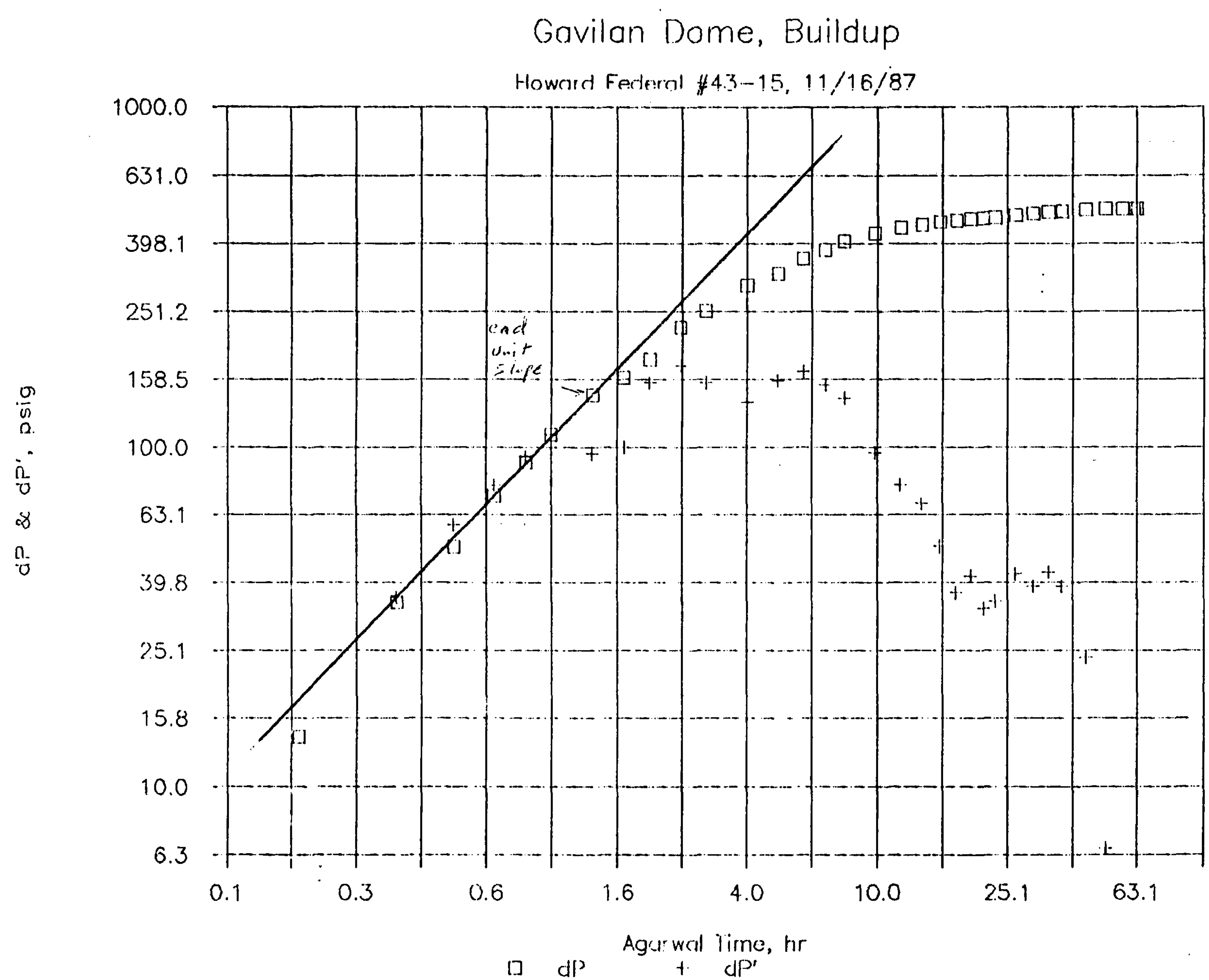

Gavilan Dome, Buildup
Howard Federal #43-15, 11/16/87
1000.0
631.0
398.1
251.2
158.5
100.0
63.1
39.8
25.1
15.8
10.0
6.3
dP & dP', psig
end unit slope
0.1
0.3
0.6
1.6
4.0
10.0
25.1
63.1
Agarwal Time, hr
dP
dP'

Fig 1

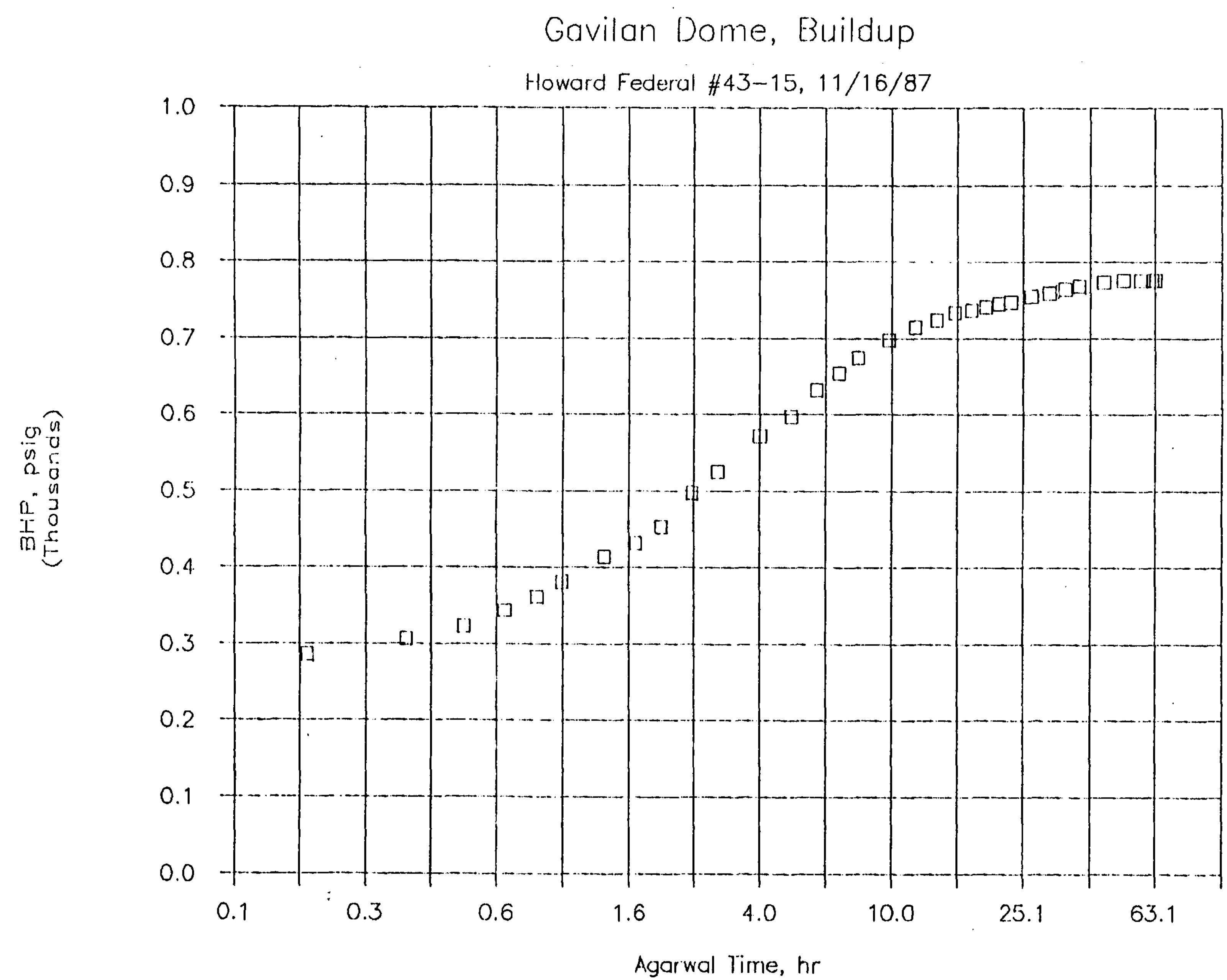
Gavilan Dome, Buildup
Howard Federal #43-15, 11/16/87
BHP, psig
(Thousands)
1.0
0.9
0.8
0.7
0.6
0.5
0.4
0.3
0.2
0.1
0.0
0.1
0.3
0.6
1.6
4.0
10.0
25.1
63.1
Agarwal Time, hr

Fig 2

Gavilan Dome, Buildup

Howard Federal #43-15, 11/16/87

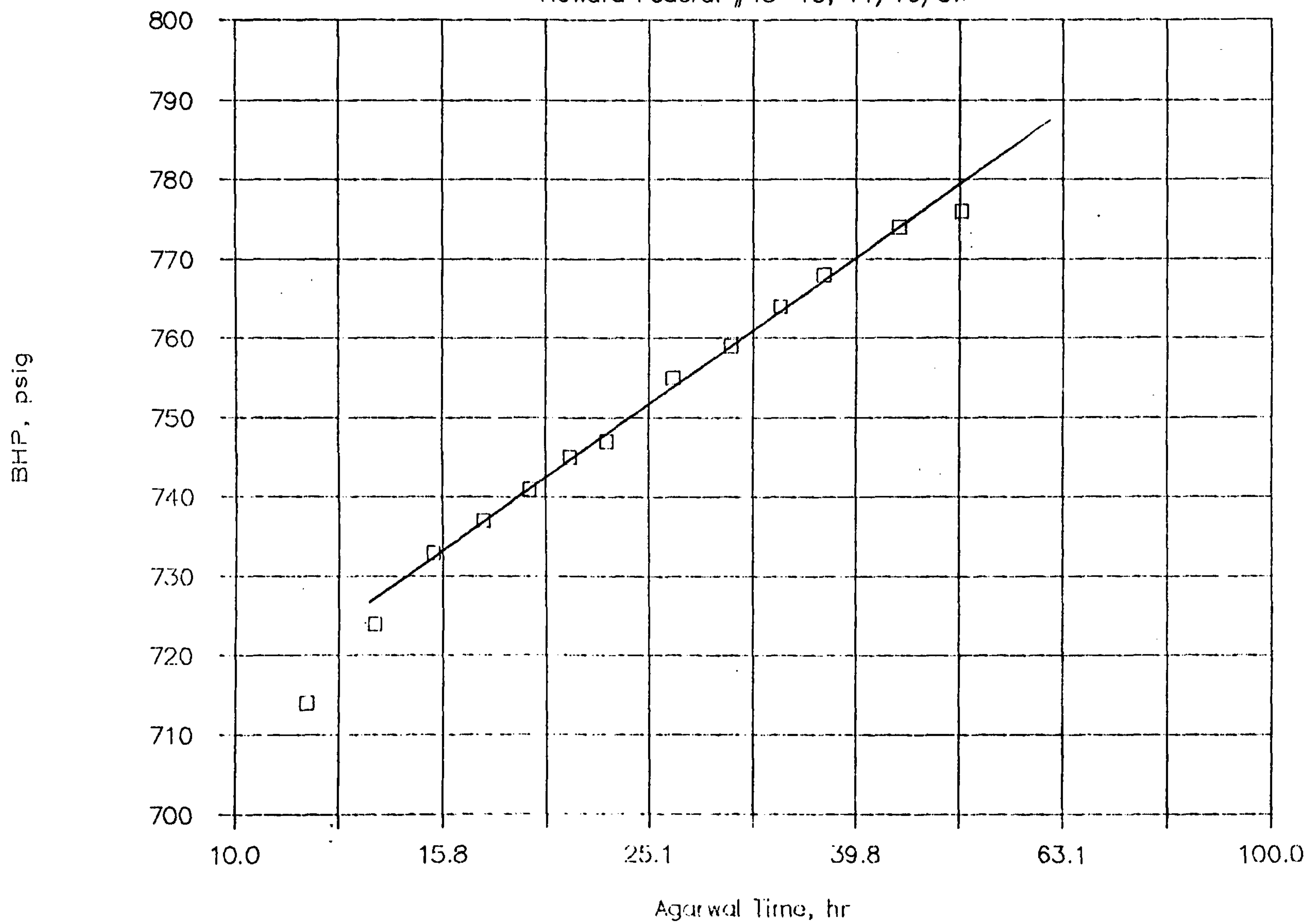

Fig 3

Reading

Howard Federal #43-15

11/19 Buildup

$q_o = 9.19$ BOPD $\quad q_g = 636.63$ Mcf/D $\quad \bar{P} = 852 \quad m = 92.77$

$B_o = 1.301 \quad B_g = 3.309 \quad R_s = 409 \quad \mu_o = .680 \quad \mu_g = 0.01375$

$$q_o = (9.19)(1.301) = 11.9$$

$$q_g = \left[636.63 - \frac{(9.19)(409)}{1000}\right]3.209 = 2094.2$$

$$q_t = 2106 \text{ RB/D}$$

$$(11.9)(.620) = 8.13$$

$$(2094.2)(0.01375) = 28.79$$

$$\mu_{average} = 0.01752 \text{ cp}$$

$$\lambda_t h = \frac{(162.6)(2106)}{92.77} = 3691 \frac{\text{md.ft}}{\text{cp}}$$

$$\bar{k} h = 64.7 \text{ md.ft}$$

$$k_o h = \frac{(162.6)(11.9)(.68)}{92.77} = 14.2$$

$$k_g h = \frac{(162.6)2094.2(.01375)}{92.77} = 50.5$$

Gavilan Dome, Buildup

High Adventure #1, 11/19/87

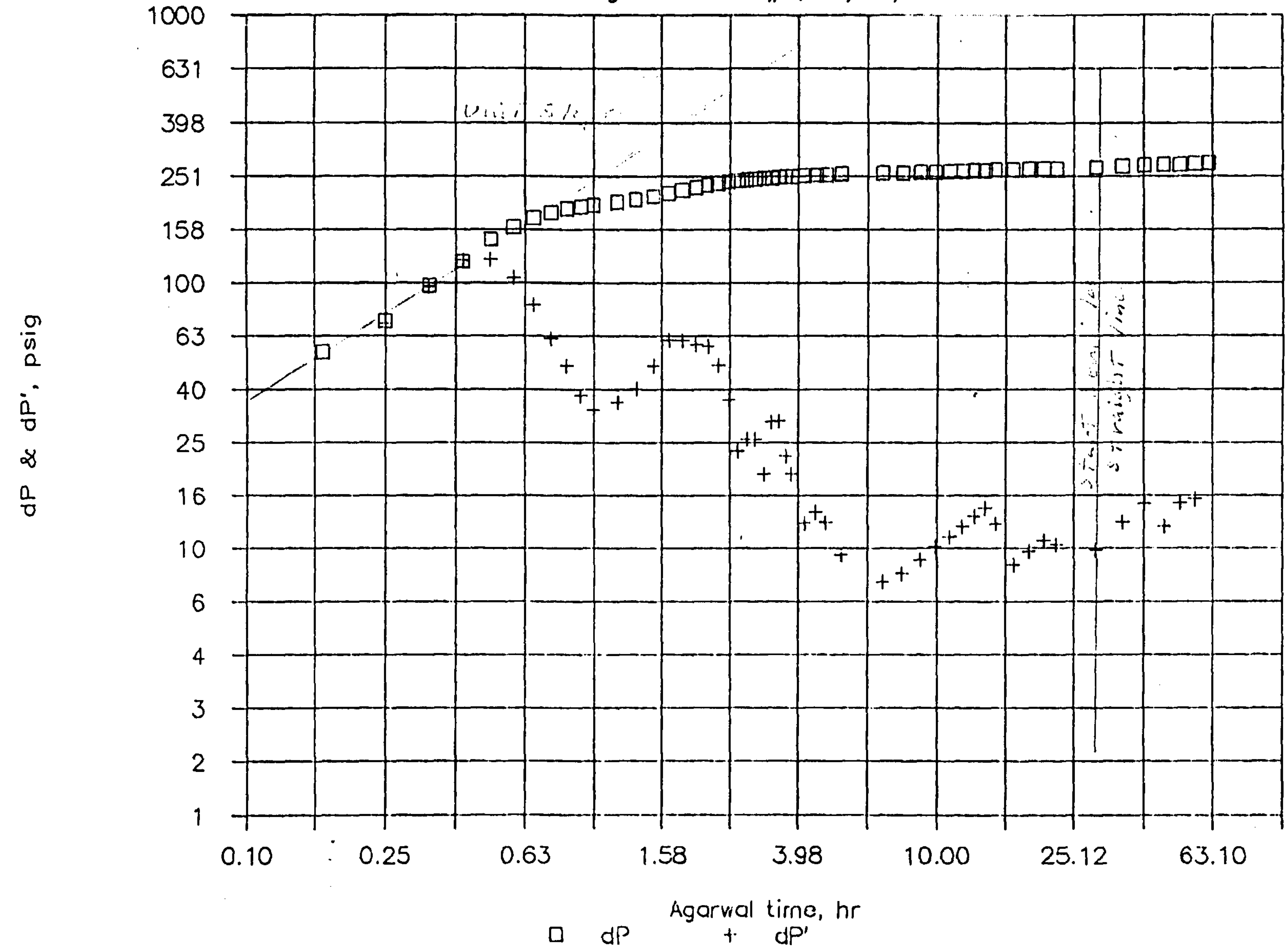

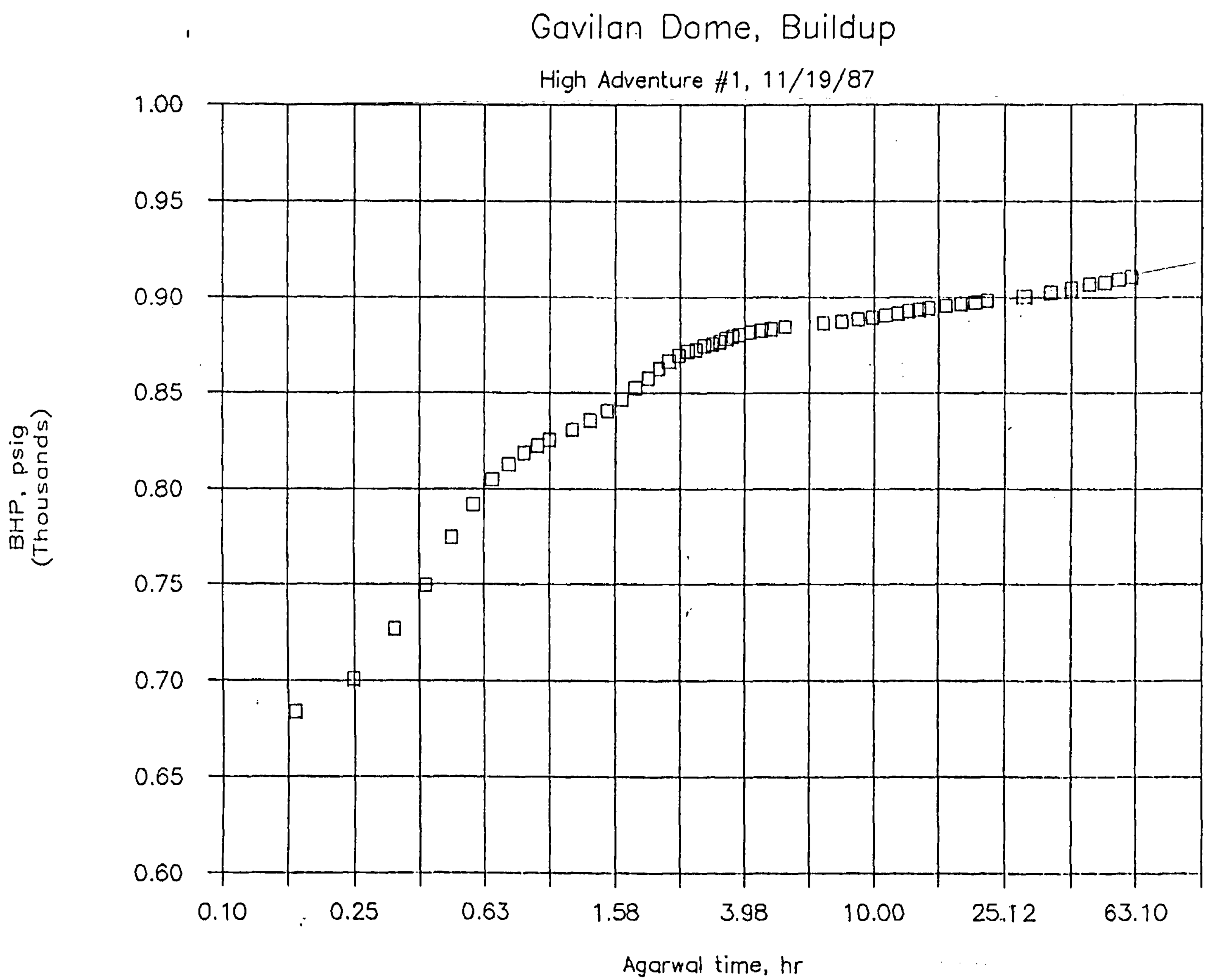
Gavilan Dome, Buildup
High Adventure #1, 11/19/87
BHP, psig
(Thousands)
1.00
0.95
0.90
0.85
0.80
0.75
0.70
0.65
0.60
0.10
0.25
0.63
1.58
3.98
10.00
25.12
63.10
Agarwal time, hr

$B_g = 722.34$

$q_o = 233$

$T = 840\ h$

Gavilan Dome Buildup Analysis
Sun High Adventure #1, Start Test 11:23 AM, 11/16/87
Flow Time, T = 840 hours q = 233 B/D

@ 910 Psig

$B_o = 1.308$ $B_g = 3.065$ $R_s = 426$ $\mu_o = .647$ $\mu_g = .01392$

dt hr	BHP psig	dP psig	T*dt/T+dt Agarwal	Agarwal' WMS Tech
0.00				
0.17	683.8	54.9	0.167	
0.25	700.8	71.9	0.250	70.4
0.33	726.8	97.9	0.333	97.3
0.42	749.7	120.8	0.416	121.4
0.50	774.7	145.8	0.500	122.4
0.58	791.6	162.7	0.583	104.8
0.67	805.0	176.1	0.666	82.9
0.75	813.0	184.1	0.749	62.0
0.83	818.9	190.0	0.832	49.0
0.92	822.9	194.0	0.916	38.0
1.00	825.9	197.0	0.999	33.5
1.17	830.9	202.0	1.168	35.7
1.33	835.9	207.0	1.328	40.3
1.50	840.9	212.0	1.497	49.1
1.67	846.9	218.0	1.667	61.0
1.83	852.8	223.9	1.826	60.8
2.00	857.8	228.9	1.995	58.9
2.17	862.8	233.9	2.164	[illegible]
2.33	866.8	237.9	2.327	49.2
2.50	869.8	240.9	2.493	36.7

hr	psig	psig	Agarwal	WMS Tech
36.00	902.7	273.8	34.521	12.6
42.00	904.7	275.8	40.000	14.7
48.00	906.7	277.8	45.405	12.1
54.00	907.7	278.8	50.738	14.9
60.00	909.7	280.8	56.000	15.5
66.00	910.7	281.8	61.192	

Reservoir bbl

$(233)(1.308) = 304.8$ RB

$\left[723 - \frac{(233)(426)}{1000}\right] 3.065$

$= 1911.8$ RBG

$q_t = 2217$ RB/D

$(304.8)(0.647) =$

$(1911.8)(.01392) =$

$\mu_{Average} = 0.1010\ cp$

6 points

CC : 99.7%

P_{1hr} : 852.9 psig

slope : 32.34 psi/cycle

$$\lambda_t h = \frac{(162.6)(2217)}{32.34} = 11,146\ \frac{md \cdot ft}{cp}$$

$$\bar{K} h = 1126\ md \cdot ft$$

$$K_o h = \frac{(162.6)(304.8)(.647)}{32.34} = 991.5$$

$$K_g h = \frac{(162.6)(1911.8)\ .01392}{32.34} = 133.8$$

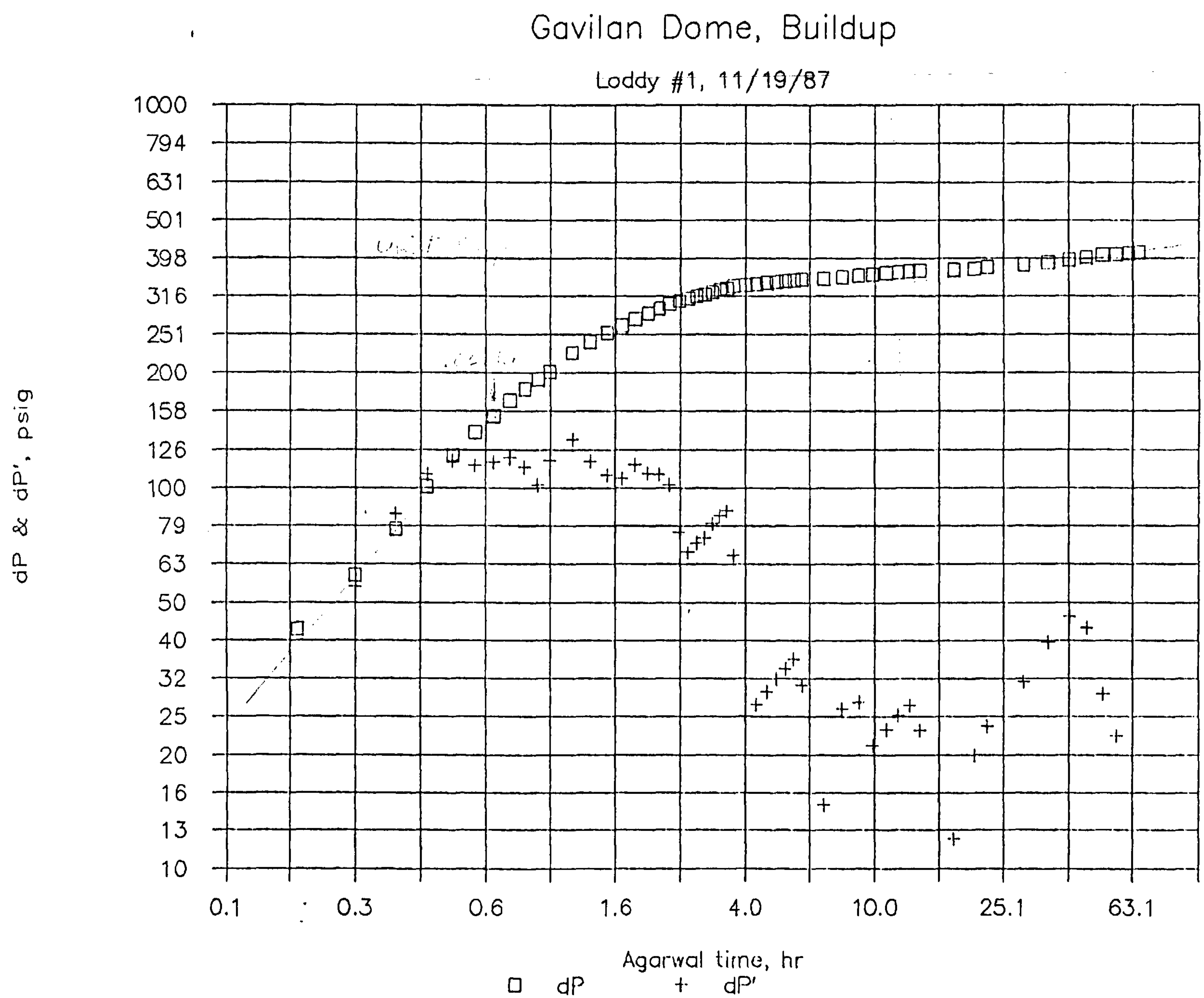

Gavilan Dome, Buildup
Loddy #1, 11/19/87
1000
794
631
501
398
316
251
200
158
126
100
79
63
50
40
32
25
20
16
13
10
dP & dP', psig
0.1
0.3
0.6
1.6
4.0
10.0
25.1
63.1
Agarwal time, hr
dP
dP'

Gavilan Dome, Buildup

Loddy #1, 11/19/87

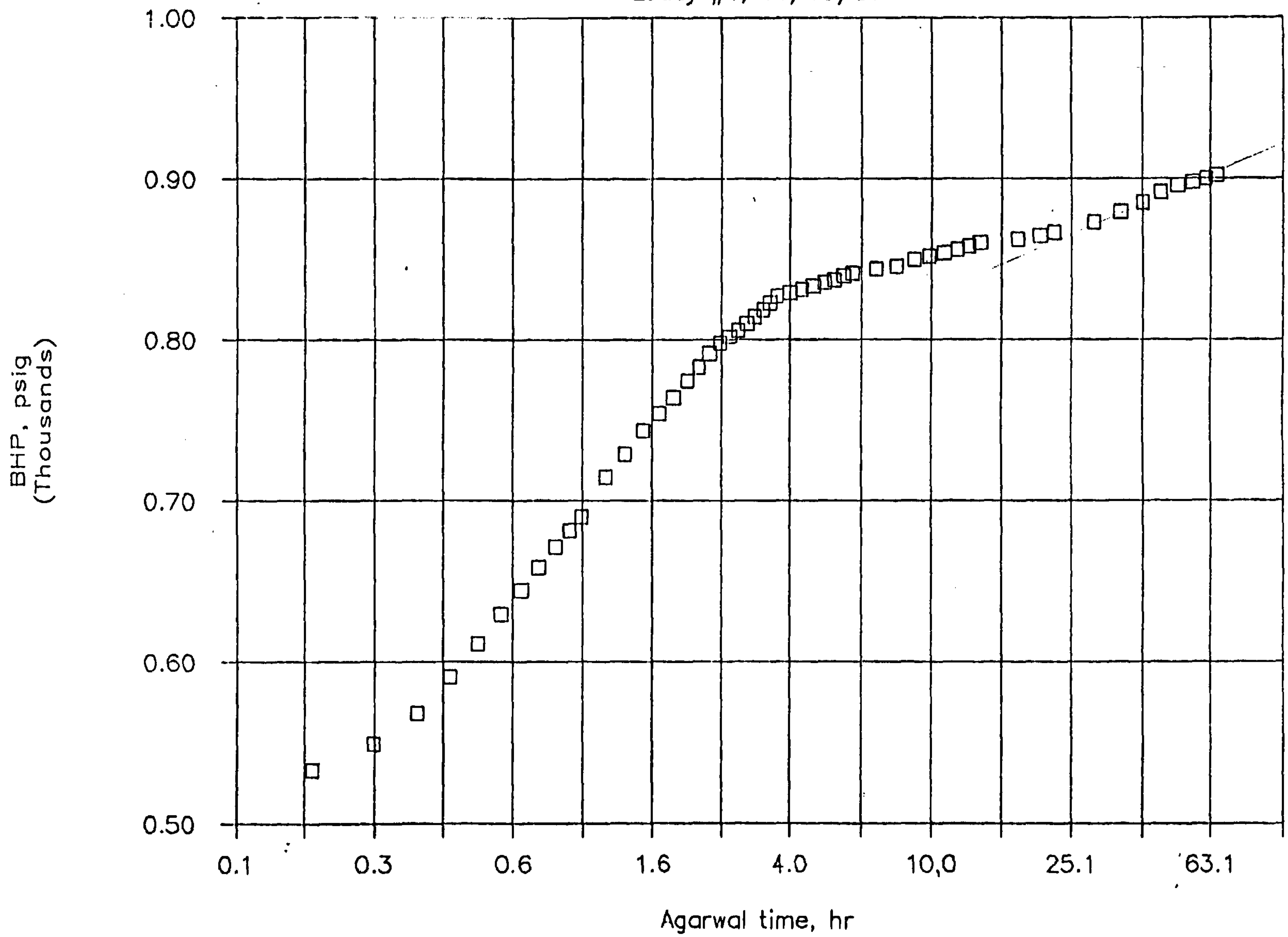

$q_g = 338.54$ Mcf/D
$q_o = 67$ BO/D
$T = 840$ hr

Gavilan Dome Buildup Analysis
Sun Loddy#1, Start Test 10:06 AM, 11/~~16~~ 19/87
Flow Time,T = ~~816~~ 840 hours q = ~~69~~ 67 B/D

$B_o = 1.307$ $B_g = 3.098$ $R_s = 423$ $\mu_o = 0.650$ $\mu_g = 0.01390$

Cartesian plot
cc = 100%
Intercept
$P_{0hr} = 490$ psig

dt hr	BHP psig	dP psig	T*dt/T+dt Agarwal	Agarwal' WMS Tech
0.00	490.0			
0.17	532.6	42.6	0.167	
0.25	549.2	59.2	0.250	55.1
0.33	567.9	77.9	0.333	85.7
0.42	590.7	100.7	0.416	108.3
0.50	611.4	121.4	0.500	117.7
0.58	630.1	140.0	0.583	114.4
0.67	644.6	154.6	0.666	116.5
0.75	659.1	169.1	0.749	120.6
0.83	671.5	181.5	0.832	113.3
0.92	681.9	191.9	0.916	101.8
1.00	690.2	200.2	0.999	117.9
1.17	715.0	225.0	1.168	133.7
1.33	729.5	239.5	1.328	117.2
1.50	744.0	254.0	1.497	108.1
1.67	754.4	264.4	1.667	105.8
1.83	764.8	274.8	1.826	115.3
2.00	775.1	285.1	1.995	109.1
2.17	783.4	293.4	2.164	108.7
2.33	791.7	301.7	2.326	102.2
2.50	797.9	307.9	2.492	76.4
hr	psig	psig	Agarwal	WMS Tech
36.00	879.2	389.2	34.479	39.4
42.00	885.4	395.4	39.944	46.2
48.00	891.7	401.7	45.333	43.1
54.00	895.8	405.8	50.648	28.9
60.00	897.9	407.9	55.890	22.4
66.00	900.0	410.0	61.061	27.7
71.00	902.1	412.1	65.317	

$(67)(1.307) = 87.57$ RB/D

$\left[338.54 - \frac{(67)(423)}{1000}\right]3.098 = 961.0$ RB/D

$q_t = 1049$ RB/D

$(87.57)(.650)$

$(961)(.01390)$

$\mu_{average} = 0.0670$ cp

7 points
cc 98.9%
$P_{1hr} = 754.7$ psig
slope = 81.82 psi/cycle

$$\lambda_t h = \frac{(162.6)(1049)}{81.82} = 2085 \frac{md.ft}{cp}$$

$$\bar{K}h = 140 \text{ md.ft}$$

$$K_o h = \frac{(162.6)(87.57)(.650)}{81.82} = 113.1$$

$$K_g h = \frac{(162.6)(961)(.01390)}{81.82} = 26.5$$

APPENDIX 3

Interference Test Analyses Worksheets

Frac Pulse Analyses
Kamal Method

(1) 5/10/88

<u>Frac D-17 Response at A-20</u> 5/27/87 $\bar{P} \sim 1240$ psi

Pump Time 1.63 hr

Signal Time 80.0 hr

Lag Time, t_l 35.5 hr

Peak $\frac{\Delta P}{q}$ 1.41×10^{-6}

Δt_{cyc} = signal time + pump time = 80.0 + 1.63 = 81.63

$$\text{Pulse Ratio} = \frac{\text{Pump time}}{\Delta t_{cyc}} = \frac{1.63}{81.63} = 0.0200$$

$$\text{Demensionless time lag, } t_{l_D} = \frac{t_l}{\Delta t_{cyc}} = \frac{35.5}{81.63} = 0.435$$

Demensionless cycle period, $\Delta t_{cycD} = C\, t_{l_D}^{\,A} + D$

$$\Delta t_{cycD} = (0.337)(.435^{-.815}) - 0.325$$

$$= 0.339$$

From Fig 10-13
A = −0.815
C = 0.337
E = −1.34
F = 0.0255
D = −0.325

Demensionless response amplitude

$$\frac{\Delta P_D}{\Delta t_{cycD}} = 1 \times \left[F \exp(E\, t_{l_D}) + 0.01\right]$$

$$= -1\left[.0285 \exp[(-1.34)(.435)] + 0.01\right]$$

$$= -0.0259$$

$$\Delta P_D = (-0.0259)(0.339) = -0.00878$$

ΔP_D = Δt [illegible]

5/13/8?

$$\Delta P_D = \frac{Kh\,\Delta P}{70.6\,B\,\mu\,q}$$

$B = 1.86$

$\mu = 0.559$

$$Kh = \frac{70.6\,B\,\mu\,\Delta P_D}{\Delta P/q}$$

$$Kh = \frac{(70.6)(1.86)(0.559)(0.00878)}{1.41 \times 10^{-6}}$$

$Kh = 457{,}000$ md.ft

$$\Delta t_{cycD} = \frac{K\,\Delta t_{cyc}}{56900\,\phi\,C_t\,\mu\,r^2}$$

$r = 12\,787$

$$\phi C_t h = \frac{Kh\,\Delta t_{cyc}}{56900\,\mu\,r^2\,\Delta t_{cycD}}$$

$$= \frac{(457{,}000)(81.63)}{(56{,}900)(.559)(12787^2)(.339)}$$

$$= 2.12 \times 10^{-5}$$

$C_{t\,1240\,psi} = S_o C_o + S_w C_w + S_g C_g + C_f$

$(.87)(3.6 \times 10^{-4}) + (0.1)(3.3 \times 10^{-6}) + (0.1)(7 \times 10^{-4}) + 100 \times 10^{-6} = 4.8 \times 10^{-4}$

$\phi h = 4.41 \times 10^{-2}$

$\phi = 2.94 \times 10^{-4} = 0.03\%$

5/13/88

Determine c_t

Assume $S_w = 0.10$ $c_w = 3.3 \times 10^{-6}$ $c_f = 100 \times 10^{-6}$

$S_g = 0.03$ $c_g :$ $S_o = 0.87$ $c_o =$

BHT = 170° = 630°

	1000	125
γ_o	.714	.71
γ_g	.0572	.0716
T	630°	630°
Z	.872	.85
R_s	452	523
B_o	1.32	1.35
B_g	$\frac{2.767}{1000}$	2.17
$\frac{dR_s}{dp}$	0.30	0.28
$\frac{dB_o}{dR_s}$	3.99×10^{-4}	4.67×1

$$c_{o_{1000psi}} = \frac{1}{B_o}\frac{dR_s}{dp}\left[B_g - \frac{dB_o}{dR_s}\right]$$

$$= \left(\frac{1}{1.32}\right)(0.30)\left[2.767 \times 10^{-3} - 3.99 \times 10^{-4}\right]$$

$$c_{o_{1000}} = 5.38 \times 10^{-4}$$

$$c_{o_{1250}} = \left(\frac{1}{1.352}\right)(28)\left[2.176 \times 10^{-3} - 4.67 \times 10^{-4}\right]$$

$$= 3.54 \times 10^{-4}$$

$$c_{o_{800}} = \left(\frac{1}{1.294}\right)(0.28)\left[3.521 \times 10^{-3} - 4.29 \times 10^{-4}\right]$$

$$c_{o_{800}} = 6.69 \times 10^{-4}$$

$$c_{o_{500}} = \frac{1}{1.253}(0.32)\left[5.804 \times 10^{-3} - 5 \times 10^{-4}\right]$$

$$c_{o_{500}} = 1.17 \times 10^{-3}$$

$$C_g = \frac{1}{p} - \left[\frac{dz}{dp}\;\frac{1}{z}\right]$$

	Z	$\frac{dz}{dp}$	C_g
$\bar{p} = 500$	0.914	1×10^{-4}	1.89×10^{-3}
$\bar{p} = 800$	0.887	8×10^{-5}	1.16×10^{3}
$\bar{p} = 1000$	0.872	6×10^{-5}	9.31×10^{-4}
$\bar{p} = 1200$	0.859	6×10^{-5}	7.63×10^{-4}
$\bar{p}$ 1300	0.852	8×10^{-5}	6.75×10^{-4}

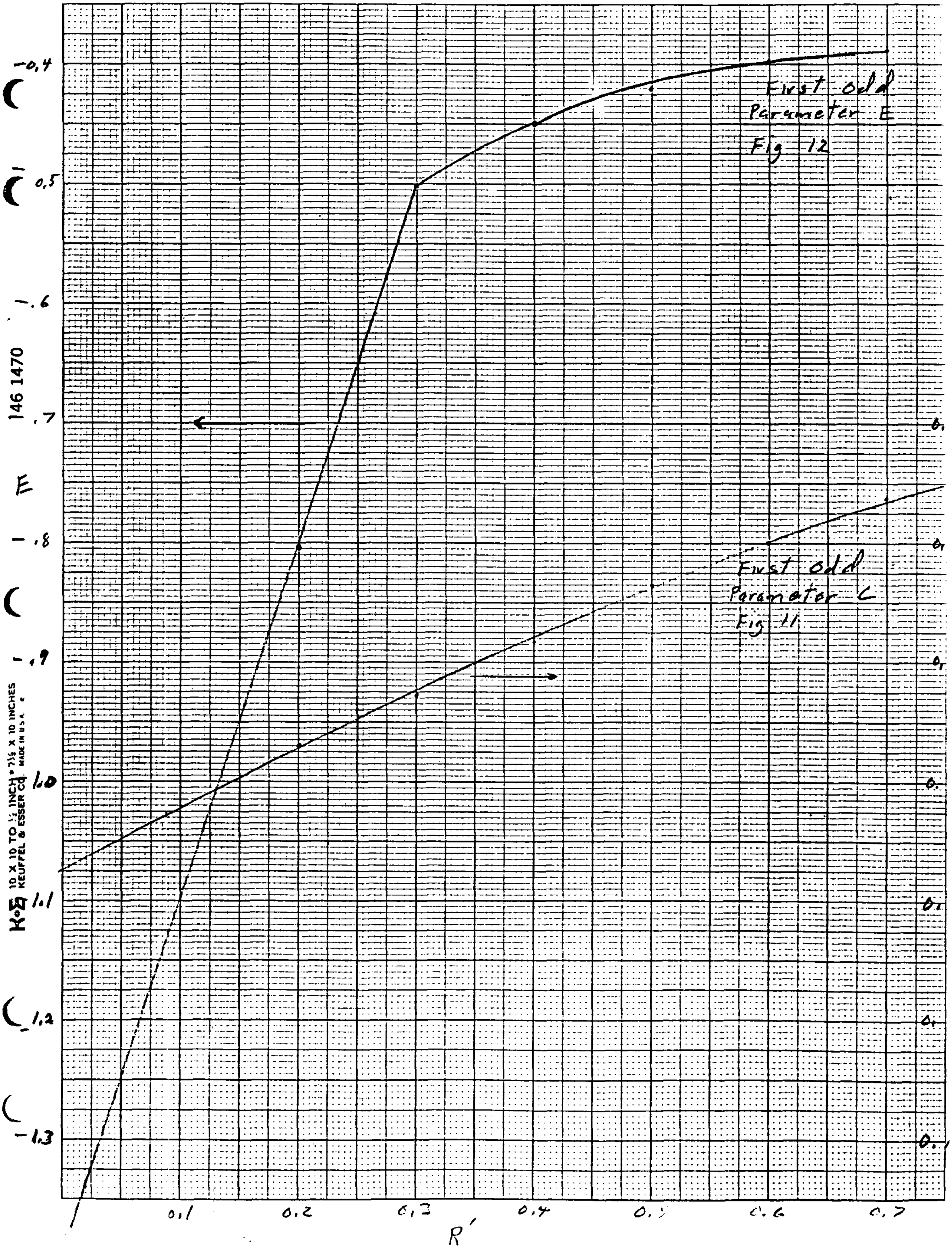

146 1470
K+E 10 X 10 TO 1/2 INCH • 7 1/2 X 10 INCHES KEUFFEL & ESSER CO. MADE IN U.S.A.

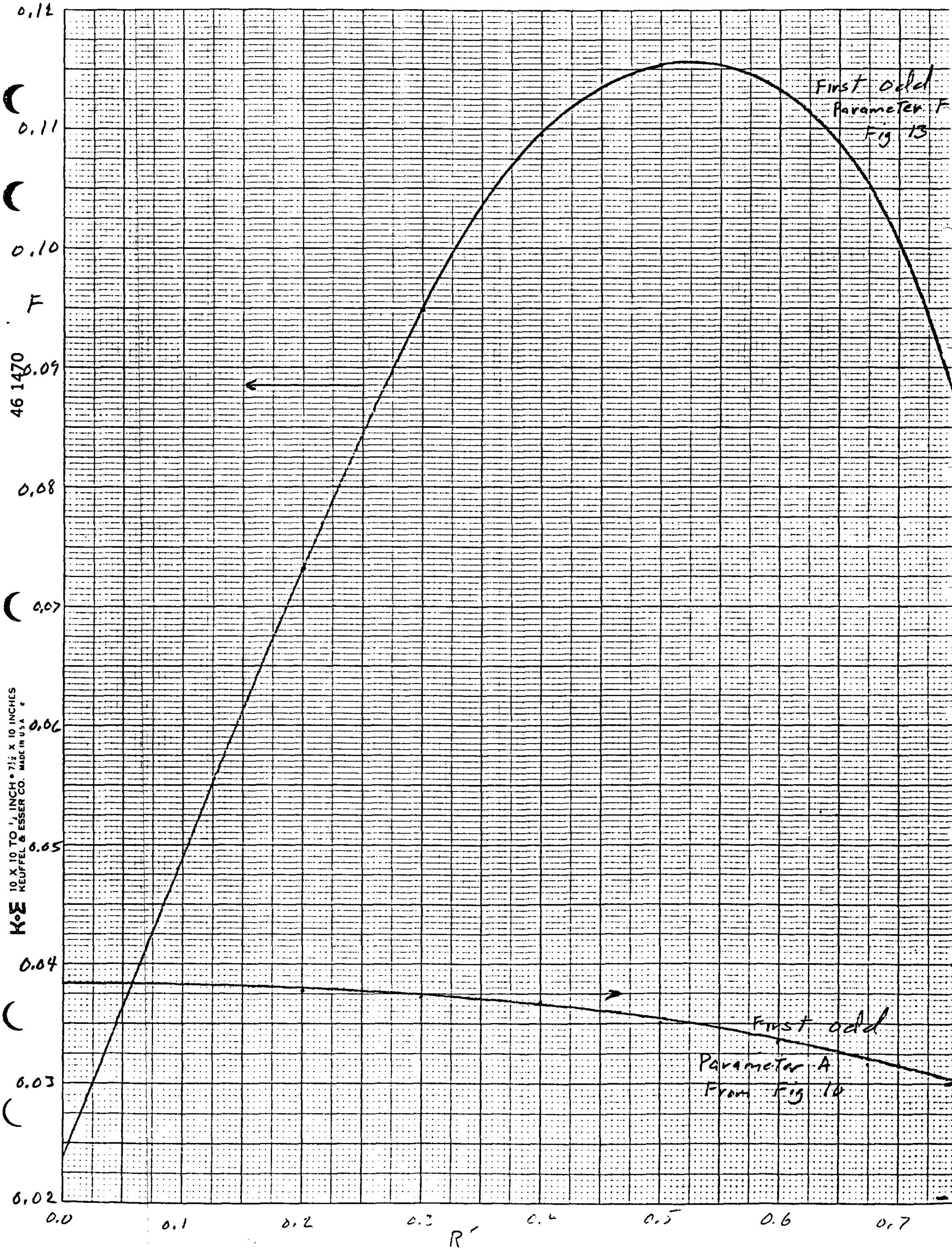

0.12
0.11
0.10
F
0.09
0.08
0.07
0.06
0.05
0.04
0.03
0.02
0.0
0.1
0.2
0.3
0.4
0.5
0.6
0.7
R'
First odd Parameter F Fig 13
First odd Parameter A From Fig 10
46 1470
K+E 10 X 10 TO 1/2 INCH • 7 1/2 X 10 INCHES KEUFFEL & ESSER CO. MADE IN U.S.A.

From Loddy #1 PVT Data

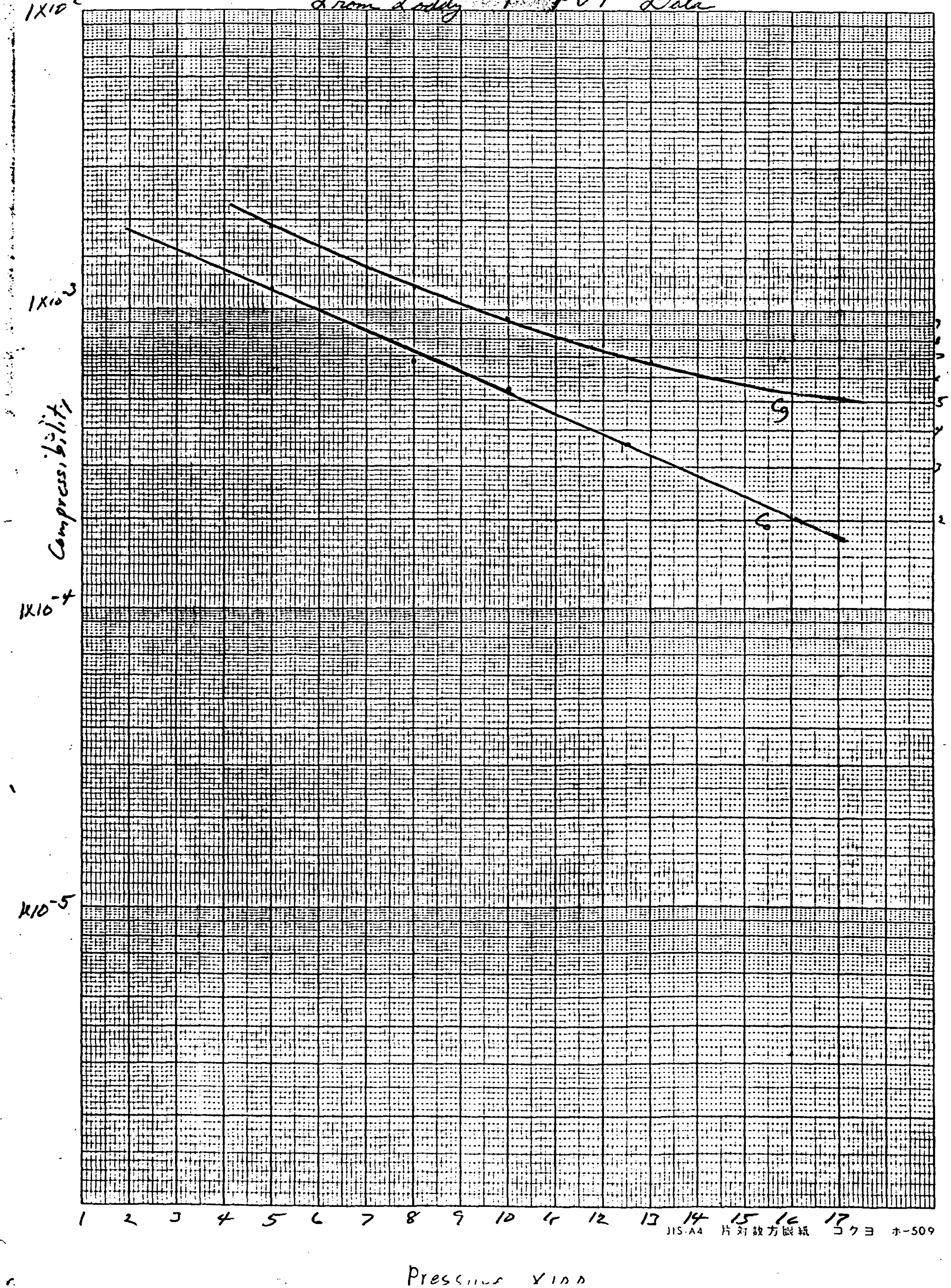

Frac Pulse Analysis
Kamal Method

Frac Well	TAP 4
Response Well	E-6
Date	2/13/86
Static Pressure, psig	1691
Pump Time, hr	0.672
Signal Time, hr	32.16
Lag Time, hr	16.08
Peak dP/q	7.09E-06
Constants from Figures 10-13	
A =	-0.815
C =	0.335
E =	-1.34
F =	0.029
D =	-0.325
Total Cycle Time, dTcyc =	32.832
Pulse Ratio, R' =	0.020467
Demensionless Time Lag, TlD =	0.489766
Demensionless Cycle Period, dTcycD =	0.274382
Demensionless Response Amplitude, dPD =	0.006871
Average Formation Volume Factor, B =	1.41
Average Viscosity, cp =	0.53
Distance Between Wells, ft	3448
kh = 70.6*B*µ*dPD/(dP/q) =	51135.35
∅Cth = kh*dTcyc/(56900*µ*r^2*dTcycD) =	1.71E-05
Oil Saturation, So =	0.87
Oil Compressibilty, Co =	1.75E-04
Gas Saturation, Sg =	0.03
Gas Compressibilty, Cg =	1.52E-04
Water Saturation, Sw =	0.1
Water Compressibility, Cw =	3.30E-06
Formation Compressibility, Cf =	1.00E-04
Total Compressibilty, Ct =	2.57E-04
∅h =	0.066369

Frac Pulse Analysis
Kamal Method

Frac Well	N-31
Response Well	E-6
Date	4/1/86
Static Pressure, psig	1660
Pump Time, hr	1.1232
Signal Time, hr	96
Lag Time, hr	42.72
Peak dP/q	4.40E-04
Constants from Figures 10-13	
A =	-0.815
C =	0.325
E =	-1.38
F =	0.0265
D =	-0.325
Total Cycle Time, dTcyc =	97.1232
Pulse Ratio, R' =	0.011564
Demensionless Time Lag, TlD =	0.439853
Demensionless Cycle Period, dTcycD =	0.309727
Demensionless Response Amplitude, dPD =	0.007570
Average Formation Volume Factor, B =	1.41
Average Viscosity, cp =	0.53
Distance Between Wells, ft	2858
kh = 70.6*B*μ*dPD/(dP/q) =	907.7466
øCth = kh*dTcyc/(56900*μ*r^2*dTcycD) =	1.16E-06
Oil Saturation, So =	0.87
Oil Compressibilty, Co =	1.85E-04
Gas Saturation, Sg =	0.03
Gas Compressibilty, Cg =	1.52E-04
Water Saturation, Sw =	0.1
Water Compressibility, Cw =	3.30E-06
Formation Compressibility, Cf =	1.00E-04
Total Compressibilty, Ct =	2.66E-04
øh =	0.004346

Frac Pulse Analysis
Kamal Method

Frac Well	F-30
Response Well	B-32
Date	9/4/86
Static Pressure, psig	1443
Pump Time, hr	1.3
Signal Time, hr	190
Lag Time, hr	90.5
Peak dP/q	6.70E-06
Constants from Figures 10-13	
A =	-0.815
C =	0.328
E =	-1.375
F =	0.025
D =	-0.325
Total Cycle Time, dTcyc =	191.3
Pulse Ratio, R' =	0.006795
Demensionless Time Lag, TlD =	0.473078
Demensionless Cycle Period, dTcycD =	0.278674
Demensionless Response Amplitude, dPD =	0.006422
Average Formation Volume Factor, B =	1.41
Average Viscosity, cp =	0.53
Distance Between Wells, ft	7000
kh = 70.6*B*µ*dPD/(dP/q) =	50570.35
ØCth = kh*dTcyc/(56900*µ*r^2*dTcycD) =	2.35E-05
Oil Saturation, So =	0.87
Oil Compressibilty, Co =	2.60E-04
Gas Saturation, Sg =	0.03
Gas Compressibilty, Cg =	5.90E-04
Water Saturation, Sw =	0.1
Water Compressibility, Cw =	3.30E-06
Formation Compressibility, Cf =	1.00E-04
Total Compressibilty, Ct =	3.44E-04
Øh =	0.068246

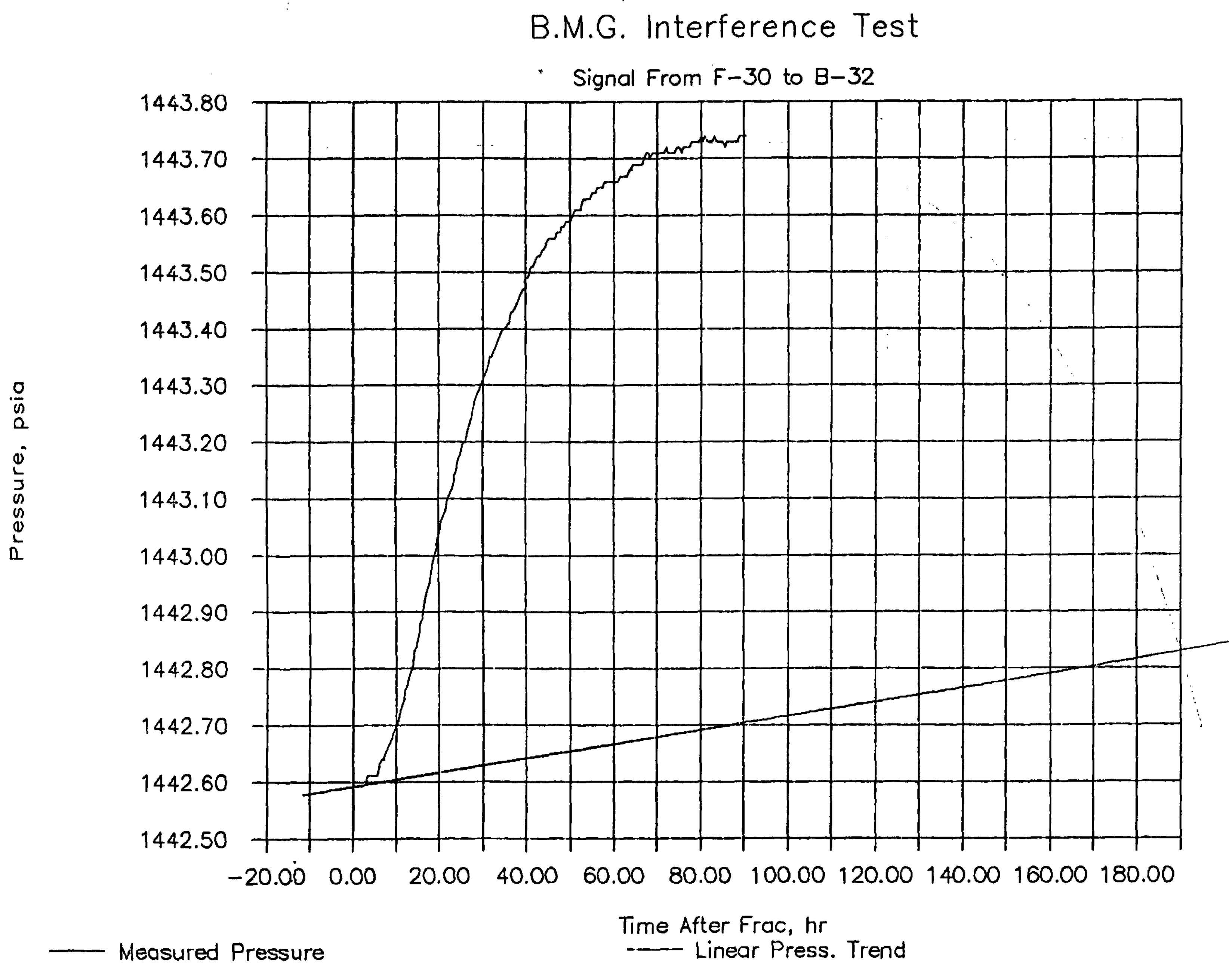
B.M.G. Interference Test
Signal From F-30 to B-32
Pressure, psia
1443.80
1443.70
1443.60
1443.50
1443.40
1443.30
1443.20
1443.10
1443.00
1442.90
1442.80
1442.70
1442.60
1442.50
-20.00
0.00
20.00
40.00
60.00
80.00
100.00
120.00
140.00
160.00
180.00
Time After Frac, hr
Measured Pressure
Linear Press. Trend

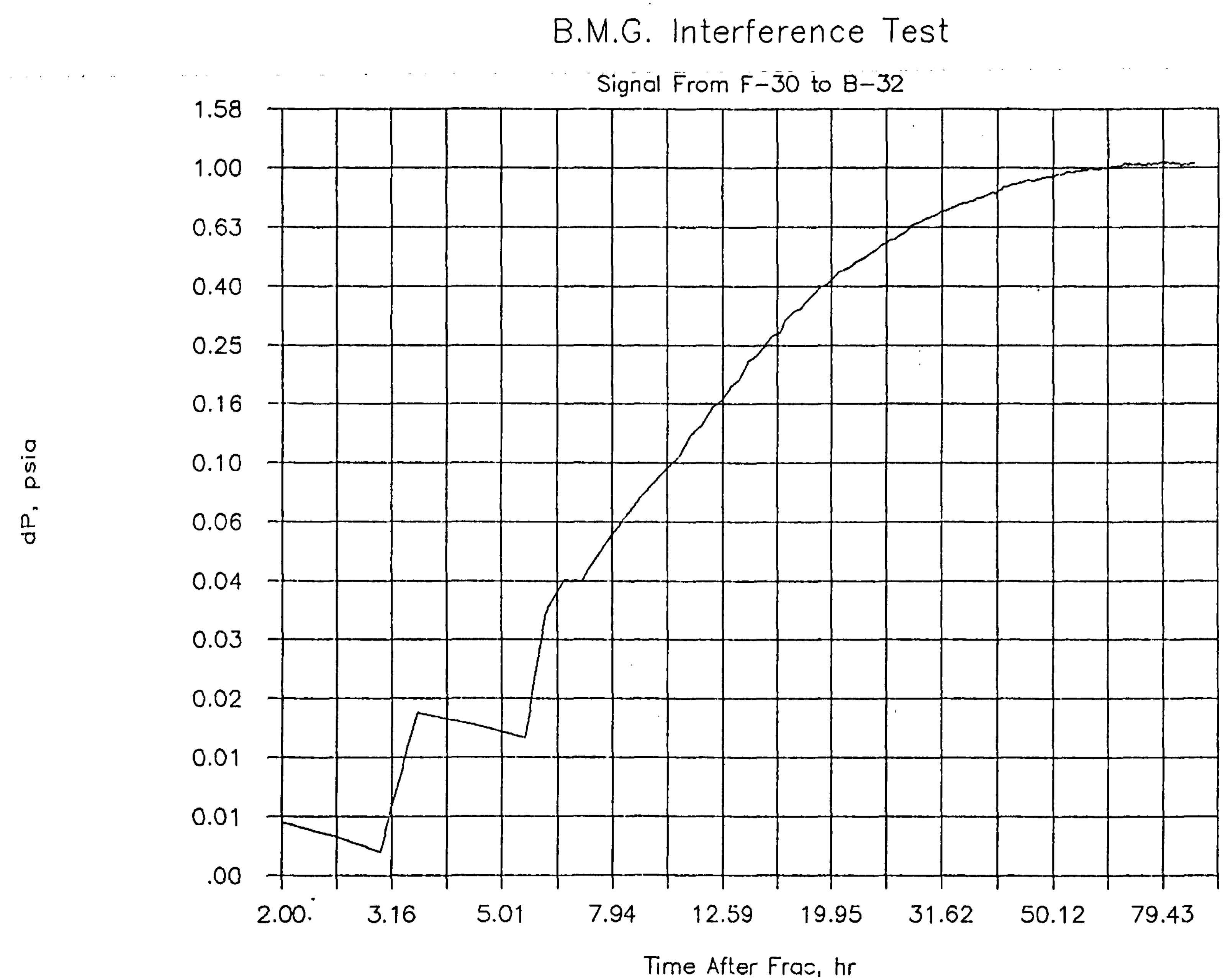
B.M.G. Interference Test
Signal From F-30 to B-32
dP, psia
1.58
1.00
0.63
0.40
0.25
0.16
0.10
0.06
0.04
0.03
0.02
0.01
0.01
.00
2.00
3.16
5.01
7.94
12.59
19.95
31.62
50.12
79.43
Time After Frac, hr

Frac Pulse Analysis
Kamal Method

Frac Well	C-34
Response Well	B-32
Date	4/23/87
Static Pressure, psig	1237
Pump Time, hr	1.7
Signal Time, hr	215
Lag Time, hr	96
Peak dP/q	8.83E-06
Constants from Figures 10-13	
A =	-0.815
C =	0.328
E =	-1.375
F =	0.025
D =	-0.325
Total Cycle Time, dTcyc =	216.7
Pulse Ratio, R' =	0.007844
Demensionless Time Lag, T1D =	0.443008
Demensionless Cycle Period, dTcycD =	0.311865
Demensionless Response Amplitude, dPD =	0.007358
Average Formation Volume Factor, B =	1.79
Average Viscosity, cp =	0.552
Distance Between Wells, ft	10411
kh = 70.6*B*μ*dPD/(dP/q) =	58134.34
ϕCth = kh*dTcyc/(56900*μ*r^2*dTcycD) =	1.19E-05
Oil Saturation, So =	0.87
Oil Compressibilty, Co =	3.60E-04
Gas Saturation, Sg =	0.03
Gas Compressibilty, Cg =	7.00E-04
Water Saturation, Sw =	0.1
Water Compressibility, Cw =	3.30E-06
Formation Compressibility, Cf =	1.00E-04
Total Compressibilty, Ct =	4.35E-04
ϕh =	0.027306

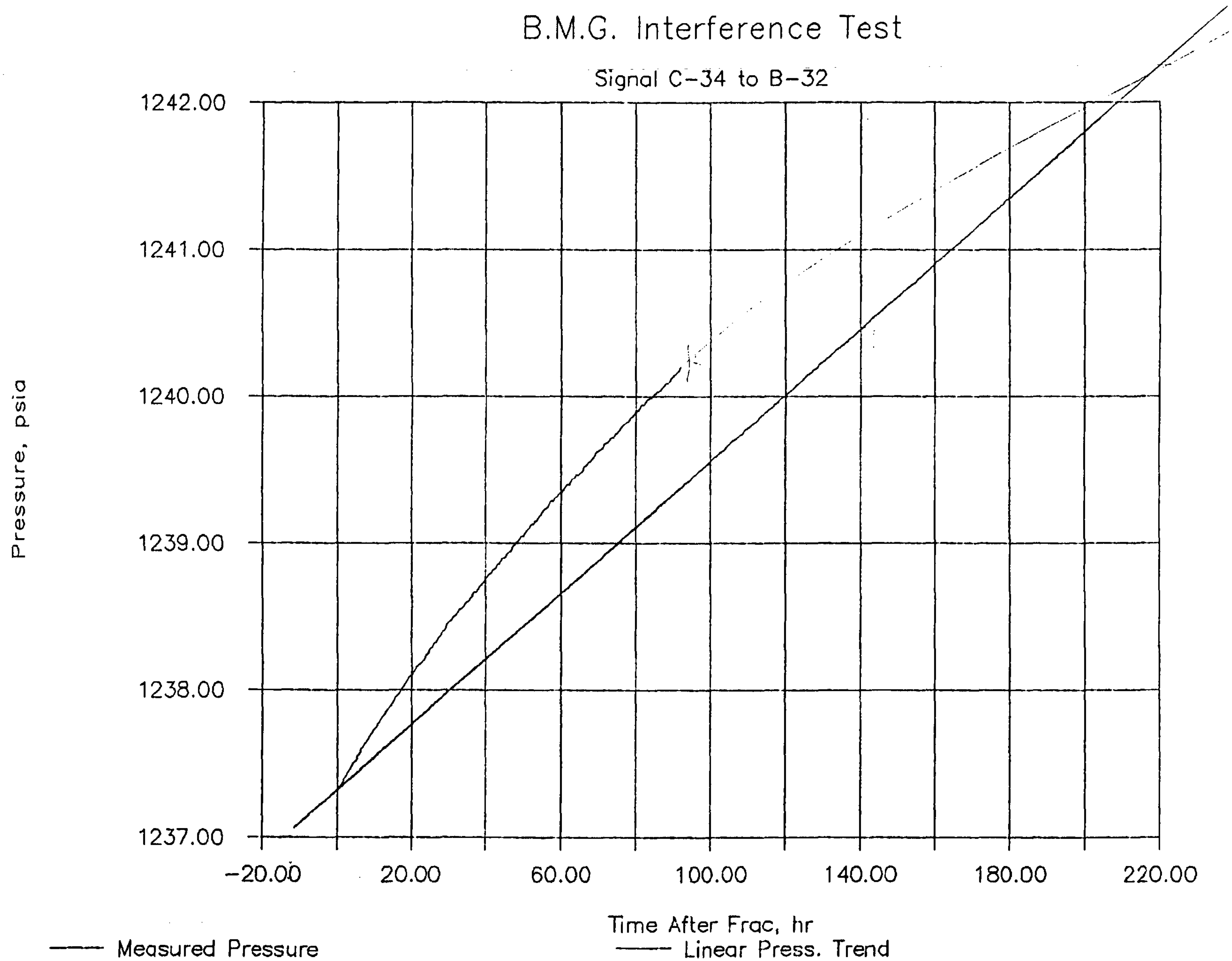

B.M.G. Interference Test
Signal C-34 to B-32
Pressure, psia
1242.00
1241.00
1240.00
1239.00
1238.00
1237.00
-20.00
20.00
60.00
100.00
140.00
180.00
220.00
Time After Frac, hr
Measured Pressure
Linear Press. Trend

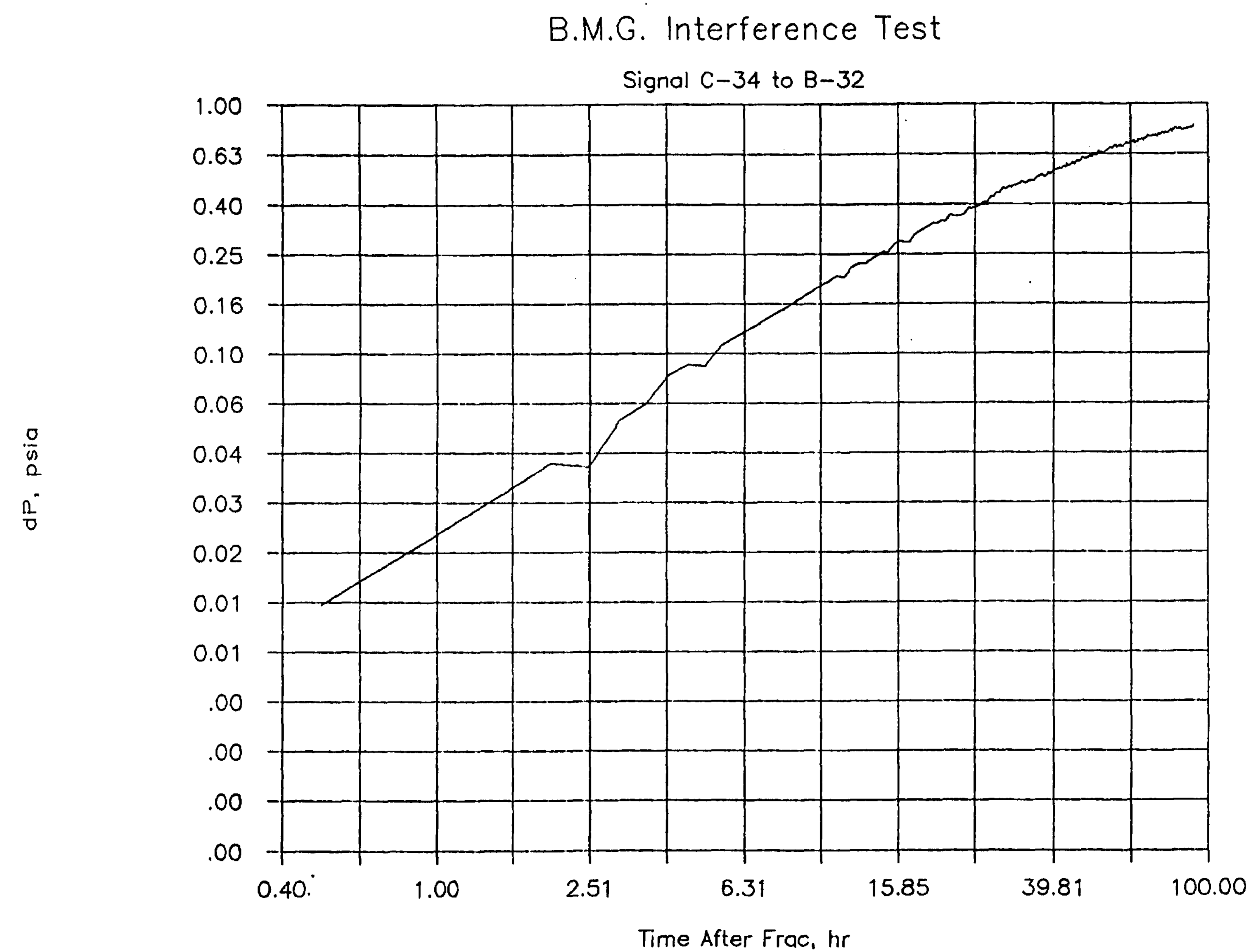
B.M.G. Interference Test
Signal C–34 to B–32
dP, psia
1.00
0.63
0.40
0.25
0.16
0.10
0.06
0.04
0.03
0.02
0.01
0.01
.00
.00
.00
.00
0.40
1.00
2.51
6.31
15.85
39.81
100.00
Time After Frac, hr

Frac Pulse Analysis
Kamal Method

Frac Well	C-34
Response Well	B-29
Date	4/23/87
Static Pressure, psig	1207
Pump Time, hr	1.7
Signal Time, hr	200
Lag Time, hr	99
Peak dP/q	7.63E-06
Constants from Figures 10-13	
A =	-0.815
C =	0.33
E =	-1.375
F =	0.026
D =	-0.325
Total Cycle Time, dTcyc =	201.7
Pulse Ratio, R' =	0.008428
Demensionless Time Lag, TlD =	0.490827
Demensionless Cycle Period, dTcycD =	0.264395
Demensionless Response Amplitude, dPD =	0.006144
Average Formation Volume Factor, B =	1.79
Average Viscosity, cp =	0.552
Distance Between Wells, ft	11222
kh = 70.6*B*µ*dPD/(dP/q) =	56176.33
ØCth = kh*dTcyc/(56900*µ*r^2*dTcycD) =	1.08E-05
Oil Saturation, So =	0.87
Oil Compressibilty, Co =	3.80E-04
Gas Saturation, Sg =	0.03
Gas Compressibilty, Cg =	7.20E-04
Water Saturation, Sw =	0.1
Water Compressibility, Cw =	3.30E-06
Formation Compressibility, Cf =	1.00E-04
Total Compressibilty, Ct =	4.53E-04
Øh =	0.023942

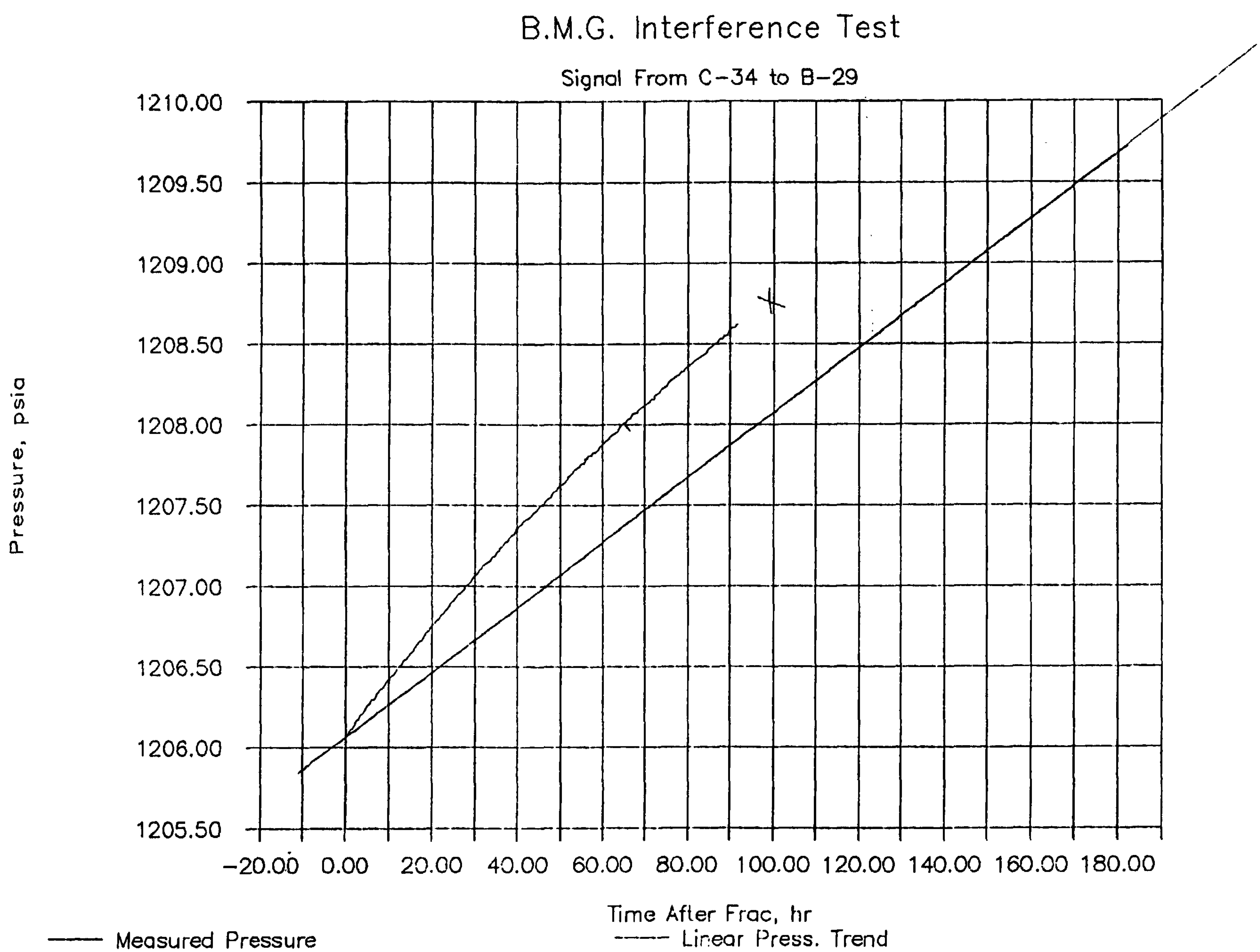

B.M.G. Interference Test
Signal From C-34 to B-29
Pressure, psia
1210.00
1209.50
1209.00
1208.50
1208.00
1207.50
1207.00
1206.50
1206.00
1205.50
-20.00
0.00
20.00
40.00
60.00
80.00
100.00
120.00
140.00
160.00
180.00
Time After Frac, hr
Measured Pressure
Linear Press. Trend

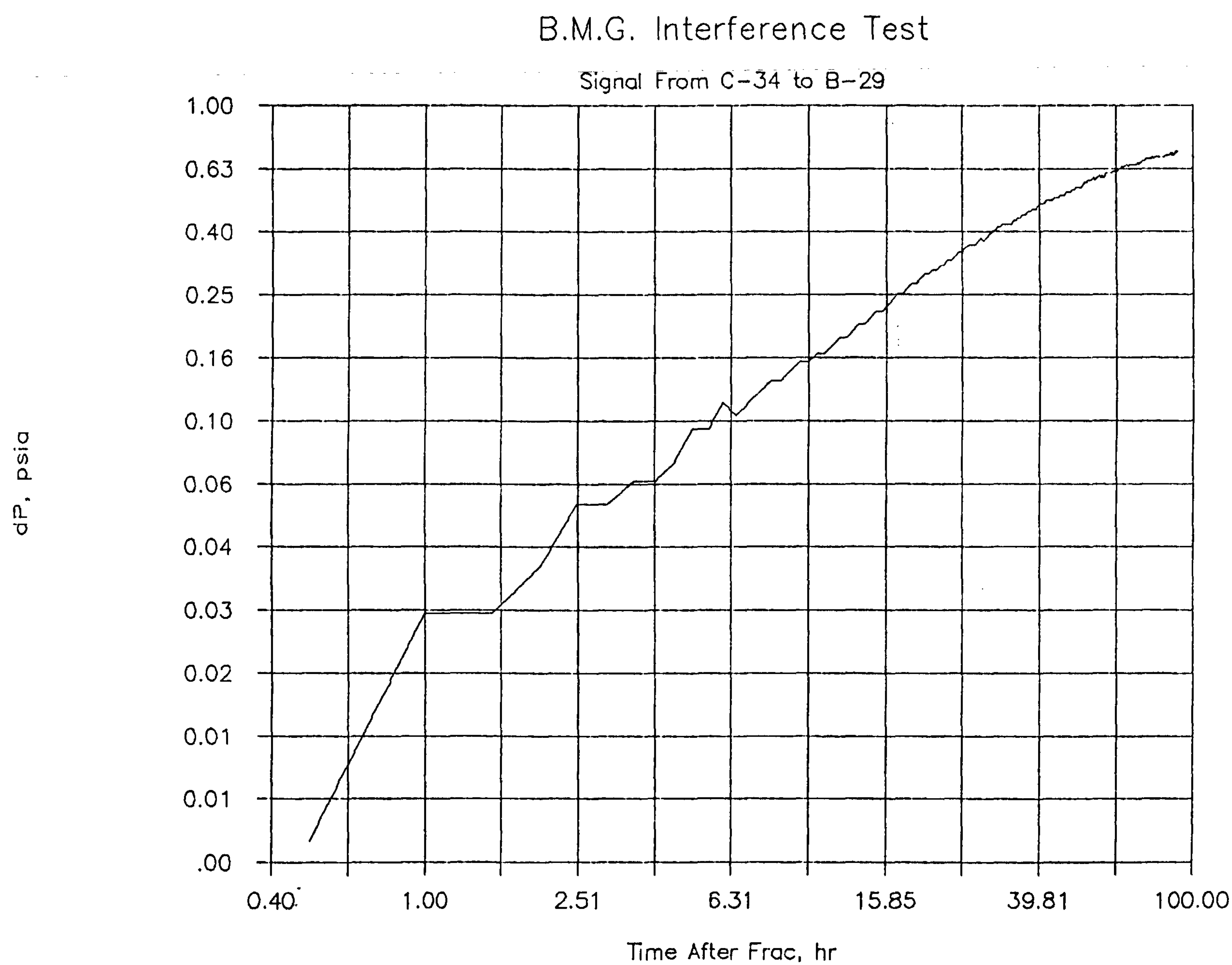
B.M.G. Interference Test
Signal From C-34 to B-29
1.00
0.63
0.40
0.25
0.16
0.10
0.06
0.04
0.03
0.02
0.01
0.01
.00
dP, psia
0.40
1.00
2.51
6.31
15.85
39.81
100.00
Time After Frac, hr

Frac Pulse Analysis
Kamal Method

Frac Well	A-16
Response Well	A-20
Date	5/11/87
Static Pressure, psig	1234
Pump Time, hr	1.6
Signal Time, hr	68
Lag Time, hr	13
Peak dP/q	1.05E-06
Constants from Figures 10-13	
A =	-0.815
C =	0.335
E =	-1.34
F =	0.029
D =	-0.325
Total Cycle Time, dTcyc =	69.6
Pulse Ratio, R' =	0.022988
Demensionless Time Lag, TlD =	0.186781
Demensionless Cycle Period, dTcycD =	0.989944
Demensionless Response Amplitude, dPD =	0.032251
Average Formation Volume Factor, B =	1.8
Average Viscosity, cp =	0.555
Distance Between Wells, ft	7312
kh = 70.6*B*μ*dPD/(dP/q) =	2166337.
øCth = kh*dTcyc/(56900*μ*r^2*dTcycD) =	9.02E-05
Oil Saturation, So =	0.87
Oil Compressibilty, Co =	3.60E-04
Gas Saturation, Sg =	0.03
Gas Compressibilty, Cg =	7.00E-04
Water Saturation, Sw =	0.1
Water Compressibility, Cw =	3.30E-06
Formation Compressibility, Cf =	1.00E-04
Total Compressibilty, Ct =	4.35E-04
øh =	0.207599

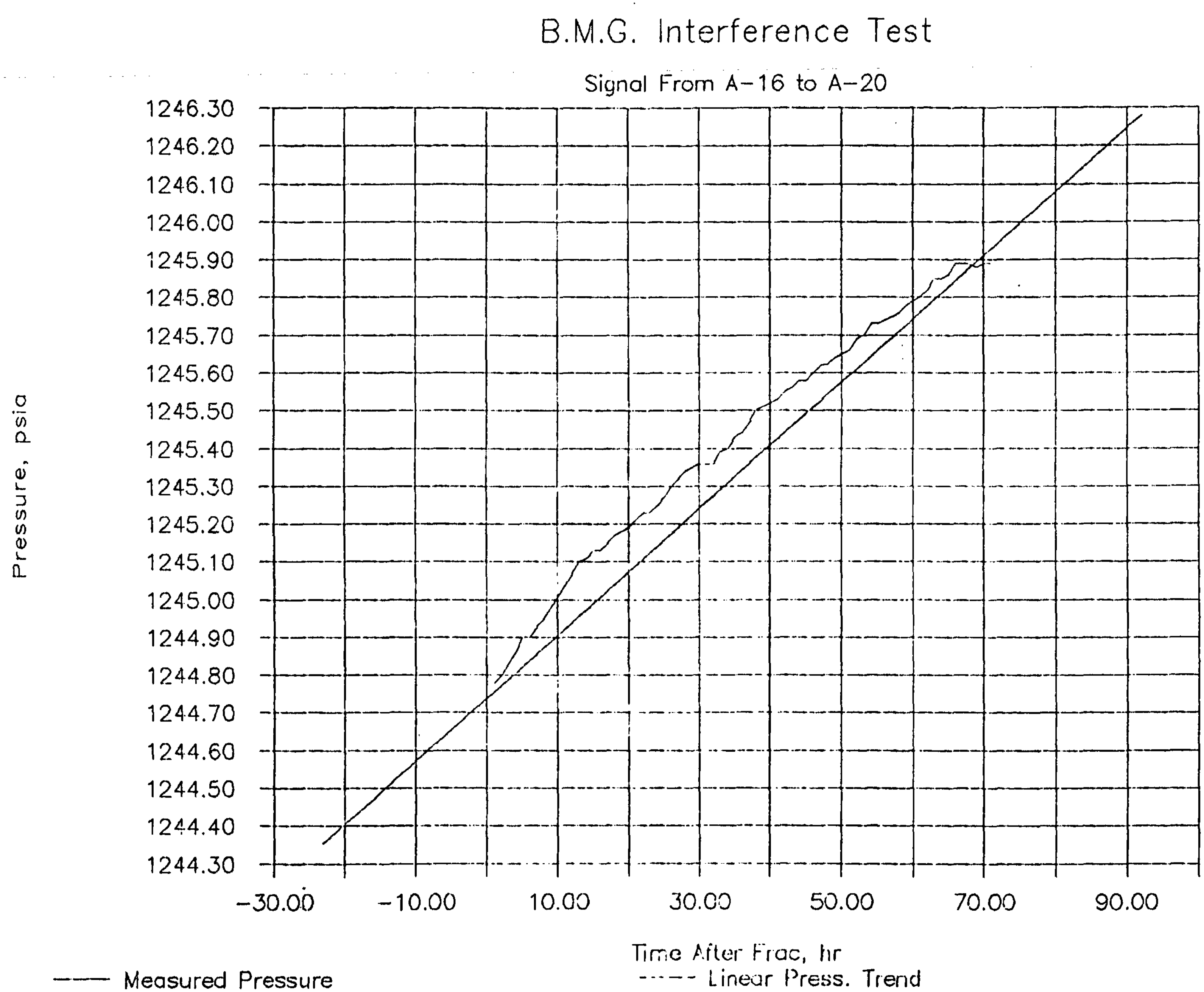
B.M.G. Interference Test
Signal From A-16 to A-20
1246.30
1246.20
1246.10
1246.00
1245.90
1245.80
1245.70
1245.60
1245.50
1245.40
1245.30
1245.20
1245.10
1245.00
1244.90
1244.80
1244.70
1244.60
1244.50
1244.40
1244.30
Pressure, psia
-30.00
-10.00
10.00
30.00
50.00
70.00
90.00
Time After Frac, hr
Measured Pressure
Linear Press. Trend

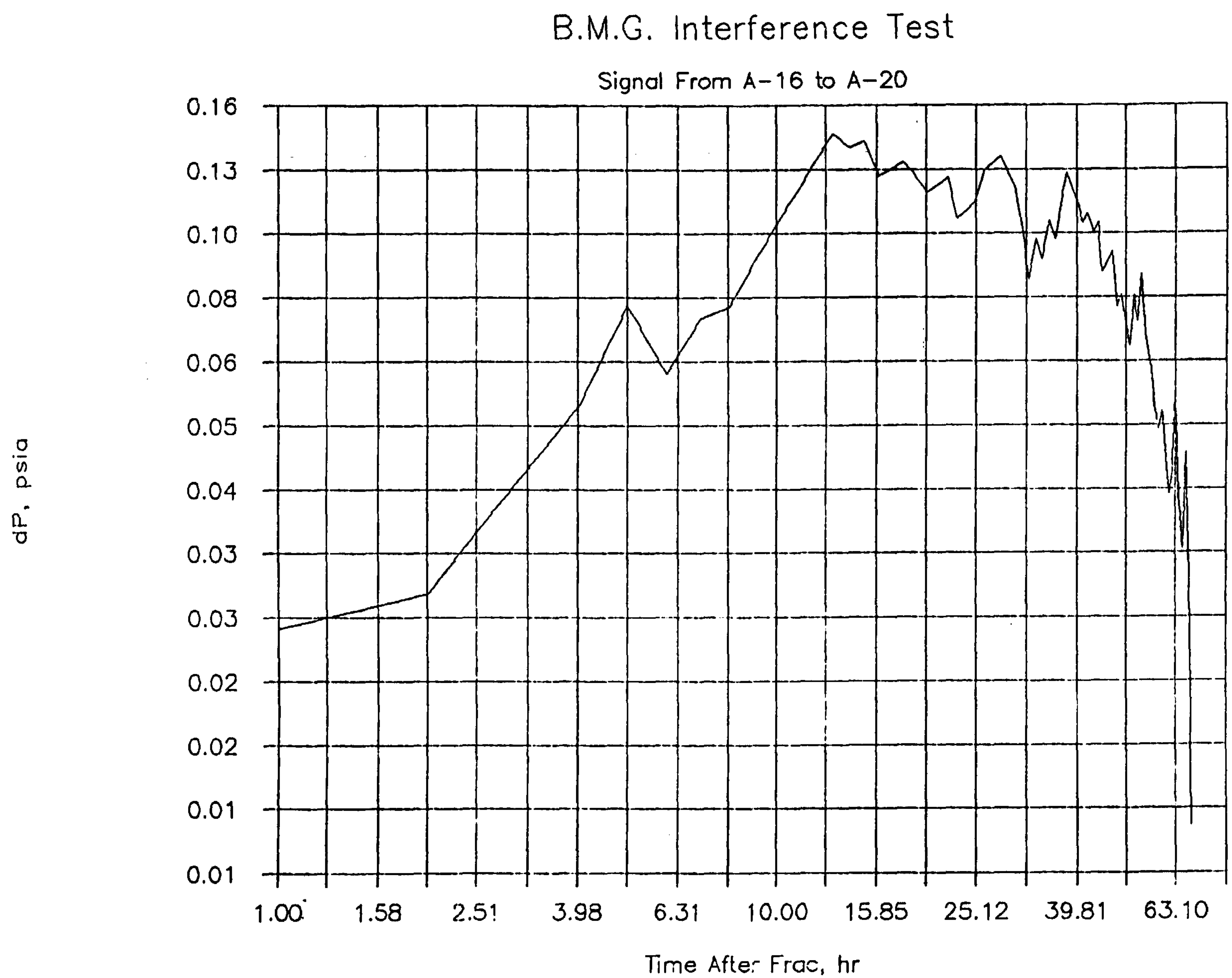
B.M.G. Interference Test
Signal From A-16 to A-20
0.16
0.13
0.10
0.08
0.06
0.05
0.04
0.03
0.03
0.02
0.02
0.01
0.01
dP, psia
1.00
1.58
2.51
3.98
6.31
10.00
15.85
25.12
39.81
63.10
Time After Frac, hr

Frac Pulse Analysis
Kamal Method

Frac Well	A-16
Response Well	B-32
Date	5/11/87
Static Pressure, psig	1240
Pump Time, hr	1.6
Signal Time, hr	470
Lag Time, hr	150
Peak dP/q	3.65E-05
Constants from Figures 10-13	
A =	-0.815
C =	0.328
E =	-1.375
F =	0.025
D =	-0.325
Total Cycle Time, dTcyc =	471.6
Pulse Ratio, R' =	0.003392
Demensionless Time Lag, TlD =	0.318066
Demensionless Cycle Period, dTcycD =	0.509299
Demensionless Response Amplitude, dPD =	0.013315
Average Formation Volume Factor, B =	1.8
Average Viscosity, cp =	0.555
Distance Between Wells, ft	16538
kh = 70.6*B*µ*dPD/(dP/q) =	25728.77
ØCth = kh*dTcyc/(56900*µ*r^2*dTcycD) =	2.76E-06
Oil Saturation, So =	0.87
Oil Compressibilty, Co =	3.60E-04
Gas Saturation, Sg =	0.03
Gas Compressibilty, Cg =	7.00E-04
Water Saturation, Sw =	0.1
Water Compressibility, Cw =	3.30E-06
Formation Compressibility, Cf =	1.00E-04
Total Compressibilty, Ct =	4.35E-04
Øh =	0.006347

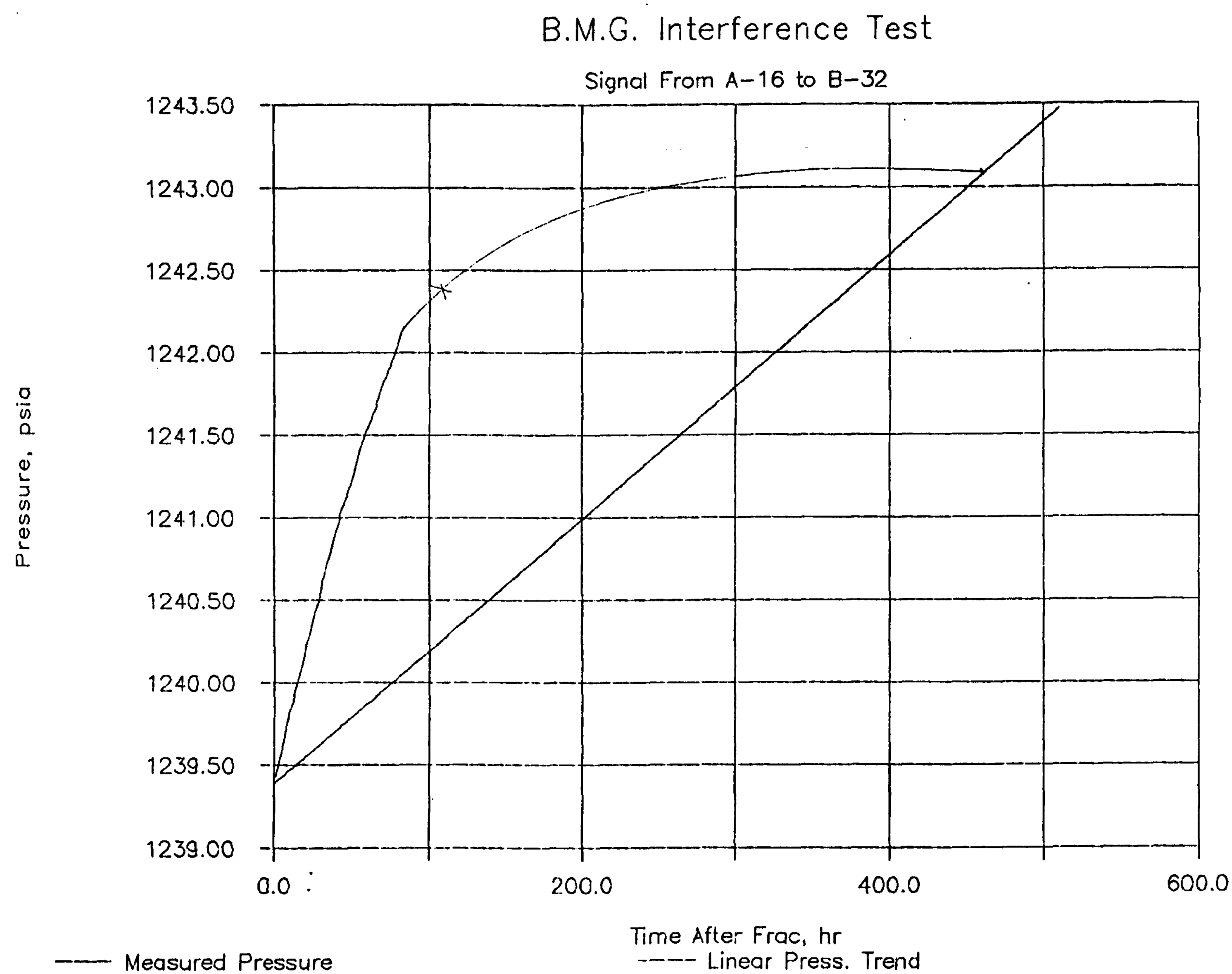
B.M.G. Interference Test
Signal From A-16 to B-32
Pressure, psia
1243.50
1243.00
1242.50
1242.00
1241.50
1241.00
1240.50
1240.00
1239.50
1239.00
0.0
200.0
400.0
600.0
Time After Frac, hr
Measured Pressure
Linear Press. Trend

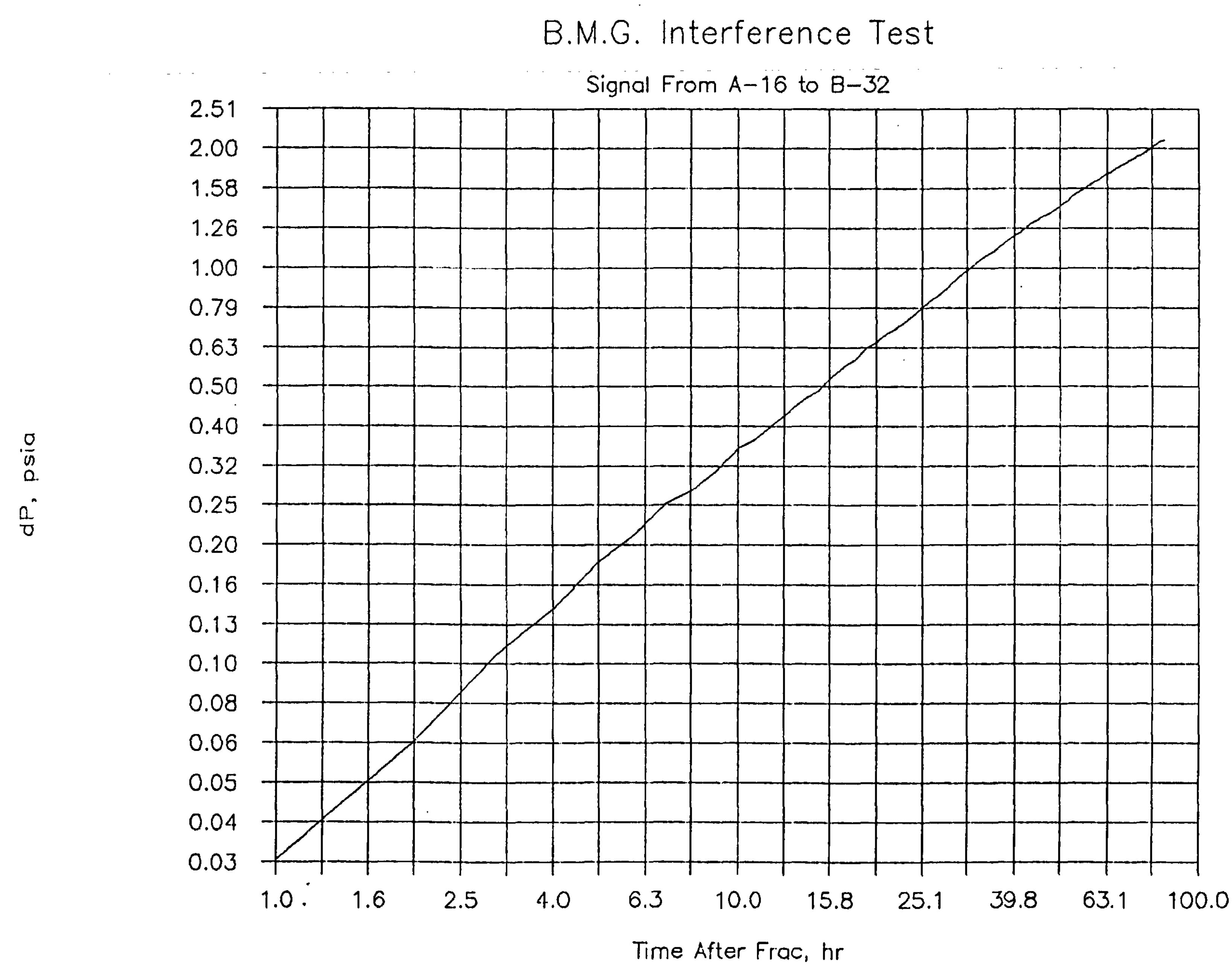
B.M.G. Interference Test
Signal From A-16 to B-32
dP, psia
2.51
2.00
1.58
1.26
1.00
0.79
0.63
0.50
0.40
0.32
0.25
0.20
0.16
0.13
0.10
0.08
0.06
0.05
0.04
0.03
1.0
1.6
2.5
4.0
6.3
10.0
15.8
25.1
39.8
63.1
100.0
Time After Frac, hr

Frac Pulse Analysis
Kamal Method

Frac Well	D-17
Response Well	A-20
Date	5/27/87
Static Pressure, psig	1240
Pump Time, hr	1.63
Signal Time, hr	80
Lag Time, hr	35.5
Peak dP/q	1.41E-06
Constants from Figures 10-13	
A =	-0.815
C =	0.337
E =	-1.34
F =	0.0285
D =	-0.325
Total Cycle Time, dTcyc =	81.63
Pulse Ratio, R' =	0.019968
Demensionless Time Lag, T1D =	0.434889
Demensionless Cycle Period, dTcycD =	0.339280
Demensionless Response Amplitude, dPD =	0.008791
Average Formation Volume Factor, B =	1.86
Average Viscosity, cp =	0.559
Distance Between Wells, ft	12787
kh = 70.6*B*μ*dPD/(dP/q) =	457710.6
ϕCth = kh*dTcyc/(56900*μ*r^2*dTcycD) =	2.12E-05
Oil Saturation, So =	0.87
Oil Compressibilty, Co =	3.60E-04
Gas Saturation, Sg =	0.03
Gas Compressibilty, Cg =	7.00E-04
Water Saturation, Sw =	0.1
Water Compressibility, Cw =	3.30E-06
Formation Compressibility, Cf =	1.00E-04
Total Compressibilty, Ct =	4.35E-04
ϕh =	0.048730

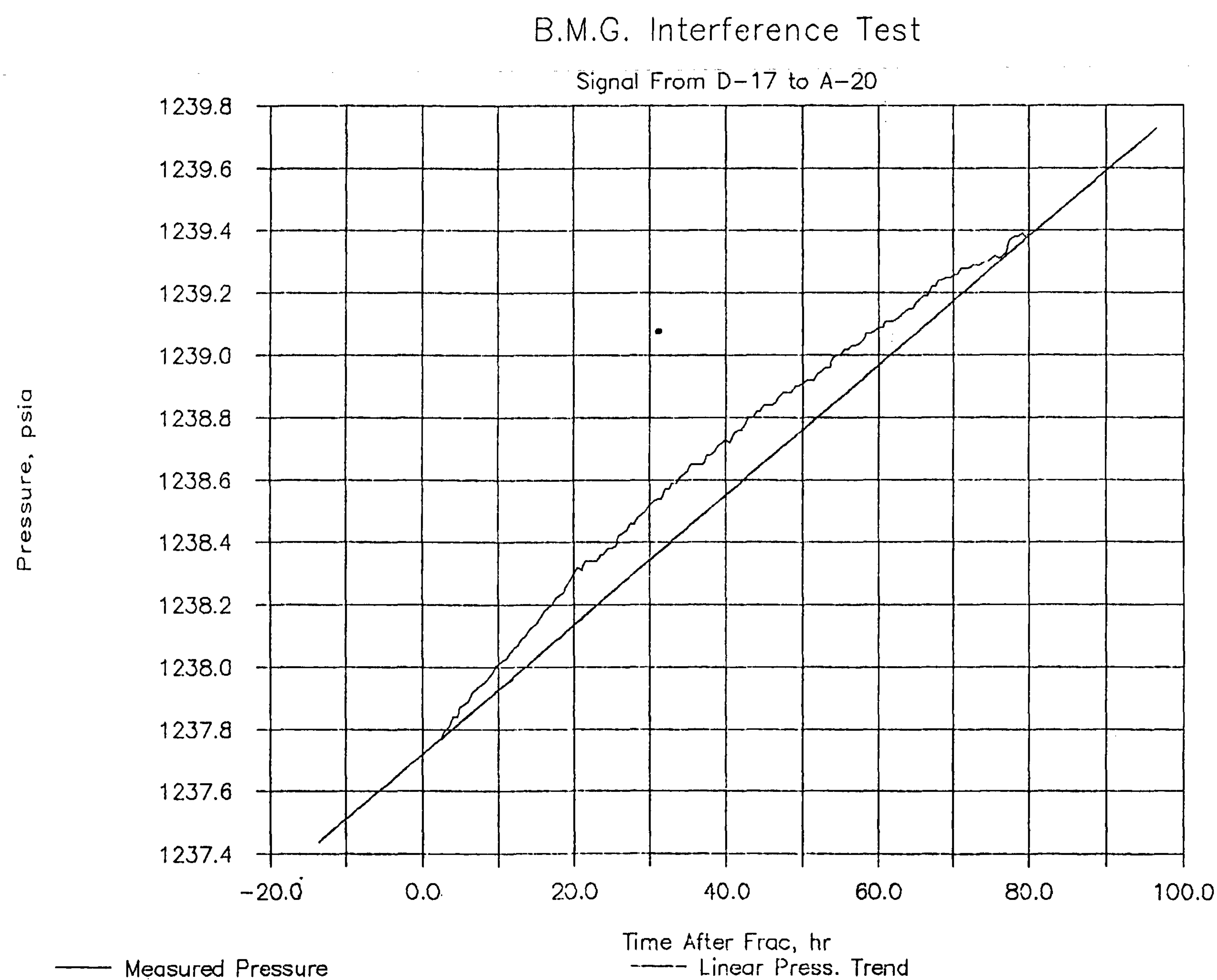
B.M.G. Interference Test
Signal From D-17 to A-20
Pressure, psia
1239.8
1239.6
1239.4
1239.2
1239.0
1238.8
1238.6
1238.4
1238.2
1238.0
1237.8
1237.6
1237.4
-20.0
0.0
20.0
40.0
60.0
80.0
100.0
Time After Frac, hr
Measured Pressure
Linear Press. Trend

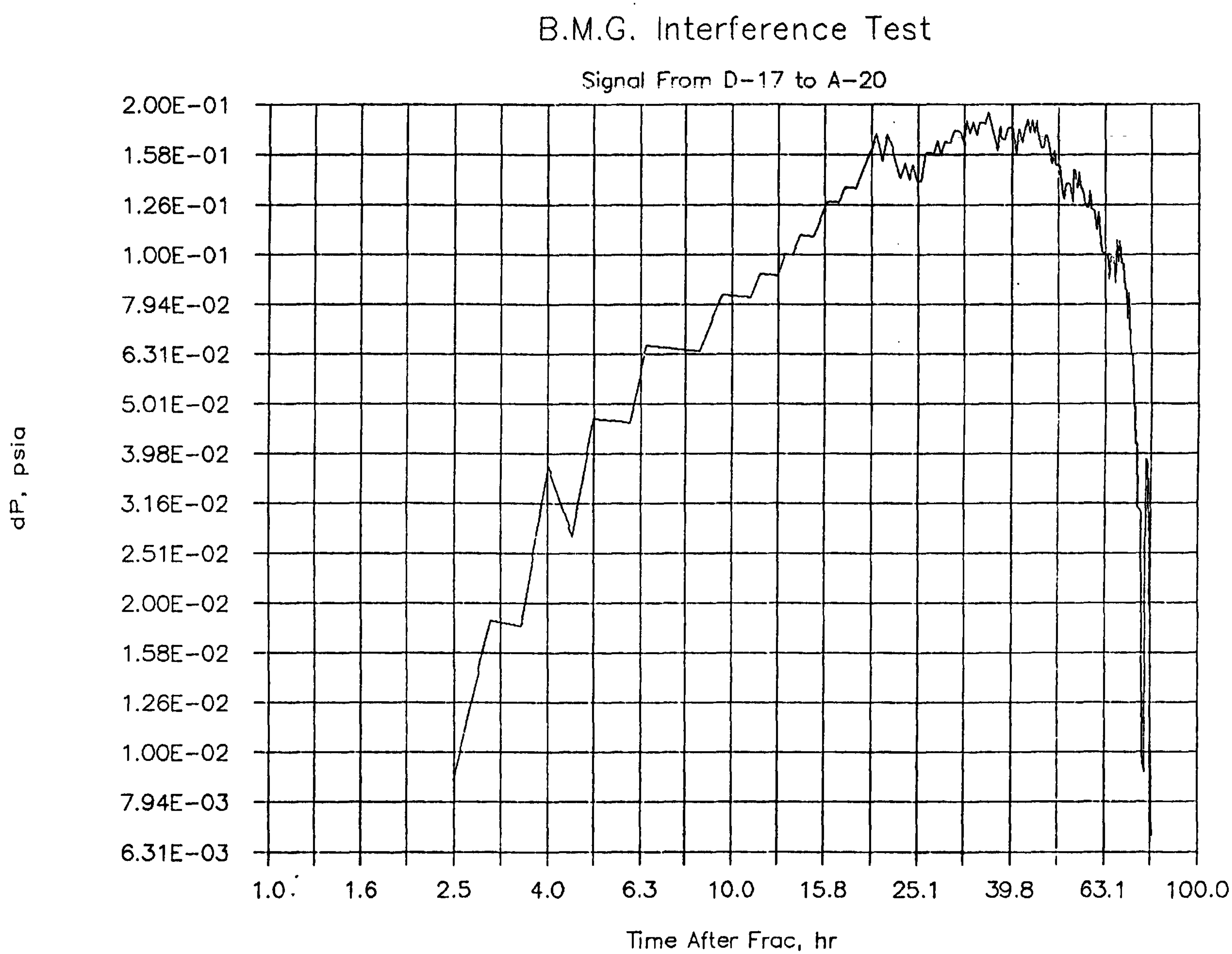

B.M.G. Interference Test
Signal From D-17 to A-20
dP, psia
2.00E-01
1.58E-01
1.26E-01
1.00E-01
7.94E-02
6.31E-02
5.01E-02
3.98E-02
3.16E-02
2.51E-02
2.00E-02
1.58E-02
1.26E-02
1.00E-02
7.94E-03
6.31E-03
1.0
1.6
2.5
4.0
6.3
10.0
15.8
25.1
39.8
63.1
100.0
Time After Frac, hr

Frac Pluse Analysis
Kamal Method

Frac Well	F-7
Response Well	D-17
Date	11/25/87
Static Pressure, psig	997
Pump Time, hr	1
Signal Time, hr	420
Lag Time, hr	115
Peak dP/q	0.000026
Constants from Figures 10-13	
A =	-0.815
C =	0.33
E =	-1.375
F =	0.024
D =	-0.325
Total Cycle Time, dTcyc =	421
Pulse Ratio, R' =	0.002375
Demensionless Time Lag, T1D =	0.273159
Demensionless Cycle Period, dTcycD =	0.625243
Demensionless Response Amplitude, dPD =	0.016559
Average Formation Volume Factor, B =	2.8867
Average Viscosity, cp =	0.48
Distance Between Wells, ft	3554
kh = 70.6*B*u*dPD/(dP/q) =	60671.99
OCth = kh*dTcyc/(56900*u*r^2*dTcycD) =	1.18E-04
Oil Saturation, So =	0.87
Oil Compressibilty, Co =	5.30E-04
Gas Saturation, Sg =	0.03
Gas Compressibilty, Cg =	9.20E-04
Water Saturation, Sw =	1.00E-01
Water Compressibility, Cw =	3.30E-06
Formation Compressibility, Cf =	1.00E-04
Total Compressibilty, Ct =	5.89E-04
Oh =	0.201045

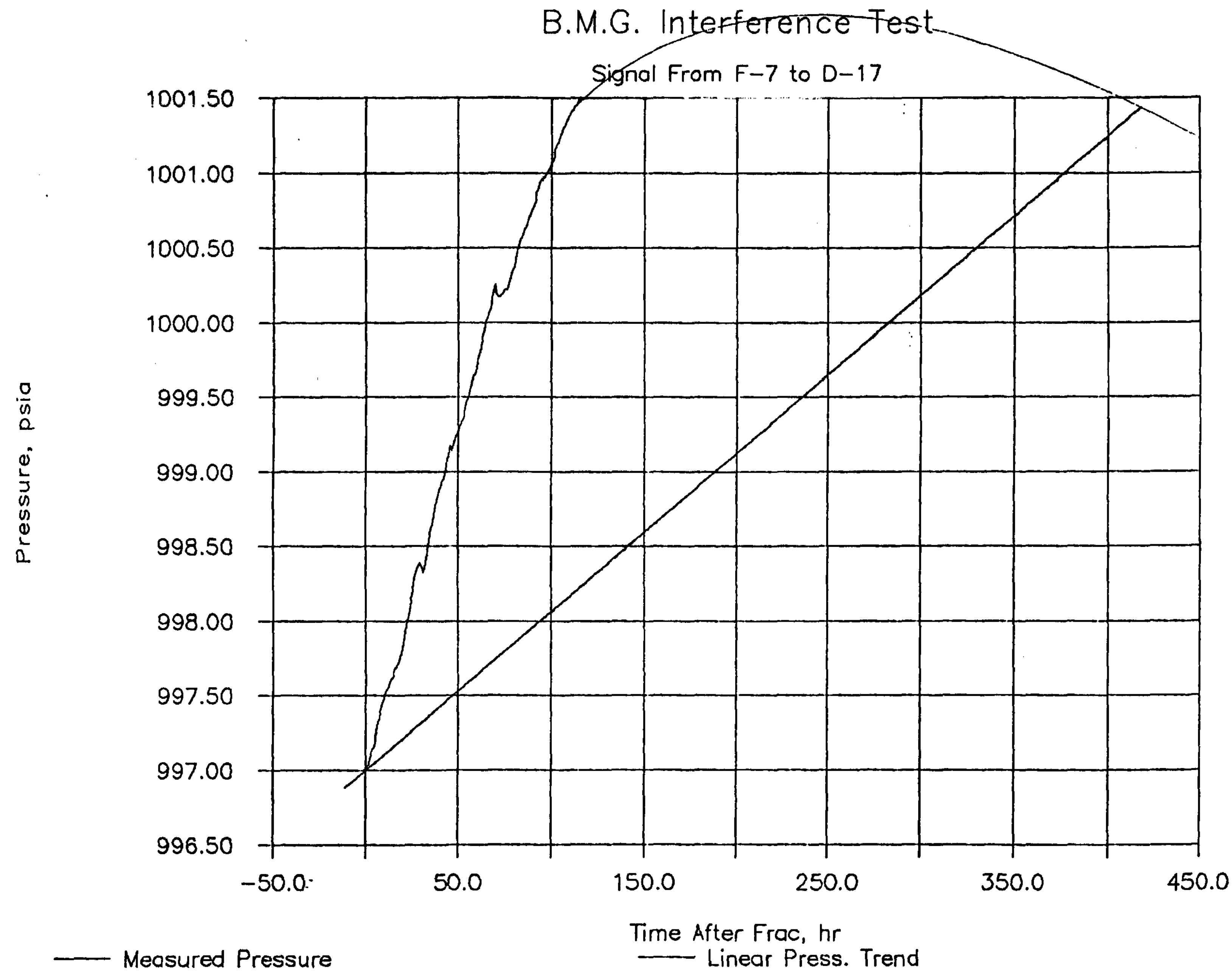
B.M.G. Interference Test
Signal From F-7 to D-17
Pressure, psia
1001.50
1001.00
1000.50
1000.00
999.50
999.00
998.50
998.00
997.50
997.00
996.50
-50.0
50.0
150.0
250.0
350.0
450.0
Time After Frac, hr
Measured Pressure
Linear Press. Trend

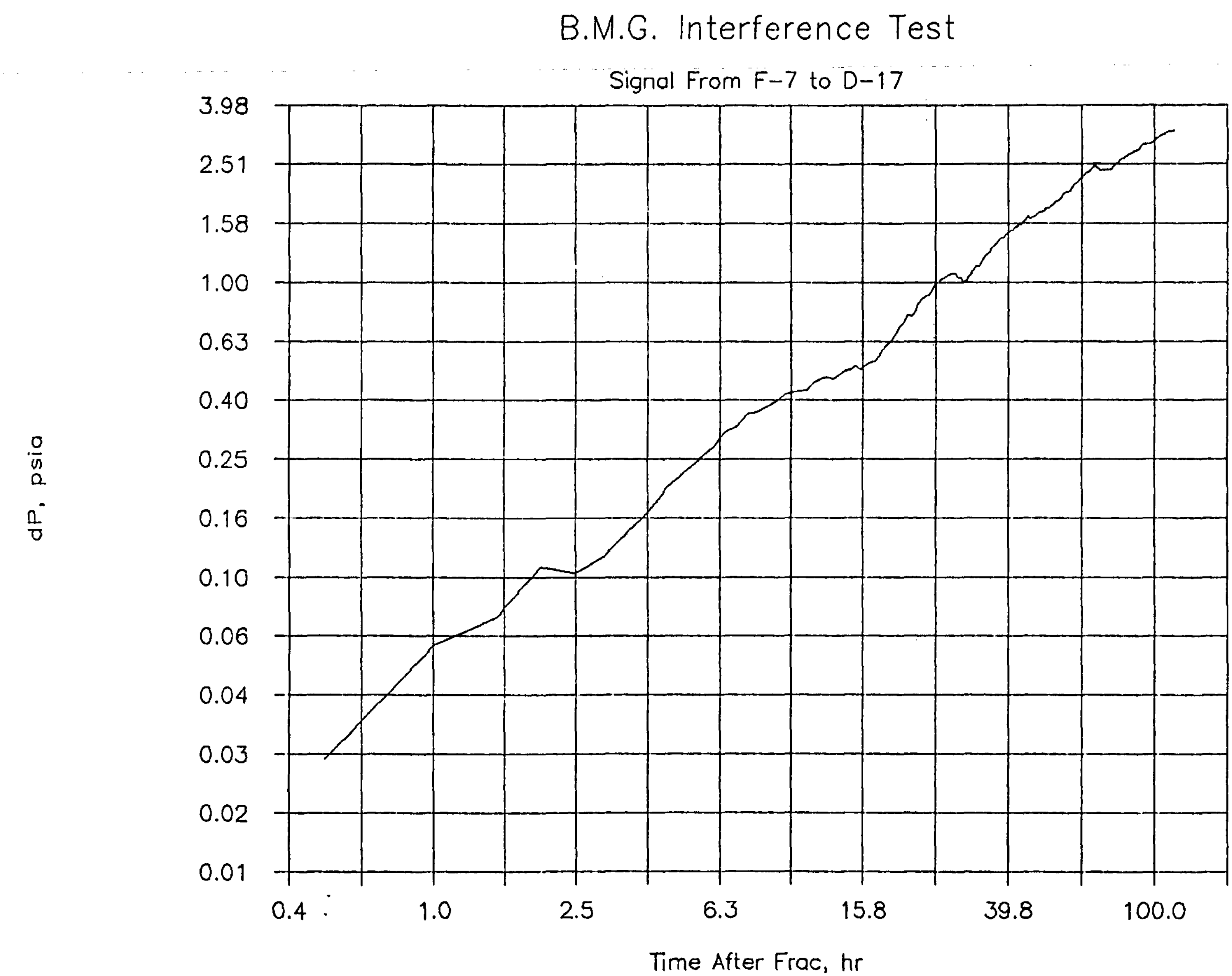
B.M.G. Interference Test
Signal From F-7 to D-17
dP, psia
3.98
2.51
1.58
1.00
0.63
0.40
0.25
0.16
0.10
0.06
0.04
0.03
0.02
0.01
0.4
1.0
2.5
6.3
15.8
39.8
100.0
Time After Frac, hr

Frac Pulse Analysis
Kamal Method

Frac Well	F-7
Response Well	E-6
Date	11/25/87
Static Pressure, psig	1032
Pump Time, hr	1
Signal Time, hr	62
Lag Time, hr	14
Peak dP/q	7.04E-06
Constants from Figures 10-13	
A =	-0.815
C =	0.335
E =	-1.35
F =	0.0225
D =	-0.325
Total Cycle Time, dTcyc =	63
Pulse Ratio, R' =	0.015873
Demensionless Time Lag, T1D =	0.222222
Demensionless Cycle Period, dTcycD =	0.816334
Demensionless Response Amplitude, dPD =	0.021770
Average Formation Volume Factor, B =	2.8867
Average Viscosity, cp =	0.4814
Distance Between Wells, ft	5280
kh = 70.6*B*µ*dPD/(dP/q) =	303392.7
øCth = kh*dTcyc/(56900*µ*r^2*dTcycD) =	3.07E-05
Oil Saturation, So =	0.87
Oil Compressibilty, Co =	5.00E-04
Gas Saturation, Sg =	0.03
Gas Compressibilty, Cg =	8.80E-04
Water Saturation, Sw =	0.1
Water Compressibility, Cw =	3.30E-06
Formation Compressibility, Cf =	1.00E-04
Total Compressibilty, Ct =	5.62E-04
øh =	0.054583

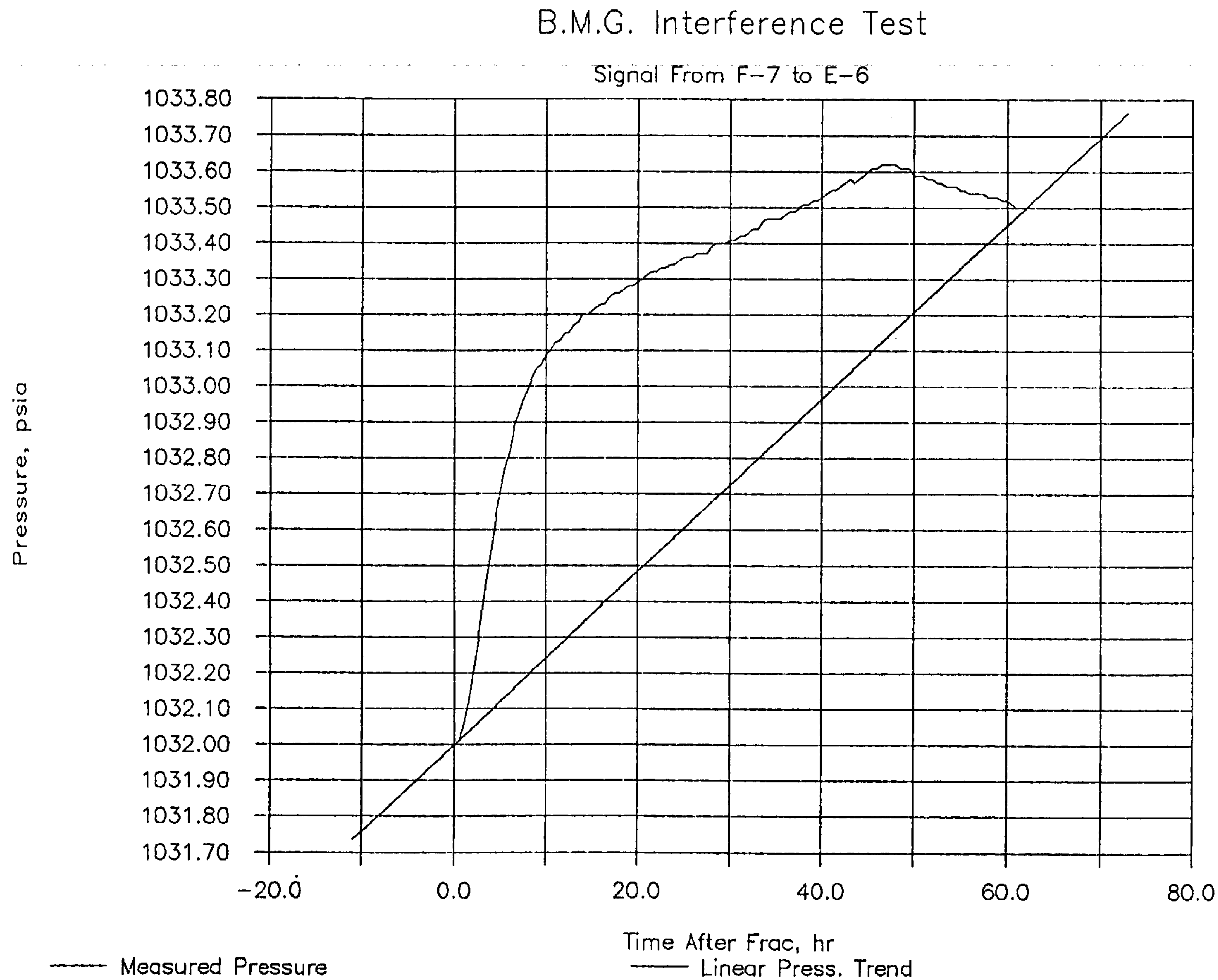

B.M.G. Interference Test
Signal From F-7 to E-6
1033.80
1033.70
1033.60
1033.50
1033.40
1033.30
1033.20
1033.10
1033.00
1032.90
1032.80
1032.70
1032.60
1032.50
1032.40
1032.30
1032.20
1032.10
1032.00
1031.90
1031.80
1031.70
Pressure, psia
-20.0
0.0
20.0
40.0
60.0
80.0
Time After Frac, hr
Measured Pressure
Linear Press. Trend

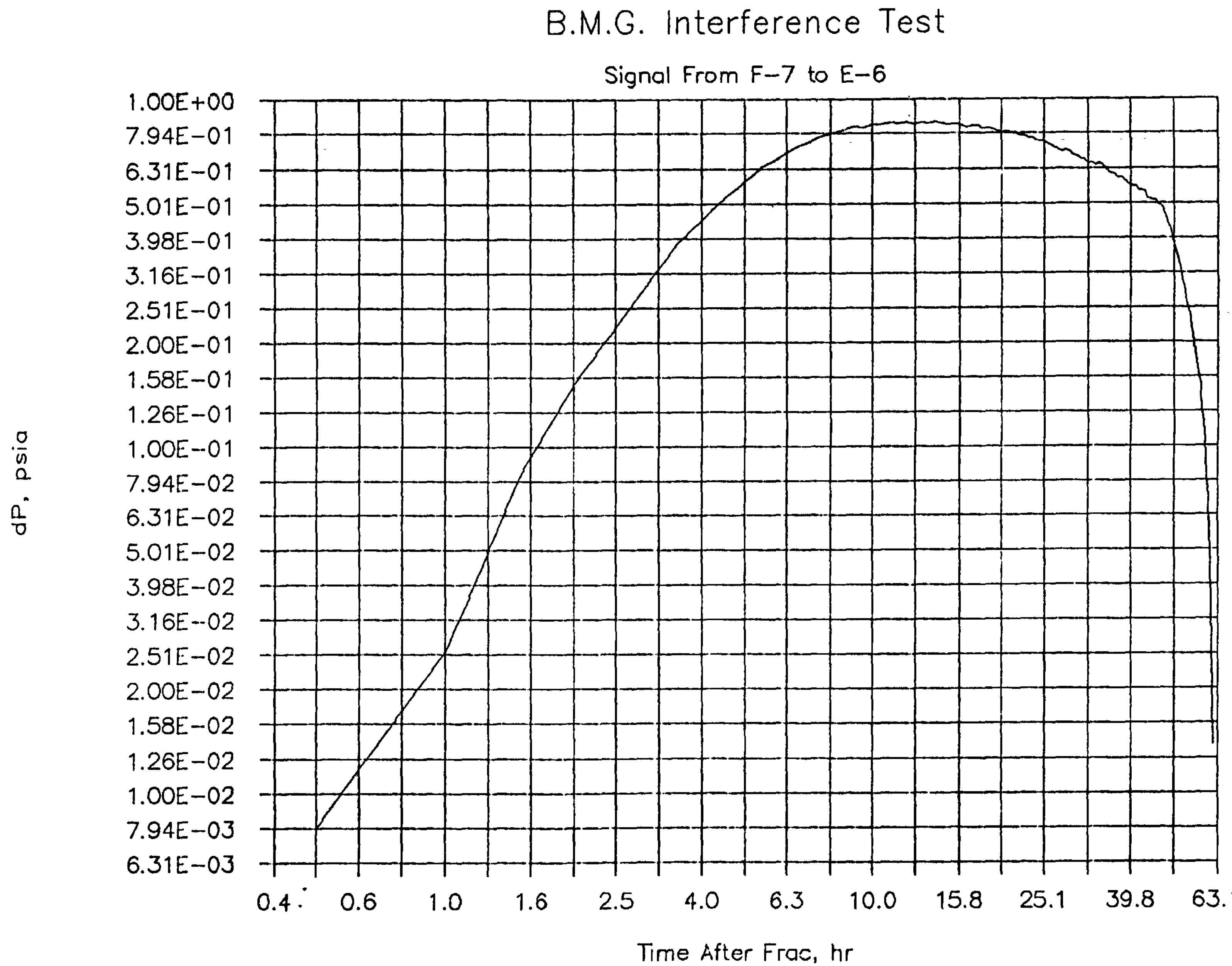
B.M.G. Interference Test
Signal From F-7 to E-6
dP, psia
1.00E+00
7.94E-01
6.31E-01
5.01E-01
3.98E-01
3.16E-01
2.51E-01
2.00E-01
1.58E-01
1.26E-01
1.00E-01
7.94E-02
6.31E-02
5.01E-02
3.98E-02
3.16E-02
2.51E-02
2.00E-02
1.58E-02
1.26E-02
1.00E-02
7.94E-03
6.31E-03
0.4
0.6
1.0
1.6
2.5
4.0
6.3
10.0
15.8
25.1
39.8
63.1
Time After Frac, hr

Frac Pulse Analysis
Kamal Method

Frac Well	F-7
Response Well	J-6
Date	11/25/87
Static Pressure, psig	1032
Pump Time, hr	1
Signal Time, hr	53.5
Lag Time, hr	3
Peak dP/q	7.01E-05
Constants from Figures 10-13	
A =	-0.815
C =	0.335
E =	-1.34
F =	0.029
D =	-0.325
Total Cycle Time, dTcyc =	54.5
Pulse Ratio, R' =	0.018348
Demensionless Time Lag, T1D =	0.055045
Demensionless Cycle Period, dTcycD =	3.234214
Demensionless Response Amplitude, dPD =	0.119465
Average Formation Volume Factor, B =	2.8867
Average Viscosity, cp =	0.4814
Distance Between Wells, ft	5830
kh = 70.6*B*µ*dPD/(dP/q) =	167199.6
øCth = kh*dTcyc/(56900*µ*r^2*dTcycD) =	3.03E-06
Oil Saturation, So =	0.87
Oil Compressibilty, Co =	5.00E-04
Gas Saturation, Sg =	0.03
Gas Compressibilty, Cg =	8.80E-04
Water Saturation, Sw =	0.1
Water Compressibility, Cw =	3.30E-06
Formation Compressibility, Cf =	1.00E-04
Total Compressibilty, Ct =	5.62E-04
øh =	0.005387

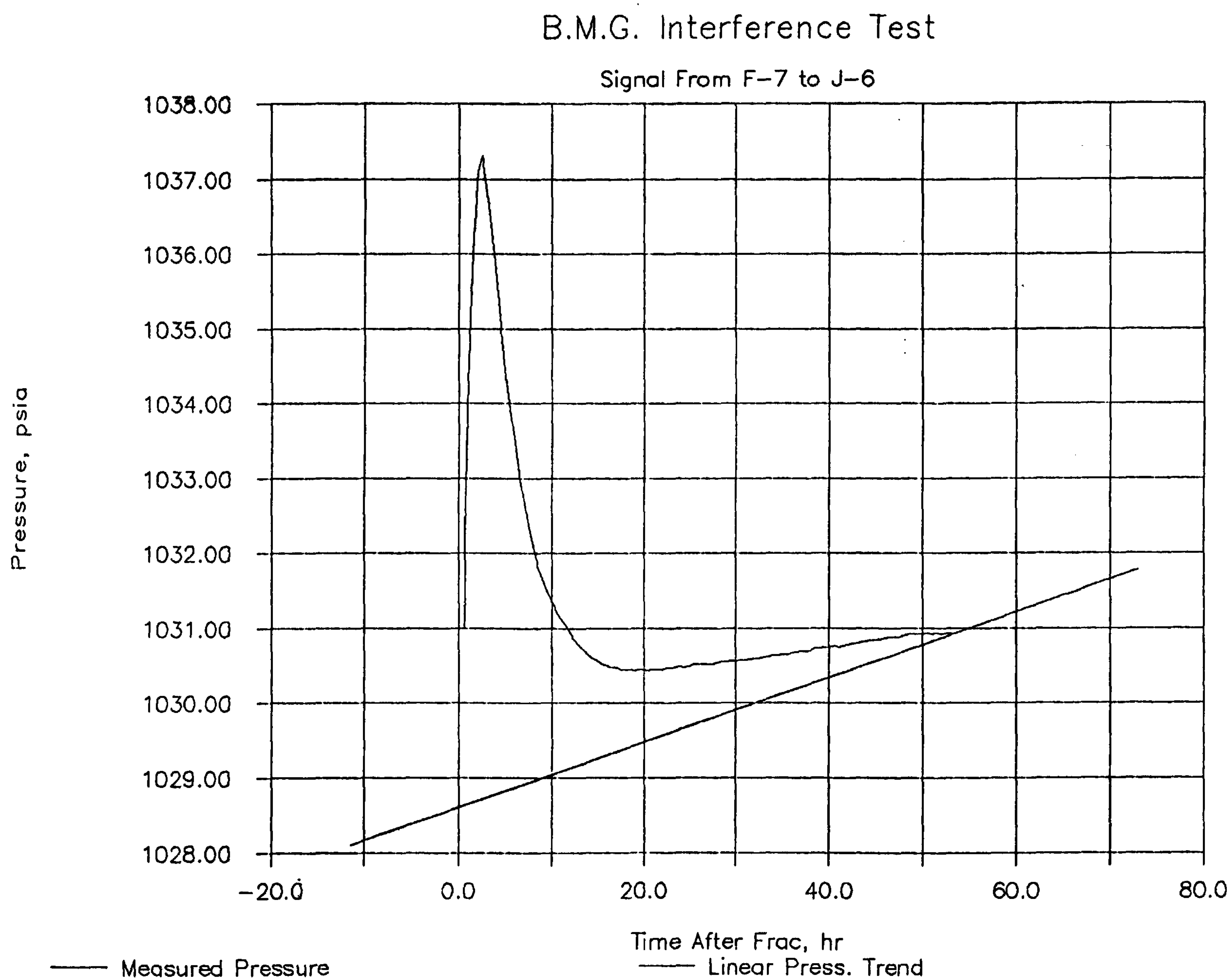
B.M.G. Interference Test
Signal From F-7 to J-6
Pressure, psia
1038.00
1037.00
1036.00
1035.00
1034.00
1033.00
1032.00
1031.00
1030.00
1029.00
1028.00
-20.0
0.0
20.0
40.0
60.0
80.0
Time After Frac, hr
Measured Pressure
Linear Press. Trend

4

Directional Perm.

Analysis of F-7 observed

at D-17 & E-6

Directional Perm. Analysis of F-7 Frac.
Observed at D-17 & E-6 on 11/25/87

$\bar{P} = 967\ psi$ $\qquad R_s = 445$

$B_o = 1.3375$ $\qquad \mu_g = 0.01428$

$B_g = 2.7845$ $\qquad \mu_o = 0.6464$

<u>E-6</u>

BOPD = 270.87

MCFPD = 1144.00

$$(270.87)(1.3375) = 362.29$$

$$\left(1144 - \frac{(270.87)(445)}{1000}\right)2.7845 = 3054.5$$

$$3416.8\ RB/D$$

$$FVF = \frac{(362.29)(1.3375) + (3054.5)(2.9845)}{3416.8} = 2.81$$

$$(270.87)(.6464) = 175.09$$

$$\left(1144 - \frac{(270.87)(445)}{1000}\right)(0.01428) = 14.62$$

$$189.71$$

$$\mu = \frac{(175.09)(.6464) + (14.62)(0.01428)}{189.71} = .59$$

J-6

BOPD = 14.9

MCFPD = 523

$(14.9)(1.3375) = 19.93$

$\left(523 - \frac{(14.9)(445)}{1000}\right) 2.9845 = 1541.10$

1561.0 PB/D

$$FVF = \frac{(19.93)(1.3375) + (1541.10)(2.9845)}{1561.0} = 2.9635$$

$(14.9)(.6464) = 9.63$

$\left(523 - \frac{(14.9)(445)}{1000}\right)(.01428) = 7.37$

17.00

$$\mu = \frac{(9.63)(.6464) + (7.37)(.01428)}{17.00} = 0.37$$

$$AVG\ FVF = \frac{2.8099 + 2.9635}{2} = 2.8867$$

$$AVG\ \mu = \frac{0.59 + 0.37}{2} = 0.48$$

Match Points

	$\frac{\Delta P}{q}$	P_D	ΔT	$\frac{t_D}{r_D^2}$	$\frac{t_{PD}}{r_D^2}$
D-17	10.0×10^{-6}	.48	100	2.2	3.0
E-6	10.0×10^{-6}	.48	100	7.8	.03

$$\bar{K} h = \frac{(141.2)\, B \mu\, P_D}{\frac{\Delta P}{q}}$$

since $h = 150$

$$\bar{K} = \frac{(141.2)(.27)(2.8867)(.48)}{(100 \times 10^{-6})(150)}$$

$\bar{K} = 3521.68$ mdarcy

$\bar{K} h = 528252.24$ md-ft

$$y^2 k_x + x^2 k_y - 2xy\, k_{xy} = \frac{(0.0002637)(\bar{K}^2)\, \Delta t}{\phi\, C_T\, \mu \left(\frac{t_D}{r_D^2}\right)}$$

Let $W = \phi C_T \mu$

D17 -

$$4880^2 K_x + 3210^2 K_y - 2(3210)(-4880) K_{xy} = \frac{.0002637(3521.68)^2(100)}{W\ (2.2)}$$

E-6

$$5090^2 K_x + 1490^2 K_y - 2(1490)(5090) K_{xy} = \frac{(.0002637)(3521.68)^2(100)}{W(7.8)}$$

$$-1(2.311\,K_x + K_y + 3.04\,K_{xy} = .0144/W)$$

E-6 $$11.67\,K_x + K_y + 6.83\,K_{xy} = .0189/W$$

$$9.359\,K_x + 0K_y + 3.79\,K_{xy} = .0045/W$$

$$\boxed{K_x = .000481/W - .4050\,K_{xy}}$$

$$K_y = \frac{.0189}{W} - 6.83\,K_{xy} - 11.67\left(\frac{.000481}{W} - .4050\,K_{xy}\right)$$

$$\boxed{K_y = \frac{.0133}{W} - 2.10\,K_{xy}}$$

$$K_x K_y - K_{xy}^2 = \bar{K}^2$$

$$\left(\frac{.000481}{W} - .4050\,K_{xy}\right)\left(\frac{.0133}{W} - 2.10\,K_{xy}\right) - K_{xy}^2 = 3521.68^2$$

$$\frac{6.40\times10^{-6}}{W^2} - \frac{1.01\times10^{-3}\,K_{xy}}{W} - \frac{5.39\times10^{-3}\,K_{xy}}{W} + 0.851\,K_{xy}^2 - K_{xy}^2 = 3521.68^2$$

assume $\phi C_T \mu = 3.5\times10^{-7}$ $\therefore$ $W = 3.5\times10^{-7}$

$$52244897.96 - 2885.71\,K_{xy} - 15400\,K_{xy} - .149\,K_{xy}^2 = 12402230.02$$

$$39842667.94 - 18285.71\,K_{xy} - .149\,K_{xy}^2 = 0$$

$K_{xy} = \frac{-B \pm \sqrt{B^2 - 4AC}}{2A}$ (5)

$$K_{xy} = \frac{18285.71 - \sqrt{18285.71^2 - 4(-.149)(39842667.94)}}{2(-.149)}$$

$$\underline{K_{xy} = 2141.53}$$

$$K_x = \frac{.006481}{3.5\times10^{-7}} - (.4050)(2141.53)$$

$$\underline{K_x = 506.97}$$

$$K_y = \frac{.0133}{3.5\times10^{-7}} - 2.10(2141.53)$$

$$K_y = 33502.79$$

$$K_{\frac{max}{min}} = .5\left((K_x + K_y) \pm \left[(K_x - K_y)^2 + 4K_{xy}^2\right]^{1/2}\right)$$

$$K_{\frac{max}{min}} = .5\left((506.97 + 33502.79) \pm \left[(506.79 - 33502.79)^2 + 4(2141.53)^2\right]^{1/2}\right)$$

$K_{max} = 33641.29$

$K_{min} = 368.47$

$$\Theta = \tan^{-1}\left(\frac{K_{max} - K_x}{K_{xy}}\right)$$ ⑥

$$\Theta = \tan^{-1}\left(\frac{33641.29 - 506.97}{2141.53}\right)$$

$$\Theta = 86.30^{\circ}$$

Fracture Responce From F-7 to D-17
Q = 122400

time hr	pressure psia	dt	dp	dp/q	shut in time hr
72	997.08	2	0.240565	1.97E-06	218
75	997.22	5	0.306970	2.51E-06	221
78	997.41	8	0.424367	3.47E-06	224
81	997.54	11	0.482730	3.94E-06	227
84	997.62	14	0.492034	4.02E-06	230
87	997.7	17	0.502254	4.10E-06	233
90	997.85	20	0.583367	4.77E-06	236
93	998.04	23	0.705350	5.76E-06	239
96	998.26	26	0.858181	7.01E-06	242
99	998.38	29	0.911840	7.45E-06	245
102	998.39	32	0.856306	7.00E-06	248
105	998.58	35	0.981561	8.02E-06	251
108	998.77	38	1.107584	9.05E-06	254
111	998.92	41	1.194359	9.76E-06	257
114	999.05	44	1.261868	1.03E-05	260
117	999.16	47	1.310093	1.07E-05	263
120	999.27	50	1.359019	1.11E-05	266
123	999.38	53	1.408631	1.15E-05	269
126	999.52	56	1.488911	1.22E-05	272
129	999.65	59	1.559847	1.27E-05	275
132	999.83	62	1.681424	1.37E-05	278
135	999.99	65	1.783628	1.46E-05	281
138	1000.12	68	1.856446	1.52E-05	284
141	1000.19	71	1.869864	1.53E-05	287
144	1000.19	74	1.813871	1.48E-05	290
147	1000.24	77	1.808455	1.48E-05	293
150	1000.37	80	1.883602	1.54E-05	296
153	1000.51	83	1.969303	1.61E-05	299
156	1000.63	86	2.035546	1.66E-05	302
159	1000.73	89	2.082321	1.70E-05	305
162	1000.81	92	2.109616	1.72E-05	308
165	1000.96	95	2.207422	1.80E-05	311
168	1001	98	2.195730	1.79E-05	314

Fracture Responce From F-7 to E-6
Q = 122400 bfpd, r = 5280 ft

time hr	pressure psia	dt hrs	dp psia	dp/q	Linear Press. Trend
69.5	1032.02	0.5	0.007916	6.47E-08	1032.012
70	1032.05	1	0.025833	2.11E-07	1032.024
70.5	1032.12	1.5	0.083749	6.84E-07	1032.036
71	1032.2	2	0.151666	1.24E-06	1032.048
71.5	1032.28	2.5	0.219583	1.79E-06	1032.060
72	1032.37	3	0.297499	2.43E-06	1032.072
72.5	1032.47	3.5	0.385416	3.15E-06	1032.084
73	1032.55	4	0.453333	3.70E-06	1032.096
73.5	1032.63	4.5	0.521249	4.26E-06	1032.108
74	1032.7	5	0.579166	4.73E-06	1032.120
74.5	1032.77	5.5	0.637083	5.20E-06	1032.132
75	1032.82	6	0.674999	5.51E-06	1032.145
75.5	1032.88	6.5	0.722916	5.91E-06	1032.157
76	1032.92	7	0.750833	6.13E-06	1032.169
76.5	1032.96	7.5	0.778749	6.36E-06	1032.181
77	1032.99	8	0.796666	6.51E-06	1032.193
77.5	1033.02	8.5	0.814583	6.66E-06	1032.205
78	1033.05	9	0.832499	6.80E-06	1032.217
78.5	1033.06	9.5	0.830416	6.78E-06	1032.229
79	1033.09	10	0.848333	6.93E-06	1032.241
79.5	1033.1	10.5	0.846249	6.91E-06	1032.253
80	1033.12	11	0.854166	6.98E-06	1032.265
80.5	1033.13	11.5	0.852083	6.96E-06	1032.277
81	1033.15	12	0.859999	7.03E-06	1032.29
81.5	1033.15	12.5	0.847916	6.93E-06	1032.302
82	1033.17	13	0.855833	6.99E-06	1032.314
82.5	1033.18	13.5	0.853749	6.98E-06	1032.326
83	1033.2	14	0.861666	7.04E-06	1032.338
83.5	1033.2	14.5	0.849583	6.94E-06	1032.350
84	1033.21	15	0.847499	6.92E-06	1032.362
84.5	1033.22	15.5	0.845416	6.91E-06	1032.374
85	1033.23	16	0.843333	6.89E-06	1032.386
85.5	1033.23	16.5	0.831249	6.79E-06	1032.398
86	1033.25	17	0.839166	6.86E-06	1032.410
86.5	1033.26	17.5	0.837083	6.84E-06	1032.422
87	1033.26	18	0.824999	6.74E-06	1032.435
87.5	1033.27	18.5	0.822916	6.72E-06	1032.447
88	1033.28	19	0.820833	6.71E-06	1032.459
88.5	1033.28	19.5	0.808749	6.61E-06	1032.471
89	1033.29	20	0.806666	6.59E-06	1032.483
89.5	1033.3	20.5	0.804583	6.57E-06	1032.495
90	1033.31	21	0.802499	6.56E-06	1032.507
90.5	1033.32	21.5	0.800416	6.54E-06	1032.519
91	1033.32	22	0.788333	6.44E-06	1032.531
91.5	1033.33	22.5	0.786249	6.42E-06	1032.543
92	1033.33	23	0.774166	6.32E-06	1032.555
92.5	1033.34	23.5	0.772083	6.31E-06	1032.567
93	1033.34	24	0.759999	6.21E-06	1032.58
93.5	1033.35	24.5	0.757916	6.19E-06	1032.592

Fracture Responce From F-7 to E-6
Q = 122400 bfpd, r = 5280 ft

time hr	pressure psia	dt hrs	dp psia	dp/q	Linear Press. Trend
94	1033.36	25	0.755833	6.18E-06	1032.604
94.5	1033.36	25.5	0.743749	6.08E-06	1032.616
95	1033.36	26	0.731666	5.98E-06	1032.628
95.5	1033.37	26.5	0.729583	5.96E-06	1032.640
96	1033.37	27	0.717499	5.86E-06	1032.652
96.5	1033.37	27.5	0.705416	5.76E-06	1032.664
97	1033.39	28	0.713333	5.83E-06	1032.676
97.5	1033.4	28.5	0.711249	5.81E-06	1032.688
98	1033.4	29	0.699166	5.71E-06	1032.700
98.5	1033.4	29.5	0.687083	5.61E-06	1032.712
99	1033.41	30	0.684999	5.60E-06	1032.725
99.5	1033.41	30.5	0.672916	5.50E-06	1032.737
100	1033.42	31	0.670833	5.48E-06	1032.749
100.5	1033.42	31.5	0.658749	5.38E-06	1032.761
101	1033.43	32	0.656666	5.36E-06	1032.773
101.5	1033.44	32.5	0.654583	5.35E-06	1032.785
102	1033.44	33	0.642499	5.25E-06	1032.797
102.5	1033.46	33.5	0.650416	5.31E-06	1032.809
103	1033.469	34	0.647333	5.29E-06	1032.821
103.5	1033.47	34.5	0.636249	5.20E-06	1032.833
104	1033.47	35	0.624166	5.10E-06	1032.845
104.5	1033.47	35.5	0.612083	5.00E-06	1032.857
105	1033.48	36	0.609999	4.98E-06	1032.87
105.5	1033.49	36.5	0.607916	4.97E-06	1032.882
106	1033.49	37	0.595833	4.87E-06	1032.894
106.5	1033.5	37.5	0.593749	4.85E-06	1032.906
107	1033.51	38	0.591666	4.83E-06	1032.918
107.5	1033.51	38.5	0.579583	4.74E-06	1032.930
108	1033.52	39	0.577499	4.72E-06	1032.942
108.5	1033.52	39.5	0.565416	4.62E-06	1032.954
109	1033.53	40	0.563333	4.60E-06	1032.966
109.5	1033.54	40.5	0.561249	4.59E-06	1032.978
110	1033.55	41	0.559166	4.57E-06	1032.990
110.5	1033.55	41.5	0.547083	4.47E-06	1033.002
111	1033.56	42	0.544999	4.45E-06	1033.015
111.5	1033.57	42.5	0.542916	4.44E-06	1033.027
112	1033.58	43	0.540833	4.42E-06	1033.039
112.5	1033.57	43.5	0.518749	4.24E-06	1033.051
113	1033.58	44	0.516666	4.22E-06	1033.063
113.5	1033.59	44.5	0.514583	4.20E-06	1033.075
114	1033.6	45	0.512499	4.19E-06	1033.087
114.5	1033.61	45.5	0.510416	4.17E-06	1033.099
115	1033.61	46	0.498333	4.07E-06	1033.111
115.5	1033.62	46.5	0.496249	4.05E-06	1033.123
116	1033.62	47	0.484166	3.96E-06	1033.135
116.5	1033.62	47.5	0.472083	3.86E-06	1033.147
117	1033.62	48	0.459999	3.76E-06	1033.16
117.5	1033.61	48.5	0.437916	3.58E-06	1033.172
118	1033.61	49	0.425833	3.48E-06	1033.184

Fracture Responce From F-7 to E-6
Q = 122400 bfpd, r = 5280 ft

time hr	pressure psia	dt hrs	dp psia	dp/q	Linear Press. Trend
118.5	1033.61	49.5	0.413749	3.38E-06	1033.196
119	1033.59	50	0.381666	3.12E-06	1033.208
119.5	1033.59	50.5	0.369583	3.02E-06	1033.220
120	1033.59	51	0.357499	2.92E-06	1033.232
120.5	1033.58	51.5	0.335416	2.74E-06	1033.244
121	1033.58	52	0.323333	2.64E-06	1033.256
121.5	1033.57	52.5	0.301249	2.46E-06	1033.268
122	1033.57	53	0.289166	2.36E-06	1033.280
122.5	1033.56	53.5	0.267083	2.18E-06	1033.292
123	1033.56	54	0.254999	2.08E-06	1033.305
123.5	1033.56	54.5	0.242916	1.98E-06	1033.317
124	1033.55	55	0.220833	1.80E-06	1033.329
124.5	1033.55	55.5	0.208749	1.71E-06	1033.341
125	1033.54	56	0.186666	1.53E-06	1033.353
125.5	1033.54	56.5	0.174583	1.43E-06	1033.365
126	1033.54	57	0.162499	1.33E-06	1033.377
126.5	1033.54	57.5	0.150416	1.23E-06	1033.389
127	1033.53	58	0.128333	1.05E-06	1033.401
127.5	1033.53	58.5	0.116249	9.50E-07	1033.413
128	1033.53	59	0.104166	8.51E-07	1033.425
128.5	1033.52	59.5	0.082083	6.71E-07	1033.437
129	1033.52	60	0.069999	5.72E-07	1033.45
129.5	1033.51	60.5	0.047916	3.91E-07	1033.462
130	1033.5	61	0.025833	2.11E-07	1033.474
130.5	1033.5	61.5	0.013749	1.12E-07	1033.486

APPENDIX 4

Rate Sensitivity

$$q_{crit} = \frac{(4.9\times10^{-4})(K K'_{rg})(A)(\Delta\gamma)(\sin\theta)}{(\mu_g)(M-1)} = RB/D$$

Page 326 Dake

$$K K'_{rg} = \frac{235}{235 ft} = 1.0 md$$

$B_o = 1.293$

$A = 139400$

$\Delta\gamma = (0.7206 - 0.0136)$

$\mu_g = 0.01359$

$\mu_o = 0.710$

$$M = \frac{K_{rg}}{K_{ro}} \frac{\mu_o}{\mu_g} \quad @ \; 800 psi \quad \frac{(0.85)(0.710)}{0.01359} = 44.4$$

$$q_{crit} = \frac{(4.9\times10^{-4})(1 md)(139400)(0.7206-0.0136)(-1)}{(0.01359)(44.4-1)(1.293)}$$

$q_{crit} = 63.3$ RB/D or 50 STB/D

GAVILAN—W. PUERTO CHIQUITO

Rate Sensitivity, All Wells

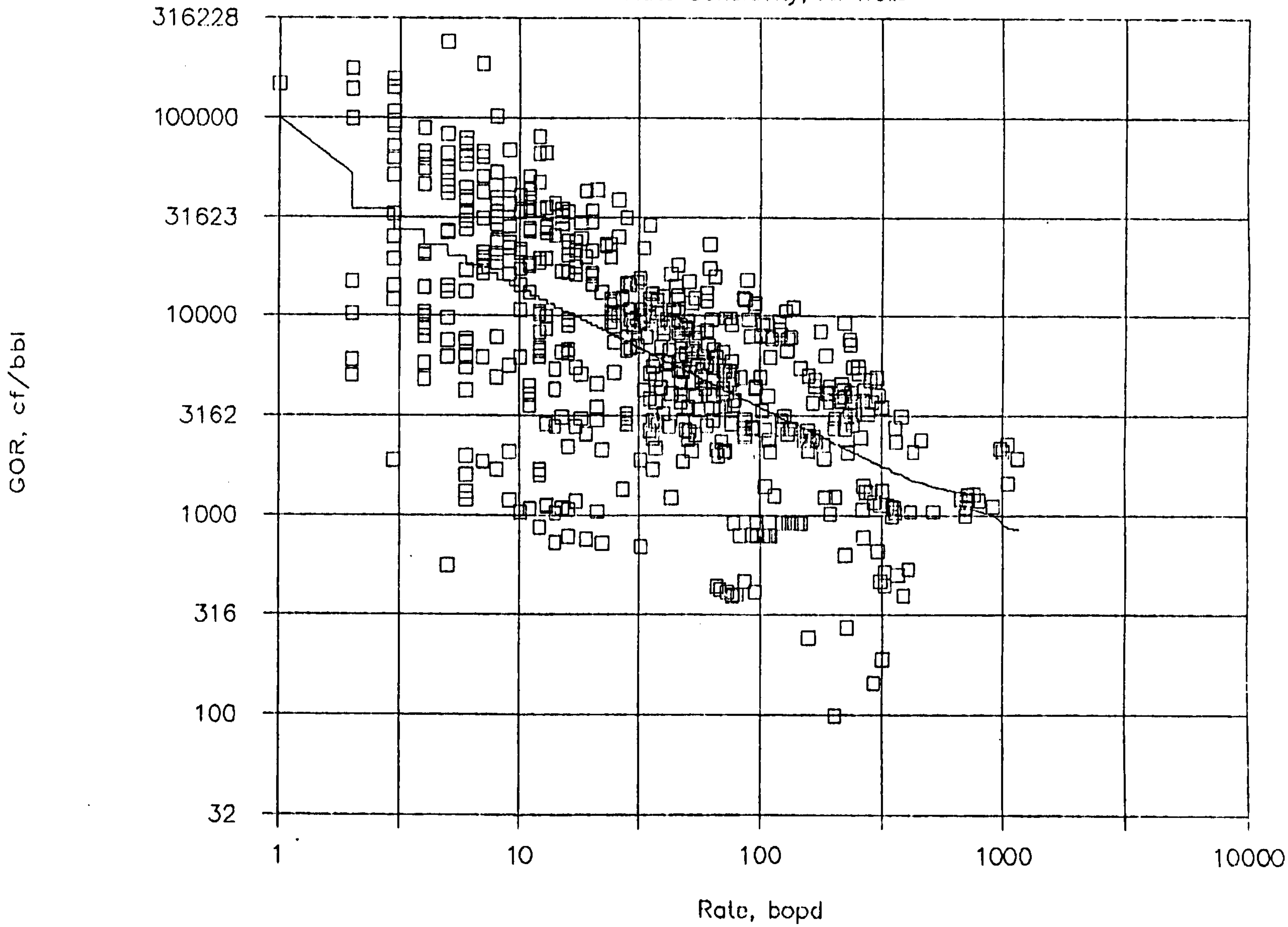

Gavilan Dome, 2/15–2/29/88

Rate Sensitivity, Amoco BCU#2

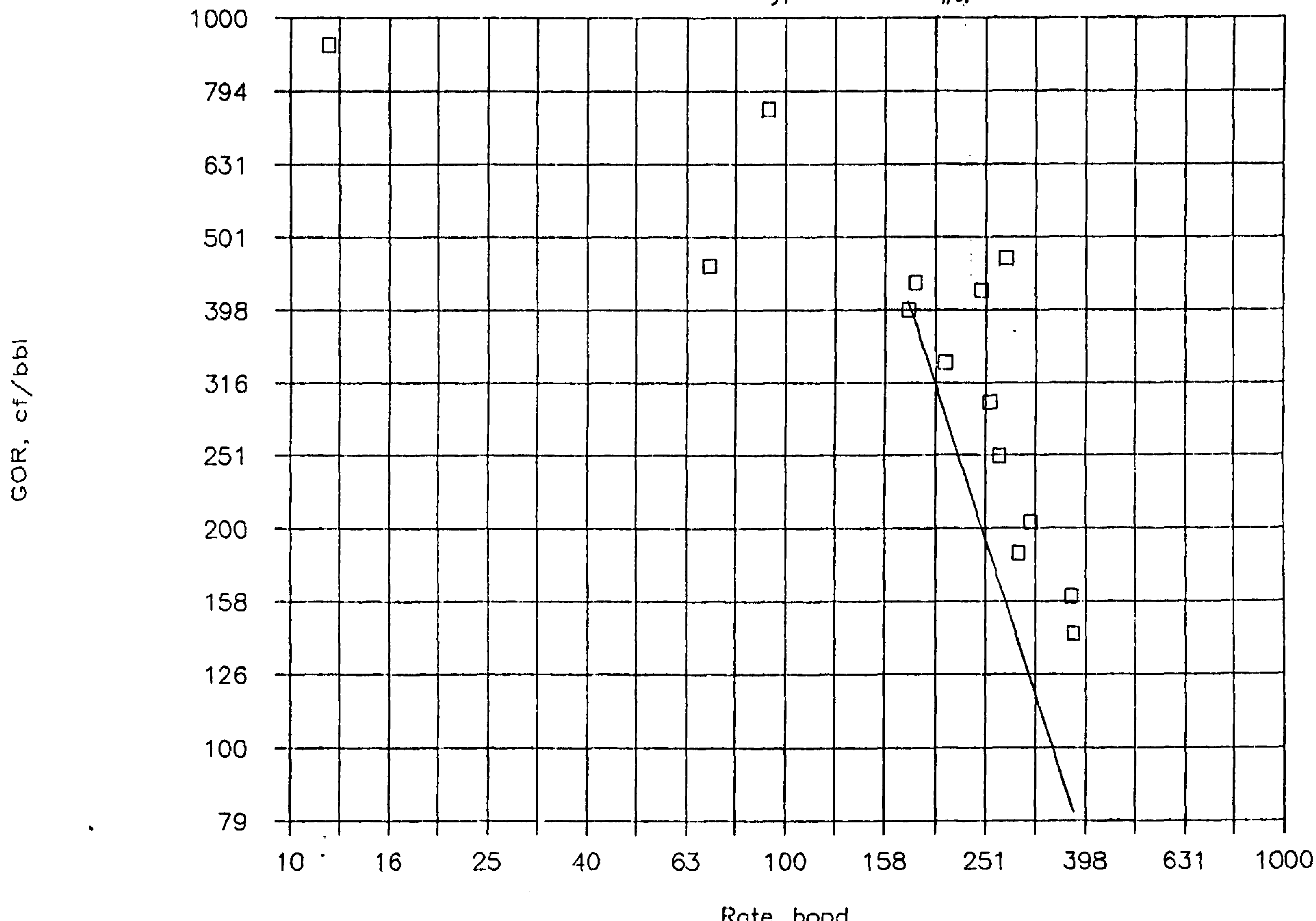

C.C. = 0.31

Gavilan Dome, 1/6–2/29/88

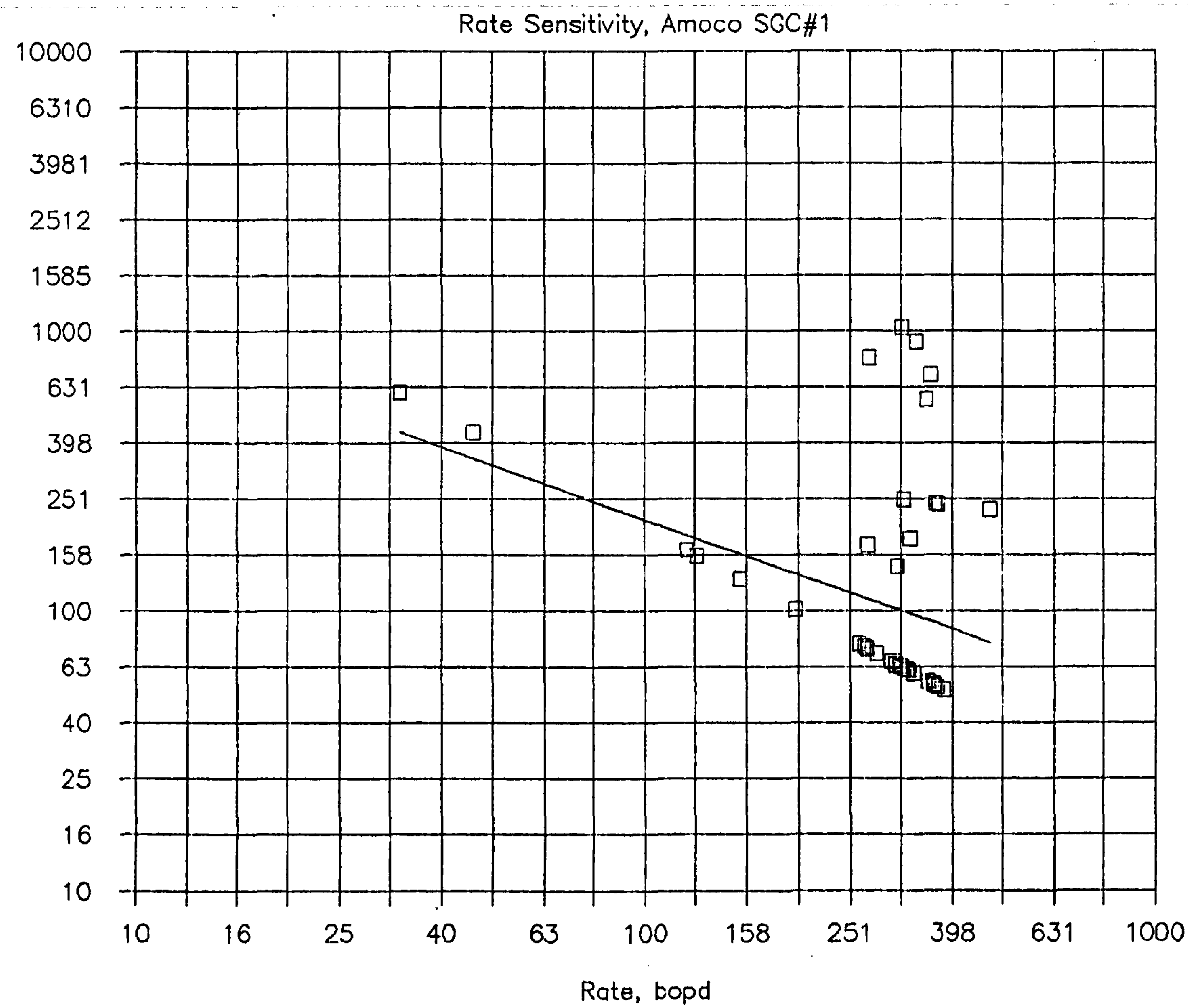

C.C. = 0.35

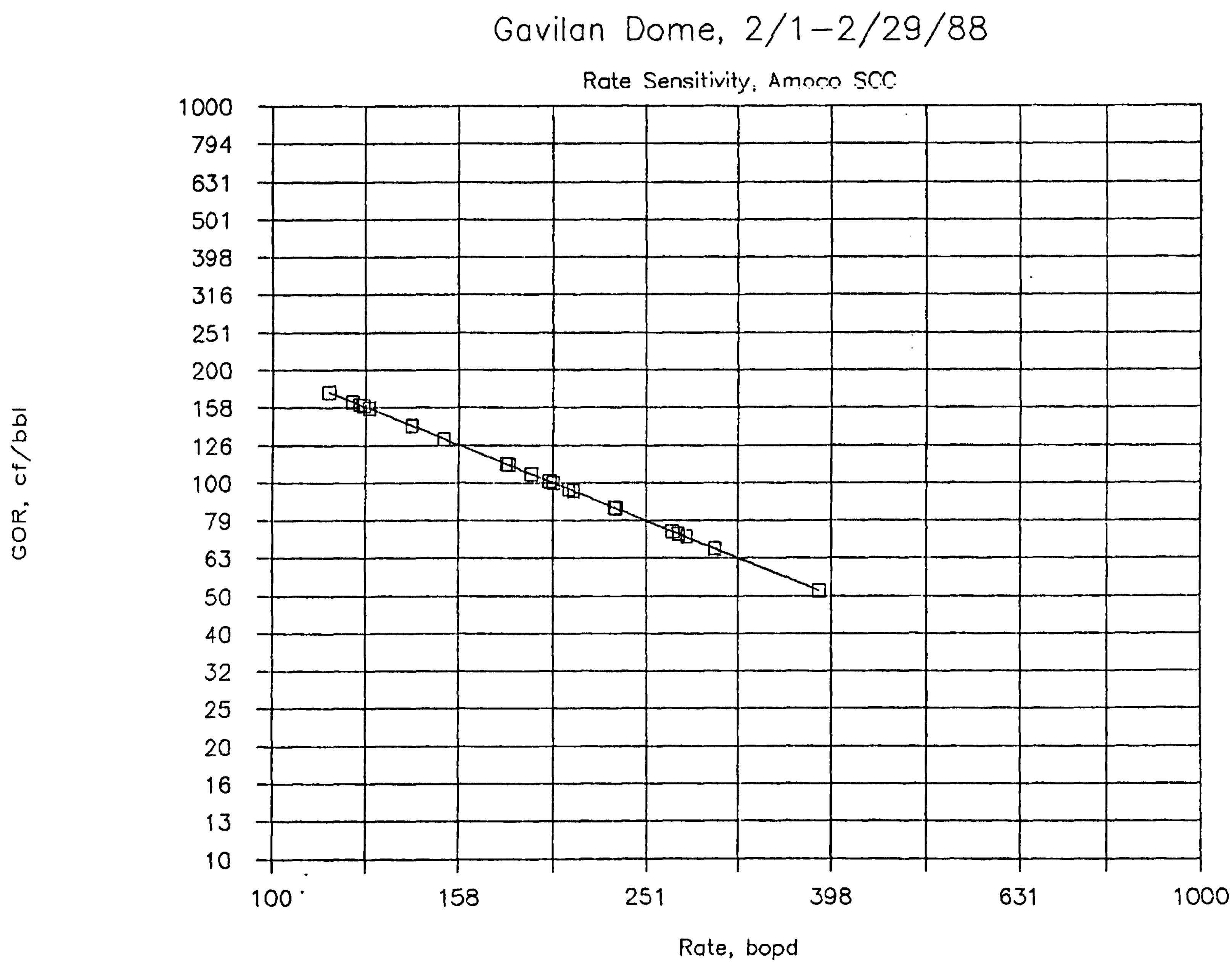
Gavilan Dome, 2/1-2/29/88
Rate Sensitivity, Amoco SCC
GOR, cf/bbl
1000
794
631
501
398
316
251
200
158
126
100
79
63
50
40
32
25
20
16
13
10
100
158
251
398
631
1000
Rate, bopd

C.C. = 1.00

W. Puerto Chiquito, July—Sept. 87

Rate Sensitivity, BMG A-16

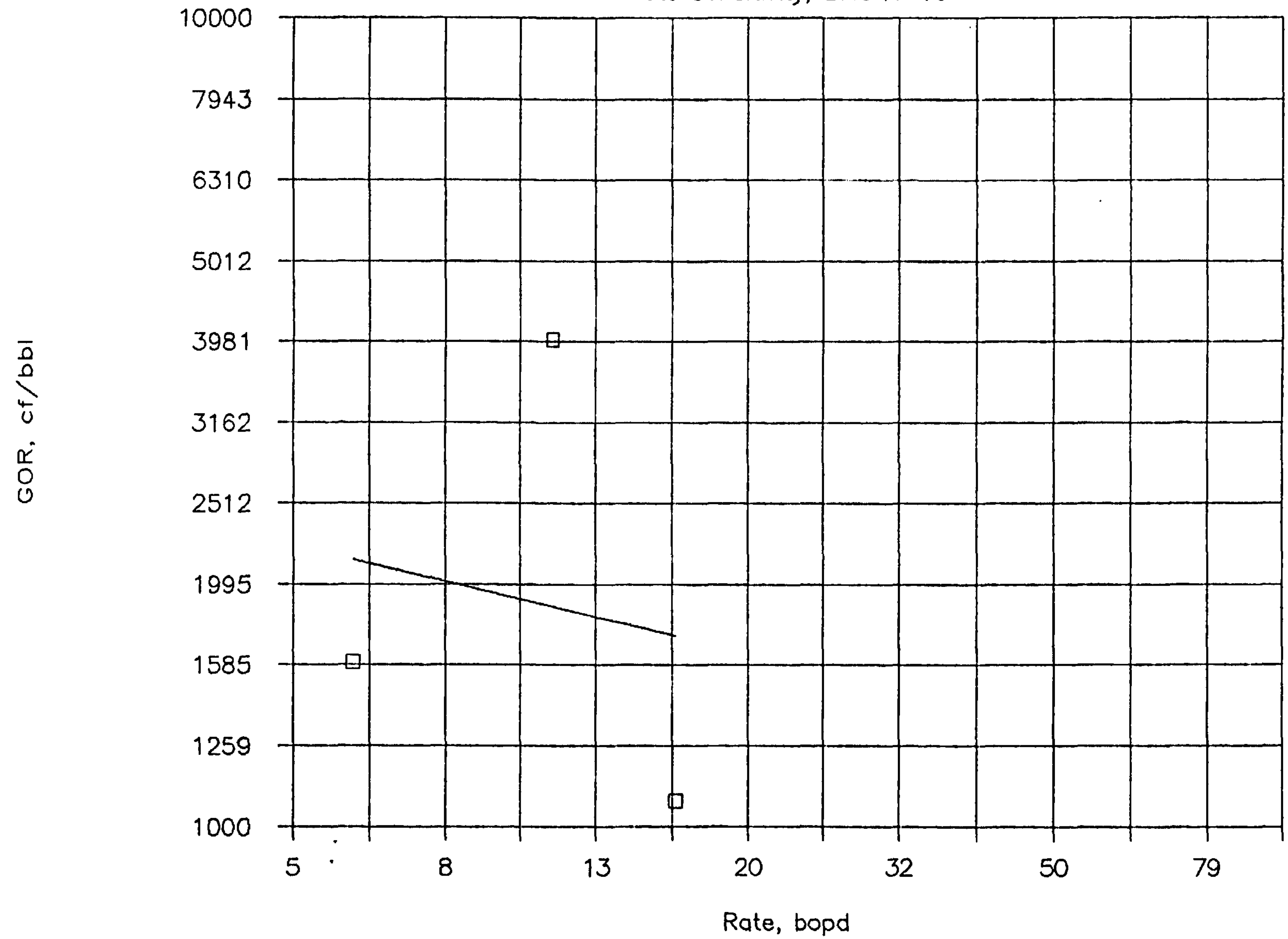

C.C. = 0.16

W. Puerto Chiquito, July 87—Feb 88

Rate Sensitivity, BMG A-20

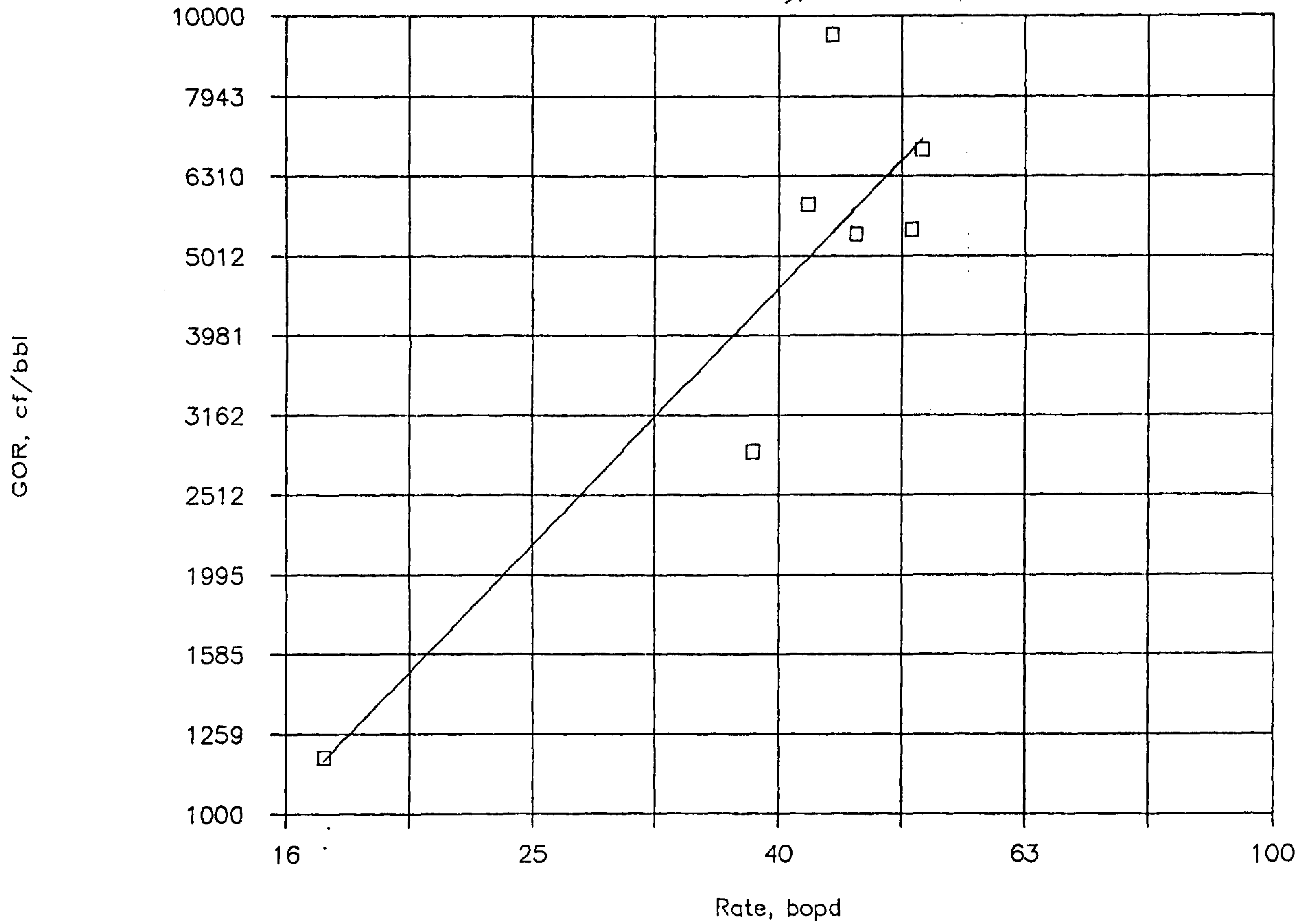

C. C. =0.90

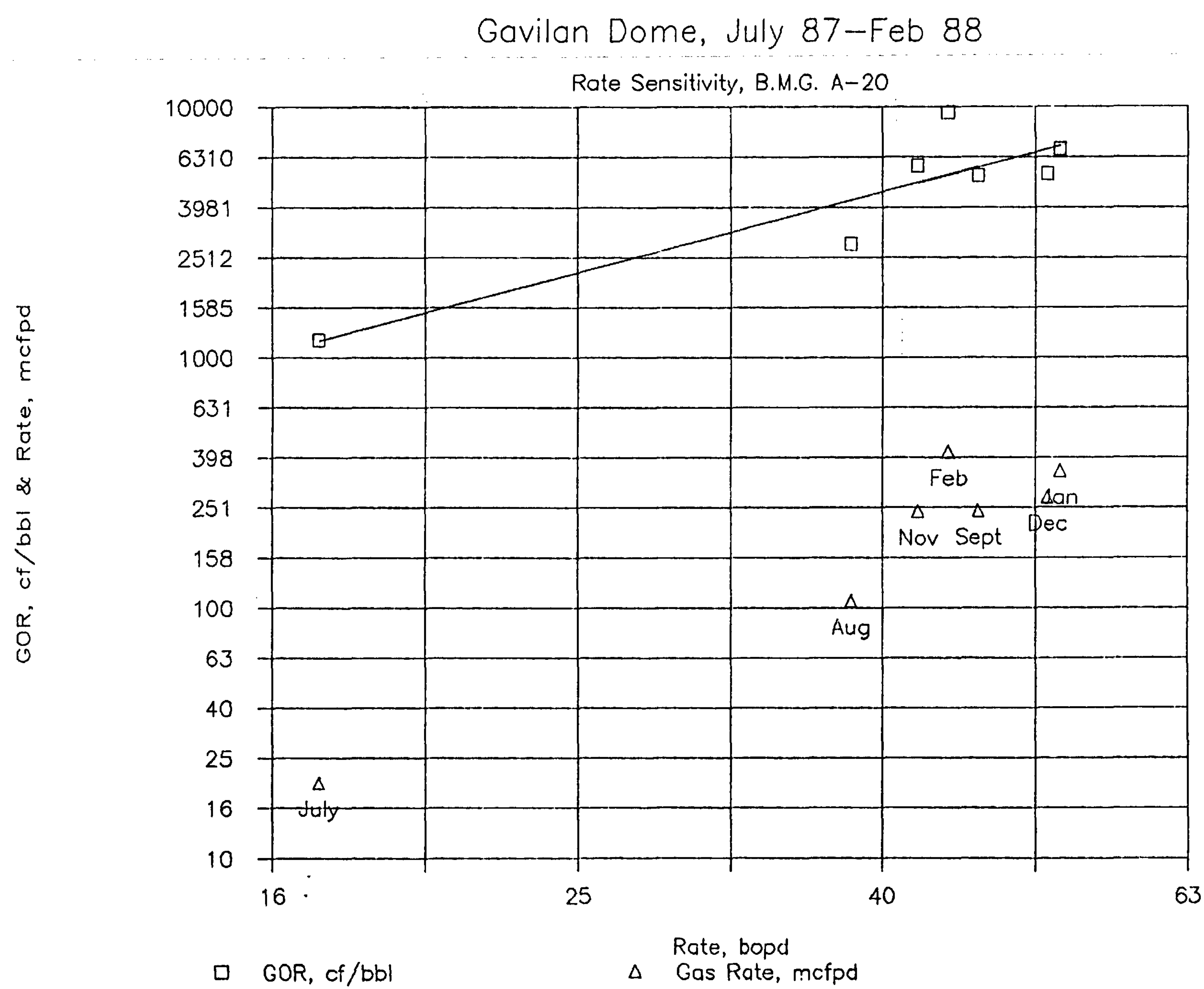
Gavilan Dome, July 87—Feb 88
Rate Sensitivity, B.M.G. A-20
GOR, cf/bbl & Rate, mcfpd
10000
6310
3981
2512
1585
1000
631
398
251
158
100
63
40
25
16
10
16
25
40
63
Rate, bopd
Feb
Jan
Dec
Nov
Sept
Aug
July
GOR, cf/bbl
Gas Rate, mcfpd

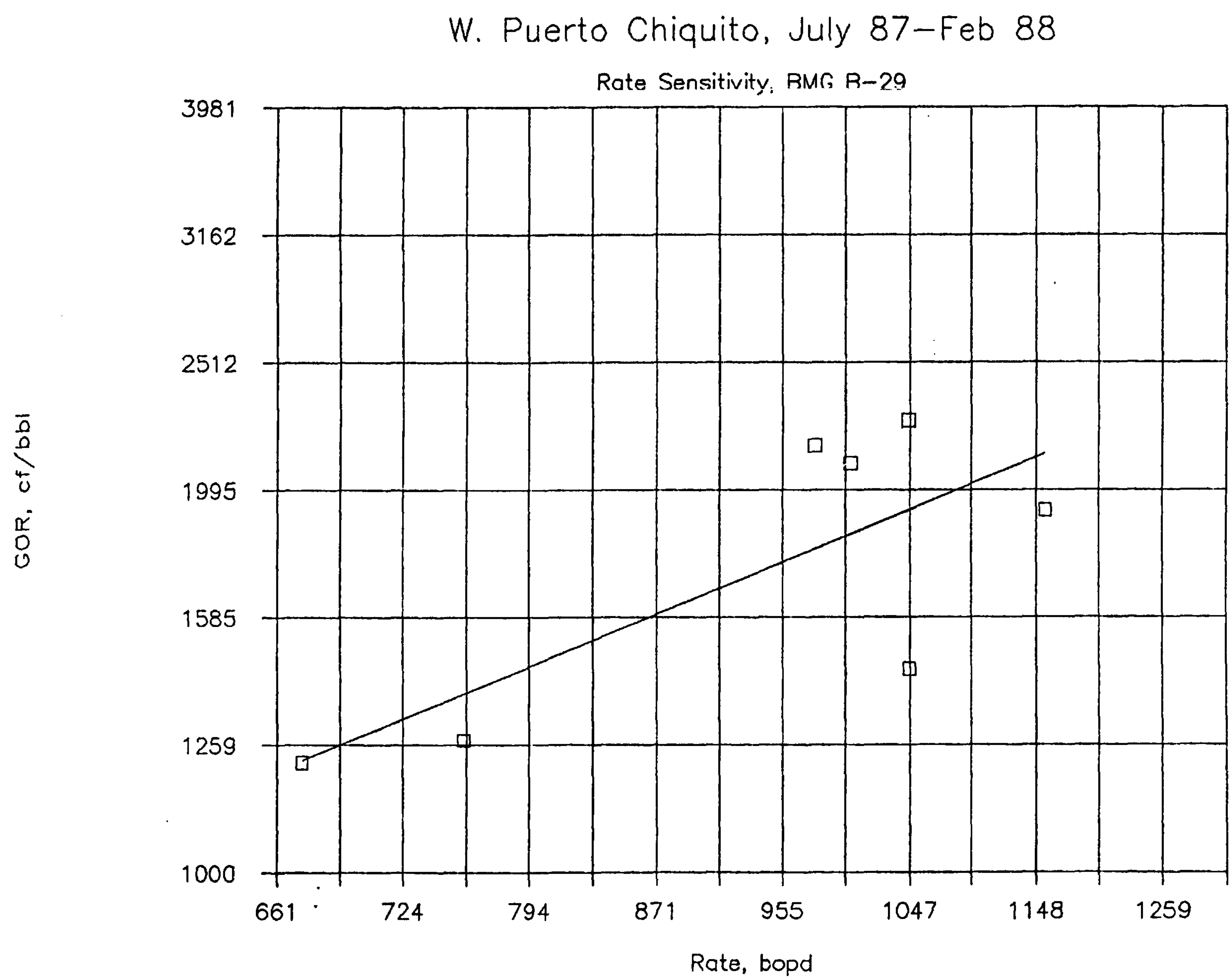
W. Puerto Chiquito, July 87–Feb 88
Rate Sensitivity, BMG B-29
GOR, cf/bbl
3981
3162
2512
1995
1585
1259
1000
661
724
794
871
955
1047
1148
1259
Rate, bopd

C. C. =0. 76

W. Puerto Chiquito, July 87—Feb 88

Rate Sensitivity, BMG B-32

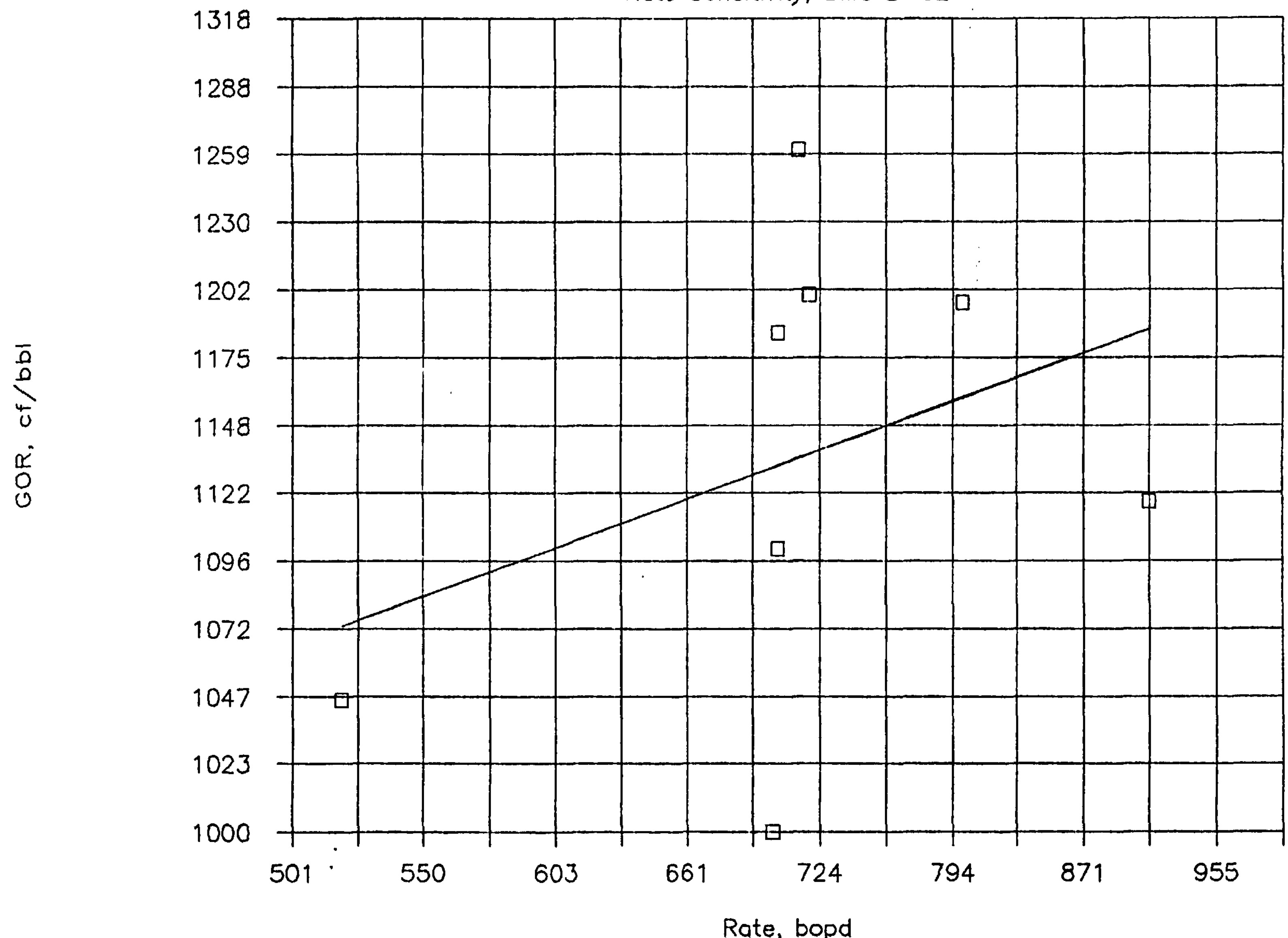

C.C. = 0.36

W. Puerto Chiquito, Dec 87—Feb 88

Rate Sensitivity, BMG C-34

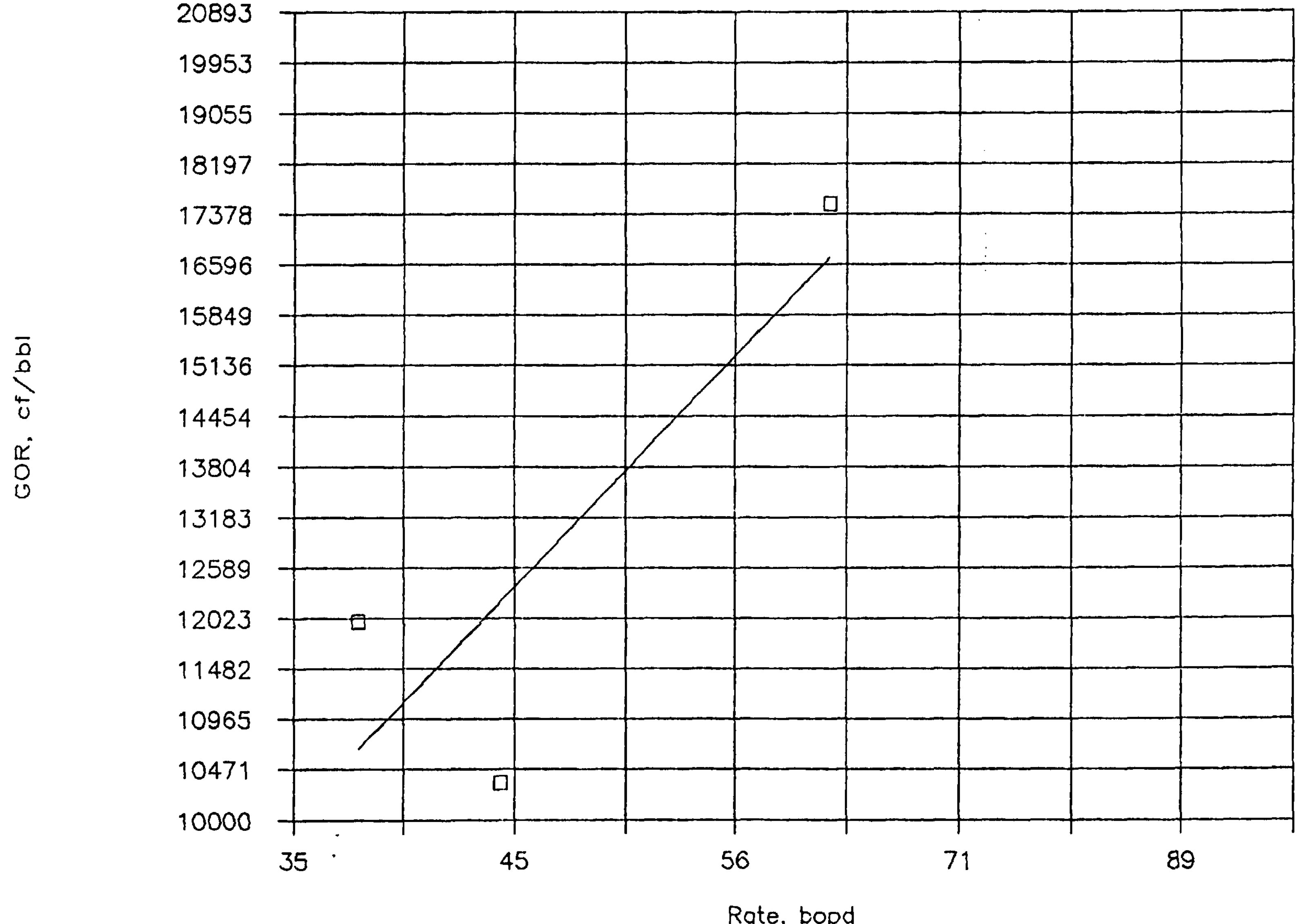

C.C. = 0.84

W. Puerto Chiquito, July 87

Rate Sensitivity, BMG D-17

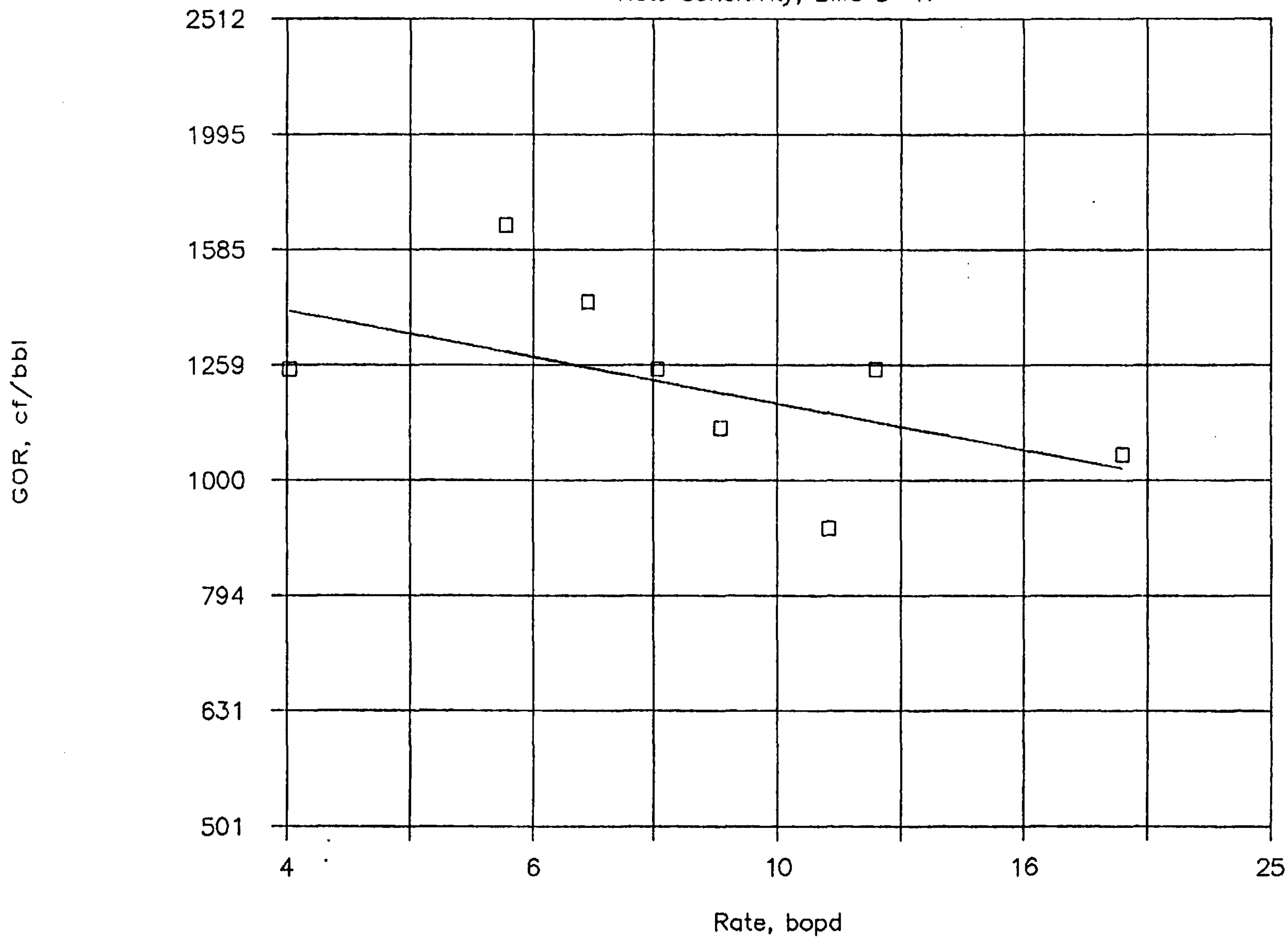

C.C. = 0.52

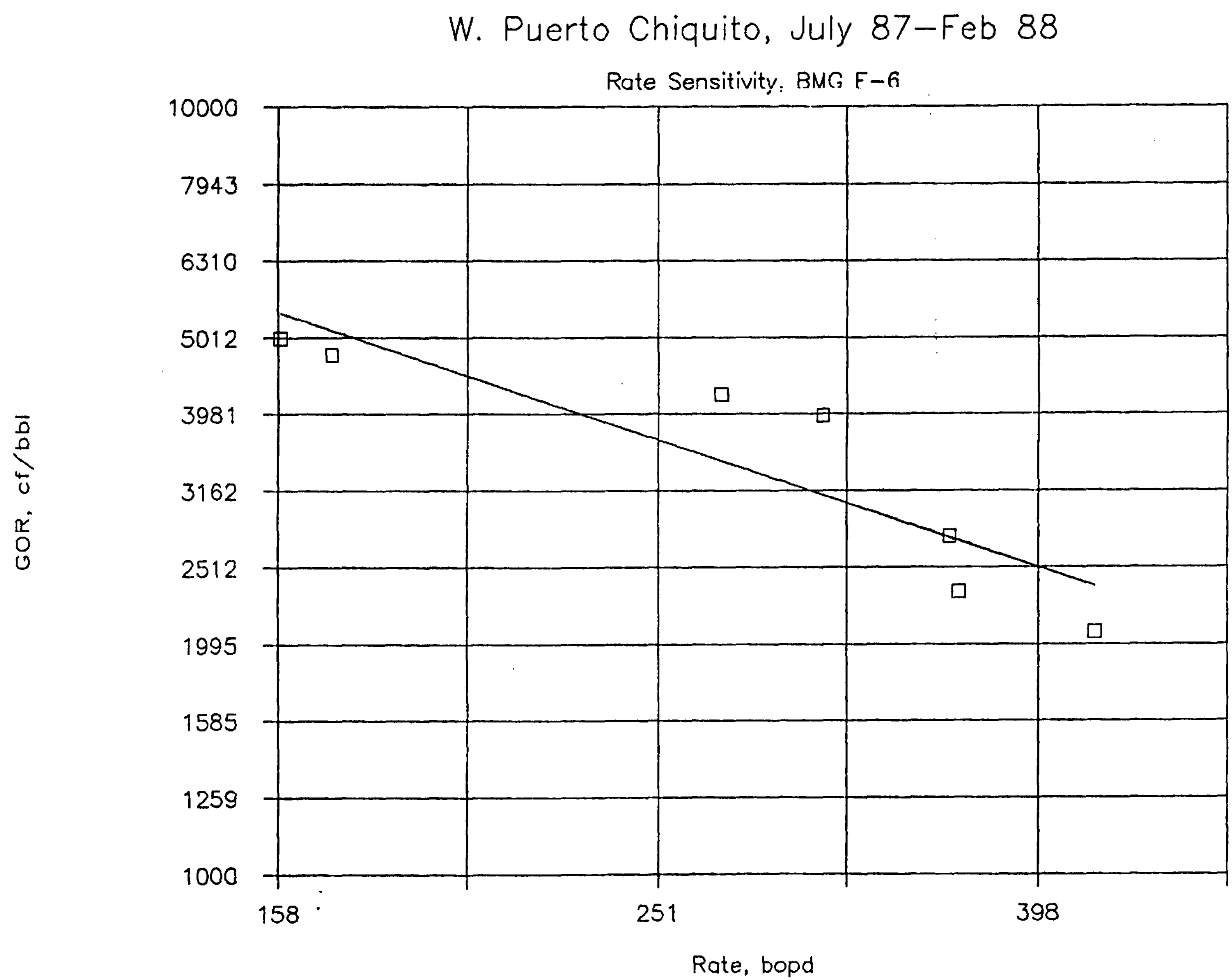
W. Puerto Chiquito, July 87–Feb 88
Rate Sensitivity, BMG F–6
10000
7943
6310
5012
3981
3162
2512
1995
1585
1259
1000
GOR, cf/bbl
158
251
398
Rate, bopd

C. C. = 0.89

W. Puerto Chiquito, July 87—Feb 88

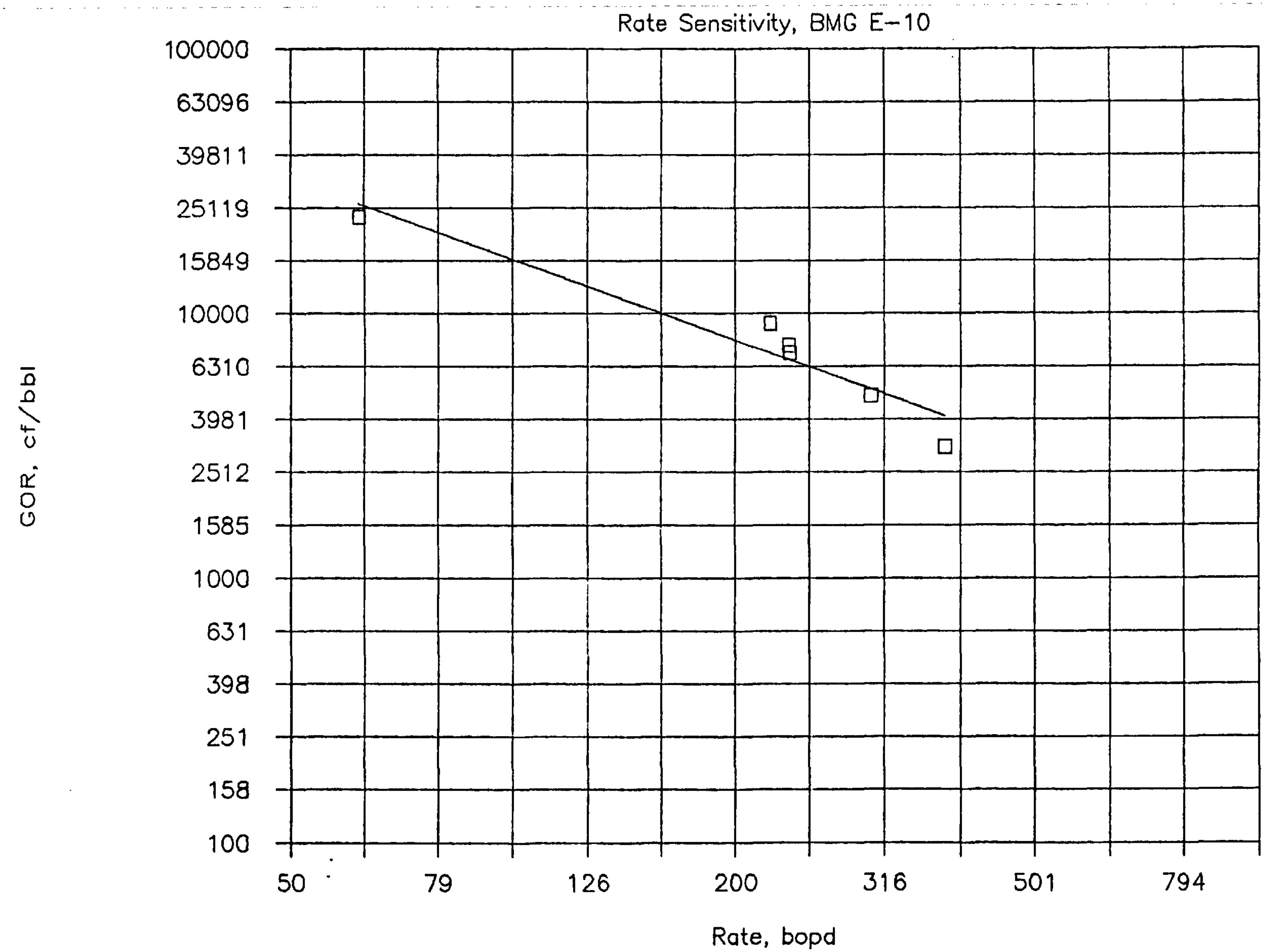

C. C. = 0.96

W. Puerto Chiquito, Dec 87—Jan 88

Rate Sensitivity, BMG F-7

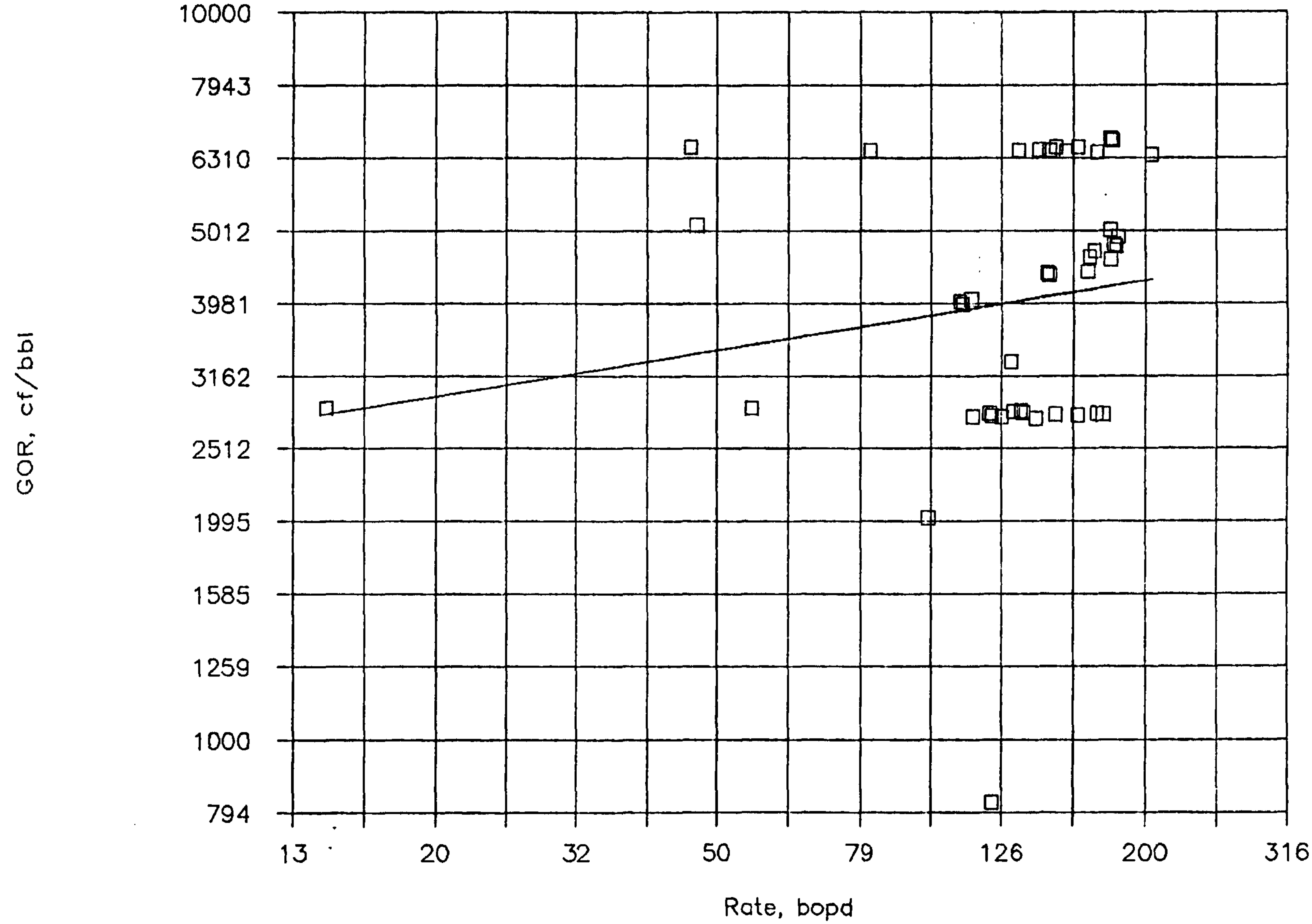

C.C. = 0.18

W. Puerto Chiquito, July 87–Feb 88

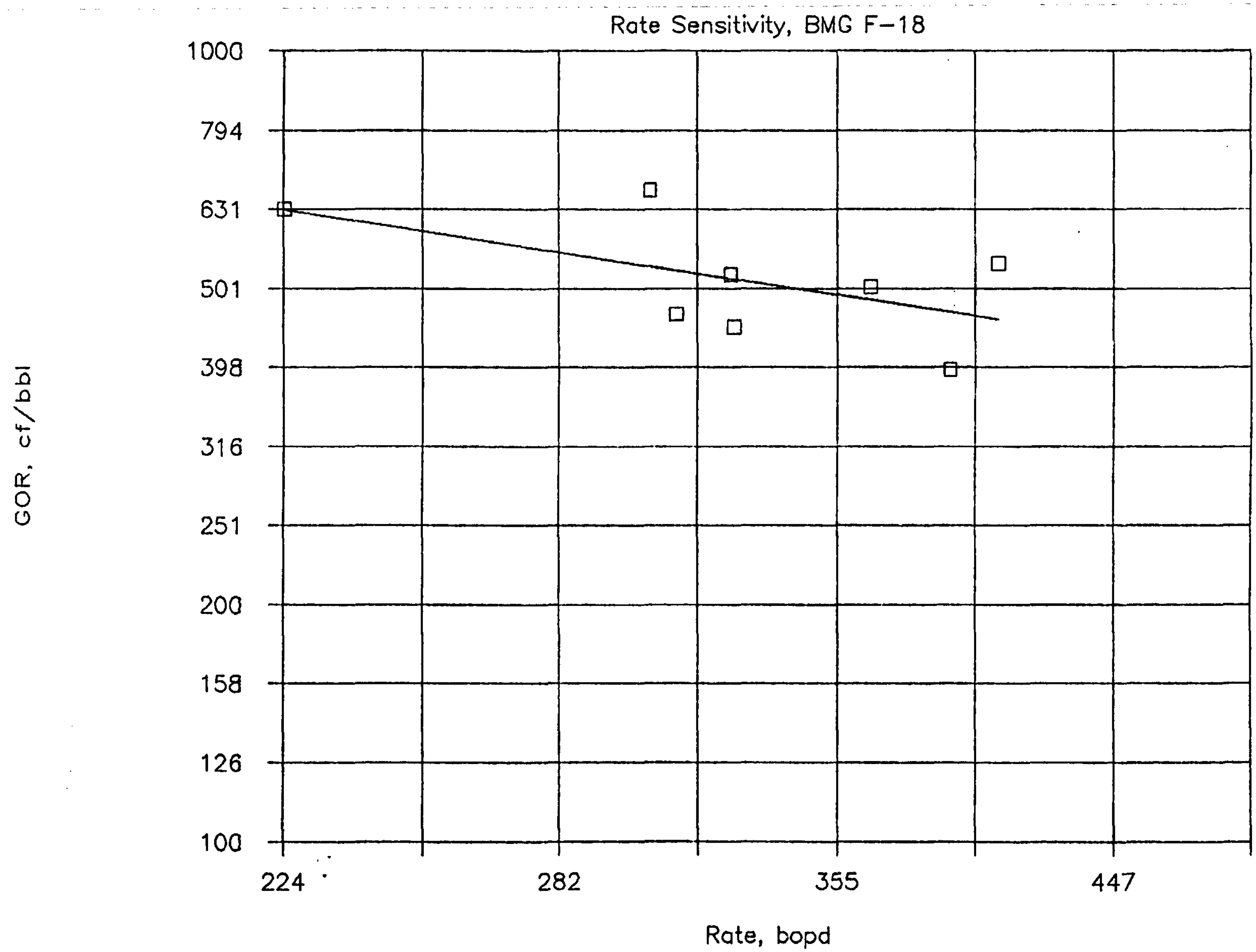

C.C. = 0.58

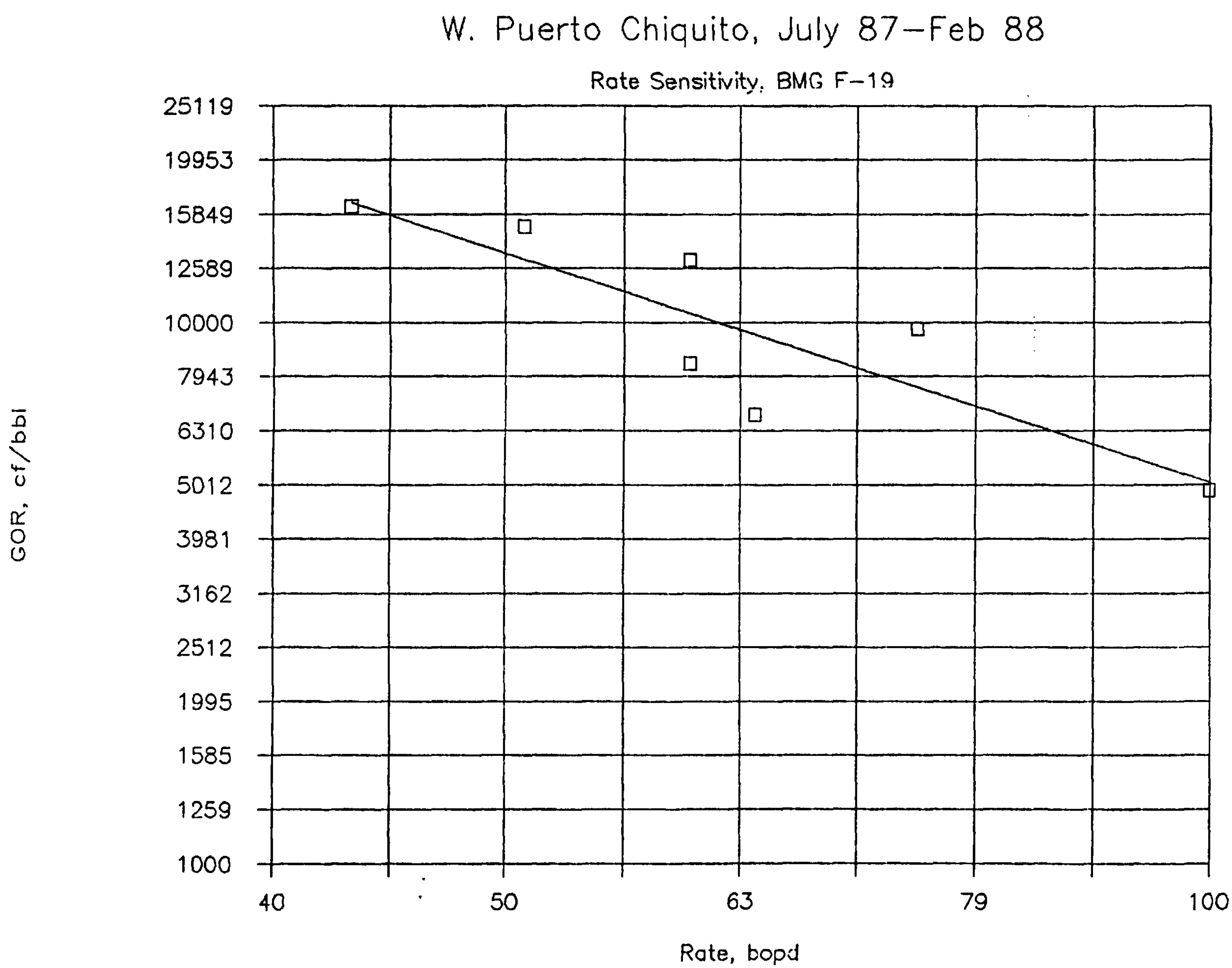
W. Puerto Chiquito, July 87–Feb 88
Rate Sensitivity, BMG F–19
GOR, cf/bbl
25119
19953
15849
12589
10000
7943
6310
5012
3981
3162
2512
1995
1585
1259
1000
40
50
63
79
100
Rate, bopd

C. C. = 0.87

W. Puerto Chiquito, July 87–Feb 88

Rate Sensitivity, BMG F-30

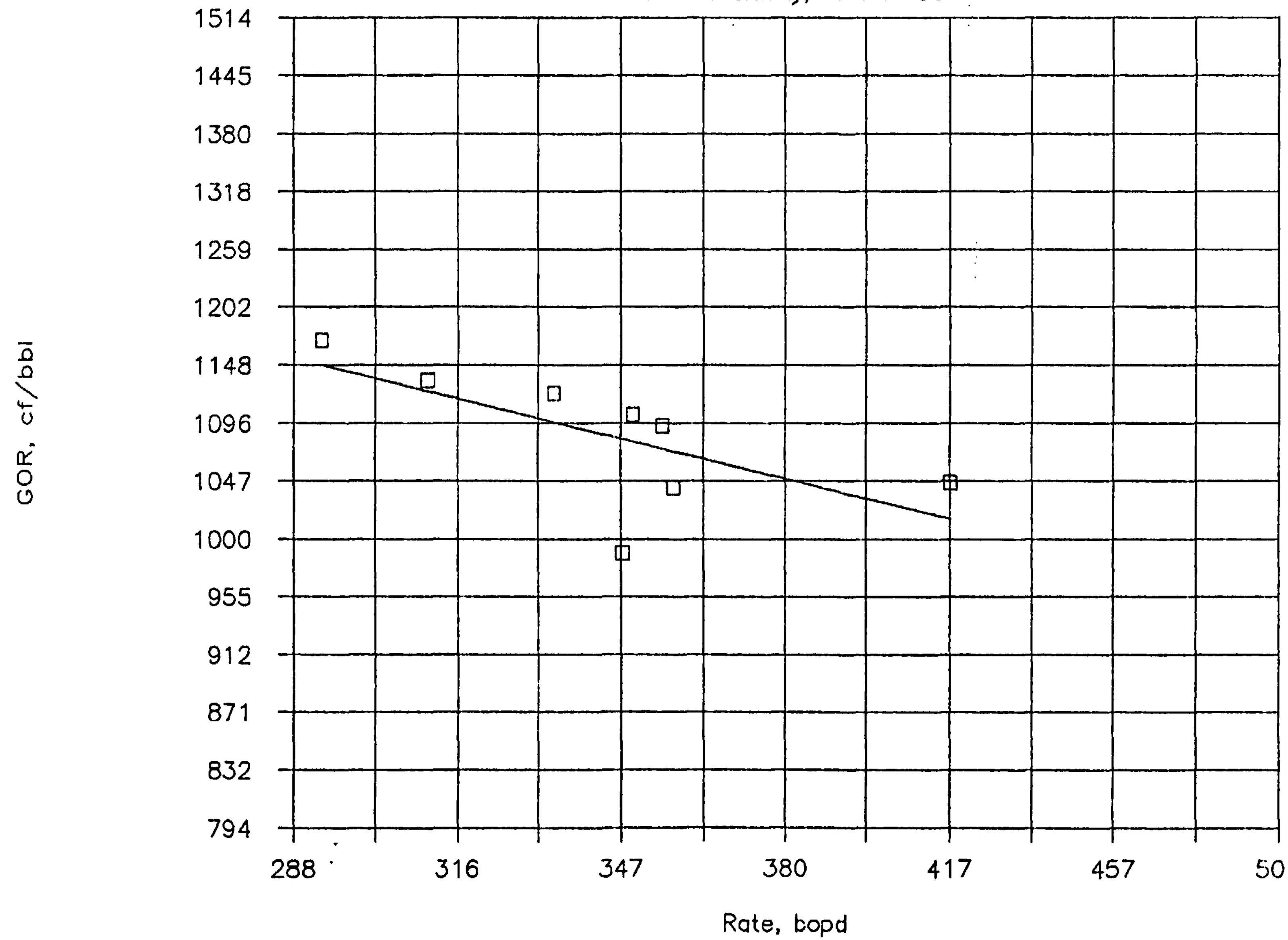

C.C. = 0.66

W. Puerto Chiquito, July 87—Feb 88

Rate Sensitivity, BMG G-5

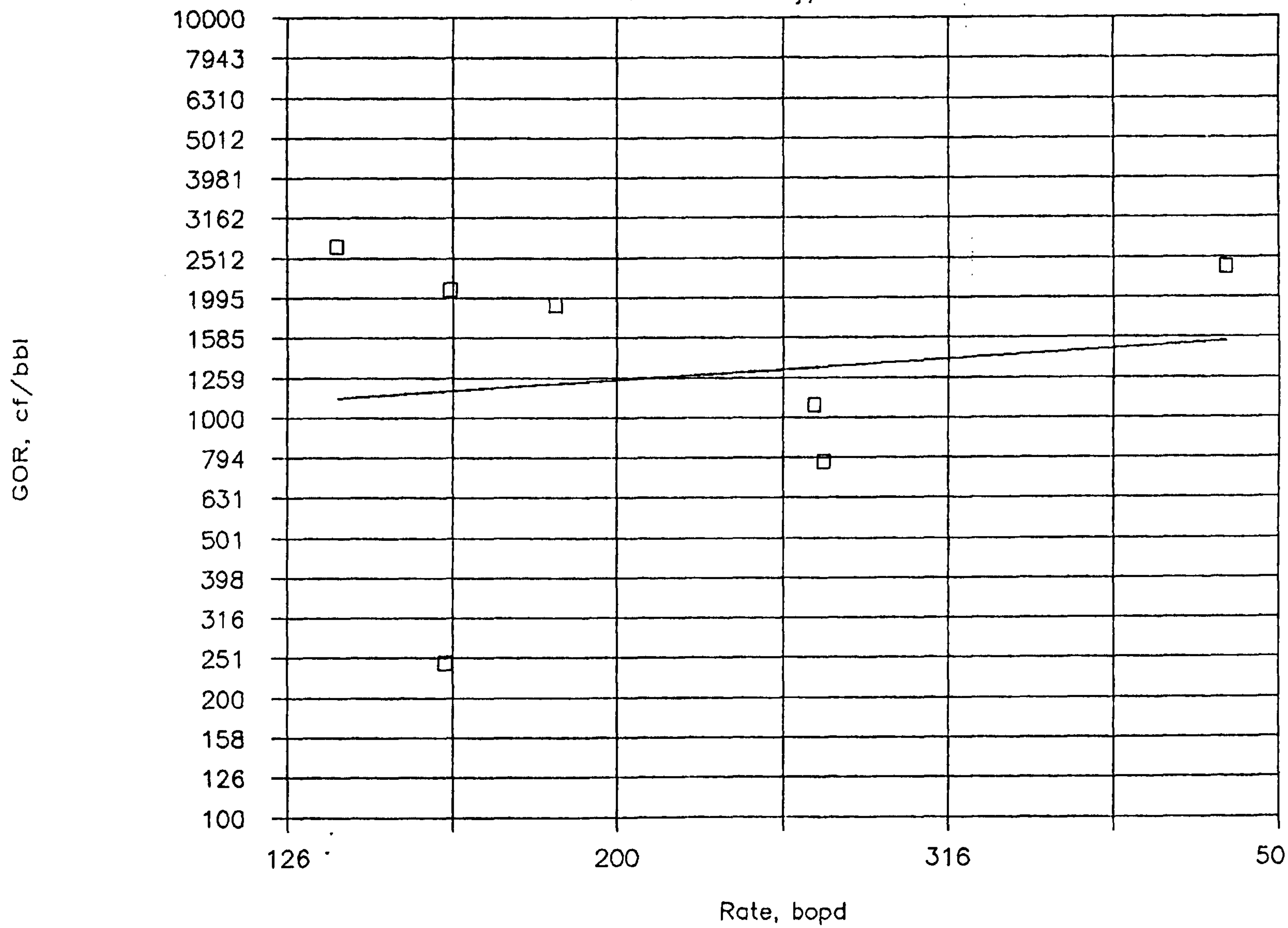

C.C. = 0.13

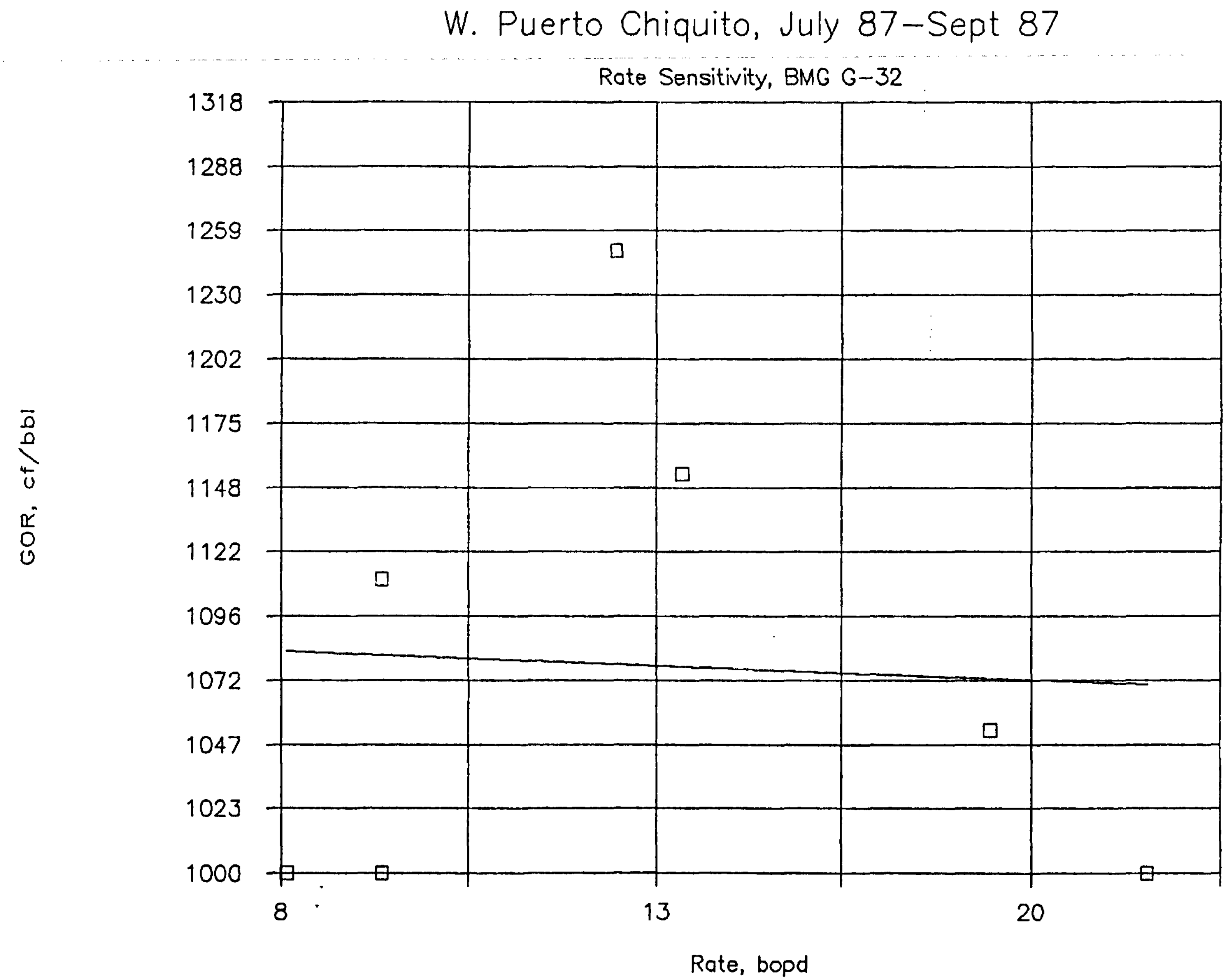

W. Puerto Chiquito, July 87–Sept 87
Rate Sensitivity, BMG G-32
GOR, cf/bbl
1318
1288
1259
1230
1202
1175
1148
1122
1096
1072
1047
1023
1000
8
13
20
Rate, bopd

C.C. = 0.05

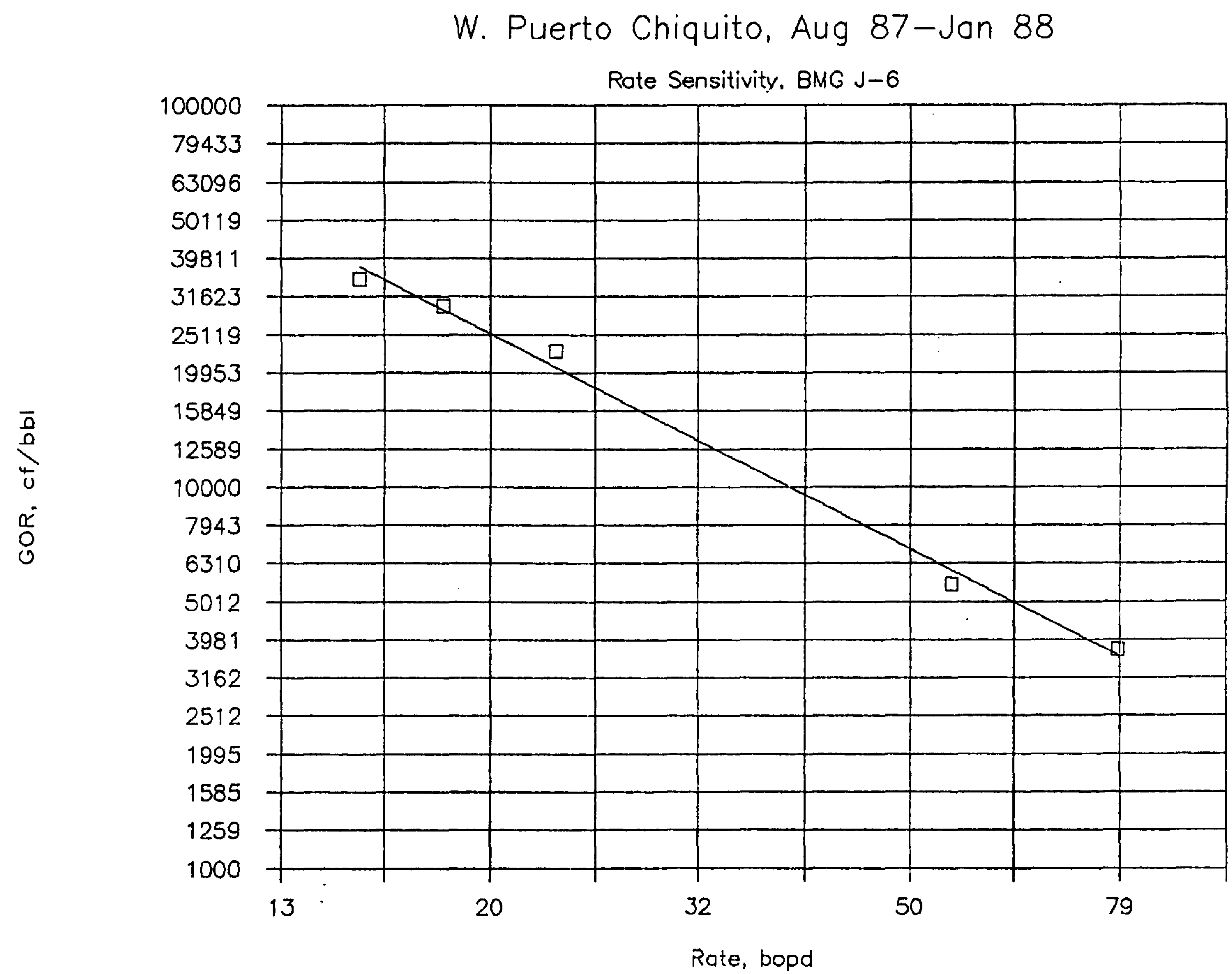

W. Puerto Chiquito, Aug 87—Jan 88
Rate Sensitivity, BMG J-6
100000
79433
63096
50119
39811
31623
25119
19953
15849
12589
10000
7943
6310
5012
3981
3162
2512
1995
1585
1259
1000
13
20
32
50
79
GOR, cf/bbl
Rate, bopd

C.C. = 1.00

Gavilan Dome, Aug 87–Jan 88

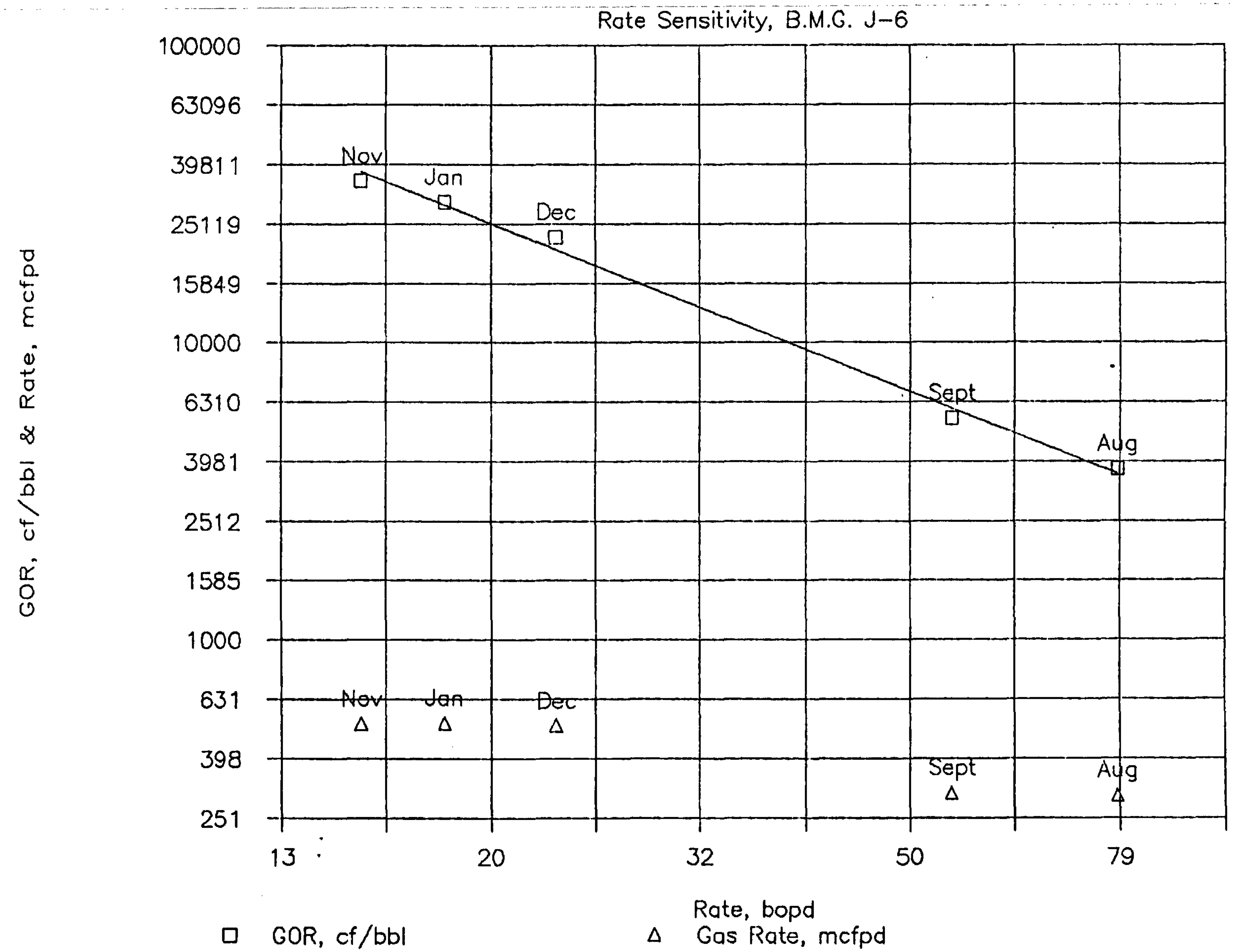

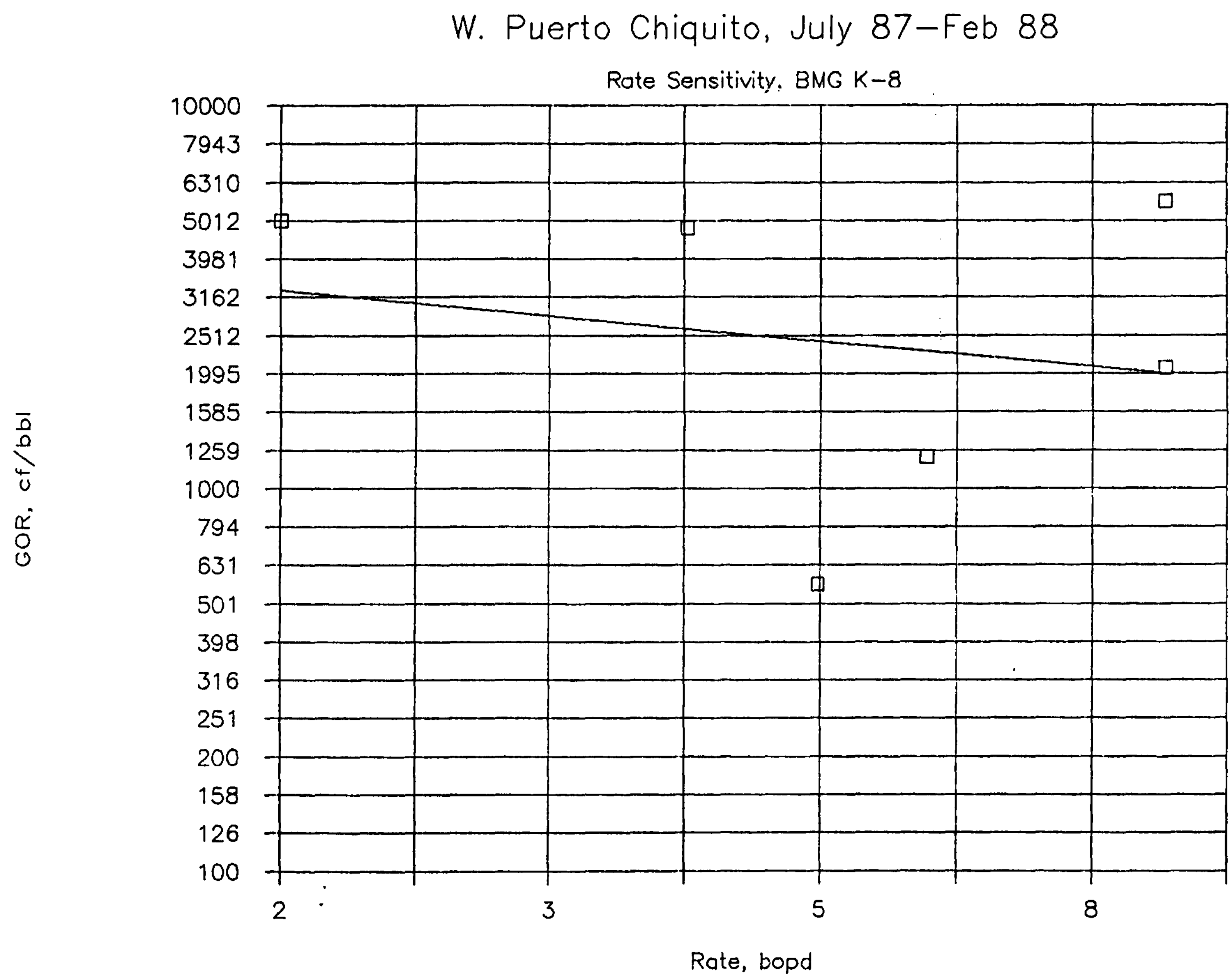
W. Puerto Chiquito, July 87—Feb 88
Rate Sensitivity, BMG K-8
GOR, cf/bbl
10000
7943
6310
5012
3981
3162
2512
1995
1585
1259
1000
794
631
501
398
316
251
200
158
126
100
2
3
5
8
Rate, bopd

C.C. = 0.20

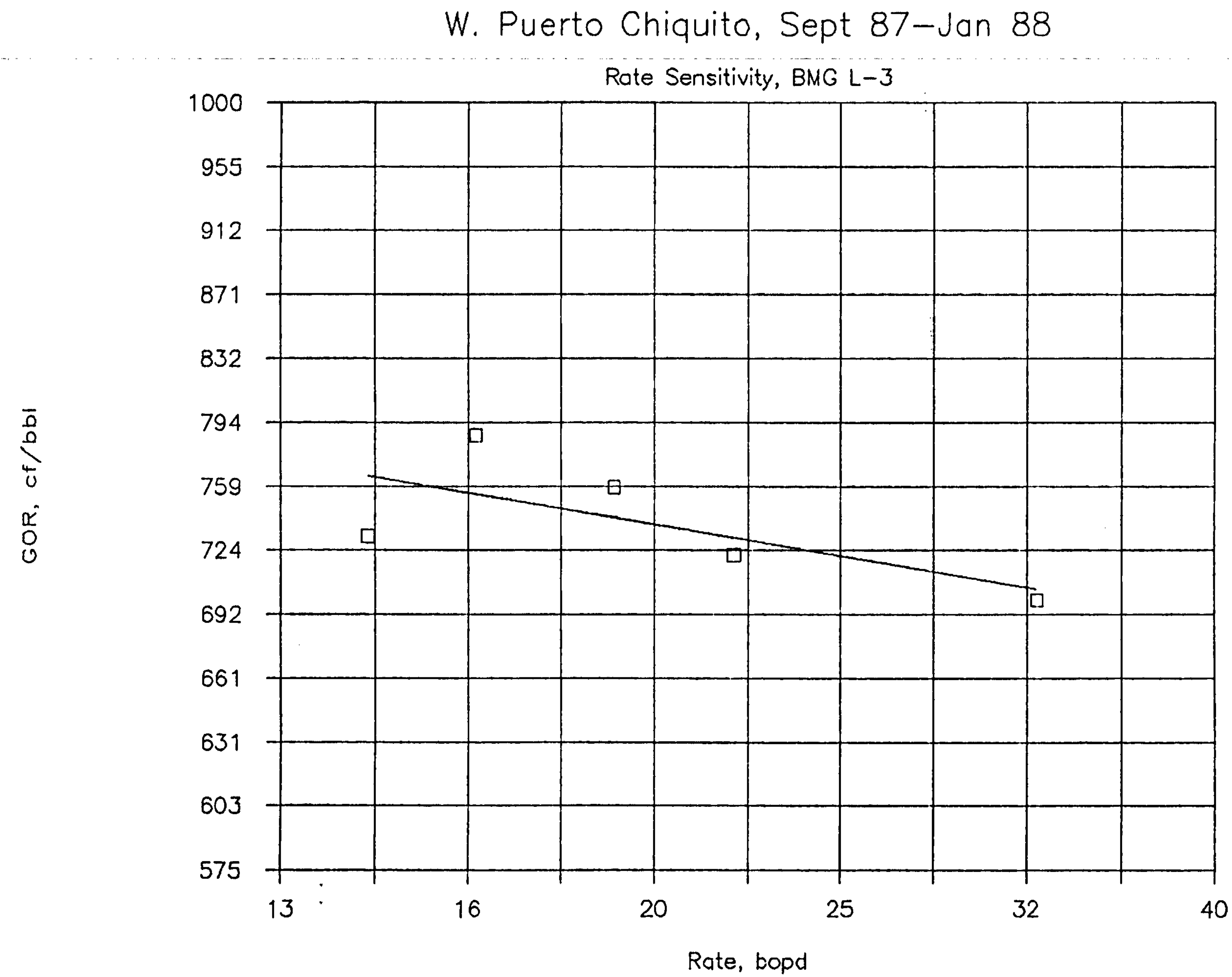

W. Puerto Chiquito, Sept 87–Jan 88
Rate Sensitivity, BMG L-3
GOR, cf/bbl
1000
955
912
871
832
794
759
724
692
661
631
603
575
13
16
20
25
32
40
Rate, bopd

C.C. = 0.68

W. Puerto Chiquito, Sept 87—Jan 88

Rate Sensitivity, BMG L—11

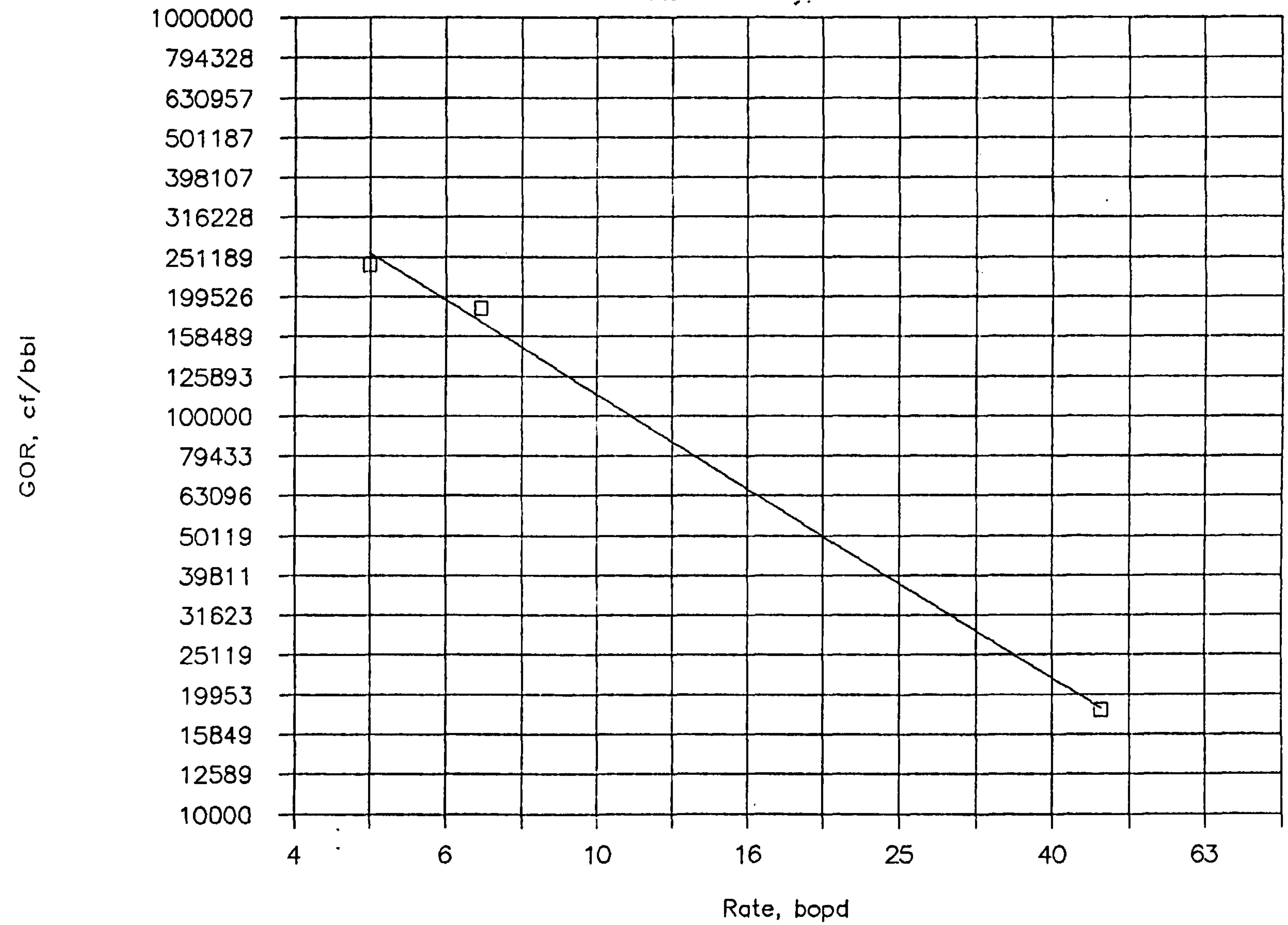

C.C. = 1.00

Gavilan Dome; Aug 87, Sept 87, & Feb 88

Rate Sensitivity, B.M.G. L-11

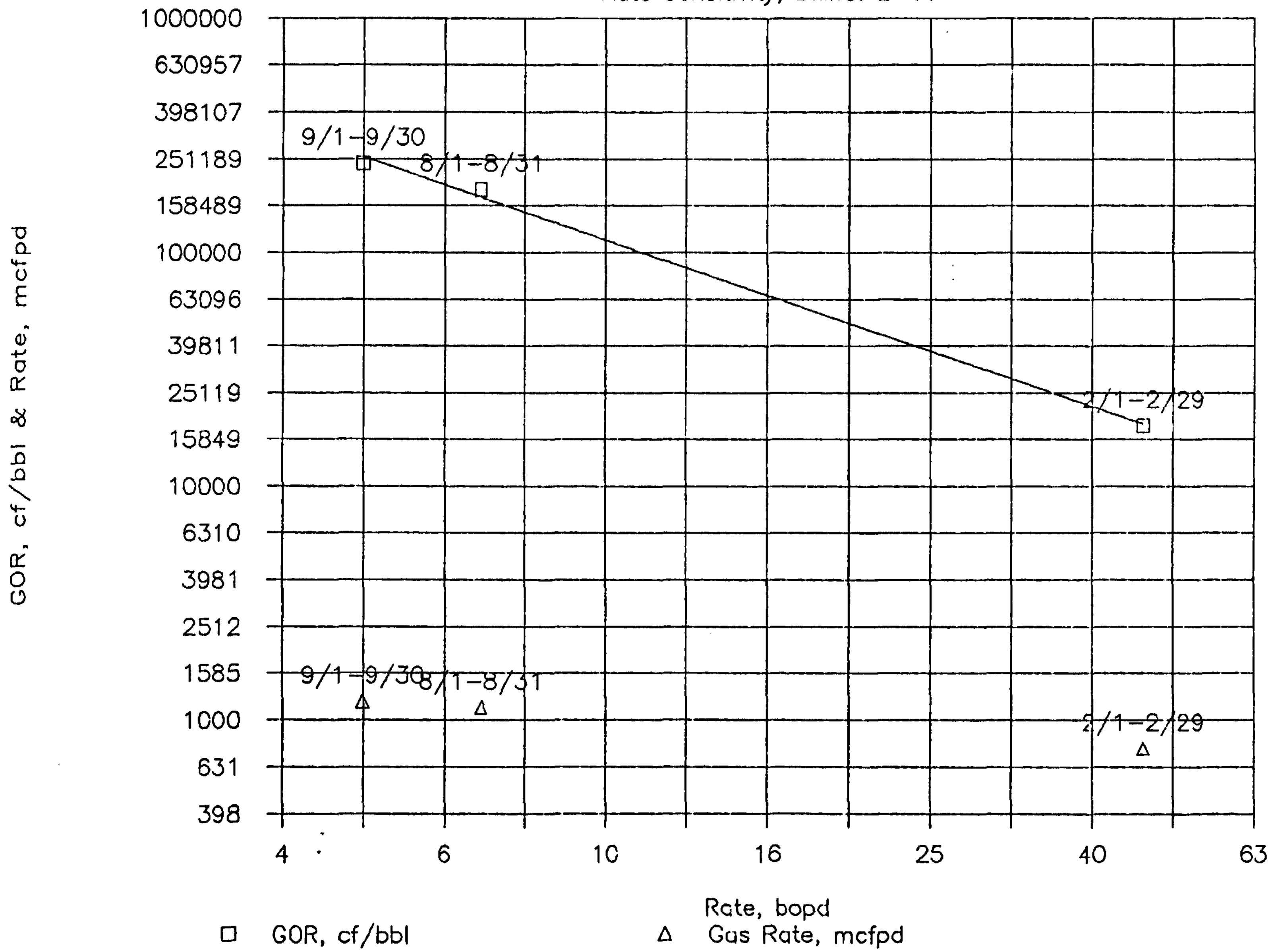

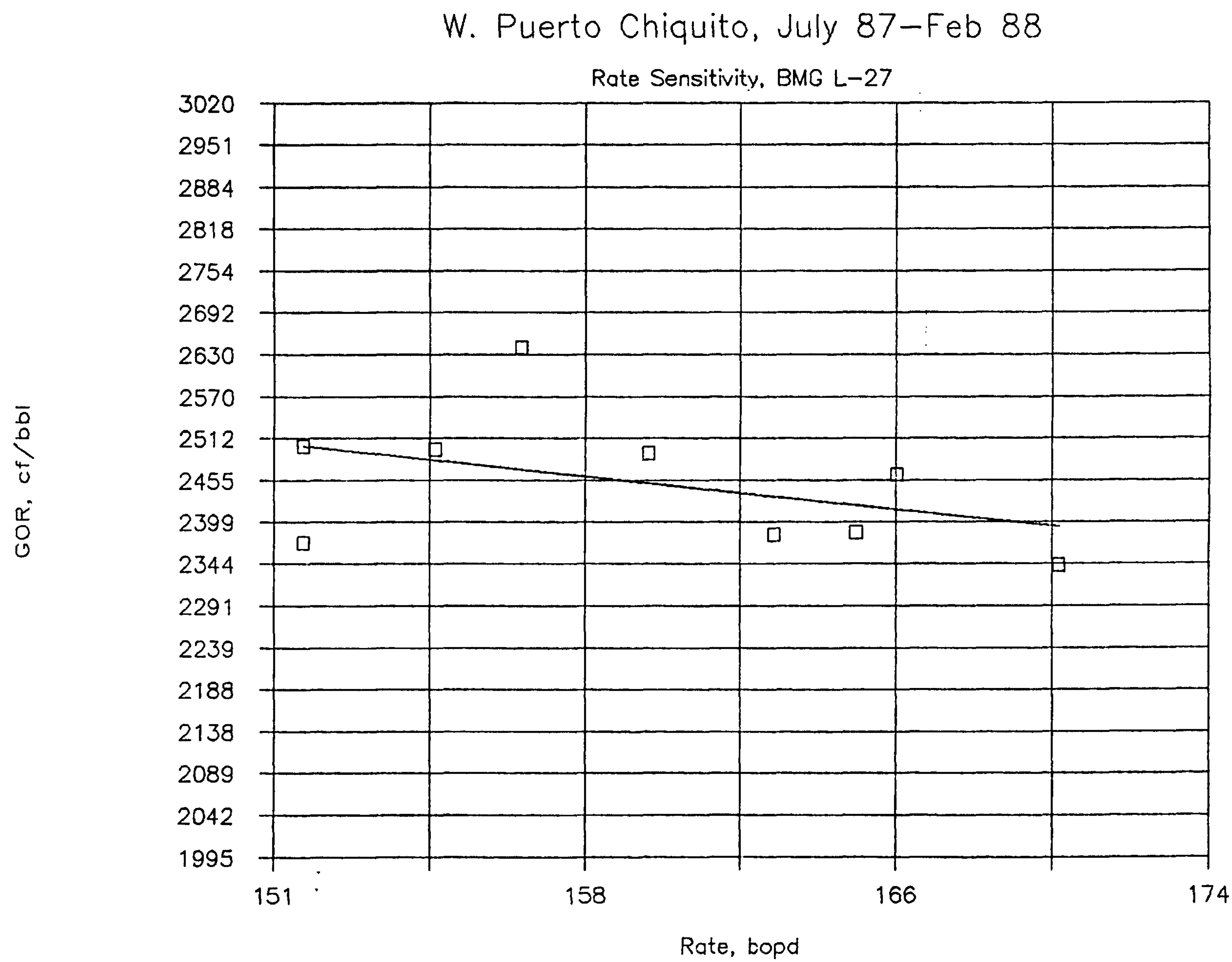
W. Puerto Chiquito, July 87–Feb 88
Rate Sensitivity, BMG L-27
GOR, cf/bbl
3020
2951
2884
2818
2754
2692
2630
2570
2512
2455
2399
2344
2291
2239
2188
2138
2089
2042
1995
151
158
166
174
Rate, bopd

C.C. = 0.43

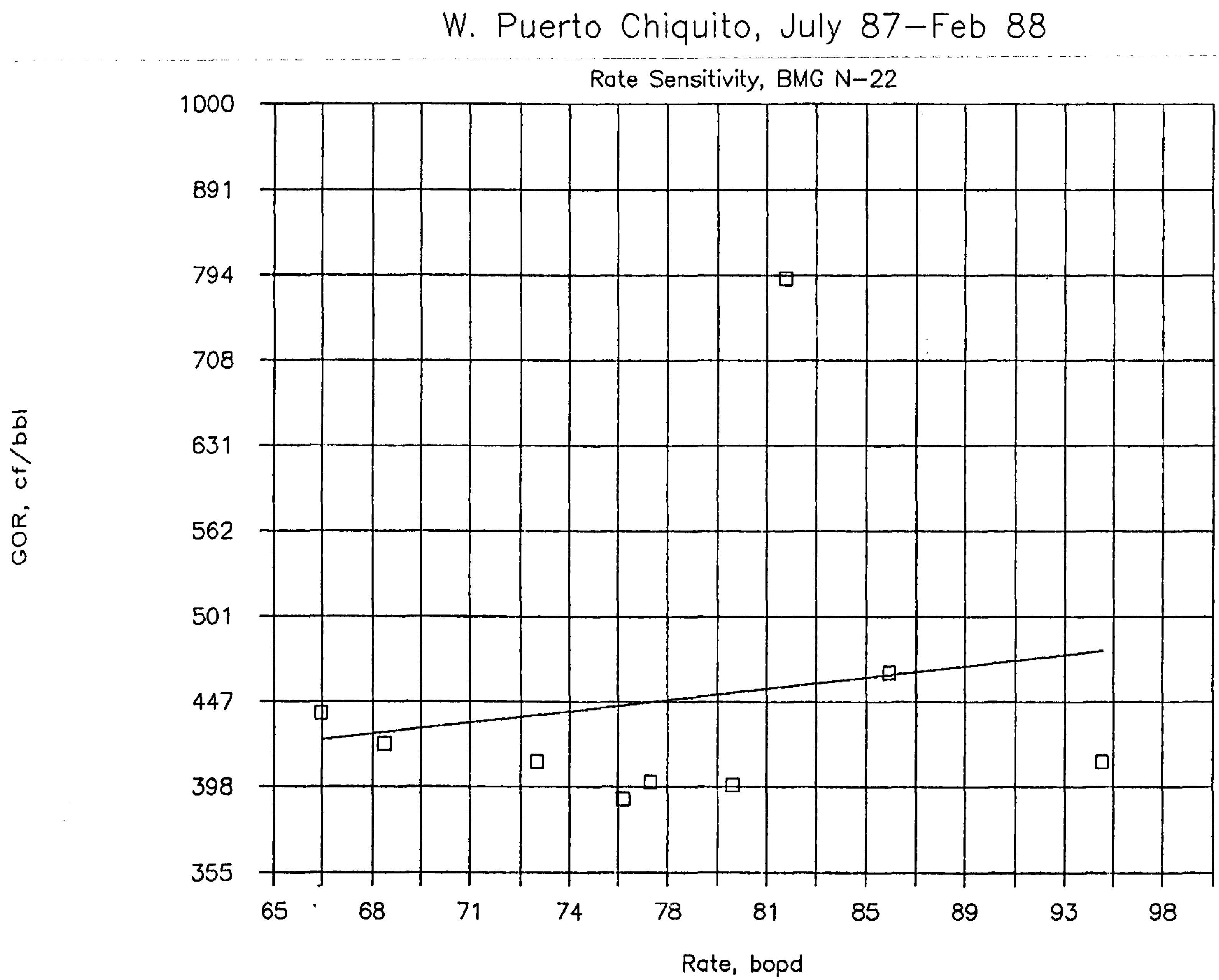
W. Puerto Chiquito, July 87–Feb 88
Rate Sensitivity, BMG N–22
GOR, cf/bbl
1000
891
794
708
631
562
501
447
398
355
65
68
71
74
78
81
85
89
93
98
Rate, bopd

C.C. = 0.17

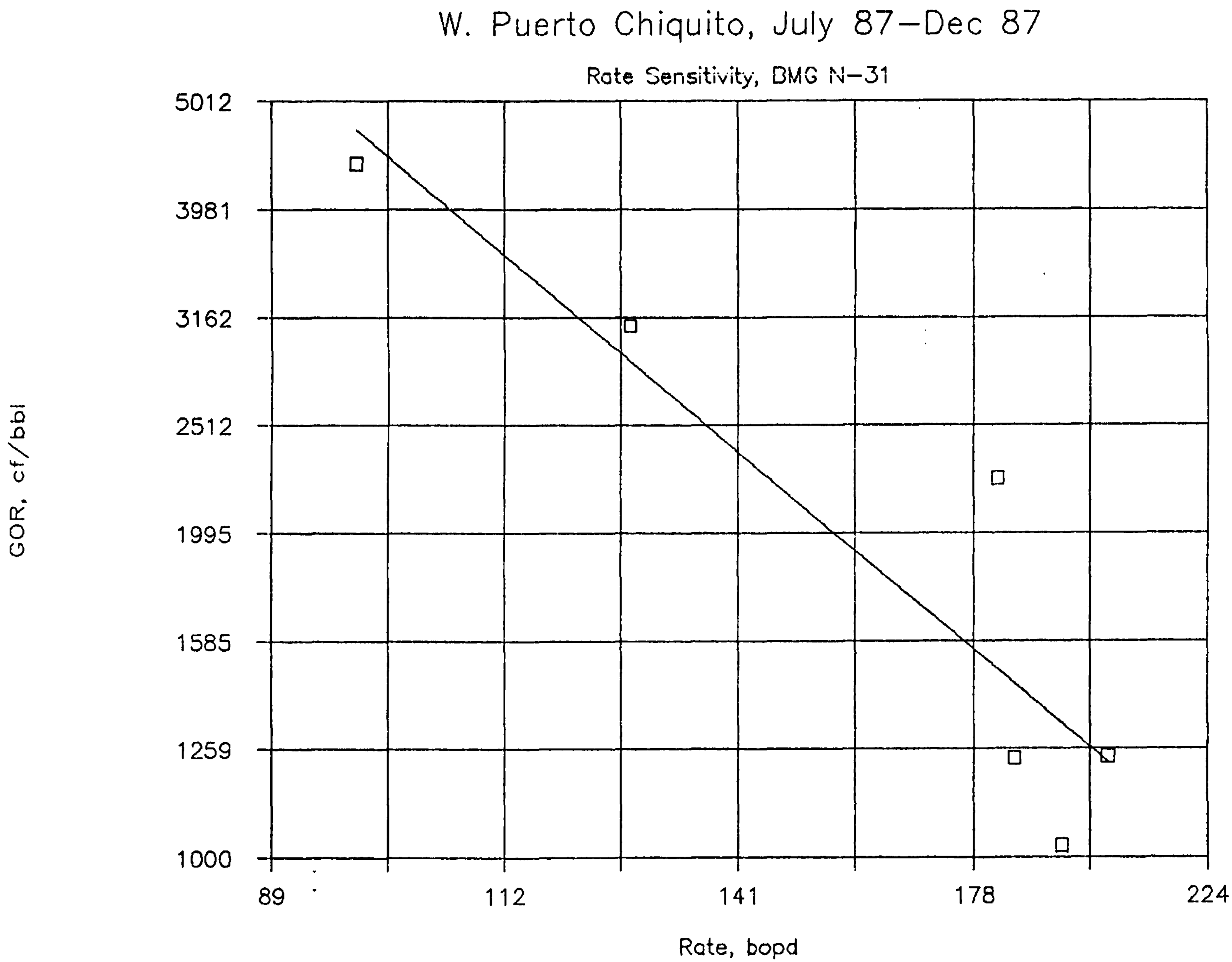
W. Puerto Chiquito, July 87–Dec 87
Rate Sensitivity, BMG N–31
5012
3981
3162
2512
1995
1585
1259
1000
GOR, cf/bbl
89
112
141
178
224
Rate, bopd

C.C. = 0.92

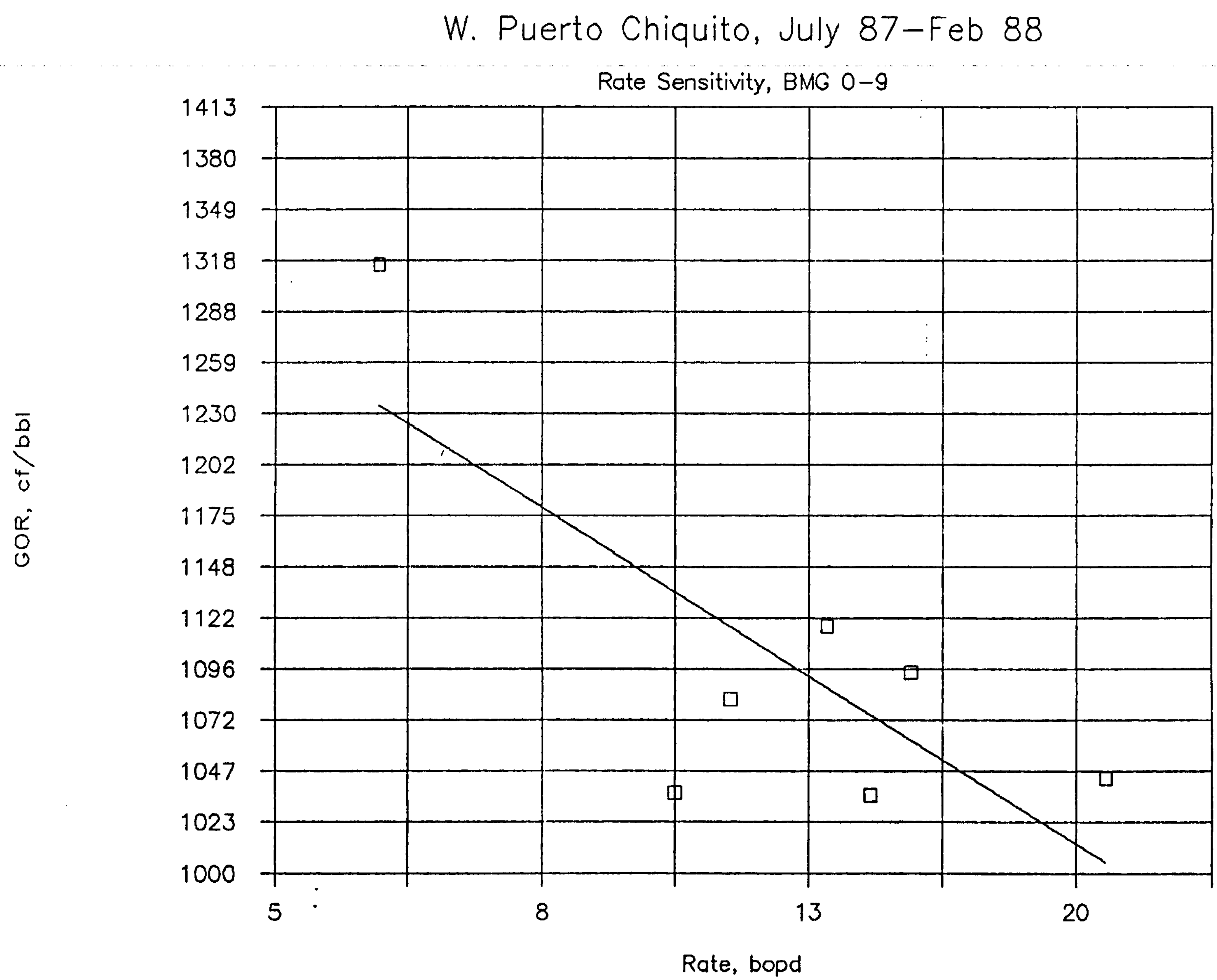
W. Puerto Chiquito, July 87—Feb 88
Rate Sensitivity, BMG 0-9
GOR, cf/bbl
1413
1380
1349
1318
1288
1259
1230
1202
1175
1148
1122
1096
1072
1047
1023
1000
5
8
13
20
Rate, bopd

C.C. = 0.76

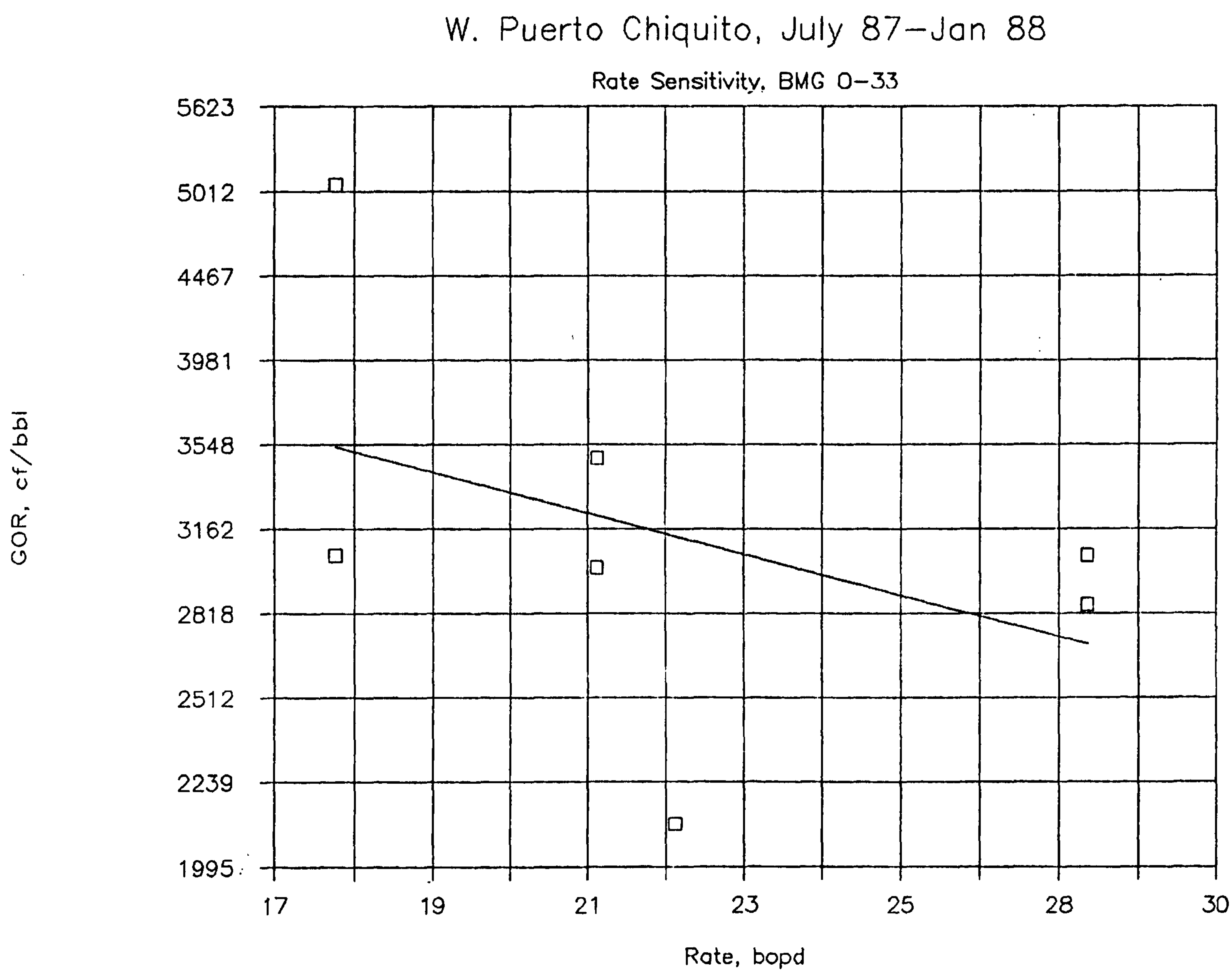

W. Puerto Chiquito, July 87–Jan 88
Rate Sensitivity, BMG 0–33
GOR, cf/bbl
5623
5012
4467
3981
3548
3162
2818
2512
2239
1995
17
19
21
23
25
28
30
Rate, bopd

C.C. = 0.43

Gavilan Dome, July 87–Feb 88

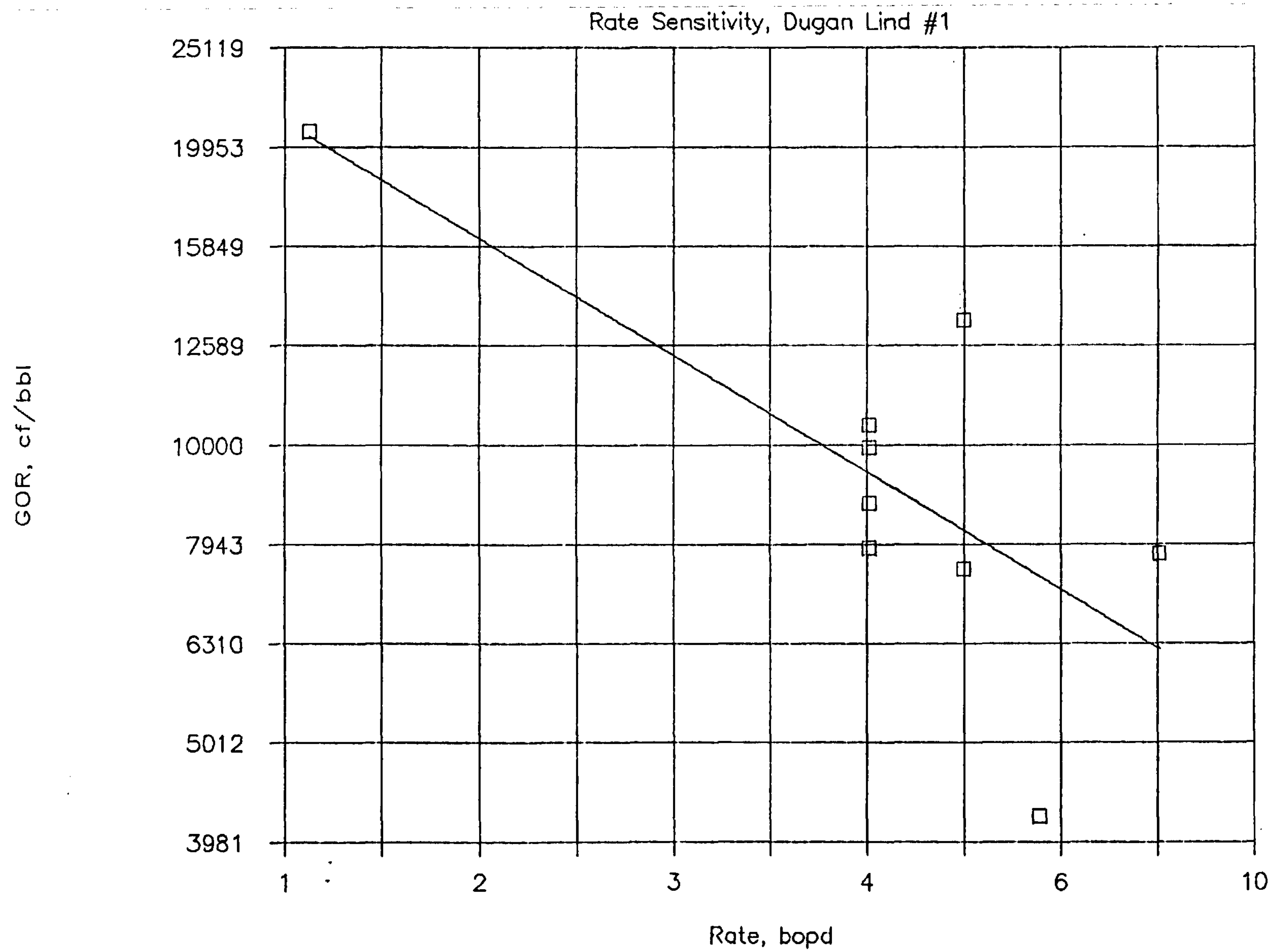

C. C. = 0.75

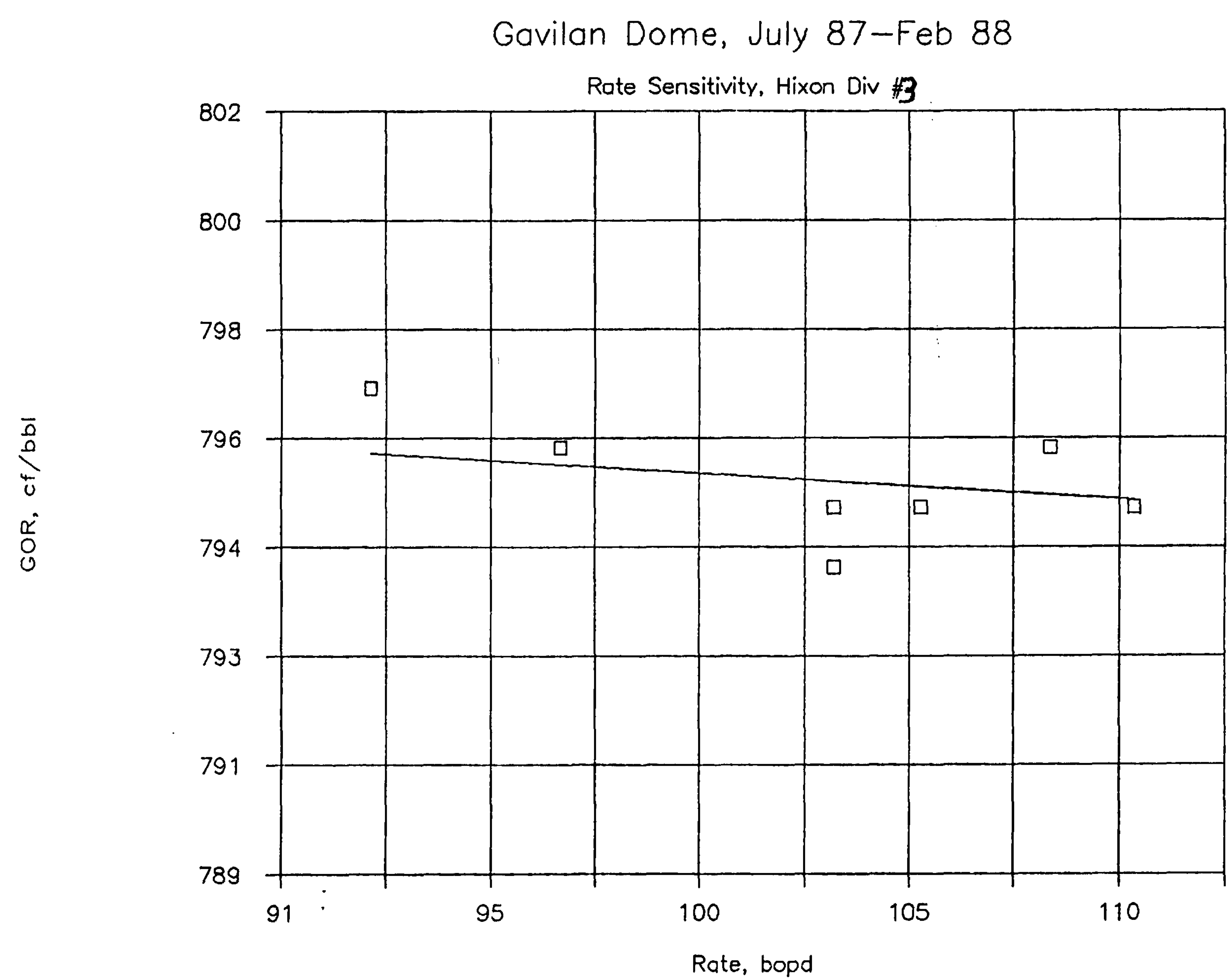
Gavilan Dome, July 87–Feb 88
Rate Sensitivity, Hixon Div #3
802
800
798
796
794
793
791
789
GOR, cf/bbl
91
95
100
105
110
Rate, bopd

C.C. = 0.06

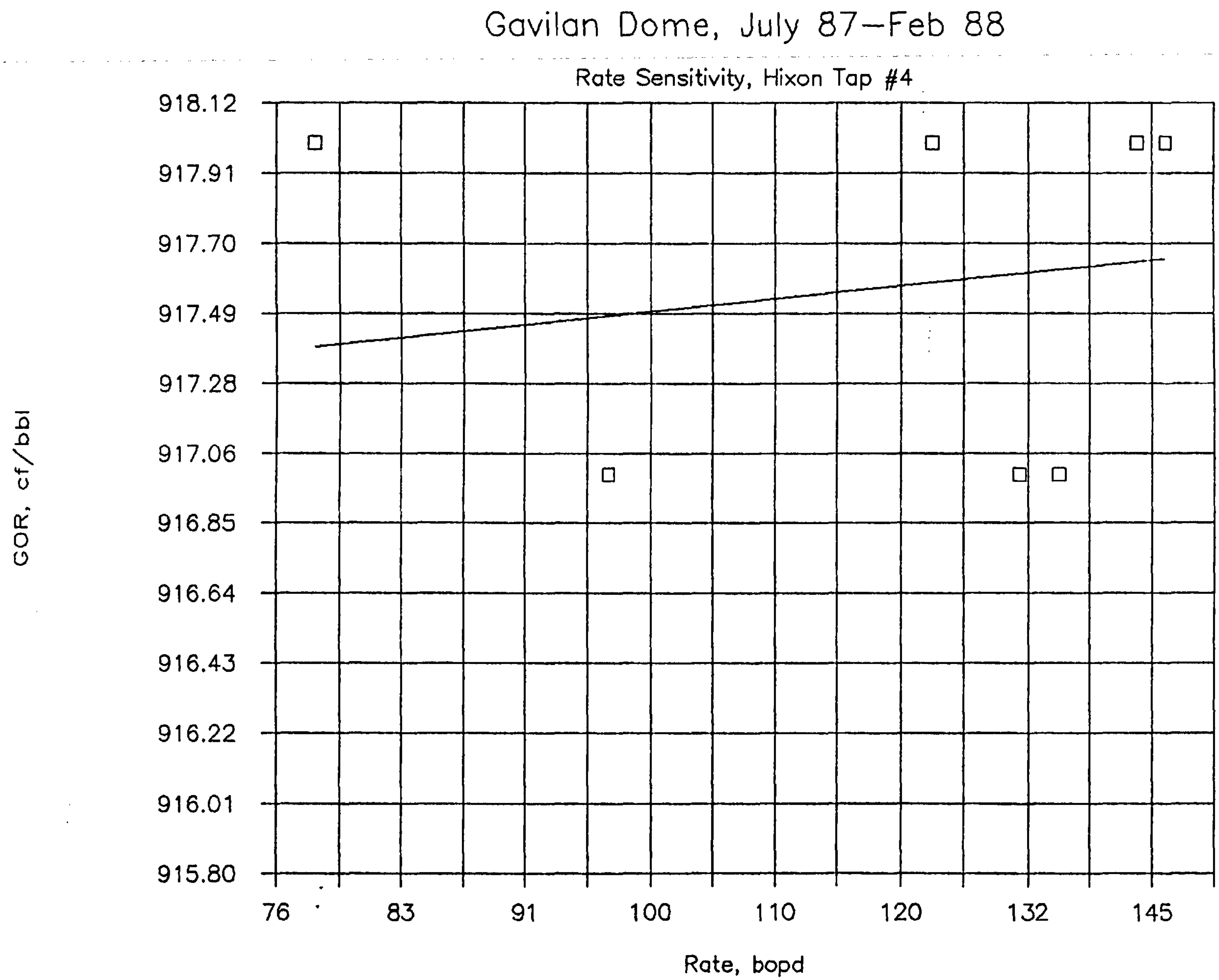
Gavilan Dome, July 87—Feb 88
Rate Sensitivity, Hixon Tap #4
918.12
917.91
917.70
917.49
917.28
917.06
916.85
916.64
916.43
916.22
916.01
915.80
GOR, cf/bbl
76
83
91
100
110
120
132
145
Rate, bopd

C.C. = 0.01

Gavilan Dome, Dec 87—Feb 88

Rate Sensitivity, Mallon DF 3#15

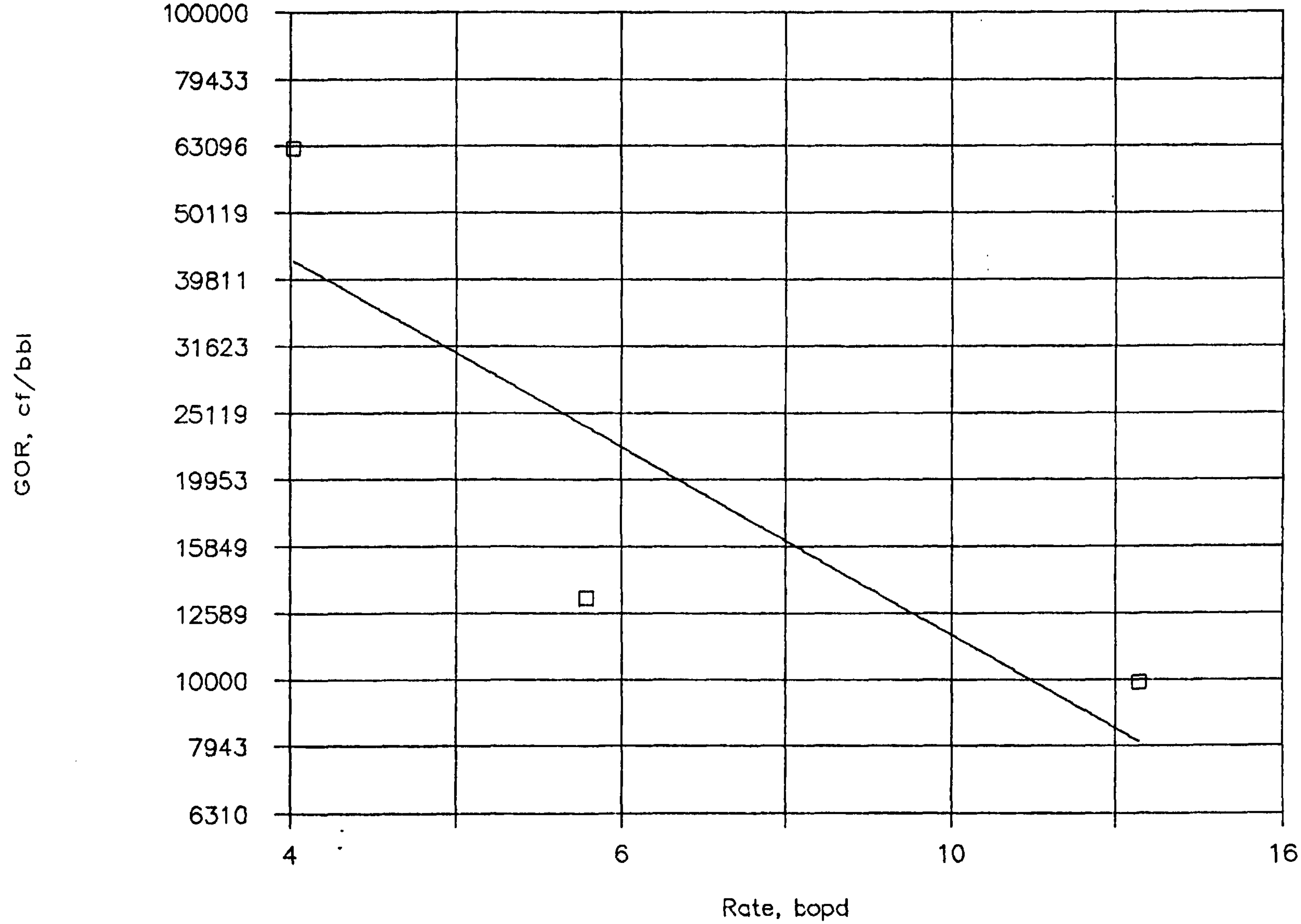

C.C.=0.85

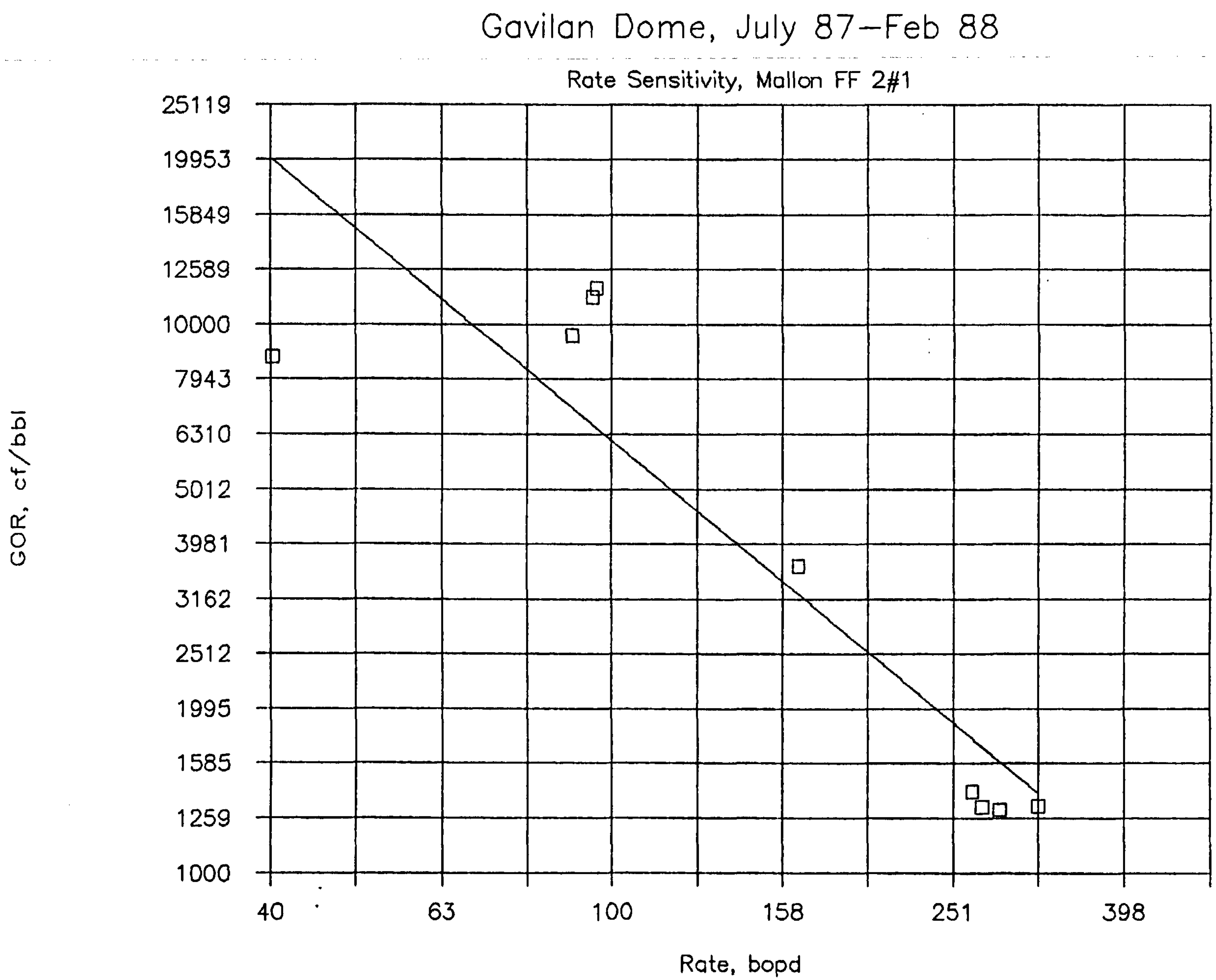

Gavilan Dome, July 87—Feb 88
Rate Sensitivity, Mallon FF 2#1
GOR, cf/bbl
25119
19953
15849
12589
10000
7943
6310
5012
3981
3162
2512
1995
1585
1259
1000
40
63
100
158
251
398
Rate, bopd

C.C. = 0.90

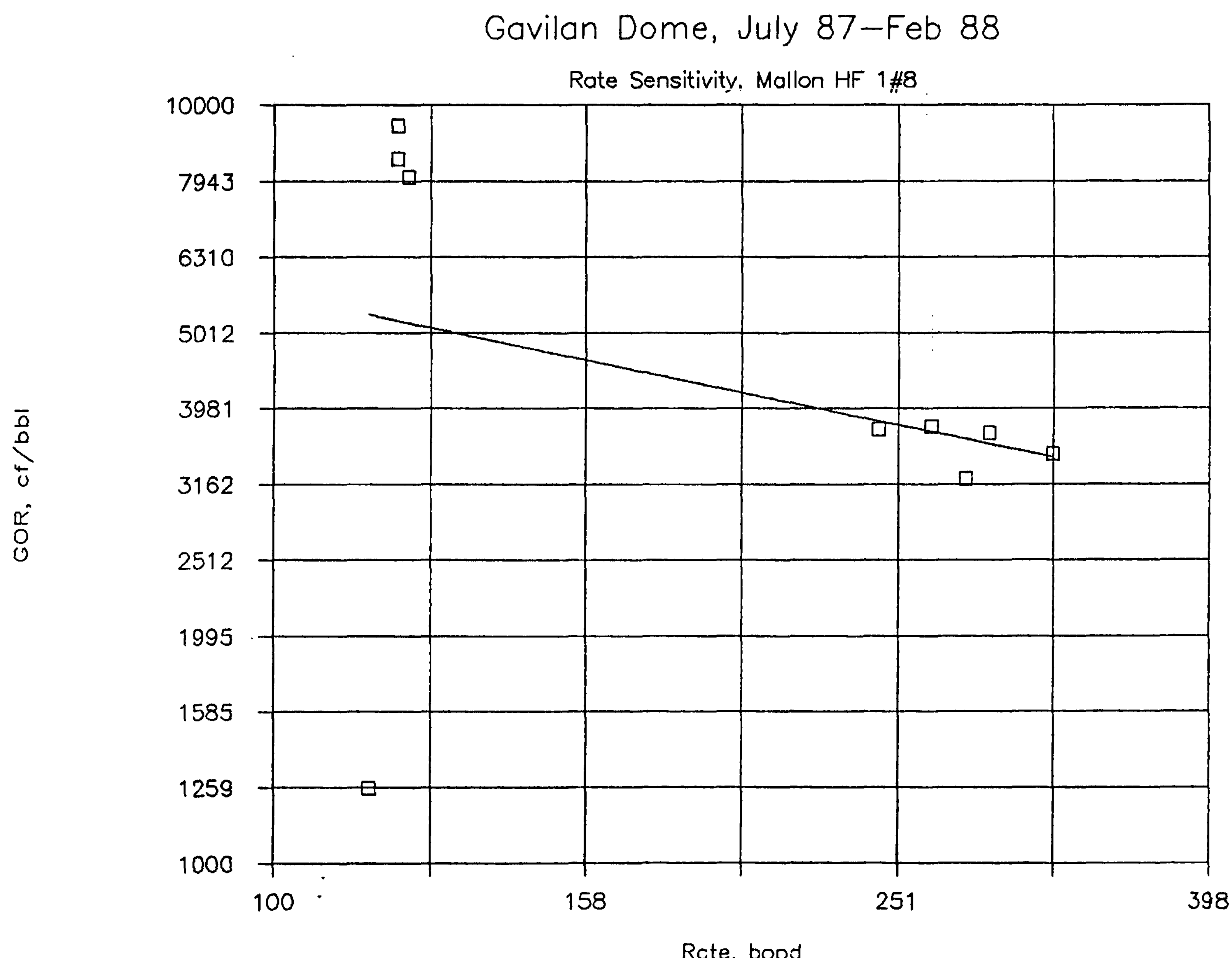

Gavilan Dome, July 87—Feb 88
Rate Sensitivity, Mallon HF 1#8
GOR, cf/bbl
10000
7943
6310
5012
3981
3162
2512
1995
1585
1259
1000
100
158
251
398
Rate, bopd

C. C. = 0.31

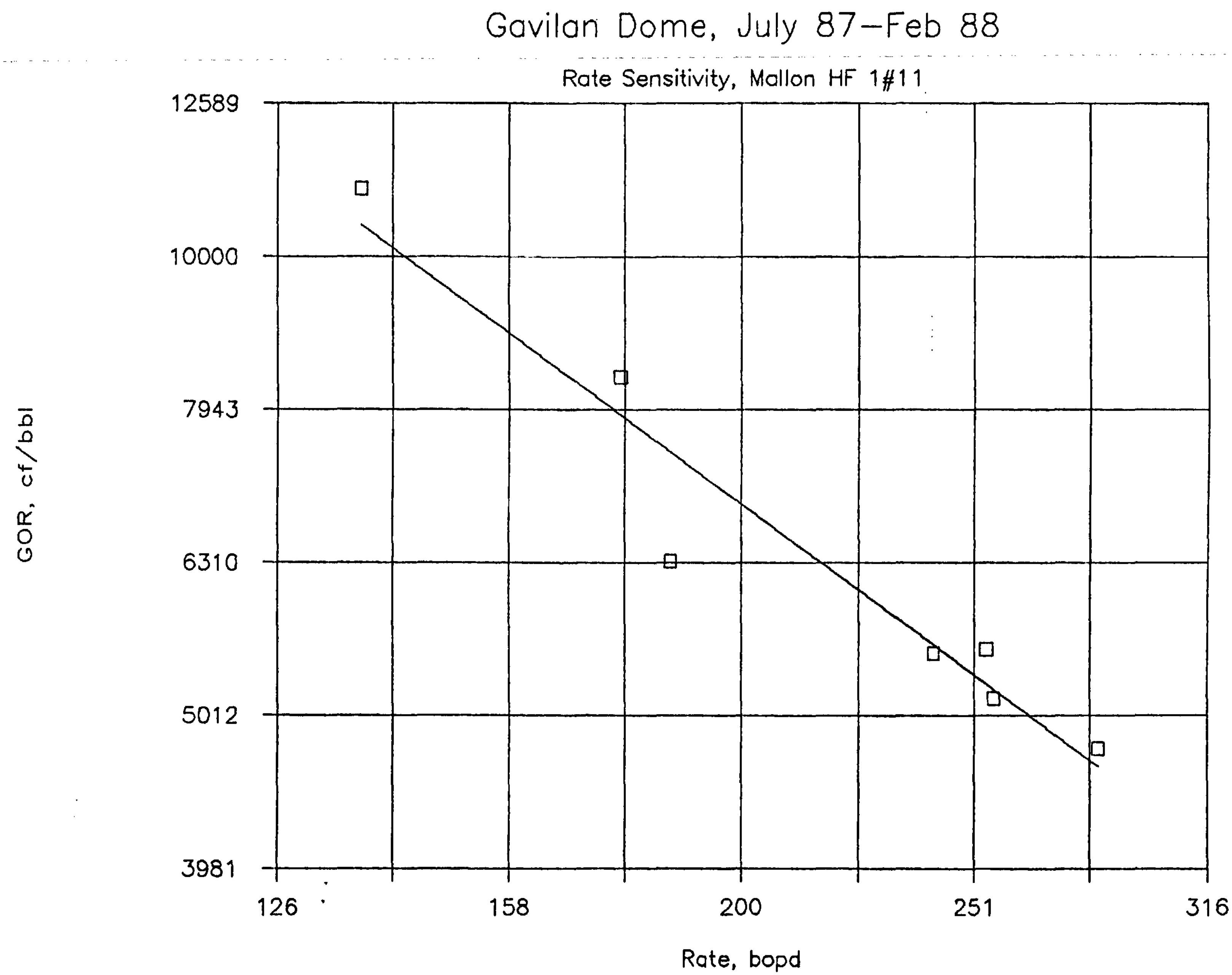

Gavilan Dome, July 87–Feb 88
Rate Sensitivity, Mallon HF 1#11
12589
10000
7943
6310
5012
3981
GOR, cf/bbl
126
158
200
251
316
Rate, bopd

C.C. = 0.97

Gavilan Dome, July 87—Feb 88

Rate Sensitivity, Mallon JF 12#5

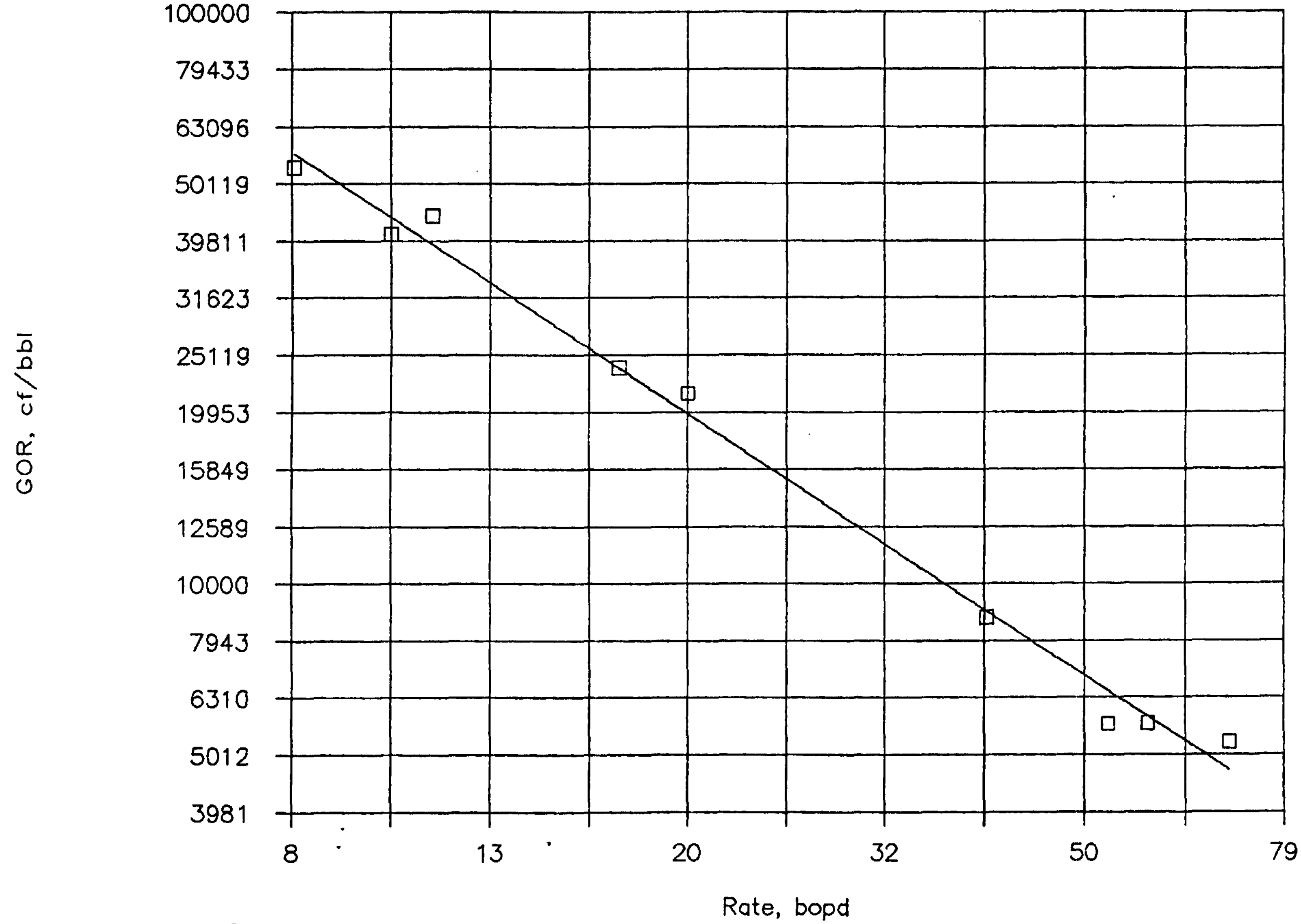

C.C. = 1.00

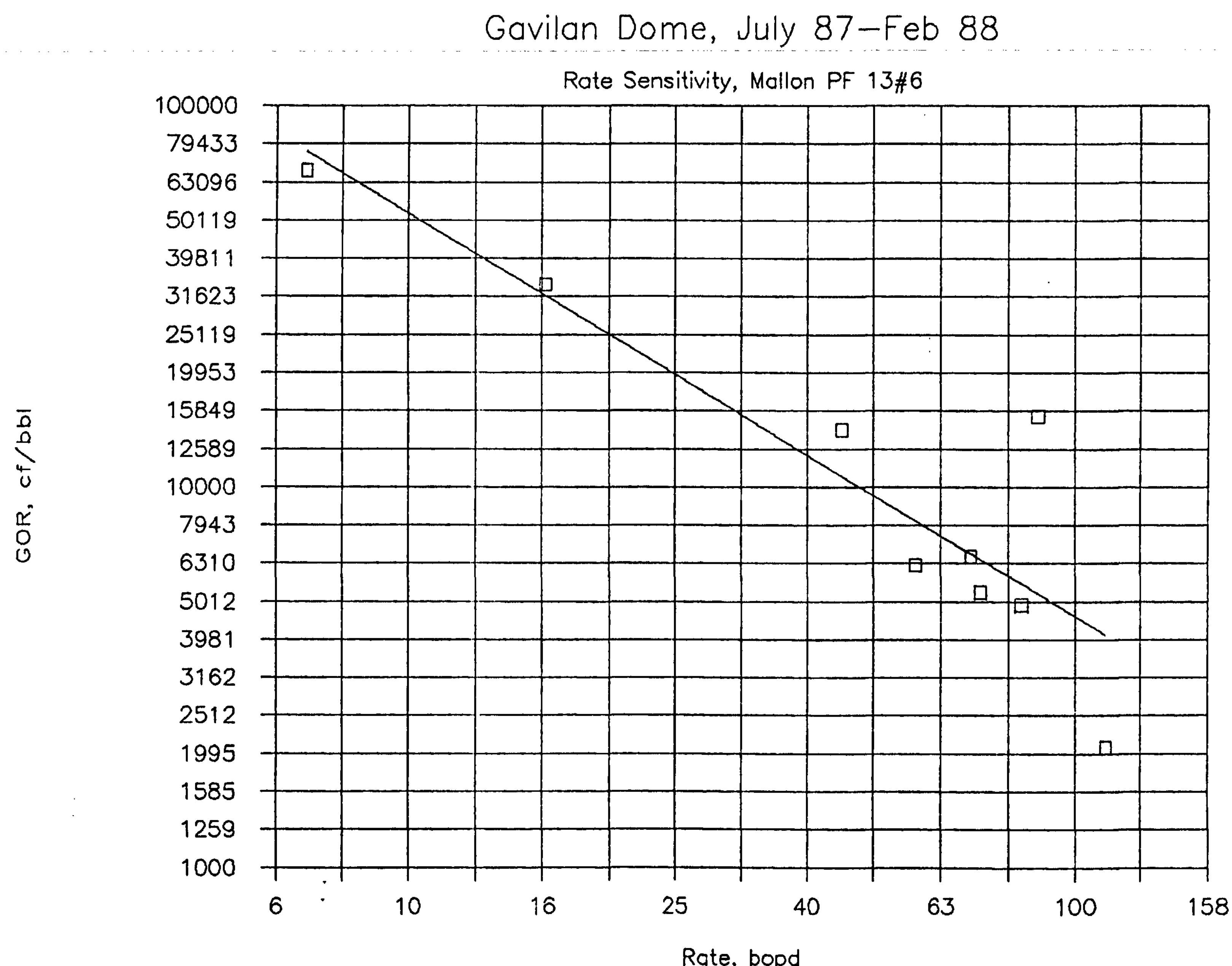

Gavilan Dome, July 87–Feb 88
Rate Sensitivity, Mallon PF 13#6
GOR, cf/bbl
100000
79433
63096
50119
39811
31623
25119
19953
15849
12589
10000
7943
6310
5012
3981
3162
2512
1995
1585
1259
1000
6
10
16
25
40
63
100
158
Rate, bopd

C. C. = 0.89

Gavilan Dome, July 87–Feb 88

Rate Sensitivity, Mallon Rf 2#16

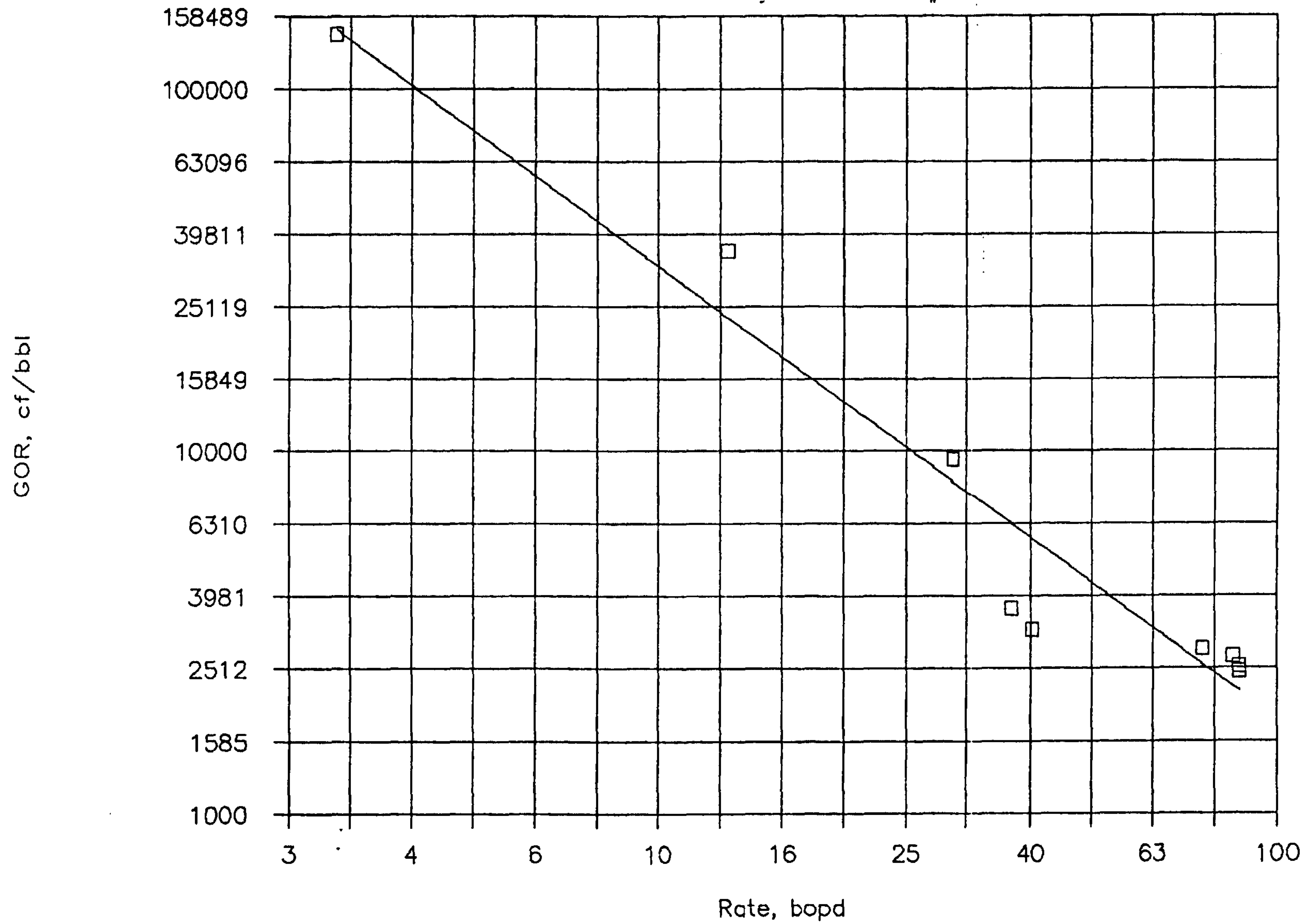

C.C. = 0.97

Gavilan Dome, July 87–Jan 88

Rate Sensitivity, Meridian HAF #2

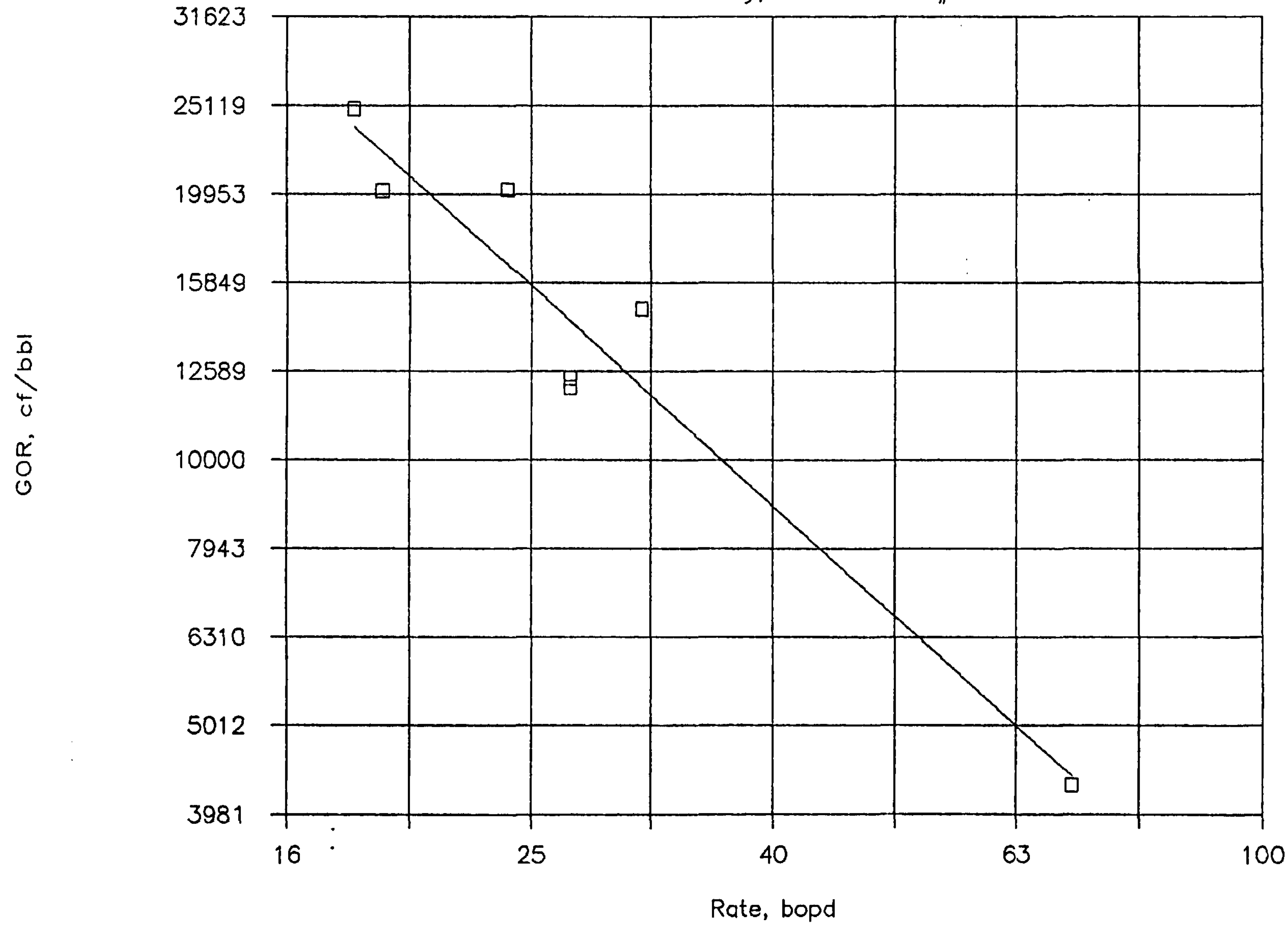

C. C. = 0.96

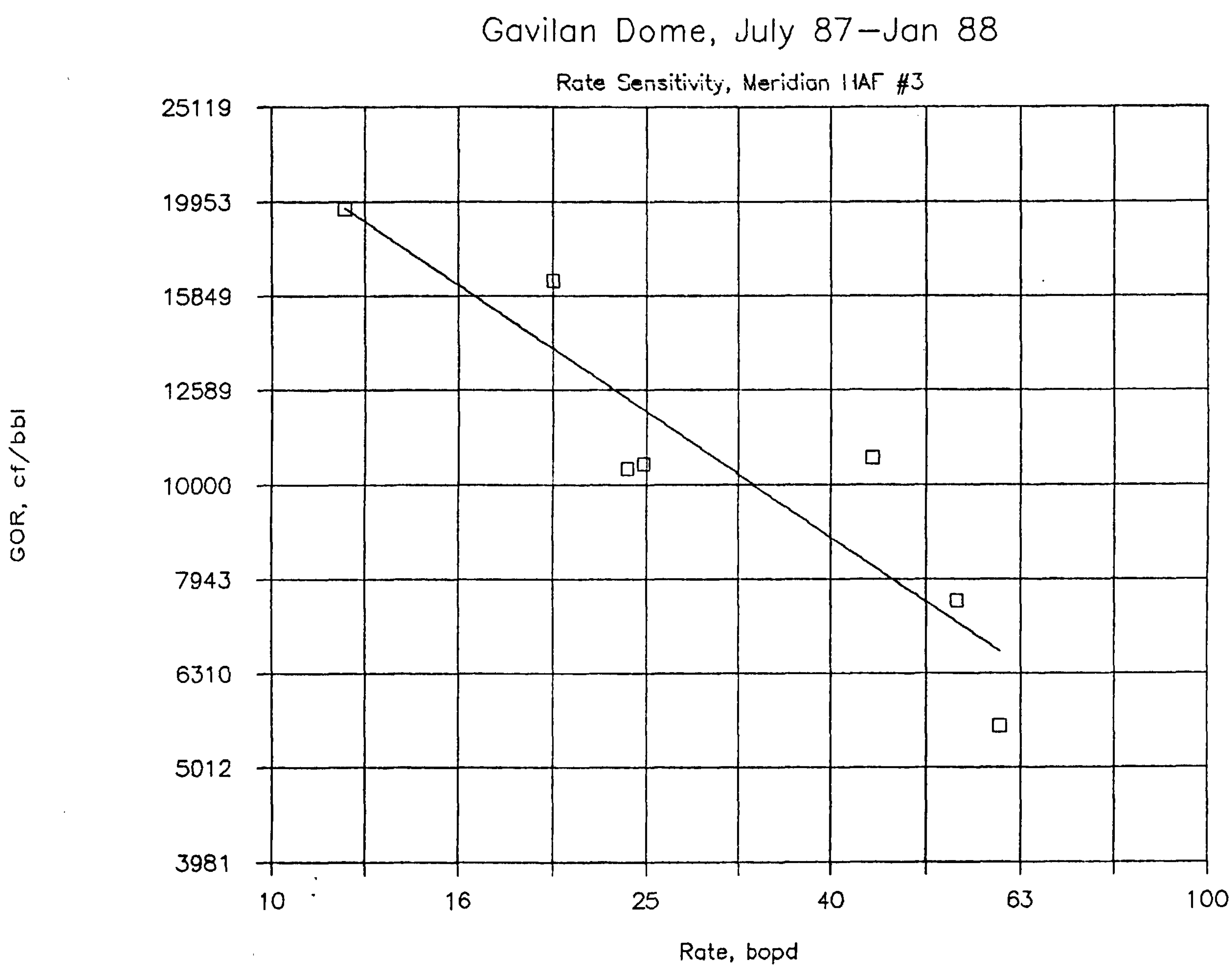
Gavilan Dome, July 87—Jan 88
Rate Sensitivity, Meridian HAF #3
GOR, cf/bbl
25119
19953
15849
12589
10000
7943
6310
5012
3981
10
16
25
40
63
100
Rate, bopd

C. C. = 0.92

Gavilan Dome, July 87–Jan 88

Rate Sensitivity, Meridian HF #1

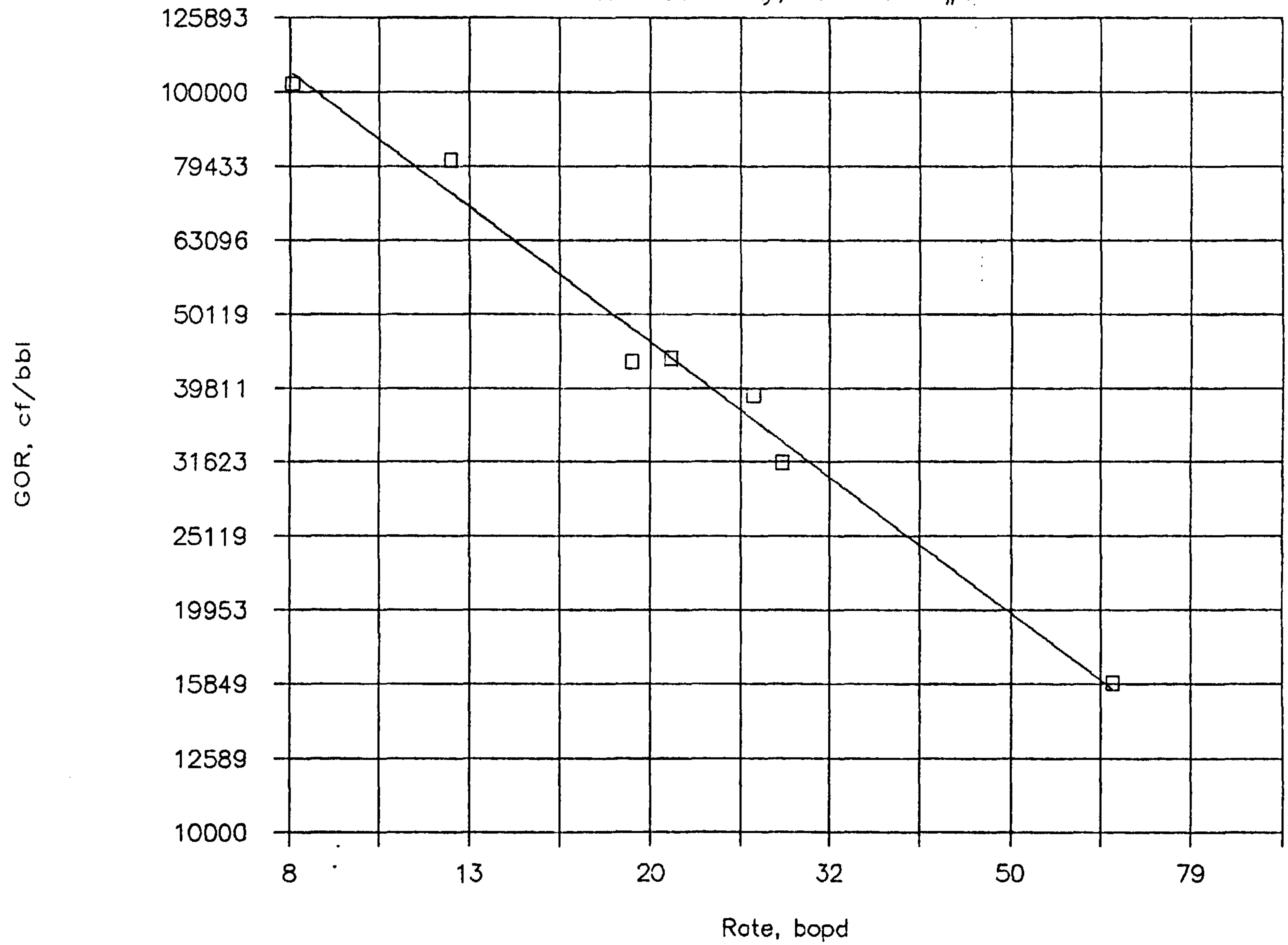

C.C. = 0.99

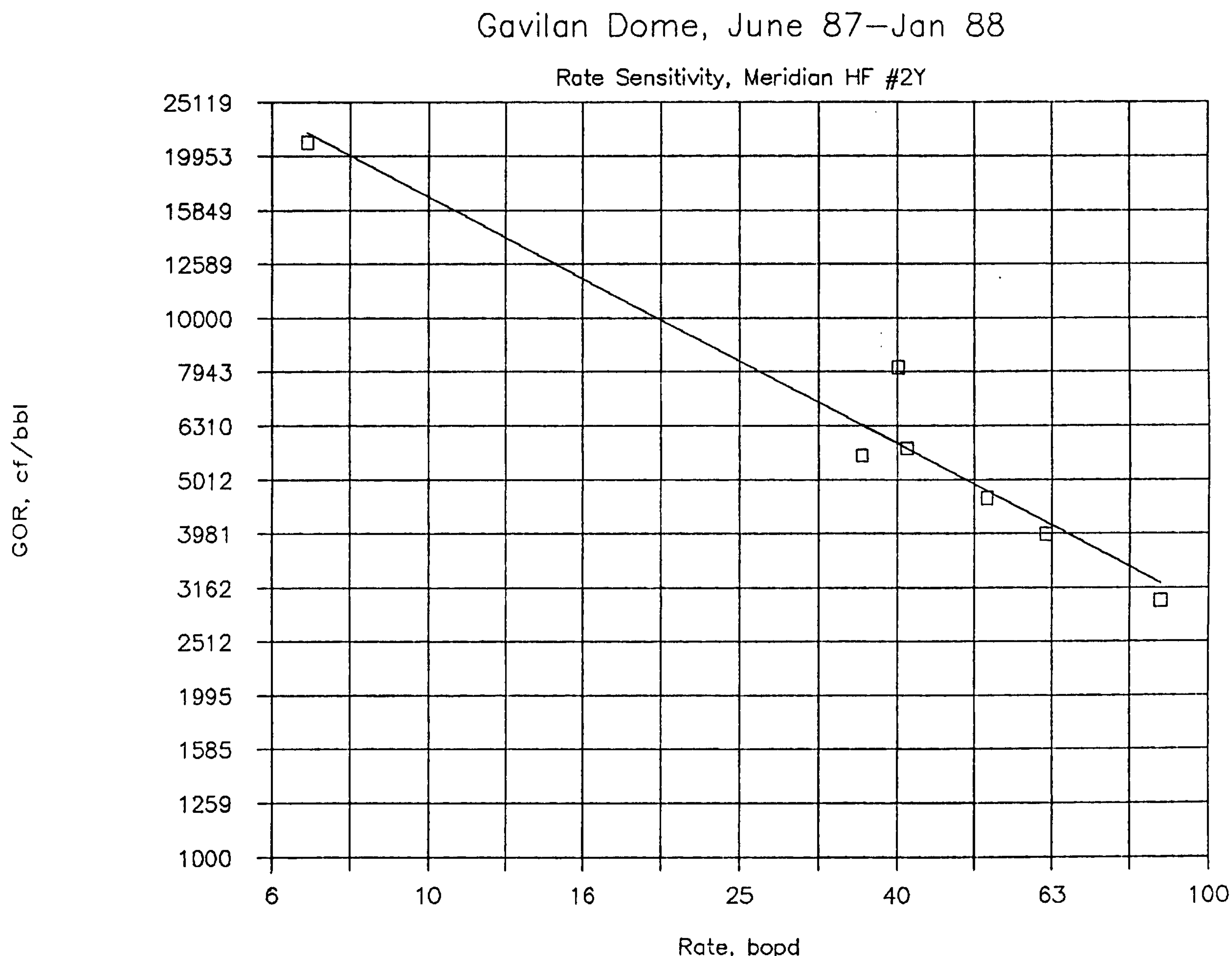

Gavilan Dome, June 87–Jan 88
Rate Sensitivity, Meridian HF #2Y
GOR, cf/bbl
25119
19953
15849
12589
10000
7943
6310
5012
3981
3162
2512
1995
1585
1259
1000
6
10
16
25
40
63
100
Rate, bopd

C.C. = 0.97

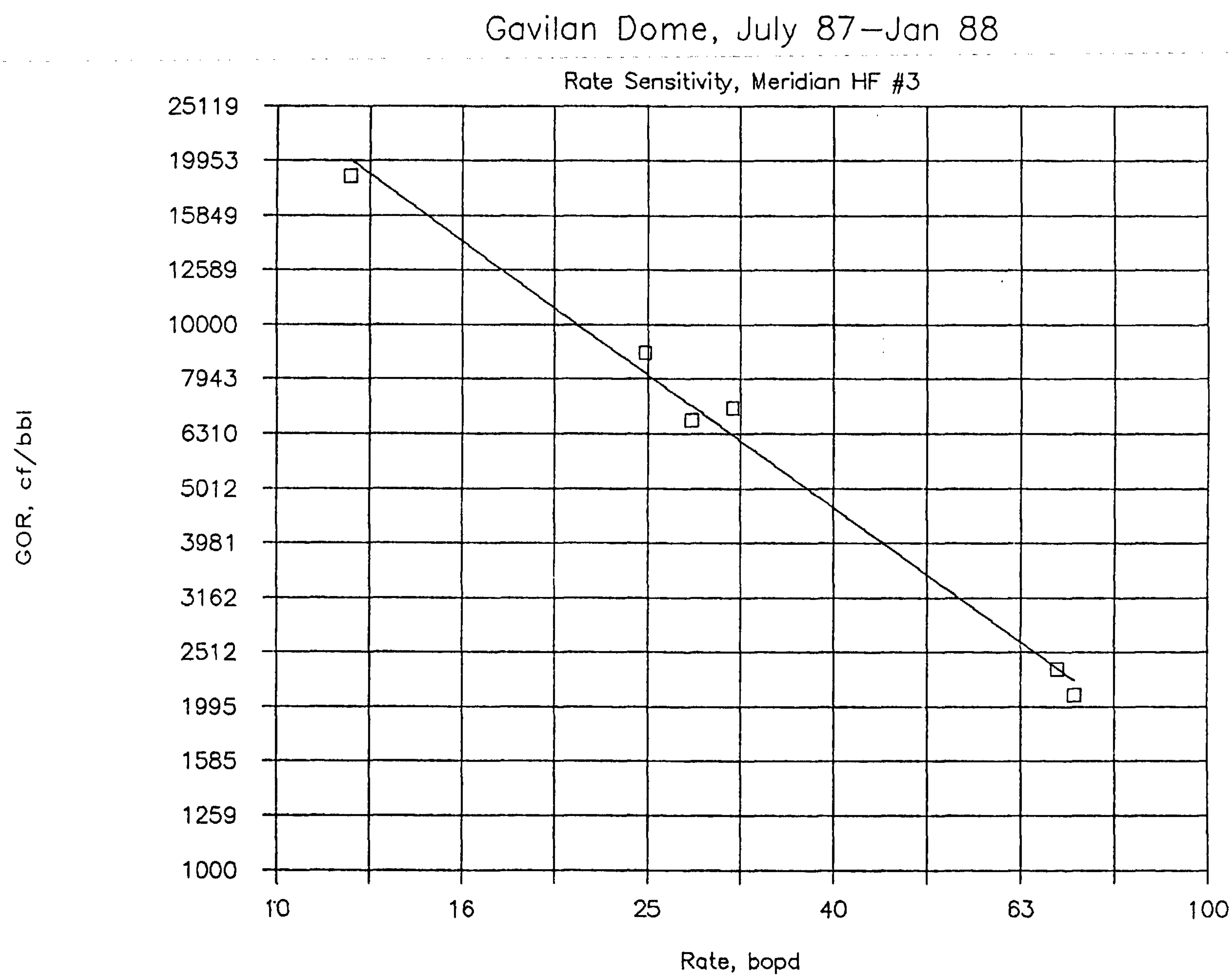

Gavilan Dome, July 87—Jan 88
Rate Sensitivity, Meridian HF #3
25119
19953
15849
12589
10000
7943
6310
5012
3981
3162
2512
1995
1585
1259
1000
GOR, cf/bbl
10
16
25
40
63
100
Rate, bopd

C. C. = 1.00

Gavilan Dome, 1/1–2/15/88

Rate Sensitivity, Merrion Kry #1

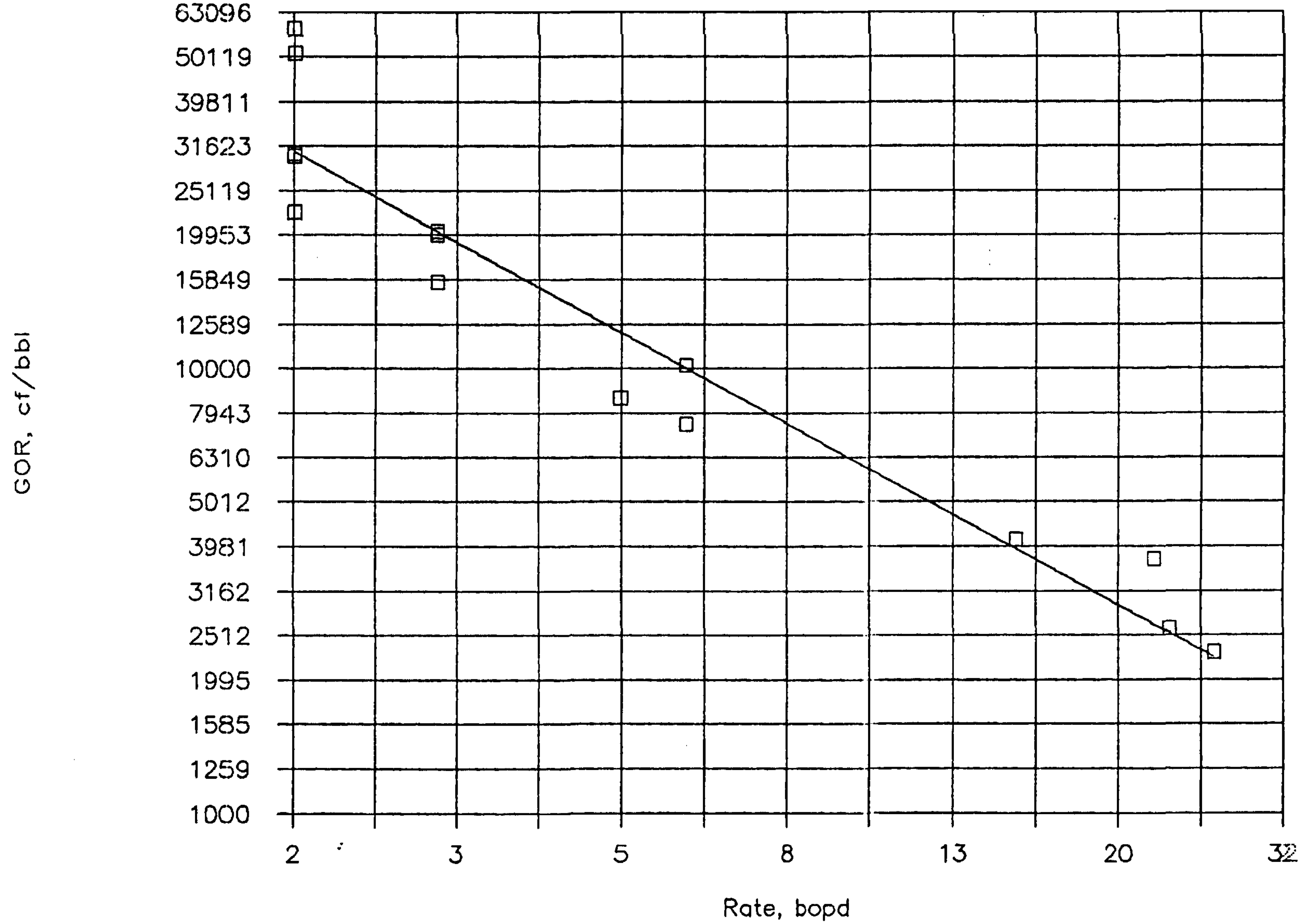

C.C. = 0.96

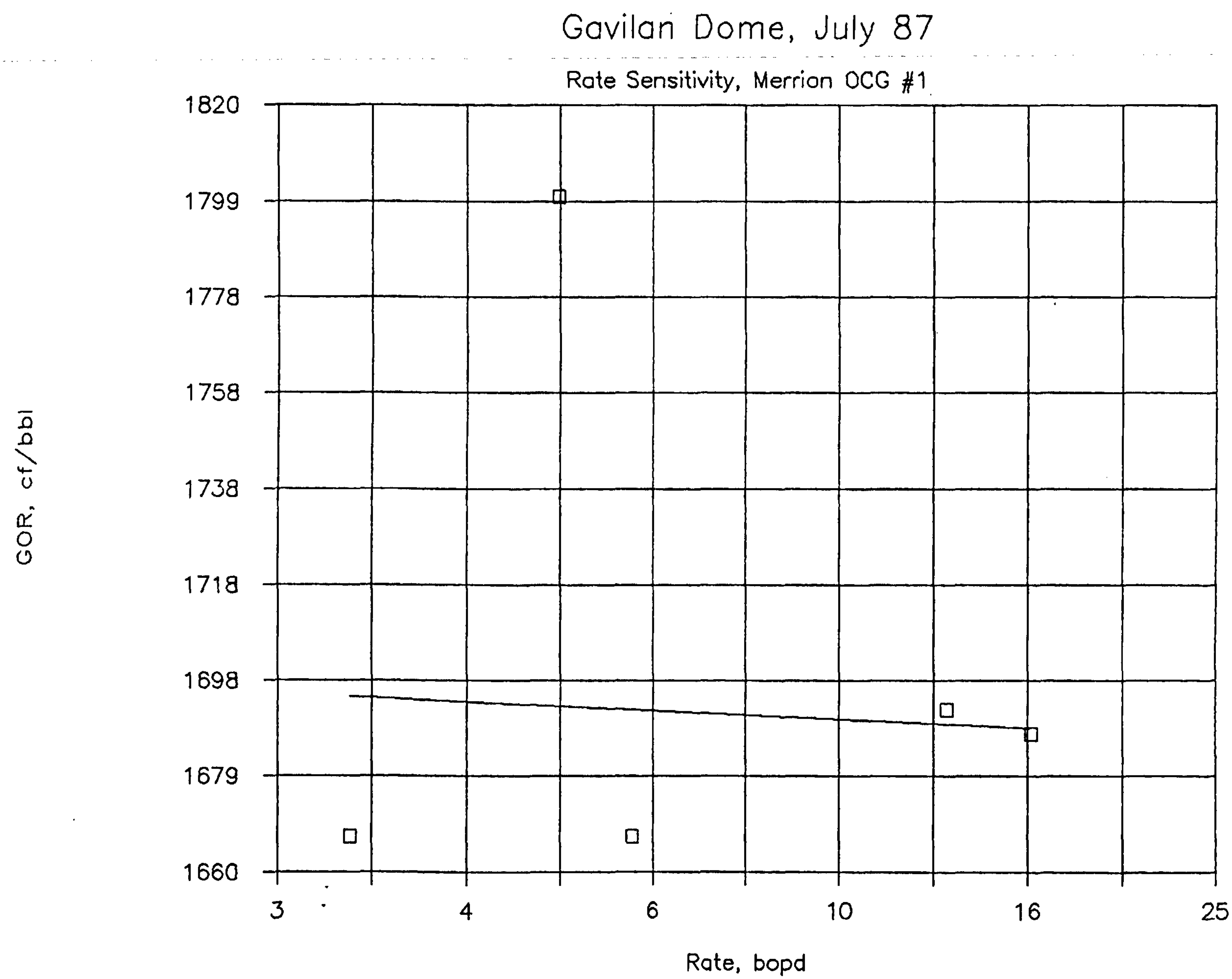

Gavilan Dome, July 87
Rate Sensitivity, Merrion OCG #1
1820
1799
1778
1758
1738
1718
1698
1679
1660
GOR, cf/bbl
3
4
6
10
16
25
Rate, bopd

C. C. = 0.15

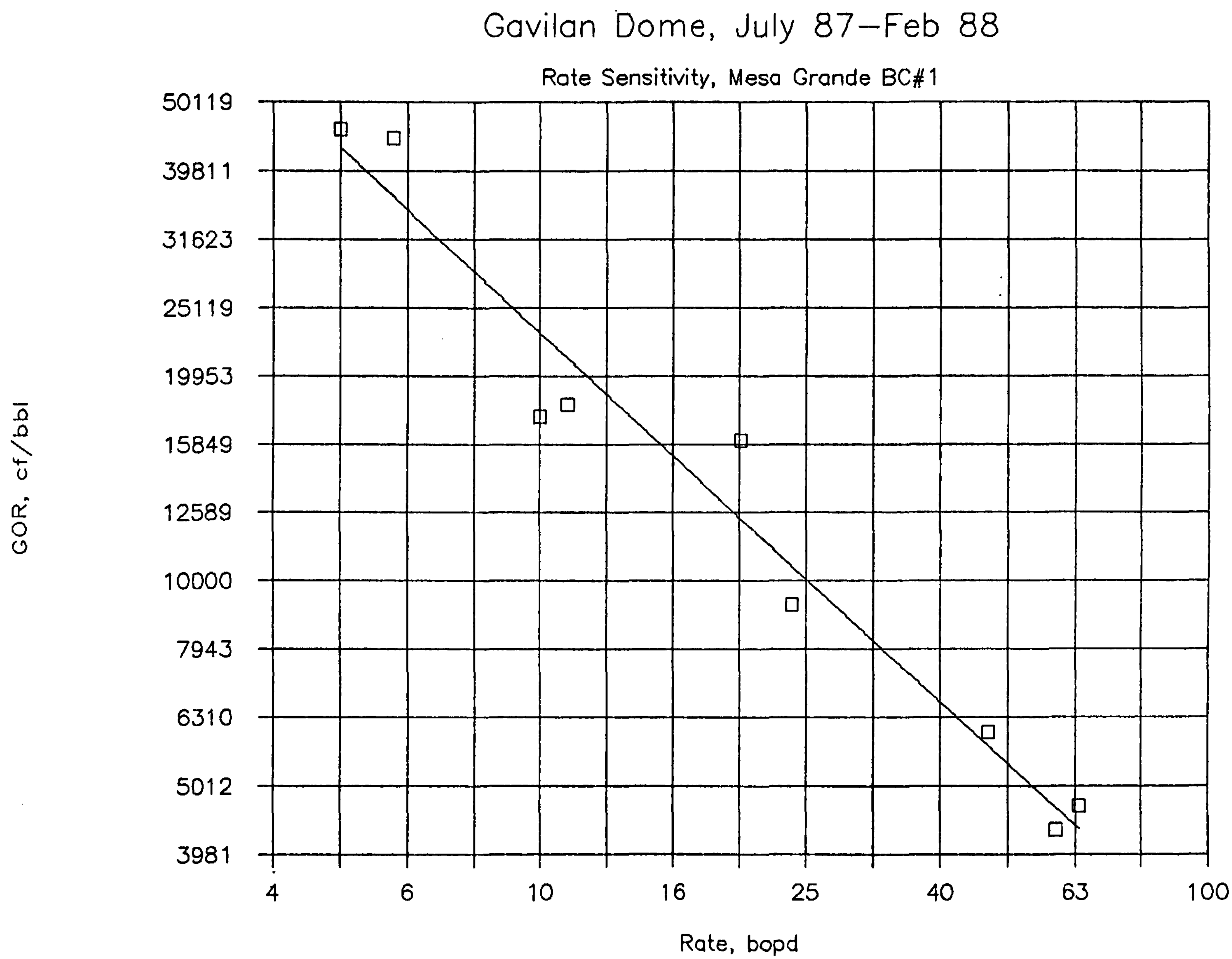
Gavilan Dome, July 87—Feb 88
Rate Sensitivity, Mesa Grande BC#1
GOR, cf/bbl
50119
39811
31623
25119
19953
15849
12589
10000
7943
6310
5012
3981
4
6
10
16
25
40
63
100
Rate, bopd

C.C. = 0.98

Gavilan Dome, July 87–Feb 88

Rate Sensitivity, Mesa Grande BRO #1

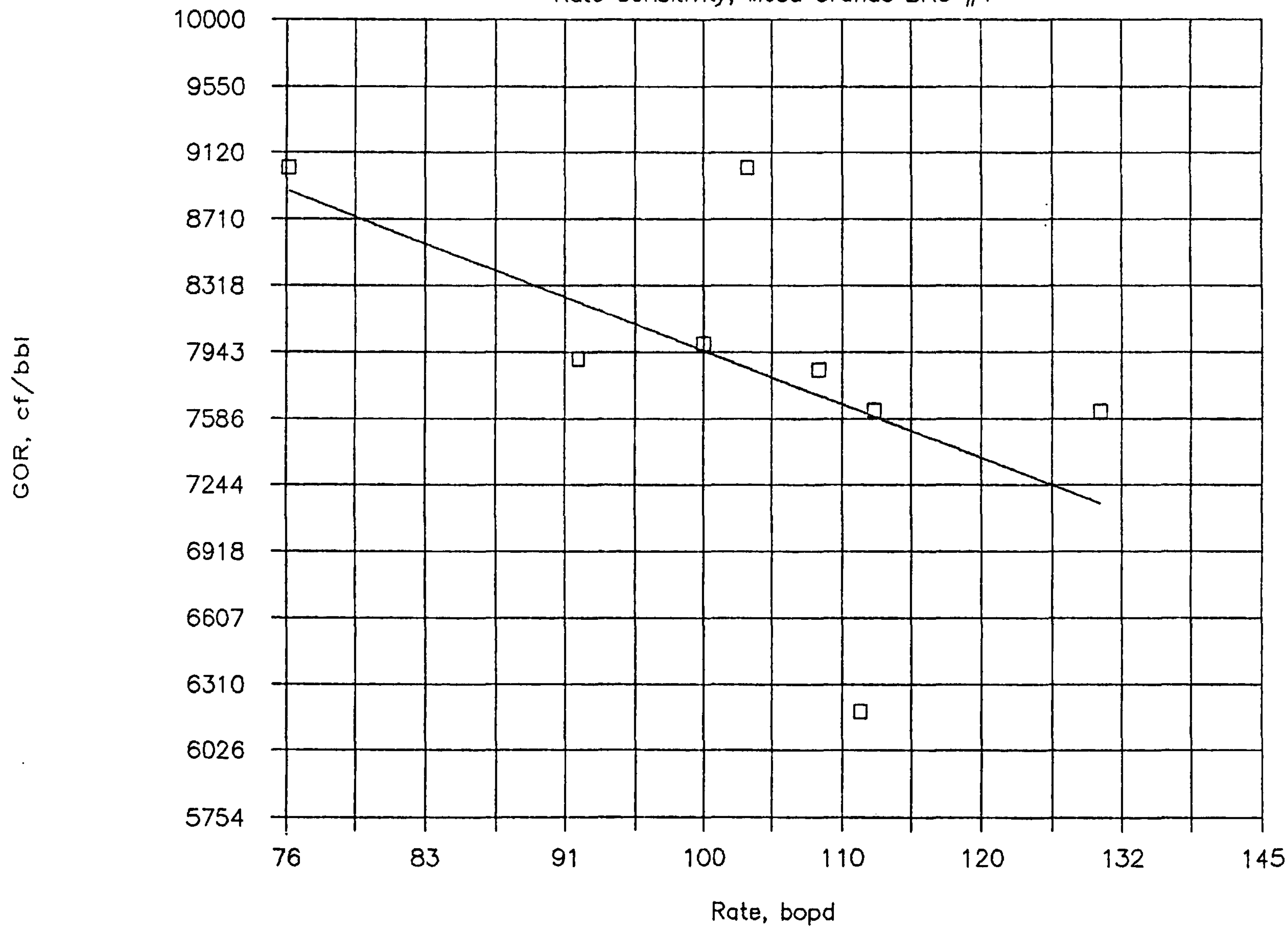

C.C. = 0.54

Gavilan Dome, July 87—Feb 88

Rate Sensitivity, Mesa Grande GAV #1

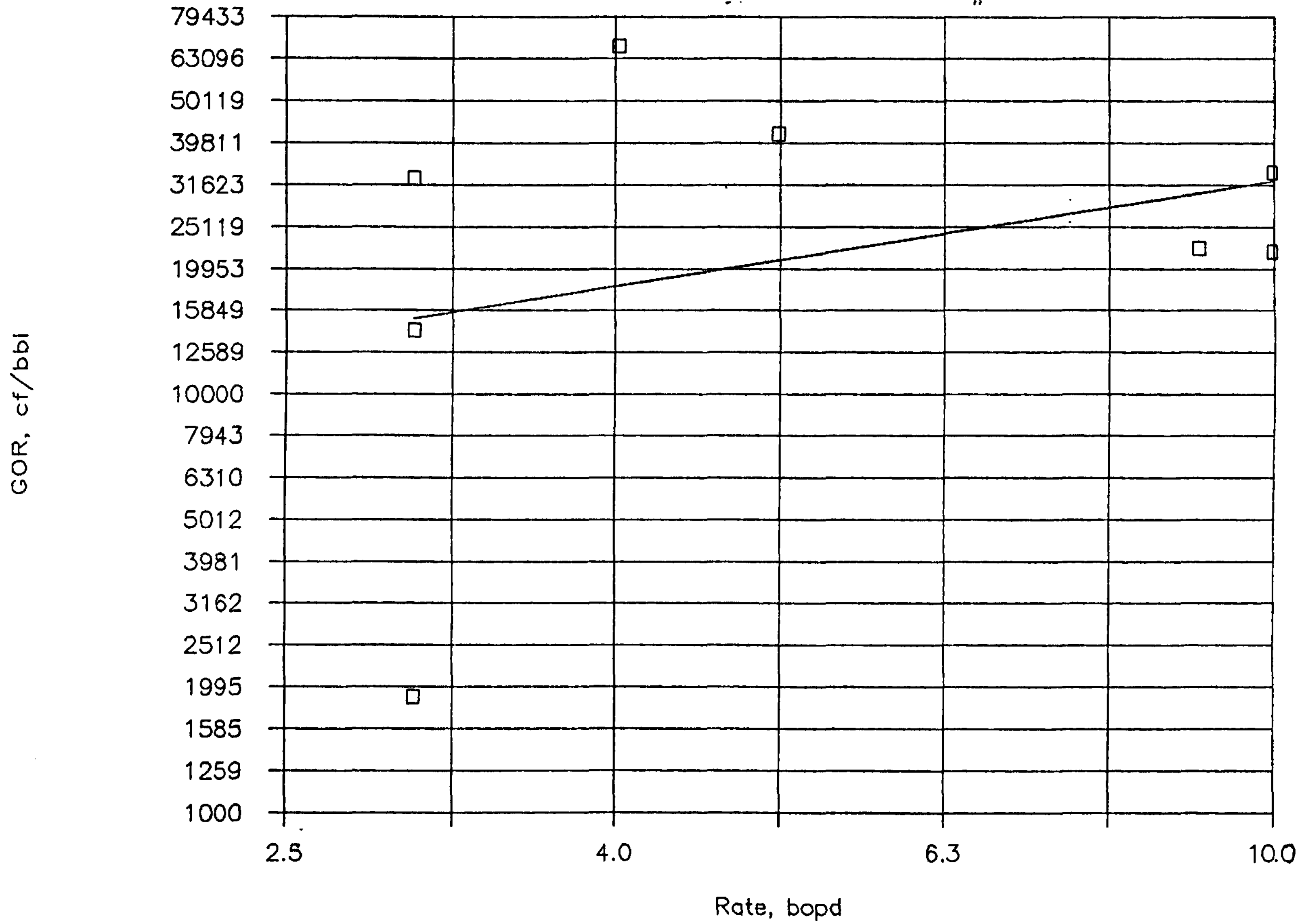

C. C. = 0.32

Gavilan Dome, July 87–Feb 88

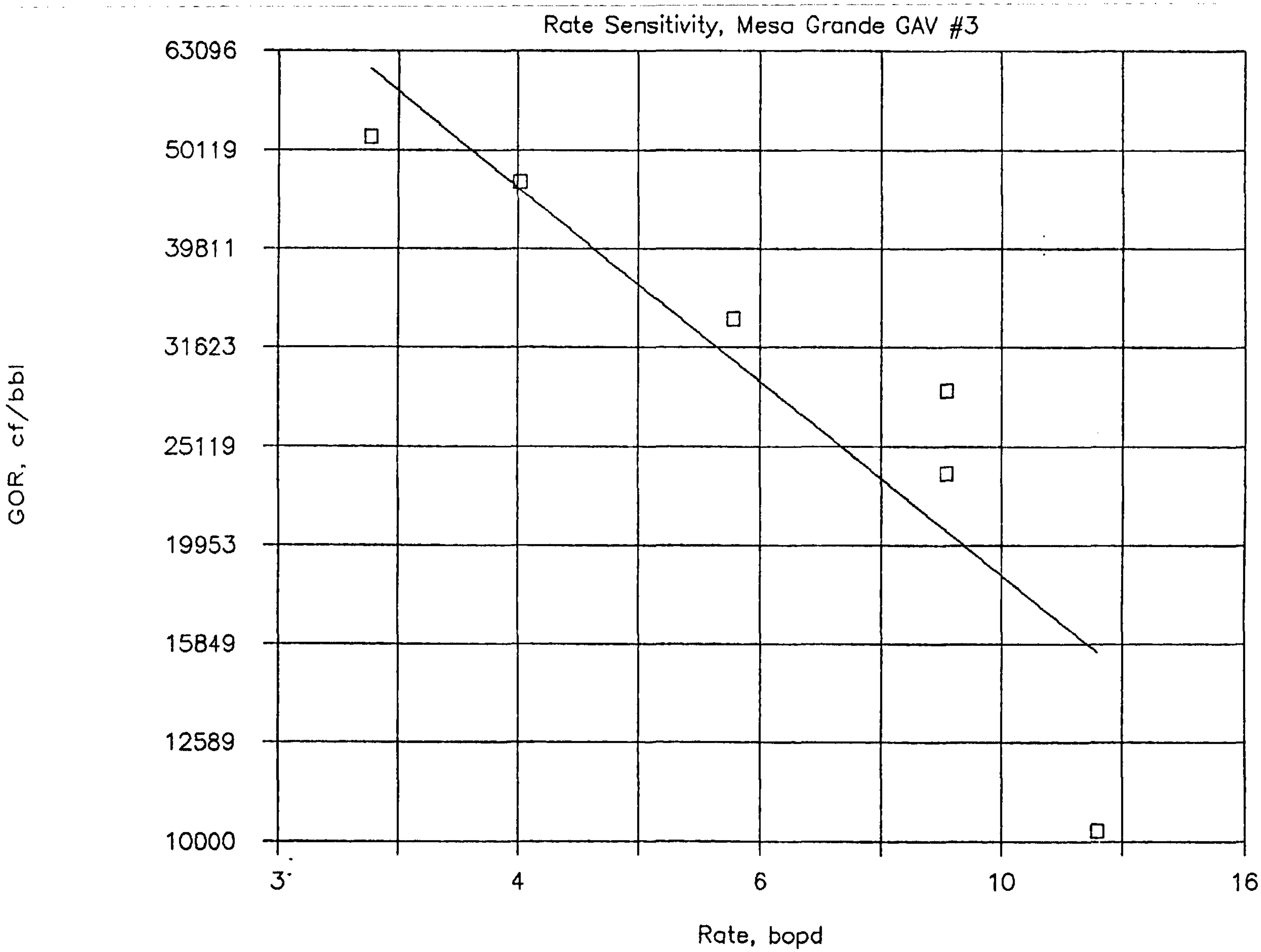

C. C. = 0.90

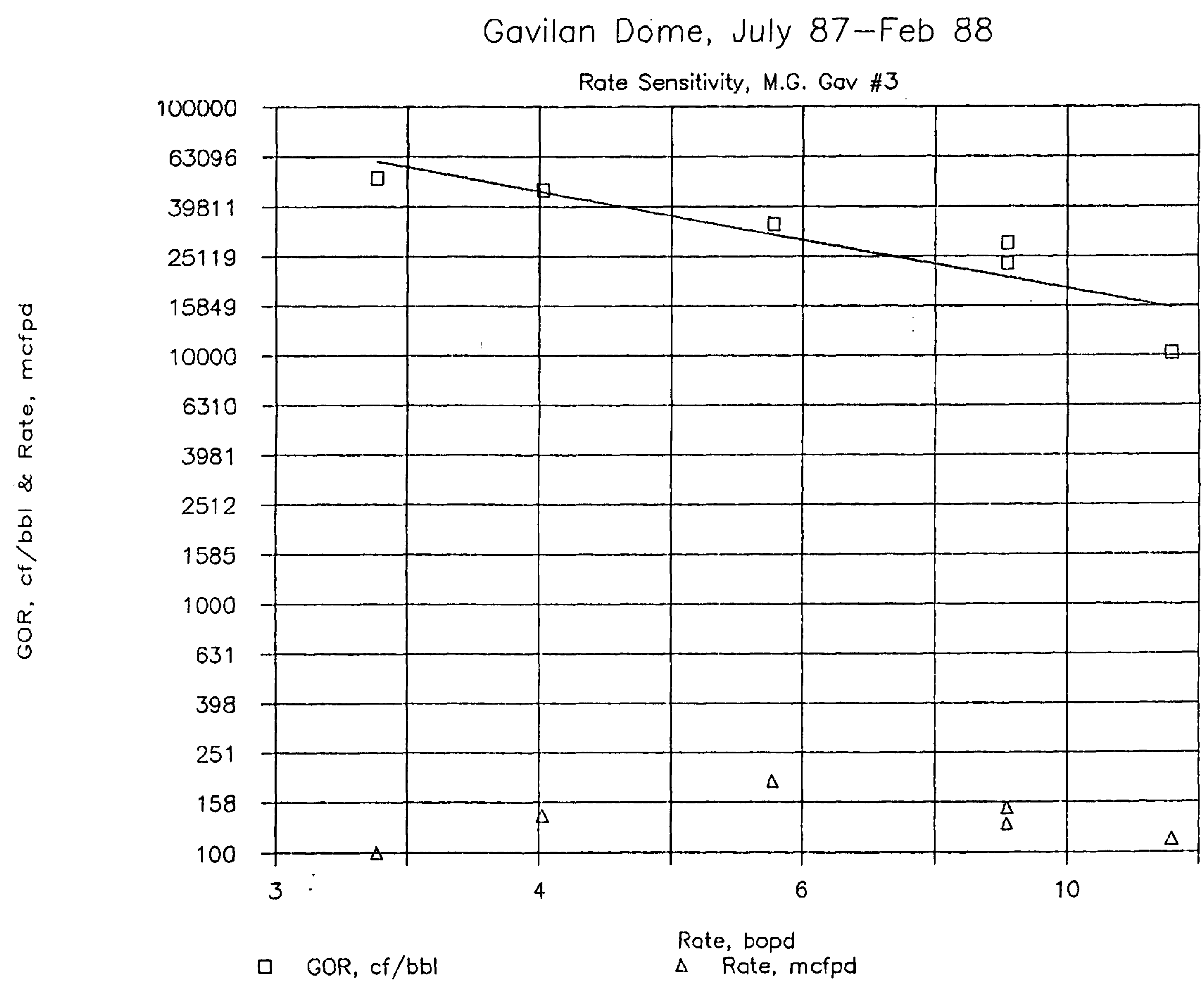

Gavilan Dome, July 87–Feb 88
Rate Sensitivity, M.G. Gav #3
GOR, cf/bbl & Rate, mcfpd
100000
63096
39811
25119
15849
10000
6310
3981
2512
1585
1000
631
398
251
158
100
3
4
6
10
Rate, bopd
□ GOR, cf/bbl
Δ Rate, mcfpd

Gavilan Dome, July 87—Feb 88

Rate Sensitivity, Mesa Grande GH #1

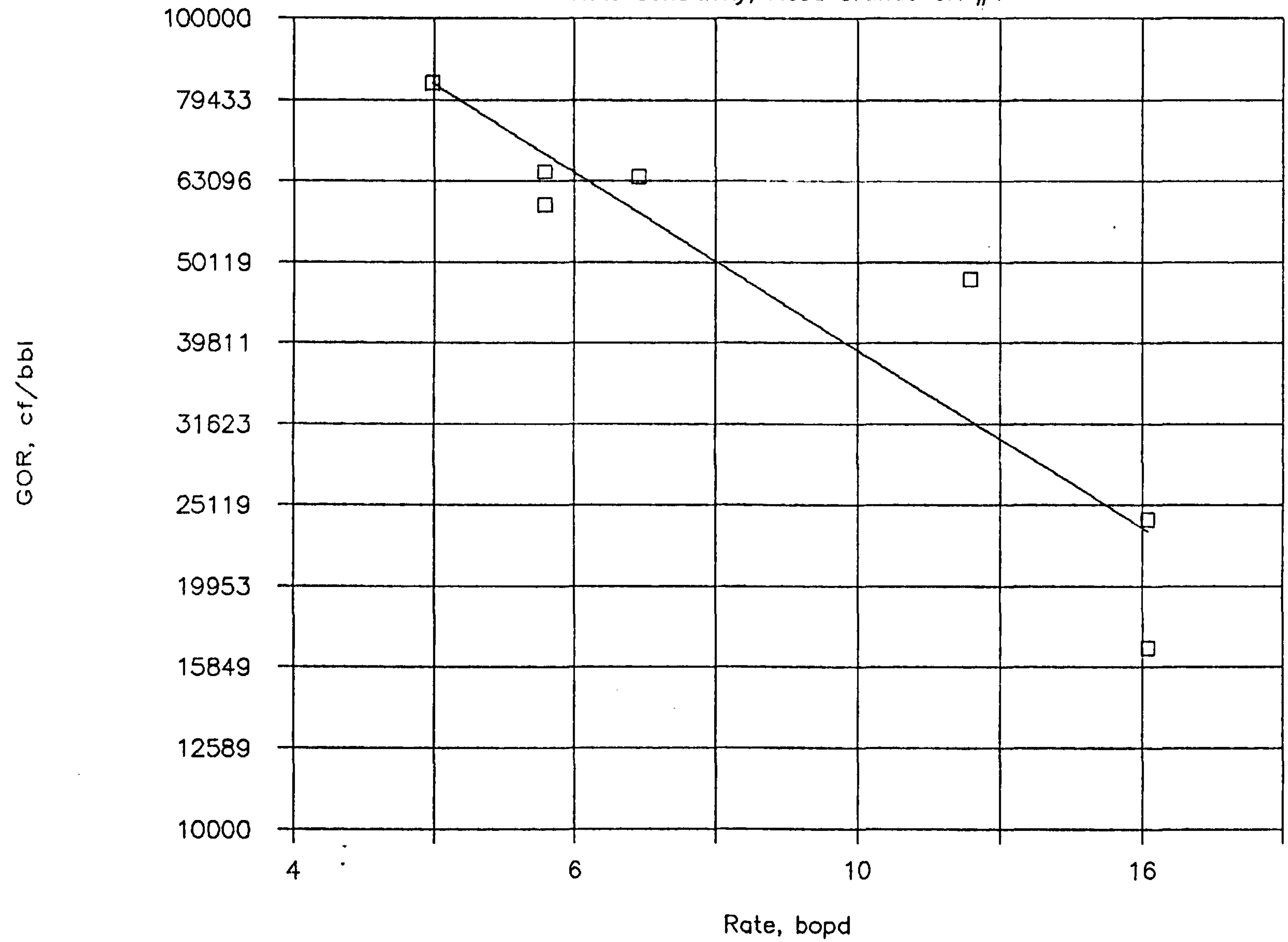

C.C. = 0.92

Gavilan Dome, Aug 87—Feb 88

Rate Sensitivity, Mesa Grande HC #1

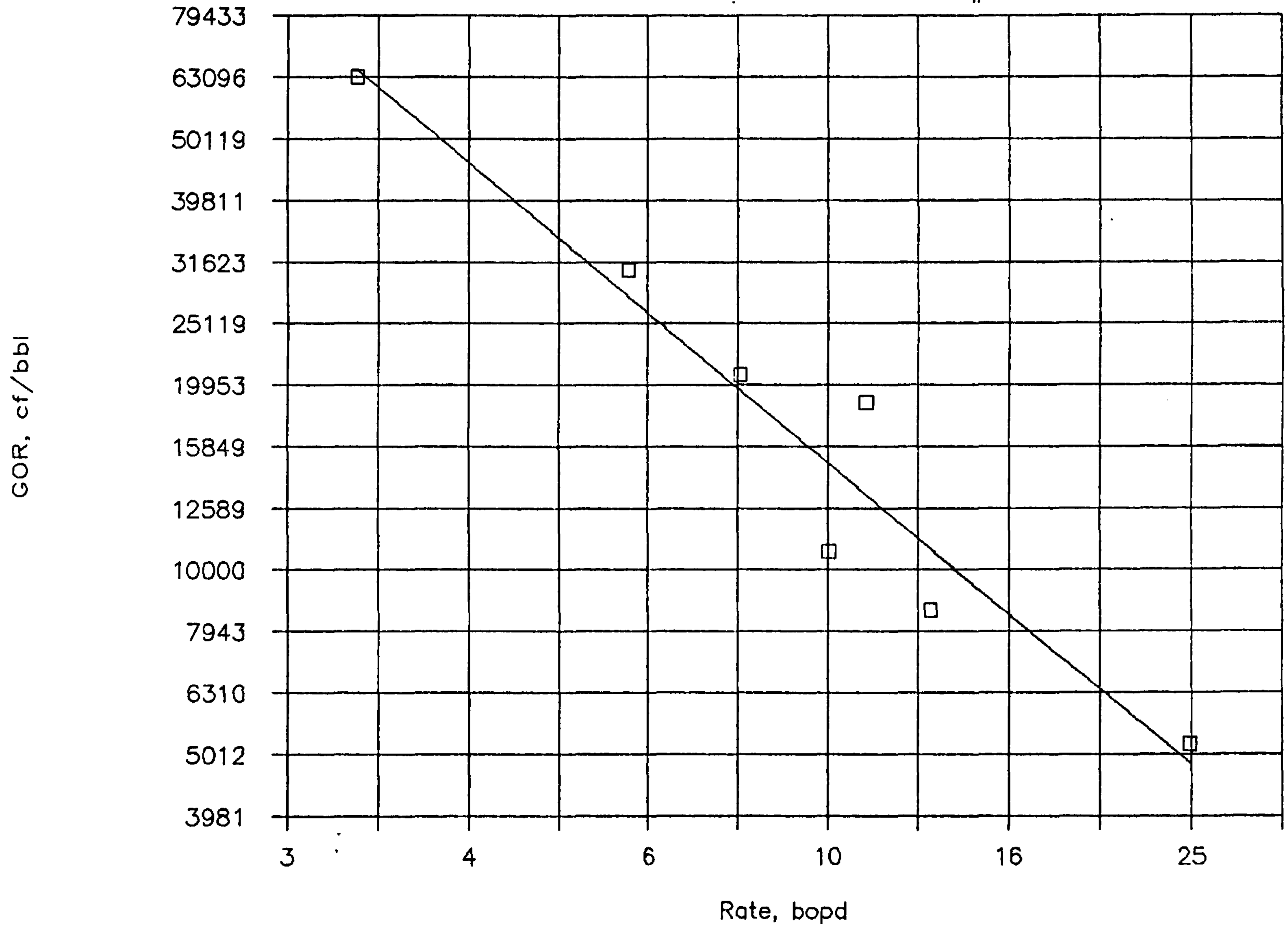

C.C. = 0.96

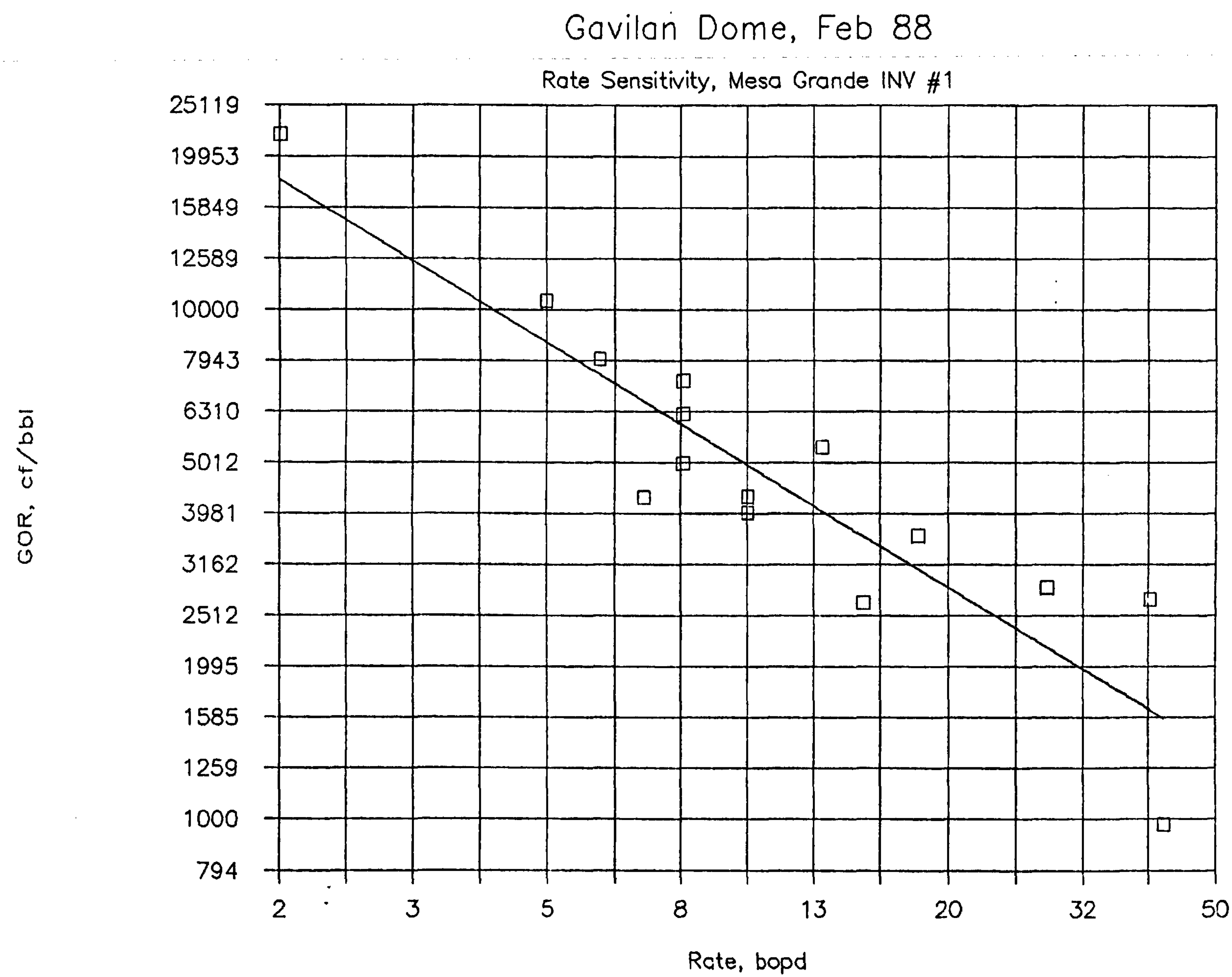

Gavilan Dome, Feb 88
Rate Sensitivity, Mesa Grande INV #1
25119
19953
15849
12589
10000
7943
6310
5012
3981
3162
2512
1995
1585
1259
1000
794
GOR, cf/bbl
2
3
5
8
13
20
32
50
Rate, bopd

C.C. = 0.91

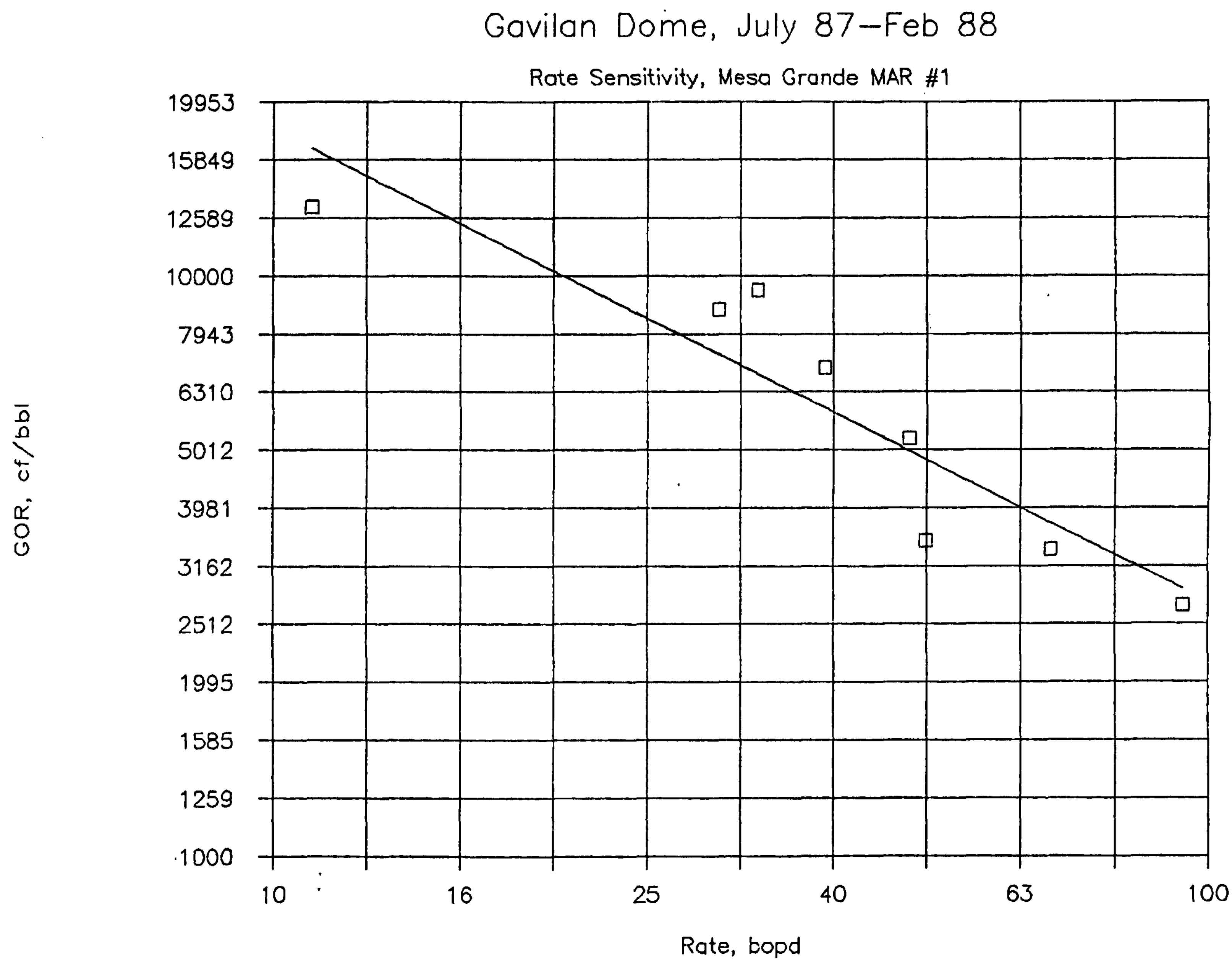
Gavilan Dome, July 87–Feb 88
Rate Sensitivity, Mesa Grande MAR #1
GOR, cf/bbl
19953
15849
12589
10000
7943
6310
5012
3981
3162
2512
1995
1585
1259
1000
10
16
25
40
63
100
Rate, bopd

C.C. = 0.92

Gavilan Dome, Feb 88

Rate Sensitivity, Mesa Grande PRO #2

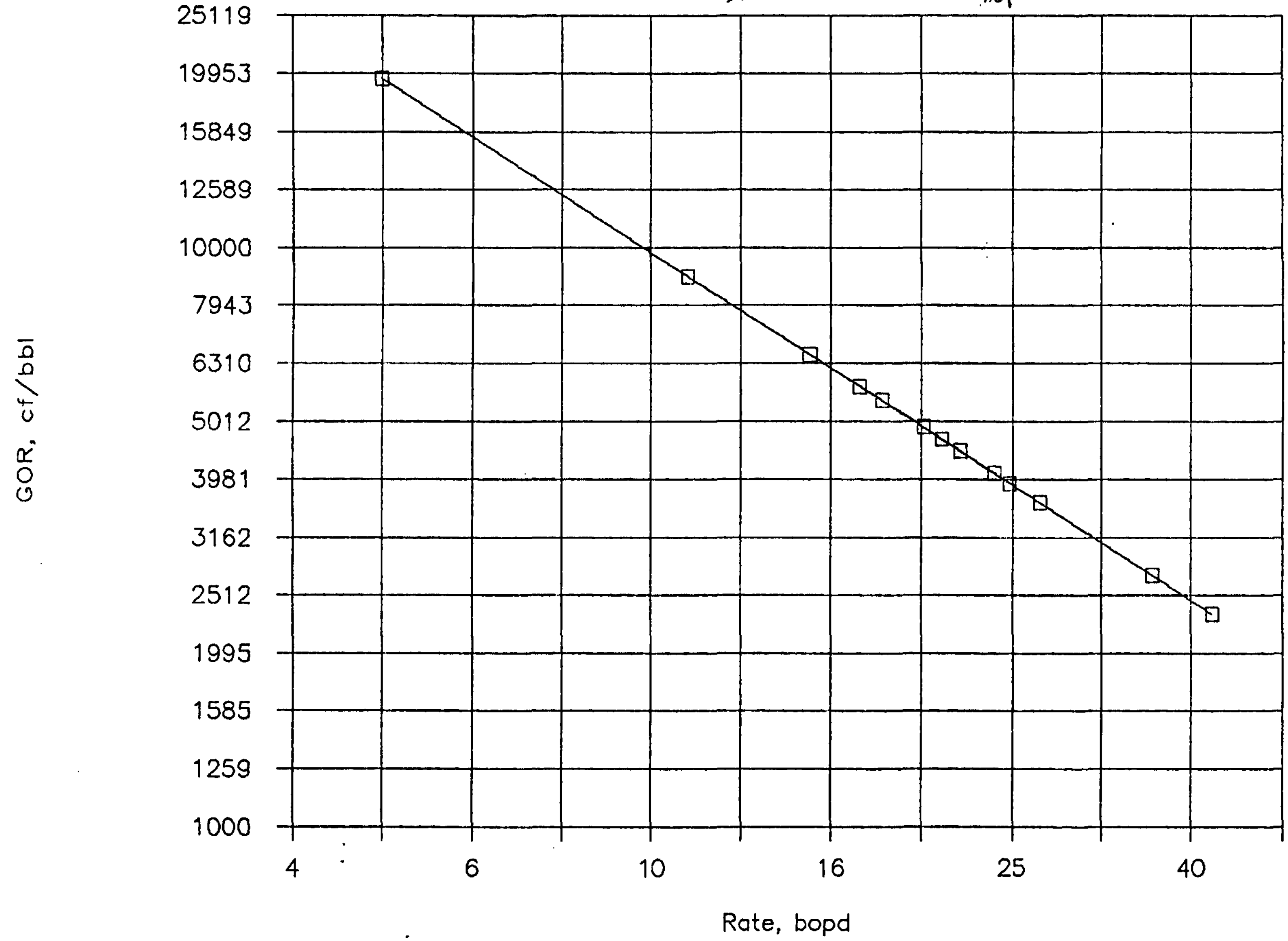

C.C. = 1.00

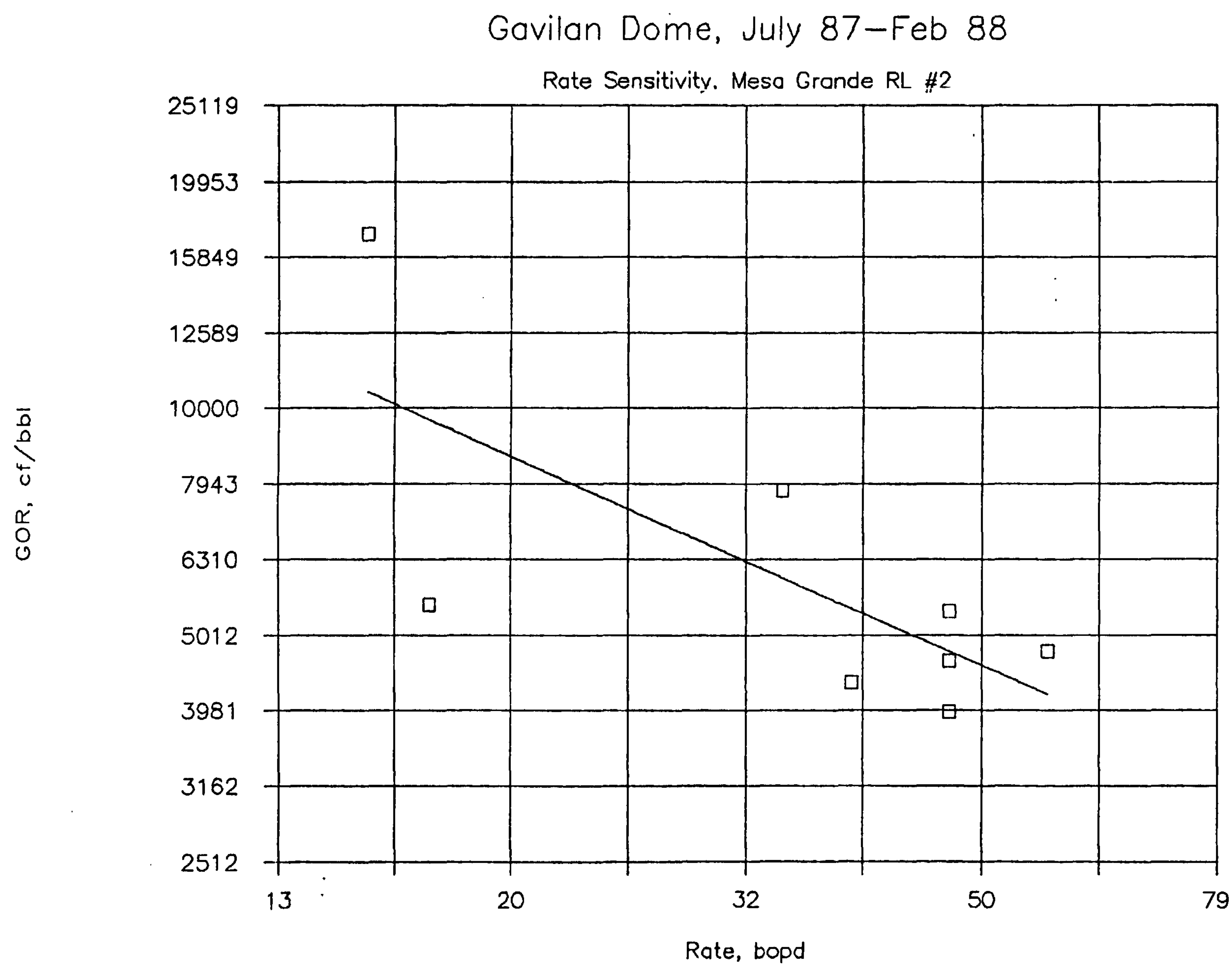

Gavilan Dome, July 87—Feb 88
Rate Sensitivity, Mesa Grande RL #2
25119
19953
15849
12589
10000
7943
6310
5012
3981
3162
2512
GOR, cf/bbl
13
20
32
50
79
Rate, bopd

C.C. = 0.73

Gavilan Dome, July 87—Feb 88

Rate Sensitivity, Mesa Grande RL #3

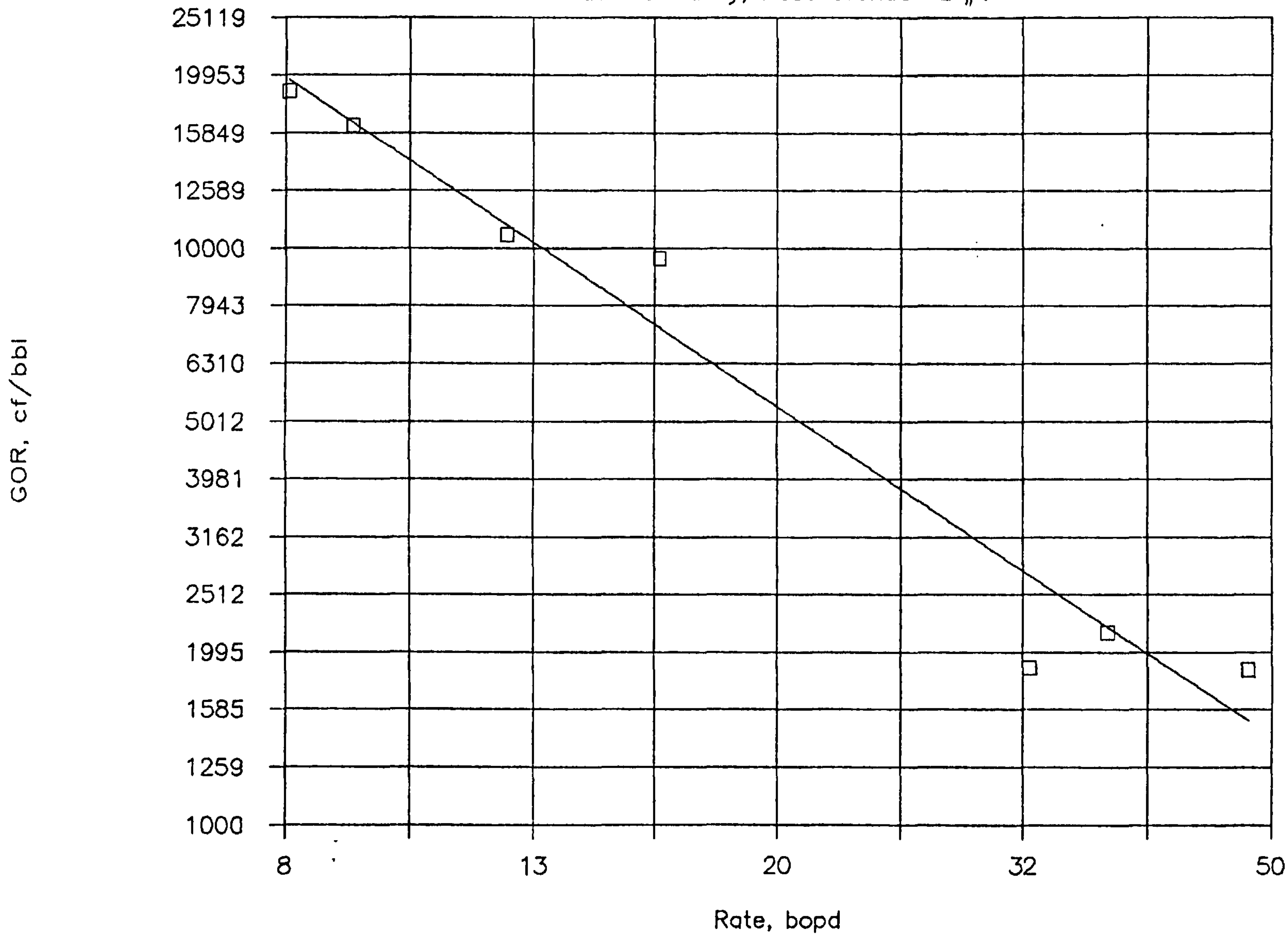

C.C.= 0.98

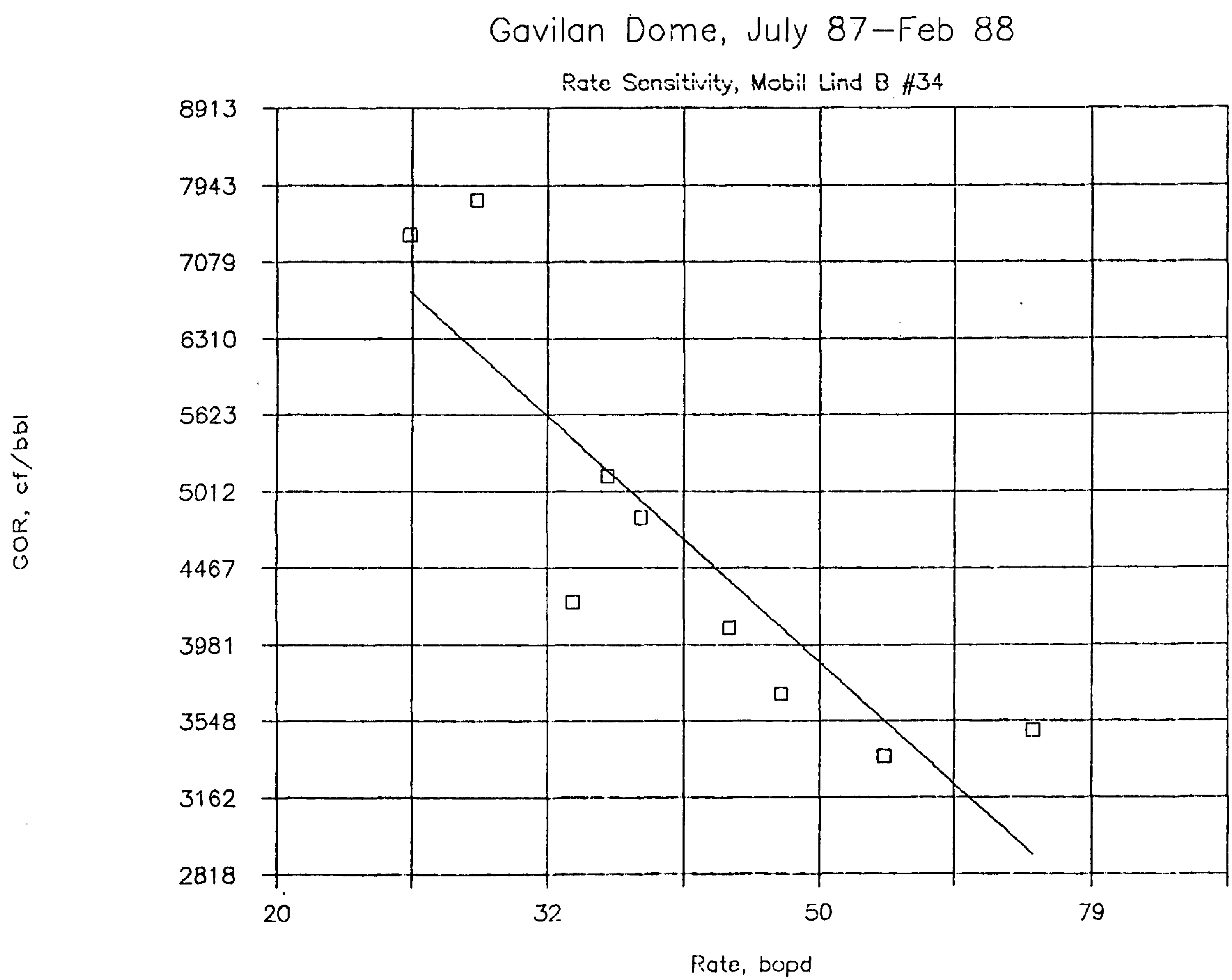
Gavilan Dome, July 87—Feb 88
Rate Sensitivity, Mobil Lind B #34
8913
7943
7079
6310
5623
5012
4467
3981
3548
3162
2818
GOR, cf/bbl
20
32
50
79
Rate, bopd

C.C. = 0.88

Gavilan Dome, July 87–Feb 88

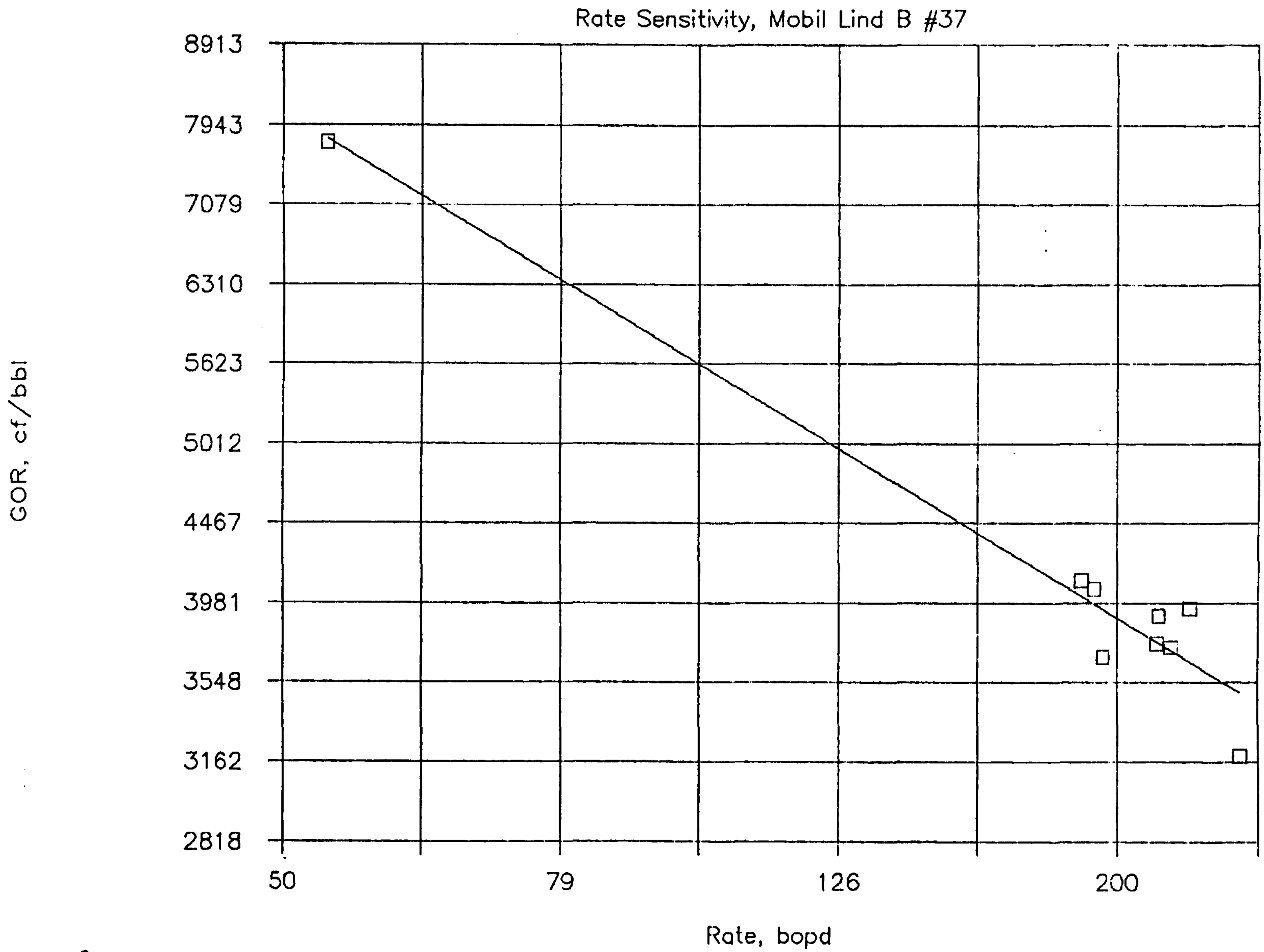

C.C. = 0.98

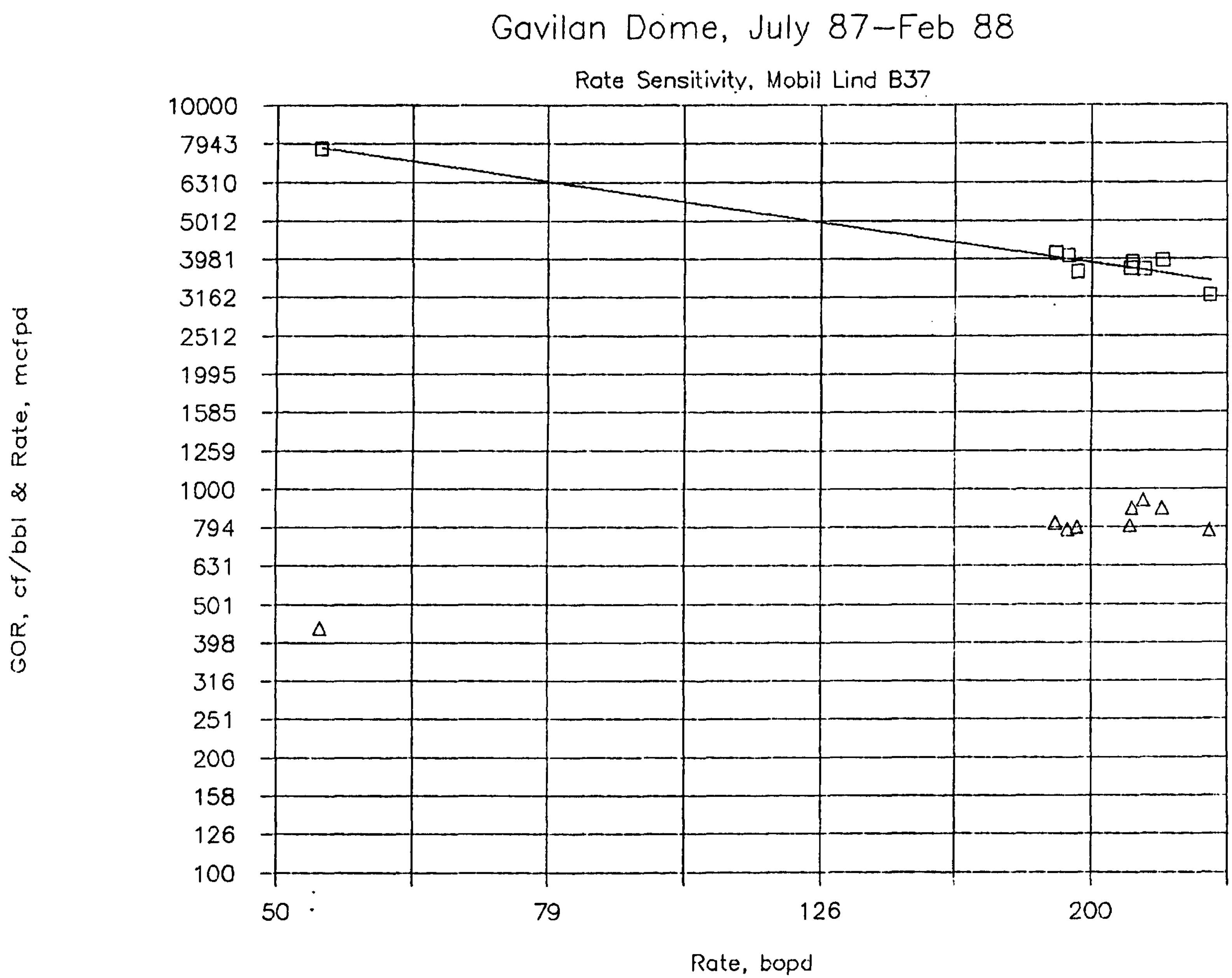
Gavilan Dome, July 87–Feb 88
Rate Sensitivity, Mobil Lind B37
GOR, cf/bbl & Rate, mcfpd
10000
7943
6310
5012
3981
3162
2512
1995
1585
1259
1000
794
631
501
398
316
251
200
158
126
100
50
79
126
200
Rate, bopd

Gavilan Dome, July 87–Nov 87

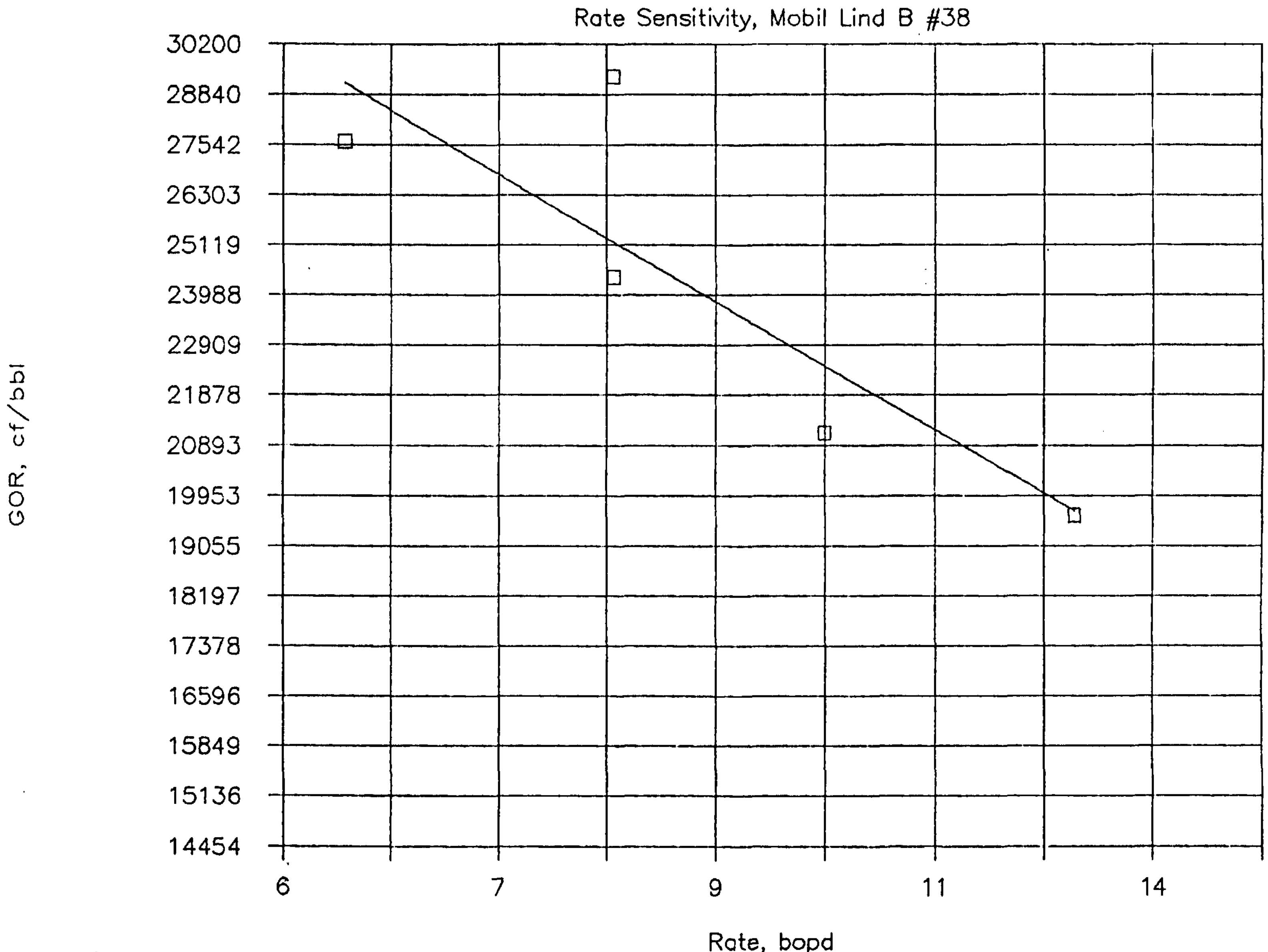

C.C. = 0.86

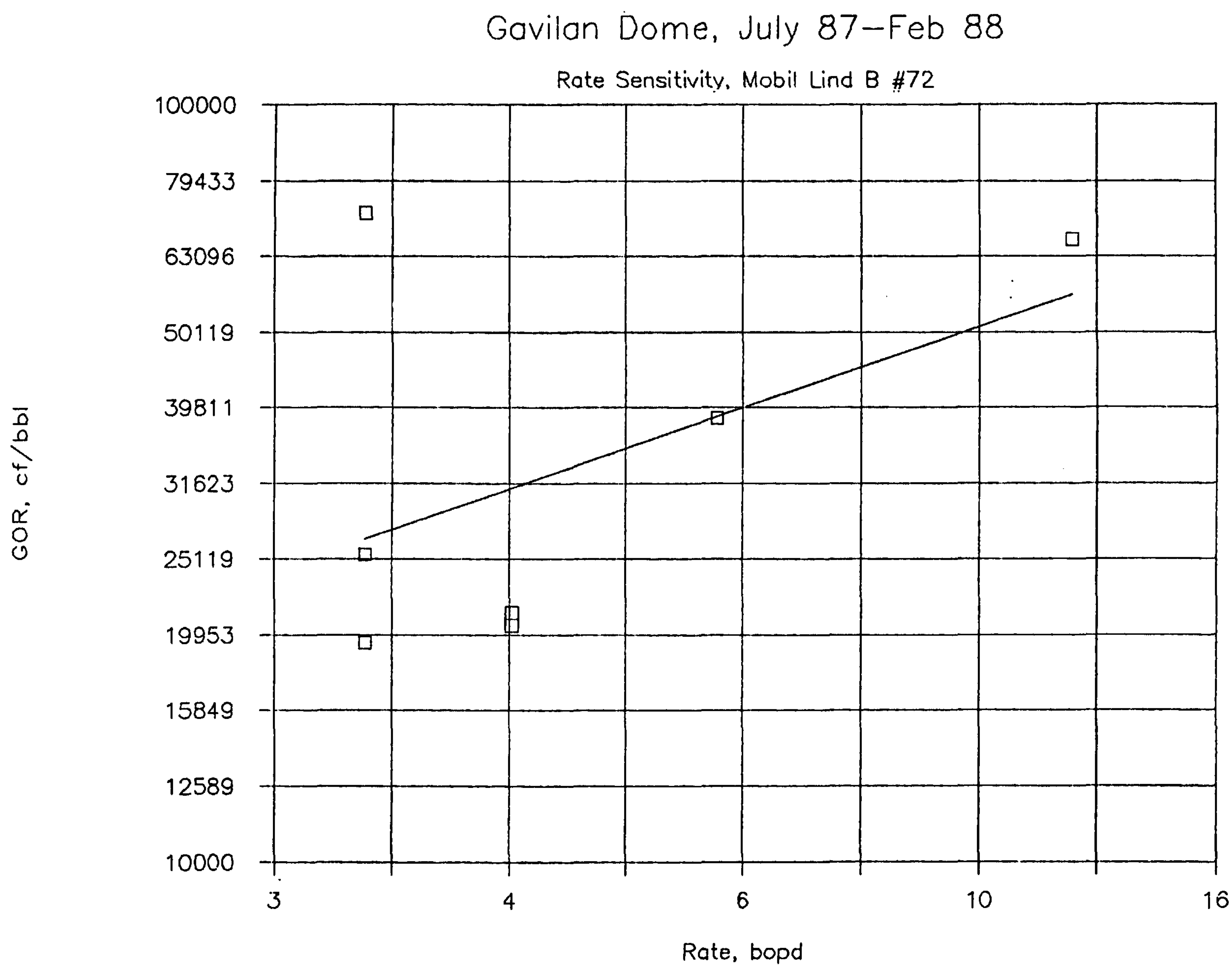
Gavilan Dome, July 87–Feb 88
Rate Sensitivity, Mobil Lind B #72
100000
79433
63096
50119
39811
31623
25119
19953
15849
12589
10000
GOR, cf/bbl
3
4
6
10
16
Rate, bopd

C.C.=0.49

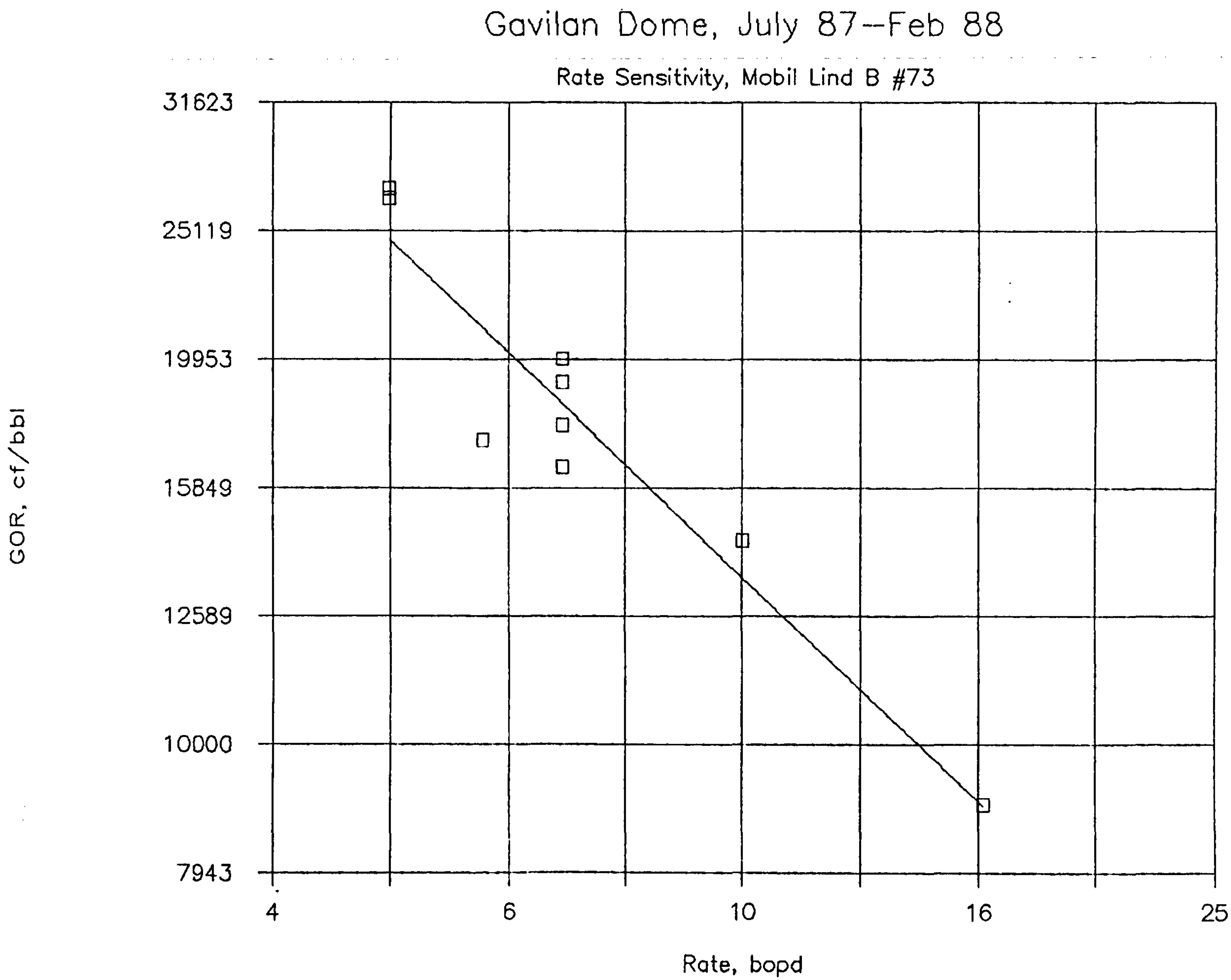
Gavilan Dome, July 87--Feb 88
Rate Sensitivity, Mobil Lind B #73
GOR, cf/bbl
31623
25119
19953
15849
12589
10000
7943
4
6
10
16
25
Rate, bopd

C.C. = 0.95

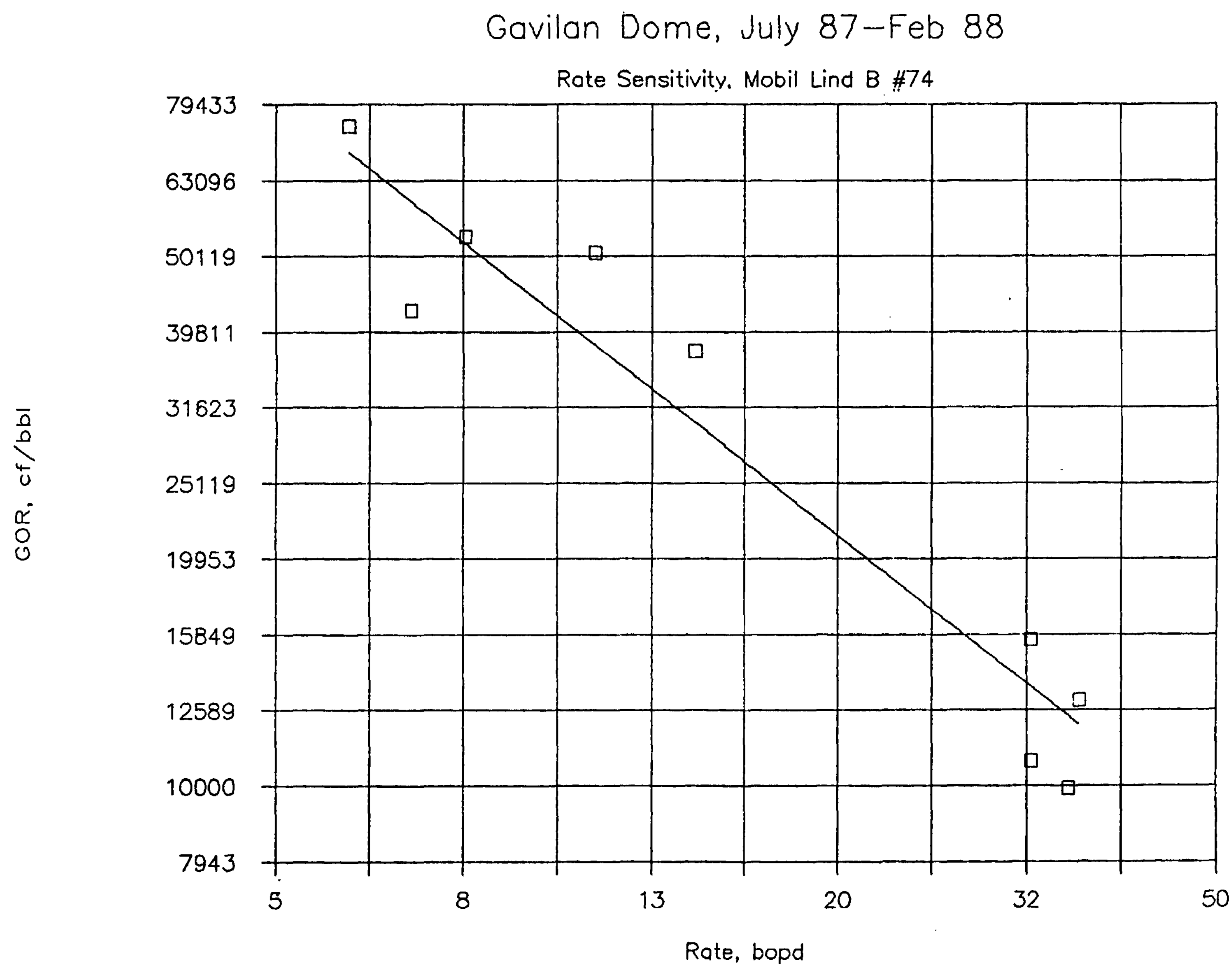

Gavilan Dome, July 87–Feb 88
Rate Sensitivity, Mobil Lind B #74
GOR, cf/bbl
79433
63096
50119
39811
31623
25119
19953
15849
12589
10000
7943
5
8
13
20
32
50
Rate, bopd

C.C. = 0.86

Gavilan Dome, June 87—Feb 88

Rate Sensitivity, R&B HF 43-15

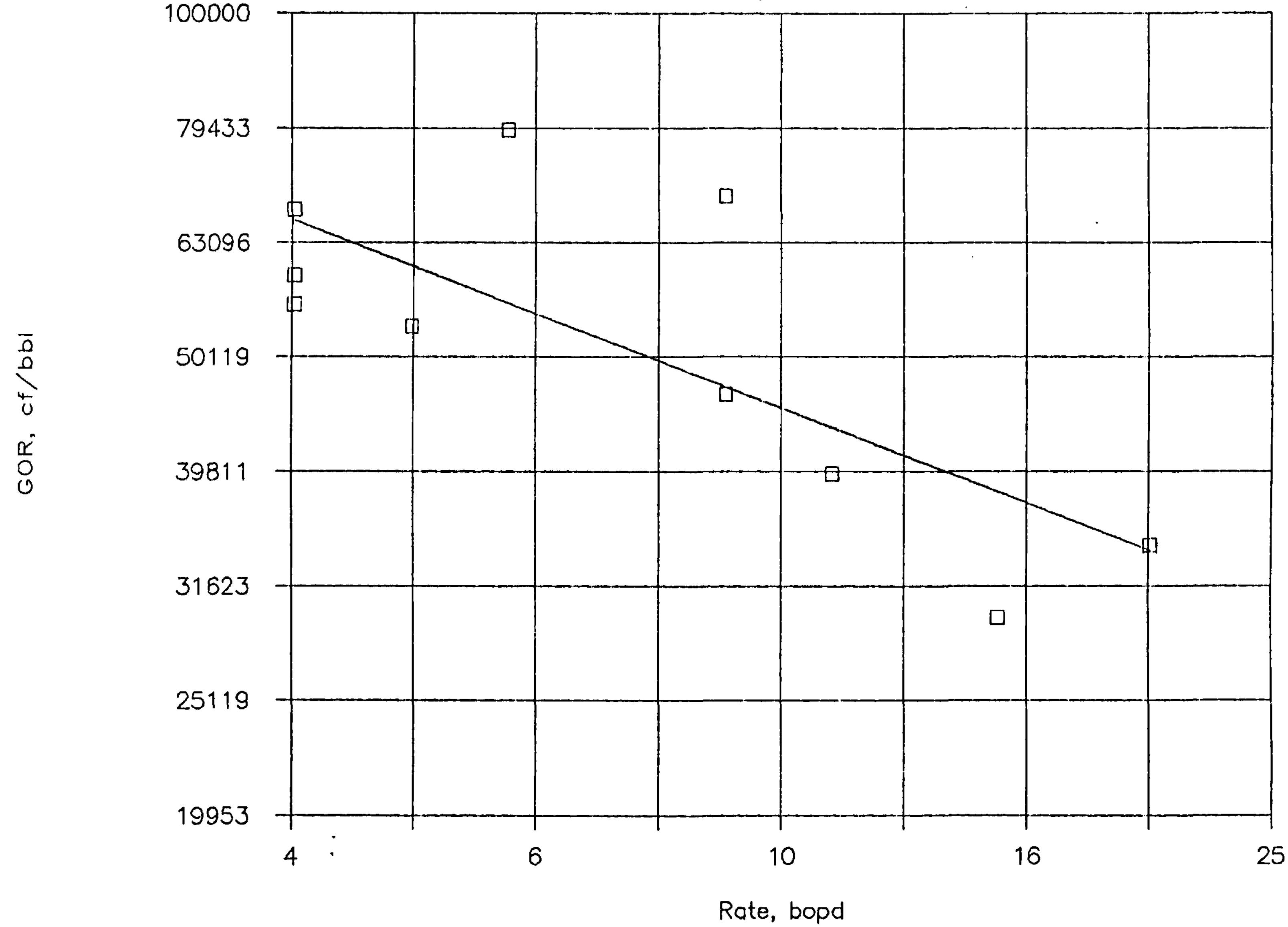

C.C. = 0.76

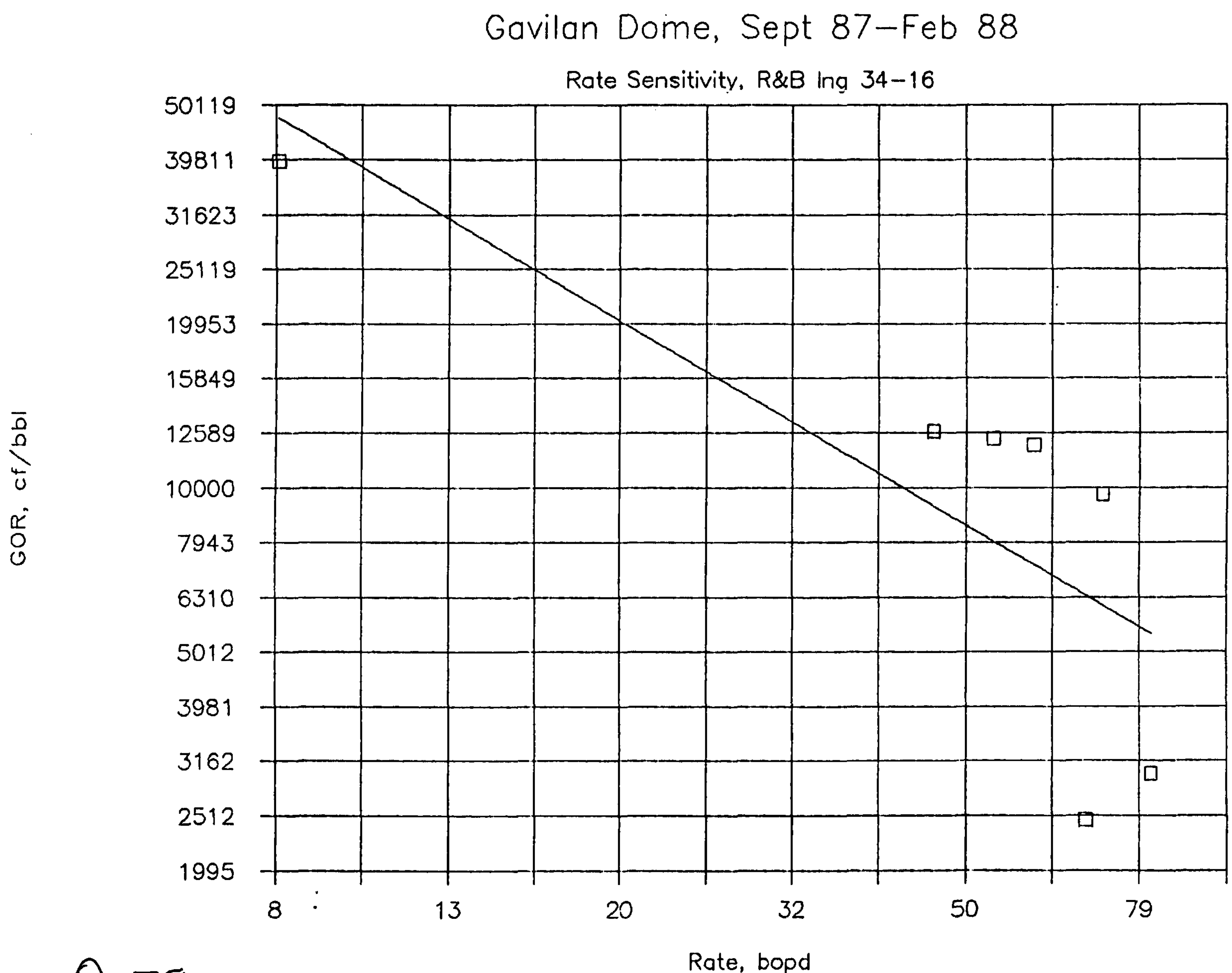
Gavilan Dome, Sept 87–Feb 88
Rate Sensitivity, R&B Ing 34-16
GOR, cf/bbl
50119
39811
31623
25119
19953
15849
12589
10000
7943
6310
5012
3981
3162
2512
1995
8
13
20
32
50
79
Rate, bopd

C.C. = 0.79

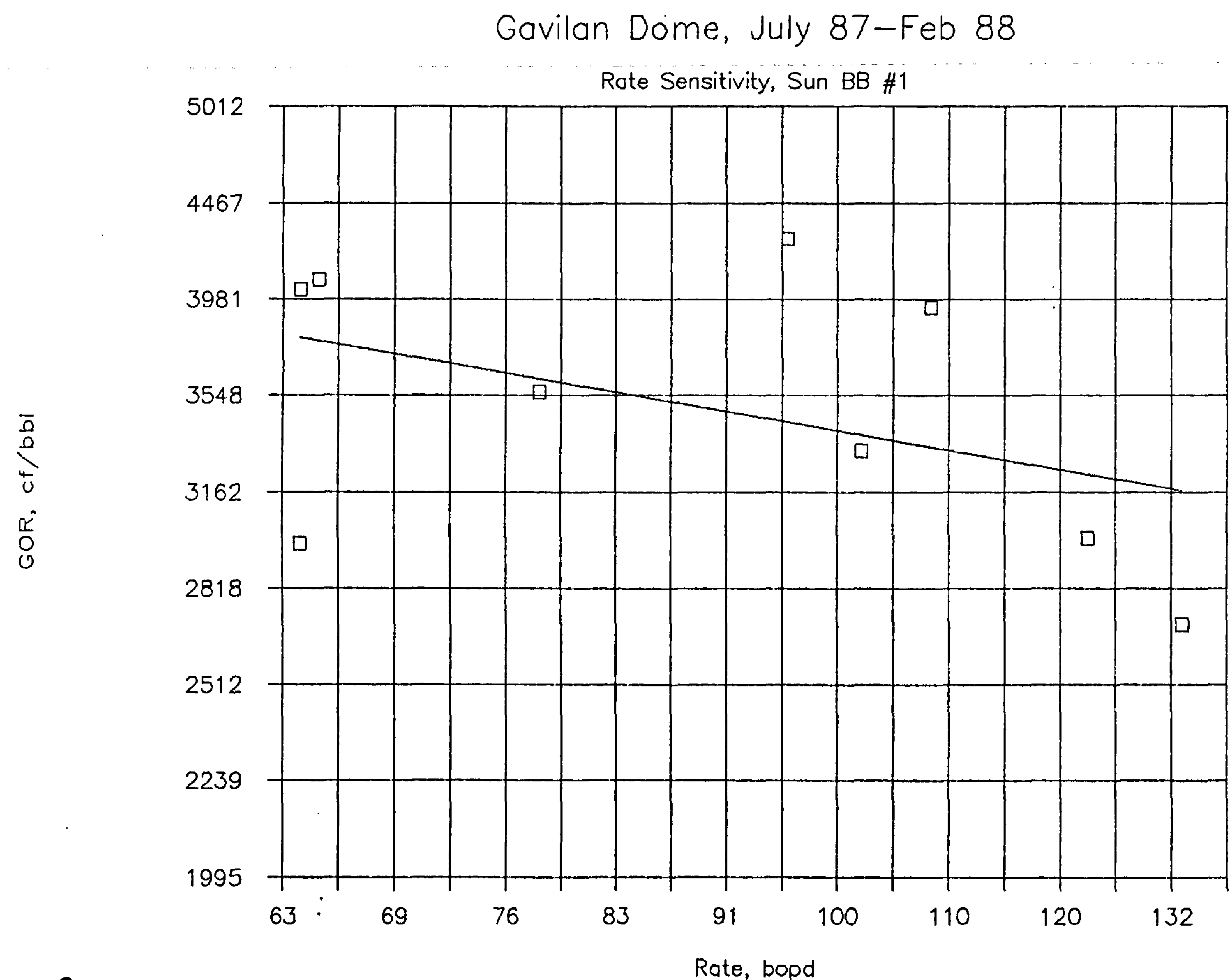
Gavilan Dome, July 87–Feb 88
Rate Sensitivity, Sun BB #1
5012
4467
3981
3548
3162
2818
2512
2239
1995
GOR, cf/bbl
63
69
76
83
91
100
110
120
132
Rate, bopd

C.C. = 0.44

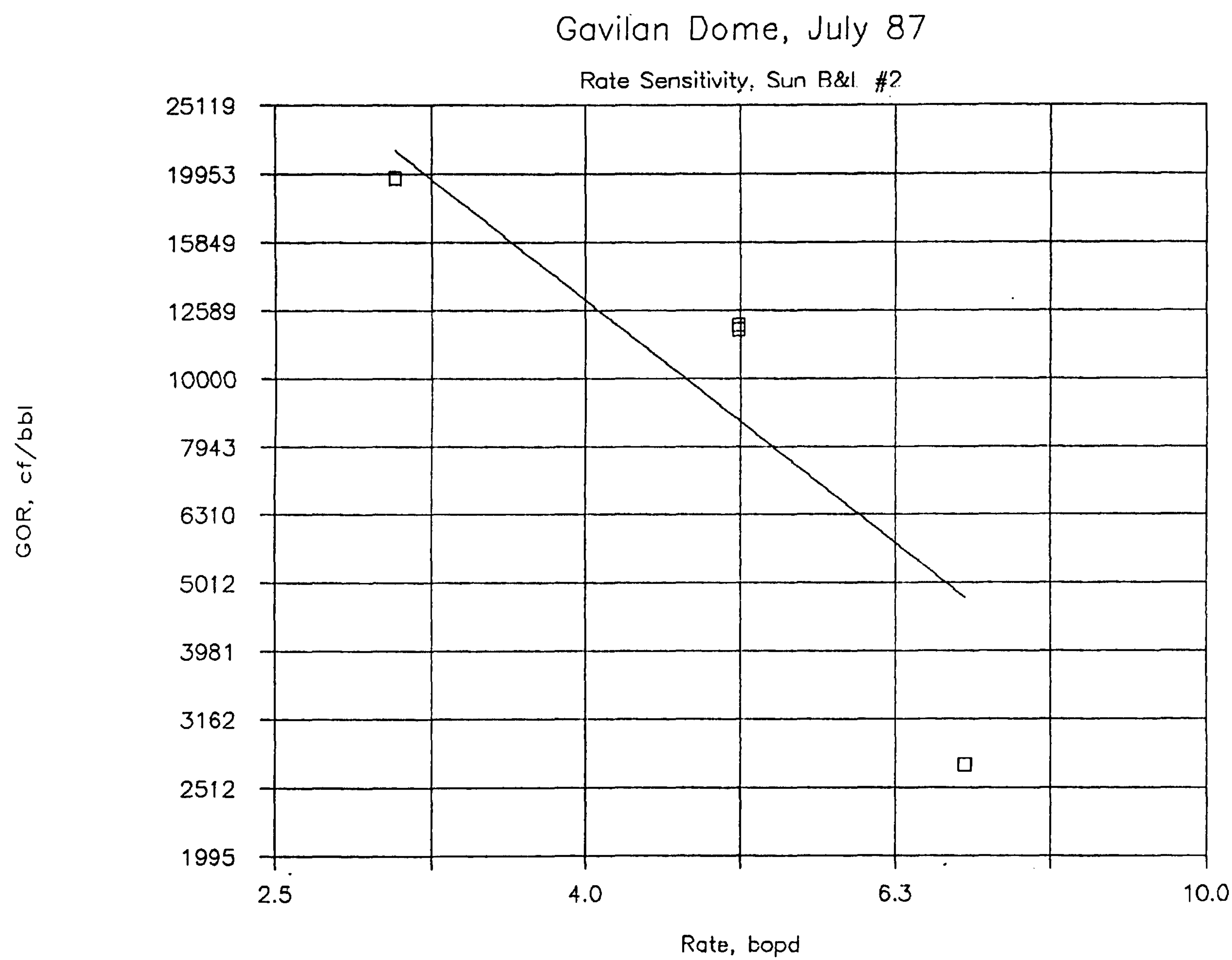
Gavilan Dome, July 87
Rate Sensitivity, Sun B&I #2
25119
19953
15849
12589
10000
7943
6310
5012
3981
3162
2512
1995
GOR, cf/bbl
2.5
4.0
6.3
10.0
Rate, bopd

C. C. = 0.89

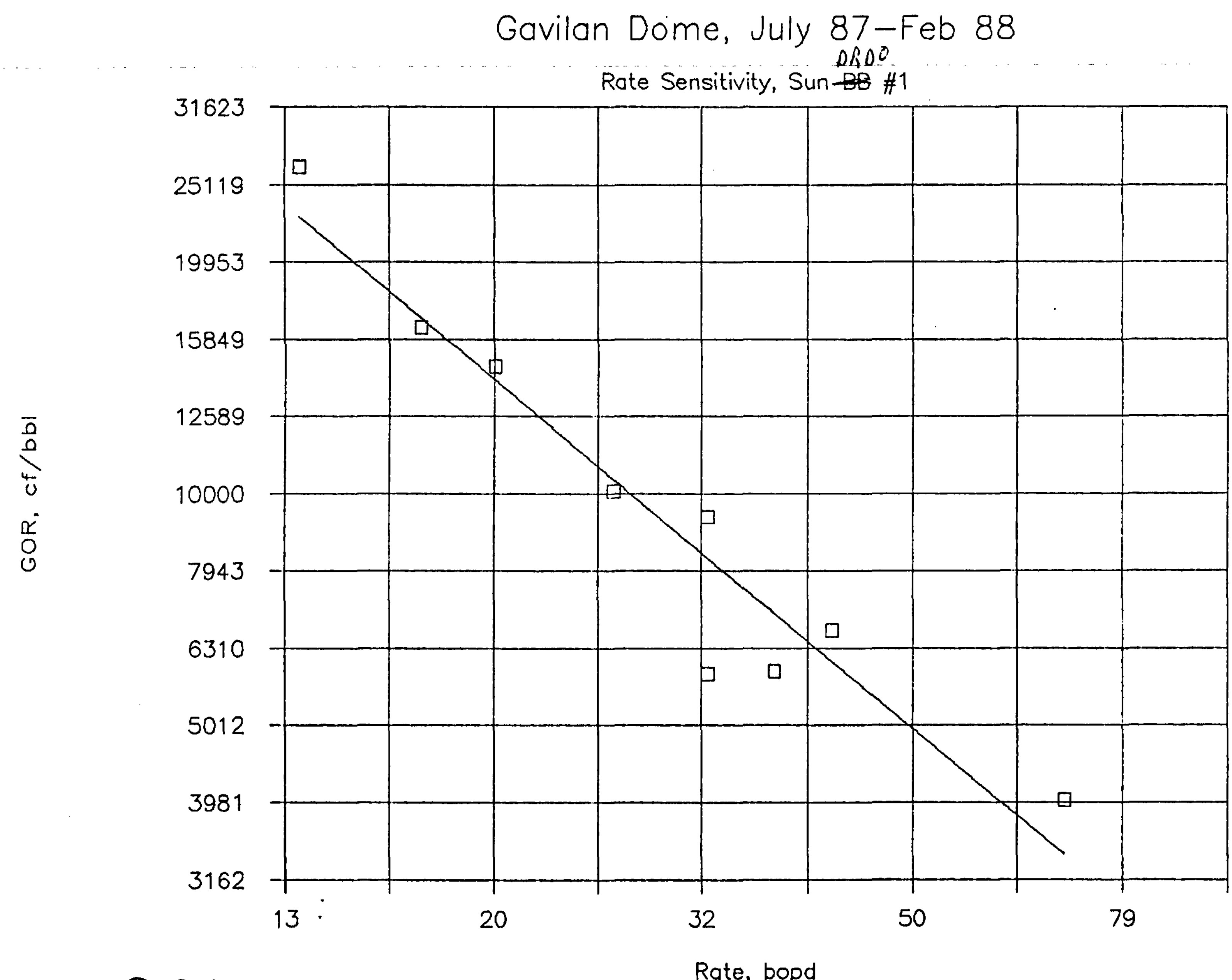
Gavilan Dome, July 87—Feb 88
Rate Sensitivity, Sun ~~BB~~ DRDO #1
31623
25119
19953
15849
12589
10000
7943
6310
5012
3981
3162
GOR, cf/bbl
13
20
32
50
79
Rate, bopd

C.C. = 0.96

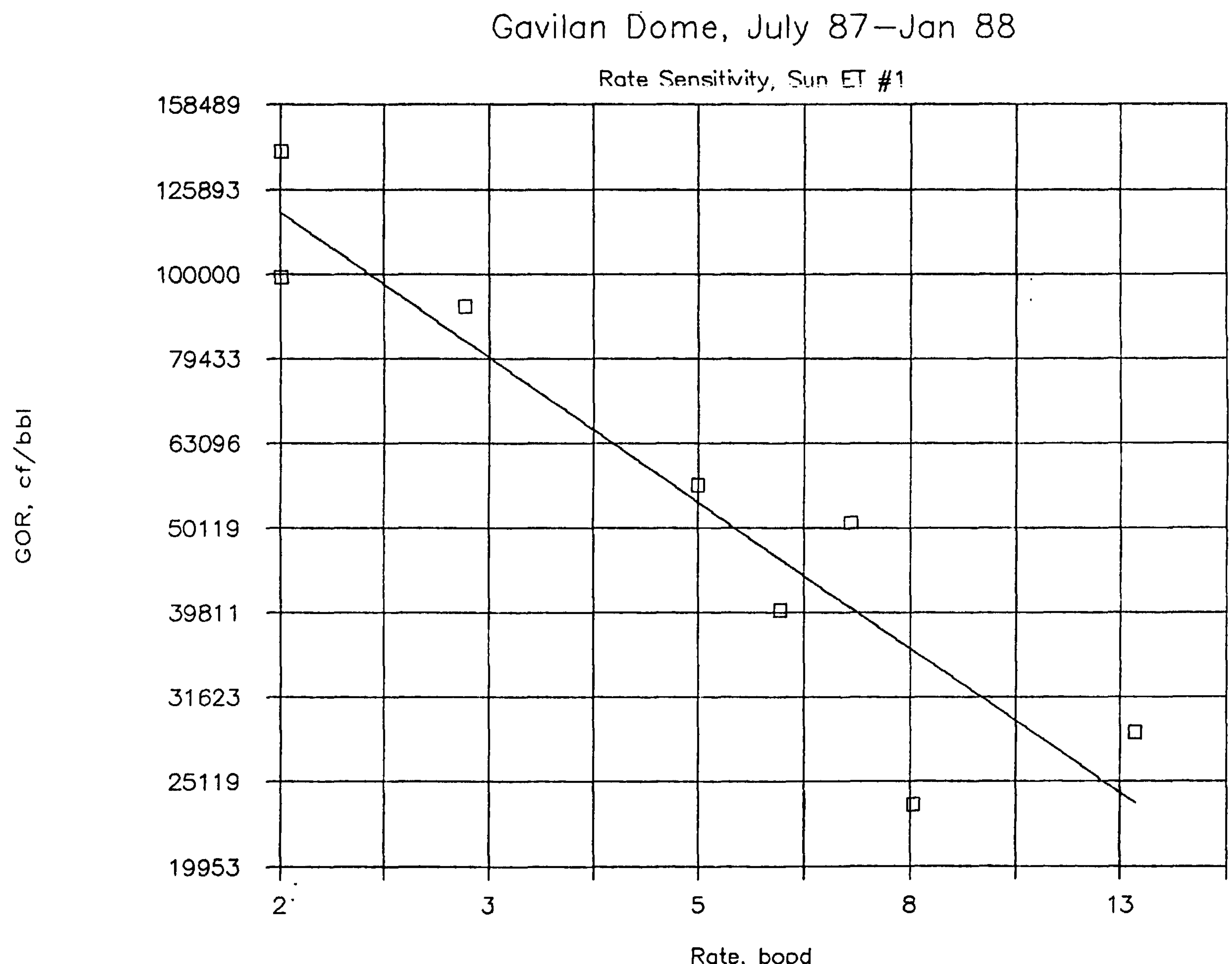
Gavilan Dome, July 87—Jan 88
Rate Sensitivity, Sun ET #1
158489
125893
100000
79433
63096
50119
39811
31623
25119
19953
GOR, cf/bbl
2
3
5
8
13
Rate, bopd

C.C. = 0.93

Gavilan Dome, July 87–Feb 88

Rate Sensitivity, Sun FS #1

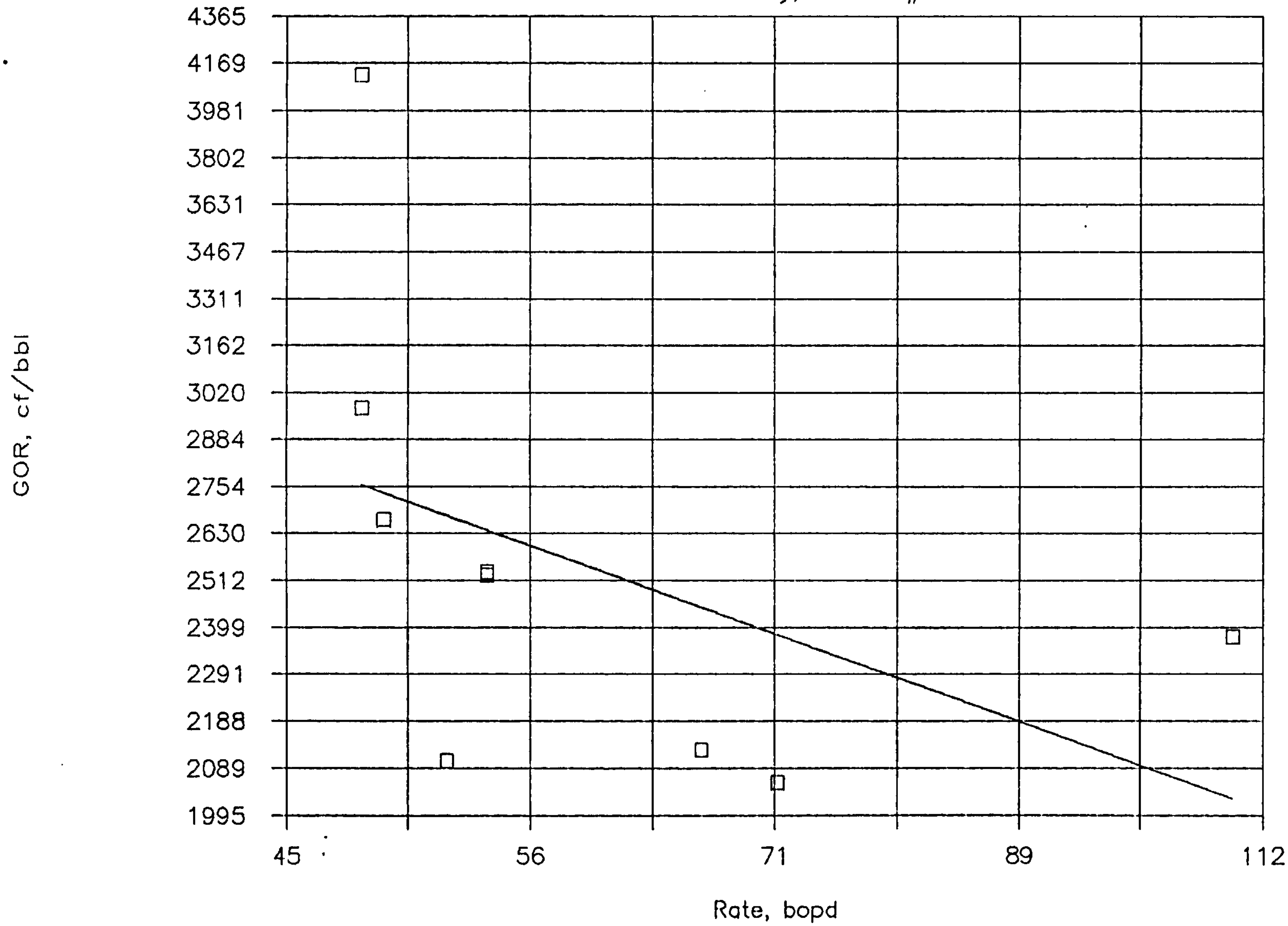

C.C. = 0.46

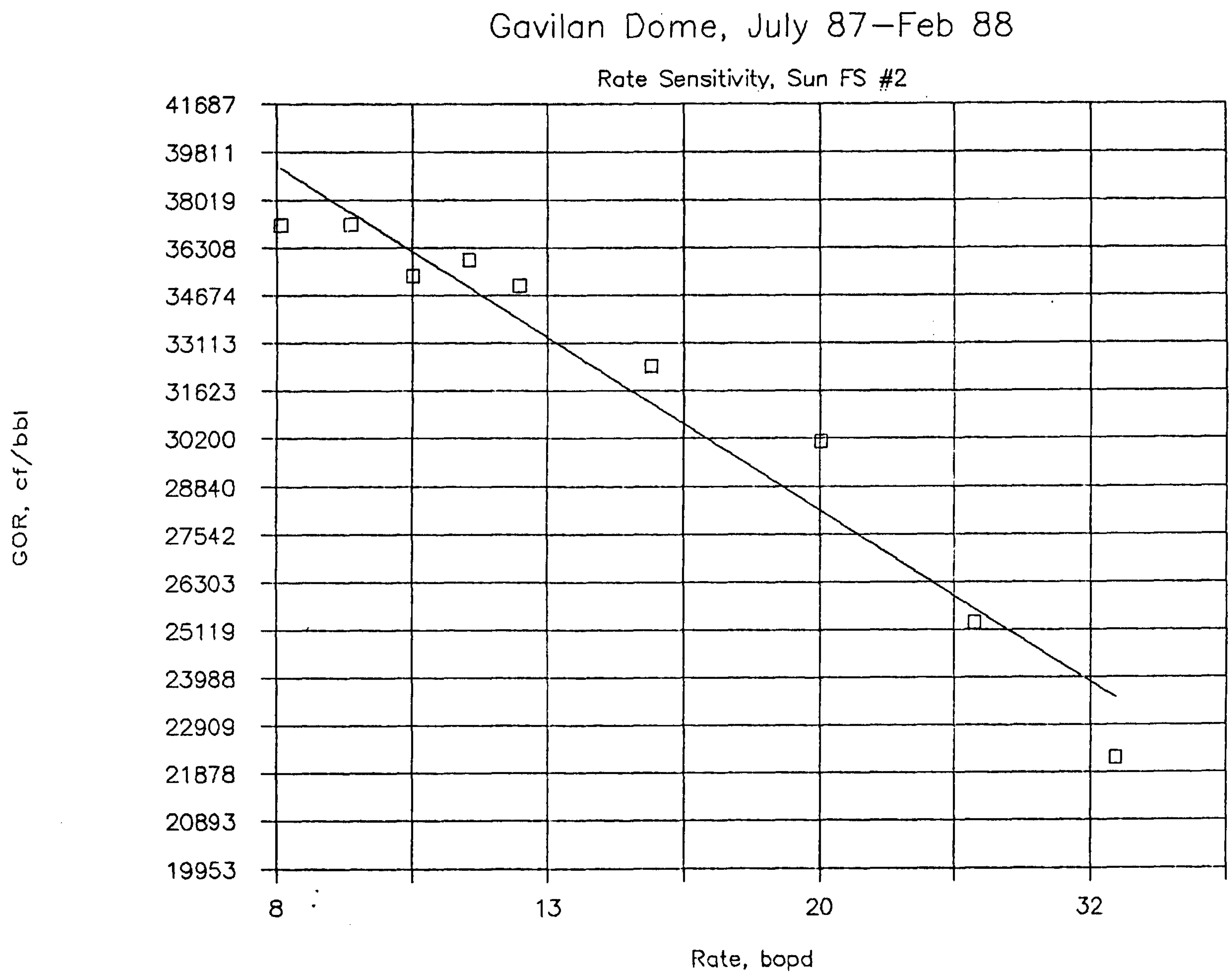
Gavilan Dome, July 87–Feb 88
Rate Sensitivity, Sun FS #2
41687
39811
38019
36308
34674
33113
31623
30200
28840
27542
26303
25119
23988
22909
21878
20893
19953
GOR, cf/bbl
8
13
20
32
Rate, bopd

C.C. = 0.97

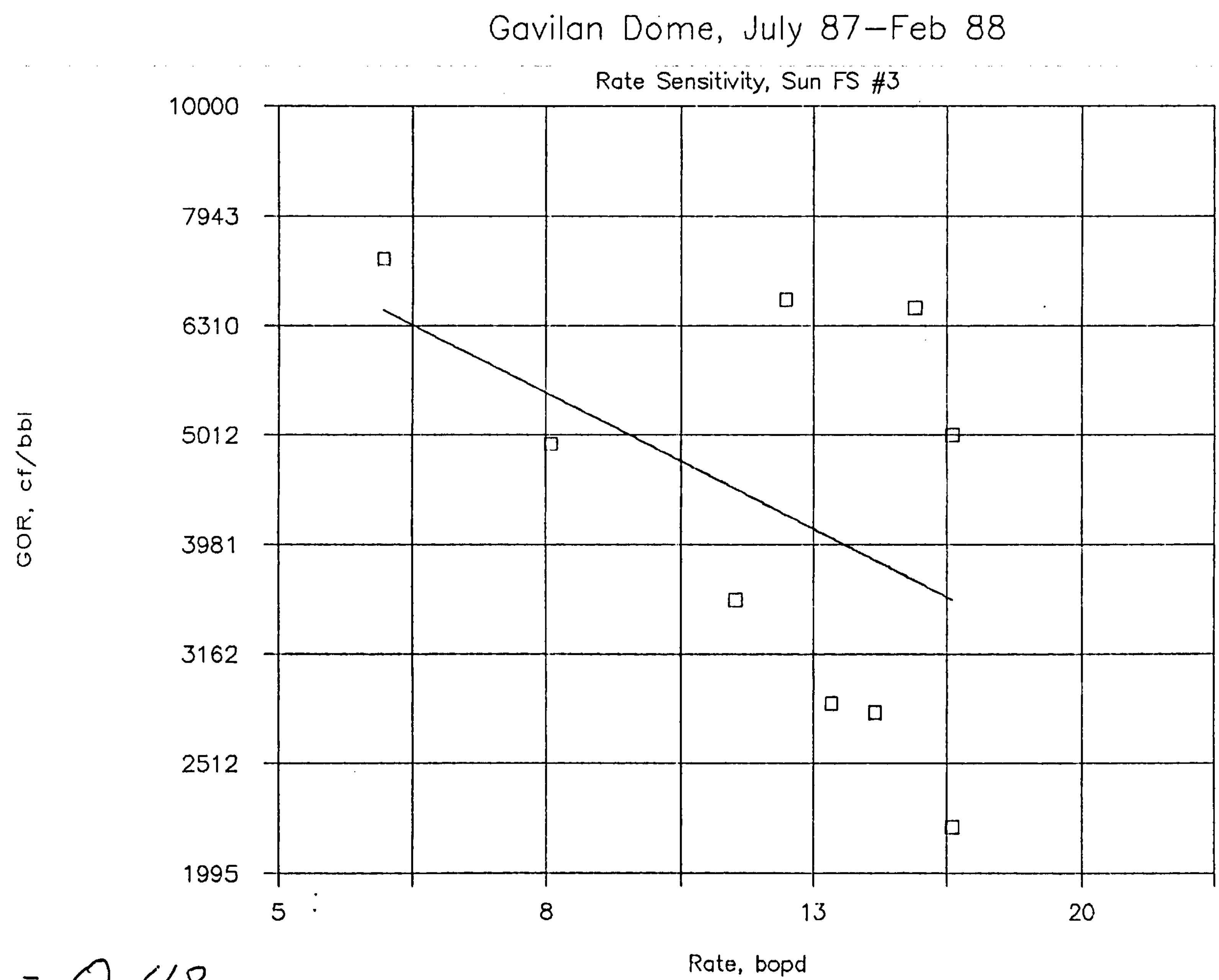
Gavilan Dome, July 87–Feb 88
Rate Sensitivity, Sun FS #3
GOR, cf/bbl
10000
7943
6310
5012
3981
3162
2512
1995
5
8
13
20
Rate, bopd

C. C. = 0.48

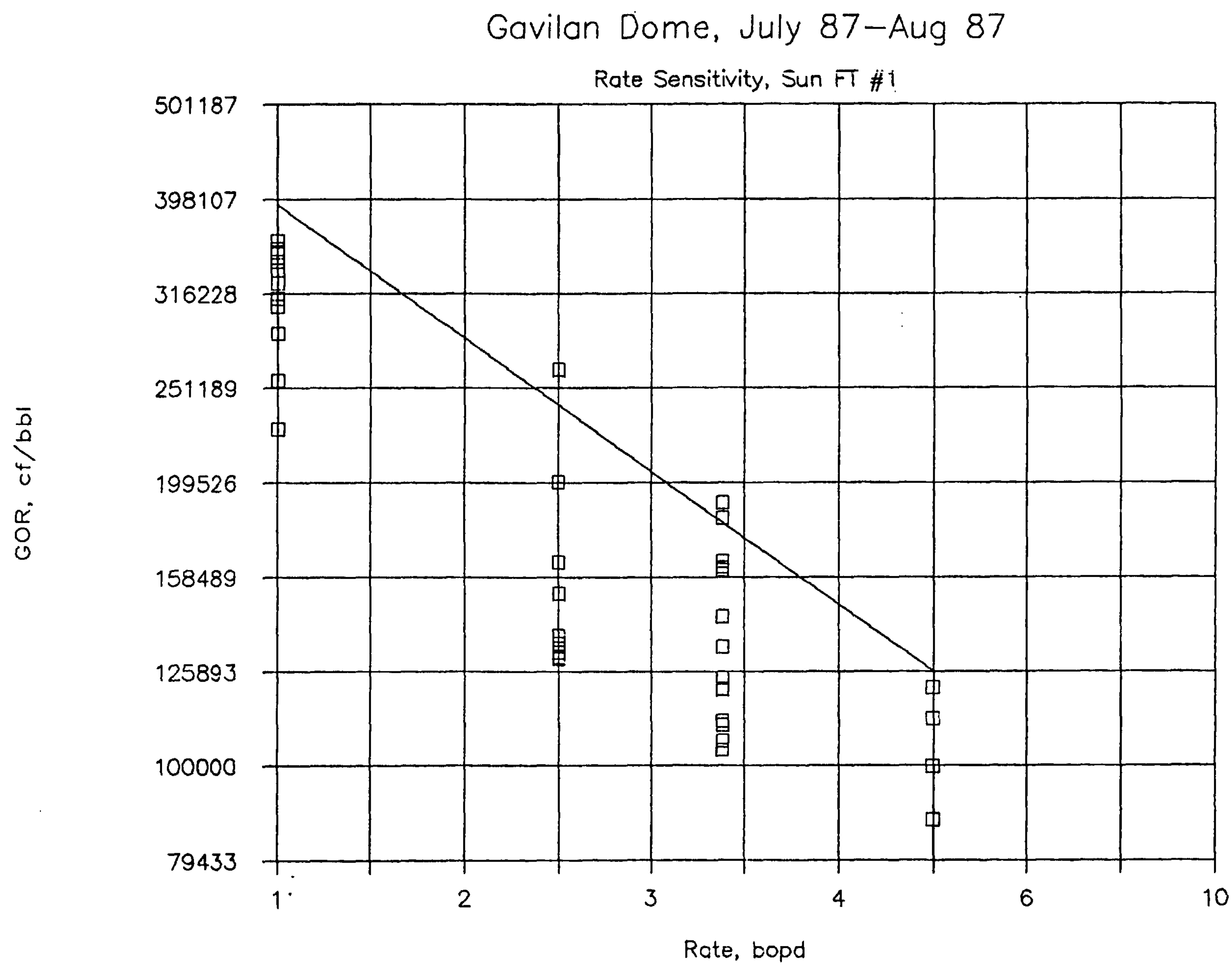

Gavilan Dome, July 87—Aug 87
Rate Sensitivity, Sun FT #1
501187
398107
316228
251189
199526
158489
125893
100000
79433
GOR, cf/bbl
1
2
3
4
6
10
Rate, bopd

C. C. = 0.88

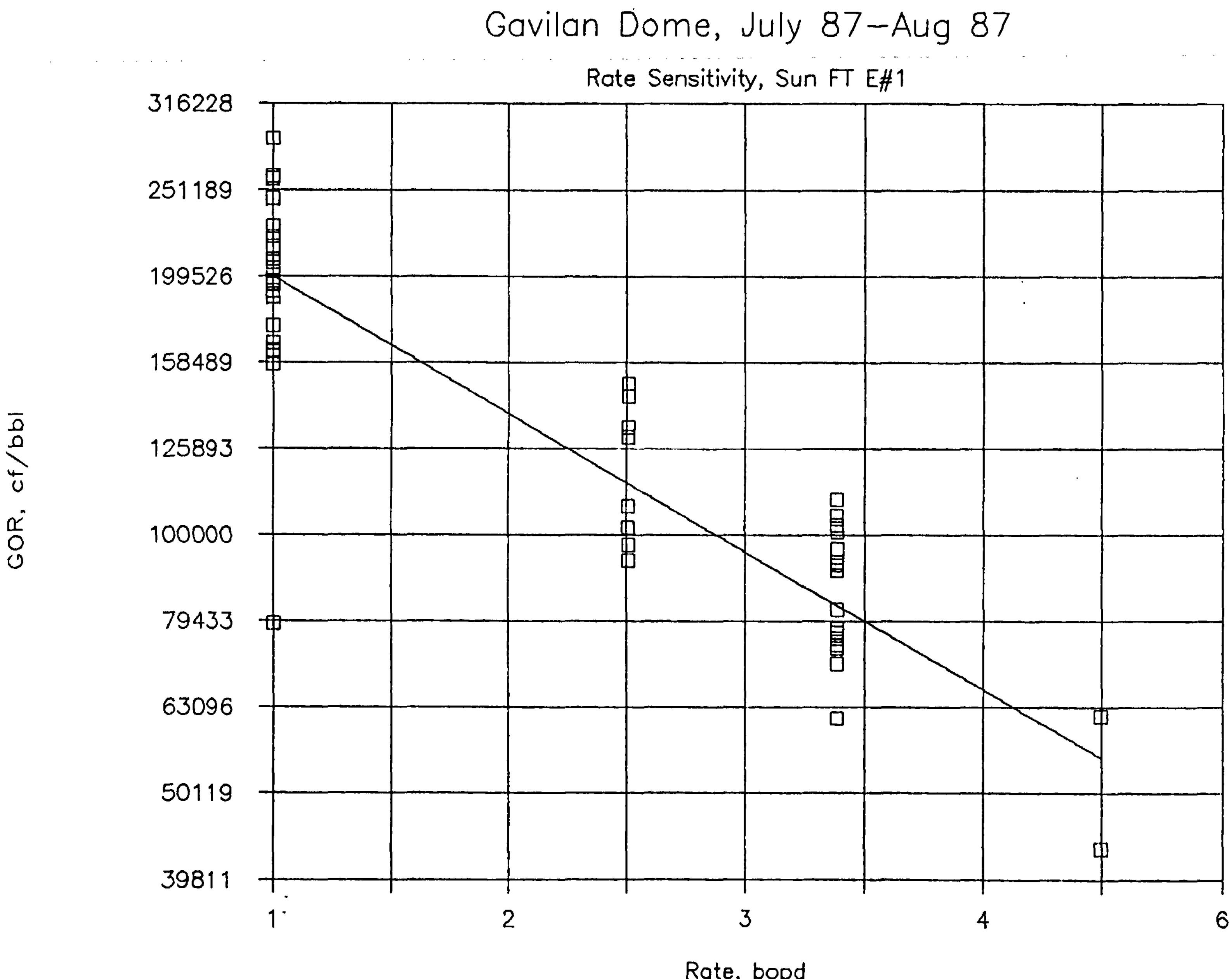

Gavilan Dome, July 87–Aug 87
Rate Sensitivity, Sun FT E#1
GOR, cf/bbl
316228
251189
199526
158489
125893
100000
79433
63096
50119
39811
1
2
3
4
6
Rate, bopd

C.C. = 0.91

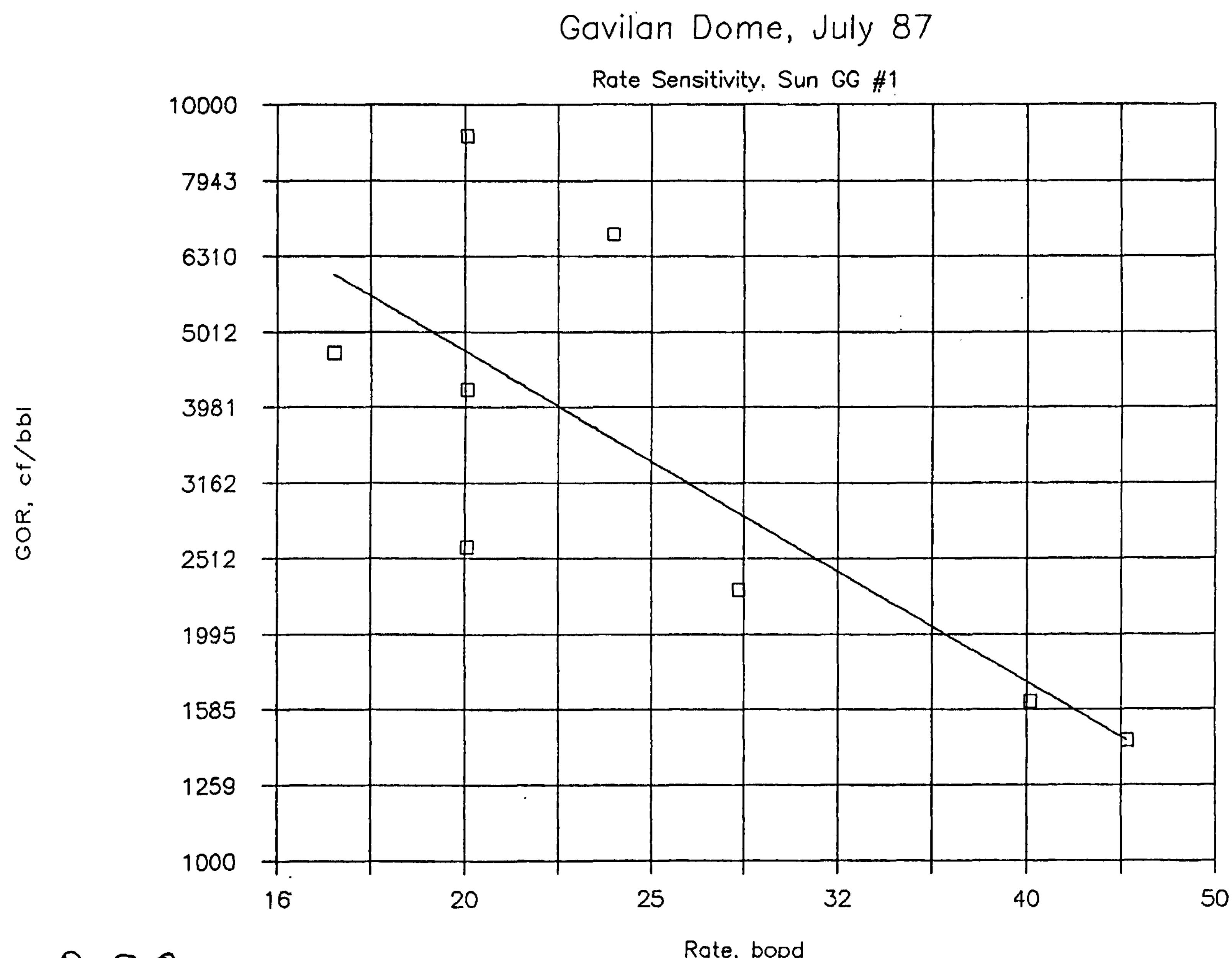
Gavilan Dome, July 87
Rate Sensitivity, Sun GG #1
GOR, cf/bbl
10000
7943
6310
5012
3981
3162
2512
1995
1585
1259
1000
16
20
25
32
40
50
Rate, bopd

C.C. = 0.80

Gavilan Dome, July 87—Feb 88

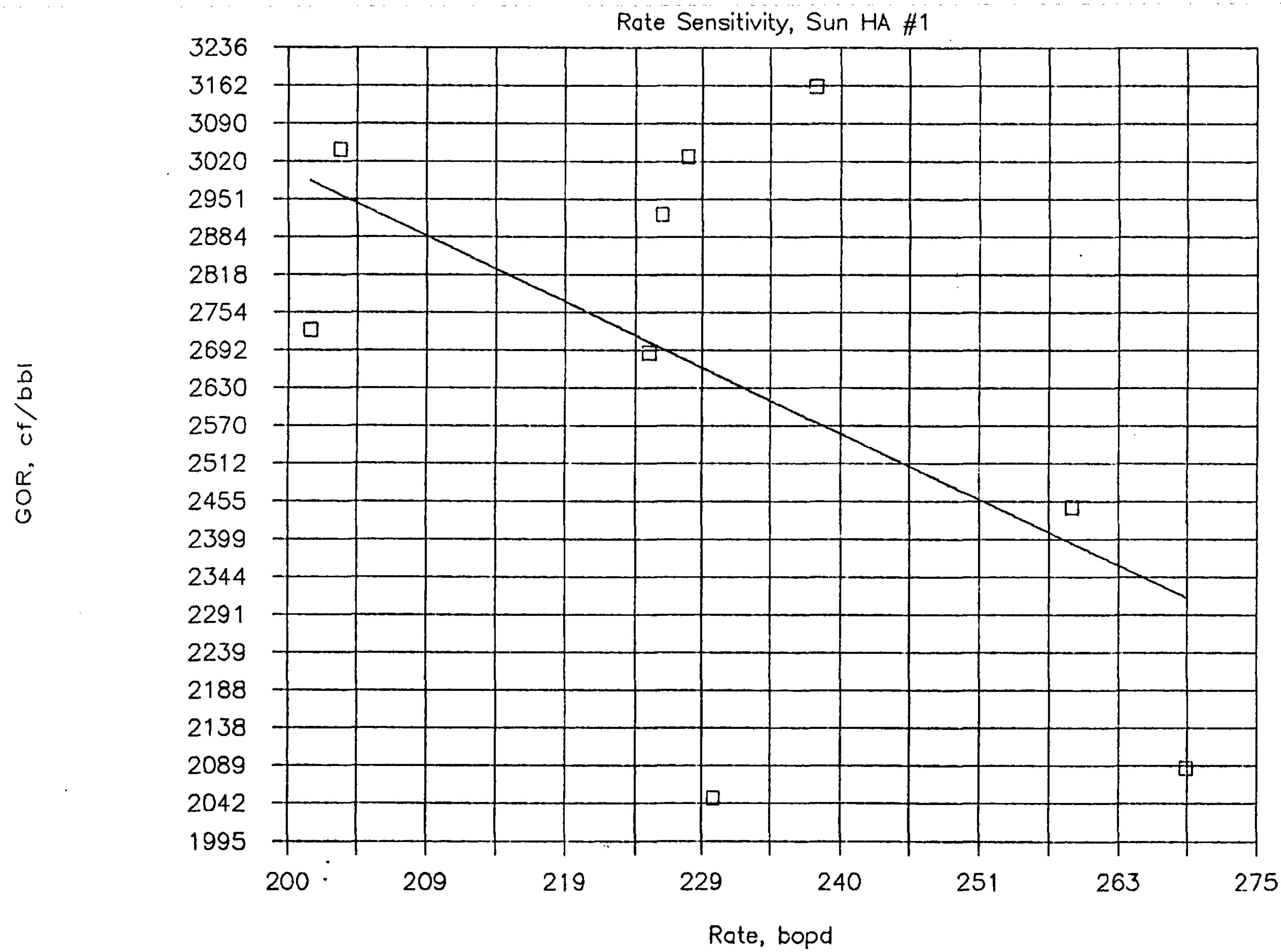

C.C. = 0.52

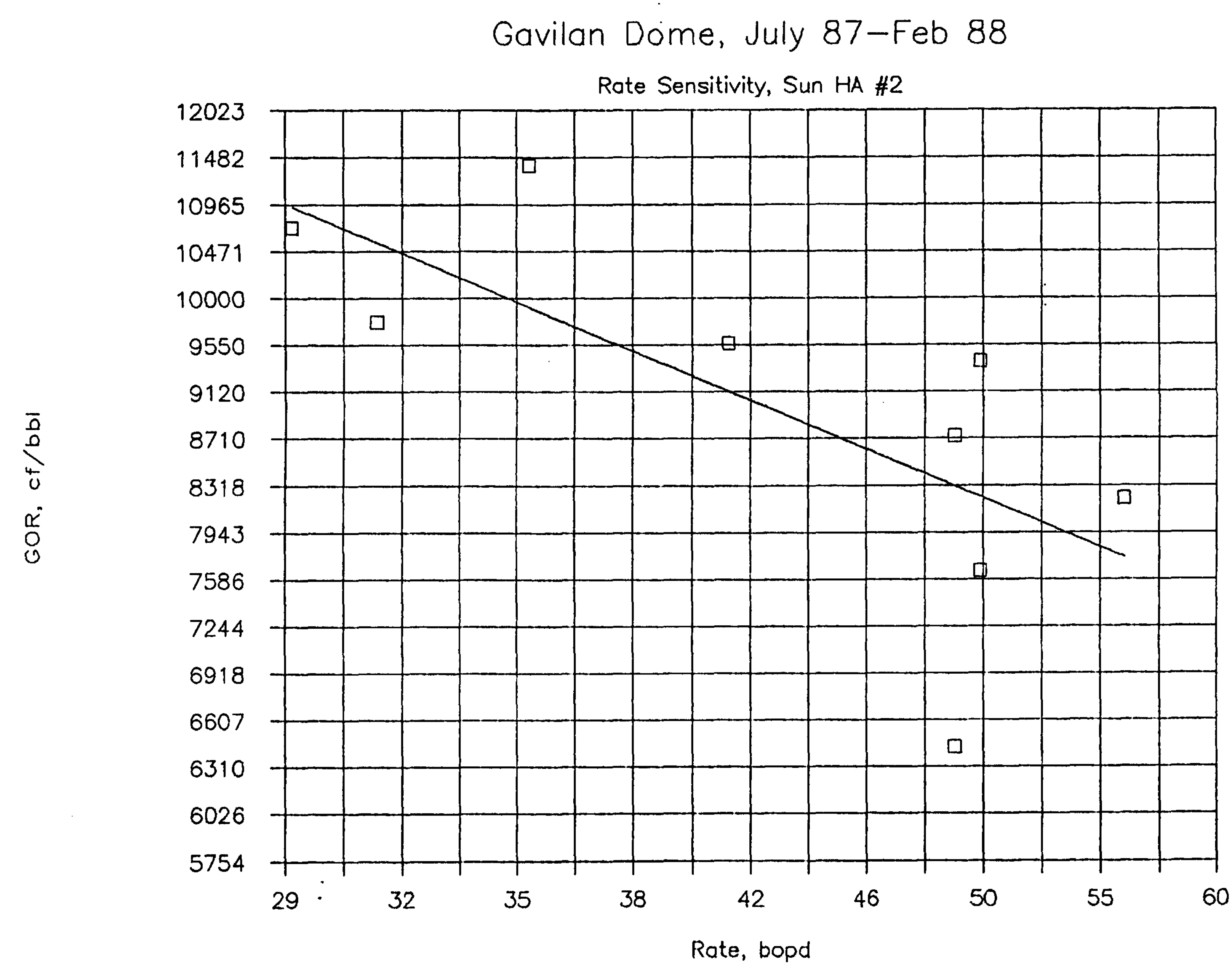
Gavilan Dome, July 87—Feb 88
Rate Sensitivity, Sun HA #2
GOR, cf/bbl
12023
11482
10965
10471
10000
9550
9120
8710
8318
7943
7586
7244
6918
6607
6310
6026
5754
29
32
35
38
42
46
50
55
60
Rate, bopd

C.C. = 0.71

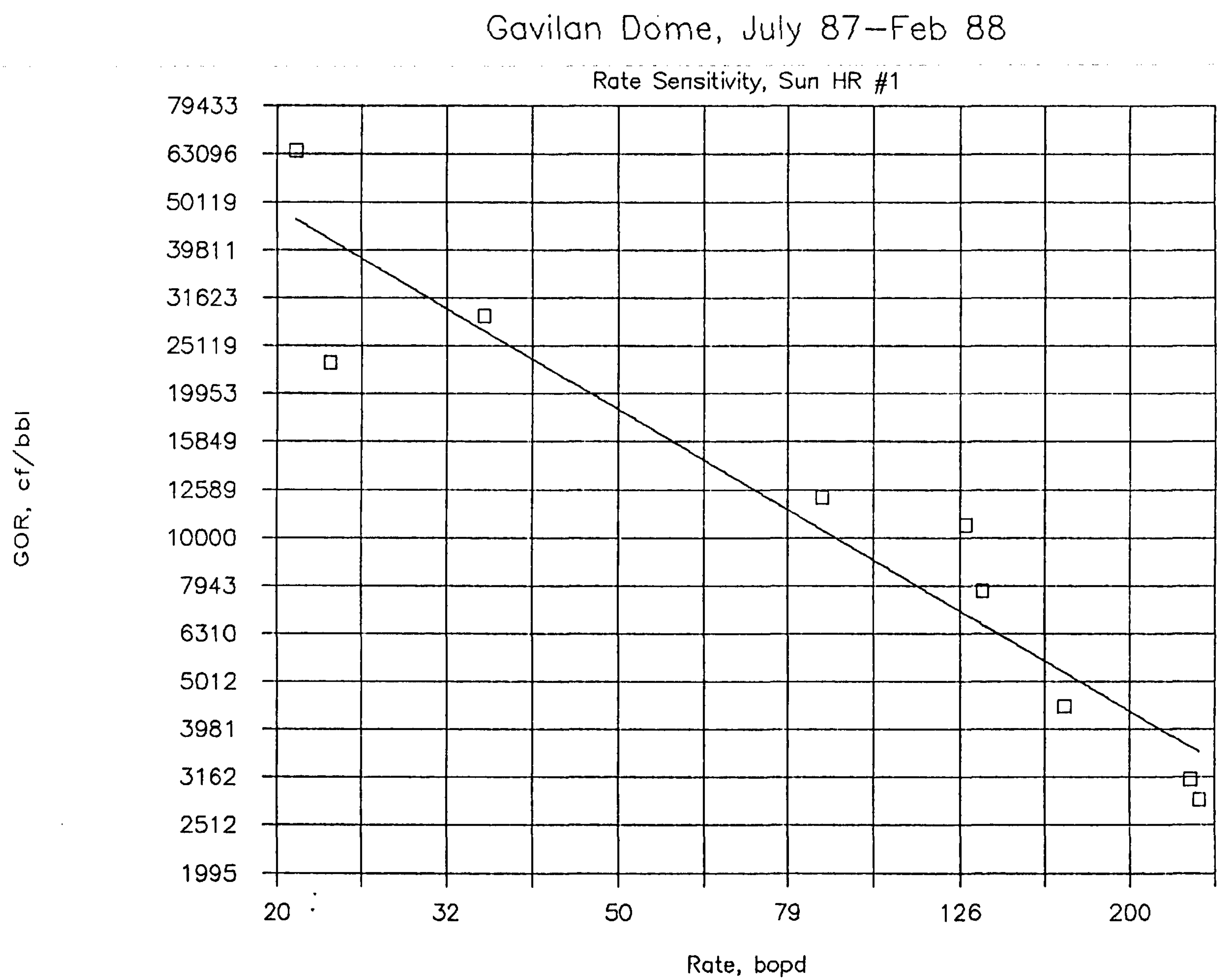

Gavilan Dome, July 87—Feb 88
Rate Sensitivity, Sun HR #1
79433
63096
50119
39811
31623
25119
19953
15849
12589
10000
7943
6310
5012
3981
3162
2512
1995
GOR, cf/bbl
20
32
50
79
126
200
Rate, bopd

C. C. = 0.95

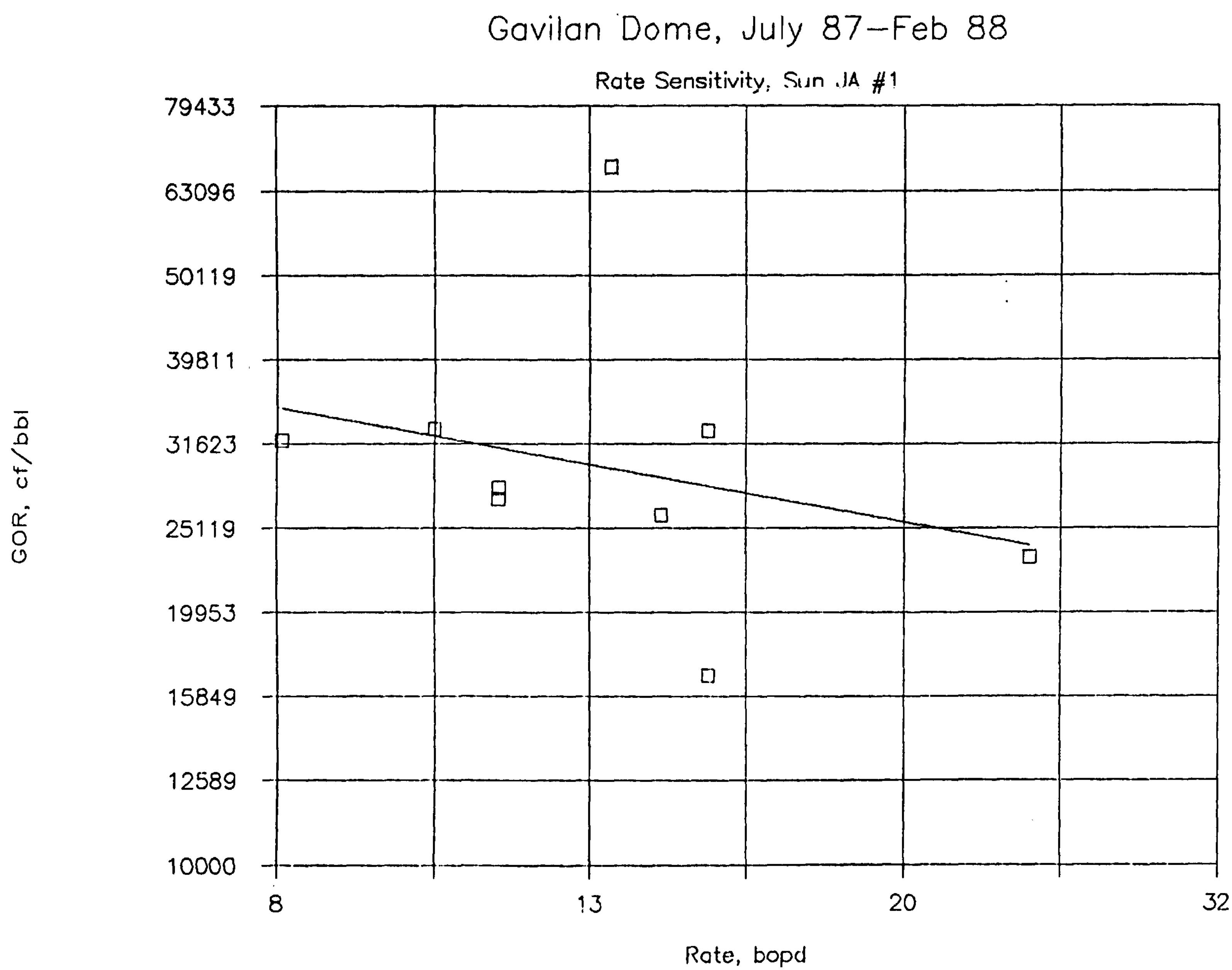

Gavilan Dome, July 87–Feb 88
Rate Sensitivity, Sun JA #1
GOR, cf/bbl
79433
63096
50119
39811
31623
25119
19953
15849
12589
10000
8
13
20
32
Rate, bopd

C.C. = 0.29

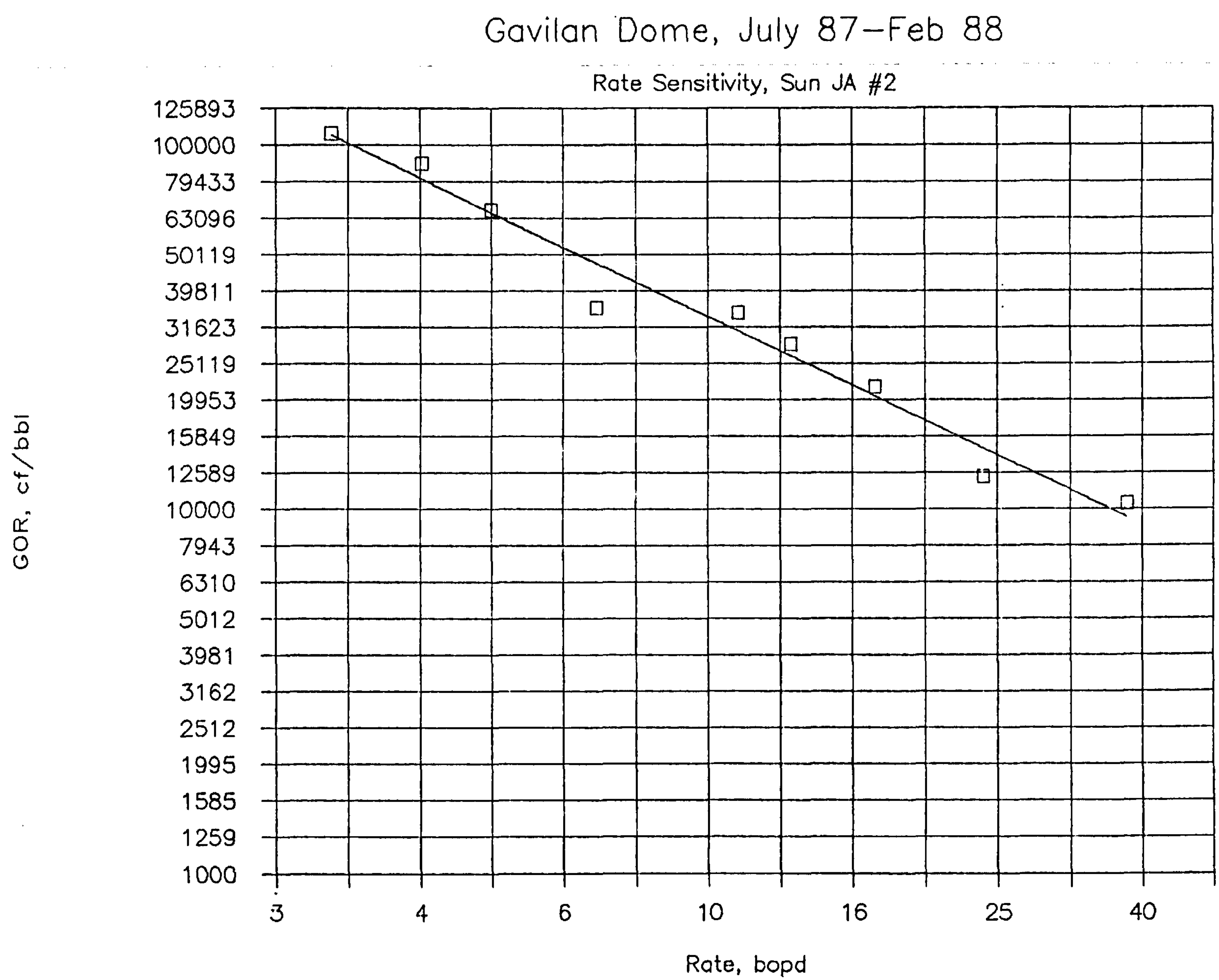

Gavilan Dome, July 87–Feb 88
Rate Sensitivity, Sun JA #2
GOR, cf/bbl
125893
100000
79433
63096
50119
39811
31623
25119
19953
15849
12589
10000
7943
6310
5012
3981
3162
2512
1995
1585
1259
1000
3
4
6
10
16
25
40
Rate, bopd

C.C. = 0.99

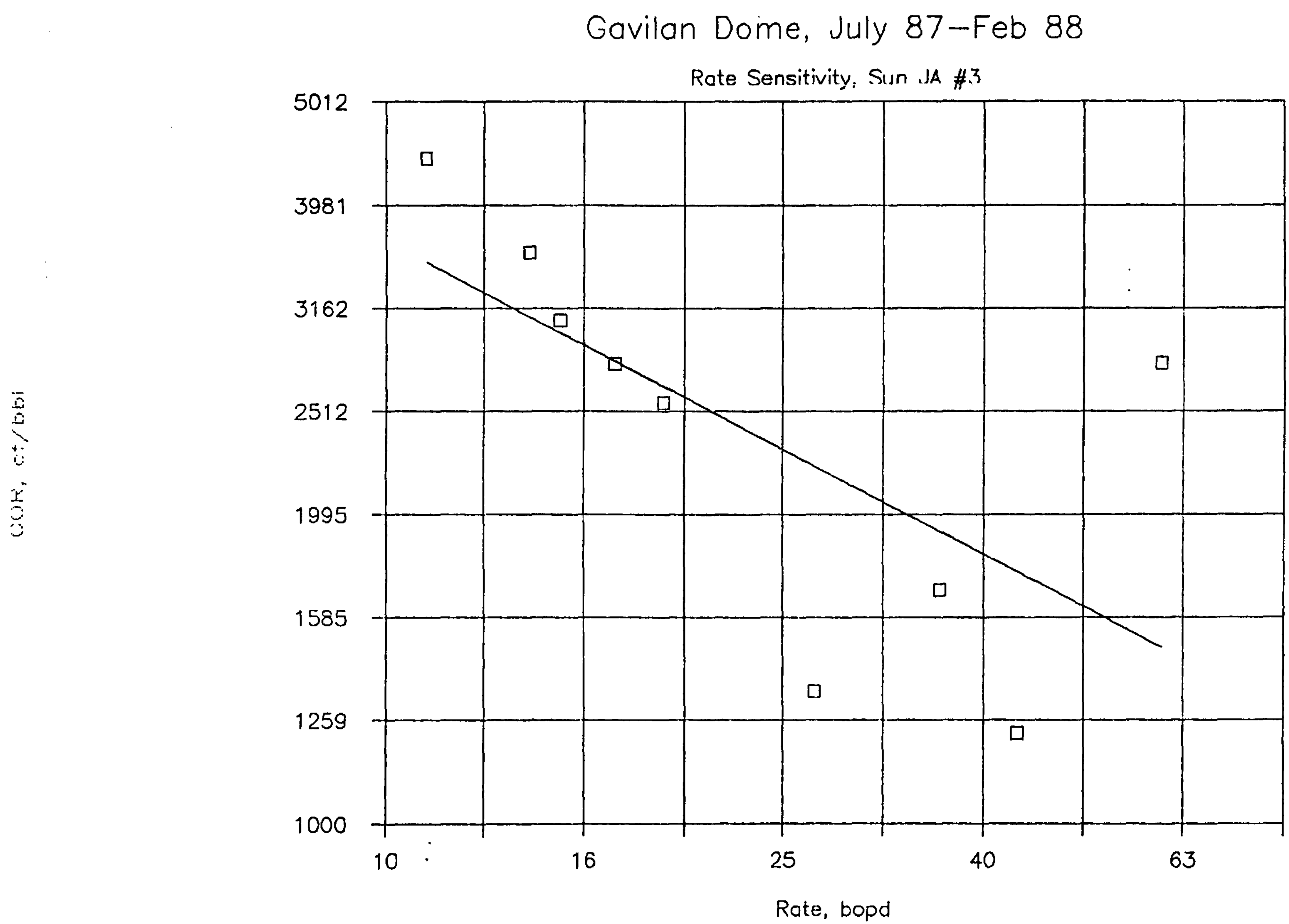
Gavilan Dome, July 87—Feb 88
Rate Sensitivity, Sun JA #3
GOR, cf/bbl
5012
3981
3162
2512
1995
1585
1259
1000
10
16
25
40
63
Rate, bopd

C.C. = 0.66

Gavilan Dome, July 87—Feb 88

Rate Sensitivity, Sun LL #1

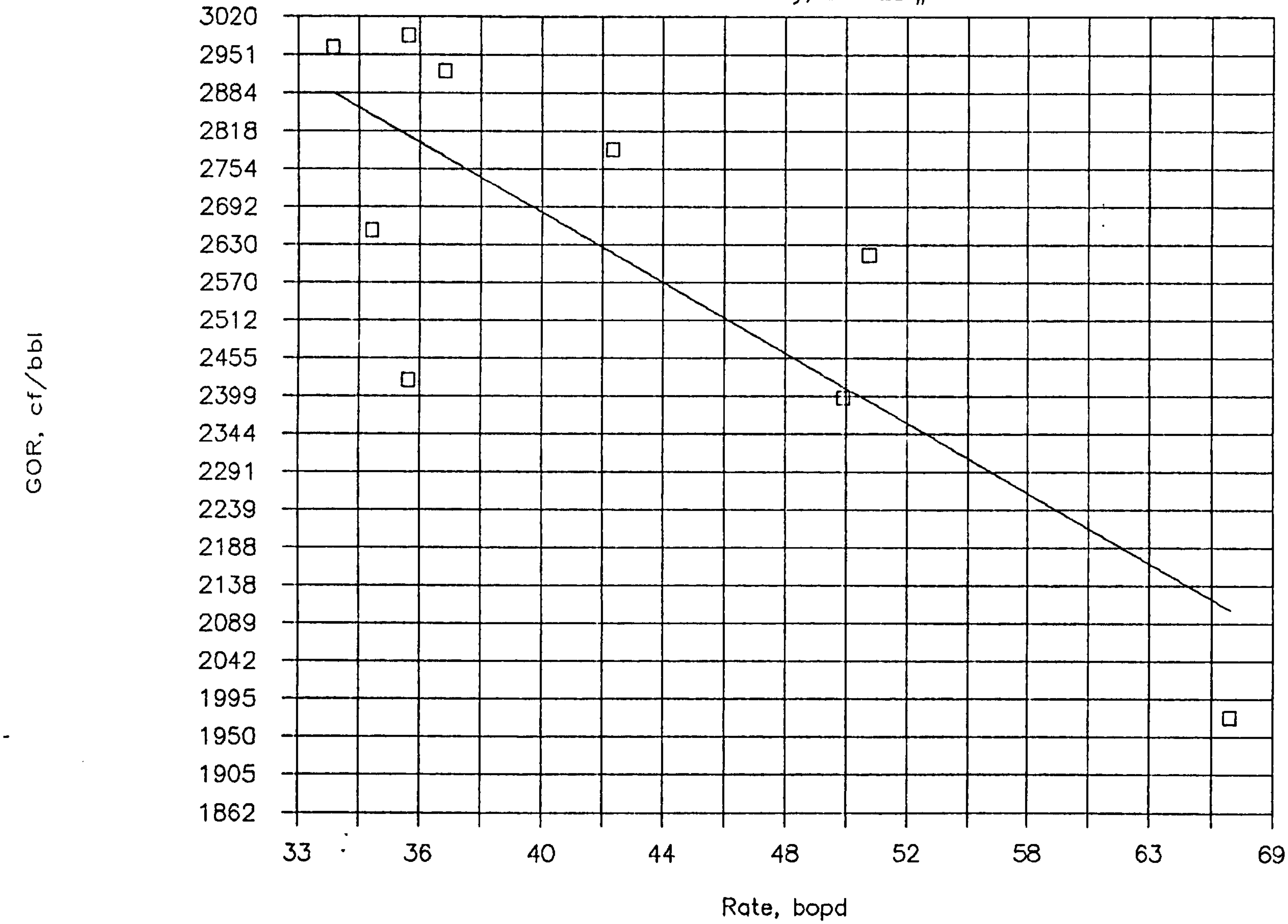

C. C. = 0.80

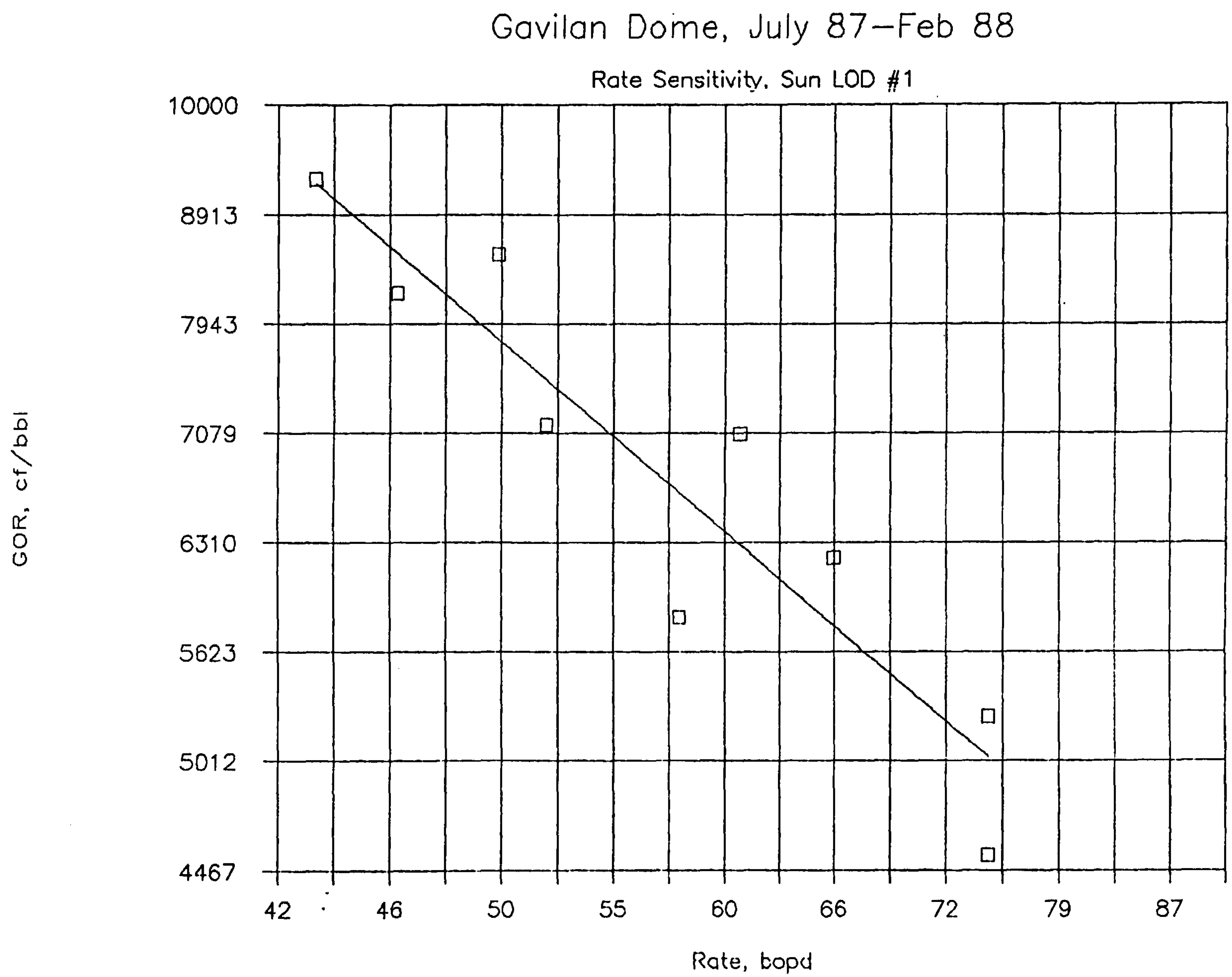
Gavilan Dome, July 87—Feb 88
Rate Sensitivity, Sun LOD #1
GOR, cf/bbl
10000
8913
7943
7079
6310
5623
5012
4467
42
46
50
55
60
66
72
79
87
Rate, bopd

C.C. = 0.93

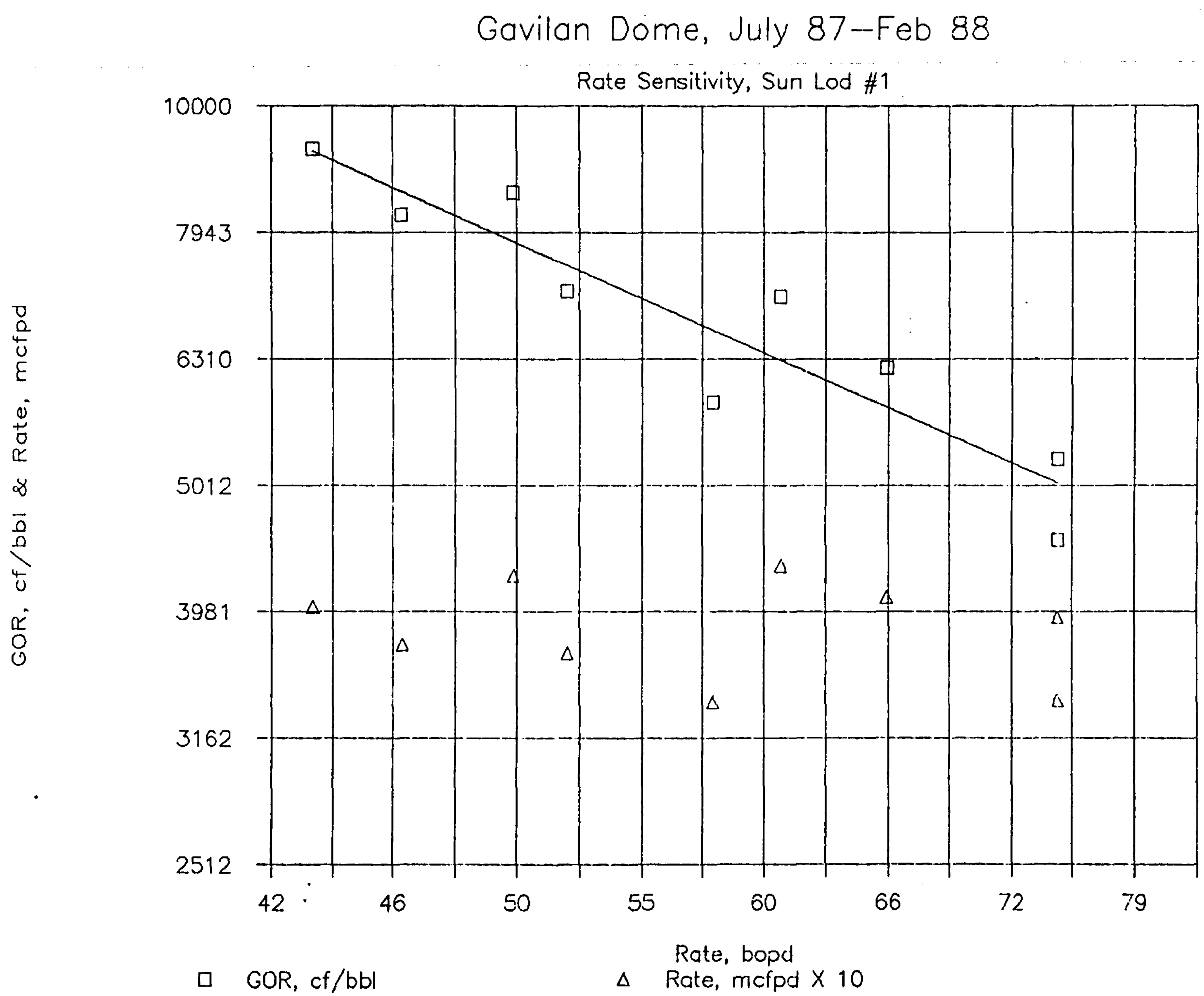

Gavilan Dome, July 87—Feb 88
Rate Sensitivity, Sun Lod #1
10000
7943
6310
5012
3981
3162
2512
GOR, cf/bbl & Rate, mcfpd
42
46
50
55
60
66
72
79
Rate, bopd
GOR, cf/bbl
Rate, mcfpd X 10

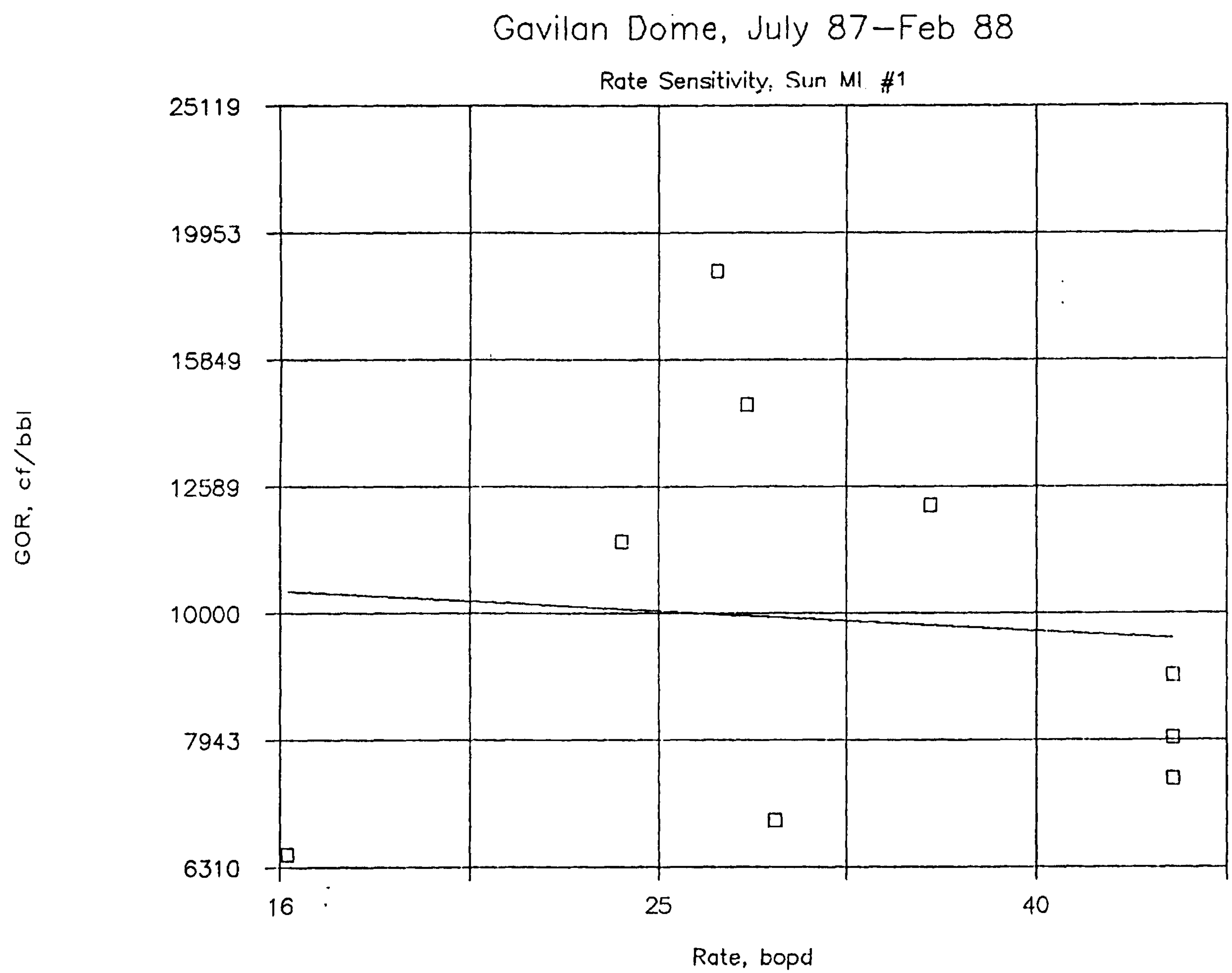
Gavilan Dome, July 87—Feb 88
Rate Sensitivity, Sun MI #1
25119
19953
15849
12589
10000
7943
6310
GOR, cf/bbl
16
25
40
Rate, bopd

C.C. = 0.08

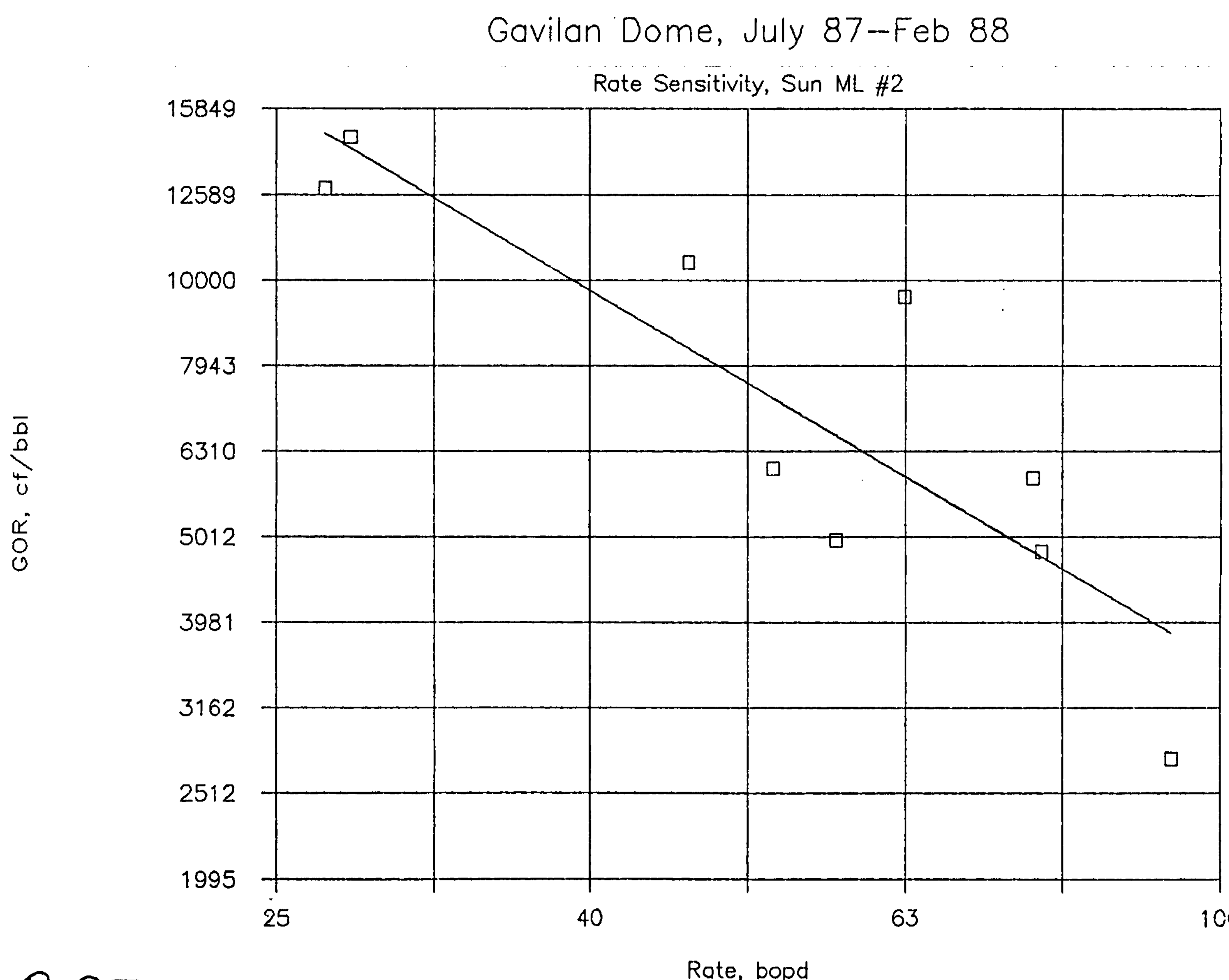

Gavilan Dome, July 87--Feb 88
Rate Sensitivity, Sun ML #2
15849
12589
10000
7943
6310
5012
3981
3162
2512
1995
GOR, cf/bbl
25
40
63
100
Rate, bopd

C. C. = 0.87

Gavilan Dome, July 87–Feb 88

Rate Sensitivity, Sun NH #1

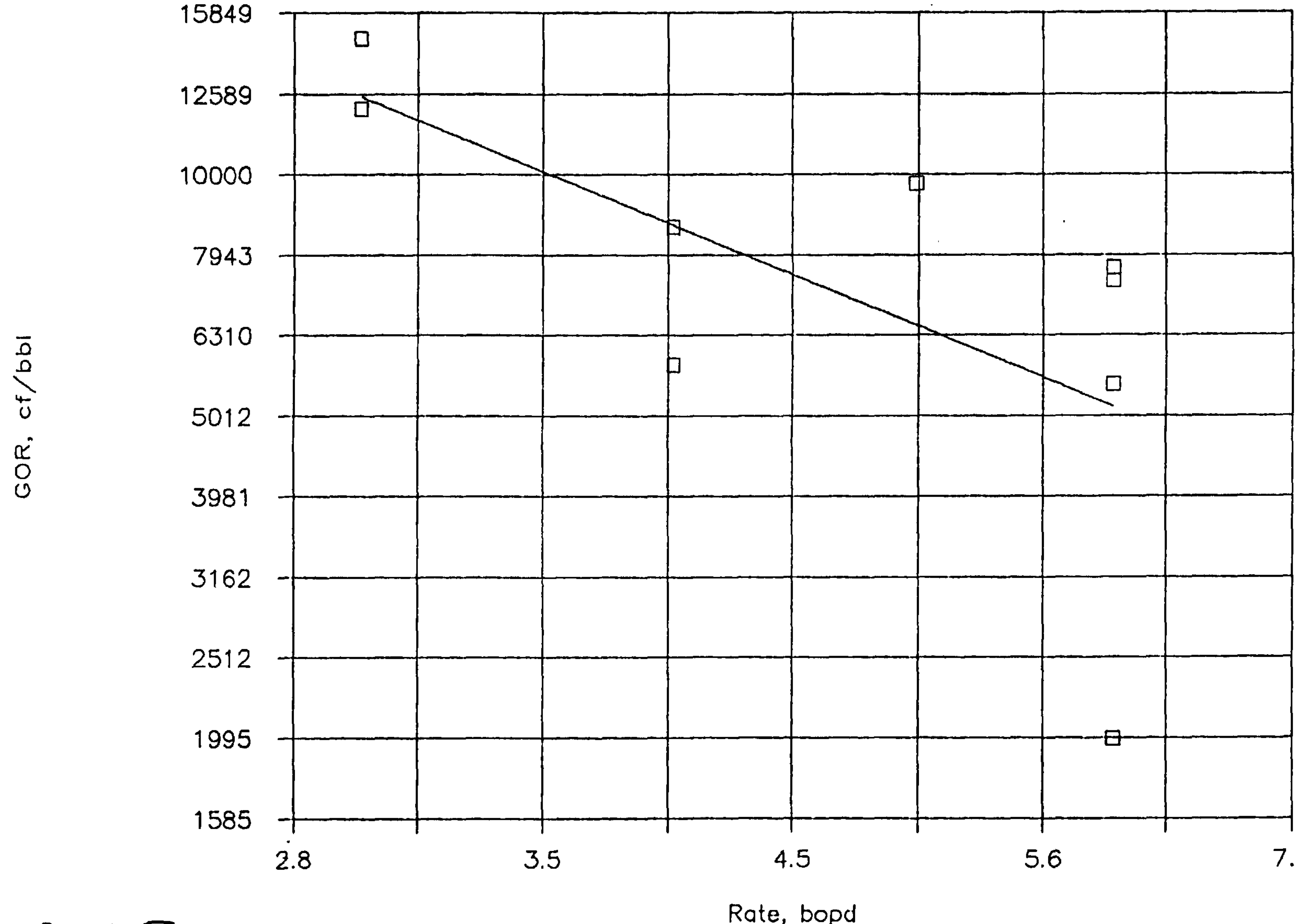

C. C. = 0.65

Gavilan Dome, July 87—Feb 88

Rate Sensitivity, Sun NS #1

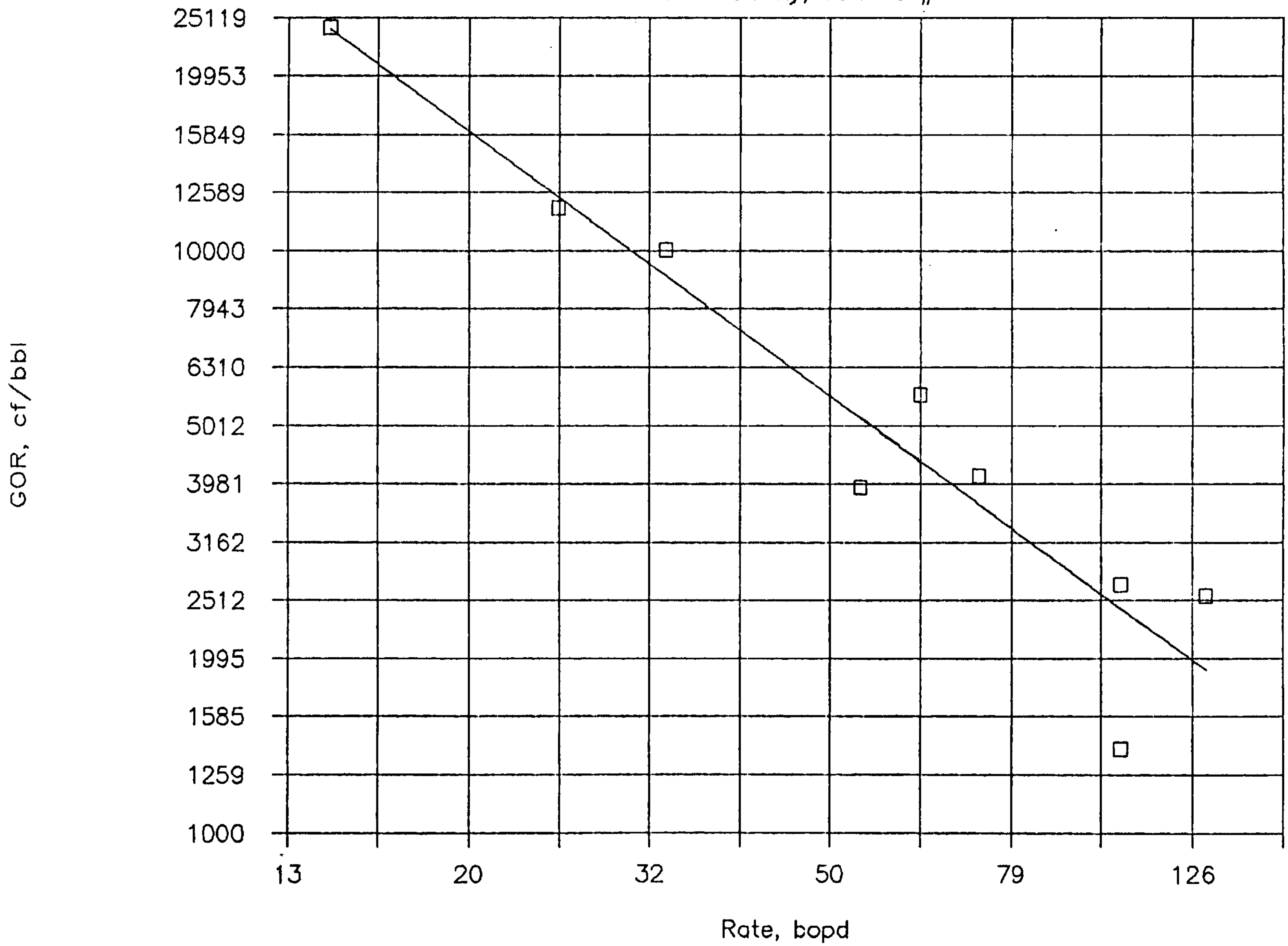

C.C. = 0.95

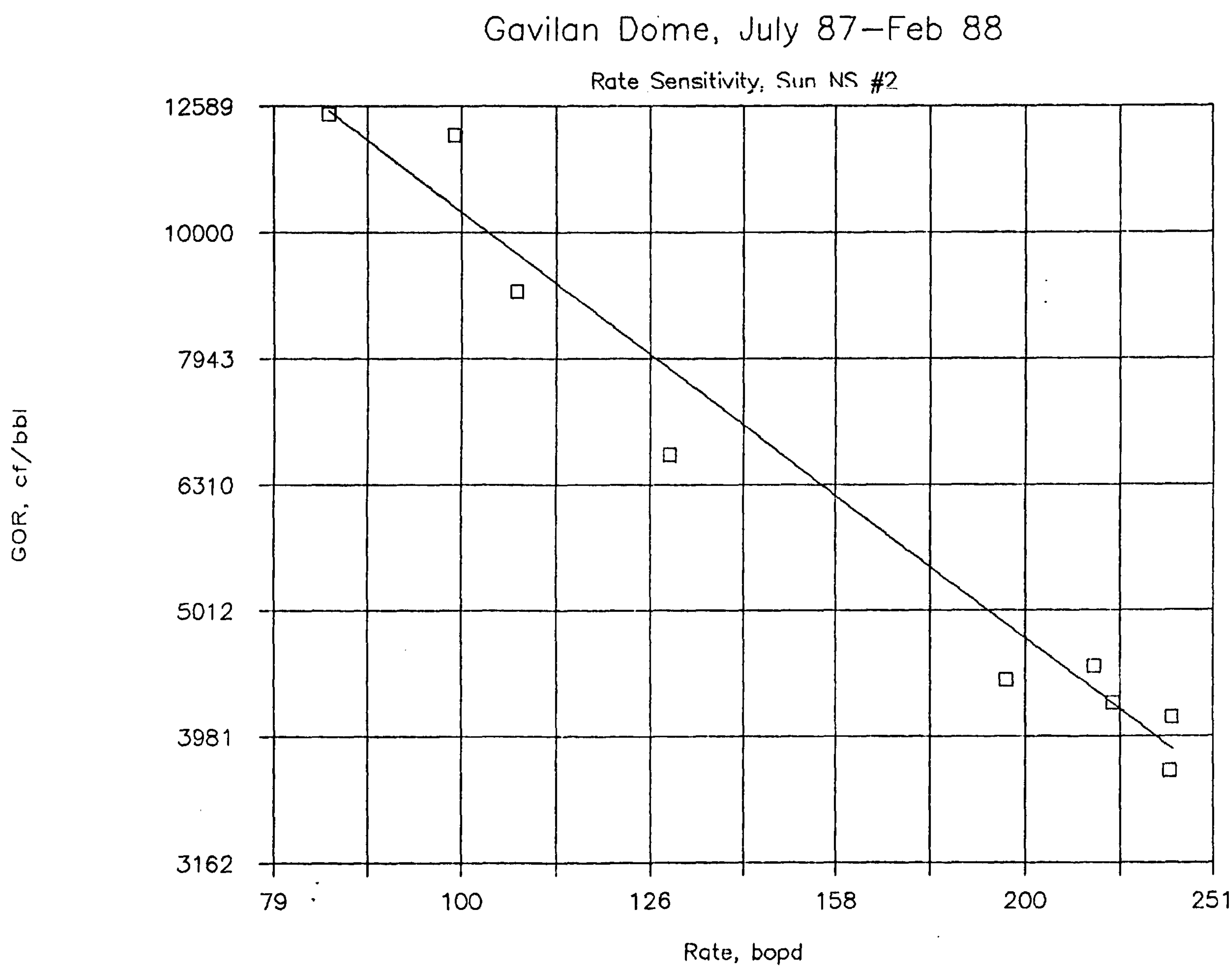

Gavilan Dome, July 87—Feb 88
Rate Sensitivity, Sun NS #2
12589
10000
7943
6310
5012
3981
3162
GOR, cf/bbl
79
100
126
158
200
251
Rate, bopd

C. C. = 0.98

Gavilan Dome, July 87–Feb 88

Rate Sensitivity, Sun NS #3

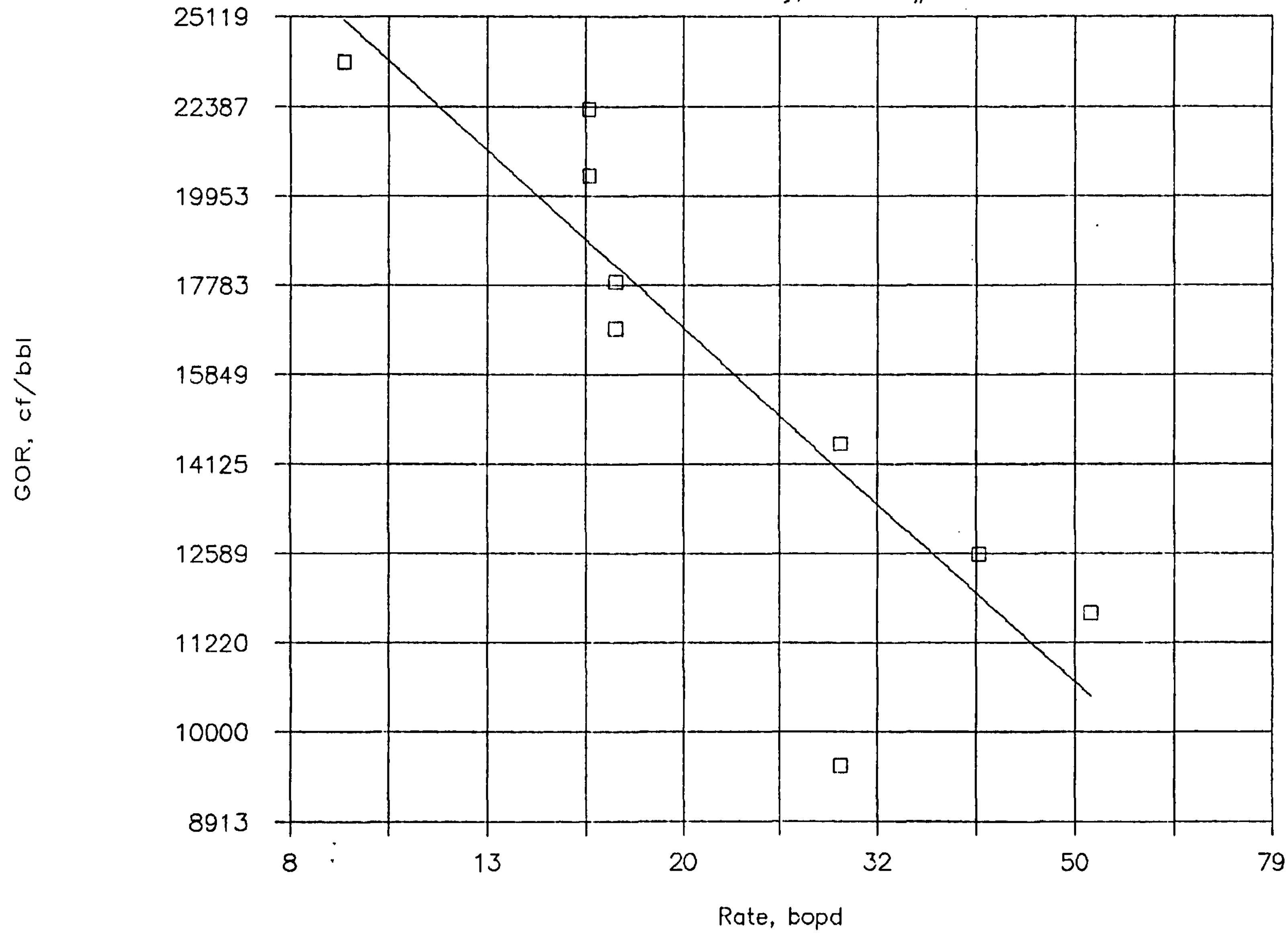

C. C. = 0.86

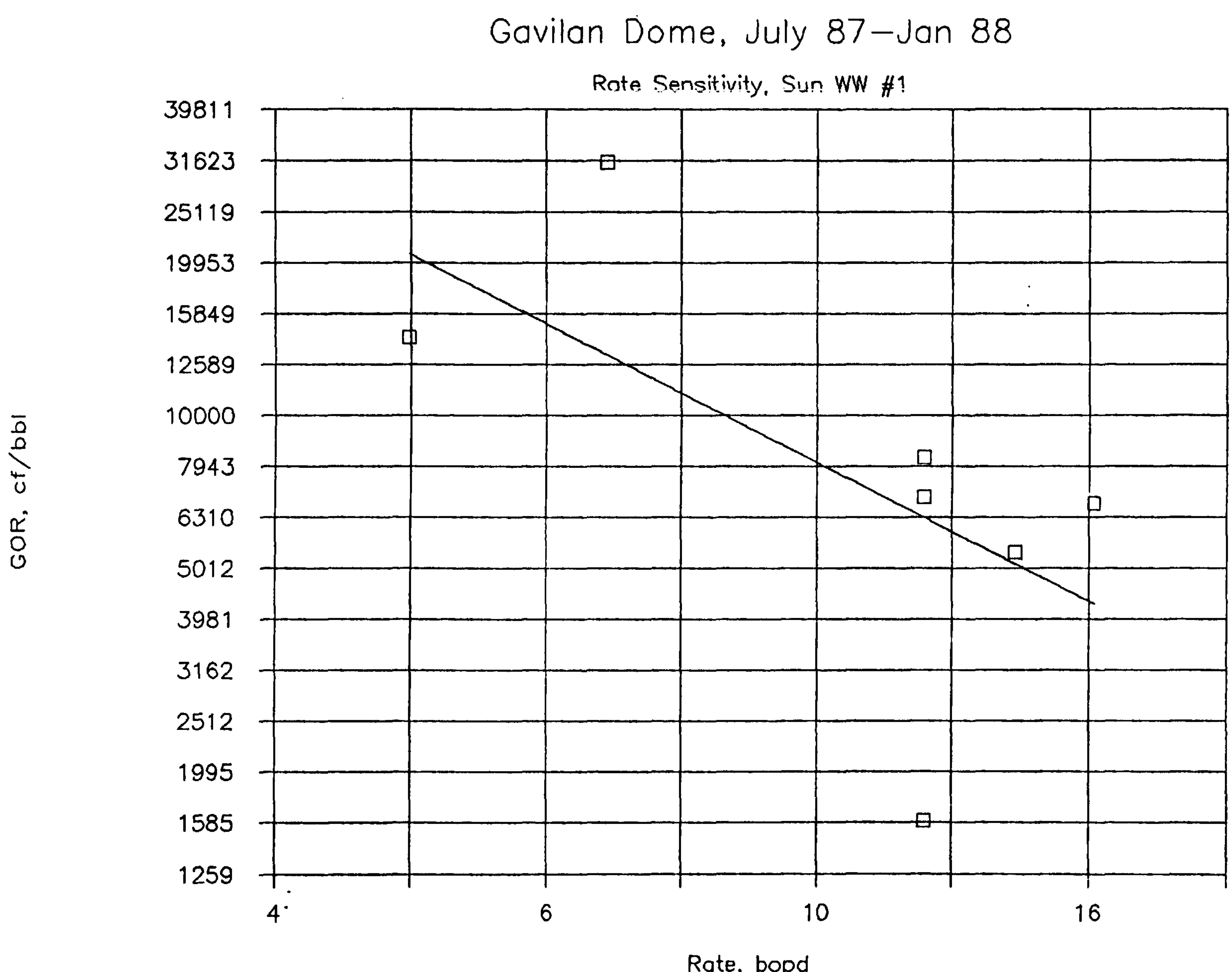
Gavilan Dome, July 87—Jan 88
Rate Sensitivity, Sun WW #1
GOR, cf/bbl
39811
31623
25119
19953
15849
12589
10000
7943
6310
5012
3981
3162
2512
1995
1585
1259
4
6
10
16
Rate, bopd

C.C. = 0.62

GAVILAN DOME DATA BASE
RATE vs. GOR SENSITIVITY

OPERATOR	WELL	DATE	AVERAGE GOR	AVERAGE BOPD	CUM OIL	CUM GAS	AVERAGE MCFPD
AMOCO	BCU#1	1/1-1/31	190	314	8173	1554	60
AMOCO	BCU#1	2/1-2/29	145	292	7297	1058	42
				606			
AMOCO	BCU#2	2/1-2/29	274	228	3421	938	67
AMOCO	HTF#1	2/1-2/29	1687	12	83	140	20
AMOCO	OCFB#1	2/1-2/29	13250	22	44	583	292
AMOCO	SGC#1	1/1-1/31	8971	30	273	2449	245
AMOCO	SGC#1	2/1-2/29	3856	35	810	3123	142
				65			
AMOCO	SCC#1	2/1-2/29	99	201	4432	440	20
BMG	A-16	7/1-7/31	1075	16	214	230	18
BMG	A-16	8/1-8/31	1600	6	25	40	10
BMG	A-16	9/1-9/30	4009	11	212	850	45
				33			
BMG	A-20	7/1-7/31	1176	17	187	220	20
BMG	A-20	8/1-8/31	2843	38	568	1615	107
BMG	A-20	9/1-9/30	5331	46	1103	5880	245
BMG	A-20	11/1-11/14	5812	42	585	3400	243
BMG	A-20	12/1-12/31	5405	51	666	3600	277
BMG	A-20	1/1-1/31	6802	52	1601	10890	351
BMG	A-20	2/1-2/29	9474	44	133	1260	420
				290			
BMG	B-29	7/1-7/31	1219	673	18176	22160	821
BMG	B-29	8/1-8/31	1269	757	21187	26887	960
BMG	B-29	9/1-9/30	1922	1156	32372	62230	2223
BMG	B-29	10/1-10/31	2092	1003	15041	31460	2097
BMG	B-29	11/1-11/16	2262	1046	16738	37860	2366
BMG	B-29	11/30-12/31	2161	977	17578	37990	2111
BMG	B-29	2/1-2/29	1444	1047	8379	12100	1513
				6659			
BMG	B-32	7/1-7/31	1046	519	12984	13575	543
BMG	B-32	8/1-8/31	1261	714	19993	25210	900
BMG	B-32	9/1-9/30	1119	911	27344	30600	1020
BMG	B-32	10/1-10/31	1197	800	11998	14360	957
BMG	B-32	11/1-11/16	1200	719	11509	13810	863
BMG	B-32	11/30-12/31	1185	704	11964	14180	834
BMG	B-32	1/1-1/31	1000	701	13319	1300	700

GAVILAN DOME DATA BASE
RATE vs. GOR SENSITIVITY

OPERATOR	WELL	DATE	AVERAGE GOR	AVERAGE BOPD	CUM OIL	CUM GAS	AVERAGE MCFPD
BMG	B-32	2/1-2/29	1101	704	16894	18605	775
				5772			
BMG	C-34	12/1-12/31	10345	44	348	3600	450
BMG	C-34	1/1-1/31	11990	38	191	2290	458
BMG	C-34	2/1-2/29	17551	62	494	8670	1084
				144			
BMG	D-17	7/1-7/31	1195	9	135	160	1067
BMG	E-6	7/1-7/31	3966	307	7687	30490	1220
BMG	E-6	8/1-8/31	2339	362	11228	26260	847
BMG	E-6	9/1-9/30	2068	426	12765	26404	880
BMG	E-6	10/1-10/31	2757	358	5375	14820	988
BMG	E-6	11/1-11/16	4223	271	4063	17160	1144
BMG	E-6	12/1-12/31	4998	159	2391	11950	797
BMG	E-6	1/1-1/31	4752	169	2033	9660	805
				2052			
BMG	E-10	7/1-7/31	3124	380	11012	34400	1186
BMG	E-10	8/1-8/31	4896	303	9384	45940	1482
BMG	E-10	9/1-9/30	7124	236	6127	43760	1750
BMG	E-10	11/1-11/16	7589	235	3754	28490	1781
BMG	E-10	1/1-1/31	9199	222	1761	16200	1800
BMG	E-10	2/1-2/29	23201	62	556	12900	1433
				1438			
BMG	F-7	12/1-12/31	2689	124	2224	5980	332
BMG	F-7	1/1-1/31	5457	147	3832	20910	804
				271			
BMG	F-18	7/1-7/31	631	224	3362	2120	141
BMG	F-18	8/1-8/31	448	326	10096	4520	146
BMG	F-18	9/1-9/30	538	406	9751	5250	219
BMG	F-18	10/1-10/31	395	390	5846	2310	154
BMG	F-18	11/1-11/16	504	365	5469	2755	184
BMG	F-18	12/1-12/31	522	325	9753	5095	170
BMG	F-18	1/1-1/31	465	311	9643	4480	145
BMG	F-18	2/1-2/29	667	304	6982	4655	202
				2651			
BMG	F-19	7/1-7/31	6754	64	1869	12624	435
BMG	F-19	8/1-8/31	9719	75	2314	22490	725
BMG	F-19	9/1-9/30	13050	60	1436	18740	781
BMG	F-19	11/1-11/14	15035	51	712	10705	765
BMG	F-19	12/1-12/31	16392	43	693	11360	757
BMG	F-19	1/1-1/31	4899	100	398	1950	488
BMG	F-19	2/1-2/29	8417	60	120	1010	505
				453			

GAVILAN DOME DATA BASE
RATE vs. GOR SENSITIVITY

OPERATOR	WELL	DATE	AVERAGE GOR	AVERAGE BOPD	CUM OIL	CUM GAS	AVERAGE MCFPD
BMG	F-30	7/1-7/31	1042	357	10009	10430	373
BMG	F-30	8/1-8/31	989	347	9703	9600	343
BMG	F-30	9/1-9/30	1046	417	12506	13080	436
BMG	F-30	10/1-10/31	1094	355	5331	5830	389
BMG	F-30	11/1-11/16	1123	334	5337	5992	375
BMG	F-30	11/30-12/31	1134	311	9963	11295	353
BMG	F-30	1/1-1/31	1171	293	8491	9940	343
BMG	F-30	2/1-2/29	1104	349	8366	9240	385
				2763			
BMG	G-5	9/1-9/30	774	266	1330	1030	206
BMG	G-5	10/1-10/31	1073	263	3952	4240	283
BMG	G-5	11/1-11/16	1912	183	2924	5590	349
BMG	G-5	11/21-11/30	2093	158	473	990	330
BMG	G-5	12/1-12/31	2688	135	2697	7250	363
BMG	G-5	1/1-1/31	244	157	4860	11880	383
BMG	G-5	2/1-2/29	2374	465	3252	7720	351
				1627			
BMG	G-32	7/1-7/31	1132	13	53	60	15
BMG	G-32	9/1-9/30	870	12	46	40	10
				25			
BMG	J-6	8/1-8/31	3764	79	1905	7170	299
BMG	J-6	9/1-9/30	5556	55	1530	8500	304
BMG	J-6	11/1-11/10	35101	15	149	5230	523
BMG	J-6	12/1-12/31	22735	23	340	7730	515
BMG	J-6	1/1-1/31	29858	18	211	6300	525
				190			
BMG	J-8	9/1-9/30	1852	7	27	50	13
BMG	K-8	7/1-7/31	562	5	146	82	3
BMG	K-8	8/1-8/31	1207	6	29	35	7
BMG	K-8	9/1-9/30	2065	9	46	95	19
BMG	K-8	12/1-12/31	5618	9	89	500	50
BMG	K-8	1/1-1/31	4789	4	95	455	20
BMG	K-8	2/1-2/29	5000	2	41	205	10
				35			
BMG	L-3	9/1-9/30	722	22	486	351	16
BMG	L-3	10/1-10/31	732	14	205	150	10
BMG	L-3	11/1-11/16	758	19	211	160	16
BMG	L-3	12/1-12/31	699	32	256	179	22
BMG	L-3	1/1-1/31	787	16	305	240	13
				103			
BMG	L-11	8/1-8/31	186207	7	116	21600	1137

GAVILAN DOME DATA BASE
RATE vs. GOR SENSITIVITY

OPERATOR	WELL	DATE	AVERAGE GOR	AVERAGE BOPD	CUM OIL	CUM GAS	AVERAGE MCFPD
BMG	L-11	9/1-9/30	240000	5	15	3600	1200
BMG	L-11	2/1-2/29	18206	46	418	7610	761
				58			
BMG	L-27	7/1-7/31	2462	166	3980	9800	408
BMG	L-27	8/1-8/31	2641	157	4863	12845	414
BMG	L-27	9/1-9/30	2386	165	4949	11810	394
BMG	L-27	10/1-10/31	2382	163	2439	5810	387
BMG	L-27	11/1-11/16	2497	155	2479	6190	387
BMG	L-27	11/21-11/30	2491	160	1443	3595	399
BMG	L-27	12/1-12/31	2343	170	3064	7180	399
BMG	L-27	1/1-1/31	2372	152	4697	11140	359
BMG	L-27	2/1-2/29	2501	152	3351	8380	381
				1440			
BMG	N-22	7/1-7/31	791	82	2365	1870	64
BMG	N-22	8/1-8/31	465	86	1634	760	40
BMG	N-22	9/1-9/30	401	77	2317	930	31
BMG	N-22	10/1-10/31	412	73	1093	450	30
BMG	N-22	11/1-11/16	392	76	1213	475	30
BMG	N-22	11/21-11/30	412	95	947	390	39
BMG	N-22	12/1-12/31	422	68	2108	890	33
BMG	N-22	1/1-1/31	440	66	1911	840	29
BMG	N-22	2/1-2/29	399	80	1753	700	32
				703			
BMG	N-31	7/1-7/31	2240	182	5291	11850	409
BMG	N-31	8/1-8/31	1238	203	6303	7800	252
BMG	N-31	9/1-9/30	1025	194	5833	5980	199
BMG	N-31	10/1-10/31	1234	185	2771	3420	228
BMG	N-31	11/1-11/16	3106	127	2035	6320	395
BMG	N-31	12/1-12/31	4393	97	1457	6400	427
				988			
BMG	O-9	7/1-7/31	1082	11	319	345	12
BMG	O-9	8/1-8/31	1316	6	19	25	8
BMG	O-9	9/1-9/30	1044	21	297	310	22
BMG	O-9	11/21-11/30	1095	15	137	150	17
BMG	O-9	12/1-12/31	1118	13	331	370	16
BMG	O-9	1/1-1/31	1037	10	270	280	10
BMG	O-9	2/1-2/29	1036	14	304	315	15
				90			
BMG	O-33	7/1-7/31	3484	21	574	2000	74
BMG	O-33	8/1-8/31	5056	18	89	450	90
BMG	O-33	9/1-9/30	3052	28	729	2225	85
BMG	O-33	10/1-10/31	3003	21	313	940	63
BMG	O-33	11/1-11/14	2115	22	260	550	46
BMG	O-33	12/1-12/31	2853	28	333	950	95
BMG	O-33	1/1-1/31	3051	18	372	1135	54

GAVILAN DOME DATA BASE
RATE vs. GOR SENSITIVITY

OPERATOR	WELL	DATE	AVERAGE GOR	AVERAGE BOPD	CUM OIL	CUM GAS	AVERAGE MCFPD
				156			
DUGAN	LIND #1	7/1-7/31	7766	8	128	994	34
DUGAN	LIND #1	8/1-8/31	7504	5	121	908	36
DUGAN	LIND #1	9/1-9/30	7884	4	95	749	31
DUGAN	LIND #1	10/1-10/31	8733	4	116	1013	33
DUGAN	LIND #1	11/1-11/16	10465	4	22	225	28
DUGAN	LIND #1	11/21-11/30	9935	4	15	152	30
DUGAN	LIND #1	12/1-12/31	13367	5	60	802	29
DUGAN	LIND #1	1/1-1/31	4227	6	22	93	23
				40			
HIXON	DIV #3	7/1-7/31	794	103	2480	1969	82
HIXON	DIV #3	8/1-8/31	795	105	3147	2501	83
HIXON	DIV #3	10/1-10/31	795	110	1759	1399	87
HIXON	DIV #3	11/1-11/15	796	108	1619	1289	86
HIXON	DIV #3	12/1-12/31	795	103	3083	2452	82
HIXON	DIV #3	1/1-1/31	796	97	3019	2404	78
HIXON	DIV #3	2/2-2/29	797	93	2322	1851	74
				719			
HIXON	TAP #2	7/1-7/31	6239	12	355	2215	73
HIXON	TAP #2	8/1-8/31	6209	10	325	2018	65
HIXON	TAP #2	10/1-10/31	6202	6	99	614	38
HIXON	TAP #2	11/1-11/15	6208	7	77	478	43
HIXON	TAP #2	12/1-12/31	6220	5	127	790	32
HIXON	TAP #2	1/1-1/31	6196	5	56	347	32
HIXON	TAP #2	2/1-2/29	6220	6	41	255	36
				51			
HIXON	TAP #4	7/1-7/31	918	143	4133	3795	131
HIXON	TAP #4	8/1-8/31	918	146	4235	3889	134
HIXON	TAP #4	10/1-10/31	917	135	2154	1976	124
HIXON	TAP #4	11/1-11/15	917	131	1970	1807	120
HIXON	TAP #4	12/1-12/31	918	123	3824	3510	113
HIXON	TAP #4	1/1-1/31	917	97	2140	1962	89
HIXON	TAP #4	2/1-2/29	918	78	1944	1784	71
				853			
MALLON	DF 3#15	12/1-12/31	62591	4	44	2754	230
MALLON	DF 3#15	1/1-1/31	9908	13	141	1397	64
MALLON	DF 3#15	2/1-2/29	13295	6	95	1263	66
				23			
MALLON	FF 2#1	7/1-7/31	1326	316	9789	12979	419
MALLON	FF 2#1	8/1-8/31	1407	265	8211	11556	373
MALLON	FF 2#1	9/1-9/30	1306	285	6844	8936	372
MALLON	FF 2#1	10/1-10/31	1321	272	8426	11134	359
MALLON	FF 2#1	11/1-11/15	8730	40	597	5212	347
MALLON	FF 2#1	11/20-11/30	3636	165	1814	6596	600

GAVILAN DOME DATA BASE
RATE vs. GOR SENSITIVITY

OPERATOR	WELL	DATE	AVERAGE GOR	AVERAGE BOPD	CUM OIL	CUM GAS	AVERAGE MCFPD
MALLON	FF 2#1	12/1-12/31	9591	90	1077	10329	861
MALLON	FF 2#1	1/1-1/31	11649	96	479	5580	1116
MALLON	FF 2#1	2/1-2/29	11232	95	1048	11771	1070
				1624			
MALLON	HF 1#8	7/1-7/31	3212	278	8609	27649	892
MALLON	HF 1#8	8/1-8/31	3691	288	8919	32922	1062
MALLON	HF 1#8	9/1-9/30	3472	316	9471	32886	1096
MALLON	HF 1#8	10/1-10/31	3771	264	8186	30871	996
MALLON	HF 1#8	11/1-11/15	3736	244	3657	13664	911
MALLON	HF 1#8	11/21-11/30	8022	122	856	6867	981
MALLON	HF 1#8	12/1-12/31	1255	115	805	1010	144
MALLON	HF 1#8	1/1-1/31	9388	120	720	6759	1127
MALLON	HF 1#8	2/1-2/29	8498	120	841	7147	1021
				1867			
MALLON	HF 1#11	7/1-7/31	6328	186	5578	35298	1217
MALLON	HF 1#11	8/1-8/31	5147	256	5368	27628	1316
MALLON	HF 1#11	9/1-9/30	4770	284	6241	29769	1294
MALLON	HF 1#11	10/1-10/31	5503	241	7472	41119	1326
MALLON	HF 1#11	11/1-11/30	5545	254	3803	21087	1406
MALLON	HF 1#11	12/1-12/31	8339	177	1415	11800	1311
MALLON	HF 1#11	2/1-2/29	11085	137	684	7582	1516
				1535			
MALLON	JF 12#5	7/1-7/31	23870	17	322	7686	452
MALLON	JF 12#5	8/1-8/31	5281	70	1260	6654	370
MALLON	JF 12#5	9/1-9/30	5689	58	1725	9813	327
MALLON	JF 12#5	10/1-10/31	5682	53	1644	9341	301
MALLON	JF 12#5	11/1-11/15	8730	40	597	5212	347
MALLON	JF 12#5	11/20-11/30	21547	20	223	4805	437
MALLON	JF 12#5	12/1-12/31	40893	10	270	11041	425
MALLON	JF 12#5	1/1-1/31	44067	11	75	3305	472
MALLON	JF 12#5	2/1-2/29	53509	8	114	6100	407
				287			
MALLON	PF 13#6	7/1-7/31	5311	72	2235	11869	383
MALLON	PF 13#6	8/1-8/31	4897	83	2558	12526	404
MALLON	PF 13#6	9/1-9/30	2071	111	3331	6899	230
MALLON	PF 13#6	10/1-10/31	15351	88	2725	41831	1349
MALLON	PF 13#6	11/1-11/15	6241	58	872	5442	363
MALLON	PF 13#6	11/20-11/30	6573	70	769	5055	460
MALLON	PF 13#6	12/1-12/31	14096	45	178	2509	627
MALLON	PF 13#6	1/1-1/31	34024	16	252	8574	536
MALLON	PF 13#6	2/1-2/29	67677	7	96	6497	406
				550			
MALLON	RF 2#16	7/1-7/31	2849	76	2366	6741	217
MALLON	RF 2#16	8/1-8/31	2468	87	2708	6683	216
MALLON	RF 2#16	9/1-9/30	2541	87	2604	6617	221

GAVILAN DOME DATA BASE
RATE vs. GOR SENSITIVITY

OPERATOR	WELL	DATE	AVERAGE GOR	AVERAGE BOPD	CUM OIL	CUM GAS	AVERAGE MCFPD
MALLON	RF 2#16	10/1-10/31	2718	85	2550	6931	224
MALLON	RF 2#16	11/1-11/15	3686	37	370	1364	136
MALLON	RF 2#16	11/20-11/30	3227	40	441	1423	129
MALLON	RF 2#16	12/1-12/31	9538	30	751	7163	276
MALLON	RF 2#16	1/1-1/31	35631	13	295	10511	350
MALLON	RF 2#16	2/1-2/29	141905	3	21	2980	373
				458			
MERIDIAN	HAF #2	7/1-7/31	20207	24	386	7800	488
MERIDIAN	HAF #2	8/1-8/31	14827	31	689	10216	464
MERIDIAN	HAF #2	9/1-9/30	4296	70	1049	4506	300
MERIDIAN	HAF #2	11/1-11/16	12074	27	27	326	326
MERIDIAN	HAF #2	11/21-11/30	12384	27	190	2353	336
MERIDIAN	HAF #2	12/1-12/31	20154	19	325	6550	364
MERIDIAN	HAF #2	1/1-1/31	24918	18	306	7625	477
				216			
MERIDIAN	HAF #3	7/1-7/31	10685	44	696	7437	465
MERIDIAN	HAF #3	8/1-8/31	7537	54	1089	8208	410
MERIDIAN	HAF #3	9/1-9/30	5551	60	907	5035	336
MERIDIAN	HAF #3	11/1-11/16	10520	25	25	263	263
MERIDIAN	HAF #3	11/21-11/30	10401	24	167	1737	248
MERIDIAN	HAF #3	12/1-12/31	19618	12	280	5493	211
MERIDIAN	HAF #3	1/1-1/31	16465	20	159	2618	154
				239			
MERIDIAN	HF #1	7/1-7/31	15915	65	1037	16504	1032
MERIDIAN	HF #1	8/1-8/31	38913	26	515	20040	1002
MERIDIAN	HF #1	9/1-9/30	43723	21	314	13729	915
MERIDIAN	HF #1	11/1-11/16	102500	8	8	820	820
MERIDIAN	HF #1	11/21-11/30	31623	28	167	5281	880
MERIDIAN	HF #1	12/1-12/31	43236	19	191	8258	751
MERIDIAN	HF #1	1/1-1/31	81011	12	95	7696	962
				179			
MERIDIAN	HF #2Y	6/1-6/30	2997	87	1819	5452	260
MERIDIAN	HF #2Y	8/1-8/31	3978	62	934	3715	219
MERIDIAN	HF #2Y	9/1-9/30	4626	52	773	3576	238
MERIDIAN	HF #2Y	11/1-11/16	21143	7	7	148	148
MERIDIAN	HF #2Y	11/21-11/30	8100	40	140	1296	216
MERIDIAN	HF #2Y	12/1-12/31	5733	41	857	4913	234
MERIDIAN	HF #2Y	1/1-1/31	5554	36	1082	6009	207
				325			
MERIDIAN	HF #3	7/1-7/31	2342	69	1105	2588	162
MERIDIAN	HF #3	8/1-8/31	2101	72	1516	3185	152
MERIDIAN	HF #3	11/1-11/16	6679	28	28	187	187
MERIDIAN	HF #3	11/21-11/30	7027	31	183	1286	214
MERIDIAN	HF #3	12/1-12/31	8861	25	624	5529	213
MERIDIAN	HF #3	1/1-1/31	18724	12	199	3726	143

GAVILAN DOME DATA BASE
RATE vs. GOR SENSITIVITY

OPERATOR	WELL	DATE	AVERAGE GOR	AVERAGE BOPD	CUM OIL	CUM GAS	AVERAGE MCFPD
				237			
MERRION	KRY #1	1/1-1/31	19631	13	65	1276	51
MERRION	OCG #1	7/1-7/31	1691	8	55	93	13

GAVILAN DOME DATA BASE
RATE vs. GOR SENSITIVITY

OPERATOR	WELL	DATE	AVERAGE GOR	AVERAGE BOPD	CUM OIL	CUM GAS	AVERAGE MCFPD
MESA GR.	BC #1	6/1-6/30	6010	47	895	5379	269
MESA GR.	BC #1	7/1-7/31	4681	64	966	4522	301
MESA GR.	BC #1	8/1-8/31	4323	59	1543	6670	267
MESA GR.	BC #1	10/1-10/31	16050	20	20	321	321
MESA GR.	BC #1	11/1-11/17	9263	24	400	3705	218
MESA GR.	BC #1	11/21-11/30	18094	11	85	1538	192
MESA GR.	BC #1	12/1-12/31	17406	10	251	4369	182
MESA GR.	BC #1	1/1-1/31	45768	5	99	4531	206
MESA GR.	BC #1	2/1-2/29	44417	6	96	4264	213
MESA GR.	BRO #1	7/1-7/31	9027	76	1135	10246	683
MESA GR.	BRO #1	8/1-8/31	9027	103	2783	25123	930
MESA GR.	BRO #1	10/1-10/31	7627	130	3912	29837	962
MESA GR.	BRO #1	11/1-11/16	7848	108	1725	13538	846
MESA GR.	BRO #1	11/21-11/30	7990	100	800	6392	799
MESA GR.	BRO #1	12/1-12/31	7631	112	2234	17047	852
MESA GR.	BRO #1	1/1-1/31	6194	111	1886	11681	687
MESA GR.	BRO #1	2/1-2/29	7907	92	1661	13133	773
MESA GR.	GAV #1	7/1-7/31	21926	10	149	3267	218
MESA GR.	GAV #1	8/1-8/31	22408	9	238	5333	190
MESA GR.	GAV #1	10/1-10/31	32875	3	104	3419	110
MESA GR.	GAV #1	11/1-11/17	14220	3	41	583	34
MESA GR.	GAV #1	11/21-11/30	42027	5	37	1555	194
MESA GR.	GAV #1	12/1-12/31	1889	3	36	68	6
MESA GR.	GAV #1	1/1-1/31	33977	10	130	4417	316
MESA GR.	GAV #1	2/1-2/29	67716	4	81	5485	219
MESA GR.	GAV #3	7/1-7/31	28595	9	79	2259	151
MESA GR.	GAV #3	8/1-8/31	10247	12	299	3064	113
MESA GR.	GAV #3	10/1-10/31	33843	6	178	6024	194
MESA GR.	GAV #3	12/1-12/31	23618	9	55	1299	130
MESA GR.	GAV #3	1/1-1/31	51710	3	31	1603	100
MESA GR.	GAV #3	2/1-2/29	46578	4	45	2096	140
MESA GR.	GH #1	7/1-7/31	16749	16	239	4003	267
MESA GR.	GH #1	8/1-8/31	24102	16	372	8966	345
MESA GR.	GH #1	10/1-10/31	47667	12	12	572	572
MESA GR.	GH #1	11/1-11/17	64780	6	109	7061	392
MESA GR.	GH #1	11/21-11/30	58909	6	44	2592	324
MESA GR.	GH #1	12/1-12/31	63796	7	152	9697	359
MESA GR.	GH #1	1/1-1/31	83186	5	118	9816	393
MESA GR.	HC #1	8/1-8/31	8604	13	371	3192	110
MESA GR.	HC #1	10/1-10/31	5200	25	25	130	130

GAVILAN DOME DATA BASE
RATE vs. GOR SENSITIVITY

OPERATOR	WELL	DATE	AVERAGE GOR	AVERAGE BOPD	CUM OIL	CUM GAS	AVERAGE MCFPD
MESA GR.	HC #1	11/1-11/16	10727	10	161	1727	108
MESA GR.	HC #1	11/22-11/30	63267	3	15	949	136
MESA GR.	HC #1	12/1-12/31	18663	11	89	1661	151
MESA GR.	HC #1	1/1-1/31	20767	8	129	2679	128
MESA GR.	HC #1	2/1-2/29	30725	6	109	3349	146
MESA GR.	INV #1	2/1-2/29	4259	14	228	971	54
MESA GR.	MAR #1	7/1-7/31	2709	94	1416	3836	256
MESA GR.	MAR #1	8/1-8/31	3376	68	1489	5027	229
MESA GR.	MAR #1	10/1-10/31	5237	48	1394	7301	243
MESA GR.	MAR #1	11/1-11/17	6948	39	620	4308	253
MESA GR.	MAR #1	11/21-11/30	8774	30	212	1860	233
MESA GR.	MAR #1	12/1-12/31	13194	11	263	3470	129
MESA GR.	MAR #1	1/1-1/31	3494	50	451	1576	197
MESA GR.	MAR #1	2/1-2/29	9449	33	750	7087	308
MESA GR.	PRO #1	2/1-2/29	4594	21	512	2352	98
MESA GR.	RL #2	7/1-7/31	4771	57	855	4079	272
MESA GR.	RL #2	8/1-8/31	5389	47	1260	6790	251
MESA GR.	RL #2	10/1-10/31	3967	47	1456	5776	186
MESA GR.	RL #2	11/1-11/17	4336	39	664	2879	169
MESA GR.	RL #2	11/21-11/31	5500	17	120	660	83
MESA GR.	RL #2	12/1-12/31	4629	47	1088	5036	187
MESA GR.	RL #2	1/1-1/31	7791	34	506	3942	141
MESA GR.	RL #2	2/1-2/29	17015	15	336	5717	249
MESA GR.	RL #3	7/1-7/31	2156	37	556	1199	80
MESA GR.	RL #3	8/1-8/31	1860	48	1250	2325	83
MESA GR.	RL #3	10/1-10/31	1875	32	933	1749	56
MESA GR.	RL #3	11/1-11/17	9625	16	32	308	62
MESA GR.	RL #3	12/1-12/31	10554	12	177	1868	75
MESA GR.	RL #3	1/1-1/31	16365	9	192	3142	101
MESA GR.	RL #3	2/1-2/29	18720	8	175	3276	131
MOBIL	LIN B#34	7/1-7/31	3501	72	2229	7804	252
MOBIL	LIN B#34	8/1-8/31	3365	56	1733	5832	216
MOBIL	LIN B#34	9/1-9/30	3697	47	1396	5161	172
MOBIL	LIN B#34	10/1-10/31	4817	37	955	4600	170
MOBIL	LIN B#34	11/1-11/16	4246	33	532	2259	141
MOBIL	LIN B#34	11/20-11/30	4083	43	384	1568	174
MOBIL	LIN B#34	12/1-12/31	5126	35	987	5059	181
MOBIL	LIN B#34	1/1-1/31	7368	25	560	4126	179
MOBIL	LIN B#34	2/1-2/29	7766	28	691	5366	215

GAVILAN DOME DATA BASE
RATE vs. GOR SENSITIVITY

OPERATOR	WELL	DATE	AVERAGE GOR	AVERAGE BOPD	CUM OIL	CUM GAS	AVERAGE MCFPD
MOBIL	LIN B#37	7/1-7/31	7750	54	1683	13044	435
MOBIL	LIN B#37	8/1-8/31	3733	218	6772	25283	936
MOBIL	LIN B#37	9/1-9/30	3192	244	7314	23349	778
MOBIL	LIN B#37	10/1-10/31	3953	225	6975	27573	889
MOBIL	LIN B#37	11/1-11/17	3907	214	3641	14225	889
MOBIL	LIN B#37	11/20-11/30	3682	195	1947	7168	796
MOBIL	LIN B#37	12/1-12/31	3757	213	3837	14417	801
MOBIL	LIN B#37	1/1-1/31	4063	192	3657	14858	782
MOBIL	LIN B#37	2/1-2/29	4112	188	3570	14679	816
MOBIL	LIN B#38	7/1-7/31	19598	13	415	8133	262
MOBIL	LIN B#38	8/1-8/31	21127	10	300	6338	235
MOBIL	LIN B#38	9/1-9/30	29320	8	219	6421	199
MOBIL	LIN B#38	10/1-10/31	24403	8	238	5808	187
MOBIL	LIN B#38	11/1-11/16	27625	6	96	2652	166
MOBIL	LIN B#72	7/1-7/31	20565	4	108	2221	74
MOBIL	LIN B#72	8/1-8/31	21349	4	86	1836	68
MOBIL	LIN B#72	9/1-9/30	25473	3	74	1885	63
MOBIL	LIN B#72	11/20-11/30	38523	6	44	1695	188
MOBIL	LIN B#72	12/1-12/31	66383	12	81	5377	199
MOBIL	LIN B#72	1/1-1/31	71987	3	79	5676	183
MOBIL	LIN B#72	2/1-2/29	19500	3	58	1131	45
MOBIL	LIN B#73	7/1-7/31	19977	7	173	3456	115
MOBIL	LIN B#73	8/1-8/31	17279	6	165	2851	106
MOBIL	LIN B#73	9/1-9/30	16449	7	187	3076	103
MOBIL	LIN B#73	10/1-10/31	17724	7	192	3403	110
MOBIL	LIN B#73	11/1-11/16	26657	5	67	1786	112
MOBIL	LIN B#73	11/20-11/30	19154	7	52	996	111
MOBIL	LIN B#73	12/1-12/31	8970	16	302	2709	113
MOBIL	LIN B#73	1/1-1/31	14429	10	219	3160	117
MOBIL	LIN B#73	2/1-2/29	27143	5	98	2660	111
MOBIL	LIN B#74	7/1-7/31	53190	8	210	11170	30
MOBIL	LIN B#74	8/1-8/31	15613	32	727	11351	437
MOBIL	LIN B#74	9/1-9/30	12994	36	980	12734	424
MOBIL	LIN B#74	10/1-10/31	9931	35	1008	10010	323
MOBIL	LIN B#74	11/1-11/16	10793	32	482	5202	325
MOBIL	LIN B#74	11/20-11/30	37495	14	109	4087	454
MOBIL	LIN B#74	12/1-12/31	50631	11	141	7139	376
MOBIL	LIN B#74	1/1-1/31	74360	6	100	7436	372
MOBIL	LIN B#74	2/1-2/29	42538	7	119	5062	281

GAVILAN DOME DATA BASE
RATE vs. GOR SENSITIVITY

OPERATOR	WELL	DATE	AVERAGE GOR	AVERAGE BOPD	CUM OIL	CUM GAS	AVERAGE MCFPD
R&B	HF 43-15	6/1-6/30	55728	4	103	5740	239
R&B	HF 43-15	7/1-7/31	29693	15	378	11224	416
R&B	HF 43-15	8/1-8/31	39632	11	353	13990	466
R&B	HF 43-15	9/1-9/30	46545	9	44	2048	410
R&B	HF 43-15	10/1-10/31	34337	20	98	3365	673
R&B	HF 43-15	11/1-11/16	69293	9	147	10186	637
R&B	HF 43-15	11/21-11/30	79180	6	61	4830	483
R&B	HF 43-15	12/1-12/31	53333	5	117	6240	240
R&B	IN 34-16	9/1-9/30	39613	8	31	1228	205
R&B	IN 34-16	10/1-10/31	12698	46	1160	14730	526
R&B	IN 34-16	11/1-11/16	12312	54	858	10564	660
R&B	IN 34-16	11/20-11/30	11991	60	663	7950	723
R&B	IN 34-16	12/1-12/31	9708	72	1231	11950	703
SUN	BB#1	7/1-7/31	2701	133	3585	9684	372
SUN	BB#1	8/1-8/31	2995	123	3309	9909	367
SUN	BB#1	9/1-9/30	3322	102	1635	5431	362
SUN	BB#1	10/1-10/31	3944	108	2054	8100	426
SUN	BB#1	11/1-11/16	4282	96	1533	6564	410
SUN	BB#1	11/22-11/30	2973	64	451	1341	192
SUN	BB#1	12/1-12/31	3563	78	2026	7219	267
SUN	BB#1	1/1-1/31	4030	64	1538	6198	258
SUN	B&L#1	7/1-7/31	10250	2	48	492	21
SUN	B&L#1	8/1-8/31	6020	2	50	301	10
SUN	B&L#1	9/1-9/30	14909	2	11	164	15
SUN	B&L#2	7/1-7/31	13971	4	34	475	53
SUN	DRDO#1	7/1-7/31	4010	70	2106	8445	282
SUN	DRDO#1	8/1-8/31	6664	42	1038	6917	266
SUN	DRDO#1	9/1-9/30	9324	32	550	5128	302
SUN	DRDO#1	10/1-10/31	14614	20	383	5597	295
SUN	DRDO#1	11/1-11/16	16424	17	264	4336	271
SUN	DRDO#1	11/21-11/30	26475	13	101	2674	334
SUN	DRDO#1	12/1-12/31	10084	26	713	7190	257
SUN	DRDO#1	1/1-1/31	5901	37	1135	6698	216
SUN	E.T.	7/1-7/31	28740	13	404	11611	387
SUN	E.T.	8/1-8/31	50890	7	172	8753	324
SUN	E.T.	9/1-9/30	56356	5	87	4903	288
SUN	E.T.	10/1-10/31	91667	3	48	440	232
SUN	E.T.	11/1-11/16	99280	2	25	2482	155

GAVILAN DOME DATA BASE
RATE vs. GOR SENSITIVITY

OPERATOR	WELL	DATE	AVERAGE GOR	AVERAGE BOPD	CUM OIL	CUM GAS	AVERAGE MCFPD
SUN	E.T.	11/21-11/30	40089	6	45	1804	226
SUN	E.T.	12/1-12/31	23621	8	214	5055	181
SUN	E.T.	1/1-1/31	139615	2	13	1815	113
SUN	FS#1	7/1-7/31	2533	54	1404	3556	142
SUN	FS#1	8/1-8/31	2060	71	1918	3952	146
SUN	FS#1	9/1-9/30	2128	66	1120	2383	140
SUN	FS#1	10/1-10/31	2525	54	1027	2593	136
SUN	FS#1	11/1-11/16	2667	49	787	2099	131
SUN	FS#1	11/21-11/30	2378	109	368	875	109
SUN	FS#1	12/1-12/31	2105	52	1405	2957	106
SUN	FS#1	1/1-1/31	2976	48	1446	4303	143
SUN	FSA#2	7/1-7/31	22195	33	990	21973	732
SUN	FSA#2	8/1-8/31	25292	26	678	17148	660
SUN	FSA#2	9/1-9/30	30122	20	345	10392	611
SUN	FSA#2	10/1-10/31	32395	15	294	9524	501
SUN	FSA#2	11/1-11/16	35884	11	138	4952	354
SUN	FSA#2	11/21-11/30	37120	8	50	1856	309
SUN	FSA#2	12/1-12/31	35008	12	244	8542	427
SUN	FSA#2	1/1-1/31	37137	9	95	3528	358
SUN	FSB#3	7/1-7/31	6550	15	447	2928	98
SUN	FSB#3	8/1-8/31	2800	14	370	1036	38
SUN	FSB#3	9/1-9/30	2197	16	254	558	35
SUN	FSB#3	10/1-10/31	2851	13	255	727	38
SUN	FSB#3	11/1-11/16	3548	11	177	628	39
SUN	FSB#3	11/21-11/30	6663	12	83	553	69
SUN	FSB#3	12/1-12/31	4919	8	222	1092	39
SUN	FSB#3	1/1-1/31	7263	6	137	995	38
SUN	FTS#1	7/1-7/31	156636	3	22	3446	431
SUN	FTS#1	8/1-8/31	177222	2	45	7975	332
SUN	FTS#1-E	7/1-7/31	96712	3	73	7060	243
SUN	FTS#1-E	8/1-8/31	147825	1	40	5913	211
SUN	GG#1	7/1-7/31	3224	28	254	819	91
SUN	HA#1	7/1-7/31	2688	225	6290	16905	604
SUN	HA#1	8/1-8/31	2924	226	6098	17831	660
SUN	HA#1	9/1-9/30	3042	203	3451	10499	618
SUN	HA#1	10/1-10/31	3160	238	4522	14288	752

GAVILAN DOME DATA BASE
RATE vs. GOR SENSITIVITY

OPERATOR	WELL	DATE	AVERAGE GOR	AVERAGE BOPD	CUM OIL	CUM GAS	AVERAGE MCFPD
SUN	HA#1	11/1-11/16	3029	228	3641	11029	689
SUN	HA#1	11/21-11/30	2446	259	1812	4433	633
SUN	HA#1	12/1-12/31	2725	201	3422	9324	548
SUN	HA#1	1/1-1/31	2049	230	3450	7068	471
SUN	HA#2	7/1-7/31	6435	49	1455	9363	312
SUN	HA#2	8/1-8/31	9774	31	810	7917	293
SUN	HA#2	9/1-9/30	10726	29	485	5202	306
SUN	HA#2	10/1-10/31	8211	56	1057	8679	457
SUN	HA#2	11/1-11/16	8733	49	776	6777	424
SUN	HA#2	11/21-11/30	9566	41	327	3128	391
SUN	HA#2	12/1-12/31	9398	50	906	8515	473
SUN	HA#2	1/1-1/31	11391	35	741	8441	384
SUN	HR#1	7/1-7/31	2837	241	7231	20516	684
SUN	HR#1	8/1-8/31	3130	235	6347	19865	736
SUN	HR#1	9/1-9/30	10617	128	1914	20321	1195
SUN	HR#1	10/1-10/31	7768	134	2538	19714	1038
SUN	HR#1	11/1-11/16	4455	167	2671	11899	744
SUN	HR#1	11/21-11/30	12157	87	611	7428	929
SUN	HR#1	12/1-12/31	29058	35	242	7032	1005
SUN	HR#1	1/1-1/31	23162	23	68	1575	525
SUN	JA#1	7/1-7/31	26019	14	420	10928	364
SUN	JA#1	8/1-8/31	28062	11	305	8559	317
SUN	JA#1	9/1-9/30	27180	11	178	4838	285
SUN	JA#1	10/1-10/31	16785	15	293	4918	259
SUN	JA#1	11/1-11/16	67333	13	39	2626	219
SUN	JA#1	11/21-11/30	23240	24	96	2231	279
SUN	JA#1	12/1-12/31	32738	15	160	5238	249
SUN	JA#1	1/1-1/31	31906	8	212	6764	251
SUN	JAA#2	7/1-7/31	10379	38	1125	11676	389
SUN	JAA#2	8/1-8/31	12279	24	655	8043	298
SUN	JAA#2	9/1-9/30	28395	13	215	6105	359
SUN	JAA#2	10/1-10/31	34693	11	212	7355	409
SUN	JAA#2	11/1-11/16	66521	5	73	4856	208
SUN	JAA#2	11/1-11/21	21660	17	103	2231	279
SUN	JAA#2	12/1-12/31	88865	4	74	6576	329
SUN	JAA#2	1/1-1/31	107549	3	51	5485	274
SUN	JAB#3	7/1-7/31	1224	43	1283	1570	52
SUN	JAB#3	8/1-8/31	1688	36	961	1622	60
SUN	JAB#3	9/1-9/30	1344	27	453	609	36
SUN	JAB#3	10/1-10/31	2560	19	368	942	50

GAVILAN DOME DATA BASE
RATE vs. GOR SENSITIVITY

OPERATOR	WELL	DATE	AVERAGE GOR	AVERAGE BOPD	CUM OIL	CUM GAS	AVERAGE MCFPD
SUN	JAB#3	11/1-11/16	2795	17	268	749	47
SUN	JAB#3	11/21-11/30	3075	15	120	369	46
SUN	JAB#3	12/1-12/31	2801	60	423	1185	44
SUN	JAB#3	1/1-1/31	4416	11	334	1475	49
SUN	LL#1	7/1-7/31	1973	67	1939	3826	125
SUN	LL#1	8/1-8/31	2615	51	1374	3593	133
SUN	LL#1	9/1-9/30	2397	50	844	2023	119
SUN	LL#1	10/1-10/31	2787	42	752	2096	116
SUN	LL#1	11/1-11/16	2986	36	574	1714	107
SUN	LL#1	11/21-11/30	2922	37	294	859	107
SUN	LL#1	12/1-12/31	2653	35	992	2632	94
SUN	LL#1	1/1-1/31	2422	36	1071	2594	84
SUN	LOD #1	7/1-7/31	7072	61	1898	13422	433
SUN	LOD #1	8/1-8/31	6212	66	1776	11033	409
SUN	LOD #1	9/1-9/30	5255	75	1276	6705	394
SUN	LOD #1	10/1-10/31	4538	75	1420	6444	339
SUN	LOD #1	11/1-11/16	5837	58	926	5405	338
SUN	LOD #1	11/21-11/30	8548	50	398	3402	425
SUN	LOD #1	12/1-12/31	8206	46	1051	8625	375
SUN	LOD #1	1/1-1/31	9252	43	1043	9650	402
SUN	ML#1	7/1-7/31	11402	24	711	8107	270
SUN	ML#1	8/1-8/31	6861	29	793	5441	202
SUN	ML#1	9/1-9/30	6460	16	63	407	136
SUN	ML#1	10/1-10/31	7402	47	894	6617	389
SUN	ML#1	11/1-11/16	7984	47	745	5948	372
SUN	ML#1	11/21-11/30	8942	47	378	3380	423
SUN	ML#1	12/1-12/31	12175	35	629	7658	450
SUN	ML#1	1/1-1/31	14617	28	847	12381	442
SUN	MLA#2	7/1-7/31	9571	63	1877	17965	599
SUN	MLA#2	8/1-8/31	2756	93	2512	6924	256
SUN	MLA#2	9/1-9/30	4973	57	910	4525	266
SUN	MLA#2	10/1-10/31	6030	52	989	5964	314
SUN	MLA#2	11/1-11/16	4815	77	1239	5966	373
SUN	MLA#2	11/21-11/30	5869	76	611	3586	448
SUN	MLA#2	12/1-12/31	10493	46	836	8772	487
SUN	MLA#2	1/1-1/31	14692	28	770	11313	435
SUN	NS#1	7/1-7/31	4105	73	2181	8952	309
SUN	NS#1	8/1-8/31	2679	105	2831	7584	281
SUN	NS#1	9/1-9/30	1395	105	210	293	147
SUN	NS#1	10/1-10/31	2556	130	518	1324	331

GAVILAN DOME DATA BASE
RATE vs. GOR SENSITIVITY

OPERATOR	WELL	DATE	AVERAGE GOR	AVERAGE BOPD	CUM OIL	CUM GAS	AVERAGE MCFPD
SUN	NS#1	11/1-11/16	3932	54	862	3389	242
SUN	NS#1	11/21-11/30	5661	63	502	2842	355
SUN	NS#1	12/1-12/31	10044	33	749	7523	289
SUN	NS#1	1/1-1/31	11837	25	711	8416	301
SUN	NSA#2	7/1-7/31	4229	222	6646	28108	937
SUN	NSA#2	8/1-8/31	3739	238	6421	24005	889
SUN	NSA#2	9/1-9/30	4125	239	4066	16774	988
SUN	NSA#2	10/1-10/31	4526	217	4127	18678	983
SUN	NSA#2	11/1-11/16	4414	195	3113	13742	859
SUN	NSA#2	11/21-11/30	6669	129	900	6002	857
SUN	NSA#2	12/1-12/31	8984	107	859	7717	965
SUN	NSA#2	1/1-1/31	12412	85	677	8403	1050
SUN	NSB#3	7/1-7/31	11665	52	1360	15865	610
SUN	NSB#3	8/1-8/31	12580	40	1087	13675	506
SUN	NSB#3	9/1-9/30	14502	29	458	6642	391
SUN	NSB#3	10/1-10/31	9581	29	520	4982	293
SUN	NSB#3	11/1-11/16	17857	17	237	4232	282
SUN	NSB#3	11/21-11/30	20477	16	109	2232	319
SUN	NSB#3	12/1-12/31	22308	16	276	6157	342
SUN	NSB#3	1/1-1/31	23718	9	163	3866	276
SUN	NH#1	7/1-7/31	5802	4	121	702	24
SUN	NH#1	8/1-8/31	1989	6	176	350	11
SUN	NH#1	9/1-9/30	5484	6	95	521	31
SUN	NH#1	10/1-10/31	8600	4	85	731	38
SUN	NH#1	11/1-11/16	12059	3	51	615	38
SUN	NH#1	11/21-11/30	9750	5	32	312	39
SUN	NH#1	12/1-12/31	7653	6	121	926	39
SUN	NH#1	1/1-1/31	7371	6	159	1172	39
SUN	WW#1	7/1-7/31	6731	16	468	3150	105
SUN	WW#1	8/1-8/31	6923	12	311	2153	80
SUN	WW#1	9/1-9/30	5406	14	219	1184	70
SUN	WW#1	10/1-10/31	8290	12	207	1716	90
SUN	WW#1	11/1-11/16	1599	12	187	299	37
SUN	WW#1	11/21-11/30	14256	5	39	556	70
SUN	WW#1	12/1-12/31	31385	7	13	408	17

APPENDIX 5

Hard-to-Find References

RESERVOIR PERFORMANCE AND WELL SPACING, SPRABERRY TREND AREA FIELD OF WEST TEXAS

LINCOLN F. ELKINS, SOHIO PETROLEUM CO., OKLAHOMA CITY, OKLA., MEMBER AIME

SUMMARY

The Spraberry Trend Field of West Texas was discovered in January, 1949. Drilling of 2,234 wells and production of some 45 million bbl of oil by January, 1953, indicated this to be an important field which will ultimately cover more than 400,000 acres. In addition to being the world's largest field in areal extent, the Spraberry has presented many problems in well completion and operation and has demonstrated unique reservoir performance characteristics.

The pay section consists primarily of a few fine grained sandstone or siltstone members in a thousand-ft thick section of shale, limestone, and siltstone. Since porosity averages only 10 per cent and nearly all permeabilities are less than 1 md, conventional core analysis does not delineate the "pay" section. Mercury injection was used as a capillary pressure test adaptable to rapid routine use to select those intervals having low enough connate water saturation to contain commercially significant oil saturation. In the central area of the field this "pay" amounts to 16 ft of Upper Spraberry and 15 ft of Lower Spraberry sands.

An interconnected system of vertical fractures, observed in cores, provides the flow channels for oil to drain into the wells but most of the oil is stored in the matrix since the void volume of fractures is estimated to be less than 1 per cent of that in the sand. Initial potentials of wells range up to 1,000 B/D after fracture treatment which should be compared with estimated capacity of 5 to 10 B/D if oil had to flow into the wells through the sand itself.

Without exception initial pressures of later drilled wells were significantly lower than initial pressures of earlier drilled nearby wells in a large area some 6 miles long. This means the earlier drilled wells had drained fluids from areas much greater than their 40-acre proration units. Since most of this performance occurred while the reservoir pressure was above the saturation pressure it was analyzed by the compressible fluid flow theory. This analysis gave calculated initial pressures which agreed within $\pm$ 30 psi of measured pressures of 60 per cent of wells in the area using 16-md permeability corresponding to a fracture system substantially that indicated by cores and using combined compressibility of rock and its contained oil and water corresponding to the core analysis data. The most important feature of this analysis was the very close agreement between effective compressibility of the rock and its contained oil and water from the field performance and that from the core tests, because it meant there are no "islands" of low permeability reservoir rock left untapped in the inter-well area and thus no additional wells are necessary to insure that at least one well penetrates each "reservoir."

Twenty-five of forty-four 40-acre spaced wells on three contiguous sections were used in a four-month interference test. Six shut-in wells were tested monthly for oil production, productivity index, gas-oil ratio and pressure buildup, and seven shut-in wells were tested for decline in reservoir pressure. Tests on 12 regularly producing wells gave comparative data for interpretation of shut-in test wells. Reduction in reservoir pressure, decline in productivity index, and increase in gas-oil ratio were found to be substantially the same in the shut-in test wells as those in the comparative regularly producing wells, meaning that the producing wells were depleting the

[1]References given at end of paper.

Manuscript received in the Petroleum Branch office Feb. 2, 1953. Paper presented at the AIME Annual Meeting in Los Angeles, Calif., Feb. 14-19, 1953.

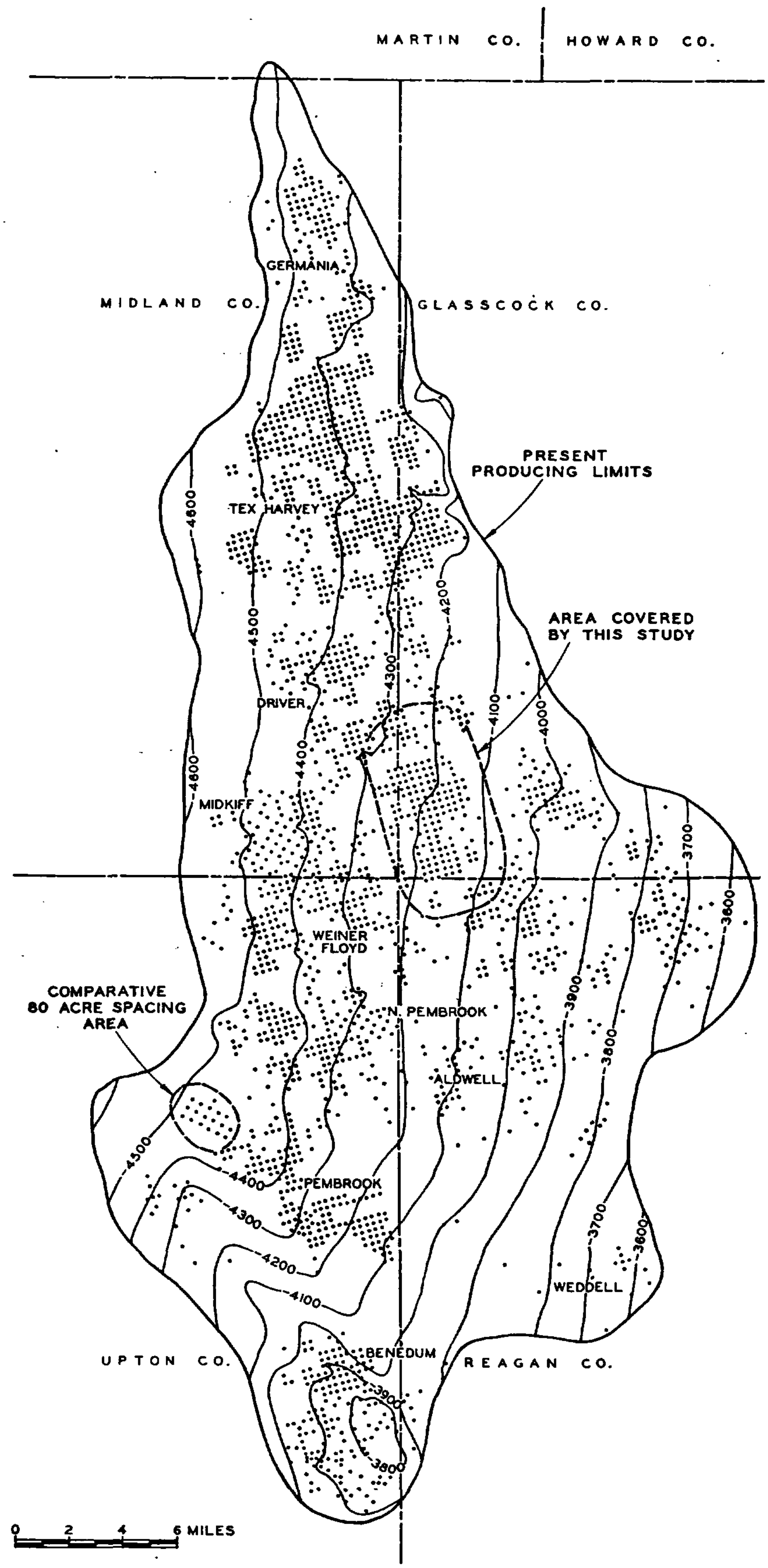

FIG. 1 — SPRABERRY TREND FIELD, CONTOURS ON TOP OF SPRABERRY FORMATION.

reservoir with the same efficiency at these points in the reservoir a quarter of a mile away as they were at points near the producing wells themselves.

Rapid decline in oil productivity and rapid increase in gas-oil ratio point to recovery of only some 7 or 8 per cent of oil in place. Laboratory tests on Spraberry cores indicate this low recovery is probably caused by capillary retention of oil due to "end effects" in the small fractured blocks of the reservoir rocks. Production rates necessary to overcome this capillary retention of oil cannot be achieved by any practicable spacing of wells.

The significance of this study is that direct experiment in the field itself demonstrates ability of a well in the Spraberry to recover oil from areas of the order of at least 160 acres as efficiently as could many wells on the same area even though the effective permeability of the reservoir including its fractures is only 16 md. It also demonstrates how modern reservoir engineering methods coupled with an enlightened management attitude can lead to an early understanding of a specific reservoir's performance and thus to proper development and operation.

HISTORY

The Spraberry sands of West Texas, named from a ranch owner on whose property they were first tested, were proved productive in January, 1949, in the Spraberry Deep Field in Dawson County. In February, 1949, the sands were proved productive in the Tex-Harvey Field in Midland County some 50 miles to the south. Development was very slow until late 1950 and early 1951 when additional fields were discovered including Germania, Driver, Midkiff, Pembrook, Benedum Spraberry, and others. Activity increased in 1951, reaching a peak at the beginning of 1952 when some 235 rotary rigs were in operation in the Trend. Thereafter drilling fell off sharply due partly to the steel shortage, but due mostly to the rapid decline in oil productivity of wells.

Development as of Jan. 1, 1953, is outlined in Fig. 1, including limits of semi-proved commercial production. More than 400,000 acres in an area nearly 40 miles in length and up to 25 miles in width are included in this one field which most likely will be proved ultimately to be continuous, making it the largest in areal extent in the world. The circled area near the center of the field indicates the area in which tests were run which are presented in this paper. History of development and production of the Spraberry Trend are shown graphically in Fig. 2.

Originally 40-acre proration units were in effect despite two concerted efforts in 1951 to obtain wider spacing. In December, 1952, however, regulations were changed to provide 80-acre proration units with 80-acre plus tolerance to each unit at the option of the operation. In addition, the various Spraberry fields covering parts of five counties were combined officially into one known as the Spraberry Trend Area Field.

GEOLOGY

The Spraberry formation is of Permian Leonard age and consists of about a thousand-ft section of sandstones, siltstones, shales and limestones with the top of the section occurring at a depth range of about 6,300 to 7,200 ft within the probable productive area. The structure is predominantly a broad regional monocline dipping westward about 50 ft per mile as illustrated in Fig. 1. Some noses are superimposed on the monocline and there is one anticline with about 200 ft of closure in the Benedum Area at the southern tip of the Spraberry Trend. Other anticlinal structures occur in Spraberry fields outside the Trend area such as Spraberry Deep in Dawson County. To the north and east the section grades primarily to a carbonate section providing the necessary seal for the stratigraphic trap. To the south and west the section becomes more shaly. Updip limits of commercial production are controlled by scarcity of vertical fracturing — the dominant feature of this unique reservoir — rather than by lack of accumulation of petroleum. Downdip production is limited both by scarcity of fractures and by water. Readers are referred to other papers for greater geological detail.[1,2,3]

DRILLING AND COMPLETION

Wells are drilled to the top of the Spraberry in about 35 days with rotary rigs using water and water-base mud. Some operators set a salt string at about 4,000 ft, followed by a liner to reduce mud costs while others set a single long oil string. Until late 1951 nearly all wells had casing set on top of the Spraberry after which the wells were drilled in with cable tools or with rotary tools using formation oil as the drilling fluid. Initially some wells were shot with nitroglycerine, but most wells have been hydrafraced to obtain satisfactory productivity. Very few wells will flow without such treatment.[4,5] Initial potentials of wells range up to 1,000 B/D and average about 250 B/D. Since late 1951 many wells have been successfully drilled through the entire Spraberry section with water-base mud, casing set through, cemented, and gun perforated. They have then been completed by hydrafrac using packers and temporary bridging plugs for selective treatment. Nearly all wells in the test area discussed in this paper were completed in the Upper Spraberry alone with casing set on top followed by cable tool and hydrafrac completion. After tests reported in this paper were completed, many of these wells were deepened to the lower Spraberry by continuous diamond drilling using oil as the drilling fluid and were completed in open hole. On new wells this same operator has changed entirely to normal rotary drilling with water-base mud and with casing set through the entire zone.

RESERVOIR CONDITIONS

Sand Properties

The Spraberry section is best illustrated by means of the composite log in Fig. 3 which includes the gamma ray and induction logs, geological description, and core analysis. Typical is the main upper pay sand about 31 ft in gross thickness productive throughout most of the field and the main lower pay sand about 27 ft in thickness productive in part of the field. In addition, numerous other thinner sands and siltstones occur distributed throughout the 900-ft section which is mostly shale. Porosity of these sands ranges up to 13 per cent and permeability ranges from less than 0.001 md to about 1 md. Shale sections also have about these same porosities and per-

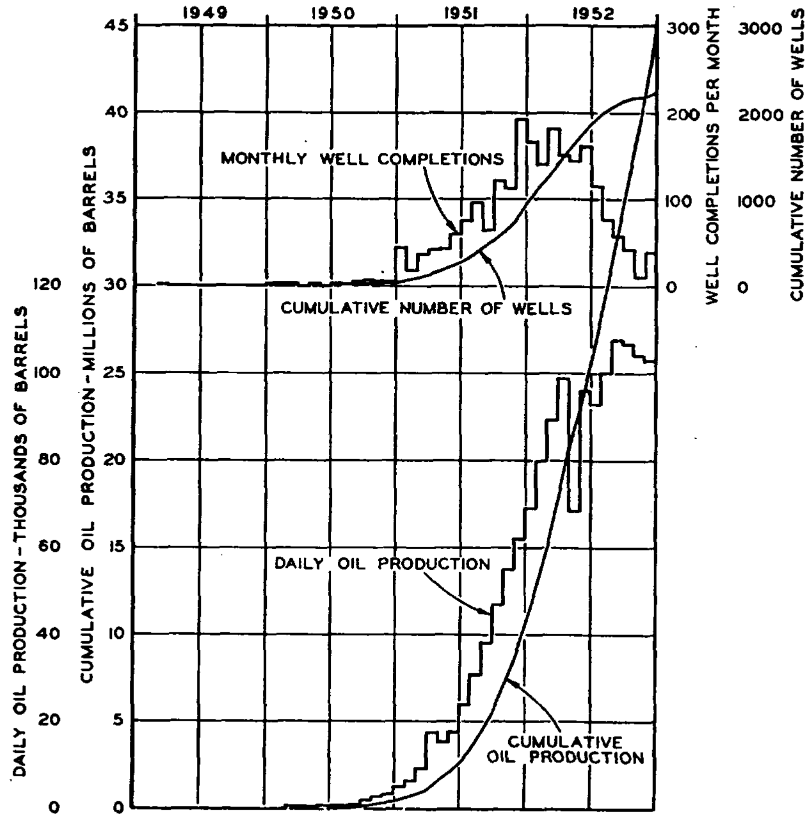

FIG. 2 — HISTORY OF DEVELOPMENT AND PRODUCTION, SPRABERRY TREND AREA FIELD.

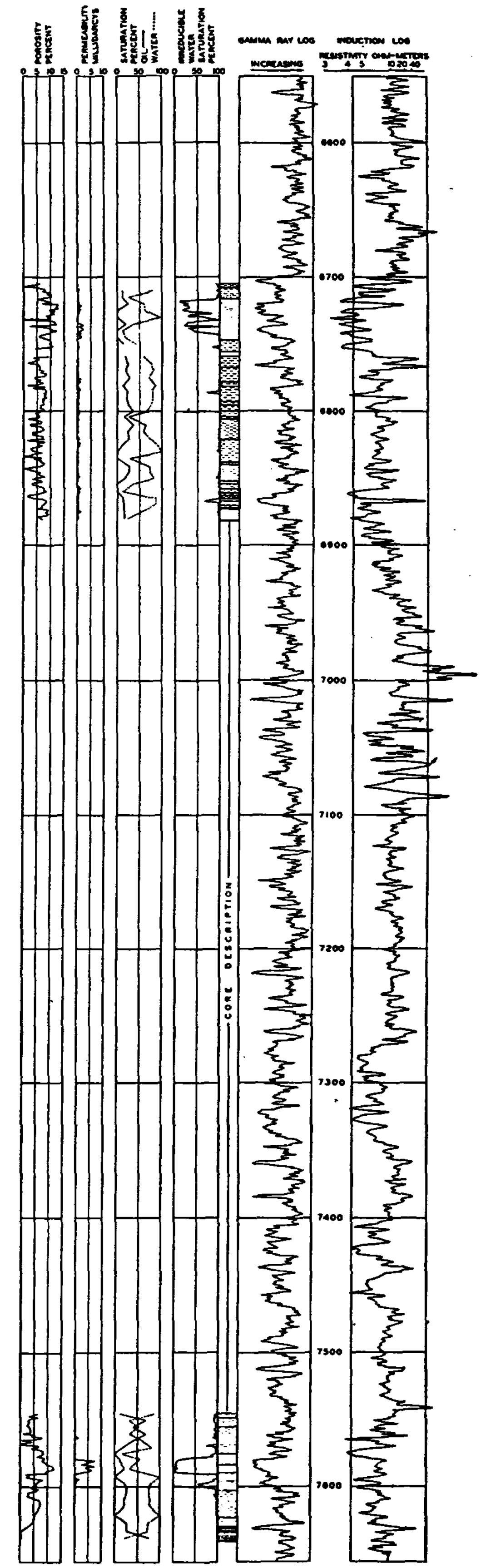

FIG. 3 — COMPOSITE LOG, SOHIO PROCTOR NO. 1, REAGAN COUNTY, TEX.

meabilities. Residual oil saturation in water-base mud cut cores determined by both retort and extraction methods ranges from about 10 per cent to 30 per cent in both shales and sands. Thus, conventional core analysis does not delineate the "pay" section.

Retorting of Spraberry shale at 400° F under vacuum yielded no oil recovery while retorting of companion samples at 1,000° F yielded recovery equivalent of 10 to 30 per cent of pore space. Vacuum distillation of Spraberry crude at 400° F gave about 50 per cent vaporization. The hydrocarbon material in the Spraberry shale thus is not ordinary crude oil but is probably a highly viscous or even semi-solid residue. It is not a commercial deposit.

Porous diaphragm, centrifuge, and mercury injection capillary pressure methods all give similar values for irreducible water saturation for Spraberry sandstones. Single point mercury injection measurements at 1,300 psi were made to determine those portions of sand which had pores large enough to permit oil entry under conditions of capillarity which probably exist in the reservoir. Typical data are included in Fig. 3 and are labeled irreducible water saturation. Similar tests by commercial service laboratories have been reported as "productive porosity." Arbitrarily selecting "pay" as that section having less than 60 per cent irreducible water saturation limits the main upper sand to an average of 16 ft and the main lower sand to an average of 15 ft. Most other sand

Table 1 — Spraberry Sand Properties, Driver Field, Glasscock County, Texas

Well	Gross* Sand Section Ft	Net** Pay Ft	Average Porosity Net Pay Per Cent	Average Irreducible Water Sat. Net Pay	Reservoir Pore Vol. Bbl/Acre Gross Sand	Hydrocarbon Pore Volume Bbl/Acre Gross Sand	Hydrocarbon Pore Volume Bbl/Acre Net Sand
Main Upper Spraberry Sand							
A	30	18	10.6	28.4	21,650	11,650	10,630
B	36	20	9.1	28.4	24,600	11,650	10,100
C***	24	15	9.8	19.4	16,550	10,100	9,230
D	29	15	10.1	25.0	20,300	9,150	8,850
E	22	10	10.2	32.8	16,400	6,280	5,280
F***	17	11	10.4	25.0	12,700	7,530	6,360
G	41	13	9.7	32.0	27,500	8,530	6,750
H	27	17	8.5	25.7	18,250	9,080	8,300
I	28	14	8.9	30.6	18,800	8,470	6,670
J	32	23	11.1	37.8	25,800	13,800	12,400
Average	31	16	9.9	30.1	21,600	9,930	8,610
Main Lower Spraberry Sand							
A	27	14	9.4	15.2	15,850	9,310	8,700
I	36	20	9.9	24.9	23,700	11,800	11,500
J	19	10	10.6	9.5	12,100	7,680	7,450
Average	27	15	10.0	16.5	17,230	9,630	9,230

*Sandstone and siltstone section by core description.
**Section having less than 60% irreducible water saturation by Mercury Injection Method.
***Complete section not cored and analyzed. Excluded from averages.

FIG. 4 — TYPICAL FRACTURES IN SPRABERRY CORES.

FIG. 5 — TOP VIEW OF VERTICAL FRACTURES IN OUTCROP OF BRUSHY CANYON FORMATION.

streaks are too fine grained to contain sufficient oil saturation to be productive in this area but some of these thinner streaks apparently are productive in some parts of the field. Data for ten wells cored in the test area are summarized in Table 1. Values for hydrocarbon pore space for each well on both the gross sand and net sand basis are not products of average values but are summation of values measured individually on a sample of each foot of core.

Vertical Fractures

The unique feature of the Spraberry formation is the extensive vertical fracturing observed in all productive wells cored. Sixty-two per cent of 2,058 ft of cores from five wells in this area had single fractures present and 4 per cent had multiple fractures, some parallel and some intersecting. Fracture spacing laterally is probably of the order of a few inches to a few feet estimated from frequency of fractures observed vertically in the 3.5 in. diameter cores. Typical fractures in cores are illustrated in Fig. 4. The vertical fracture pattern may very well be similar to that occurring in the outcrop of the Spraberry equivalent Brushy Canyon Formation some 70 miles south of Carlsbad, New Mexico, as illustrated in Fig. 5.

One hundred eleven measurements of fracture openings were made on these cores by comparing core diameter normal to the fracture with that parallel to the fracture after matching the core pieces by bedding planes, bit scratches, and fracture irregularities. These fracture measurements ranged up to 0.013 in. and averaged 0.002 in. Some large fractures exist as demonstrated by cement in cores cut below casing but these are infrequent. Productivity of wells indicates some of the fractures must be open because the actual initial potentials of wells often exceed the potential calculated from core analysis permeability by a factor of about 25. Fractures exist in the shales but pressure-production data discussed later indicate

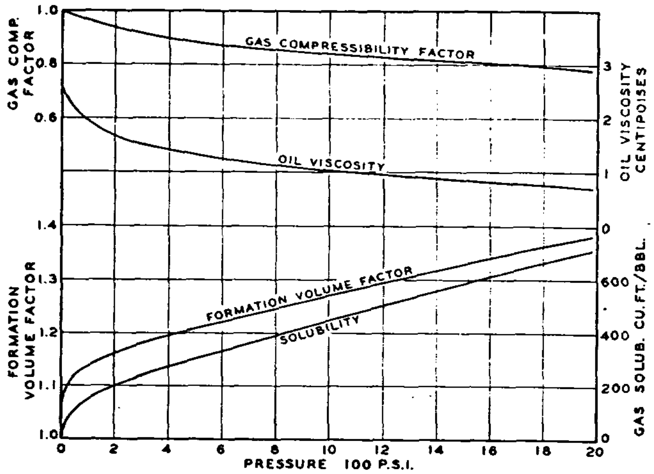

FIG. 6 — AVERAGE SUBSURFACE OIL SAMPLE, UPPER SPRABERRY SAND, DRIVER FIELD, GLASSCOCK COUNTY, TEX. TEMPERATURE, 136° F.

flow is mainly limited to the sand section and vertical communication through fractures in shale is negligible.

Fracture void volume in the main upper Spraberry sand is estimated to be about 110 bbl per acre based on fracture opening and probable fracture spacing just discussed. Fractures thus contribute little to reservoir void volume but do serve as conduits for flow of oil and gas from the reservoir to the wells.

Properties of Oil at Reservoir Conditions

Subsurface samples of oil were obtained from ten newly completed upper Spraberry wells in this area. Properties of each oil sample at saturation pressure are summarized in Table 2 and average properties at various pressures are presented graphically in Fig. 6. Of greatest significance for analysis of upper Spraberry reservoir performance observed is the approximate 300 psi undersaturation of oil initially. Formation volume factor is 1.385 and gas in solution is 713 cu ft per bbl at the 136° F reservoir temperature. Lower Spraberry oil in this area was saturated initially at a pressure of about 2,535 psi. Formation volume factor is 1.58 and gas in solution is 1.047 cu ft per bbl at the 144° F reservoir temperature.

Oil in Place Initially

Tank oil in place initially in the Upper Spraberry, estimated from these various core analysis, fracture opening, and subsurface sample data, is 7,250 bbl per acre on the gross section basis and 6,300 bbl per acre on the net section basis considering only those intervals having less than 60 per cent irreducible water saturation. Similar estimates for the main lower Spraberry sand are 6,150 bbl per acre on the gross basis and 5,900 bbl on the net basis respectively.

MEASUREMENT AND INTERPRETATION OF INITIAL PRESSURES IN WELLS

After hydrafrac treatment each well in the subject area was produced just a few hours for clean up and was then shut in for a minimum of 72 hours prior to measurement of reservoir pressure. Production during clean up ranged from 100 to 400 bbl generally. Wells so tested are identified in Fig. 7 and data obtained are presented graphically in Fig. 8 with appropriate corresponding circular symbols. Subsequent 72-hour shut in pressures of some producing wells are shown as X's, and lines connect pressures of an individual well. Within each closely associated group the later drilled wells had lower initial pressures without exception than did the earlier drilled wells, and in nearly all cases the initial pressures of later drilled wells correspond closely with 72-hour shut in pressures of nearby regularly producing wells. Each later drilled well was at least 1,320 ft from any previously producing well, and one, Davenport C-14, in Section 11, was over half a mile from any producing well. This latter well reflected some 130 psi reduction in reservoir pressure at this distance even though it was completed within about three months of the wells first drilled in the area.

This rapid equalization of pressure over such wide area means the fractures observed in cores are a sample of an

Table 2 — Properties of Reservoir Oil, Upper Spraberry Sand, Driver Field, Glasscock County, Texas

Well	Reservoir Pressure Psi (−4400′ Datum)	Reservoir Temp. °F	Pressure at Sampling Depth Psi	Sat. Press. Psi	Formation Volume Factor	Gas Sol. Cu Ft Per Bbl	Oil Visc. at Sat. Press. Cent.	Compressibility of Oil Vol/Vol/Psi	Gravity Residual Oil °API
A	2330	135	2111	1944	1.398	721	0.77	12.7 x 10^{-6}	37.7
B	2231	136	2110	1982	1.391	719	—	12.0 x 10^{-6}	37.0
C	2263	137	2185	2008	1.362	685	0.66	12.7 x 10^{-6}	36.6
D	2251	137	2130	2090	1.356	679	0.62	11.9 x 10^{-6}	37.4
E	2212	138	2109	1797	1.365	666	0.78	11.7 x 10^{-6}	37.3
F	2325	137	2111	1959	1.396	714	—	12.1 x 10^{-6}	37.1
G	2341	137	2108	2016	1.397	726	—	12.0 x 10^{-6}	37.3
H	2308	136	2175	2124	1.370	740	—	11.2 x 10^{-6}	37.3
I	2074	136	1847	1935	1.441	768	—	12.9 x 10^{-6}	37.5
J	2218	136	2002	1958	1.376	711	—	12.4 x 10^{-6}	37.0
Average		136		1981	1.385	713	.71	12.2 x 10^{-6}	37.2

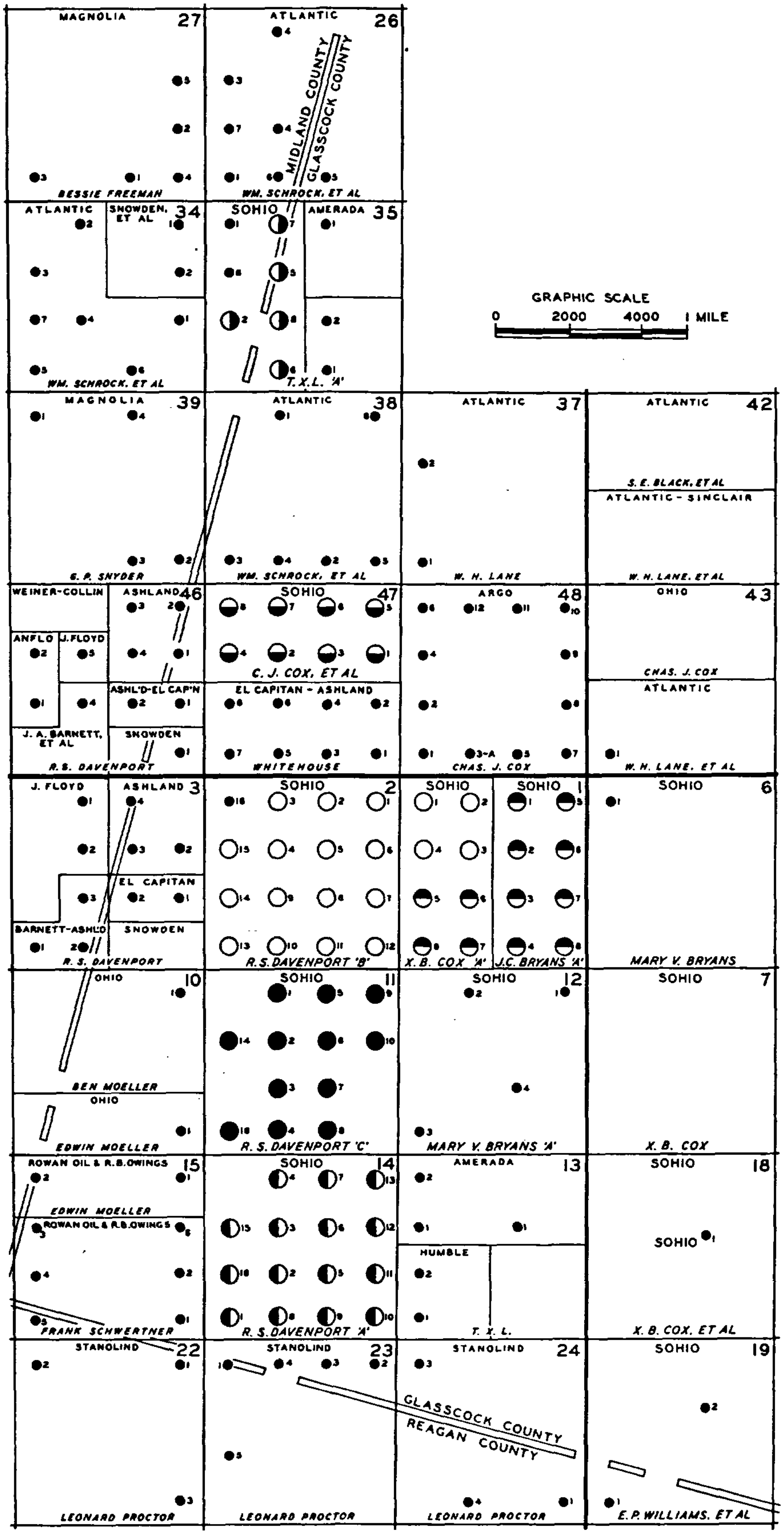

FIG. 7 — GROUPING OF WELLS FOR COMPARISON OF DECLINE OF INITIAL PRESSURE IN WELLS WITH DATE OF COMPLETION.

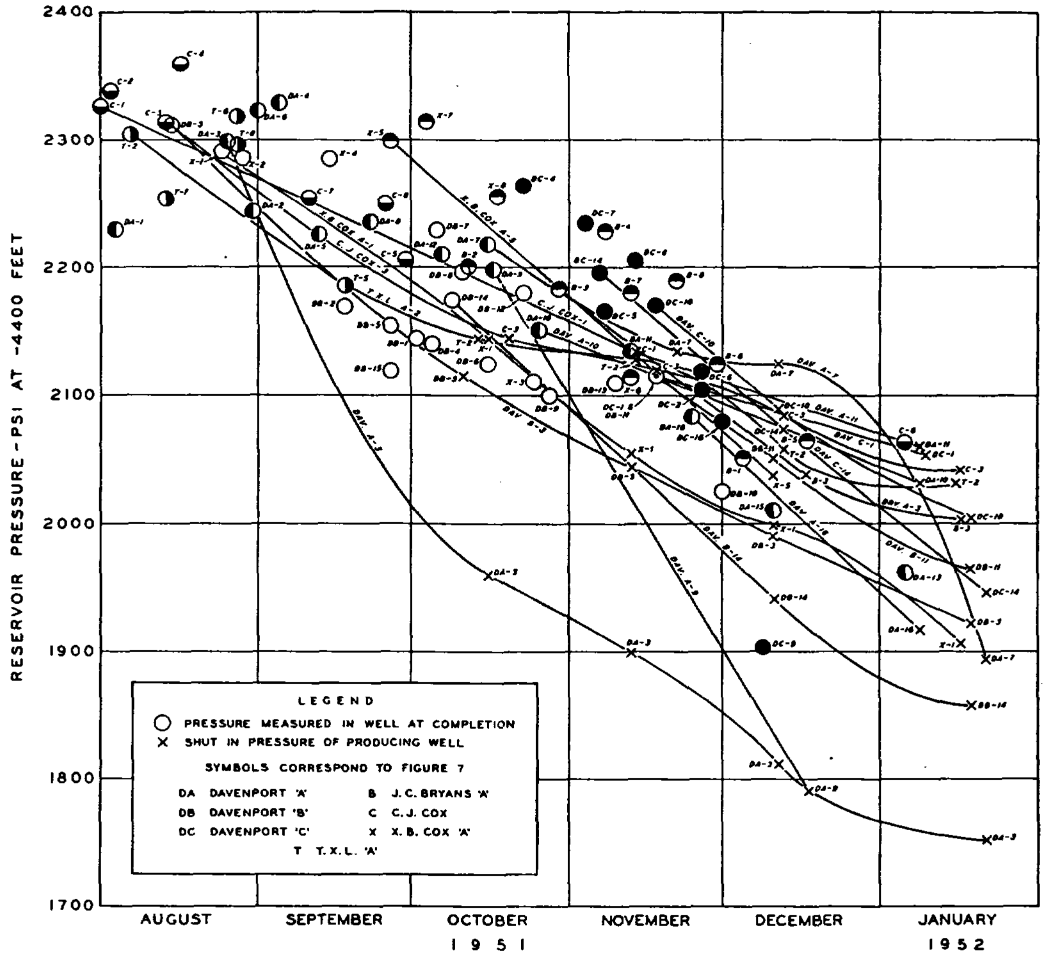

FIG. 8 — COMPARISON OF INITIAL PRESSURES IN WELLS WITH DATE OF COMPLETION.

extensive well interconnected system of fractures covering this entire area. Since without exception reduced pressures were observed in all later drilled wells in each area, many wells drilled were unnecessary because they did not connect to fractures not already being drained by previously drilled wells.

Since reservoir pressures were above the saturation pressure of the oil until about Dec. 1, 1951, the performance was analyzed by the theory of flow compressible fluids by considering each well as a point sink in an infinite reservoir of uniform thickness, porosity, and permeability, and calculating the pressure drawdown at locations of each new well by Equation (1).[6,7]

$$P_o - P = \frac{QUB}{4\pi KH\,1.127}\,Ei\left(-\frac{R^2}{4\frac{KT}{UCF}\,6.32}\right) \quad . . . \quad (1)$$

where:

P_o — Initial pressure, psi
P — Pressure at R at time T
Q — Constant production rate, B/D
U — Oil viscosity, centipoise
B — Formation volume factor
K — Effective permeability, darcys
H — Thickness, feet
R — Distance, feet
C — Weighed average compressibility of oil, connate water, and rock
F — Porosity, fraction
T — Time, days
$Ei()$ — Exponential integral
1.127, 6.32 — Conversion factors

Total pressure drawdown is the summation of effects of all producing wells using their appropriate production rates, distances, times on production, etc. Production from 143 wells within three miles of key wells indicated in Figs. 7 and 8 was used in calculation of expected initial pressures of 65 wells completed by Dec. 1, 1951.

Because the correct diffusivity factor is unknown and is in implicit form in the relation it was necessary to assume various values of $\frac{K}{UCF}$ and calculate pressures of each well. Deviations between measured and calculated pressures are shown for three values of diffusivity in Fig. 9 leading to selection of 2.77×10^4 as the "best" value of $\frac{K}{UCF}$ based on most

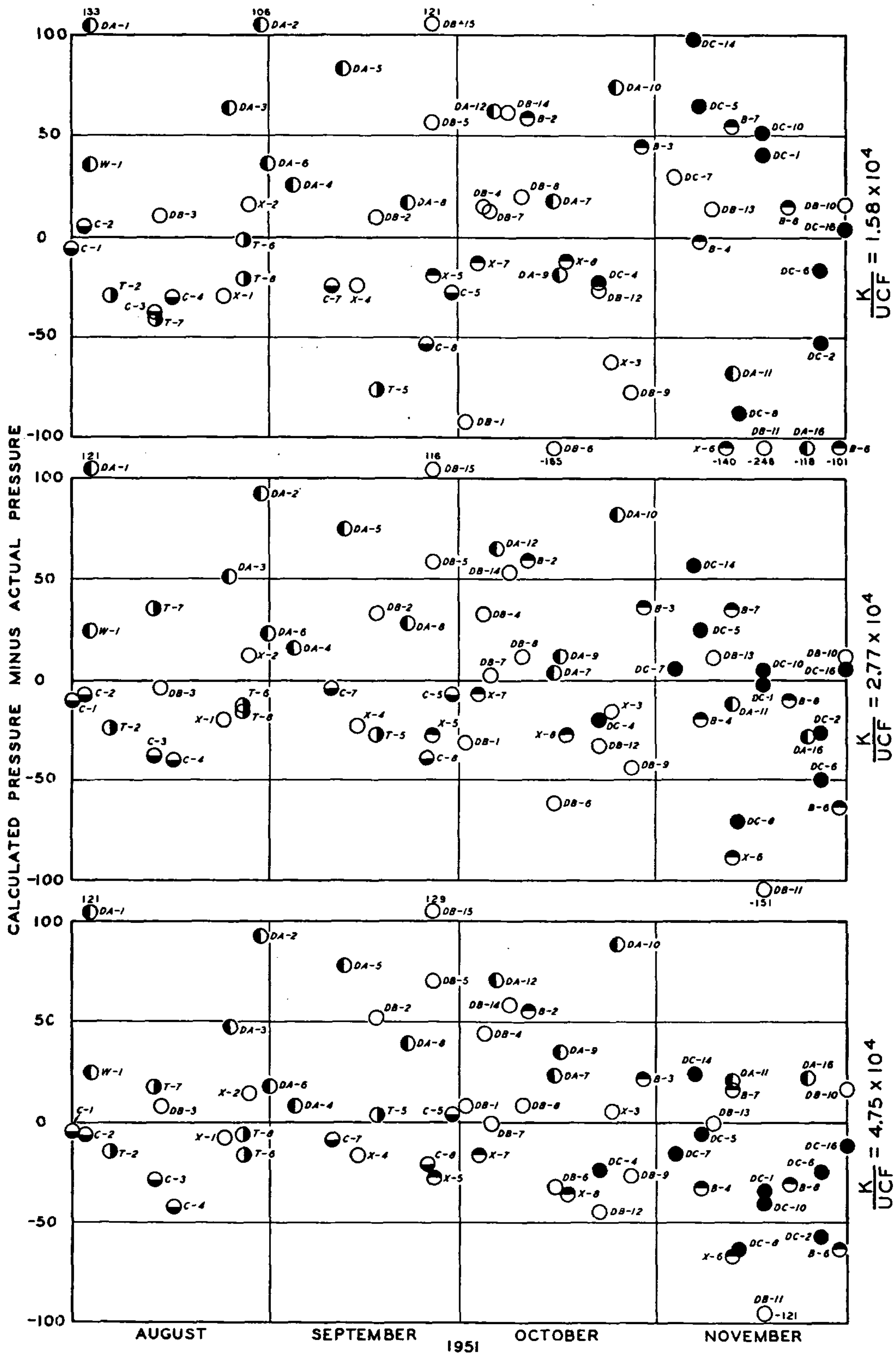

SYMBOLS CORRESPOND TO FIGURE 7

DA	DAVENPORT 'A'	B	J. C. BRYANS 'A'
DB	DAVENPORT 'B'	C	C. J. COX
DC	DAVENPORT 'C'	X	X. B. COX 'A'
	T	T. X L. 'A'	

FIG. 9 — COMPARISON OF CALCULATED INITIAL PRESSURES WITH ACTUAL INITIAL PRESSURES OF WELLS.

Table 3 — Expansibility of Rock, Oil and Water Derived from Pressure — Production Analysis Upper Spraberry Sand

Diffusivity $\frac{K}{UCF}$	Expansibility Bbl/Acre/Psi
1.58×10^4	0.186
2.77×10^4	0.204
4.75×10^4	0.197

uniform distribution of plus and minus errors on the basis of both time and geographical distribution. Sixty per cent of calculated pressures are within plus or minus 30 psi of measured initial pressures of wells, which is very excellent considering the working accuracy of pressure gauges in field application, difference in clean-up production and build-up characteristics of wells and the necessary assumption that all wells on each lease had equal production during any particular month.

Average effective permeability in this area was approximately 16 md for the 31-ft gross section as determined by this analysis, corresponding to productivity index of 0.48 B/D per psi and initial potential of 520 B/D. Actual productivity indices ranged from about 0.1 to 2.5 initially and initial potentials ranged from 31 to 960 B/D in this area. This effective permeability in millidarcy-feet is also of the same order of magnitude as that determined by build-up curve analysis in an adjacent area.[8] Considering the flow to be primarily in two sets of equally spaced mutually perpendicular uniform fractures permits calculation of average fracture opening by Equation (2).[9]

$$W = \left(\frac{12\,KS}{6.45 \times 10^8} \right)^{1/3} \quad \ldots\ldots\ldots\ldots \quad (2)$$

where

W — Fracture opening, inch
K — Effective permeability, darcys
S — Fracture spacing, inches

For average fracture spacing of 10 in. corresponding to frequency of fractures seen vertically in 3.5 in. diameter cores the fracture opening is calculated to be 0.0015 in. For 4-in. spacing the opening would be 0.0011 in., and for 2-ft spacing 0.0020 in. These calculated fracture openings compare favorably with the average opening of 0.002 in. actually observed in cores.

The factor HCF, obtained by elimination of $\frac{K}{U}$ from $\frac{KH}{U}$ and $\frac{K}{UCF}$ in Equation (1), multiplied by 7,758 is combined expansibility of rock and its contained oil and water in bbl per acre per psi. Expansibility so calculated is summarized in Table 3 for a three-fold range of diffusivity used in the analysis of the pressure-production performance.. It is significant that the calculated expansibility varies only 9 per cent for this range and thus little error is introduced even though the resolving power of the analysis is not high in selecting the most probable value of the diffusivity factor. The corresponding combined expansibility of rock, oil, and water calculated from core analyses and subsurface samples is summarized in Table 4. Certainly the almost perfect agreement between expansibility calculated from the pressure-production analysis and that from the cores is partly fortuitous because data from individual core wells have an average deviation of $\pm$ 15 per cent from the mean. But the good agreement of all factors in the analysis including calculated individual well pressures, calculated permeability and fracture opening versus well tests and core measurement, and calculated expansibility of rock, oil, and water versus core data must mean these values quite accurately represent average conditions in this area of the field. Close agreement of expansibility of oil, water and rock derived from the analysis with that from cores using only sand intervals probably means production comes only from the sand and vertical migration through fractures in shale is not significant. At least this lack of migration through large vertical intervals was confirmed by a large increase in production when nearly depleted upper Spraberry wells were deepened to the lower Spraberry.

Observation of reduced reservoir pressure initially in all later drilled wells in each area certainly leads to the conclusion that there exists an interconnected system of fractures tapped by all wells drilled. But the almost perfect agreement between combined expansibility of rock, oil and water derived

Table 4 — Expansibility of Rock, Oil and Water Derived from Cores and Subsurface Fluid Samples Upper Spraberry Sand

	Volume Bbl/Acre	Unit Expansibility Vol/Vol/Psi	Gross Expansion Bbl/Acre/Psi
Oil	10,060	12.2×10^{-6}	0.124
Water	11,650	3.2×10^{-6}	0.037
Rock	240,000	1.88×10^{-7}*	0.045
			0.206

*Pore Vol. Change/Bulk Vol/Psi.

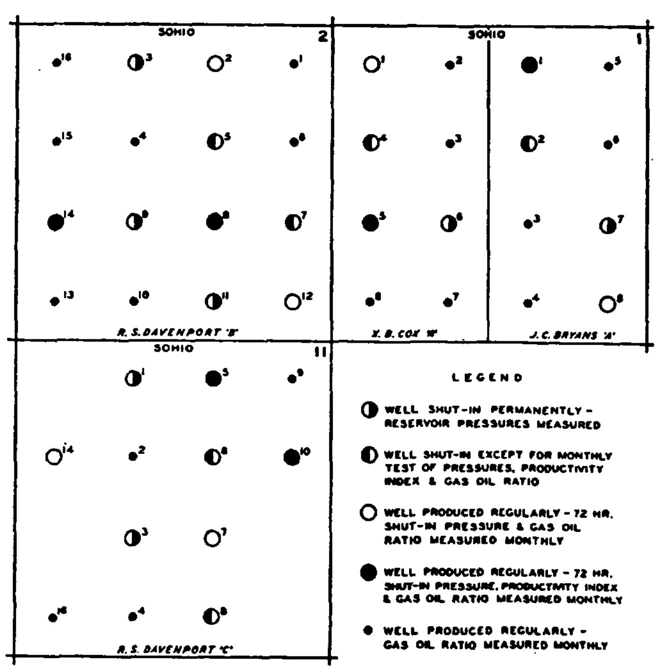

FIG. 10 — KEY TO WELLS IN LARGE SCALE INTERFERENCE TEST.

using only production and initial pressures of wells and expansibility of rock, oil, and water obtained from core analyses indicate the chance is nil that the interwell area has untapped "islands" of reservoir containing commercially significant amounts of oil. Thus additional wells, and for that matter many existing wells, are unnecessary to insure that each part of the reservoir is permeably connected to some well.

INTERFERENCE TEST

In order to continue to observe interference and other features of reservoir performance in the inter-well area, indicated initially by reduced reservoir pressure of later drilled wells, Sohio Petroleum Co. obtained permission from the Texas Railroad Commission to conduct a large scale long time interference test. The test area included three contiguous sections of land upon which 44 wells almost completed uniform 40-acre spacing development. Alternate wells in the center rows were shut in and their allowable production transferred to other wells on each lease in such manner as to protect correlative rights among all leases involved in the test area. The test area is outlined in Fig. 10.

Seven of the wells were shut in throughout the test and had reservoir pressure measurements made monthly. Six of the shut-in wells had production rate, gas-oil ratio, and flowing bottom hole pressure measured after which they were then shut in for a 72-hour pressure buildup test. Additional spot measurements of reservoir pressure were made after the wells had been shut in for one week and for one month. The wells were then returned to production for a 48-hour test period during which gas and oil production were measured and the flowing bottom hole pressure was measured in each well during the last six hours of the test period. The wells were then shut in again for 72-hour pressure buildup tests and for spot readings of reservoir pressure after shut-in periods of one week and one month, etc. Each of the six wells so tested was shut in for three successive months each followed by the 48-hour production test and pressure tests just described. Shut-in wells so tested are illustrated by appropriate symbols in Fig. 10.

To provide a basis for evaluating the observations in the shut-in wells, various tests were made in regularly producing wells. Seventy-two hour shut-in pressures were measured at monthly intervals in six regularly producing wells. Production rate, gas-oil ratio, and flowing bottom hole pressure measurements followed by 72-hour reservoir pressure buildup tests were conducted at monthly intervals in six additional regularly producing wells. Wells so tested are illustrated by appropriate symbols in Fig. 10. In addition, oil production rate and gas-oil ratio were measured on all regularly producing wells in the test area at least once each month.

Decline in Reservoir Pressure

Although the reservoir was below the saturation pressure in the area during the interference test, reservoir pressure continued to decline rapidly due to continued development and due to rapidly increasing gas-oil ratios. Pressure data of the shut-in wells and of the producing wells are presented graphically in Fig. 11 with appropriate symbols to designate test program of each well. Some of the wells shut in permanently showed build up in reservoir pressure for a short time, but soon all shut in wells demonstrated significant decline in reservoir pressure at these points 1,320 ft from any producing well. In wells shut in except for 48-hour production tests monthly, the reservoir pressure built up to a maximum and then declined within each 30-day shut-in period. Only the 30-day shut-in pressures of these wells are included in Fig. 12. These wells also demonstrated significant decline in reservoir pressures at points in the reservoir 1,320 ft from regularly producing wells. Shut-in wells had approximately the same rate of pressure decline as did the producing wells and none of the shut-in wells failed to indicate some significant decline in pressure. During March and April, 1952, the pressure declined about 3 psi per day. During May and June, 1952, the rate of decline of reservoir pressure was reduced to about 2 psi per day due to curtailed production during the oil strike.

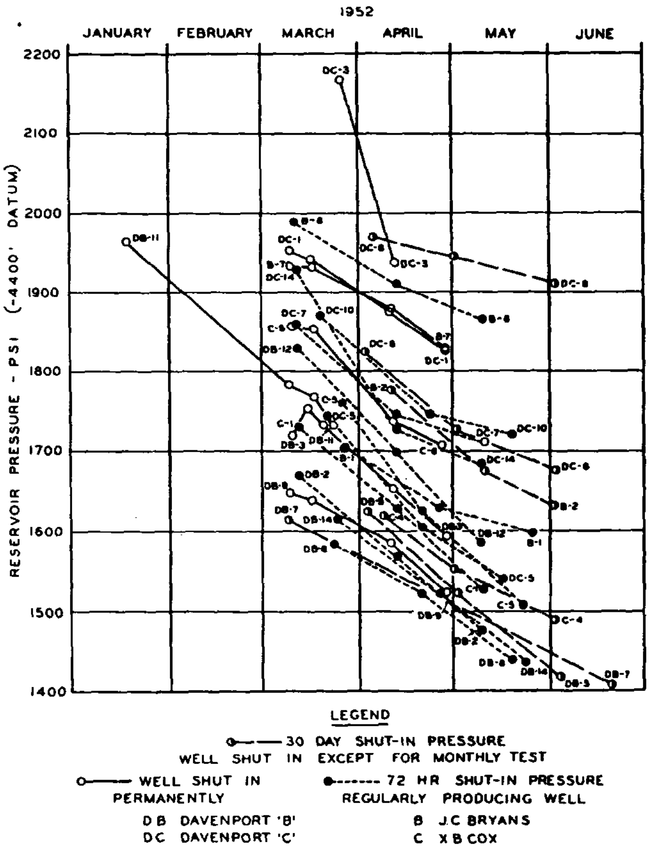

FIG. 11 — COMPARISON OF DECLINE IN RESERVOIR PRESSURE, SHUT-IN WELLS VS REGULARLY PRODUCING WELLS.

Reservoir pressures in the test area covered a range of some 500 psi due partly to difference in date of development of various areas and due partly to variations in density of drilling surrounding particular wells. Thus wells on the Davenport "B" lease drilled earlier and most completely surrounded by areas approaching complete development on a uniform 40-acre spacing pattern reflect the lowest reservoir pressure. Such regional variation in reservoir pressure makes it difficult to determine lag of pressure decline in the inter-

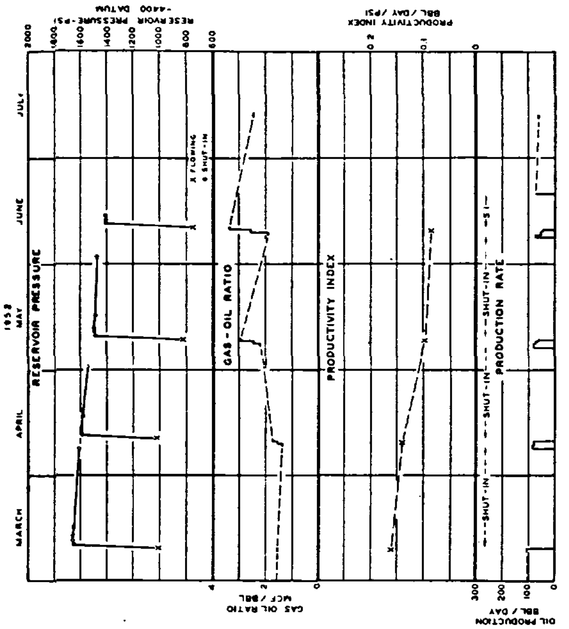

FIG. 12-E — PERFORMANCE OF X. B. COX A-4 SHUT-IN TEST WELL.

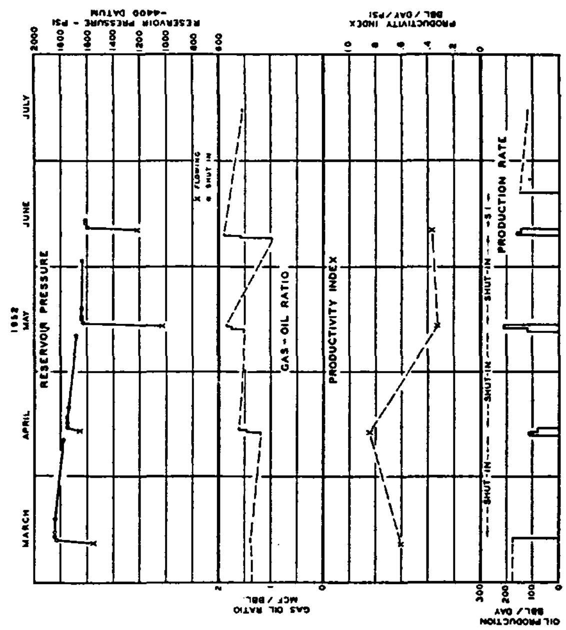

FIG. 12-F — PERFORMANCE OF J. C. BRYANS A-2 SHUT-IN TEST WELL.

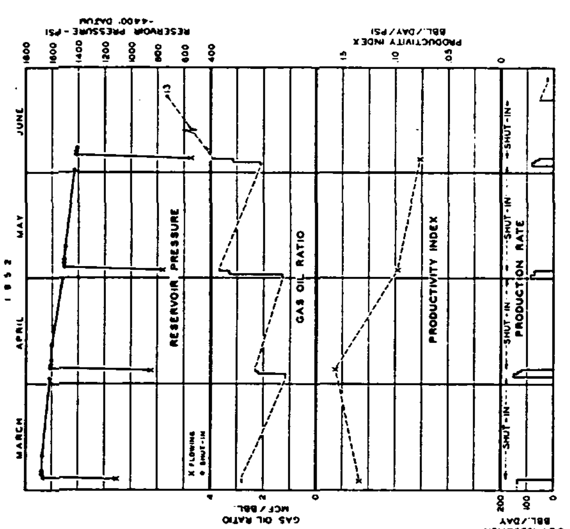

FIG. 12-C — PERFORMANCE OF DAVENPORT B-5 SHUT-IN TEST WELL.

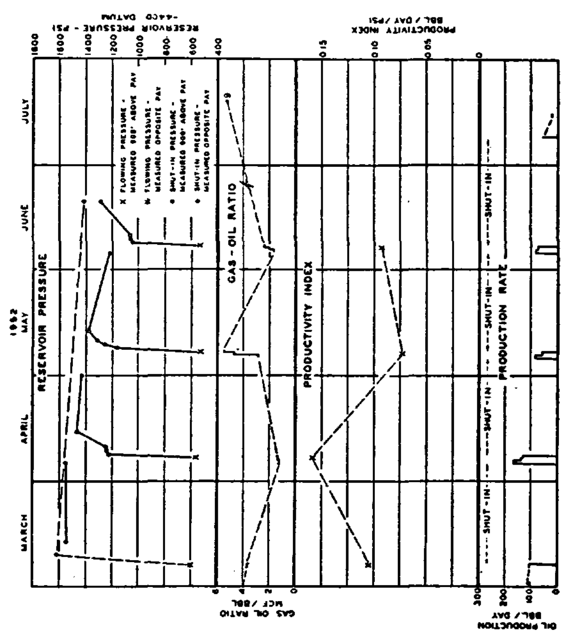

FIG. 12-D — PERFORMANCE OF DAVENPORT B-7 SHUT-IN TEST WELL.

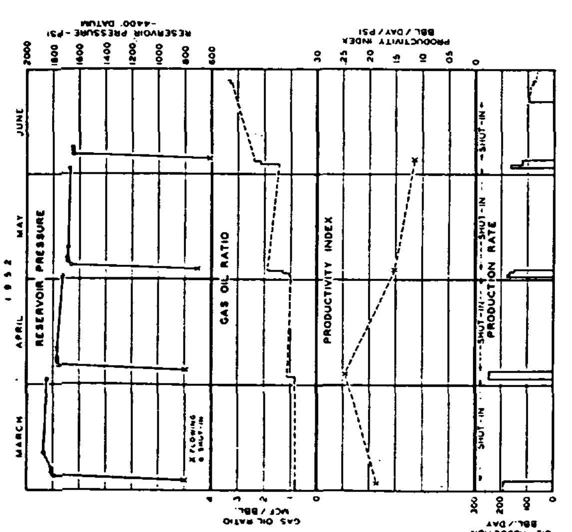

FIG. 12-A — PERFORMANCE OF DAVENPORT C-6 SHUT-IN TEST WELL.

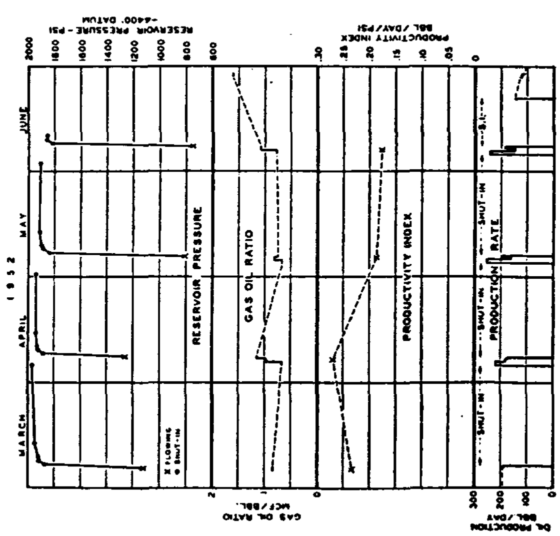

FIG. 12-B — PERFORMANCE OF DAVENPORT C-8 SHUT-IN TEST WELL.

well area behind that of the area close to the producing wells. One good example, however, is Davenport B-11 which had been shut in long before the test program started. Five of the eight surrounding wells had 72-hour shut-in pressures measured in March, 1952. Average of these pressures was 1,725 psi or about 40 psi below the 1,765 psi pressure of Davenport B-11 when all pressures were corrected to a common date.

These data show that, on the average, the pressure declined in shut-in observation wells 1,320 ft from any producing well at almost exactly the same rate as it did in the producing wells. As should be expected, the pressure in the shut-in wells was slightly higher than in the nearby producing wells but this lag which ranges at most up to 200 psi indicates depletion of the area of shut-in wells lagged only a few weeks behind the depletion of the area near the producing wells.

Most of the observations of lower initial pressures in later drilled newly completed wells were made while reservoir pressure was above or very near the saturation pressure of the formation oil. Under those conditions large pressure changes occurred with removal of quite small volumes of oil due to the expansibility of oil above the saturation pressure. These observations during the interference test have shown that without exception production from wells has continued to affect reservoir conditions at points up to at least 1,320 ft away from the producing wells while the reservoir pressure has declined hundreds of psi below the saturation pressure of the formation oil. And this occurred during a period when much larger amounts of oil and gas must be removed to effect reservoir pressure changes due to the much larger expansibility of fluids below the saturation pressure.

Gas-Oil Ratios and Productivity Indices

In previous discussions of well spacing and recovery efficiency, proponents of wider spacing have often stated that interference between wells demonstrated by changes in pressure means efficient recovery of oil over the distance pressure drawdown was observed. Opponents of wider spacing have argued that reduction of pressure did not necessarily mean recovery of oil. The proponents have had to rely on theoretical considerations involving assumptions which were not acceptable to all concerned. It would indeed be fortunate if methods were available by which a well could be drilled and the oil content of the reservoir determined accurately. The well could then be shut in while other wells are produced and later could be resampled to determine oil recovery from the reservoir by difference. However, such techniques have not yet been developed and it is necessary to rely on indirect observations of depletion such as changes in oil productivity and gas-oil ratios in shut-in wells compared with such changes as occur in regularly producing wells to judge relative recovery efficiency.

As previously mentioned, gas-oil ratios and productivity indices were measured for six wells shut in except for a 48-hour production test each month. Data obtained in the series of tests on each of the wells are presented graphically in Fig. 12A-F, inclusive. With one exception the reservoir pressure in each well reached a maximum and then declined during each 30-day shut-in test period, and all of the wells had significant decline in pressure from month to month as discussed previously. Circled pressure points represent 1, 2, 3, 7, and 30 days shut-in pressures. In three shut-in wells the gas-oil ratio decreased during the first month it was shut in and in all six shut-in wells it was higher at the end of the four-month test period than it was at the beginning. In five of the six shut-in wells the productivity index was higher following the first one-month shut-in period than it had been at the beginning of the test. In all of the six shut-in wells the productivity index was lower at the end of the three-month test period than it was at the beginning of the test.

During each 48-hour production test of the shut-in wells, oil production was gauged for the first 24 hours, the next 18 hours, and finally for each of the last six one-hour periods. Flowing bottom hole pressures were recorded during this last six-hour period just prior to shutting in the well for a pressure buildup test. Gas production was measured throughout the 48 hours by orifice meters. Production data and gas-oil ratio calculated for the first 24 hours, the next 18 hours, and the last six hour periods included in Fig. 12A-F, inclusive, show that oil production declined generally and gas-oil ratio increased generally for each of the wells such that 48 hours was insufficient for the wells to be completely stabilized. Thus actual changes in productivity and gas-oil ratios in these shut-in wells probably were more severe than the 48-hour tests indicate. Additional gas-oil ratio and oil production tests were made within one to two weeks after the wells had been returned to regular production and four of the six wells showed further significant increase in gas-oil ratio. Data of these latter tests are included in each well performance chart.

Results obtained in six regularly producing wells tested for comparison are presented in Fig. 13A-F, inclusive. These charts show the oil production rate, gas-oil ratio, and productivity index data along with the flowing pressure and static reservoir pressure measured after 24 hours, 48 hours, and 72 hours shut-in periods. These 72-hour shut-in pressures, summarized in Fig. 11, were discussed previously. Gas-oil ratios of all six of these regularly producing test wells increased during the period and productivity indices of all six of these wells declined significantly throughout the test period.

Productivity indices of all shut-in and regularly producing test wells are summarized in Table 5. The tabulation includes ratio of the last test to the first test of each well to illustrate relative decline in productivity. For the regular producing wells this ratio averaged 0.56 representing 44 per cent decline in productivity during a two month period. For the shut-in test wells this ratio averaged 0.66 representing 34 per cent decline in productivity. As mentioned in discussion of well performance records in Fig. 12A-F these shut in test wells were still declining in production at the end of the 48-hour test following each one-month shut-in period. The last three tests were not comparable to the stabilized test following regular production before the well was shut in but they should be comparable to each other since all were measured at comparable times on production. For the group of shut-in wells the ratio of last productivity index to that measured after the first one-month shut-in period averaged 0.54 representing 46 per cent decline during a two-month period during which only enough oil was produced to test the wells. Production of these six wells during the 48-hour tests totalled less than 2 per cent of production from the four leases involved and average production of each of the shut-in wells was less than 10 per cent of average production of each of the regularly producing wells during the test period.

Reservoir pressure declined about 150 to 185 psi during the test and the corresponding increase in viscosity of oil should have been about 10 per cent from 0.82 to 0.90 cp. Thus, only 10 per cent of the 45 per cent decline in productivity index is attributable to changes in oil viscosity and the remaining 35 per cent must be due to actual reduction of oil saturation in the reservoir. Since over three-fourths of the decline in productivity index observed is due to reduction in oil saturation and since the same percentage decline in productivity index occurred in shut-in wells as did in regularly producing wells, it can only be concluded that a well in the Spraberry effects recovery of oil as efficiently at points in the reservoir at least

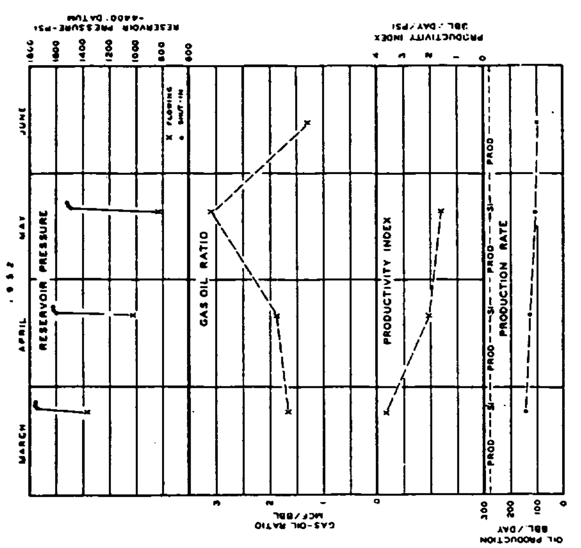

FIG. 13-E — PERFORMANCE OF X. B. COX A-5 REGULARLY PRODUCING WELL.

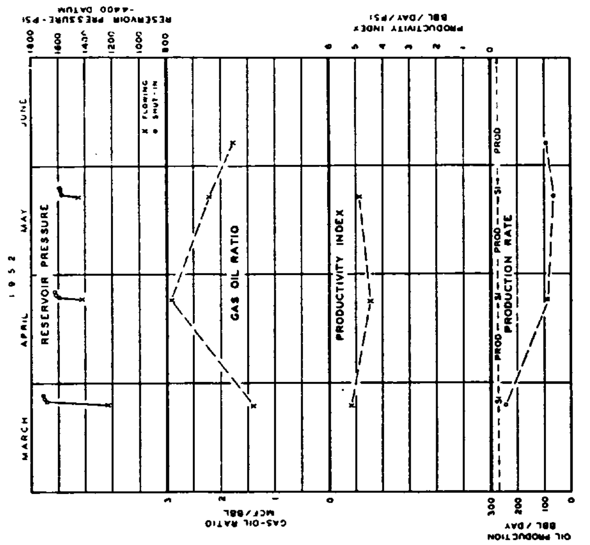

FIG. 13-F — PERFORMANCE OF J. C. BRYANS A-1 REGULARLY PRODUCING WELL.

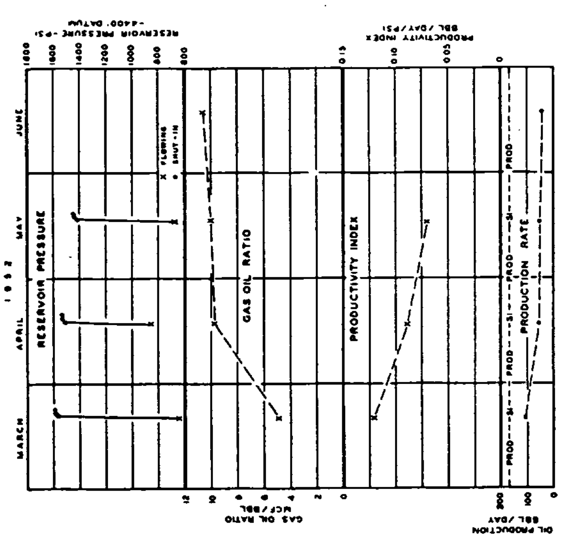

FIG. 13-C — PERFORMANCE OF DAVENPORT B-8 REGULARLY PRODUCING WELL.

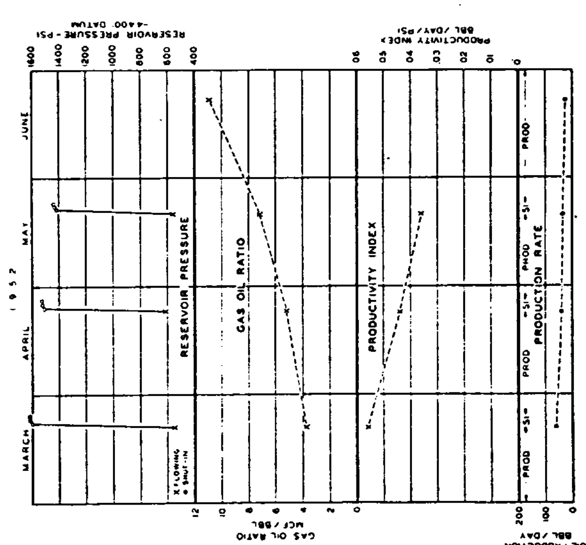

FIG. 13-D — PERFORMANCE OF DAVENPORT B-14 REGULARLY PRODUCING WELL.

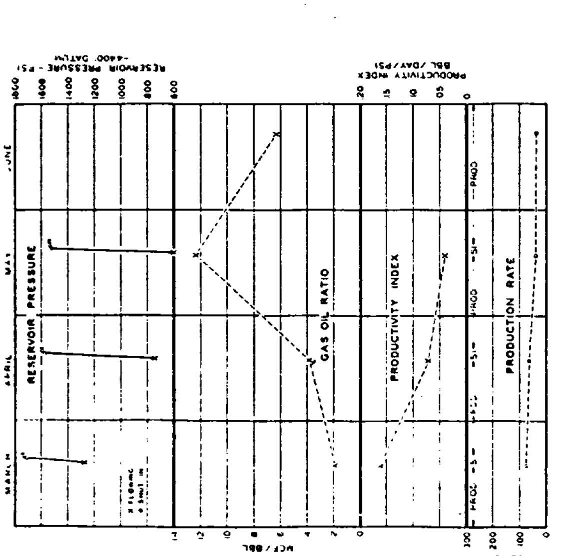

FIG. 13-A — PERFORMANCE OF DAVENPORT C-5 REGULARLY PRODUCING WELL.

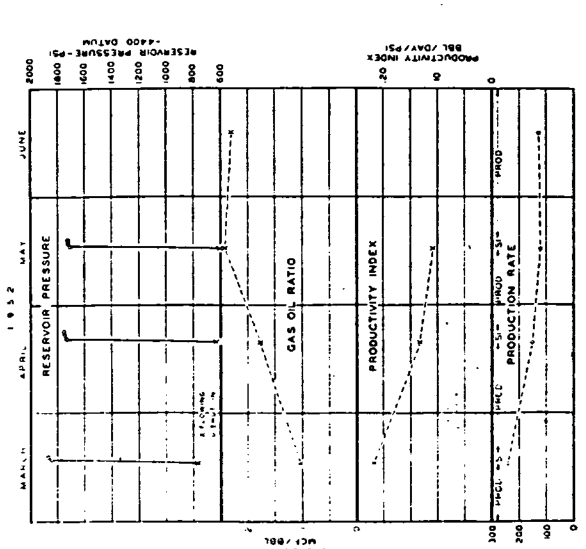

FIG. 13-B — PERFORMANCE OF DAVENPORT C-10 REGULARLY PRODUCING WELL.

Table 5 — Decline in Productivity Index

Shut-In Wells Tested Monthly

Well	Productivity Index — Bbl/Day/Psi				Ratio June Test / March Test	Ratio June Test / April Test
	March*	April**	May**	June**		
Davenport C-6	0.187	0.248	0.150	0.114	0.61	0.46
Davenport C-8	0.235	0.269	0.185	0.176	0.75	0.65
Davenport B-5	0.134	0.157	0.098	0.077	0.57	0.49
Davenport B-7	0.105	0.158	0.073	0.093	0.88	0.59
Cox A-4	0.160	0.140	0.099	0.087	0.54	0.62
Bryans A-2	0.59	0.82	0.32	0.36	0.61	0.44
				Average	0.66	0.54

Wells Produced Regularly

Well	Productivity Index — Bbl/Day/Psi			Ratio May Test / March Test
	March	April	May	
Davenport C-5	0.163	0.073	0.043	0.26
Davenport C-10	0.219	0.133	0.111	0.51
Davenport B-8	0.120	0.088	0.070	0.58
Davenport B-14	0.056	0.044	0.036	0.64
Cox A-5	0.365	0.202	0.152	0.42
Bryans A-1	0.52	0.45	0.49	0.94
			Average	0.56

*Test taken after regular production before well shut-in.
**Test taken last 6 hours of 48-hour production test following one month shut-in period.

1,320 ft from the well as it does from points near the well itself.

Since gas-oil ratios in the Spraberry have increased rapidly after the reservoir pressure declined below 1,600-1,700 psi, it is best to compare gas-oil ratios of the shut-in wells with those of the producing wells at common pressures rather than at common dates. Gas-oil ratios of the six regularly producing wells having productivity index tests and the gas-oil ratios of the six shut-in test wells are plotted versus 72-hour shut-in reservoir pressure in Fig. 14. The last gas-oil ratio point for each shut-in well plotted at the lowest reservoir pressure represents the test one to two weeks after the well had been returned to production. It is included because it represents more stabilized production than do the other measurements made during the 48-hour production tests following each one-month shut-in period. Similarly the last gas-oil ratio point for each of the regularly producing wells represents a test in June, 1952, most nearly corresponding in date to the last tests of the shut-in wells.

Although gas-oil ratios of individual wells varied irregularly during the test, there is good general agreement between the trend of gas-oil ratios of shut-in wells and the trend of gas-oil ratios of regularly producing wells. This is particularly true when it is recalled that shut-in wells were not stabilized within the 48-hour production test following each one-month shut-in period. This is best illustrated by Davenport B-5 and Davenport B-7 wells, whose gas-oil ratios increased from 3,364 to 13,077 cu ft per bbl and from 2,414 to 9,160 cu ft per bbl. respectively, within one to two weeks after the wells had been returned to regular production. These compare with gas-oil ratios 14,250 cu ft per bbl for Davenport B-8 and 11,130 cu ft per bbl for the Davenport B-14 at approximately the same date.

Since change in gas-oil ratio is an index of depletion of oil and since approximately the same changes in gas-oil ratios occurred in the shut-in wells as did in the regularly producing wells, it can only be concluded that oil saturation was reduced by substantially the same amount in the vicinity of the shut-in wells as it was in the vicinity of the producing wells.

These various comparisons of performance of shut-in wells with performance of nearby producing wells have shown by three indices of depletion, decline in reservoir pressure, decline in productivity index, and increase in gas-oil ratio, that substantially the same reduction in oil saturation was occurring in the vicinity of the shut-in wells as was occurring in the vicinity of the producing wells. These detailed tests were conducted in an area drilled on a uniform 40-acre spacing pattern so the tests of shut-in wells are limited to points 1,320 ft from some regularly producing well. But the previous observations of reduced pressure in newly completed wells in this same area included many step out developmental wells 1,870 ft from any producing well and one over half a mile from any

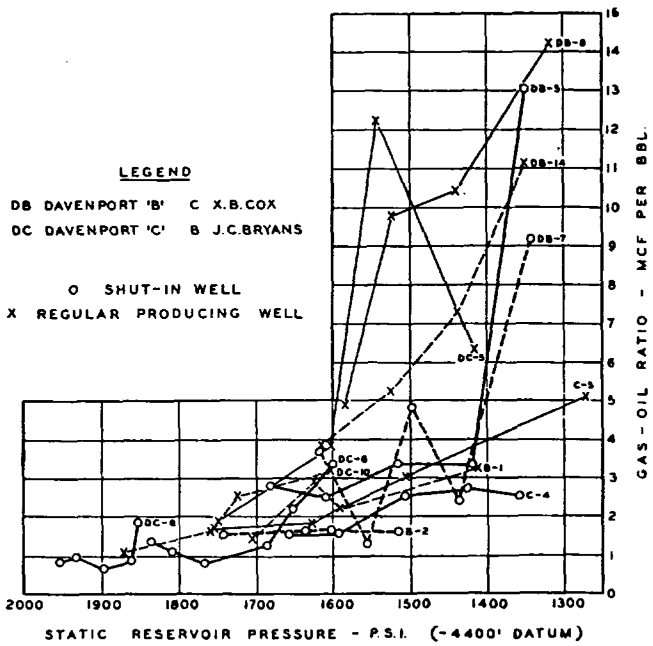

FIG. 14 — COMPARISON OF GAS-OIL RATIOS OF SHUT-IN AND PRODUCING WELLS.

producing well. There is no reason to believe reduction in productivity index and increase in gas-oil ratio would be limited to distances of 1,320 ft when reductions in reservoir pressures have occurred over much greater distances. From these various observations, it can only be concluded that one well can effect recovery of oil from an area of at least 160 acres in the Spraberry Trend as efficiently as could many wells drilled on the same tract.

GENERAL RESERVOIR PERFORMANCE

Production History

This extensive program of obtaining cores, subsurface oil samples, initial pressures of each well and the conduct of an extensive interference test in this area has yielded the most complete record of performance of any area in the Spraberry Trend. History of oil production, gas-oil ratio, and reservoir pressure of the 16-well Davenport "B" lease covering Section 2 in this area is presented in Fig. 15. Production began in August, 1951, and reached a maximum in January, 1952, when full development on a 40-acre spacing pattern had been completed. During this period average reservoir pressure declined from 2,350 psi initially to about 1,900 psi and gas-oil

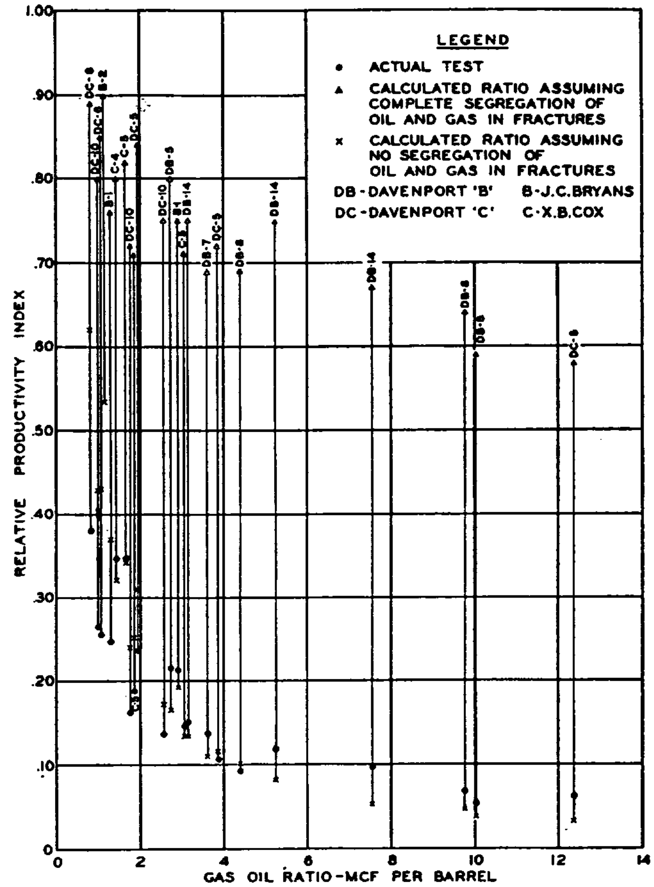

FIG. 16 — RELATION BETWEEN DECLINE IN PRODUCTIVITY INDEX AND GAS-OIL RATIO AND DEGREE OF SEGREGATION OF OIL AND GAS IN FRACTURES.

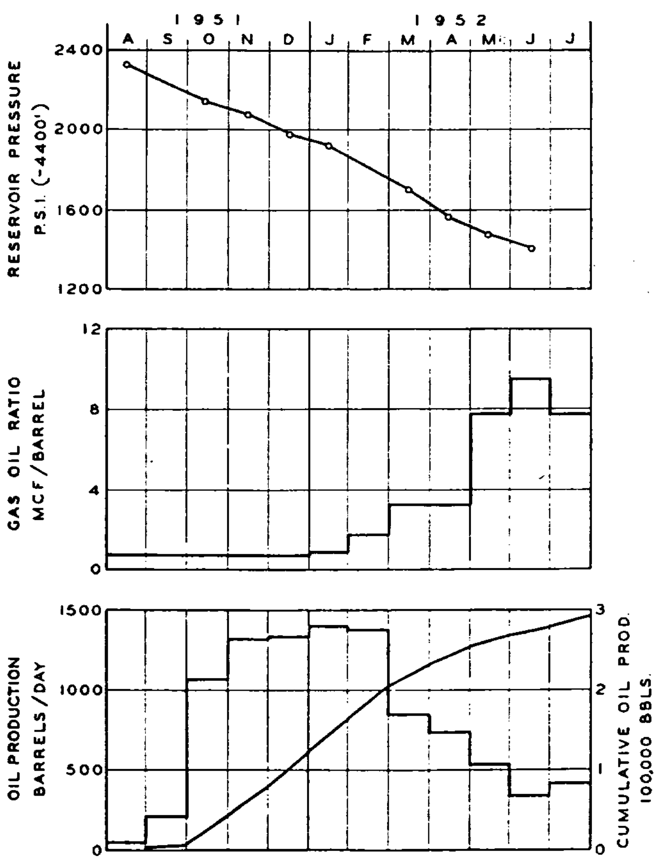

FIG. 15 — RESERVOIR PERFORMANCE, SPRABERRY SAND, DAVENPORT B LEASE (16 WELLS), DRIVER FIELD, GLASSCOCK COUNTY, TEX.

ratios remained below 1,000 cu ft per bbl at or near the solution ratio. Cumulative recovery was 170,000 bbl, or 265 bbl per acre. Production declined sharply in March due partly to some wells being shut in for the test program just described and due partly to some wells being dead and shut in for installation of gas lift equipment. Radical changes in reservoir conditions caused production to continue to decline sharply through June when it averaged only 25 bbl per well per day even though additional wells were returned to production each month. In February gas-oil ratios started to increase rapidly such that by June the average gas-oil ratio for the lease was about 9,500 cu ft per bbl and ratios for some wells were as high as 30,000 cu ft per bbl. Reservoir pressure had declined to about 1,400 psi in June and cumulative lease production was only 280,000 bbl, equivalent to 17,500 bbl per well or 440 bbl per acre. Four wells on the lease were deepened to the lower Spraberry, accounting for the increase in production and decrease in gas-oil ratio in July, 1952. Extrapolation of production decline from the upper Spraberry alone on this lease would not indicate future production to be a large percentage of past production, and this points to very low ultimate recovery in barrels per acre and in percentage of oil in place initially.

Other leases in the test area have experienced the same type decline in oil productivity and increase in gas-oil ratio, although such changes have lagged slightly behind that of the Davenport "B' lease due partly to later development and due partly to the Davenport "B" lease being most completely surrounded by areas of complete development on the 40-acre spacing pattern.

Decline in Well Productivity

Many factors affecting production change very rapidly in the Spraberry, as indicated by the decline in production of this typical lease and by the decline in productivity indices of various test wells in the interference program. For example, one well near the test area had a productivity index of 0.46 B/D per psi in a test taken within a few days after completion of the well. Two months later in a second test the productivity index declined from 0.23 to 0.09 B/D per psi in a 14-day test while the gas-oil ratio was still less than 1,000 cu ft per bbl. Such decline in productivity is much greater than that corresponding to normal relative permeability - saturation relations.

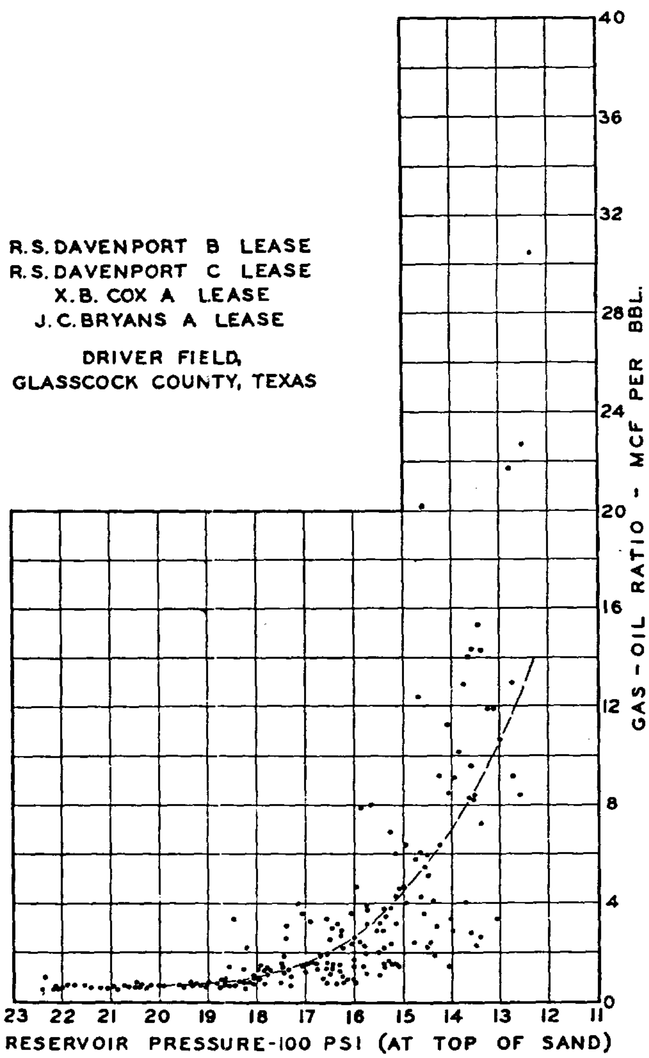

FIG. 17 — GAS-OIL RATIO VS RESERVOIR PRESSURE, PERIODIC INDIVIDUAL WELL TESTS.

Since the fracture openings are paper thin, gravity segregation of oil and gas may be very incomplete — particularly in the vicinity of the wells where velocities are highest, where considerable additional gas is being continually released from solution as the fluids flow into the area of reduced pressure, and where the converging flow concentrates pressure loss due to friction. With complete segregation of oil and gas in uniform fractures the relative permeabilities to oil and gas would correspond ideally to the relative saturations in the fractures (diagonals of a permeability - saturation plot). With no segregation in the fractures, gas would be transported as bubbles dispersed in the oil phase and the friction effects would be about the same as if only oil were present. Relative permeability to oil would correspond to the fractional composition of oil in the flowing mixture and relative permeability to gas would have no meaning in the normal concept of permeability.

Theoretical productivity index was calculated for each test of the wells in the interference test program both for the case of complete segregation of oil and gas in the fractures and for the case of no segregation of oil and gas using relative permeability - saturation relations just previously defined and using Equation (3) developed by Evinger and Muskat.[10]

$$PI = \frac{2\pi K_s H}{(P_s - P_f)\ ln\ r_e/r_w} \int_{P_f}^{P_s} \frac{K_o/K_s}{U} \frac{dP}{B} \quad . \ . \ . \ . \ . \ . \quad (3)$$

where:

PI Productivity index
K_s Specific permeability
H Thickness
K_o Effective permeability to oil
P_s Static reservoir pressure
P_f Flowing bottom hole pressure
U Oil viscosity
B Formation volume factor
r_e Drainage radius
r_w Well radius

Initial productivity indices of these test wells were calculated from initial potential tests, measured initial shut in reservoir pressures, and flowing bottom hole pressures estimated from a simple linear average of tubing pressure versus flowing bottom hole pressure from 16 tests of other new Spraberry wells. Error in flowing bottom hole pressure is estimated to have been less than 100 psi, and pressure drawdown was greater than 500 psi in all but one of the 12 test wells. Actual relative productivity indices, using these as starting points, and theoretical relative productivity indices for 23 tests of the 12 wells are plotted versus gas-oil ratio in Fig. 16. Assumption of no segregation of oil and gas in the fractures gives approximately ten times closer agreement with the actual productivity tests than does assumption of complete segregation of oil and gas in the fractures. At gas-oil ratios greater than 5,000 cu ft per bbl actual productivity is consistently greater than that calculated assuming no segregation of oil and gas in the fractures but still many fold less than that assuming complete segregation. Some deviation is not surprising because oil volume fraction of the flowing gas-oil mixture is less than 10 per cent and at least some segregation should be expected.

In addition to explaining the abnormal decline in productivity of Spraberry wells this analysis has one very practical application in considering installation of artificial lift to increase production rate of flowing wells. This theory indicates only nominal increase in production by lowering flowing bot-

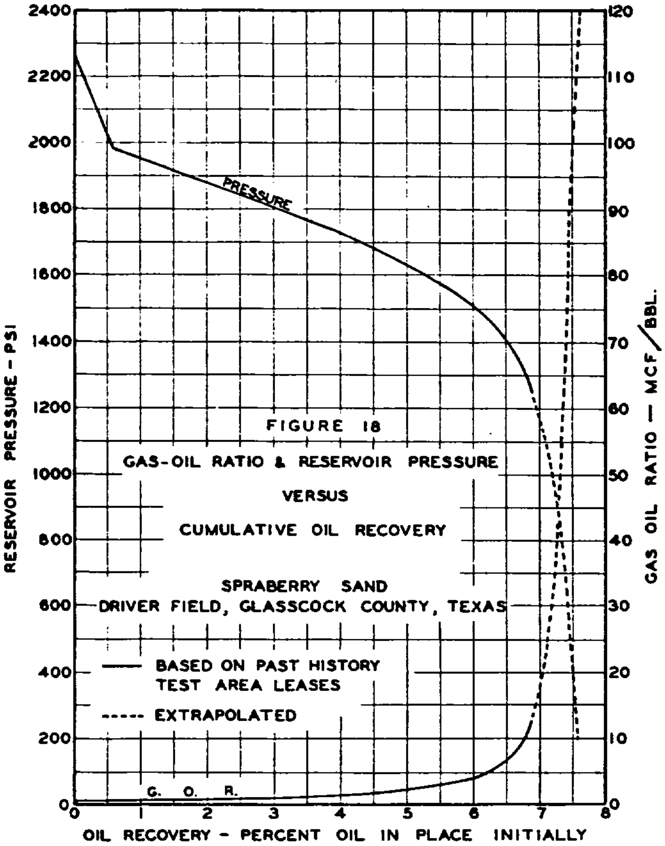

FIG. 18 — GAS-OIL RATIO AND RESERVOIR PRESSURE VS CUMULATIVE OIL RECOVERY.

tom hole pressure from say 500 psi to 100 psi when the well is capable of flowing steadily at the higher pressure. Many wells tested under these conditions have flowed at substantially the same rates as they could be pumped.

Gas-Oil Ratio, Pressure and Recovery

Individual gas-oil ratios of the various wells on the test leases are plotted versus reservoir pressure in Fig. 17. Gas-oil ratios remained at or near the solution gas-oil ratio until the pressure declined below 1,900 psi. With further reduction in pressure they then increased rapidly and averaged about 11,000 cu ft per bbl at 1,250 psi reservoir pressure. Gas-oil ratios of many wells in the test area have increased further to the range of 20,000 to 80,000 cu ft per bbl at reservoir pressure in excess of 900 psi although insufficient pressure data are available to plot the trend accurately.

Because of the rapid changes in Spraberry wells and differences in depletion of the wells, the relation between pressure decline, gas-oil ratio, and cumulative recovery cannot be accurately determined simply by averaging lease data. Such a comparison can be made, however, by material balance methods using the gas-oil ratio - pressure trend in Fig. 17, and the properties of the reservoir oil in Fig. 6. Calculations of percentage recovery of oil were made for increments of pressure decline such that gas-oil ratio corresponded to the average in that pressure range and the material balance was satisfied. Results of these calculations are presented in Fig. 18, which shows calculated gas-oil ratio and pressure versus percentage recovery of oil in place initially. The solid line corresponds with the gas-oil ratio - pressure trend in Fig. 17 and the dashed line corresponds with extrapolation of the gas-oil ratio trend.

This relation between pressure and oil recovery per cent permits an approximate indirect material balance estimate of oil in place initially in the main upper Spraberry sand in the test area. Recovery percentages corresponding to May 20, 1952, reservoir pressures of 18 wells in the three-section test area ranged from 2.45 per cent to 6.65 per cent and averaged 5.72 per cent. Combining this recovery percentage with oil in place initially in the main upper Spraberry sand indicates expected recovery of 360 to 415 bbl per acre by May 20, 1952, depending upon whether net sand oil content or gross sand oil content is applicable. Actual recovery of the four leases to that date totalled 735,000 bbl, or 418 bbl per acre on the basis of 40 acres per well.

The comparison cannot be exact because analytical methods have not yet been developed which will account for the complex flow behavior when the reservoir is below the saturation pressure and both free gas and oil are present. Equalization of pressure between the undeveloped area and the test area should be much slower than that observed in newly completed wells during development when the reservoir was above the saturation pressure. Reduction in effective permeability to oil, demonstrated by the two-fold reduction in productivity indices of wells in the interference test, and seven-fold increase in expansibility of the oil-gas mixture when the pressure declines below the saturation pressure should reduce this rate of pressure equalization.

Considering these factors, the agreement between the expected recovery and the actual recovery is good. Not only does this mean that the pressure-recovery relation in Fig. 18 reasonably represents basic performance of the Spraberry, but it also re-affirms the previous conclusion that the fracture system provides permeable contact with all reservoir blocks containing oil. Thus "islands" of reservoir rock containing commercial quantities of oil do not remain untapped by fractures in the inter-well area.

Unique Reservoir Performance

The relations between gas-oil ratio, pressure, and oil recovery percentage in Fig. 18 show that gas-oil ratios had increased significantly above the solution ratio when only 3 or 4 per cent of the oil in place had been recovered and that they had increased to about 12,000 cu ft per bbl when less than 7 per cent of oil in place had been recovered. Such trend to very high gas-oil ratio at very low percentage recovery of oil is not the performance normally expected in sandstone reservoirs where recoveries are often 15 to 25 per cent of oil in place before high average gas-oil ratios are reached. This performance of the Spraberry results from the unique properties of the reservoir, including the exceedingly fine grained low permeability matrix and the high degree of fracturing. With such conditions, retention of oil within the pores of the rock due to unbalanced capillary forces, well known as end effects in laboratory fluid-flow experiments, is important. Normally this end effect, which may be expressed as a capillary pressure difference, is at most a few psi and it is unimportant when compared with total pressure difference from a distant point in the reservoir to the well bore where the oil and gas must flow the entire length through chains of pores. In the Spraberry where the reservoir rock is divided into segments a few inches to a few feet in size, the total pressure gradient from the center of a block to the fracture face is of

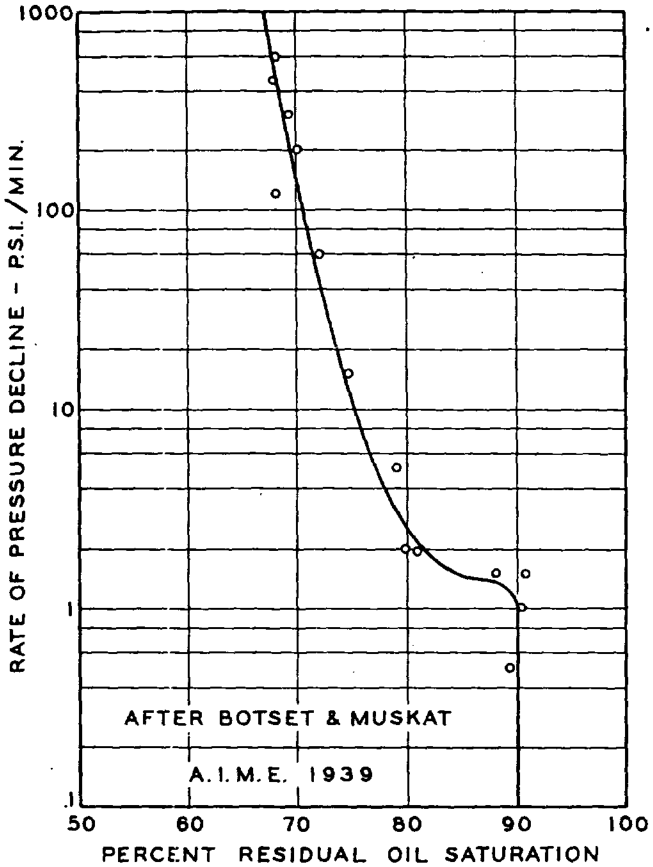

FIG. 19 — EFFECT OF RATE OF PRESSURE DECLINE ON FINAL SATURATION (SMALL CORE TESTS).

the same order of magnitude as the force of capillary retention and lower recoveries of oil result. The inter-relation between permeability, flow rate, capillary pressure, fluid properties, etc., is complex but the characteristic performance of small samples of reservoir rock is illustrated by an experiment conducted by Botset and Muskat, reported in 1939.[11] These investigators performed experiments in which a small core filled with gas-saturated oil was allowed to produce by pressure depletion at different rates in successive experiments. Results of these experiments are summarized in Fig. 19, which is a plot of residual oil saturation versus rate of pressure decline. With pressure decline of 600 psi per minute, the residual oil saturation was 67 per cent of pore space. At successively lower rates of pressure decline, the residual oil saturation was higher until the pressure decline rate reached about 1.5 psi per minute. Below this rate of production, recovery was independent of rate within experimental limits of accuracy. At high rates of production, the pressure gradient within the core was sufficient largely to overcome the capillary retention of oil. At lower rates of production, the pressure gradient was less and effects of capillarity were more pronounced. At very low rates of production, a certain minimum oil recovery was attained regardless of production rate. This latter phenomenon is due to necessity of removal of enough oil so that gas bubbles forming within individual pores could grow in size to connect with gas bubbles in adjacent pores such that it could flow readily out of the core. When this equilibrium saturation had been reached the gas flow rate was low enough that the viscous drag of gas on oil was insufficient to overcome the capillary retention and no more oil was produced.

Since the relation between the various factors involved are very complex and many of them not known quantitatively for the Spraberry, similar laboratory experiments were performed directly upon a Spraberry core sample. A core 2 in. in diameter and 6 in. in length was machined to fit closely a steel cylinder. The core containing 28.5 per cent water saturation was placed in the cell and filled with gas-saturated Spraberry oil from a subsurface sample. Gas and oil were removed from the core at such a rate to result in pressure decline of about 200 psi per minute. The core was removed and oil saturation determined to be 2 per cent by difference in weight between the core with its residual oil and water saturation and the weight of the core with its initial water saturation. Oil recovery was calculated to be 52 per cent of oil in place initially in the core.

After being cleaned, the same core containing 13.4 per cent water saturation was replaced in the cell and again filled with gas-saturated Spraberry crude oil. Withdrawal of fluids was slowed to a constant rate of pressure decline of about 100 psi per day. Residual oil similarly determined by weight difference was 57.5 per cent of pore space and the oil recovery similarly calculated to be 7 per cent of oil in place initially. Data for both tests are summarized in Table 6. Practically all production of oil occurred before pressure declined to 1,000 psi. Thereafter only gas was produced.

Pressure decline of 100 psi per day in the slower experiment reported is some 30 to 100 times faster than the reservoir pressure decline rate in presently developed areas of the Spraberry Trend, which is of the order of 1 to 3 psi per day. Recovery performance of fracture blocks of size and properties similar to that used in the laboratory experiment should certainly be no better than that of the laboratory core. In addition, recovery performance of blocks a few feet in size at pressure decline rates of the order of 1 to 3 psi should be about the same as that observed in the laboratory core test at a pressure decline rate of 100 psi per day. This is based on assumption from theory of relative permeability and capillarity that similar end effects occur in different sized blocks when production rates are such that total pressure drop from the center to the face of the block is the same in all blocks. Frequency of fractures and opening of fractures observed in cores coupled with determination of reservoir permeability from analysis of the pressure-production relation indicates

Table 6 — Results of Laboratory Experiments Pressure Depletion of Oil Saturated Spraberry Cores

CORE PROPERTIES	
Porosity	8.15%
Permeability	1.1 md
Size	2.18" diam. x 6.1" length
TEST NO. 1	
Simulated Connate Water Saturation	28.5 %
Saturation Pressure of Crude Oil	2000 Psi
Average Rate Pressure Drawdown	200 Psi/Min.
Residual Oil Saturation by Weight Difference	25 %
Calculated Oil Recovery — Per cent of Oil in Place Initially	52 %
TEST NO. 2	
Simulated Connate Water Saturation	13.4 %
Saturation Pressure of Crude Oil	1990 Psi
Average Rate of Pressure Drawdown	100 Psi/Day
Residual Oil Saturation by Weight Difference	57.5 %
Calculated Oil Recovery — Per cent of Oil in Place Initially	7 %

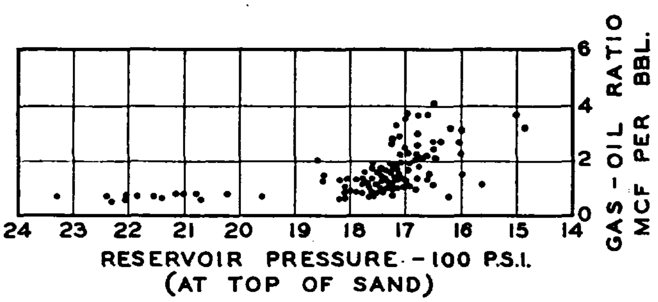

FIG. 20 — GAS-OIL RATIO VS RESERVOIR PRESSURE, PERIODIC INDIVIDUAL WELL TESTS. E. D. BERNSTEIN LEASE, R. W. CLARK LEASE, R. PEMBROOK LEASE, PEMBROOK FIELD, UPTON COUNTY, TEX.

fracture blocks are probably in this size range, and it appears that this recovery mechanism greatly influenced by capillary retention is the proper explanation of early trend to high gas-oil ratios and very low percentage recovery of oil in place indicated by performance to date in the Spraberry.

Since most Spraberry wells have been produced at near capacity and very low recovery percentage is indicated even in the areas of 40-acre spacing, no practical method exists by which the rate of pressure decline could be greatly accelerated to achieve more efficient natural recovery.

The possibility that recovery is affected by production rate in the Spraberry cannot be ruled out on the basis of the two Spraberry core tests by analogy to the Botset-Muskat experiments. However, a portion of the Pembrook Field was developed on uniform 80-acre spacing. With proration based on 40-acre units, the production rate per acre in this portion of the Pembrook Field has been half the production rate per acre of the portion of the Driver Field drilled on 40-acre spacing, which has been discussed in this paper. Relation between gas-oil ratio and reservoir pressure for this portion of the Pembrook Field is presented in Fig. 20.

Core analyses, oil characteristics including solubility, shrinkage and saturation pressure, and reservoir pressure initially in this area of the Pembrook Field were very similar to those in the Driver Field. Comparison of data in Fig. 20 with that in Fig. 17 shows the relation between gas-oil ratio and pressure — and thus recovery efficiency — are substantially the same for the 80-acre spacing area and the 40-acre spacing area. In addition oil recovery per acre attained when reservoir pressure had declined to 1,650 psi was about the same in both areas. These factors demonstrate reduced withdrawal rate per acre should have no adverse effect on ultimate recovery if the remainder of the field is developed on wider spacing.

Applicability to Entire Field

Reservoir performance data included in this paper come entirely from the two areas outlined. However, reservoir conditions and reservoir performance are qualitatively similar to this throughout the Spraberry Trend. Those readers interested in any other particular area are referred to the testimony presented by W. O. Keller at the recent hearing on the Spraberry Trend.[12] This includes summaries of core analyses, subsurface sample analyses, potentials and productivity indices of wells, examples of reduced reservoir pressure in later drilled wells, decline curve estimates of ultimate recoveries, etc., for various areas in the field.

CONCLUSIONS

1. Spraberry oil is stored primarily in pores of sand matrix of very limited section. Paper-thin vertical fractures provide flow channels for oil in this extremely low permeability reservoir.
2. That a well can deplete an area of at least 160 acres in the Spraberry as efficiently as could many wells in the same area was confirmed by direct experiment in the field.
3. Capillary "end effects" in the small fractured blocks of rock limit recovery to only a few per cent of oil in place initially.

ACKNOWLEDGMENT

Just as important as the particular facts reported here regarding reservoir performance and well spacing in the Spraberry Trend is the demonstration of co-operation that can be achieved through thorough understanding at all levels from field personnel to corporate management in solving a pressing problem. While space does not permit individual acknowledgment, the tireless efforts of pumpers, pressure unit operators, field engineers and supervisors, laboratory personnel, and others are gratefully appreciated for making the thousands of measurements accurately and on time which made this analysis possible.

The author wishes to express his appreciation to the management of Sohio Petroleum Co. for its support in the conduct of this extensive field research program and for its permission to publish the data included in this paper.

REFERENCES

1. McLennan, Lamar, Jr., and Bradley, H. W.: "Spraberry and Dean Sandstones of West Texas," *Bull.* AAPG, (April, 1951).
2. Wilkinson, W. M.: "Fracturing in the Spraberry Reservoir, West Texas." Presented at Los Angeles Meeting AAPG, March 28, 1952.
3. Bartley, J. H.: "Geology of the Spraberry Trend of the Permian Basin of West Texas." Presented at Shreveport Meeting API, March 5, 1952.
4. Franklin, Leonard O.: "Drilling and Completion Practices, Spraberry Trend." Presented at Shreveport Meeting API, March 5, 1952.
5. *Spraberry Symposium*, Third Oil Recovery Conference, Texas Petroleum Research Committee.
6. Muskat, M.: *Flow of Homogeneous Fluids through Porous Media*, McGraw-Hill. (1937) 667.
7. Bruce, W. A.: "Pressure Prediction for Oil Reservoirs," *Trans.* AIME. (1943) 151, 73.
8. Dyes, A. B., and Johnston, O. C.: "Spraberry Permeability from Build-up Curve Analysis." *Trans.* AIME, (1953) 198, 135. (*Jour. of Pet. Tech.*, May, 1953.)
9. Muskat, M.: *op. cit.*, 425.
10. Evinger, H. H., and Muskat, M.: "Calculation of Theoretical Productivity Factor," *Trans.* AIME, (1942) **146**, 126.
11. Botset, H. G., and Muskat, M.: "Effect of Pressure Reduction on Core Saturation." *Trans.* AIME, (1939) **132**, **172**.
12. Keller, W. O.: Testimony presented before Texas Railroad Commission at hearing on Spraberry Trend, Sept. 11-17, 1952.

A DRAWDOWN AND BUILD-UP TYPE CURVE FOR INTERFERENCE TESTING

H. J. Ramey, Jr.
Stanford University
Stanford, California

ABSTRACT

Interference testing is a powerful method for in situ measurement of transmissivity, storativity, and quantitative identification of anisotropy and system boundaries. The log-log type-curve matching procedure can be used for analysis of interference data taken during production or drawdown. Once production is terminated, observation well pressures return toward the initial pressure. This recovery, or pressure build-up, has been interpreted by differencing the extrapolated drawdown and measured build-up. This procedure extracts the "injection" well which causes the build-up. A new type curve for both the drawdown and build-up portion of the test has been prepared. Application of the new type curve shows that the older differencing procedure may obscure detection of system boundaries. The principal of the build-up type curve may be extended to other flow problems.

INTRODUCTION

The initial assessment of geothermal reservoirs usually has two main objectives. One is determination of the deliverability from the reservoir, and the other is estimation of the reserves, or the economically producible amount of steam in the system. Many geothermal reservoirs are complicated by the fact that neither the porosity-thickness product nor producible area are known, either early in the life or after extended production. One means of determining the deliverability is a pressure transient test. Pressure transient tests can be conducted in a short period of time, and early in the life of a geothermal development. However, estimation of steam reserves requires an extended period of production with observation of mean reservoir pressure at various stages of production. Material and energy balance performance matching with a detectable decline in pressure following production is the minimum information for performance matching. Thus it is necessary to produce a reservoir for an extended period of time before performance matching can be accomplished with acceptable risk.

The dilemma is that single-well pressure tests of fairly short duration are needed to provide accurate information on deliverability (permeability thickness or transmissivity) and well condition, while long-term production testing is required to establish reserves. Fortunately, an interference test is a type of pressure transient test that can be accomplished in a reasonable period of time, and yet provide important information concerning apparent reserves early in the life of a geothermal development. At least two wells are required for an interference test. More than two wells is desirable.

The main problem with single-well pressure transient tests is that distances in the reservoir are measured in units of the wellbore radius. A test of an individual well can yield important information concerning the condition of the well, the formation conductivity, and drainage boundaries of the well. However, long periods of production are required prior to pressure build-up testing for boundaries to be evident, when distances are measured in units of wellbore radius. An alternate procedure is to observe pressure effects transmitted between two or more wells. This kind of test is called an interference test. The theory of interference testing was explained by C.V. Theis (1935). A modern discussion of interference testing procedures has been presented by Earlougher (1977). There are many recent publications on this important subject in both the groundwater and the petroleum engineering literatures. An example of application of interference testing to geothermal systems has been published by Chang and Ramey (1979).

One simple basis for interference test analysis is the continuous line source solution. This model assumes that a single well is produced at a constant rate in an infinitely large slab reservoir of constant properties. The pressure effects caused by the producing well may be observed at one or more distant wells, which are not produced but used simply as pressure observation stations. The solution to this problem can be displayed on a piece of log-log coordinate paper. Figure 1 is a type-curve for this problem as used commonly in the petroleum literature. Figure 1 presents the analytical solution for the conventional line-source well (exponential integral solution).

$$p_D = -\frac{1}{2}\,\mathrm{Ei}\left(-\frac{r_D^2}{4t_D}\right). \tag{1}$$

where

$$p_D = \frac{kh}{141.2\,qB\mu}(p_i - p_{r,t}) \tag{2}$$

$$r_D = r/r_w \tag{3}$$

$$t_D = \frac{0.000264kt}{\phi\mu c r_w^2} \tag{4}$$

In Eqs. 2-4, English engineering units are used: permeability in millidarcies, lengths in feet, pressures in psi, viscosity in centipoise, flow rates in stock tank barrels per day, time in hours, porosity in fraction of bulk volume, formation volume factor in reservoir volumes per standard volume, and total system effective compressibility in reciprocal psi.

Figure 1 presents a dimensionless pressure which is directly proportional to an observed pressure drawdown versus the ratio of a dimensionless time to the dimensionless distance between the production and observation well squared. The dimensionless time is directly proportional to real time, and the dimensionless distance is directly proportional to real distance. An important characteristic of the logarithmic scale is that quantities proportional to the plotted scale are simply displaced linearly along the scale. Thus it is possible to graph the field data observed in an interference test as a pressure drop on the ordinate versus time on the abscissa, and make a direct comparison with the analytic solution represented by Fig. 1. This procedure is called log-log type-curve matching, and has been outlined in detail in many references, such as Earlougher (1977).

Once a set of field data has been matched with the line-source type curve, it is possible to equate the pressure difference point with the dimensionless pressure from the type-curve to make quantitative calculations. In the usual case, the net formation thickness (h), the flowrate (q), the formation volume factor (B), and the viscosity (μ) of the produced fluid would be known. The objective of the pressure matchpoint would be calculation of the effective permeability to the flowing phase (k). From the time matchpoint, it would be possible then to calculate the porosity-compressibility product. In the ordinary case, the porosity would be known, and thus it would be possible to obtain a check on the average compressibility of the formation and fluid. An alternative would be to determine the in-place porosity under the assumption that the average compressibility of the rock-fluid system were known. This step is frequently done in petroleum engineering work as a check upon porosity derived either from core analyses or from well logging methods. In petroleum engineering application, one frequently obtains both effective permeabilities and porosities which agree with information known from other sources. For example, the effective permeability will frequently agree with that obtained from a pressure buildup test on a single well, while the porosity obtained from an interference test will frequently agree with porosities obtained from core analyses.

In the case of interference testing of geothermal systems, analysis is often more complex. In the use of the pressure matchpoint, it is often observed that the net formation thickness for the geothermal system is not known. This may be a result of the fact that the formation has not been fully penetrated by drilling, or that the system is fractured and characteristics are not readily apparent. In this case, the product of permeability and formation thickness is obtained, a useful quantity for deliverability and well condition determination. In the case of the time matchpoint, frequently the porosity is not known. Since the thickness also is not known, there is a dilemma as to the kind of useful calculation available from the time matchpoint. Fortunately, important and useful information can be obtained from the time matchpoint. The product of porosity, compressibility, and thickness can be computed. This product is sufficient to estimate the mass of geothermal fluid in the system per unit area. An estimate of the system area and recovery factor for the fluid is then sufficient to make an initial estimate of the capacity of the system.

The result obtained by this method is definitely preliminary, and should be checked by material-energy balance performance matching as production follows. Several uncertainties have been identified which render the results of the test uncertain. The Theis line-source method depends on a single-phase fluid flow model. There may be carbon dioxide or steam caps in geothermal systems. In this case, the compressibility of the system may be close to that of gas, rather than liquid. Another problem is that geothermal systems are often fractured systems. Recently, Deruyck (1980) studied interference testing in fractured (two-porosity) systems, and Kucuk (1980) has offered a similar study. It appears that this sort of system should be studied further.

Both show that two-porosity system interference results may resemble the Theis curve for a homogeneous system, but the parameters which result from type-curve matching can be uncertain.

We have established the potential importance of an interference test in the early evaluation of geothermal steam systems. Because an interference test involves producing a geothermal system from an initially static condition for some time, it is obvious that the test must eventually be terminated. When this happens, there is an opportunity to obtain additional information as pressures return toward the initial state. Most discussions of interference testing deal mainly with the pressure drawdown period. But the ensuing shut-in period, when pressures recover toward the initial state, can provide important information concerning drainage boundaries of the system. One discussion of this kind of procedure was presented by Ramey in 1975. In general, the procedure involves extrapolating the initial drawdown portion of the test and differencing the pressure recovery from the extrapolation from the drawdown. The result is extraction of the effect of an injection well which caused the pressure shut-in. An example of this kind of differencing is given by Ramey (1975). Fortunately, it is possible to prepare a new log-log type-curve which contains both the drawdown and build-up portions of the test on a single graph.

Pressure-Build-up Type Curves

We consider that a well is produced at constant rate for a period of time, t_p, and then shut in. During the initial drawdown portion, the pressures at adjacent shut-in observation wells are represented by Fig. 1 and Eqs. 1-4. After the producing well is shut in, it is necessary to employ the principle of superposition to generate a relationship which describes the shut-in period properly. This results in:

$$\frac{kh}{141.2\ qB\mu} (P_i - P_{ws_{r,t+\Delta t}}) = P_D(r_D, t_p+\Delta t) - P_D(r_D, \Delta t) \tag{5}$$

t_{pD}/r_D^2

Equation 5 can be evaluated generally by replacing the dimensionless pressures by their appropriate line-source values for a particular producing time, t_p, and a range of shut-in times, Δt. Fig. 2 presents such a graph. The format is similar to Fig. 1, except the pressure build-up lines are shown as a family of curves dropping below the line-source solution, each displaying the parameter of dimensionless producing time divided by the dimensionless distance squared.

Figure 2 is the general solution for both pressure drawdown and pressure build-up measured at a shut-in observation well caused by a well producing at a constant rate for time, t_p. Obviously, a single type-curve match between field data and Fig. 2 can be made with the match involving both the production and the build-up data.

Field Example

In 1975 Ramey presented several sets of pressure drawdown and build-up interference data. We will select one example from this reference for purposes of discussion. The example will be the production of well 5-D with an interference effect measured in well 1-E, 700 ft away from well 5-D. This test actually involved injection rather than production, but the principle is the same. The injection into well 5-D caused a pressure rise in 1-E, and after shut-in, the pressure rise declined, approaching the initial pressure at an extended period of shut-in.

The details of the field example will not be given completely here. The results for well 1-E were selected by Ramey in 1975 to illustrate the principle of differencing pressure build-up data to extract the effect of the well causing the shut-in. As found in this study, well 1-E appeared to provide a reasonable match with the line-source solution for both the drawdown and pressure build-up data. (See Wentzel, 1942, for rate change differencing.)

Table 1 provides the field data for the example interference fall-off test at well 1-E. Fig. 3 is a log-log type curve of both the drawdown and build-up pressure drops as a function of the total test time. This sort of field data graph can be matched directly with the new drawdown-build-up line-source type-curve presented in Fig. 2. Fig. 4 is an illustration of the kind of match that can be obtained between the well 1-E example and the new drawdown-build-up type curve. In the match shown in Fig. 4, the same matchpoint found by Ramey in 1975 has been maintained. It is evident by comparing the field data with the new type-curve that although the drawdown portion matches the line-source reasonably well, the build-up portion of the curve after shut-in does not appear to match the computed buildup curves in Fig. 2 ideally. This may represent an indication of some sort of boundary effect becoming evident during the build-up portion of the test.

On the other hand, in the 1975 publication by Ramey, the differencing procedure was used to analyze the pressure build-up portion of the test. The build-up portion was found to match the line-source solution reasonably well. We suspect that the differencing procedure involves enough trial and error that data may be forced to match the line-source even when the field data are not a good match for the line-source solution. On the other hand, a number of other field cases have been found which appear to provide reasonably good matches with the new drawdown-build-up type curve shown in Fig. 2.

ACKNOWLEDGMENT

This work was conducted at Stanford University under DOE Grant # LBL Subcontract # 1673500.

REFERENCES

1. Chang, C.R.Y., and Ramey, H.J., Jr.: "Well Interference Test in the Chingshui Geothermal Field," Proc., Fifth Workshop on Geothermal Engineering, Stanford University, Dec. 12-14, 1978, 71.

2. Deruyck, B.G.: "Interference Well Test Analysis for a Naturally Fractured Reservoir," MS report, Stanford University, June 1980.

3. Earlougher, R.C.: Advances in Well Test Analysis, Society of Petroleum Engineers of AIME Monograph No. 5 (1977).

4. Kucuk, F.: "Transient Flow in Naturally Fractured Reservoirs and Its Application to Devonian Gas Shales," paper SPE No. 9397, presented at the 55th Annual Fall Meeting, SPE of AIME, Dallas, Texas, Sept. 21-24, 1980.

5. Theis, C.V.: "The Relation Between the Lowering of the Piezometric Surface and the Rate and Duration of Discharge of a Well Using Groundwater Storage," Trans., AGU (1935), 16, 519.

6. Ramey, H.J., Jr.: "Interference Analysis for Anisotropic Formations--A Case History," Jour. Pet. Tech. (Oct. 1975), 1290.

7. Wenzel, L.K.: "Methods for Determining Permeability of Water Bearing Materials," Geol. Survey Water Supply Paper 887, US Government Printing Office, Washington, 1942, 93.

TABLE 1--FIELD EXAMPLE INTERFERENCE FALL OFF
Well 1-E

Total Time, (hours)*	Δt, (hours)	Δp, (psi)**
27.5		3
47		5
72		11
95		13
115	14	16
125	24	16
142	41	13
192	91	10
215	114	10
240	139	6
295	194	5.8

*$t+\Delta t$ after shut-in at 101 hours.
**Actual measured pressure rise.

$q = 115$ b/d $\qquad r = 700$ ft
$B = 1$ res b/Stb $\qquad h = 25$ ft
$\mu = 1$ cp $\qquad t_p = 101$ hrs

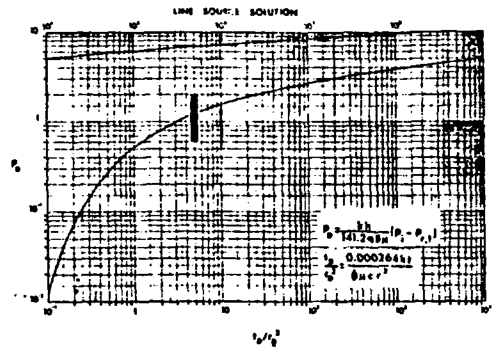

Fig. 1--The Continuous Line-Source Solution Type Curve

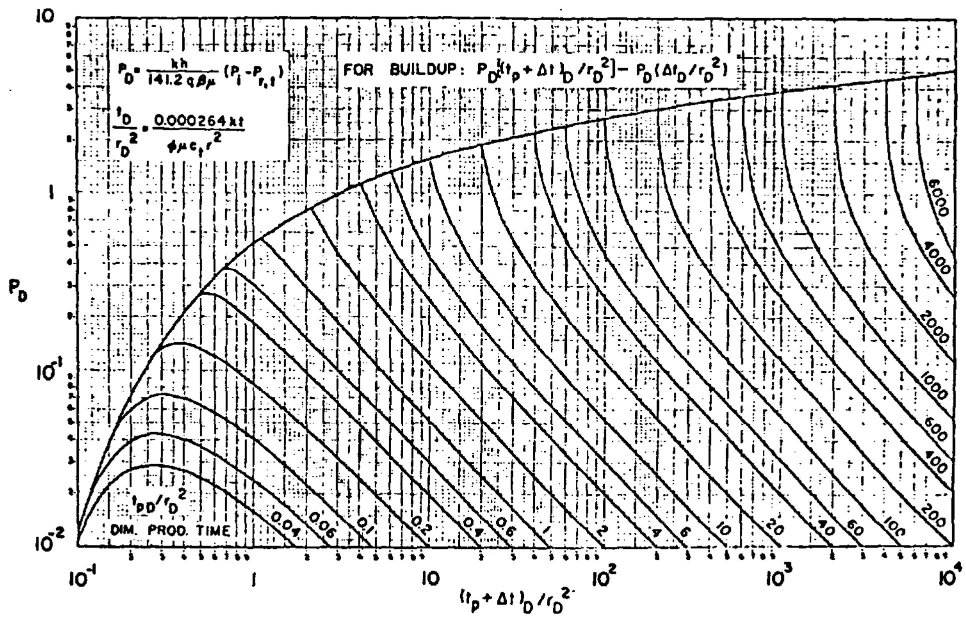

Fig. 2--Drawdown and Buildup Interference Test for a Line Source Well

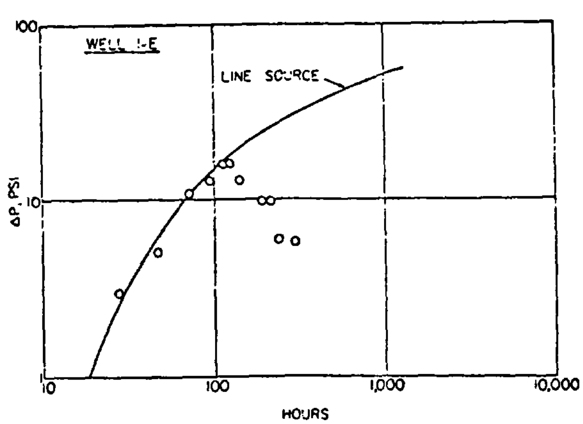

Fig. 3--Field Data Graph for Well 1-E

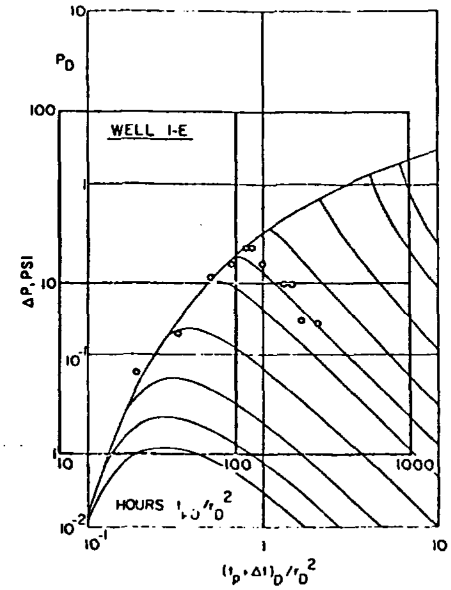

Fig. 4--Type-Curve Match for Well 1-E

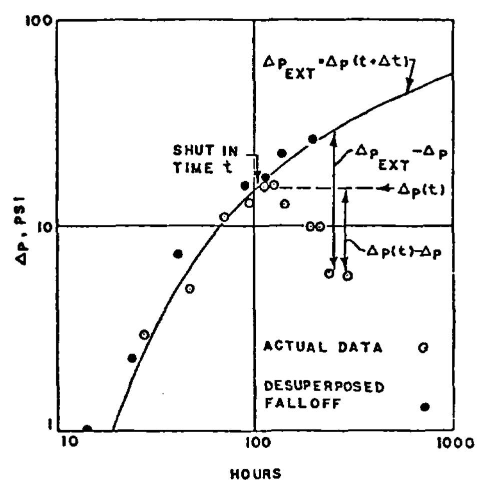

Fig. 5--Field Example Interference Falloff Analysis, Well 1-E

BUBBLE FORMATION IN SUPERSATURATED HYDROCARBON MIXTURES

IARVEY T. KENNEDY, A AND M COLLEGE OF TEXAS, COLLEGE STATION, TEX., MEMBER AIME, AND CHARLES R. OLSON, OHIO OIL CO., SHREVEPORT, LA., JUNIOR MEMBER AIME

ABSTRACT

In many investigations of the performance of petroleum reservoirs the assumption is made that the liquid, if below its bubble-point pressure, is at all times in equilibrium with gas. On the other hand, observations by numerous investigators have indicated that gas-liquid systems including hydrocarbon systems, may exhibit supersaturation to the extent of many hundred psi in the laboratory. Up to the present, there has been no reliable data on which to judge the actual extent of supersaturation under conditions approaching those existing in petroleum reservoirs.

The work reported here deals with observations and measurements on mixtures of methane and kerosene in the presence of silica and calcite crystals. Bubbles were observed to form on crystal-hydrocarbon surfaces in preference to the glass-hydrocarbon interface or to the body of the liquid. Statistically, it was found that the number of bubbles formed per second per square centimeter of crystal surface was a function of the supersaturation only, and the function was evaluated graphically.

Supersaturations were observed up to 770 psi, under which condition bubbles formed quickly and with considerable violence. With decreasing degrees of supersaturation, the frequency of bubble formation became less, until at 30 psi supersaturation and lower, no bubbles were observed to form, even though the observation at 30 psi was continued for 138 hours. It was found that silica and calcite crystals had identical effects, within experimental error, in accelerating the formation of bubbles, and that small amounts of water and crude oil had no effect on the results.

It is shown that the maximum supersaturation that can exist in a reservoir may be calculated from the data presented and from the area of the rock surface. It is also shown that the number of bubbles formed in the reservoir, in order of magnitude, may be calculated for any rate of pressure decline imposed on the reservoir by production. The bearing of the number and distribution of bubbles on reservoir performance is discussed.

INTRODUCTION

A liquid system is supersaturated with gas when the amount of gas dissolved exceeds that corresponding to equilibrium at the existing pressure and temperature. The degree of supersaturation may be conveniently expressed as the difference between the bubble-point of the mixture and the prevailing pressure. Thus, if a mixture having a bubble-point of 1,000 psi at a given temperature exists in single liquid phase at 700 psi at the same temperature, it is supersaturated to the extent of 300 psi.

There are many examples of high supersaturations, mostly in aqueous solutions, reported in the literature. Thus, Kenrick, Wismer and Wyatt[1] showed that water may be saturated with oxygen, nitrogen or carbon dioxide at 100 atmospheres, and the pressure reduced to one atmosphere without producing bubbles immediately. When liquids are in a state of tension, they may be considered as supersaturated at least to the extent of the tension. The tensile strength of water has been reported as 30 atmospheres by Meyer,[2] 60 atmospheres by Budgett,[3] 30 to 50 atmospheres by Temperley and Chambers,[4,5] 200 atmospheres by Dixon,[6] and 223 atmospheres by Briggs.[7]

Vincent[8,9] determined the tensile strength of a mineral oil as 45 psi. Gardescu[10] maintained pressures for short times in a model reservoir at 115 psi below the bubble-point.

It should be noted that the high supersaturations observed were obtained on systems carefully purified to remove particles or surfaces which might promote the formation of bubbles. These "nuclei" were considered as contaminants which interfered with the determination of a property of the liquid. In

[1]References given at end of paper.

Manuscript received in the Petroleum Branch office June 10, 1952. Paper presented at the Petroleum Branch Fall Meeting in Houston, Tex., Oct. 1-3, 1952.

petroleum reservoirs, the mineral and water surfaces with which oil is in contact must be accepted as essential parts of the system under investigation. Further, the data, to be of greatest utility for engineering purposes, should deal quantitatively with the number of bubbles formed in the reservoir under prevailing conditions. It is clear that observations of the maximum supersaturations that can be maintained for unspecified short periods, cannot yield this type of information.

In the direction of developing a quantitative approach to the phenomenon of supersaturation, it was noted that bubbles are always formed on a solid surface rather than in the liquid phase. Their formation appears to be distributed at random both as regards time and location on the solid surface. It would therefore be expected that a sufficiently large number of observations would give, at a fixed supersaturation, a constant average number of bubbles formed per square centimeter of surface per second. This theory of random formation of bubbles is in accord with the wide variation of supersaturations reported in the literature on apparently identical systems, and is supported by the data obtained in this investigation.

EXPERIMENTAL METHOD

Methane used in this investigation was the commercial material, obtained in 1,500 psi cylinders and rated as 96 per cent pure, the impurities being ethane, propane, nitrogen and oxygen. The kerosene had an API gravity of 46.3°, with an average boiling point (10 per cent intervals) of 344°F. The quartz and calcite minerals used were accurately cut from large natural crystals. The crude oil used was from the East Texas Field.

The choice of test methods was complicated by the fact that at high supersaturations, glass was the only solid found which did not accelerate bubble formation. In a steel observation cell, bubbles were observed to form repeatedly at certain points on the steel surface and on the exposed surfaces of the gaskets. The slightest scum on a mercury surface would promote bubble formation at high supersaturations, although no trouble from this source was observed in the lower range of values. However, at low supersaturations, due to the longer periods of observation required, the greater effect of diffusion of gas across gas-liquid boundaries eliminated the possibility of employing such surfaces.

Two methods were therefore employed. In the first method, used at high supersaturations, the system was confined in a glass tube with a gas-liquid contact as an upper boundary. For lower supersaturations, the system was confined above carefully purified mercury. As will be shown later, diffusion was not a factor for the periods of observation required in the first method, while no bubbles were observed to form on the mercury surface in the low supersaturation tests for which the second method was used.

In both methods, filtered kerosene and methane were agitated together in an Aminco mixing bomb for several hours, at 500 psi or 1,000 psi and room temperature. An amount of gas was released that would cause a slight drop in pressure, and shaking continued. A rise in pressure to the original value indicated that saturation was complete. The gas phase was bled off from the mixture at constant pressure, and the pressure then raised to 2,000 psi, to give an unsaturated solution of accurately known bubble-point.

In the first test method, used for high supersaturation values, quartz or calcite crystals were stacked in a test tube within a Penberthy visual cell as shown in Fig. 1. The crystals had rectangular faces of accurately known areas, the total area for each crystal averaging about 4.5 sq cm. Sufficient kerosene containing no dissolved gas was introduced into the tube to cover the bottom and one-half of the sides of the lowest crystal. The pressure in the cell was then raised to the test pressure, usually 1,000 psi, by introducing methane, and enough saturated kerosene was added to raise the liquid level to the center of the next higher crystal, holding the pressure constant.

A valve, connecting the cell to a fixed and calibrated orifice, was then opened, and the pressure allowed to fall. An electric timer was started when the valve was opened, and the time at which the first bubble appeared was noted. In conjunction with the calibration curve, the time indicated the pressure, and thus the supersaturation pressure, at which the bubble formed. A typical calibration curve is shown in Fig. 2. Where warranted by temperature fluctuations, corrections based on several calibration curves made at different room temperatures, were applied.

The appearance of a bubble terminated a run, since considerable mixing and evolution of gas generally accompanied its formation. To prepare for the next run, the cell was then allowed to fall to atmospheric pressure to desaturate its contents. It was then again brought to the test pressure by the induction of gas, and live kerosene was added until the liquid level rose to the center of the next higher crystal. The pressure was allowed to fall by opening the valve to the calibrated orifice, and the observation repeated. After the glass tube containing the crystals was filled above the top crystal, the tube was emptied, and another set made. Normally, 85 observations constituted a series, which could be analyzed

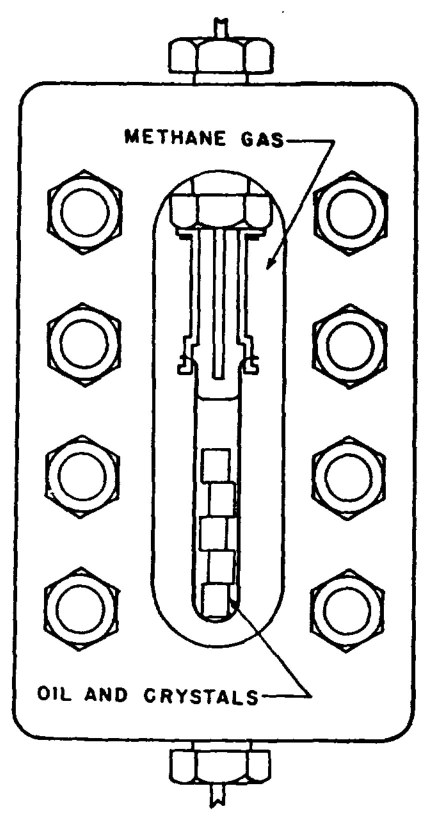

FIG. 1 — WINDOWED CELL FOR HIGH SUPERSATURATION TESTS.

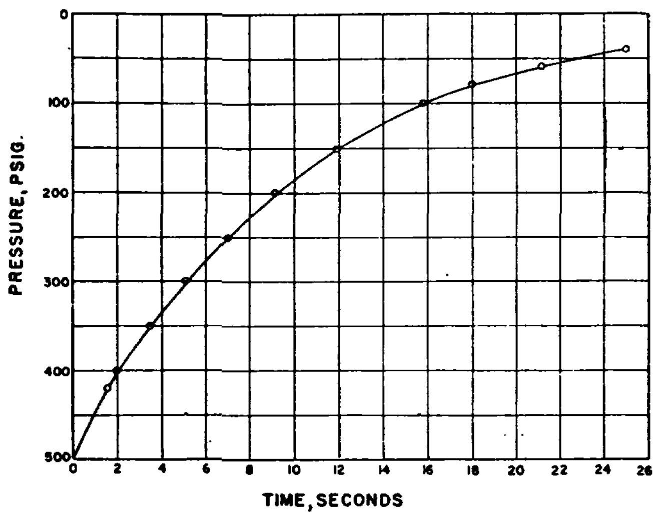

FIG. 2 — TYPICAL ORIFICE CALIBRATION CURVE.

statistically. On one series (Series E), in which the crystal area was twice the usual area, 170 observations were made to provide more points in the high supersaturation range.

The data desired from this method were (1) the number of bubbles formed in a definite narrow range of supersaturation values, (2) the total number of seconds during which the system was in this range, and (3) the area of crystal-oil interface involved. To obtain (1), the supersaturation ranges were selected to correspond to two-second intervals on the orifice calibration curve, and the number of bubbles observed in each of these intervals totaled. To obtain (2) for a given interval, two seconds for each test that went through the interval were added to the time spent in the interval by those tests terminating in the interval; (3) was determined as the average crystal-oil area for the tests terminating in the interval involved.

An example of the calculation of the number of bubbles formed per second per square centimeter (termed the frequency) by this method follows. In the interval zero to two seconds, corresponding to the supersaturation range of 0-95 psi supersaturation, no bubbles were formed and the frequency is zero. In the interval two to four seconds, corresponding to 95-165 psi supersaturation, nine bubbles were formed, and 76 tests passed through the interval without forming bubbles. The actual time spent in the interval in those tests terminated by bubble formation in the interval is shown in the first nine terms in the first bracket of the denominator below.

$$F = \frac{9}{[1.1+1.2+0.9+1.5+0.3+1.4+0.7+1.5+0.6+(76)\,2]\,[4.47]} = 0.0125$$

The term 4.47 represents an average of the crystal areas exposed to live oil. The frequency, thus determined, represents the probability that a bubble will form in one second on one square centimeter of crystal surface, at the average supersaturation in the interval.

In the second method, employed where the degree of supersaturation was so low that long times of standing were required, mixtures were confined above mercury as shown in Fig. 3. In order that no reaction products between kerosene and mercury could be formed and act as nuclei, the kerosene was distilled over sodium. After this precaution was taken no bubbles formed on the mercury surface.

In determining the frequency of bubble formation by this method the cell was assembled as shown in Fig. 3 with a single crystal inside the glass tube. The cell was then evacuated to less than 1 mm mercury pressure and purified mercury was drawn into the cell through the bottom connection until the inverted test tube was completely immersed in and filled with mercury. Water was then pumped into the top of the cell, with mercury being withdrawn from the bottom, until the test tube could be observed to a position well below the crystal, which had floated to the top of the test tube. The pressure in the cell was then adjusted to 1,000 psi which was 500 psi above the bubble-point of the mixture. A sample of kerosene-methane mixture was then introduced into the open lower end of the test tube, and then collected above the mercury.

Then the pressure on the system was lowered by bleeding off water from the top of the cell until the desired supersaturation was reached. The system was then allowed to stand until a bubble was observed to form, or in one case, until 138 hours had elapsed without bubble formation. After a bubble had been observed, the pressure was quickly raised to 1,700 psi, so as to redissolve the bubble before appreciable diffusion had taken place. One filling could thus be used for a number of tests without refilling the tube.

To correct for small variations of bubble-point with temperature, which could not be considered as negligible in this method, the magnitude of the bubble-point variation was

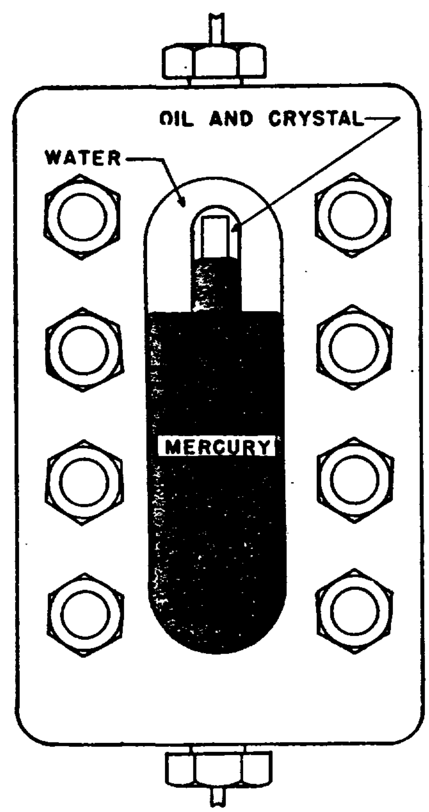

FIG. 3 — WINDOWED CELL FOR LOW SUPERSATURATION TESTS.

estimated by using available K-value charts for methane in a 200 molecular weight solvent. Correction was then applied by raising or lowering the pressure in the cell to keep the supersaturation of the liquid constant.

The frequency, as measured by this method, was simply the reciprocal the time which elapsed at a given supersaturation before a bubble was observed, divided by the crystal area.

DISCUSSION OF RESULTS

At any vapor-liquid interface in a supersaturated system vaporization is taking place. In the first method employed, such an interface existed and it was necessary to determine what influence, if any, this process exerted on the measured frequencies. To this end, two series of tests, "A" and "B," were run, the first involving an initial rate of pressure decline of 55 psi per second while the initial pressure decline rate for Series "B" was 30 psi per second. If the loss of gas at the interface were effective in lowering the supersaturation, it should be more pronounced in the second series, and the frequency of bubble formation should be lower. Reference to Tables I and II, and to Fig. 4, in which the average frequencies for all series are plotted against the supersaturation, shows no effect in this direction. All subsequent runs by Method 1 were made with pressure decline rates higher than those used in Series "B," so as to eliminate the possibility of this source of error.

Both Series "A" and "B" were made with kerosene saturated with methane at 500 psi in the presence of quartz crystals. The temperature of saturation and testing ranged from 84°F to 86°F. As in the other series investigated, the errors introduced by this variation did not exceed others inherent in the method and no correction for temperature was applied.

Series "C" was made with a mixture of kerosene and methane with a bubble-point of 1,000 psi, to determine the effect of absolute saturation pressure on bubble frequency. The data are contained in Table III and are plotted in Fig. 4. It is seen that, within the error involved in statistical observations of this type, there is no difference between liquids of different bubble-point at the same supersaturation. The crystals used in this series were quartz, as in the two previous series.

Series "D" was made with 1,000 psi bubble-point oil, and in all respects was similar to Series "C" except that calcite crystals were substituted for quartz. The data are shown in Table IV and are plotted on Fig. 4. It is seen that the composite curve drawn fits the data of this series as well as the previous data, and that calcite must be considered as equivalent to quartz as an accelerator of bubble formation.

In Series "E," a volume of saturated oil sufficient to cover twice the area of crystal as in previous tests was introduced. In other respects the runs were identical with those of Series "D." An examination of Table V, and the points for this series plotted on Fig. 4 indicates that the frequency of bubble formation, in terms of bubbles formed per second per square centimeter of crystal surface, is comparable to that obtained in the other runs. In order that sufficient data for statistical purposes should be available, twice as many runs as usual were made under the conditions of this series.

Undiluted crude oil could not be used in the tests described, because its dark color interfered with the observation of bubbles. However, it was thought possible that nuclei might be present in crude oil and might influence the frequency data obtained. In Series "F," therefore, the maximum amount of East Texas crude oil which would still allow visibility, 1.6 per cent, was added to the system. Other conditions were the same as in Series "E," *i.e.*, 1,000 psi bubble-point oil in contact with calcite. As shown in Table VI and Fig. 4, there is no discernible effect of the addition of crude oil to the system.

Data on frequencies at supersaturations below 50 psi, where effects of diffusion at the gas-liquid interface were considered to render results by the first method of investigating unreliable, are shown in Table VII. The frequencies are also

Table I — Summary of Test Data for Series "A"

Time Interval Sec.	Average Supersaturation psi	No. Bubbles Observed	Bubble Frequency Bubbles/cm²/sec x 100
0- 2	48	0	0
2- 4	130	9	1.25
4- 6	194	13	2.08
6- 8	249	16	3.34
8-10	295	14	3.50
10-12	333	9	3.44
12-14	364	7	3.79
14-16	391	6	4.96
16-18	412	4	5.14
18-20	427	3	6.04
20-22	439	2	6.21
22-24	449	0	0
24-26	458	1	10.15

Table II — Summary of Test Data for Series "B"

Time Interval Sec.	Average Supersaturation psi	No. Bubbles Observed	Bubble Frequency Bubbles/cm²/sec x 100
0- 2	32	0	0
2- 4	86	0	0
4- 6	129	7	.962
6- 8	166	10	1.52
8-10	197	9	1.55
10-12	227	11	2.26
12-14	254	11	2.86
14-16	278	8	2.68
16-18	301	8	3.52
18-20	321	7	4.30
20-22	338	5	4.76
22-24	354	3	5.20
24-26	369	3	7.89
26-28	382	1	3.99
28-30	394	1	6.38
30-32	405	1	44.7

Table III — Summary of Test Data for Series "C"

Time Interval Sec.	Average Supersaturation psi	No. Bubbles Observed	Bubble Frequency Bubbles/cm²/sec x 100
0- 2	80	0	0
2- 4	216	10	1.39
4- 6	318	21	3.68
6- 8	406	22	5.22
8-10	484	15	7.26
10-12	550	9	7.51
12-14	609	5	12.85
14-16	663	2	15.96
16-18	709	0	0
18-20	747	1	18.61

Table IV — Summary of Test Data for Series "D"

Time Interval Sec.	Average Supersaturation psi	No. Bubbles Observed	Bubble Frequency Bubbles/cm²/sec x 100
0- 2	80	0	0
2- 4	216	14	2.01
4- 6	318	17	3.08
6- 8	406	18	4.71
8-10	484	16	6.63
10-12	550	12	9.95
12-14	609	5	10.25
14-16	663	2	12.09
16-18	709	0	0
18-20	747	0	0
20-22	778	1	76.5

Table V — Summary of Test Data for Series "E"

Time Interval Sec.	Average Supersaturation psi	No. Bubbles Observed	Bubble Frequency Bubbles/cm²/sec x 100
0- 2	81	0	0
2- 4	220	43	1.69
4- 6	322	51	2.98
6- 8	406	42	4.68
8-10	481	21	6.15
10-12	548	8	7.68
12-14	605	4	11.13
14-16	656	1	16.46

Table VI — Summary of Test Data for Series "F"

Time Interval Sec.	Average Supersaturation psi	No. Bubbles Observed	Bubble Frequency Bubbles/cm²/sec x 100
0- 2	81	0	0
2- 4	220	12	1.71
4- 6	322	18	3.13
6- 8	406	20	4.98
8-10	481	17	7.71
10-12	548	9	8.49
12-14	605	4	7.85
14-16	656	4	14.2
16-18	700	1	17.2

Table VII — Summary of Low Supersaturation Tests by Second Method

Supersaturation psi	Dry Quartz Crystal			Water-Wet Crystal		
	No. Bubbles Observed	Time Before First Bubble, Sec. Range	Average	No. Bubbles Observed	Time Before First Bubble, Sec. Range	Average
50	10	36.3-87.2	56.7	10	39.1-77.2	58.1
40	4	104-600	287.4	6	102-343	236.5
30	None in 138 hours			None in 27 hours		

plotted on Fig. 4. As indicated in the table, 14 observations on dry quartz crystals were made and 16 on quartz crystals which had been wet with water. It is seen that the presence of water has no discernible effect. It should also be noted that the data obtained by this method fit very well on the composite curve obtained by the method employed for investigation systems of high supersaturation. The conformity of the data by the two methods in the region of low supersaturation is further evidence that the error due to diffusion in the first method is not appreciable under the conditions employed.

The composite curve shown in Fig. 4 was drawn as the best curve to fit all of the data obtained. It is of interest to note, however, that this curve fits the points for each series almost as well as any that could be drawn.

SIGNIFICANCE OF DATA IN PETROLEUM RESERVOIR STUDIES

In the work described, an effort was made to duplicate the essential conditions which affect the formation of bubbles in petroleum reservoirs, insofar as these conditions are known. It is appropriate, therefore, to discuss some of the implications of the results in regard to a reservoir to which they may apply.

When oil is produced from a reservoir, the pressure normally declines, even if an effective water-drive is present. Some reservoirs, such as the East Texas reservoir, are so undersaturated, that substantially their entire recoverable contents may be produced at restricted rates without the pressure falling below the bubble-point of the oil. More commonly, however, the oil becomes supersaturated in the early stages of production, even though it may have been highly undersaturated initially.

On the basis of data presented here, bubbles would be expected to form only after the supersaturation exceeds 30 psi. Supersaturation in excess of this figure and bubbles will naturally occur first in the low-pressure regions in the immediate vicinity of the producing wells. Because of the comparatively high velocities and intimate contact between gas and oil, substantial equilibrium should exist between the two phases at this location under normal flowing conditions.

As the reservoir pressure declines, and the isobar corresponding to 30 psi supersaturation moves outward from the wells, bubble formation will follow it. If the reservoir oil is uniform in composition and subject to normal gravitational pressure distribution, the surfaces connecting the bubbles farthest from the wells will be an inverted and truncated cone, with sides of constant slope. The expanding cone will follow the isobar to the limit of the reservoir or to the region of interference with another well.

When a bubble is formed, diffusion of gas from the surrounding oil begins, decreasing the supersaturation in its immediate vicinity and expanding the bubble. Surface forces, tending to compress the bubble, become negligible when its radius exceeds about .01 mm. (If the surface tension is taken as five dynes per centimeter, and bubble radius, or the radius of the pore through which the bubbles are expanding, is .01 mm the excess pressure in the bubble is only .15 psi.) Due to the phenomenon of supersaturation, the equilibrium pressure of the gas dissolved in the oil is at least 30 psi higher than the pressure inside the bubble initially, and rapid evolution of gas occurs. This situation accounts for the observation that bubbles expand to about 1 mm in radius almost instantly after they are formed on crystal surfaces.

Aspects of reservoir behavior on which the data presented may shed some light may be listed as follows:

1. The extent to which reservoir fluids may be considered to be truly at equilibrium. This is a function of the number of bubbles formed and the rate of diffusion from the oil into the gas phase as well as the rate of pressure decline imposed by production from the reservoir.

2. The order of magnitude of the number, size and distribution of bubbles formed in reservoirs.

As a first step in estimating the departure from equilibrium, the maximum supersaturation possible in the reservoir may be estimated. It is evident that this maximum will occur in the early life of the reservoir as bubbles are forming, rather than at a later date when concentration gradients have been lowered by diffusion. As an example, consider a reservoir rock with a surface area of 450 sq cm per cu cm. (The unit area assumed corresponds to a rock made up of spheres .01 cm in diameter with rhombohedral packing.) From the slope of the frequency curve, Fig. 4, we may estimate the bubble frequency, as the curve approaches its intercept, as 10^{-4} bubbles per second per square centimeter per psi supersaturation. Thus, if a supersaturation of only 31 psi could persist for one day, more than four thousand bubbles would be formed in each cubic centimeter of rock. The aggregate volume of gas, if each bubble were the equivalent of one mm in diameter, would be more than twice the entire rock volume. It is clear, therefore, that the maximum supersaturation is less than one psi in excess of the intercept value on Fig. 4, and differs from this value by less than the uncertainty in our measurement of the intercept. The intercept value of 30 psi will therefore be taken as the maximum value of supersatuartion that can exist more than momentarily in a reservoir.

It should be noted that while 30 psi represents the maximum supersaturation in a reservoir, the reservoir as a whole will never have an average supersaturation approaching this figure. While bubbles are forming in one position, oil in contact with bubbles already formed in another position will be substantially at equilibrium with them. If the reservoir pressure remains constant for a time, the oil and gas phases will approach complete equilibrium due to diffusion. If the pressure is declining at a uniform rate, supersaturation in excess of 30 psi and bubble formation will occur only if the diffusion rate into bubbles already formed is insufficient to prevent such supersaturations at all points. We thus have a criterion and a means of determining the number of bubbles that is necessary and sufficient to provide the amount of diffusion required for a given rate of pressure decline. This requirement may be expressed

$$\frac{dp}{dt} = \frac{dp_s}{dt} = \frac{Q}{V_o} \cdot \frac{dp_s}{ds} \quad . \; . \; . \; . \; . \; . \; . \; . \quad (1)$$

where $\frac{dp}{dt}$ is the rate of pressure decline imposed by production from the reservoir;

$\frac{dp_s}{dt}$ is the rate of decline of saturation pressure due to

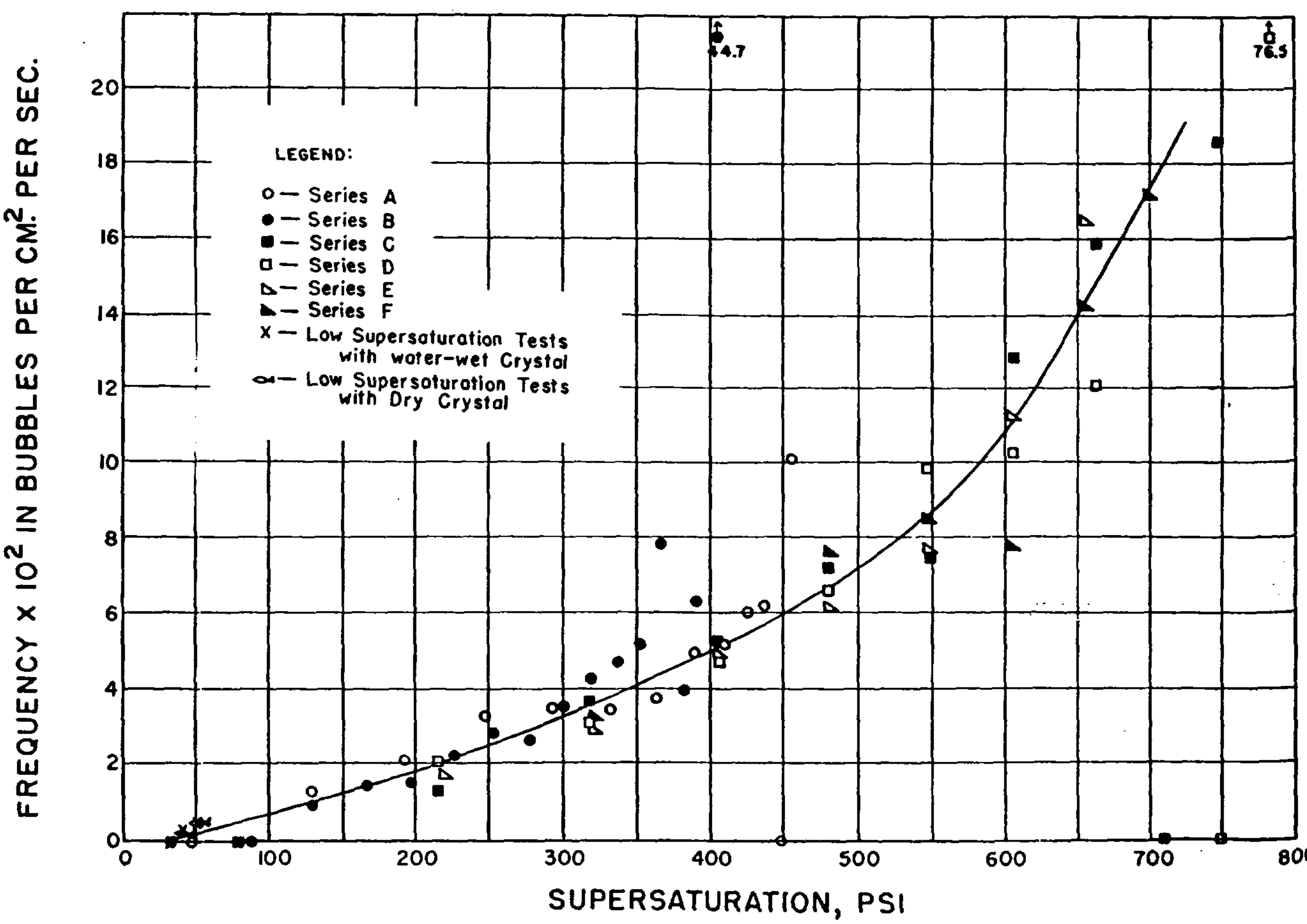

FIG. 4 — COMPOSITE BUBBLE FREQUENCY CURVE.

diffusion at the point in the region of influence of a bubble farthest removed from the bubble;

Q is the volume of gas, in surface measure, which diffuses through the volume V_o of oil in unit time;

$\frac{dp_s}{ds}$ is the decrease in equilibrium pressure due to the evolution of unit volume, in surface measure, of dissolved gas.

In determining the number of bubbles required to reduce the maximum saturation pressure at a rate equal to the reservoir pressure decline, steady state spherical flow is assumed. As shown by Bertram and Lacey,[11] the entire effect of the reservoir rock on diffusion may be expressed as a factor of about 0.8, representing the increased length of path attributable to the presence of the aggregate. (The truth of this statement is evident when it is remembered that both the amount of diffusible gas and the cross section available for diffusion are decreased by a factor representing the fractional porosity. Except for the above correction, therefore, the presence of the reservoir rock will be ignored.)

We may write, for each bubble in the reservoir,

$$Q = 0.8\frac{4\pi D(S_e - S_b)}{\frac{1}{r_b} - \frac{1}{r_e}} \quad . \; . \; . \; . \; . \; . \; . \; . \quad (2)$$

where D is the diffusion constant, and r_b and r_e are respectively the radius of the bubble and of the region of influence of the bubble, and S_b and S_e are the concentrations of gas at r_b and r_e, respectively. Each cubic foot of the reservoir may be assumed to contain N bubbles, each of which has a region of influence comprising $\frac{1}{N}$ cu ft. r_e may be expressed in terms of N as

$$r_e = \sqrt[3]{\frac{3}{4\pi N}} \quad . \; . \; . \; . \; . \; . \; . \; . \; . \; . \; . \quad (3)$$

V_o in equation (1) is simply $\frac{1}{N} = \frac{4}{3}\pi r_e^3$.

Equations (1), (2) and (3) may then be combined to give

$$\frac{dp}{dt} = \frac{dp_s}{dt} = \frac{3.2\pi ND(S_e - S_b)}{\frac{1}{r_b} - \sqrt[3]{\frac{4\pi N}{3}}}\,\frac{dp_s}{ds} \quad . \; . \quad (4)$$

If the relation between the saturation pressure, p_s, and the gas dissolved at this pressure S, be linear, then $\frac{S}{p_s} = K_s$, and

$$S_e - S_b = K_s(p_{se} - p_{sb})$$

where K_s is the slope of the pressure-solubility curve, and p_{se} and p_{sb} are respectively, the equilibrium pressures at r_e and r_b. Further, $\frac{dp_s}{ds}$, for a linear solubility relation, may be represented by $\frac{1}{K_s}$. For a reservoir in which the maximum supersaturation is 30 psi, the maximum value of $K_s(p_{se} - p_{sb})$ must equal 30 K_s. As a final equation, relating the number of bubbles with the rate of pressure decline, we may write

$$\frac{dp}{dt} = \frac{dp_s}{dt} = \frac{96\pi ND}{\frac{1}{r_b} - \sqrt[3]{\frac{4\pi N}{3}}} = \frac{301\ ND}{\frac{1}{r_b} - \sqrt[3]{4.2N}} \quad . \; . \quad (5)$$

If, in accordance with our observation that bubbles almost instantly reach the radius of 1 mm we assign this value to r_b, and let D equal 10^{-4} sq ft per hour as an average value,[12] we may calculate the number N for a typical reservoir, for any value of $\frac{dp}{dt}$. Fig. 5 shows a plot of N against the right-hand term of Equation (5). For reservoir pressure declines of 0.1, 1 and 10 psi per day, we may read corresponding numbers of bubbles per cu ft of reservoir satisfying the imposed conditions 40, 400 and 4,000. Due to the assumptions made in determining the diffusion rate, particularly the assumption of the value of r_b, the calculation must be considered correct only as to order of magnitude.

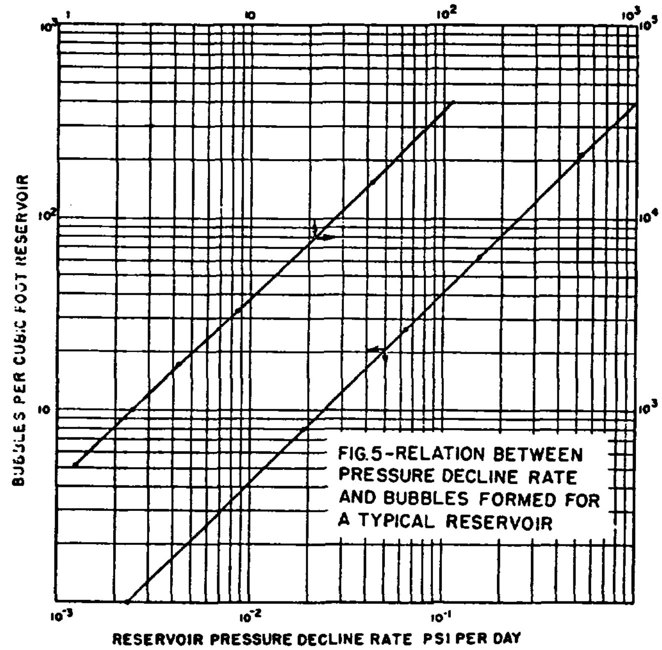

FIG. 5 — RELATION BETWEEN PRESSURE DECLINE RATE AND BUBBLES FORMED FOR A TYPICAL RESERVOIR.

For a rock consisting of grains averaging 0.1 mm in diameter, there are about 10^6 pores per centimeter cube, or some $3 \cdot 10^{10}$ pores per cu ft. It is clear that even at the most rapid reservoir pressure decline rates, only about one pore in a million will have a bubble originating in it. Where unaffected by flow, the gas will be present as a continuous enlarged bubble, encompassing many pores, surrounded by oil which is free of gas. When gradients are applied, the gas inside the continuous bubble will flow with a relative permeability characteristic of a much higher gas saturation than corresponds to the overall reservoir content, while the oil will be characterized by a relative permeability equal to the homogeneous fluid permeability of the rock. Equilibrium gas saturations, at which gas exhibits zero relative permeability, should not exist in a reservoir with gas distributed in this manner. It is noteworthy that such behavior, although detectable by a decline in gas/oil ratio in the early life of gas-drive reservoirs and generally reported in laboratory studies, has been reported absent in all field measurements.[13]

CONCLUSIONS

The data and calculations presented support the following conclusions:

1. Supersaturations as high as 770 psi are possible for short periods in a system consisting of kerosene, methane and crystals such as silica and calcite.

2. When crystals such as silica or calcite are present, bubbles invariably form on their surfaces rather than in the oil itself.

3. The tendency of bubbles to form in systems of this kind may be measured by the frequency, *i.e.*, the number of bubbles formed per second per square centimeter of crystal surface in contact with liquid.

4. Under the conditions of the tests, the frequency varied from .22 at 800 psi to zero at 30 psi saturation. No bubbles were observed to form at 30 psi supersaturation or lower, even though the test at 30 psi supersaturation was continued for 138 hours.

5. Calcite and silica surfaces are equally effective in promoting bubble formation.

6. The presence of water or crude oil, when added to the above system, had no measurable effect on bubble frequency.

7. From the bubble frequency measured, it may be calculated that maximum supersaturations in reservoirs cannot exceed 30 psi by more than a fraction of one psi, and that average supersaturations will be substantially less than this amount.

8. It is shown that the number of bubbles formed per cu ft of reservoir depends on the rate of diffusion of gas through oil and on the pressure decline rate imposed by production. For decline rates of 0.1, 1 and 10 psi per day, the number of bubbles formed will be 40, 400 and 4,000 per cu ft respectively, in order of magnitude.

9. Even at the higher rates of pressure decline, only one bubble is formed per million pores in the rock, suggesting that the increase of gas saturation in reservoirs takes place by the enlargement of gas bubbles into gas masses encompassing many rock pores.

10. Variations in the manner in which gas is distributed in permeable media may account for different relative permeabilities for the same gas saturation, and may explain discrepancies between laboratory and field data on the same type of rock.

ACKNOWLEDGMENT

It is a pleasure to acknowledge the financial support of the Tennessee Gas Transmission Co., under whose fellowship this work was done, and the encouragement given by Herman A. Otto and O. H. Moore of this company. The interest taken in this project and the advice freely given by Harold Vance, head of the petroleum engineering department, A. and M. College of Texas, is also gratefully acknowledged.

REFERENCES

1. Kenrick, F. B., Wismer, K. L., and Wyatt, K. S.: "Supersaturation of Gases in Liquids," *J. Phys. Chem.*, (Dec., 1924), 28, 1308.
2. Meyer, J.: *Zeits f. Electrochemie*, (1911), **17**, 743.
3. Budgett, H. M.: "The Adhesion of Flat Surfaces," *Proc. Roy. Soc.*, London, (1912), **A-86**, 25.
4. Temperley, H. N. V., and Chambers, L. G.: "The Behavior of Water under Hydrostatic Tension, Part I," *Proc. Phys. Soc.*, London, (July, 1946), **58**, 420.
5. Temperley, H. N. V.: "The Behavior of Water under Hydrostatic Tension, Part II," *Proc. Phys. Soc.*, London, (July, 1946), **58**, 436.
6. Dixon, H. H.: "On the Tensile Strength of Sap," *Proc. Roy. Soc.*, Dublin (1914), **14**, 229.
7. Briggs, L. J.: "A New Method for Measuring the Limiting Negative Pressure in Liquids," *Science*, (April 29, 1949), **109**, 440.
8. Vincent, R. S.: "Measurement of Tension in Liquids by Means of a Metal Bellows," *Proc. Phys. Soc.*, London, (1941), **53**, 126.
9. Vincent, R. S.: "The Viscosity Tonometer — A New Method of Measuring Tension in Liquids," *Proc. Phys. Soc.*, London, (1943), **55**, 41.
10. Gardescu, I. I.: "Experiments on Natural Gas in Oil Sand," *Oil and Gas Jour.*, (Feb. 25, 1932), **30**, (41), **22**.
11. Bertram, E. A., and Lacey, W. N.: "Rates of Solution of Gases in Oils," *Ind. and Eng. Chem.*, (March, 1936), **28**, 316.
12. Hill, E. S., and Lacey, W. N.: "Rate of Solution of Propane in Quiescent Liquid Hydrocarbons," *Ind. and Eng. Chem.*, (Dec., 1934), **26**, 1327.
13. Muskat, Morris: *Physical Principles of Oil Production*, McGraw-Hill Book Co., Inc., (1949), 464.

★ ★ ★

Determination of Fracture Orientation from Pressure Interference

LINCOLN F. ELKINS
MEMBER AIME
ARLIE M. SKOV
JUNIOR MEMBER AIME

SOHIO PETROLEUM CO.
OKLAHOMA CITY, OKLA.

ABSTRACT

Inclusion of anisotropic permeability in mathematical analysis of pressure transients observed during development of the huge Spraberry field indicates a major fracture trend which is in good agreement with that observed by fluid-injection tests spread over a 12- by 17-mile area. Delineation of this trend is important in selecting a pattern of injection for the pending large-scale water flooding in this field. Determination of reservoir parameters yielding best agreement between calculated pressures and observed reservoir pressures in newly completed wells was made using an IBM 650 computer.

INTRODUCTION

The Spraberry field covering 400,000 acres is a tight sand of less than 1-md permeability cut by an extensive system of vertical fractures. Primary recovery dominated by capillary retention of oil in the fractured sand matrix blocks is less than 10 per cent of oil in place. Strong forces of capillary imbibition of water into the sand, coupled with water flow under dynamic pressure gradient, indicate considerable increase in oil recovery can be achieved through water flooding. Best results will occur if the pattern of water injection is selected to force the water flow across the grain of the major fracture system.

Existence of an oriented vertical fracture system in the Spraberry, observed first in cores, was highlighted more recently by the 144-fold contrast in permeability along and at right angles to the major fracture trend required to match relative water breakthrough times in Humble Oil & Refining Co.'s waterflood test there. Spraberry operators since have conducted two gas-injection tracer tests for further areal confirmation of the fracture trend. Re-analysis of early reservoir pressure transients for evidence of anisotropic permeability has permitted many more local determinations of major fracture trend without resort to further field tests.

This paper is limited to updating analysis of reservoir pressure transients to include anisotropic permeability as a test for orientation of the major fracture trend in the Spraberry. The reader is referred to Refs. 1 and 2 for information about general Spraberry reservoir performance and to Refs. 3 and 4 for information about significance of fracture orientation in selection of the injection-well pattern for water flooding the Spraberry.

RESERVOIR PRESSURE DATA—DRIVER AREA

During early development of the Spraberry Driver area, Sohio Petroleum Co. made the extra effort to measure the initial pressure in each of the 71 wells in a 5-mile-long area immediately after completion. Progressively greater reductions in pressure ranging up to 400 psi were observed throughout the six-month development period. Detailed data are presented in Ref. 1.

Since the reservoir oil was undersaturated some 300 psi initially, early reservoir performance involving 55 new well pressures is subject to analysis as flow of a single compressible fluid in a porous media. Assumption of uniform permeability in all directions yielded good agreement between calculated pressures and observed pressures of these wells in the earlier study,[1] but subsequent, additional, mathematical development to include anisotropic permeability in the transient pressure considerations and present availability of electronic computers to perform the much more extensive arithmetical calculations now yield even better agreement.

The previous analysis, assuming uniform permeability, consisted essentially of calculating pressure reduction expanding circularly around each producing well and summing these effects at the time and location of each newly completed well for comparison with the measured pressure reduction. Permeability, effective fluid and rock compressibility, and permeability × thickness were varied until the best match with measured pressures was obtained. The present analysis, assuming anisotropic

Original manuscript received in Society of Petroleum Engineers office July 12, 1960. Revised manuscript received Nov. 1, 1960. Paper presented at 35th Annual Fall Meeting of SPE, Oct. 2-5, 1960, in Denver.

Discussion of this and all following technical papers is invited. Discussion in writing (three copies) may be sent to the office of the *Journal of Petroleum Technology*. Any discussion offered after Dec. 31, 1960, should be in the form of a new paper.

[1]References given at end of paper.

permeability, is similar except that, in effect, the pressure reduction caused by production of a well expands in elliptical form with length/width varying as the square root of the ratio of permeability along and at right angles to the fracture trend. This adds fracture azimuth and permeability ratio to the other significant factors affecting performance. Values of certain of these variables were assumed and one other altered until a "best" fit was obtained. It was then "fixed" and a second one adjusted, then a third, etc., until no new combination could be found to improve the agreement between calculated and actual pressures. Seventy complete sets of calculations involving 155 producing wells and 55 new well pressure points were performed.

Results of this series of calculations with respect to the orientation of fractures and contrast in permeability — factors most pertinent to water flooding — are summarized in Figs. 2 and 3 which show average (root mean square) error in pressure vs these variables. Deviation between calculated pressures and measured pressures of individual wells are presented in Fig. 4 both for assumption of directional permeability and of uniform permeability. While the resolving power of the analysis is not high, indicated by comparison of error with and without consideration of permeability contrast, there is little doubt that orientation of the fractures so calculated has sufficient accuracy to serve as a starting point for planning Spraberry waterflood injection-well patterns. They indicate an average fracture trend of N 56° E and a thirteen-fold ratio of effective permeability along and at right angles to the main fractures. Corresponding flow capacities are 3,220 and 248 md-ft, or about 104- and 8-md effective permeabilities based on 31-ft gross Upper Spraberry sand thickness. Matrix permeability is less than 1 md.

Since these pressure data of 55 new wells cover an

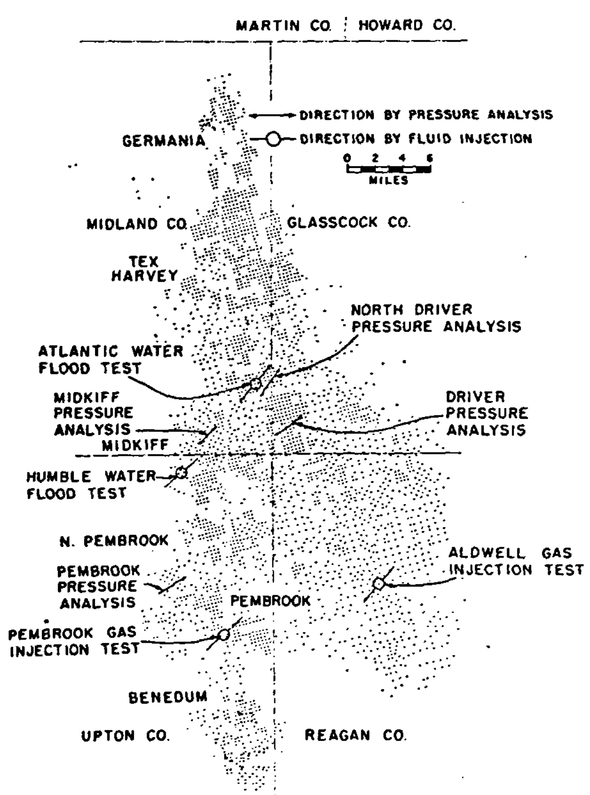

Fig. 1—Fracture Orientation, Spraberry Trend.

area 5 miles in length, they permit a determination of consistency of fracture orientation. Results of four subarea analyses also are presented in Fig. 2, with indicated

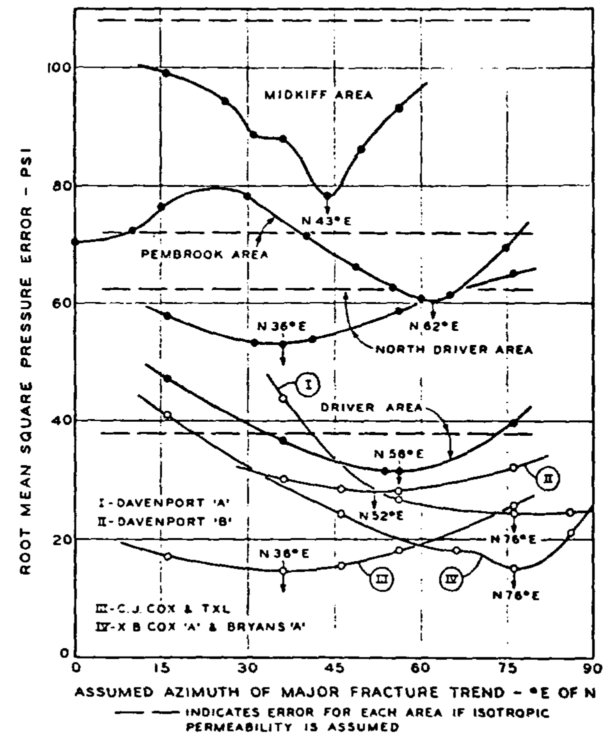

Fig. 2—Fracture Orientation by Area and by Lease in the Driver Area.

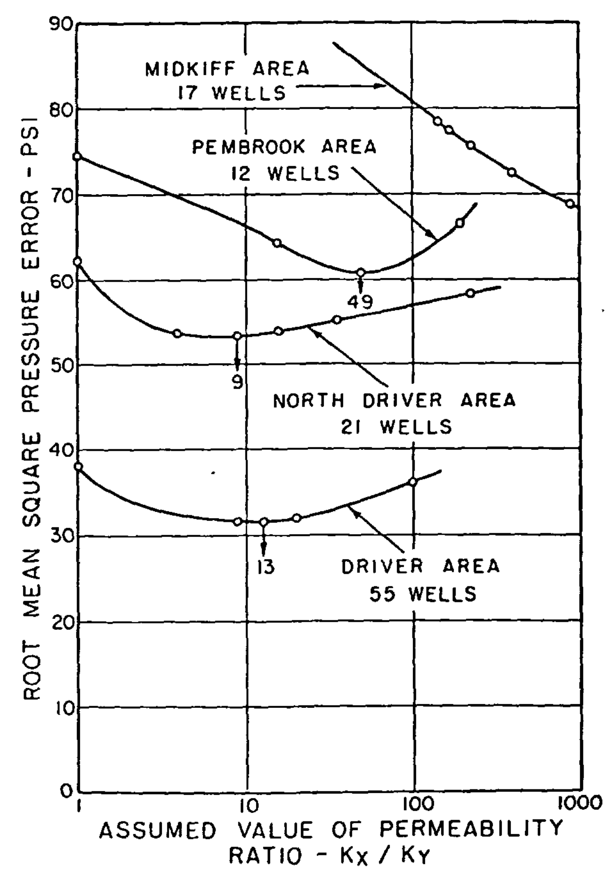

Fig. 3—Effects of Changing Magnitude of Permeability Ratio — k_x/k_y.

fracture orientation varying between N 36° E and N 76° E or ± 20° from the average direction determined using all 55 wells.

RESERVOIR PRESSURE STUDIES— OTHER SPRABERRY AREAS

Early pressures for four other areas in the Spraberry[2] have been analyzed similarly, and results are included in Figs. 2 and 3. Due possibly to the fact that three of these sets were not truly "initial" pressures of new wells but were pressures measured after as much as two months' production, there is significantly greater deviation between "best fit" calculated pressures and measured pressures than in the previously discussed results based on pressures measured immediately upon completion of new wells. Nevertheless, it is significant that fracture orientations calculated for the Midkiff and North Driver areas are in good agreement with those determined by the Humble[3] and Atlantic[4] waterflood tests, respectively. Similarly there is good agreement between the fracture orientation determined from one pressure analysis and that from the gas-injection test in the Pembrook area.[5] An attempt to determine fracture orientation from pressure data of another group of wells near the Pembrook gas-injection test resulted in such very large deviation between calculated pressures and measured pressures that no conclusion is warranted. Quite possibly this is due again to the fact that these pressures were not measured upon completion of the wells but were simply first tests available.

Fracture orientations determined by these various analyses of pressure interference between wells and by water injection and by gas injection are summarized in Fig. 1 and in Table 1. They show a range in direction from N 36° E to N 76° E over an area about 17 miles in length by 15 miles in width. Similarly, the ratio of permeability along the fracture trend to that perpendicular to it ranges from about 6 to 144 or higher.

CONCLUSIONS

Inclusion of anisotropic permeability in analysis of pressure transients in the Spraberry gives somewhat better agreement between calculated pressures and observed pressures of new wells than does assumption of uniform permeability. Close agreement between the many fracture orientations so determined and those indicated by field injection tests spread over a 15- by 17-mile area demonstrate the anisotropy is real — not merely a chance variation in the statistics. This evidence of wide-spread uniformity of fracture trend is helpful in planning the injection pattern for forthcoming Spraberry water floods.

ACKNOWLEDGMENTS

The authors wish to thank R. E. Collins of the U. of Houston and H. H. Rachford, Jr. of Humble Oil & Refining Co. for advice on the mathematical treatment of transient flow in anisotropic reservoirs. The original derivation of Eq. 1 is included in a book, *Flow of Fluids Through Porous Materials*, soon to be published by Collins. The authors also wish to thank the Pembrook Unit Operators Committee for permission to publish results of the Pembrook gas-injection fracture orientation test.

Ellen Kilpatrick developed the computer program and performed the calculations which serve as the basis for this paper.

REFERENCES

1. Elkins, L. F.: "Reservoir Performance and Well Spacing, Spraberry Trend Area Field of West Texas", *Trans.*, AIME (1953) 198, 177.
2. Testimony before Texas Railroad Commission, (Sept. 11-17, 1952) Oil and Gas Docket Nos. 125 and 126, Nos. 7 and 8 — 24360.
3. Barfield, E. C., Jordan, J. K. and Moore, W. D.: "An Analysis of Large Scale Flooding in The Fractured Spraberry Trend Area Reservoir", *Jour. Pet. Tech.* (April, 1959) XI, No. 4, 15.
4. Elkins, L. F.: "Spraberry Waterflood Possibilities", Talk presented to National Oil Scouts and Landmen's Assoc. (June 6, 1958); summary in *Oil and Gas Jour.* (June 30, 1958); *World Oil* (Aug. 1, 1958).
5. Pembrook Unit Operator: Personal Communication.
6. U. S. Bureau of Mines: Report to Southland Royalty Co. on Radioactive Gas Tracer Survey, Spraberry Trend, Aldwell Area, Reagan County, Tex. (Feb., 1960).
7. R. E. Collins: Personal Communication.

APPENDIX

The pressure drawdown at the location of a new well due to constant production of another well in an extensive reservoir of uniform thickness having aniso-

TABLE 1—FRACTURE ORIENTATION AND PERMEABILITY CONTRAST, SPRABERRY TREND AREA FIELD

	Fracture Trend	Ratio of Permeabilities*	Avg. Deviation Calculated vs Measured Pressures (psi)	Equivalent Permeability** (md-ft)
Midkiff Area				
Humble Water Flood	N 50° E	144		
Pressure Analysis (17 wells)	N 43° E	100 to 1000	78.4	443
North Driver Area				
Atlantic Water Flood***	N 42° E	—		
Pressure Analysis (21 wells)	N 36° E	9	53.3	406
Pembrook Area				
Gas Injection test	N 48° E	—		
Pressure Analysis (16 wells)	N 62° E	49	60.6	446
Aldwell Area				
Radioactive Gas Tracer[6]	N 53° E	about 16		
Driver Area†				
Pressure Analysis				
55-Well Composite	N 56° E	13	31.6	888
14-Well Davenport A Lease	N 76° E	36	24.7	1130
15-Well Davenport B Lease	N 52° E	6	28.4	968
13-Well X. B. Cox and J. C. Bryans A Leases	N 76° E	36	15.2	1020
12-Well C. J. Cox and T.X.L. Leases	N 36° E	7	14.7	481

*Ratio of permeability along major fracture trend to permeability perpendicular to fracture trend.

**$h\sqrt{k_x k_y}$

***Orientation determined by general pattern of reduction of gas-oil ratio and water breakthrough.

†See Ref. 1 for identification of leases.

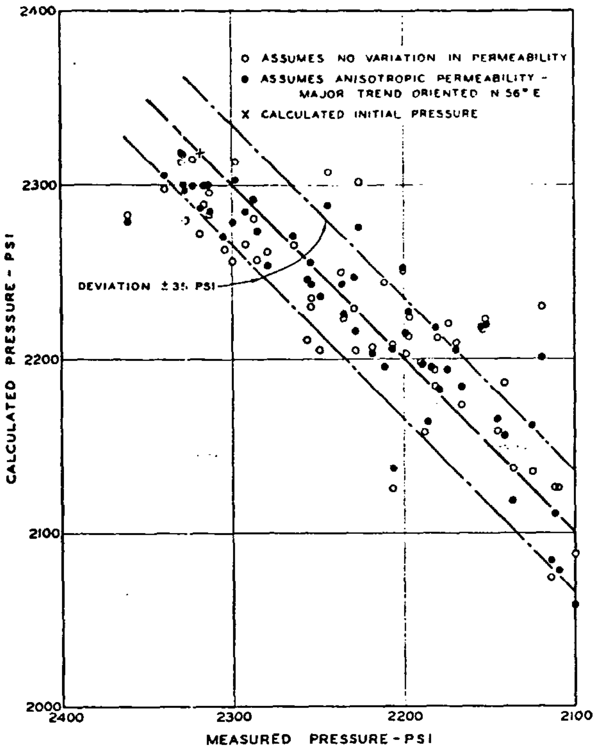

FIG. 4—CALCULATED PRESSURE VS MEASURED PRESSURES, DRIVER AREA, SPRABERRY TREND FIELD.

tropic permeability is given by Eq. 1 for conditions of single-phase flow.[7]

$$p_i - p = \frac{(-)\, q\, \mu\, B}{4\,\pi \sqrt{k_x\, k_y}\, h\ 1.127}\ \mathrm{Ei}\left(- \frac{\dfrac{(x - x_o)^2}{k_x} + \dfrac{(y - y_o)^2}{k_y}}{\dfrac{4\,t}{\mu\, c\, \phi}\quad 6.32} \right) \quad . \ . \ . \ (1)$$

where p_i = initial pressure (psi),
p = pressure at x, y at time t (psi),
q = production rate (B/D),
μ = viscosity of oil (cp),
B = formation volume factor,
h = thickness (ft),
t = time (days),
c = effective compressibility of oil, water and rock (vol/vol/psi),
ϕ = porosity (fraction),
Ei(— —) = exponential integral,
k_x = effective permeability in x direction (darcies),
k_y = effective permeability in y direction (darcies),
$(x - x_o)$ = distance from producing well to pressure point in x direction (ft),
$(y - y_o)$ = distance from producing well to pressure point in y direction (ft), and
1.127 and 6.32 = conversion factors.

The pressure reductions at a point due to production of different wells are additive. For uniform permeability, Eq. 1 reduces to the simpler, well known form involving r^2 and k.

Since significant reservoir properties including effective compressibility of rock and its contained fluids and permeability, whether uniform or anisotropic, appear implicitly in this relation they can be determined only by trial solutions until the set of values is found which gives the best match between calculated pressures and measured pressures. Fracture orientation, diffusivity parallel to the main fractures and diffusivity perpendicular to the main fractures are related implicitly in Eq. 1, and geometric mean permeability $\sqrt{k_x k_y}$ and p_i are explicit. Determination of the best set of these factors requires the following sequence.

1. Determine x and y coordinates of all producing wells and pressure observation wells.

2. Rotate these coordinates to an assumed fracture orientation since axes in Eq. 1 correspond to directions of maximum and minimum permeabilities.

3. Calculate $\Sigma\, q$ Ei (— —) for each pressure observation well using assumed values of diffusivity in the new x and y directions and determine the associated values of $\sqrt{k_x k_y}$ and p_i by least-squares method.

4. Successively modify the fracture orientation and diffusivities in the x and y directions until a set of values of these factors is found such that any further modification increases the sum of squares of the difference between measured and calculated pressures of the individual observation wells. ★★★

WELL INTERFERENCE AND PULSE TESTS

MED M. KAMAL
Amoco Production Company

SPE Mid-Continent Section
Continuing Education Course
On
Well Test Analysis

April 21, 1975

5. Using some <u>approximate</u> known values of the formation permeability, porosity, and thickness, the viscosity of the oil and the total compressibility, together with the dimensionless cycle period, the dimensionless response amplitude, and Eqs. 30 and 32, calculate the cycle period and the response amplitude.

6. Using the pulse ratio and the cycle period, calculate the pulsing period and the shut-in period.

ANALYZING THE PULSE TEST GRAPHICALLY

After running the test and measuring the time lags and the response amplitudes, the following method may be used to determine the values of the two groups $(kh/\mu)$and $(\phi c_t h)$.

1. Calculate the dimensionless time lag using Eq. 31.

2. Determine the dimensionless cycle period using the dimensionless time lag and the appropriate curve in Figs. 17, 18, 21, and 22.

3. Determine the dimensionless response amplitude using the dimensionless time lag and the appropriate curve in Figs. 19, 20, 23, or 24.

4. Calculate the value of (kh/μ) from Eq. 32 and the value of $(\phi c_t h)$ from Eq. 30.

DESIGNING THE PULSE TEST ANALYTICALLY

1. Select the pulse ratio as in the graphical method.

2. Calculate the dimensionless time lag using Eqs. 22 and 23.

3. Using Figs. 25 and 26, find A and C.

4. Using Figs. 27 and 28, find E and F.

5. Calculate the dimensionless cycle period using Eq. 33 and the dimensionless response amplitude using Eq. 34.

6. Using some approximate known values of the formation permeability, porosity and thickness, the viscosity of the oil, and the total compressibility, calculate the cycle period and the response amplitude using Eqs. 30 and 32.

ANALYZING THE PULSE TEST ANALYTICALLY

1. Using Eq. 31, calculate the dimensionless time lag.

2. Calculate the dimensionless cycle period using Eq. 33.

3. Calculate the dimensionless amplitude using Eq. 34.

4. Calculate the value of (kh/μ) using Eq. 32 and the value of $(\phi c_t h)$ using Eq. 30.

A WORKED EXAMPLE ON THE DESIGN AND ANALYSIS OF PULSE TESTS GRAPHICALLY AND ANALYTICALLY

The following is an example of the steps to be taken to design and analyze a pulse test:

Assume that the most convenient pulse ratio is 0.6 and that the reservoir has the following approximate properties: